University of Cyprus

DEPARTMENT OF CIVIL AND ENVIRONMENTAL ENGINEERING

GENERAL PLANAR-MOTION DYNAMICS OF BASE ISOLATED RIGID BLOCKS

DOCTOR OF PHILOSOPHY DISSERTATION

SPYROULLA S. ODYSSEOS

2016

University of Cyprus

DEPARTMENT OF CIVIL AND ENVIRONMENTAL ENGINEERING

GENERAL PLANAR-MOTION DYNAMICS OF BASE ISOLATED RIGID BLOCKS

SPYROULLA S. ODYSSEOS

A Dissertation Submitted to the University of Cyprus in Partial Fulfillment of the Requirements for the Degree of Doctor of Philosophy

MAY 2016

Validation Page

Doctoral Candidate: Spyroulla S. Odysseos

Doctoral Thesis Title: General Planar-Motion Dynamics of Base Isolated Rigid Blocks

The present Doctoral Dissertation was submitted in partial fulfillment of the requirements for the Degree of Doctor of Philosophy at the Department of Civil and Environmental Engineering and was approved on the 15th of April, 2016 by the members of the Examination Committee.

Examination Committee:

Research Supervisor: ΠΡΟΣΩΠΙΚΑ ΔΕΔΟΜΕΝΑ

Dr. Panayiotis Roussis, *Assistant Professor, Department of Civil and Environmental Engineering, University of Cyprus*

Committee Member: ΠΡΟΣΩΠΙΚΑ ΔΕΔΟΜΕΝΑ

Dr. Panos Papanastasiou, *Professor, Department of Civil and Environmental Engineering, University of Cyprus*

Committee Member: ΠΡΟΣΩΠΙΚΑ ΔΕΔΟΜΕΝΑ

Dr. Dimitrios Loukidis, *Assistant Professor, Department of Civil and Environmental Engineering, University of Cyprus*

Committee Member: ΠΡΟΣΩΠΙΚΑ ΔΕΔΟΜΕΝΑ

Dr. Christis Chrysostomou, *Professor, Department of Civil Engineering and Geomatics, Cyprus University of Technology*

Committee Member: ΠΡΟΣΩΠΙΚΑ ΔΕΔΟΜΕΝΑ

Dr. Panos Tsopelas, *Associate Professor, School of Applied Mathematical and Physical Science, National Technical University of Athens*

Declaration of Doctoral Candidate

The present doctoral dissertation was submitted in partial fulfillment of the requirements for the degree of Doctor of Philosophy of the University of Cyprus. It is a product of original work of my own, unless otherwise mentioned through references, notes, or any other statements.

Spyroulla S. Odysseos

Περίληψη

Η διατριβή αυτή επικεντρώνεται στη διερεύνηση της γενικής πολυμορφικής κίνησης σεισμικά μονωμένων άκαμπτων μπλοκ στο επίπεδο, όταν υπόκεινται σε εδαφικές διεγέρσεις. Το μοντέλο που αναπτύχθηκε αποτελείται από ένα συμμετρικά άκαμπτο μπλοκ το οποίο εδράζεται σε μία σεισμικά μονωμένη άκαμπτη βάση. Κάτω από μία σεισμική διέγερση, το σύστημα μπορεί να αποκριθεί δυναμικά με τέσσερις διαφορετικούς τρόπους: (α) απλή οριζόντια μετακίνηση, κατά την οποία το σύστημα μετακινείται οριζόντια ως μία οντότητα, (β) ολίσθηση, κατά την οποία το μπλοκ ολισθαίνει πάνω στη μετακινούμενη βάση, (γ) λικνισμός, κατά τον οποίο το μπλοκ περιστρέφεται γύρω από τις δύο γωνίες καθώς μετακινείται η βάση οριζόντια και (δ) ολίσθηση-λικνισμός, κατά την οποία το μπλοκ ολισθαίνει και ταυτόχρονα λικνίζεται πάνω στη μετακινούμενη βάση. Οι εξισώσεις κίνησης που περιγράφουν την κίνηση του συστήματος μορφώθηκαν με τη βοήθεια της μεθόδου Lagrange. Για την ανάλυση του μοντέλου χρησιμοποιήθηκαν δύο τύποι σεισμικής μόνωσης, ένα γραμμικό με βισκοελαστική συμπεριφορά και ένα μη-γραμμικό με διγραμμική συμπεριφορά.

Η πολυπλοκότητα του μαθηματικού μοντέλου διέπεται κυρίως από την κρούση που μπορεί να συμβεί μεταξύ του λικνιζόμενου μπλοκ και της μετακινούμενης βάσης, όπως επίσης και από την πιθανή εναλλασόμενη μετάβαση από τη μία κίνηση σε άλλη, αλλάζοντας έτσι και τους βαθμούς ελευθερίας του συστήματος. Συνεπώς, στη διατριβή αυτή αναπτύχθηκε ένα αναλυτικό μοντέλο που περιγράφει την κρούση, κατά τη διάρκεια των κινήσεων του λικνισμού και της ολίσθησης-λικνισμού, με βάση την κλασική θεωρία. Η έρευνα εξετάζει εις βάθος την κίνηση του συστήματος, συνδυάζοντας τις μη-γραμμικές εξισώσεις κίνησης με το μοντέλο της κρούσης. Επίσης, στη διατριβή αυτή διατυπώθηκαν και τα κριτήρια τα οποία καθορίζουν τις συνθήκες κάτω από τις οποίες μπορεί να γίνει η εναλλαγή της κίνησης.

Για τη διερεύνηση της δυναμικής συμπεριφοράς του συστήματος, αναπτύχθηκε ένας υπολογιστικός κώδικας που προσδιορίζει τη δυναμική απόκριση του σεισμικά μονωμένου ή μη-σεισμικά μονωμένου συστήματος, λαμβάνοντας υπόψη τους διαφορετικούς τρόπους απόκρισης, την κρούση, τα κριτήρια εναλλαγής της κίνησης και τη σεισμική διέγερση. Έγινε μια εκτεταμένη διερεύνηση αλλάζοντας τα γεωμετρικά χαρακτηριστικά του μπλοκ και τις παραμέτρους της σεισμικής μόνωσης. Ως σεισμικές διεγέρσεις χρησιμοποιήθηκαν απλοί

τριγωνομετρικοί παλμοί και πραγματικοί σεισμοί που καταγράφηκαν κοντά στο επίκεντρο. Στόχος της έρευνας είναι η μελέτη της επίδρασης της σεισμικής μόνωσης στη δυναμική συμπεριφορά και στην ευστάθεια του συστήματος.

Η έρευνα κατέδειξε ότι η σεισμική μόνωση βελτιώνει την ευστάθεια του μπλοκ όταν υπόκειται σε παλμούς με μικρή περίοδο. Συγκεκριμένα, η χρήση της σεισμικής μόνωσης βελτιώνει την ευστάθεια του μπλοκ καθώς μειώνεται το μέγεθος του, με την προϋπόθεση ότι δεν υπόκειται σε παλμούς με μεγάλη περίοδο. Σε αντίθεση, η χρήση της σεισμικής μόνωσης δε βελτιώνει την ευστάθεια του μπλοκ, σε σύγκριση με το μη-σεισμικά μονωμένο μπλοκ, όταν υπόκειται σε παλμούς με μεγάλη περίοδο. Παρόλα αυτά, για να ανασηκωθεί ένα σεισμικά μονωμένο μπλοκ απαιτείται μεγαλύτερη εδαφική επιτάχυνση σε σχέση με ένα μη-σεισμικά μονωμένο μπλοκ, ανεξαρτήτως της περιόδου του παλμού. Ο συντελεστής τριβής μεταξύ του μπλοκ και της βάσης έχει καθοριστική επίδραση στη δυναμική συμπεριφορά του σεισμικά μονωμένου μπλοκ.

Abstract

This dissertation presents a comprehensive investigation on the general planar-motion dynamics of base-isolated rigid blocks subjected to ground excitation. The system considered consists of a symmetric rigid block standing free on a seismically isolated rigid base. The response of the system is described in terms of four distinct oscillation regimes: system translation, in which the base-block system translates as a whole; sliding, in which the block slides relative to the horizontally-moving base; rocking, in which the block pivots on its edges with respect to the horizontally-moving base; and slide-rocking, in which the block simultaneously slides and pivots on its edges with respect to the horizontally-moving base. The governing equations of motion are obtained for each oscillation regime using the Lagrange method. Two models for the isolation system are considered, a linear model with viscoelastic behavior and a nonlinear model with bilinear hysteretic behavior.

The mathematical description of the system dynamics is profoundly complex, primarily due to the inherent nonlinear nature of the impact phenomenon and the potential transition from one oscillation pattern to another, each one governed by a different set of differential equations. A rigorous model governing impact from rocking and slide-rocking regimes is formulated using classical impact theory. The study examines in depth the motion of the system with a large-displacement formulation that combines the nonlinear equations of motion along with the developed model governing impact. Moreover, transition criteria that specify the conditions under which switching between the various oscillation regimes are established.

On the basis of the proposed analytical model, a computer program was developed to determine numerically the dynamic response of the system, being either isolated or not, by considering the different possible oscillation regimes, impact occurrence(s), transition criteria, and arbitrary excitation. An extensive numerical investigation was carried out under idealized base-acceleration pulses and recorded pulse-type earthquake motions with a wide range of amplitude and frequency content, for varying block geometric characteristics and isolation-system parameters, with the aim of identifying potential trends in the response and stability of the system.

The investigation has shown that the use of isolation results in better system performance, with respect to the initiation of rocking and overturning, for short-period pulses. In particular,

the use of isolation improves the stability of blocks with decreasing block size, provided that the system is not subjected to long-period acceleration pulses. On the contrary, for long-period pulses, the use of isolation is not beneficial in improving the stability of the block, compared with the non-isolated case. Nevertheless, the use of isolation results in an increase in the acceleration required to initiate rocking in comparison with the non-isolated block, regardless the pulse-period. In addition, the value of coefficient of friction between the block and the supporting base has a significant impact on the performance of the isolated block.

Acknowledgements

This dissertation would not have been possible without the support of many people. I wish to express my gratitude to my supervisor, Dr. Panayiotis Roussis, Assistant Professor at the Department of Civil and Environmental Engineering at the University of Cyprus, who was abundantly helpful and offered invaluable assistance, support, and guidance. Deepest gratitude is also due to the members of the examining committee, Dr. Panos Papanastasiou, Dr. Dimitrios Loukidis, Dr. Christis Chrysostomou, and Dr. Panos Tsopelas.

I am also grateful to my family, my beloved husband and my lovely daughter for their patient, understanding and support that showed all these years.

To my parents Sotiris and Chrystalla,

my sister Despo, my husband Christos

and to my lovely daughter Sotia

Table of Contents

List of Figures

List of Tables

List of Symbols

a	- Parameter which controls the variation of the coefficient of friction with velocity
A_{g0}	- Pulse amplitude
A_p	- Area of lead plug
A_r	- Area of rubber layer
A'	- Overlap area between the displaced top and bottom faces of elastomeric bearing
B	- Width of rigid block
c_b	- Coefficient of viscous damper
D	- Diameter of a cylindrical elastomeric bearing
$D_{\max}$	- Maximum displacement of the FPS isolator
e	- Coefficient of restitution
F_b	- Shear force mobilized at FPS isolator
$f_{\max}$	- Coefficient of friction of FPS isolator at large velocity of sliding and under constant pressure
$f_{\max 0}$	- Maximum value of the coefficient of friction at zero pressure
$f_{\max\ p}$	- Maximum value of the coefficient of friction at very high pressure
$f_{\min}$	- Coefficient of friction of FPS isolator at small velocity of sliding and under constant pressure
f_x, f_z	- Normal reaction force
F_y	- Yield force of lead-rubber bearing
$\int F_x dt$	- Horizontal impulses
$\int F_z dt$	- Vertical impulses

g - Acceleration of gravity

G_p - Shear modulus of lead

G_r - Shear modulus of rubber

H - Height of rigid block

$\boldsymbol{H}$ - Vector of angular momentum

H_C^-, H_C^+ - Pre- and post-impact angular momentum about the mass center

ΔH_C - Change in the angular momentum about the mass center

h_r - Total rubber height

I - Centroid mass moment of inertia

k_b - Lateral stiffness of bearing

$k_{b\ tot}$ - Total lateral stiffness of all elastomeric bearings

k_{eff} - Effective stiffness of FPS isolator

k_v - Vertical stiffness of an elastomeric bearing

$k_{v\gamma}$ - Sum in series of the vertical stiffness due to the rubber shear strain without volume change

k_{vV} - Vertical stiffness caused by the volume change of the rubber without shear

k_1 - Elastic stiffness of lead-rubber bearing

k_2 - Post-yield stiffness of lead-rubber bearing

$\boldsymbol{L}$ - Vector of linear momentum

L_x^-, L_x^+ - Pre- and post-impact horizontal linear momentum

L_z^-, L_z^+ - Pre- and post-impact vertical linear momentum

$\left(L_{sys}\right)_x^-$, $\left(L_{sys}\right)_x^+$ - Pre- and post-impact horizontal linear momentum of the system

$(\Delta L)_x$, $(\Delta L)_z$ - Changes in horizontal and vertical linear momentum

$(\Delta L_{sys})_x$ - Change in horizontal linear momentum of the system

M - Total mass above isolation system

m - Mass of symmetric rigid block

m_b - Mass of rigid base

$\int M_C dt$ - Angular impulse

M_{over} - Overturning moment

M_{res} - Restoring moment

N - Normal load on FPS bearing

p - Instantaneous bearing pressure

P_s - Additional seismic load on FPS isolator due to overturning moments

Q_i - Generalized non-conservative forces, $i = 1, 2, 3...$

q_i - Generalized coordinate, $i = 1, 2, 3...$

R - Distance between one corner and the mass center of the rigid block

R_b - Radius of curvature

$\boldsymbol{r}_{C/O}$ - Position vector of center-of-mass relative to point O

$\boldsymbol{r}_{C/O'}$ - Position vector of center-of-mass relative to point O'

S - Shape factor of each rubber layer

sgn - Signum function

T - Kinetic energy of the system

T_b - Period of isolation system

t_d - Pulse half-cycle duration

T_p - Pulse period

t_r - Thickness of rubber layers

T_{rot} - Kinetic energy due to the rotation of the block

T_{tr} - Kinetic energy due to the translation of the system

u - Horizontal displacement of isolation system

$\dot{u}$ - Velocity of isolation system

$\dot{u}^-$, $\dot{u}^+$ - Pre- and post impact horizontal velocity of the isolator

V - Potential energy of the system

v - Velocity of the center-of-mass of the block

$\boldsymbol{v}^-$, $\boldsymbol{v}^+$ - Pre- and post-impact translational velocities of center-of mass

V_{el} Potential energy due to elastic deformation of spring

V_{gr} - Potential energy due to gravity

W - Gravity load

W_{max} - Maximum allowable vertical load that can be carried by an elastomeric bearing

W_{tot} - Total weight of rigid superstructure

$x(t)$ - Horizontal displacement of the mass center of the block measured from the original at-rest position of the mass center

$\dot{X}^-$, $\dot{X}^+$ - Absolute pre- and post-impact horizontal velocities of the mass center of the block

x_b - Displacement of the top face of elastomeric bearing

$x_{b\,all}$ - Allowable lateral displacement of elastomeric bearing

$\ddot{x}_g$ - Horizontal component of ground acceleration

$\dot{x}_{rot}$ - Horizontal velocity of the mass center of the block due to rocking of the block.

$\dot{x}_s$ - Horizontal velocity of the mass center of the block due to sliding between the block and the supporting base

$\ddot{x}_s$ - Horizontal acceleration of the mass center of the block due to sliding between the block and the supporting base

Y - Yield displacement of FPS isolator

$\boldsymbol{Z}$ - Dimensionless variable describing the rigid-plastic behavior

$z(t)$ - Vertical displacement of the mass center of the block measured from the original at-rest position of the mass center

$\dot{Z}^-$, $\dot{Z}^+$ - Absolute pre- and post-impact vertical velocities of the mass center of the block

$\ddot{z}_g$ - Vertical component of ground acceleration

$\dot{z}_{rot}$ - Vertical velocity of the mass center of the block due to rocking of the block.

Greek Symbols

α - Angle measured between R and the vertical when the body is at rest

β, γ - Dimensionless parameters that control the shape of the hysteresis loop

γ_w - Allowable shear strain of an elastomeric bearing under gravity load

ε - Angular restitution

ε_v - Short-term failure strain of the rubber in pure tension

$\theta(t)$ - Angular rotation of the block, positive in the clockwise direction

$\dot{\theta}$ - Angular velocity of the block

$\ddot{\theta}$ - Angular acceleration of the block

$\dot{\theta}^-$, $\dot{\theta}^+$ - Pre- and post impact angular velocity

ξ_b - Damping ratio of isolation system

κ_r - Compression modulus of rubber

λ - Geometric aspect ratio or slenderness ratio

μ_b - Coefficient of friction of the FPS isolator

μ_k - Coefficient of kinetic friction between the block and the foundation $0.8\mu_s$

μ_s - Coefficient of static friction between the block and the foundation

ρ - Mass ratio m / m_b

τ_{py} - Shear yield strength of the lead

$\boldsymbol{\omega}^-$, $\boldsymbol{\omega}^+$ - Pre- and post-impact vector angular velocities of the block

ω_p - Pulse half-cycle frequency

CHAPTER 1
Introduction

1.1 Motivation

Base isolation is worldwide accepted as one of the most effective strategies for seismic protection of civil structures. Particular attention has been given to date to the application of seismic isolation in earthquake-resistant design to safeguard engineering structures in their entirety. The effectiveness of this innovative technology paved the way for extending the concept to individual elements of high importance such as high-value building contents, mechanical/electrical equipment, computer servers, and irreplaceable museum artifacts. This dissertation concentrates on the case of nonstructural components, which behave as rigid blocks.

The aim of this dissertation is to present the two-dimensional nonlinear formulation of the general response of base-isolated rigid blocks subjected to ground excitation. The system response is described in terms of four distinct oscillation regimes: system translation, sliding, rocking, and slide-rocking. Two models of the isolation system is considered; a linear model with viscoelastic behavior and a nonlinear model with bilinear hysteretic behavior. The dissertation examines in depth the motion of the system with a large-displacement formulation that combines the exact (nonlinear) equations of motion together with a rigorous model governing impact. An extensive numerical investigation is carried out for varying block geometric characteristics and isolation-system parameters, with the aim of identifying potential trends in the response and stability of the system.

1.2 Objectives

This dissertation presents a comprehensive mathematical formulation of the general planar-motion of seismically isolated free-standing rigid blocks to base excitation. The main objectives of the dissertation can be summarized as follows:

- to give a brief description of the literature relevant to the dynamics of a rigid block,
- to develop a comprehensive 2D mathematical model for the general planar nonlinear response of seismically-isolated free-standing rigid blocks to base excitation,

- to formulate the equations of motion for each oscillation pattern,
- to formulate a rigorous model governing impact between the block and the supporting base during rocking motions,
- to calculate the transition criteria which are responsible for the potential transition from one oscillation regime to another
- to develop a computer program to determine the response of the system considering the different possible oscillation regimes, impact, transition criteria and arbitrary excitation, and
- to investigate the system dynamics through an extensive parametric study with the aim of revealing interrelations among the problem variables and identifying potential trends in the response and stability of the system.

1.3 Outline

The dissertation is organized into 10 chapters. The introductory chapter embraces the prime motivation, objectives, and organization of the dissertation.

Chapter 2 describes in brief the main work and findings of the literature relevant to the dynamics of a rigid block. The review is focused on studies considering the rigid-body motion of free-standing or base-isolated symmetric blocks, on the assumption of rigid foundation and perfectly inelastic point impact.

Chapter 3 highlights the concept of seismic isolation, as an innovative approach aiming to mitigate the damaging effects of earthquakes on engineering structures. Typical seismic-isolation systems are outlined and their mechanical behavior and mathematical modeling is presented.

Chapter 4 presents the dynamics of a single rigid block free-standing on a rigid foundation as established in the literature. The review presents the various possible oscillation patterns of a rigid block along with their governing equations of motion, the criteria for the initiation of motion in each oscillation pattern, and an impact model based on classical impact theory.

Chapter 5 presents the analytical formulation of the general response of seismically isolated

rigid blocks, free-standing on the isolation base, subjected to ground excitation. The response of the system is classified into four oscillation regimes: (i) system translation, in which the system in its entirety oscillates horizontally; (ii) sliding, in which the block slides relative to the supporting base, which translates horizontally; (iii) rocking, in which the rigid block pivots on its edges as the supporting base translates horizontally; and (iv) slide-rocking, in which the block simultaneously slides and pivots on its edges, as the supporting base translates horizontally. Two models for the isolation system are considered; a linear model with viscoelastic behavior and a nonlinear model with bilinear hysteretic behavior. Equations of motion for each oscillation pattern are formulated by using the Lagrange method. Moreover, this chapter presents the criteria that govern the potential transition from one oscillation regime to another.

Chapter 6 addresses the impact problem through a rigorous formulation, whereby an analytical model governing impact from the rocking and slide-rocking regimes is derived from first principles using classical impact theory. This model assumes point-impact of short duration, zero coefficient of restitution (perfectly inelastic impact) and impulses acting only at the impacting corner. Changes in position and orientation are neglected, and changes in velocity are considered instantaneous.

Chapter 7 describes an ad hoc computational scheme developed to calculate the response of the system under ground excitation. The numerical integration of the equations of motion is pursued in MATLAB through a state-space formulation. In each time step, close attention is paid to the eventuality of transition from one pattern of motion to another due to the satisfaction of transition criteria or the impact event and to the accurate evaluation of the initial conditions for the next pattern of oscillation.

Chapter 8 and 9 present numerical results from an extensive numerical investigation of the dynamic response of the system under simple base-acceleration pulses and horizontal near-fault ground motions, aiming to identify potential trends in the response and stability of the system. The numerical investigation is carried out based on two assumptions: (a) sufficient friction to prevent sliding between the block and the supporting base, entailing rocking response, Chapter 8, and (b) insufficient friction to permit sliding between the block and the supporting base, entailing multi-pattern response, Chapter 9.

Chapter 10 presents a summary and conclusions drawn from this dissertation and a discussion on the future work that may follow from this study.

CHAPTER 2

Literature Review

A review focused on studies considering the rigid-body motion of free-standing non-isolated and isolated blocks are presented in this section.

Housner's landmark study (1963) is perhaps the first systematic work that provided basic understanding on the rocking response of a rigid block and motivated further scientific interest. Considering a slender rigid block resting upon a rigid foundation he investigated the free- and forced-vibration rocking response to a rectangular pulse, a half-sine pulse, and an earthquake-type excitation, based on the assumption of a perfectly-inelastic impact and sufficient friction to prevent sliding of the block during impact.

Following Housner, many researchers have dealt with various aspects of the complex dynamics of the single rigid block. Yim et al. (1980) adopted a probabilistic approach to conducting a numerical study using artificially-generated ground motions. This research shows that the rocking response of a block depends on the characteristics of the ground motion and the system parameters, namely the coefficient of restitution, the aspect ratio, and the size of the block.

Aslam el al. (1980) performed experimental and analytical studies on slender rigid blocks subjected to artificially-generated ground motion. Their work, confirmed that the rocking response of rigid bodies is sensitive to system parameters.

Ishiyama (1982) examined the motions of rigid bodies resting on a rigid foundation and subjected to earthquake excitations. His work included classification of the motion of rigid bodies (i.e. rest, slide, rotation, slide-rotation, translation jump, and rotation jump), derivation of the equations of each type of motion, study of the transition between them, solution of the nonlinear equations of motion for different types of ground acceleration and proposition of criteria for the overturning of rigid bodies. One of the features of his investigation was the introduction of the tangent restitution coefficient in order to estimate the magnitude of the tangent impulse at the instant of impact.

Spanos and Koh (1984) linearized the nonlinear equations of rocking of a slender rigid block,

resting on a rigid foundation harmonically excited in the horizontal direction. Moreover, they plotted stability diagrams that can be used to estimate the prospective of topple of a known amplitude and frequency rigid-block structure under harmonic excitation. Additionally, they detected several possible modes of the steady-state response and developed analytical procedures in order to determine the amplitudes of the predominant modes and perform stability analyses.

Shenton III and Jones (1991) formulated the generalized response of free-standing rigid bodies to base excitation, assuming rigid body, rigid foundation, and Coulomb friction. Their formulation takes into account the five possible modes of response (rest, slide, rock, slide-rock, and free flight) and the impact between the block and foundation. In their work, Shenton III and Jones (1991) derived a model governing impact from a rock, slide-rock or free-flight mode based on the classical impact theory, assuming point-impact, nonzero coefficient of restitution and finite value of friction.

Considering cycloidal impulsive excitation, Makris and Roussos (2000) and Zhang and Makris (2001) examined in depth the transient rocking response of free-standing rigid blocks. Making linear approximations, Makris and Roussos (2000) set up the conditions and the expression for the minimum acceleration required for the overturning of a block. Zhang and Makris (2001) derived relations for the dynamic horizontal and vertical reactions exerted at the point of rotation of a rocking rigid block. They showed that the coefficient of friction needed to maintain pure rocking motion generally increases with the acceleration level of the pulse. Subsequently, they identified a safe region on the acceleration-frequency plane where the block overturns without experiencing any impact and they showed that the shape of this region depends on the coefficient of restitution.

Yang et al. (2000) examined the dynamic response of a rigid block standing unrestrained on a rigid foundation which shakes horizontally. Their formulation takes into account four modes of motion: rest, slide, rock and slide and rock. A general two-dimensional theory is presented for dealing with the various modes of a free-standing rigid block, considering in particular the impact occurring during the rocking motion. Numerical examples demonstrate the occurrence of each of the four modes and the transition between different modes.

Taniguchi (2002) investigated the nonlinear seismic response of free-standing rectangular

rigid bodies on horizontally and vertically accelerating rigid foundations. Three modes of response are considered in his formulation: liftoff, slip, and liftoff-slip. This study concluded that the body is sensitive to small changes in the friction coefficient and slenderness, and to the wave properties and intensity of ground motions.

Apostolou et al. (2007) examined the rocking of rigid structures uplifting from their support under strong earthquake shaking. The structure is resting on the surface of either a rigid base or a linearly elastic continuum. A large-displacement approach is adopted to extract the governing equations of motion allowing for a rigorous calculation of the nonlinear response even under near-overturning conditions. Directivity affected near-fault ground motions, idealized as Ricker wavelets or trigonometric pulses are used as excitation. The conditions, under which uplifting leads to large angles of rotation and eventually to overturning, are investigated. It is concluded that the practice of estimating ground accelerations from overturning observations is rather misleading and meaningless.

Chatzis and Smyth (2012) studied the rocking motion of a solid block on a moving deformable base. Two new models were developed for the simulation of a rigid body experiencing a 2D rocking motion on a moving deformable base. The first model, the concentrated springs model, simulates the ground as tensionless vertical springs with vertical dampers placed at each of the two bottom corners of the body, whereas the second, the Winkler model, simulates the ground as a continuous medium of tensionless vertical springs with vertical dampers. Both models take into consideration sliding and uplift and both are geometrically nonlinear. The behavior of the two models is discussed and compared with the classic theory proposed by Housner.

Dimitrakopoulos and DeJong (2012) investigated the use of viscous damping to limit the rocking motion by characterizing the fundamental behavior of damped rocking structures through analytical modeling. A rocking block model is used to determine the viscous damping characteristics, which exploit the beneficial aspects of the rocking motion, while dissipating energy and preventing overturning collapse.

Voyagaki et al. (2013) examined the classical problem of rocking behavior of a rigid, free-standing block to earthquake shaking containing significant pulses, as is the case in near-field ground motions. A rectangular block resting on a perfectly rigid base is considered, subjected

to a suite of idealized acceleration pulses expressed by a generalized function controlled by a single shape parameter. The problem is treated analytically in the realm of the linearized equations of motion, under the assumption of slender block geometry and rocking without slippage. Simple overturning criteria for different earthquake waveforms are presented in the form of dimensionless closed-form expressions and graphs that provide insight into the physics of the response.

The studies reported on the dynamics of rigid blocks are not limited to the case of a single rigid block but are expanded on the dynamics of rigid-block assemblies. Psycharis (1990) and Spanos et al. (2001), for instance, dealt with the dynamics of systems consisting of two blocks, one placed on top of the other, free to rock without sliding. Their work has included classification of the possible regimes of response, study of the impact either between two blocks or between the base block and the ground, and derivation of criteria for the initiation of motion and for the transition between modes. Moreover, they derived equations governing the rocking response of the system under horizontal and vertical ground accelerations and developed an impact model.

Motivated by the increasing challenge to preserve elements of cultural heritage worldwide, which can be modeled as rigid blocks, a great deal of attention is received in recent years.

One of the earliest studies that explicitly relate to the protection of museum artifacts against earthquakes is attributed to Agbabian et al. (1988). This study aimed at the development of analytical and experimental procedures for the evaluation of the seismic mitigation of various museum objects, at the Jean Paul Getty Museum in Malibu, California. For this purpose they created an art object database in which selected art objects of the museum were categorized according to their type, their support type, the probable earthquake response mode, and the seismic mitigation method (if used). Each art/support system was characterized by applicable structural parameters. Using the developed database, generic art/support systems were established for which simplified analytical models were formulated. The analytical models were verified experimentally and they were parametrically studied in order to evaluate the performance of each type of generic system.

Following the work by Agbabian and coworkers, further research efforts have been made toward the protection of the integrity of museum contents from the destructive effects of

earthquakes. In their study on the response of rigid art objects subjected to earthquake-induced oscillations, Augusti et al. (1992) and (1995) proposed simple rules for the design of the display cases in order to mitigate the seismic risk of valuable exhibits.

Only recently has base-isolation strategy been implemented for the preservation of important elements of cultural heritage. In particular, Vestroni and Di Cintio (2000), introduced base-isolation devices consisting of multi-stage high-damping laminated rubber bearings and studied the response of the isolated system, modeled as a single-degree-of-freedom system with the isolator characterized by a hysteretic force-displacement law, in the frequency and time-domain. In order to identify the influence of the characteristics of the devices and seismic forces, they performed a parametric study on the response of an isolated statue.

Moreover, Myslimaj et al. (2003) proposed the installation of Tuned Configuration Rail (TCR), a rolling type base-isolation system, underneath showcases, preservation racks, shelves and statues to control their seismic response.

The protection of art objects was also an issue of interest for Caliò and Marletta (2003), who examined the vibrations of art objects modeled as rigid blocks simply supported on a movable mass support isolated with viscoelastic devices. In their study, they performed numerical investigations under impulsive and seismic excitations and evaluated analytically the minimum values of the horizontal support acceleration impulse that cause rocking of the object in the cases of damped and undamped systems. Furthermore, Caliò and Marletta (2004) studied the seismic vulnerability of isolated and non-isolated ancient Greek vessels and stone statues.

More recently, Di Egidio and Contento (2009) analyzed the behavior of a work of art modeled as non-symmetrical rigid block isolated with a viscoelastic device. The model applied was an extension of the model studied by Caliò and Marletta (2003), considering eccentricity of the mass center of the rigid block and existence of security stops to limit the displacement of the oscillating base to a maximum safety value, thus protecting the isolator. The analysis was performed considering both impulsive and seismic excitations.

Roussis et al. (2008) investigates the dynamic response of base-isolated block-like slender objects, such as statues, subjected to horizontal ground excitation. The structural model employed consists of a rigid block supported on a rigid base, beneath which the isolation

system is accommodated. Assuming no sliding of the block relative to the supporting base, when subjected to ground excitation the system may exhibit two possible regimes of motion, namely pure translation, in which the system in its entirety oscillates horizontally, and rocking, in which the rigid block pivots on its edges with respect to the horizontally-moving base. The dynamic response of the system is strongly affected by the occurrence of impact between the block and the horizontally-moving base, as impact can modify not only the energy but also the degrees of freedom of the system by virtue of the discontinuity introduced in the response. A model governing impact from the rocking mode is derived from first principles using classical impact theory. Numerical results are obtained via an ad hoc computational scheme developed to determine the response of the system under horizontal ground excitation.

Vassiliou and Makris (2012) examines the rocking response and stability of rigid blocks standing free on an isolated base supported on linear viscoelastic, single concave and double concave spherical sliding bearing. This study concludes that seismic isolation improves the stability of small blocks only. It suggests that free-standing ancient classical columns exhibit superior stability as they are built rather than if they were seismically isolated.

CHAPTER 3

Seismic Isolation Technique

3.1 The concept

In general, most structures have low flexibility and low vibration damping and under typical design-level earthquakes, they develop large horizontal forces. The seismic forces can be reduced by supporting the structure on systems with high horizontal flexibility and high vibration damping. Such system is the seismic isolation which is a developing technology aiming at limiting the seismic energy transfer to the structure. The system decouples the structure from the foundation by interposing seismic isolators between them. Seismic isolators have much lower lateral stiffness than the lateral stiffness of the structure. The low lateral stiffness gives the structure a natural period that is much higher than predominant periods of typical earthquakes and reduces the spectral demands, Figure 3-1a. The displacement of an isolation system increases, as the period is getting larger. Therefore, an isolation system should also dissipate energy in order to decrease the induced displacements (Figure 3-1b).

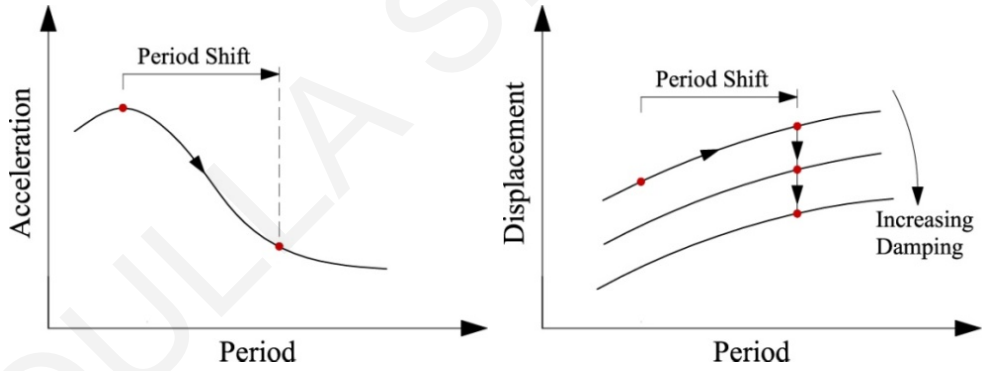

(a) (b)

Figure 3-1: a) Effect of period lengthening on floor accelerations b) Effect of damping on displacement.

3.2 Brief History

Based on Christopoulos and Filiatrault's research (2006), John Milne, a British scientist, is the inventor of the modern seismic isolation concept in 1885. He built a wood house on 6-mm diameter cast-iron shots at the top of the piles, which performed well under real earthquake

ground motions.

In 1909, J.A. Calantarients, an English medical doctor, invented a new method in which buildings could be built on lubricated “free joints” on a layer of fine material. Hence, the building during an earthquake would slide free reducing the forces transmitted to the structure.

In the late sixties, the development of modern materials brought to the surface the modern application of seismic isolation. Rubber and thin steel sheets were used to make the multi-layer elastomeric bearings that are very stiff in the vertical direction but are very flexible in the horizontal direction.

In 1969, in Skopje, Yugoslavia, was the first application of rubber isolation system on a three-storey concrete elementary school structure (Naeim and Kelly (1999)). After this installation, seismic isolation technology was spread worldwide. Nowadays, many types of seismic isolations are available such as elastomeric bearings, lead-rubber bearings, and friction pendulum bearings.

3.3 Seismic Isolation Systems

This section gives a description of the main types of seismic isolation systems and their mechanical properties.

3.3.1 Elastomeric bearings

Elastomeric Bearings or Laminated-rubber bearings were used mostly for bridges to control movements and deformations due to changes in temperature. More recently, their use has been extended to seismic isolation of buildings and other structures. Based on (Naeim and Kelly (1999)), the first use of elastomeric bearing to structure was in 1969 for the Pestalozzi in Skopje, Yugoslavia.

A typical laminated-rubber bearing is composed of elastomeric rubber with internal steel reinforcing plates solidly joined together under high pressure and temperature, Figure 3-2. Using steel and rubber layers, the gravity load resisting capacity of the bearing is increased by reducing the thickness of individual rubber layers. The steel reinforcing plates reduce the lateral bulging of the bearings and increase the vertical stiffness.

The most important parameters of elastomeric bearings are the gravity load carrying capacity,

the lateral stiffness and the maximum achievable relative displacement between the top and the base of the bearing.

Based on Christopoulos and Filiatrault (2006), the maximum allowable vertical load that can be carried by a bearing $W_{\max}$ is given by

$$W_{\max} = A' G_r S \gamma_w \tag{3.1}$$

where: A' is the overlap area between the displaced top and bottom faces of the bearing when the top of the bearing is displaced an amount x_b relative to its base as shown in Figure 3-3; G_r is the shear modulus of rubber which is between 0.5 to $1\,\text{MPa}$; S is the shape factor of each rubber layer, equal to the loaded area of the bearing divided by the load-free area of the bearing; γ_w is the allowable shear strain under gravity load.

The shape factor, S, for a cylindrical bearing of diameter D and made of rubber layers of thickness t_r is given by

$$S = \frac{\text{loaded area}}{\text{load free area}} = \frac{\left(\pi D^2\right)/4}{\pi D t_r} = \frac{D}{4t_r} \tag{3.2}$$

The shape factor, S, for a rectangular bearing of sides b x d and made of rubber layers of thickness t_r is given by

$$S = \frac{\text{loaded area}}{\text{load free area}} = \frac{bd}{2t_r\left(b+d\right)} \tag{3.3}$$

The allowable shear strain, γ_w, can be estimated as a ratio of the short-term failure strain of the rubber in pure tension ε_v such as:

$$\begin{aligned} &\gamma_w \approx 0.2\varepsilon_v \\ &\gamma_w \approx 0.4\varepsilon_v \text{ for design base earthquakes} \\ &\gamma_w \approx 0.7\varepsilon_v \text{ for maximum credible earthquakes} \end{aligned} \tag{3.4}$$

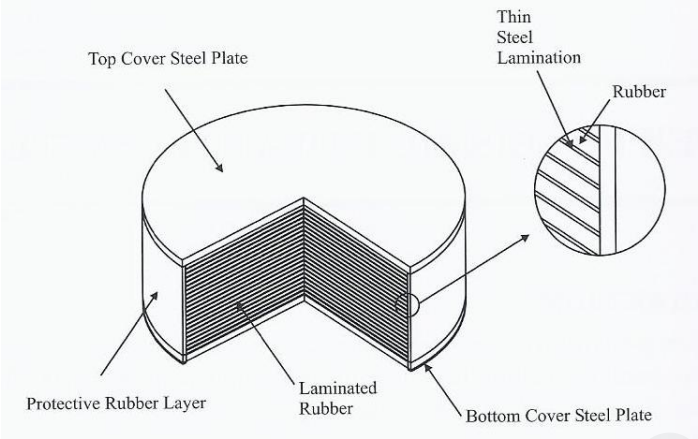

Figure 3-2: Laminated-rubber bearing (elastomeric bearing) (Christopoulos and Filiatrault (2006)).

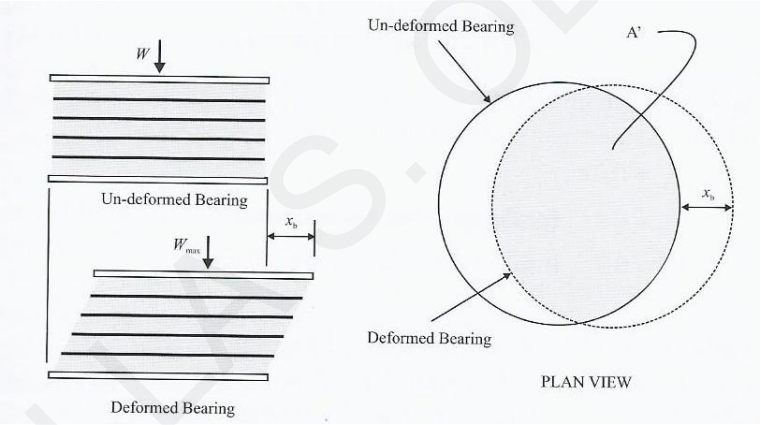

Figure 3-3: Circular Laminated-rubber bearing under gravity and lateral loads (Christopoulos and Filiatrault (2006)).

The lateral stiffness of a laminated-rubber bearing k_b is given by

$$k_b = \frac{G_r A_r}{h_r} \tag{3.5}$$

where G_r is the shear modulus of rubber; A_r is the rubber layer area; h_r is the total rubber height.

The period of vibration, T_b, of the bearings equals with

$$T_b = 2\pi\sqrt{\frac{W_{tot}}{g k_{b\ tot}}} \tag{3.6}$$

where W_{tot} is the total weight of the rigid superstructure; $k_{b\ tot}$ is the total lateral stiffness of all bearings that is calculated by summing the individual lateral stiffness of each bearing.

The vertical stiffness, k_v, of an elastomeric bearing is given by

$$k_v = \frac{k_{v\gamma} k_{vV}}{k_{v\gamma} + k_{vV}} \tag{3.7}$$

where $k_{v\gamma}$ is the sum in series of the vertical stiffness due to the rubber shear strain without volume change; k_{vV} is the vertical stiffness caused by the volume change of the rubber without shear.

Based on Skinner et al. (1993) the condition $k_{v\gamma}$ is given by

$$k_{v\gamma} = \frac{6 G_r S^2 A_r}{h_r} \tag{3.8}$$

and k_{vV} is given by

$$k_{vV} = \frac{\kappa_r A_r}{h_r} \tag{3.9}$$

where κ_r is the compression modulus of the rubber ($\kappa_r \approx 2000$ MPa for typical rubber.

Based on Christopoulos and Filiatrault (2006), the allowable lateral displacement, $x_{b\ all}$, is given by

$$x_{b\ all} = h_r \gamma_s \tag{3.10}$$

where γ_s is the allowable seismic shear strain that depends on how much shear strain is mobilized be the vertical load, see (3.1).

In addition, the limit of the overlap factor A'/A_r is important for the allowable lateral

displacement, $x_{b\,all}$. For design basis earthquakes, a limit of about 0.6 is typically used.

3.3.2 Lead-rubber bearings

The lead-rubber bearing was invented in New Zealand in 1975 (Robinson and Tucker (1977), (1983)) and has been extensively used in New Zealand, Japan and United States. It is composed of a laminated-rubber bearing with a cylindrical lead plug inserted in its center, Figure 3-4, to increase the damping of the bearing. Based on Skinner et al. (1993), the lead, at room temperature, behaves approximately as an elastic-plastic solid and yields in shear at relatively low stress of about 10 MPa. In addition, lead has fatigue resistance properties as they restored when cycled in the inelastic range and it is commonly available.

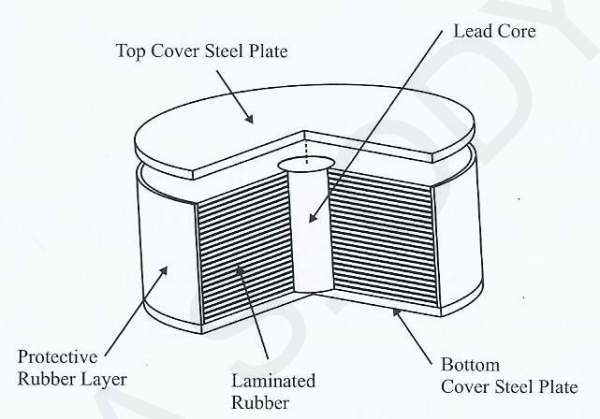

Figure 3-4: Lead-Rubber Bearing (Christopoulos and Filiatrault (2006)).

Based on Christopoulos and Filiatrault (2006), the lead-rubber bearing has a bilinear behavior with elastic stiffness k_1, a post-yield stiffness k_2 and a yield force F_y. The elastic stiffness k_1 is given by

$$k_1 \approx \frac{1}{h_r}\left(G_p A_p + G_r A_r\right) \approx 10 k_b \tag{3.11}$$

where h_r is the total rubber height, A_p is the area of the lead plug, A_r is the area of the rubber, G_p is the shear modulus of lead ≈ 150 MPa at room temperature, G_r is the shear modulus of rubber ≈ 0.5 to 1 MPa and k_b is the lateral stiffness of the laminated-rubber bearing (see Equation (3.5)).

The post-yield stiffness k_2 is equal with the lateral stiffness of the laminated-rubber bearing, Equation(3.5).

The yield force F_y is given by

$$F_y = \tau_{py} A_p \left(1 + \frac{G_r A_r}{G_p A_p} \right) \approx \tau_{py} A_p \tag{3.12}$$

where $\tau_{py} \approx 10$ MPa is the shear yield strength of the lead.

3.3.3 Friction pendulum systems

Friction Pendulum System (FPS) is a sliding isolator and it is composed of two parts: the articulated slider and the concave sliding stainless steel surface (Figure 3-5). The spherical surface provides restoring force using gravity and friction to dissipate energy. The FPS isolator is manufactured by Earthquake Protection Systems in Richmond California (Christopoulos and Filiatrault (2006)).

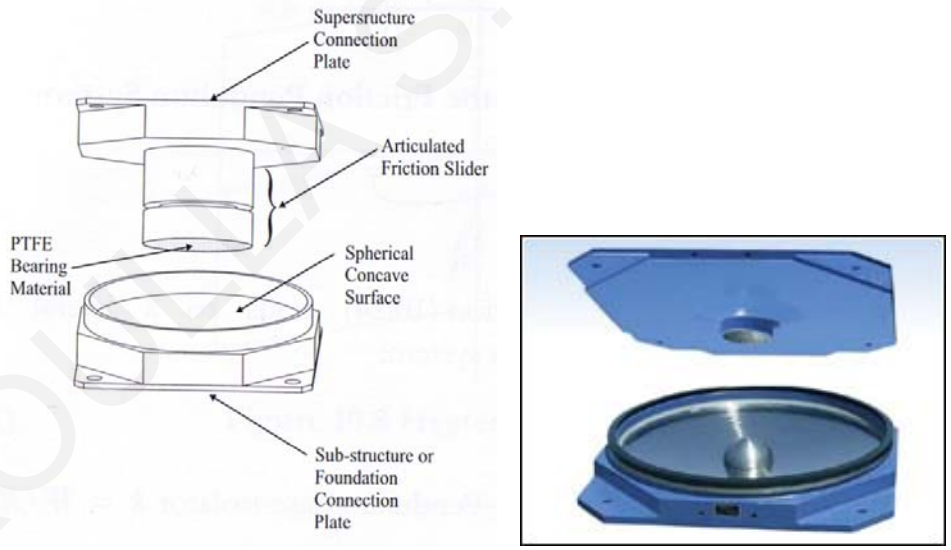

Figure 3-5: Friction Pendulum System (Christopoulos and Filiatrault (2006)).

The FPS bearing is activated when the earthquake forces overcome the static value of friction. When set in motion, the slider slides over the concave spherical surface causes the supported mass to rise. The component of the gravitational force acting parallel to the spherical surface provides the necessary restoring force. Because of the induced rising of the structure along the

spherical surface (Figure 3-6), the bearing develops a lateral force equal to the combination of the mobilized frictional force and the restoring force that develops. This restoring force is proportional to the displacement and the weight carried by the bearing, and it is inversely proportional to the radius of curvature of the spherical surface (Mokha et al. (1990)). The stiffness of the FPS isolator is the restoring force during sliding motion. The friction force between the articulated slider and the spherical surface generates damping in the isolators (Al-Hussaini et al. (1994)).

(a) (b)

Figure 3-6: Single pendulum bearing (a) center position, (b) maximum credible earthquake.

The FPS is based on the principles of pendulum motion and the friction force. During sliding motion the shear force,

Figure 3-6, mobilized at each FPS isolator is given by

$$F_b = \frac{N}{R_b}u + \mu_b Mg\boldsymbol{Z} \tag{3.13}$$

where N is the normal load on bearing, R_b is the radius of curvature, μ_b is the coefficient of friction of the friction-pendulum (FP) isolators, u is the bearing displacement and $\boldsymbol{Z}$ is a dimensionless variable describing the rigid-plastic behavior, being governed by the following differential equation

$$Y\dot{\boldsymbol{Z}} + \gamma|\dot{u}|\boldsymbol{Z}|\boldsymbol{Z}| + \beta\dot{u}\boldsymbol{Z}^2 - \dot{u} = 0 \tag{3.14}$$

in which Y is the yield displacement, and β, γ are dimensionless parameters that control the shape of the hysteresis loop, with assigned values: $\beta = 0.1$, $\gamma = 0.9$ and $Y = 0.3\text{mm}$ (Constantinou et al. (1990)).

The normal load, N, is defined by

$$N = W\left(1 + \frac{\ddot{z}_g}{g} + \frac{P_s}{W}\right) \tag{3.15}$$

in which W is the gravity load, $\ddot{z}_g$ is the vertical ground acceleration, P_s is the additional seismic load due to overturning moments, and g is the gravitational acceleration.

In Equation (3.13), the coefficients of u and $\boldsymbol{Z}$ represent the second slope of the bilinear model and the strength of the system, respectively. This corresponds to an isolator period of

$$T_b = 2\pi\sqrt{\frac{W}{gk_b}} = 2\pi\sqrt{\frac{R_b}{g}} \tag{3.16}$$

The second term in Equation (3.1) is the friction force between the slider and sliding surface. The single-curvature spherical sliding surface is typically made of PTFE or PTFE-based composites in contact with polished stainless steel. The shape of the sliding surface allows large contact areas that, depending on the materials used, are loaded to average bearing pressures in the range of 7 to 70 MPa.

For bearings with large contact area, and in the absence of liquid lubricants, the coefficient of friction depends on a number of parameters, of which the three most important are the composition of the sliding interface, bearing pressure and velocity of sliding. For interfaces composed of polished stainless steel in contact with PTFE or PTFE-based composites, the coefficient of sliding friction may be described by (Constantinou et al. (1990))

$$\mu_b = f_{\max} - \left(f_{\max} - f_{\min}\right)\exp\left(-a\left|\dot{u}\right|\right) \tag{3.17}$$

where $f_{\max}$ is the coefficient of friction at large velocity of sliding and under constant pressure, $f_{\min}$ is the coefficient of friction at small velocity of sliding and under constant pressure and a is the parameter that controls the variation of the coefficient of friction with velocity

The variation of the coefficient of friction with velocity is illustrated in Figure 3-7.

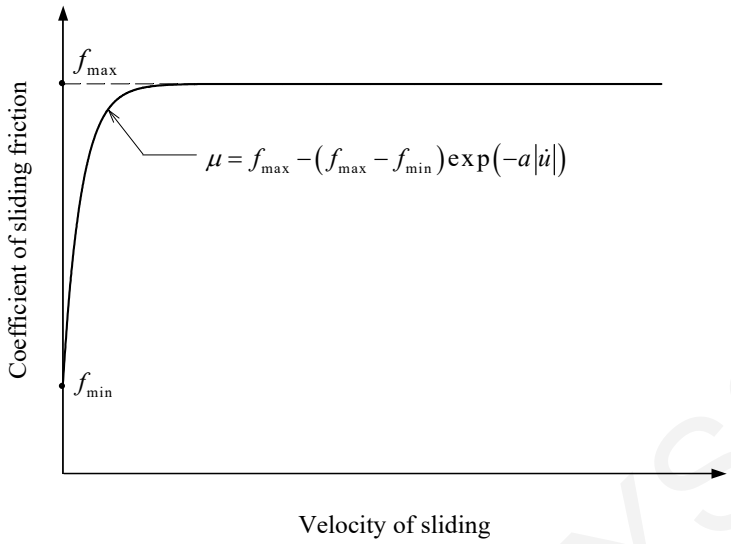

Figure 3-7: Variation of coefficient of friction with velocity (Tsopelas et al. (1994)).

Generally, the parameters f_{max}, f_{min} and a depend on bearing pressure and temperature. However, the dependency of f_{min} and a is not as significant as the dependency of f_{max} and can be neglected (Tsopelas et al. (1994)). The variation of parameter f_{max} with pressure can be expressed by the equation

$$f_{max} = f_{max\,0} - \left(f_{max\,0} - f_{max\,p}\right)\tanh\left(\varepsilon p\right) \tag{3.18}$$

where $f_{max\,0}$ is the maximum value of the coefficient of friction at zero pressure, $f_{max\,p}$ is the maximum value of the coefficient of friction at very high pressure, ε is the constant that controls the variation of f_{max} between very low and very high pressures and p is the instantaneous bearing pressure, which is equal to the normal load N (Equation (3.15)) divided by the contact area.

Figure 3-8 presents the assumed variation of friction parameter f_{max} with pressure, which is typical of the behavior of sliding bearings (Soong and Constantinou (1994)).

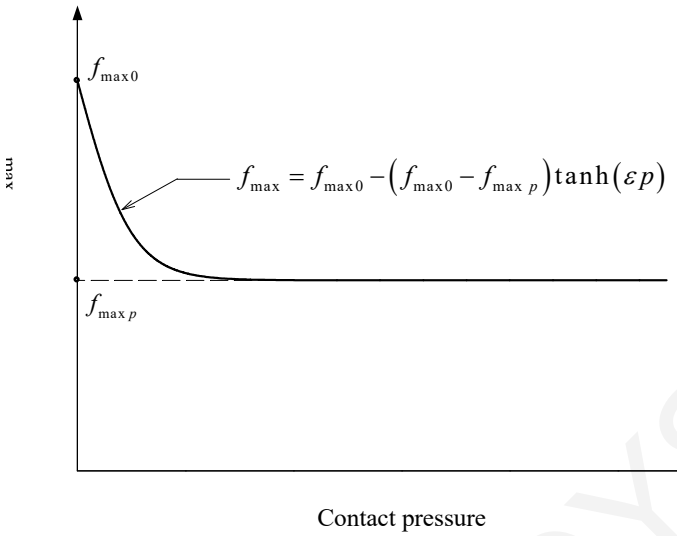

Figure 3-8: Variation of coefficient of friction with pressure (Soong and Constantinou (1994)).

Based on Christopoulos and Filiatrault (Christopoulos and Filiatrault (2006)), in reality, friction forces are present at the sliding interface and must be overcome before the bearing can slide. The energy dissipation occurring in the isolators is represented by the area enclosed by the hysteresis loops. Figure 3-9 shows a typical hysteresis response of a FPS bearing where a certain amount of friction is present at the sliding interface. The system is near rigid until the friction force is overcome. Then the force increase is proportional to the lateral stiffness of the FPS, Equation (3.1). The force required to overcome the initial friction is equal to $\mu_b W$. Because of the initial breakaway friction, the effective stiffness of the isolator is dependent on the friction coefficient of the system μ_b and the maximum displacement of the isolator $D_{\max}$. This effective stiffness k_{eff}, which is larger than $k_b = W / R$, is given by:

$$k_{eff} = W\left(\frac{1}{R} + \frac{\mu_b}{D_{\max}}\right) \tag{3.19}$$

Figure 3-10 represents an experimentally hysteretic response of an FPS system (Zayas et al. (1990)).

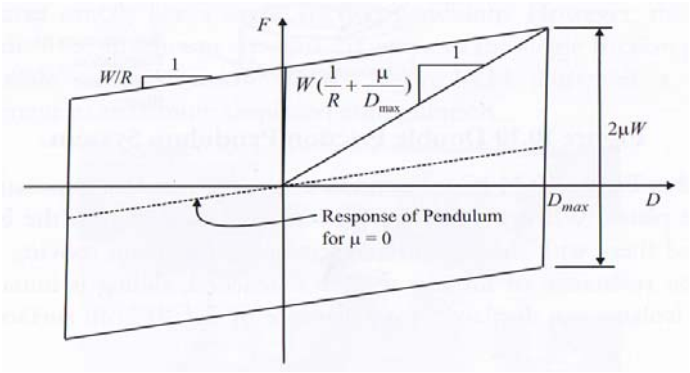

Figure 3-9: Hysteresis Loops of FPS (Christopoulos and Filiatrault (2006)).

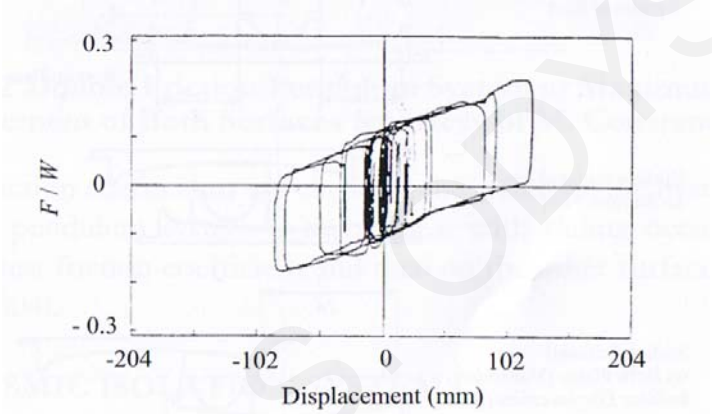

Figure 3-10: Experimental Response of FPS (Zayas et al. (1990)).

3.4 Mechanical Behavior of Isolation Systems

Generally, the seismic isolation system provides horizontal flexibility and damping to the superstructure during an earthquake. There are isolation systems that are composed of linear flexibility and linear damping namely as linear isolation systems with viscoelastic behavior. However, in most cases, isolation systems have nonlinear behavior, which can be described simply as a combination of viscoelastic and hysteretic behavior, Figure 3-11. Referring to previous section, the only isolation system with linear restoring force and linear damping is the laminated-rubber bearing. For this dissertation, two types of isolation systems are used for the analysis: a) a linear system with viscoelastic behavior Figure 3-12(a) and b) a nonlinear system with bilinear behavior Figure 3-12(b).

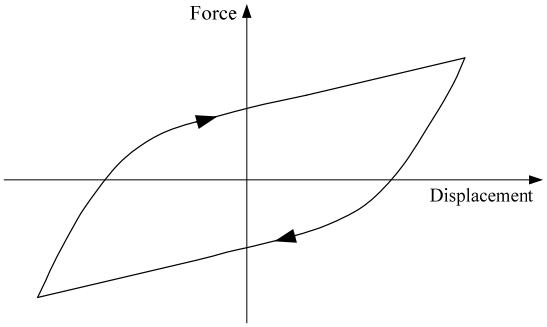

Figure 3-11: Idealized force-displacement relation of isolation systems.

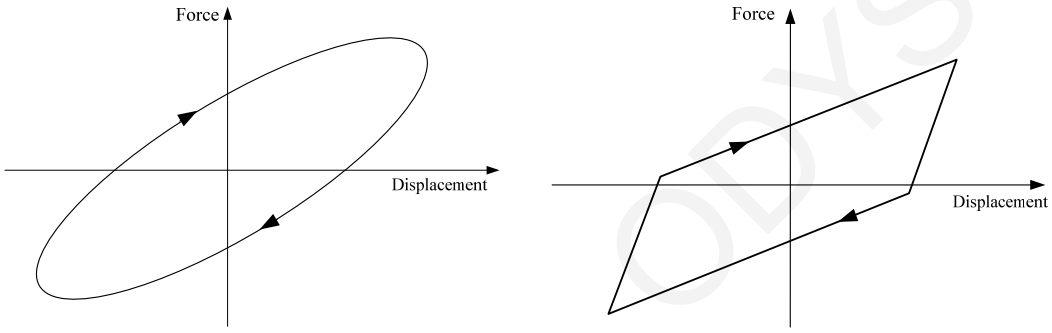

(a) (b)

Figure 3-12: a) Viscoelastic behavior, b) Bilinear Hysteretic Behavior.

3.4.1 Linear isolation system

A linear isolation system is composed of a linear spring with stiffness k_b and a linear viscous damper with coefficient c_b, Figure 3-13. The behavior of such a linear viscoelastic model, Figure 3-12(a), in terms of the lateral force developed in the isolation system is described by

$$F_b = k_b u + c_b \dot{u} \tag{3.20}$$

where u and $\dot{u}$ is the horizontal displacement and velocity of the isolation system.

The (isolation) system period T_b and damping ratio ξ_b are given respectively by

$$T_b = 2\pi\sqrt{\frac{M}{k_b}} \tag{3.21}$$

$$\xi_b = \frac{c_b}{2\sqrt{k_b M}} \tag{3.22}$$

where M is the total mass above the isolation system.

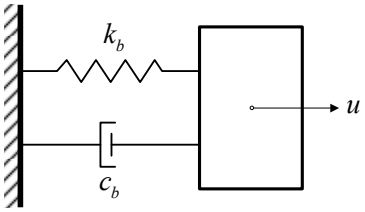

Figure 3-13: Schematic diagram of a linear isolation system.

3.4.2 Nonlinear isolation system - bilinear

A bilinear isolation system, Figure 3-12(b), is composed of a linear spring and a slider (Coulomb) that provides restoring force and friction force to the system, respectively, Figure 3-14. For this dissertation, the friction pendulum system (FPS) represents the nonlinear isolation system, (see Section 3.3.3), with a constant friction coefficient (static), μ_b, based on Coulomb friction. This type of friction is also called dry friction. Coulomb friction or dry friction occurs when the un-lubricated surfaces of two solids are in contact under a condition of sliding or a tendency to slide (Meriam and Kraige (2008)). The principles of Coulomb friction were developed from the experiments of Coulomb in 1781 and from the work of Morin from 1831 to 1834. Some typical values of coefficients of friction under normal working conditions are given in Table 3-1 (Meriam and Kraige (2008)).

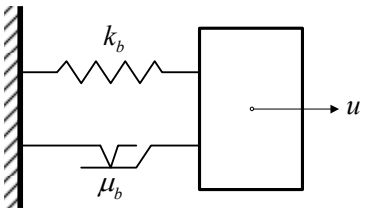

Figure 3-14: Schematic diagram of a nonlinear isolation system (FPS).

Table 3-1: Typical values of coefficient of Coulomb static friction (Meriam and Kraige (2008)).

Contacting Surface	Coefficient of static friction, μ_b
Steel on steel (dry)	0.6
Steel on steel (greasy)	0.1
Teflon on steel	0.04
Steel on babbitt (dry)	0.4
Steel on babbitt (greasy)	0.1
Brass on steel (dry)	0.5
Brake lining on cast iron	0.4
Rubber tures on smooth pavement (dry)	0.9
Wipe rope on iron pulley (dry)	0.2
Hemp rope on metal	0.3

CHAPTER 4

Dynamic Analysis of a Free Standing Rigid Block

4.1 Introduction

In this section a review of the rocking analysis of a rigid block resting on a rigid ground is presented, based on the works done by Housner (1963) and Shenton III and Jones (1991). In particular, the work discussed includes classifications of the different oscillation patterns of a rigid block and definitions of the criteria for the initiation of motion. Moreover, a model governing the impact between the block and the rigid ground during rocking and slide-rocking motions is also presented.

4.2 Model Description

Consider a symmetric rigid block of mass m and centroid mass moment of inertia I, supported on a horizontal rigid foundation (Figure 4-1). The rigid block of height $H = 2h$ and width $B = 2b$ is assumed to rotate about the base corners O and O'. The distance between one corner of its base and the mass center is denoted by R and the angle measured between R and the vertical when the body is at rest is denoted by α, where $\alpha = \tan^{-1}(b/h)$.

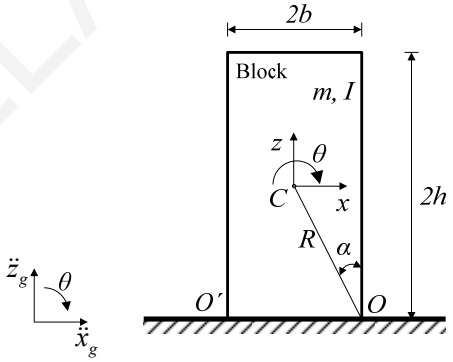

Figure 4-1: Model at rest.

The horizontal and vertical absolute displacements of the mass center of the block measured from the original at-rest position of the mass center are denoted by $x(t)$ and $z(t)$ respectively. The angular rotation of the block is denoted by $\theta(t)$, positive in the clockwise

direction. The ground motion is prescribed by a horizontal acceleration, $\ddot{x}_g(t)$, and vertical acceleration, $\ddot{z}_g(t)$.

4.3 Oscillation Regimes

When subjected to ground acceleration with horizontal and vertical components $\ddot{x}_g$ and $\ddot{z}_g$ respectively, the block can be set into sliding, rocking, slide-rocking, or free-flight regime. The five possible oscillation regimes are illustrated schematically in Figure 4-2.

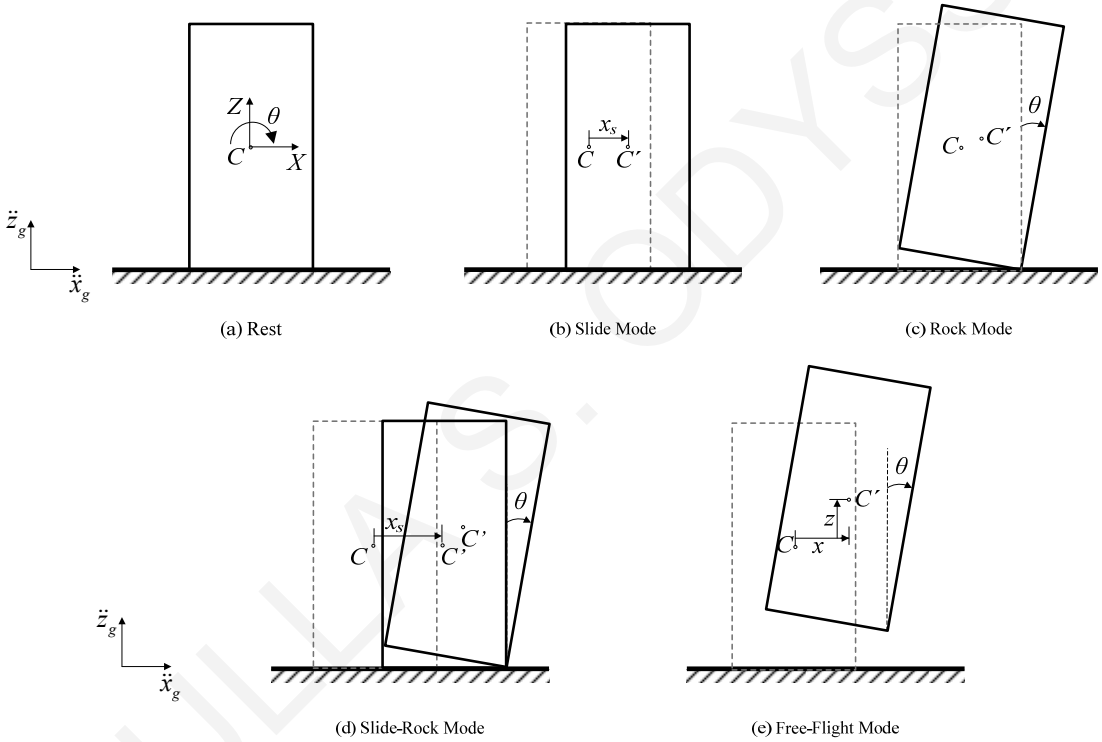

Figure 4-2: Oscillation patterns of a rigid block under ground acceleration.

At rest (Figure 4-2a), the block is assumed to be in full contact with the foundation at all times, with no relative motion between them. The rest mode is characterized by a normal reaction force greater than zero ($f_z > 0$), a friction force owed to Coulomb friction acting between the block and the foundation ($f_x > 0$), zero translation relative to the ground, and zero rotation.

During the sliding regime (Figure 4-2b), contact is still made with the foundation but the block

translates horizontally with displacement $x_s(t)$ relative to the ground. The sliding mode is characterized by a normal reaction force greater than zero ($f_z > 0$), a friction force depent on the normal force and the velocity of the center of mass, and zero rotation $\left(\theta(t) = 0\right)$.

In the rocking mode the rigid block pivots on its edges with rotation angle $\theta(t)$ (Figure 4-2c). This is true under the assumption that the block has small legs of negligible size and mass, or a slightly concave bottom.

In the slide-rocking mode (Figure 4-2d) the block rotates about either corner O or O' with rotation angle $\theta(t)$, and simultaneously slides with displacement $x_s(t)$ relative to the foundation. The friction force acting on the block is a function of the normal reaction and the velocity of the corner in contact.

Free-flight (Figure 4-2e) is characterized by zero normal reaction force, which results in loss of contact between the block and the foundation. The rigid block translates horizontally and vertically with displacements $x(t)$ and $z(t)$ relative to the ground, as it rotates with rotation angle $\theta(t)$.

4.3.1 Sliding regime

Assuming that the rigid block is initially at rest, a sliding regime (Figure 4-2b) is initiated once the inertia force of the mass exceeds the resistance provided by friction, which yields

$$\left|\ddot{x}_g\right| > \mu_s\left(\ddot{z}_g + g\right) \tag{4.1}$$

where μ_s is the coefficient of static friction between the block and the foundation, $\ddot{x}_g$ and $\ddot{z}_g$ are the horizontal and vertical components of ground acceleration respectively, and g is the gravitational acceleration.

The equation of motion during sliding regime can be derived by taking the equilibrium of horizontal forces acting on the block, yielding

$$\ddot{x}_s + \operatorname{sgn}\left(\dot{x}_s\right)\mu_k\left(g + \ddot{z}_g\right) = -\ddot{x}_g \tag{4.2}$$

in which, $\dot{x}_s$ and $\ddot{x}_s$ are respectively the horizontal velocity and the acceleration of the center of mass of the block relative to the foundation and μ_k is the coefficient of kinetic friction between the block and the foundation.

4.3.2 Rocking regime

Rocking of the block on the supporting foundation (Figure 4-2c) is initiated from rest once the overturning moment of the horizontal inertia force about one base corner, $M_{over} = m\ddot{x}_g h$, exceeds the restoring moment due to the weight of the block and the vertical inertia force, $M_{res} = mgb + m\ddot{z}_g b$, yielding

$$\left|\ddot{x}_g\right| > \left(\ddot{z}_g + g\right)\frac{b}{h} \tag{4.3}$$

If the acceleration $\ddot{x}_g$ of the block is positive, then rocking takes place about corner O', otherwise if it is negative rocking takes place about corner O.

The equation of motion during rocking mode can be derived by taking the equilibrium of moments about the corner being the center of rotation, O or O', yielding

$$I_O\ddot{\theta} = mR\cos\left(a - |\theta|\right)\ddot{x}_g - mR\,\mathrm{sgn}\,\theta\sin\left(a - |\theta|\right)\left(\ddot{z}_g + g\right) \tag{4.4}$$

where I_O is the mass moment of inertia of the block about the corner O. For rectangular blocks, $I_O = \frac{4}{3}mR^2$, and the equation (4.4) can be expressed as

$$\ddot{\theta} = \frac{3g}{4R}\left[\cos\left(a - |\theta|\right)\frac{\ddot{x}_g}{g} - \mathrm{sgn}\,\theta\sin\left(a - |\theta|\right)\frac{\left(\ddot{z}_g + g\right)}{g}\right] \tag{4.5}$$

According to Housner (1963), the term $\frac{3g}{4R} \equiv p^2$ can be used as a measure of the dynamic characteristics of the block.

Note that Equation (4.4) holds only in the absence of impact ($\theta \neq 0$). At that instant, both corner points O and O' are in contact with the base, rendering the equation of motion invalid.

The impact problem is presented separately in Section 4.4.

4.3.3 Slide-rocking regime

The conditions governing the initiation of slide-rocking regime (Figure 4-2d) are not altogether clear (Shenton and Jones (1991)). Slide-rocking is perhaps initiated from rest in the singular case when

$$\left|\ddot{x}_g\right| > \left[\mu_s\left(\ddot{z}_g + g\right), \frac{b}{h}\left(\ddot{z}_g + g\right)\right] \tag{4.6}$$

and thus the sliding and rocking regime conditions are satisfied simultaneously.

However, a slide-rocking mode may be initiated by transition from another mode of response, for example, from rocking mode when friction is not sufficient to sustain pure rocking.

Once the slide-rocking motion has been initiated, the response is governed by the following equations:

$$\begin{aligned} &m\ddot{x}_s + m\left[h\cos\theta + \operatorname{sgn}\theta\left(b\sin\theta\right)\right]\ddot{\theta} + m\left[\operatorname{sgn}\theta\left(b\cos\theta\right) - h\sin\theta\right]\dot{\theta}^2 \\ &+\operatorname{sgn}(\dot{x}_s)\mu_k m\left\{g + \ddot{z}_g + \left[\operatorname{sgn}\theta\left(b\cos\theta\right) - h\sin\theta\right]\ddot{\theta} - \left[h\cos\theta + \operatorname{sgn}\theta\left(b\sin\theta\right)\right]\dot{\theta}^2\right\} = -m\ddot{x}_g \end{aligned} \tag{4.7}$$

$$\begin{aligned} &\left(mr^2 + I\right)\ddot{\theta} + m\ddot{x}_s\left[h\cos\theta + \operatorname{sgn}\theta\left(b\sin\theta\right)\right] + mg\left[\operatorname{sgn}\theta\left(b\cos\theta\right) - h\sin\theta\right] \\ &= -m\left[h\cos\theta + \operatorname{sgn}\theta\left(b\sin\theta\right)\right]\ddot{x}_g - m\left[\operatorname{sgn}\theta\left(b\cos\theta\right) - h\sin\theta\right]\ddot{z}_g \end{aligned} \tag{4.8}$$

where $\dot{x}_s$ and $\ddot{x}_s$ are respectively the horizontal velocity and the acceleration of the mass center of the block relative to the foundation, and μ_k is the coefficient of kinetic friction between the block and the foundation. Equations (4.7) and (4.8) are valid only in the absence of impact ($\theta \neq 0$).

4.3.4 Free-flight regime

Free-flight occurs when the normal reaction force equals zero ($f_z = 0$). Assuming that the block is initially at rest or in a slide mode, free-flight is initiated when

$$\ddot{z}_g\left(t\right) = -g \tag{4.9}$$

If the block is in a rock or slide-rock mode, free-flight is initiated when

$$\ddot{z}_g = -R \operatorname{sgn}\theta \sin\left(a - |\theta|\right)\ddot{\theta} + R\cos\left(a - |\theta|\right)\dot{\theta}^2 - g \tag{4.10}$$

where $\dot{\theta}$ and $\ddot{\theta}$ are the angular velocity and acceleration of the block respectively and $\operatorname{sgn}\theta$ denotes the signum function in θ defined by

$$\operatorname{sgn}\theta = \begin{cases} 1 & \theta > 0 \\ -1 & \theta < 0 \end{cases} \tag{4.11}$$

The equations of motion for a block in a free-flight mode are

$$m\left(\ddot{x} + \ddot{x}_g\right) = 0 \tag{4.12}$$

$$m\left(\ddot{z} + \ddot{z}_g + g\right) = 0 \tag{4.13}$$

$$I\ddot{\theta} = 0 \tag{4.14}$$

where $\ddot{x}$ and $\ddot{z}$ are the horizontal and vertical accelerations of the mass center of the block relative to the foundation, respectively. Equations (4.12) through (4.14) are valid until an impact of the block with the foundation occurs.

4.4 The Impact Model

The impact problem is one of the most complicated problems in dynamics and it refers to the collision between two bodies. Impact is characterized by the generation of relatively large contact forces which act over a very short interval of time. The interrelationship of the transfer of energy and momentum, energy dissipation, elastic and plastic deformation, relative impact velocity and body geometry is quite complicated. Small changes in the impact conditions may cause large changes in the impact process and thus in the conditions immediately following the impact.

During rocking or slide-rocking motions, the block may experience one or more impacts with the foundation. At the instant of impact, both corners of the block are in contact with the base, rendering the governing equation of motion invalid. The instantaneous change of the block's

velocity must be taken into account for the integration of the equation governing the post-impact motion.

The formulation of the impact problem presented herein is based on the classical impact theory based on the following assumptions:

(i) Point-impact

(ii) Short duration of impact

(iii) Large impulsive forces relative to the other forces acting on the block

(iv) Negligible impulses at the rotating corner (impulses act only at the impacting corner)

(v) Instantaneous changes in velocity

(vi) Negligible changes in position and orientation of the block

(vii) Perfectly inelastic impact

Under the assumption of perfectly inelastic impact, the coefficient of restitution, e, that relates pre- to post-impact *translational* velocities (normal to the impact surface) of the impacting corner is zero $(e = 0)$.

The theoretical background of the classical impact theory is described analytically in Chapter 6.

4.4.1 Impact in rocking regime

Based on the assumption of perfectly inelastic impact, there is only one possible response mechanism following the impact: tilting about the impacting corner while the block re-uplifts (no bouncing).

The formulation of impact is divided into three phases: pre-impact, impact, and post-impact as illustrated schematically in Figure 4-3 and Figure 4-4. In the following, a superscript "-" refers to a pre-impact quantity and a superscript "+" to a post-impact quantity.

Consider the block at the instant when it hits the foundation from rocking about O and re-uplifts pivoting about the impacting corner O' (Figure 4-3). Impact is accompanied by an

instantaneous change in velocities, with the block displacements being unchanged. Therefore, the impact analysis is reduced to the computation of the block's post-impact angular velocity, $\dot{\theta}^{+}$, given its position and pre-impact angular velocity, $\dot{\theta}^{-}$.

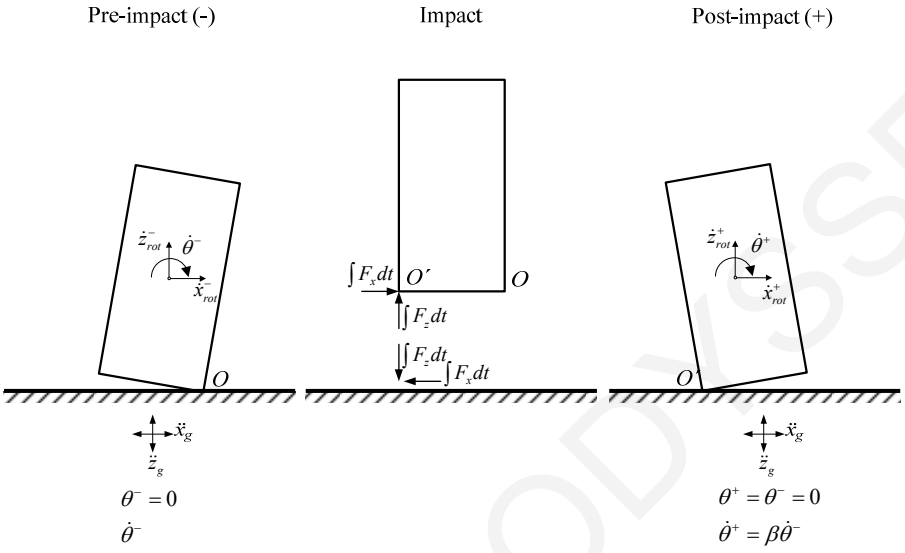

Figure 4-3: Impact from rocking about O followed by re-uplift about O'.

With regard to the block, the principle of linear impulse and momentum in the x and z directions states that

$$\int F_x dt = \left(\Delta L\right)_x = L_x^{+} - L_x^{-} : \quad \int F_x dt = m\dot{X}^{+} - m\dot{X}^{-} \tag{4.15}$$

$$\int F_z dt = \left(\Delta L\right)_z = L_z^{+} - L_z^{-} : \quad \int F_z dt = m\dot{Z}^{+} - m\dot{Z}^{-} \tag{4.16}$$

in which $\int F_x dt$ and $\int F_z dt$ are the horizontal and vertical impulses (assumed to act at O'); $\dot{X}^{-} = \dot{x}_g + \dot{x}_{rot}^{-}$, $\dot{X}^{+} = \dot{x}_g + \dot{x}_{rot}^{+}$ and $\dot{Z}^{-} = \dot{z}_g + \dot{z}_{rot}^{-}$, $\dot{Z}^{+} = \dot{z}_g + \dot{z}_{rot}^{+}$ are the absolute pre- and post-impact horizontal and vertical velocities of the mass center of the block respectively; $\dot{x}_{rot}^{-}$, $\dot{x}_{rot}^{+}$ and $\dot{z}_{rot}^{-}$, $\dot{z}_{rot}^{+}$ are the relative pre- and post-impact horizontal and vertical velocities of the mass center of the block due to the rocking, relative to the foundation; L_x^{-}, L_x^{+}, L_z^{-} and L_z^{+} are the pre- and post-impact horizontal and vertical linear momentum, respectively; $\left(\Delta L\right)_x$ and $\left(\Delta L\right)_z$ are the changes in horizontal and vertical linear momentum, respectively.

Substituting these expressions into Equations (4.15) and (4.16), we obtain

$$\int F_x dt = m\left(\dot{x}_g + \dot{x}_{rot}^{+}\right) - m\left(\dot{x}_g + \dot{x}_{rot}^{-}\right) \Rightarrow \int F_x dt = m\dot{x}_{rot}^{+} - m\dot{x}_{rot}^{-} \tag{4.17}$$

$$\int F_z dt = m\left(\dot{z}_g + \dot{z}_{rot}^{+}\right) - m\left(\dot{z}_g + \dot{z}_{rot}^{-}\right) \Rightarrow \int F_z dt = m\dot{z}_{rot}^{+} - m\dot{z}_{rot}^{-} \tag{4.18}$$

In addition, the principle of angular impulse and momentum states that

$$\int M_C dt = \Delta H_C = H_C^{+} - H_C^{-}: \;\; b\left(\int F_z dt\right) - h\left(\int F_x dt\right) = I\dot{\theta}^{+} - I\dot{\theta}^{-} \tag{4.19}$$

in which $\int M_C dt$ is the angular impulse; H_C^{-} and H_C^{+} are the pre- and post-impact angular momentum about the mass center respectively; ΔH_C is the change in the angular momentum about the mass center.

In Equations (4.17) and (4.18), the pre- and post-impact horizontal and vertical components of the relative translational velocity of the mass center can be expressed in terms of the pre- and post-impact angular velocity of the block $\left(\dot{\theta}^{-},\ \dot{\theta}^{+}\right)$ as follows.

For the pre-impact state, the translational velocity vector of the mass center can be expressed as

$$\boldsymbol{v}^{-} = \boldsymbol{v}_O^{-} + \boldsymbol{\omega}^{-} \times \boldsymbol{r}_{C/O} \tag{4.20}$$

where $\boldsymbol{v}^{-}$ is pre-impact translational velocity vector of center-of mass, $\boldsymbol{v}_O^{-}$ is pre-impact translational velocity vector of point O, $\boldsymbol{\omega}^{-}$ is pre-impact angular velocity vector of the block, and $\boldsymbol{r}_{C/O}$ is position vector of the mass center relative to point O.

Expressions for these vector quantities are given below:

$$\boldsymbol{v}^{-} = \dot{X}^{-}\hat{\boldsymbol{i}} + \dot{Z}^{-}\hat{\boldsymbol{k}} = \left(\dot{x}_g + \dot{x}_{rot}^{-}\right)\hat{\boldsymbol{i}} + \dot{z}_{rot}^{-}\hat{\boldsymbol{k}} \tag{4.21}$$

$$\boldsymbol{v}_O^{-} = \dot{x}_g\hat{\boldsymbol{i}} \tag{4.22}$$

$$\boldsymbol{\omega}^{-} = \dot{\theta}^{-}\hat{\boldsymbol{j}} \tag{4.23}$$

$$\boldsymbol{r}_{C/O} = -r\sin\left(a-\theta\right)\hat{\boldsymbol{i}} + r\cos\left(a-\theta\right)\hat{\boldsymbol{k}} \tag{4.24}$$

At impact, the angular rotation of the block becomes zero $\left(\theta = 0\right)$ and the position vector of the mass center can be rewritten as

$$\boldsymbol{r}_{C/O} = -\left(r\sin a\right)\hat{\boldsymbol{i}} + \left(r\cos a\right)\hat{\boldsymbol{k}} = -b\hat{\boldsymbol{i}} + h\hat{\boldsymbol{k}} \tag{4.25}$$

On substituting Equations (4.21) through (4.25) into Equation (4.20), the pre-impact translational velocity becomes

$$\boldsymbol{v}^{-} \equiv \left(\dot{x}_g + \dot{x}_{rot}^{-}\right)\hat{\boldsymbol{i}} + \dot{z}_{rot}^{-}\hat{\boldsymbol{k}} = \left(\dot{x}_g\right)\hat{\boldsymbol{i}} + \left(\dot{\theta}^{-}\hat{\boldsymbol{j}}\right)\times\left(-b\hat{\boldsymbol{i}} + h\hat{\boldsymbol{k}}\right) \tag{4.26}$$

which reduces to

$$\dot{x}_{rot}^{-}\hat{\boldsymbol{i}} + \dot{z}_{rot}^{-}\hat{\boldsymbol{k}} = \left(b\dot{\theta}^{-}\right)\hat{\boldsymbol{k}} + \left(h\dot{\theta}^{-}\right)\hat{\boldsymbol{i}} \tag{4.27}$$

from which the pre-impact horizontal and vertical components of $\boldsymbol{v}^{-}$ can be retrieved as

$$\dot{x}_{rot}^{-} = h\dot{\theta}^{-} \tag{4.28}$$

$$\dot{z}_{rot}^{-} = b\dot{\theta}^{-} \tag{4.29}$$

For the post-impact state, the translational velocity vector of the mass center is

$$\boldsymbol{v}^{+} = \boldsymbol{v}_{O'}^{+} + \boldsymbol{\omega}^{+}\times\boldsymbol{r}_{C/O'} \tag{4.30}$$

where $\boldsymbol{v}^{+}$ is post-impact translational velocity vector of center-of-mass, $\boldsymbol{v}_{O'}^{+}$ is post-impact translational velocity vector of point O', $\boldsymbol{\omega}^{+}$ is post-impact angular velocity vector of the block, and $\boldsymbol{r}_{C/O'}$ is position vector of the mass center relative to point O'.

Expressions for these vector quantities are given below:

$$\boldsymbol{v}^{+} = \dot{X}^{+}\hat{\boldsymbol{i}} + \dot{Z}^{+}\hat{\boldsymbol{k}} = \left(\dot{x}_g + \dot{x}_{rot}^{+}\right)\hat{\boldsymbol{i}} + \dot{z}_{rot}^{+}\hat{\boldsymbol{k}} \tag{4.31}$$

$$\boldsymbol{v}_{O'}^{+} = \dot{x}_g \hat{\boldsymbol{i}} \tag{4.32}$$

$$\boldsymbol{\omega}^{+} = \dot{\theta}^{+} \hat{\boldsymbol{j}} \tag{4.33}$$

$$\boldsymbol{r}_{C/O'} = r\sin\left(a-\theta\right)\hat{\boldsymbol{i}} + r\cos\left(a-\theta\right)\hat{\boldsymbol{k}} \tag{4.34}$$

At impact $\left(\theta = 0\right)$ the position vector of the mass center is

$$\boldsymbol{r}_{C/O'} = \left(r\sin a\right)\hat{\boldsymbol{i}} + \left(r\cos a\right)\hat{\boldsymbol{k}} = b\hat{\boldsymbol{i}} + h\hat{\boldsymbol{k}} \tag{4.35}$$

On substituting Equations (4.31) through (4.35) into Equation (4.30), the post-impact translational velocity becomes

$$\boldsymbol{v}^{+} \equiv \left(\dot{x}_g + \dot{x}_{rot}^{+}\right)\hat{\boldsymbol{i}} + \dot{z}_{rot}^{+}\hat{\boldsymbol{k}} = \left(\dot{x}_g\right)\hat{\boldsymbol{i}} + \left(\dot{\theta}^{+}\hat{\boldsymbol{j}}\right)\times\left(b\hat{\boldsymbol{i}} + h\hat{\boldsymbol{k}}\right) \tag{4.36}$$

which simplifies to

$$\dot{x}_{rot}^{+}\hat{\boldsymbol{i}} + \dot{z}_{rot}^{+}\hat{\boldsymbol{k}} = \left(-b\dot{\theta}^{+}\right)\hat{\boldsymbol{k}} + \left(h\dot{\theta}^{+}\right)\hat{\boldsymbol{i}} \tag{4.37}$$

From Equation (4.37), the post-impact horizontal and vertical components of $\boldsymbol{v}^{+}$ can be retrieved as

$$\dot{x}_{rot}^{+} = h\dot{\theta}^{+} \tag{4.38}$$

$$\dot{z}_{rot}^{+} = -b\dot{\theta}^{+} \tag{4.39}$$

Substitution of Equations (4.28), (4.29), (4.38) and (4.39) into Equations (4.15) through (4.19) yields

$$\int F_x dt = m\left(h\dot{\theta}^{+}\right) - m\left(h\dot{\theta}^{-}\right) \tag{4.40}$$

$$\int F_z dt = m\left(-b\dot{\theta}^{+}\right) - m\left(b\dot{\theta}^{-}\right) \tag{4.41}$$

$$b\left(\int F_z dt\right) - h\left(\int F_x dt\right) = I\left(\dot{\theta}^{+}\right) - I\left(\dot{\theta}^{-}\right) \tag{4.42}$$

in which the centroid mass moment of inertia for the rectangular block is given by

$$I = \frac{m}{3} r^2 = \frac{m}{3}\left(b^2 + h^2\right) \tag{4.43}$$

Equations (4.40) through (4.42) constitutes a set of three equations in three unknowns: $\int F_x dt$, $\int F_z dt$, $\dot{\theta}^+$.

Equivalently, the three equations can be combined in one (by eliminating the two impulses) in one unknown:

$$b\left(-mb\dot{\theta}^+ - mb\dot{\theta}^-\right) - h\left(mh\dot{\theta}^+ - mh\dot{\theta}^-\right) = \frac{m}{3}\left(b^2 + h^2\right)\left(\dot{\theta}^+ - \dot{\theta}^-\right) \tag{4.44}$$

which yields the post-impact angular velocity of the block as

$$\dot{\theta}^+ = \frac{\left(4h^2 - 2b^2\right)}{\left(4h^2 + 4b^2\right)}\dot{\theta}^- \tag{4.45}$$

Equation (4.45) can be written in the form

$$\dot{\theta}^+ = \frac{\left(2\lambda^2 - 1\right)}{\left(2\lambda^2 + 2\right)}\dot{\theta}^- \equiv \beta\dot{\theta}^- \tag{4.46}$$

in which $\lambda = h/b$ is the geometric aspect ratio of the block and $\beta = \dfrac{\left(2\lambda^2 - 1\right)}{\left(2\lambda^2 + 2\right)}$ is the coefficient of angular restitution.

Following the same procedure, it can be shown that the post-impact velocity for impact from rocking about O' (Figure 4-4) (realized when $\dot{\theta} > 0$) is identical to that given by Equation (4.46), which was derived considering impact from rocking about O (realized when $\dot{\theta} < 0$).

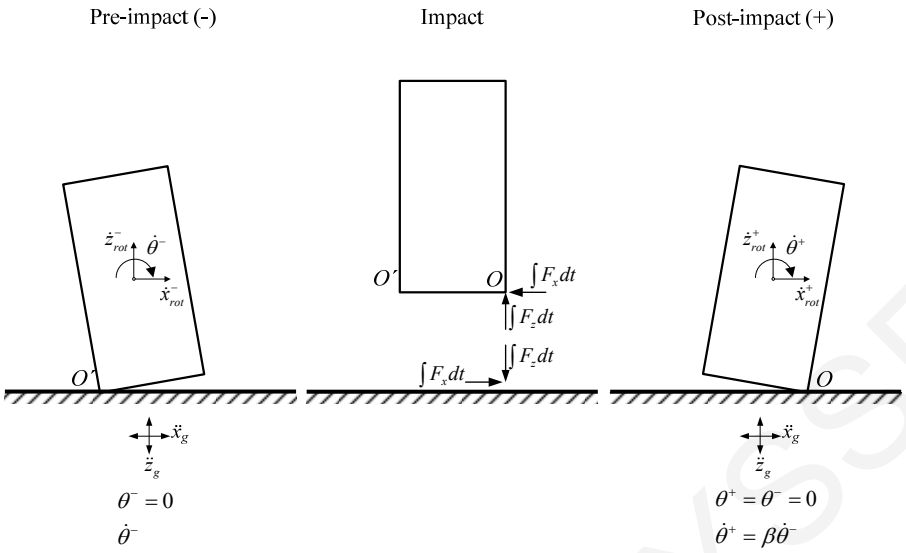

Figure 4-4: Impact from rocking about O' followed by re-uplift about O.

4.4.2 Impact in slide-rocking regime

Under the assumption of perfectly inelastic impact, there are three possible response mechanisms following impact: (a) pure rocking about the impacting corner, when sliding motion ceases after impact, Figure 4-5, (c) pure sliding, when rocking ceases after impact, Figure 4-6, and (d) simultaneous sliding and rocking about the impacting corner, Figure 4-7. As explained earlier, a superscript "-" refers to a pre-impact quantity and a superscript "+" to a post-impact quantity.

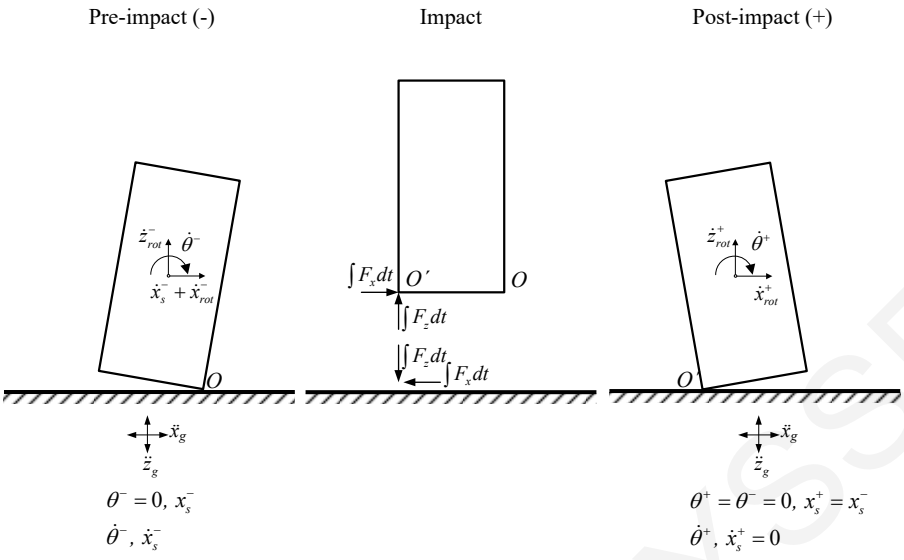

Figure 4-5: Impact from slide-rocking about *O* followed by pure rocking about *O′* (sliding ceases).

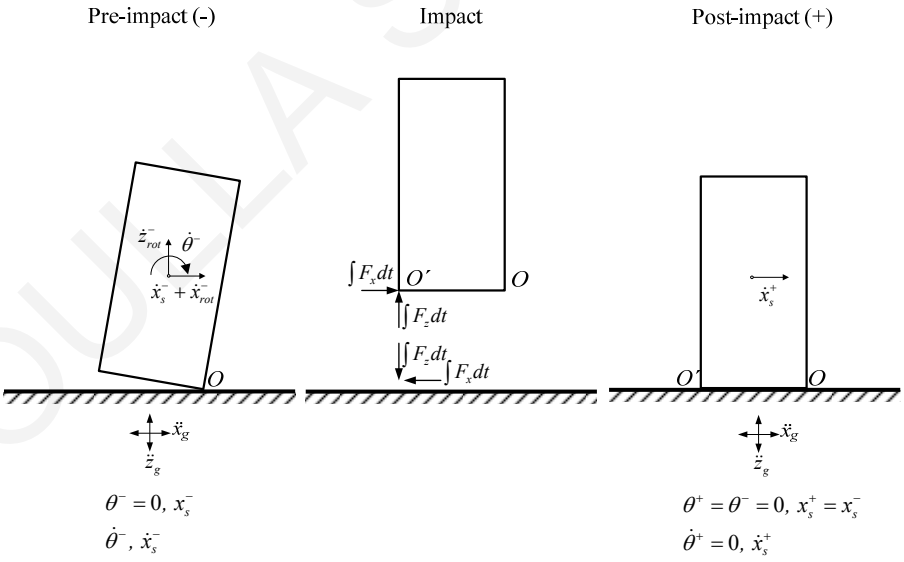

Figure 4-6: Impact from slide-rocking about *O* followed by pure sliding (rocking ceases).

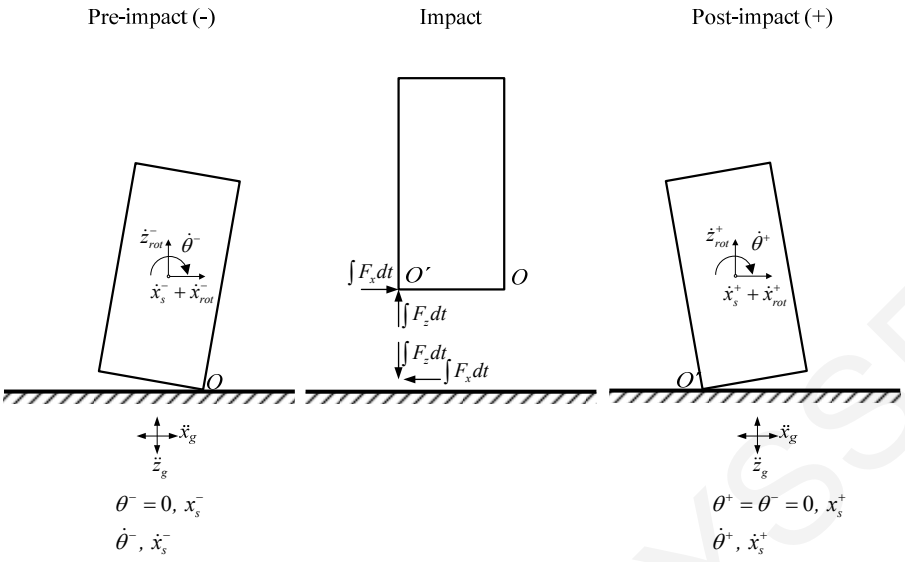

Figure 4-7: Impact from slide-rocking about *O* followed by slide-rocking about *O'*.

4.4.2.1 Pure rocking occurs after impact

Derivation for the case of impact during rocking about point O

Consider the system at the instant when the block hits the moving base from rocking about O and re-uplifts pivoting about the impacting corner, O'. As aforementioned, impact is accompanied by an instantaneous change in velocities, with the system displacements being unchanged. Therefore, the impact analysis is reduced to the computation of the initial conditions for the post-impact motion $\dot{\theta}^{+}$, given the position and the pre-impact velocities, $\dot{x}_s^{-}$, and $\dot{\theta}^{-}$.

With regard to the block, the principle of linear impulse and momentum in the x and z direction states that

$$\int F_x dt = \left(\Delta L\right)_x = L_x^{+} - L_x^{-}: \quad \int F_x dt = m\dot{X}^{+} - m\dot{X}^{-} \tag{4.47}$$

$$\int F_z dt = \left(\Delta L\right)_z = L_z^{+} - L_z^{-}: \quad \int F_z dt = m\dot{Z}^{+} - m\dot{Z}^{-} \tag{4.48}$$

in which $\int F_x dt$ and $\int F_z dt$ are the horizontal and vertical impulses (assumed to act at O'); $\dot{X}^{-} = \dot{x}_g + \dot{x}_s^{-} + \dot{x}_{rot}^{-}$, $\dot{X}^{+} = \dot{x}_g + \dot{x}_s^{+} + \dot{x}_{rot}^{+}$ and $\dot{Z}^{-} = \left(\dot{z}_{rot}^{-} + \dot{z}_g\right)$, $\dot{Z}^{+} = \left(\dot{z}_{rot}^{+} + \dot{z}_g\right)$ are the absolute pre- and post-impact horizontal and vertical velocities of the mass center of the block,

respectively; $\dot{x}_{rot}^{-}$, $\dot{x}_{rot}^{+}$ and $\dot{z}_{rot}^{-}$, $\dot{z}_{rot}^{+}$ are the relative pre- and post-impact horizontal and vertical velocities of the mass center of the block due to the rocking, relative to the foundation; $\dot{x}_{s}^{-}$ and $\dot{x}_{s}^{+}$ are the relative pre- and post-impact horizontal velocities of the mass center of the block due to the sliding, relative to the foundation; L_x^-, L_x^+, L_z^- and L_z^+ are the pre- and post-impact horizontal and vertical linear momentum, respectively; $(\Delta L)_x$ and $(\Delta L)_z$ are the changes in horizontal and vertical linear momentum, respectively.

Substituting these expressions into Equations (4.47) and (4.48), we obtain

$$\int F_x dt = m\dot{x}_s^+ + m\dot{x}_{rot}^+ - m\dot{x}_s^- - m\dot{x}_{rot}^- \tag{4.49}$$

$$\int F_z dt = m\dot{z}_{rot}^+ - m\dot{z}_{rot}^- \tag{4.50}$$

In addition, the principle of angular impulse and momentum states that

$$\int M_C dt = \Delta H_C = H_C^+ - H_C^- :\ b\left(\int F_z dt\right) - h\left(\int F_x dt\right) = I\dot{\theta}^+ - I\dot{\theta}^- \tag{4.51}$$

in which $\int M_C dt$ is the angular impulse; H_C^- and H_C^+ are the pre- and post-impact angular momentum about the mass center, respectively; ΔH_C is the change in the angular momentum about the mass center.

In Equations (4.49) and (4.50), the pre- and post-impact horizontal and vertical components of the relative translational velocity of the mass center can be expressed in terms of the pre- and post-impact angular velocity of the block, $\dot{\theta}^-$ and $\dot{\theta}^+$ as follows.

For the pre-impact state, the translational velocity vector of the mass center (Figure 4-8) can be expressed as

$$\boldsymbol{v}^- = \boldsymbol{v}_O^- + \boldsymbol{\omega}^- \times \boldsymbol{r}_{C/O} \tag{4.52}$$

where $\boldsymbol{v}^-$ is pre-impact translational velocity vector of center-of-mass, $\boldsymbol{v}_O^-$ is pre-impact translational velocity vector of point O, $\boldsymbol{\omega}^-$ is pre-impact angular velocity vector of the block, and $\boldsymbol{r}_{C/O}$ is position vector of the mass center relative to point O.

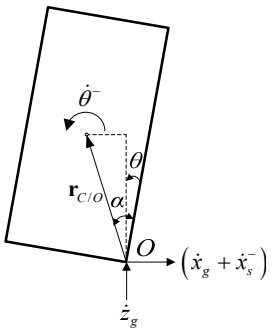

Figure 4-8: Components of pre-impact translational velocity of the non-isolated block for the case of impact during slide-rocking about point *O*.

Expressions for these vector quantities are given below:

$$\boldsymbol{v}^- = \dot{X}^-\hat{\boldsymbol{i}} + \dot{Z}^-\hat{\boldsymbol{k}} = \left(\dot{x}_g + \dot{x}_s^- + \dot{x}_{rot}^-\right)\hat{\boldsymbol{i}} + \left(\dot{z}_{rot}^- + \dot{z}_g\right)\hat{\boldsymbol{k}} \tag{4.53}$$

$$\boldsymbol{v}_O^- = \left(\dot{x}_g + \dot{x}_s^-\right)\hat{\boldsymbol{i}} + \left(\dot{z}_g\right)\hat{\boldsymbol{k}} \tag{4.54}$$

$$\boldsymbol{\omega}^- = \dot{\theta}^-\hat{\boldsymbol{j}} \tag{4.55}$$

$$\boldsymbol{r}_{C/O} = -r\sin\left(a-\theta\right)\hat{\boldsymbol{i}} + r\cos\left(a-\theta\right)\hat{\boldsymbol{k}} \tag{4.56}$$

At impact, the angular rotation of the block becomes zero $\left(\theta = 0\right)$ and the position vector of the mass center relative to point O, $\boldsymbol{r}_{C/O}$, can be rewritten as

$$\boldsymbol{r}_{C/O} = -\left(r\sin a\right)\hat{\boldsymbol{i}} + \left(r\cos a\right)\hat{\boldsymbol{k}} = -b\hat{\boldsymbol{i}} + h\hat{\boldsymbol{k}} \tag{4.57}$$

in which $\hat{\boldsymbol{i}}$ and $\hat{\boldsymbol{k}}$ are the horizontal and vertical unit vectors, respectively.

On substituting Equations (4.53) through (4.57) into Equation (4.52), the pre-impact translational velocity becomes

$$\boldsymbol{v}^- \equiv \left(\dot{x}_g + \dot{x}_s^- + \dot{x}_{rot}^-\right)\hat{\boldsymbol{i}} + \left(\dot{z}_{rot}^- + \dot{z}_g\right)\hat{\boldsymbol{k}} = \left(\dot{x}_g + \dot{x}_s^-\right)\hat{\boldsymbol{i}} + \left(\dot{z}_g\right)\hat{\boldsymbol{k}} + \left(\dot{\theta}^-\hat{\boldsymbol{j}}\right)\times\left(-b\hat{\boldsymbol{i}} + h\hat{\boldsymbol{k}}\right) \tag{4.58}$$

which reduces to

$$\dot{x}_{rot}^{-}\hat{\boldsymbol{i}} + \dot{z}_{rot}^{-}\hat{\boldsymbol{k}} = \left(b\dot{\theta}^{-}\right)\hat{\boldsymbol{k}} + \left(h\dot{\theta}^{-}\right)\hat{\boldsymbol{i}} \tag{4.59}$$

from which the pre-impact horizontal and vertical components of $\boldsymbol{v}^{-}$ can be retrieved as

$$\dot{x}_{rot}^{-} = h\dot{\theta}^{-} \tag{4.60}$$

$$\dot{z}_{rot}^{-} = b\dot{\theta}^{-} \tag{4.61}$$

For the post-impact state, the translational velocity vector of the mass center (Figure 4-9) can be expressed as

$$\boldsymbol{v}^{+} = \boldsymbol{v}_{O'}^{+} + \boldsymbol{\omega}^{+} \times \boldsymbol{r}_{C/O'} \tag{4.62}$$

where $\boldsymbol{v}^{+}$ is post-impact translational velocity vector of center-of-mass, $\boldsymbol{v}_{O'}^{+}$ is post-impact translational velocity vector of point O', $\boldsymbol{\omega}^{+}$ is post-impact angular velocity vector of the block, and $\boldsymbol{r}_{C/O'}$ is position vector of the mass center relative to point O'.

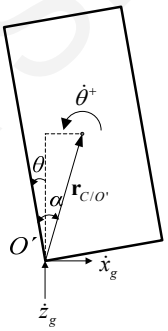

Figure 4-9: Components of post-impact translational velocity of the non-isolated block for the case of impact during slide-rocking about point *O'*.

Expressions for these vector quantities are given below:

$$\boldsymbol{v}^{+} = \dot{X}^{+}\hat{\boldsymbol{i}} + \dot{Z}^{+}\hat{\boldsymbol{k}} = \left(\dot{x}_g + \dot{x}_{rot}^{+}\right)\hat{\boldsymbol{i}} + \left(\dot{z}_{rot}^{+} + \dot{z}_g\right)\hat{\boldsymbol{k}} \tag{4.63}$$

$$\boldsymbol{v}_{O'}^{+} = \left(\dot{x}_g\right)\hat{\boldsymbol{i}} + \left(\dot{z}_g\right)\hat{\boldsymbol{k}} \tag{4.64}$$

$$\boldsymbol{\omega}^{+} = \dot{\theta}^{+}\hat{\boldsymbol{j}} \tag{4.65}$$

$$\boldsymbol{r}_{C/O'} = r\sin\left(a-\theta\right)\hat{\boldsymbol{i}} + r\cos\left(a-\theta\right)\hat{\boldsymbol{k}} \tag{4.66}$$

At impact $\left(\theta = 0\right)$ the position vector of the mass center relative to point O', $\boldsymbol{r}_{C/O'}$, becomes

$$\boldsymbol{r}_{C/O'} = \left(r\sin a\right)\hat{\boldsymbol{i}} + \left(r\cos a\right)\hat{\boldsymbol{k}} = b\hat{\boldsymbol{i}} + h\hat{\boldsymbol{k}} \tag{4.67}$$

On substituting Equations (4.63) through (4.67) into Equation (4.62), the post-impact translational velocity becomes

$$\boldsymbol{v}^{+} \equiv \left(\dot{x}_g + \dot{x}_{rot}^{+}\right)\hat{\boldsymbol{i}} + \left(\dot{z}_{rot}^{+} + \dot{z}_g\right)\hat{\boldsymbol{k}} = \left(\dot{x}_g\right)\hat{\boldsymbol{i}} + \left(\dot{z}_g\right)\hat{\boldsymbol{k}} + \left(\dot{\theta}^{+}\hat{\boldsymbol{j}}\right)\times\left(b\hat{\boldsymbol{i}} + h\hat{\boldsymbol{k}}\right) \tag{4.68}$$

which simplifies to

$$\dot{x}_{rot}^{+}\hat{\boldsymbol{i}} + \dot{z}_{rot}^{+}\hat{\boldsymbol{k}} = \left(-b\dot{\theta}^{+}\right)\hat{\boldsymbol{k}} + \left(h\dot{\theta}^{+}\right)\hat{\boldsymbol{i}} \tag{4.69}$$

from which the post-impact horizontal and vertical components of $\boldsymbol{v}^{+}$ can be retrieved as

$$\dot{x}_{rot}^{+} = h\dot{\theta}^{+} \tag{4.70}$$

$$\dot{z}_{rot}^{+} = -b\dot{\theta}^{+} \tag{4.71}$$

Substituting Equations (4.60), (4.61), (4.70) and (4.71) into Equations (4.47) through (4.51) yields

$$\int F_x dt = m\dot{u}^{+} + m\left(h\dot{\theta}^{+}\right) - m\dot{u}^{-} - m\dot{x}_s^{-} - m\left(h\dot{\theta}^{-}\right) \tag{4.72}$$

$$\int F_z dt = m\left(-b\dot{\theta}^{+}\right) - m\left(b\dot{\theta}^{-}\right) \tag{4.73}$$

$$b\left(\int F_z dt\right) - h\left(\int F_x dt\right) = I\left(\dot{\theta}^{+}\right) - I\left(\dot{\theta}^{-}\right) \tag{4.74}$$

in which block the centroid mass moment of inertia for the rectangular block is given by

$$I = \frac{m}{3} r^2 = \frac{m}{3}\left(b^2 + h^2\right) \tag{4.75}$$

Equations (4.72), (4.73) and (4.74) constitute a set of three equations in three unknowns, namely $\int F_x dt$, $\int F_z dt$, $\dot{\theta}^+$.

Equivalently, the three Equations (4.72), (4.73) and (4.74) can be combined in one (by eliminating the two impulses) with two unknowns:

$$\left(4b^2 + 4h^2\right)\dot{\theta}^+ = \left(4h^2 - 2b^2\right)\dot{\theta}^- + 3h\dot{x}_s^- \tag{4.76}$$

which yields the post-impact angular velocity of the block as

$$\dot{\theta}^+ = \frac{\left(4h^2 - 2b^2\right)\dot{\theta}^- + 3h\dot{x}_s^-}{\left(4b^2 + 4h^2\right)} \tag{4.77}$$

An identical expression can be derived for the case of impact during rocking about point O' .

4.4.2.2 Pure sliding occurs after impact

When rocking of the block on top of the moving base ceases, the system attains a sliding regime. In this case, the impact analysis is reduced to the computation of the post-impact translational velocity of the system, $\dot{x}_s^+$, given the position and the pre-impact velocities, $\dot{x}_s^-$, and $\dot{\theta}^-$.

Derivation for the case of impact during rocking about point O

Consider the system at the instant when the block hits the moving base from rocking about O.

With regard to the block, the principle of linear impulse and momentum in the x and z directions states that

$$\int F_x dt = \left(\Delta L\right)_x = L_x^+ - L_x^- : \quad \int F_x dt = m\dot{X}^+ - m\dot{X}^- \tag{4.78}$$

$$\int F_z dt = \left(\Delta L\right)_z = L_z^+ - L_z^- : \quad \int F_z dt = m\dot{Z}^+ - m\dot{Z}^- \tag{4.79}$$

in which $\int F_x dt$ and $\int F_z dt$ are the horizontal and vertical impulses (assumed to act at O'); $\dot{X}^- = \dot{x}_g + \dot{x}_s^- + \dot{x}_{rot}^-$, $\dot{X}^+ = \dot{x}_g + \dot{x}_s^+ + \dot{x}_{rot}^+$ and $\dot{Z}^- = \left(\dot{z}_{rot}^- + \dot{z}_g\right)$, $\dot{Z}^+ = \left(\dot{z}_{rot}^+ + \dot{z}_g\right)$ are the absolute pre- and post-impact horizontal and vertical velocities of the mass center of the block, respectively; $\dot{x}_{rot}^-$, $\dot{x}_{rot}^+$ and $\dot{z}_{rot}^-$, $\dot{z}_{rot}^+$ are the relative pre- and post-impact horizontal and vertical velocities of the mass center of the block due to the rocking, relative to the foundation; $\dot{x}_s^-$ and $\dot{x}_s^+$ are the relative pre- and post-impact horizontal velocities of the mass center of the block due to the sliding, relative to the foundation; L_x^-, L_x^+, L_z^- and L_z^+ are the pre- and post-impact horizontal and vertical linear momentum, respectively; $\left(\Delta L\right)_x$ and $\left(\Delta L\right)_z$ are the changes in horizontal and vertical linear momentum, respectively.

Substituting these expressions into Equations (4.78) and (4.79), we obtain

$$\int F_x dt = m\dot{x}_s^+ + m\dot{x}_{rot}^+ - m\dot{x}_s^- - m\dot{x}_{rot}^- \tag{4.80}$$

$$\int F_z dt = m\dot{z}_{rot}^+ - m\dot{z}_{rot}^- \tag{4.81}$$

In Equations (4.80) and (4.81), the pre- and post-impact horizontal components of the relative translational velocity of the mass center can be expressed in terms of the pre-impact angular velocity of the block, $\dot{\theta}^-$ as follows

For the pre-impact state, the translational velocity vector of the mass center (Figure 4-8) can be expressed as

$$\boldsymbol{v}^- = \boldsymbol{v}_O^- + \boldsymbol{\omega}^- \times \boldsymbol{r}_{C/O} \tag{4.82}$$

where $\boldsymbol{v}^-$ is pre-impact translational velocity vector of center-of-mass, $\boldsymbol{v}_O^-$ is pre-impact translational velocity of point O, $\boldsymbol{\omega}^-$ is pre-impact angular velocity of the block, and

$\boldsymbol{r}_{C/O}$ is position vector of center-of-mass relative to point O.

Expressions for these vector quantities are given below:

$$\boldsymbol{v}^- = \dot{X}^-\hat{\boldsymbol{i}} + \dot{Z}^-\hat{\boldsymbol{k}} = \left(\dot{x}_g + \dot{x}_{rot}^- + \dot{x}_s^-\right)\hat{\boldsymbol{i}} + \left(\dot{z}_{rot}^- + \dot{z}_g\right)\hat{\boldsymbol{k}} \tag{4.83}$$

$$\boldsymbol{v}_O^- = \left(\dot{x}_g + \dot{x}_s^-\right)\hat{\boldsymbol{i}} + \left(\dot{z}_g\right)\hat{\boldsymbol{k}} \tag{4.84}$$

$$\boldsymbol{\omega}^- = \dot{\theta}^-\hat{\boldsymbol{j}} \tag{4.85}$$

$$\boldsymbol{r}_{C/O} = -r\sin\left(a-\theta\right)\hat{\boldsymbol{i}} + r\cos\left(a-\theta\right)\hat{\boldsymbol{k}} \tag{4.86}$$

At impact, the angular velocity of the block becomes zero $\left(\theta = 0\right)$ and the position vector of the mass center relative to point O can be rewritten as

$$\boldsymbol{r}_{C/O} = -\left(r\sin a\right)\hat{\boldsymbol{i}} + \left(r\cos a\right)\hat{\boldsymbol{k}} = -b\hat{\boldsymbol{i}} + h\hat{\boldsymbol{k}} \tag{4.87}$$

On substituting Equations (4.83) through (4.87) into Equation (4.82), the pre-impact translational velocity therefore becomes

$$\boldsymbol{v}^- \equiv \left(\dot{x}_g + \dot{x}_{rot}^- + \dot{x}_s^-\right)\hat{\boldsymbol{i}} + \left(\dot{z}_{rot}^- + \dot{z}_g\right)\hat{\boldsymbol{k}} = \left(\dot{x}_g + \dot{x}_s^-\right)\hat{\boldsymbol{i}} + \left(\dot{z}_g\right)\hat{\boldsymbol{k}} + \left(\dot{\theta}^-\hat{\boldsymbol{j}}\right)\times\left(-b\hat{\boldsymbol{i}} + h\hat{\boldsymbol{k}}\right) \tag{4.88}$$

which reduces to

$$\dot{x}_{rot}^-\hat{\boldsymbol{i}} + \dot{z}_{rot}^-\hat{\boldsymbol{k}} = \left(b\dot{\theta}^-\right)\hat{\boldsymbol{k}} + \left(h\dot{\theta}^-\right)\hat{\boldsymbol{i}} \tag{4.89}$$

from which the pre-impact horizontal and vertical components of $\boldsymbol{v}^-$ can be retrieved as

$$\dot{x}_{rot}^- = h\dot{\theta}^- \tag{4.90}$$

$$\dot{z}_{rot}^- = b\dot{\theta}^- \tag{4.91}$$

For the post-impact state, the translational velocity vector of the mass center can be expressed as

$$\boldsymbol{v}^+ = \boldsymbol{v}_{O'}^+ + \boldsymbol{\omega}^+ \times \boldsymbol{r}_{C/O'} \tag{4.92}$$

where $\boldsymbol{v}^+$ is post-impact translational velocity vector of center-of-mass, $\boldsymbol{v}_{O'}^+$ is post-impact translational velocity vector of point O', $\boldsymbol{\omega}^+$ is post-impact angular velocity vector of the

block, and $\boldsymbol{r}_{C/O'}$ is position vector of the mass center relative to point O'.

Expressions for these vector quantities are given below:

$$\boldsymbol{v}^{+} = \dot{X}^{+}\hat{\boldsymbol{i}} + \dot{Z}^{+}\hat{\boldsymbol{k}} = \left(\dot{x}_g + \dot{x}_{rot}^{+} + \dot{x}_s^{+}\right)\hat{\boldsymbol{i}} + \left(\dot{z}_{rot}^{+} + \dot{z}_g\right)\hat{\boldsymbol{k}} \tag{4.93}$$

$$\boldsymbol{v}_{O'}^{+} = \left(\dot{x}_g + \dot{x}_s^{+}\right)\hat{\boldsymbol{i}} + \left(\dot{z}_g\right)\hat{\boldsymbol{k}} \tag{4.94}$$

$$\boldsymbol{\omega}^{+} = \dot{\theta}^{+}\hat{\boldsymbol{j}} = 0\hat{\boldsymbol{j}} \tag{4.95}$$

$$\boldsymbol{r}_{C/O'} = r\sin\left(a-\theta\right)\hat{\boldsymbol{i}} + r\cos\left(a-\theta\right)\hat{\boldsymbol{k}} \tag{4.96}$$

At impact $\theta = 0$, the position vector of the mass center relative to point O' becomes

$$\boldsymbol{r}_{C/O'} = \left(r\sin a\right)\hat{\boldsymbol{i}} + \left(r\cos a\right)\hat{\boldsymbol{k}} = b\hat{\boldsymbol{i}} + h\hat{\boldsymbol{k}} \tag{4.97}$$

On substituting Equations (4.93) through (4.97) into Equation (4.92), the post-impact translational velocity becomes

$$\boldsymbol{v}^{+} \equiv \left(\dot{x}_g + \dot{x}_{rot}^{+} + \dot{x}_s^{+}\right)\hat{\boldsymbol{i}} + \left(\dot{z}_{rot}^{+} + \dot{z}_g\right)\hat{\boldsymbol{k}} = \left(\dot{x}_g + \dot{x}_s^{+}\right)\hat{\boldsymbol{i}} + \left(\dot{z}_g\right)\hat{\boldsymbol{k}} + \left(0\hat{\boldsymbol{j}}\right)\times\left(b\hat{\boldsymbol{i}} + h\hat{\boldsymbol{k}}\right) \tag{4.98}$$

which simplifies to

$$\dot{x}_{rot}^{+}\hat{\boldsymbol{i}} + \dot{z}_{rot}^{+}\hat{\boldsymbol{k}} = 0\hat{\boldsymbol{k}} + 0\hat{\boldsymbol{i}} \tag{4.99}$$

From Equation (4.98) the post-impact horizontal and vertical components of $\boldsymbol{v}^{+}$ can be retrieved as

$$\dot{x}_{rot}^{+} = 0 \tag{4.100}$$

$$\dot{z}_{rot}^{+} = 0 \tag{4.101}$$

Substituting Equations (4.90) through (4.101) into Equations (4.80) and (4.81) yields

$$\int F_x dt = m\dot{x}_s^{+} - m\left(h\dot{\theta}^{-}\right) - m\dot{x}_s^{-} \tag{4.102}$$

$$\int F_z dt = -mb\dot{\theta}^- \tag{4.103}$$

which constitutes one equation with two unknowns: $\int F_x dt$, $\dot{x}_s^+$.

One additional equation is therefore required to uniquely determine the post-impact velocity $\dot{x}_s^+$.

With regard to the block, the principle of frictional impulse in the x and z directions states that

$$\int F_x dt = -\text{sgn}\left(\dot{x}_s^+\right)\mu_k \left|\int F_z dt\right| \tag{4.104}$$

Substituting Equations (4.102) and (4.103) in Equation (4.104) gives

$$m\dot{x}_s^+ - m\left(h\dot{\theta}^-\right) - m\dot{x}_s^- = -\text{sgn}\left(\dot{x}_s^+\right)\mu_k \left|-mb\dot{\theta}^-\right| \tag{4.105}$$

Assuming that $\text{sgn}\left(\dot{x}_s^+\right) > 0$, Equation (4.105) can be rewritten as

$$\dot{x}_s^+ = -\mu_k \left|-b\dot{\theta}^-\right| + h\dot{\theta}^- + \dot{x}_s^- \tag{4.106}$$

Once Equation (4.106) is solved and $\dot{x}_s^+$ is calculated positive, then the assumption and Equation (4.106) are correct, else a second assumption must be computed, $\text{sgn}\left(\dot{x}_s^+\right) < 0$ and Equation (4.105) can be rewritten as

$$\dot{x}_s^+ = \mu_k \left|-b\dot{\theta}^-\right| + h\dot{\theta}^- + \dot{x}_s^- \tag{4.107}$$

The absolute value in Equations (4.106) and (4.107) can be dropped since the impulse in the z direction must be positive.

Derivation for the case of impact during rocking about point O'

Consider the system at the instant when the block hits the moving base from rocking about O' .

With regard to the block, the principle of linear impulse and momentum in the x and z

direction states that

$$\int F_x dt = \left(\Delta L\right)_x = L_x^+ - L_x^- : \quad \int F_x dt = m\dot{X}^+ - m\dot{X}^- \tag{4.108}$$

$$\int F_z dt = \left(\Delta L\right)_z = L_z^+ - L_z^- : \quad \int F_z dt = m\dot{Z}^+ - m\dot{Z}^- \tag{4.109}$$

in which $\int F_x dt$ and $\int F_z dt$ are the horizontal and vertical impulses (assumed to act at O'); $\dot{X}^- = \dot{x}_g + \dot{x}_s^- + \dot{x}_{rot}^-$, $\dot{X}^+ = \dot{x}_g + \dot{x}_s^+ + \dot{x}_{rot}^+$ and $\dot{Z}^- = \left(\dot{z}_{rot}^- + \dot{z}_g\right)$, $\dot{Z}^+ = \left(\dot{z}_{rot}^+ + \dot{z}_g\right)$ are the absolute pre- and post-impact horizontal and vertical velocities of the mass center of the block, respectively; $\dot{x}_{rot}^-$, $\dot{x}_{rot}^+$ and $\dot{z}_{rot}^-$, $\dot{z}_{rot}^+$ are the relative pre- and post-impact horizontal and vertical velocities of the mass center of the block due to the rocking, relative to the foundation; $\dot{x}_s^-$ and $\dot{x}_s^+$ are the relative pre- and post-impact horizontal velocities of the mass center of the block due to the sliding, relative to the foundation; L_x^-, L_x^+, L_z^- and L_z^+ are the pre- and post-impact horizontal and vertical linear momentum, respectively; $\left(\Delta L\right)_x$ and $\left(\Delta L\right)_z$ are the changes in horizontal and vertical linear momentum, respectively.

Substituting these expressions into Equations (4.108) and (4.109), we obtain

$$\int F_x dt = m\dot{x}_s^+ + m\dot{x}_{rot}^+ - m\dot{x}_s^- - m\dot{x}_{rot}^- \tag{4.110}$$

$$\int F_z dt = m\dot{z}_{rot}^+ - m\dot{z}_{rot}^- \tag{4.111}$$

In Equations (4.110) and (4.111), the pre- and post-impact horizontal components of the relative translational velocity of the mass center can be expressed in terms of the pre-impact angular velocity of the block, $\dot{\theta}^-$ as follows.

For the pre-impact state, the translational velocity vector of the mass center can be expressed as

$$\boldsymbol{v}^- = \boldsymbol{v}_{O'}^- + \boldsymbol{\omega}^- \times \boldsymbol{r}_{C/O'} \tag{4.112}$$

where $\boldsymbol{v}^-$ is pre-impact translational velocity vector of center-of-mass, $\boldsymbol{v}_{O'}^-$ is pre-impact translational velocity of point O', $\boldsymbol{\omega}^-$ is pre-impact angular velocity of the block, and $\boldsymbol{r}_{C/O'}$ is position vector of center-of-mass relative to point O'.

Expressions for these vector quantities are given below:

$$\boldsymbol{v}^- = \dot{X}^-\hat{\boldsymbol{i}} + \dot{Z}^-\hat{\boldsymbol{k}} = \left(\dot{x}_g + \dot{x}_{rot}^- + \dot{x}_s^-\right)\hat{\boldsymbol{i}} + \left(\dot{z}_{rot}^- + \dot{z}_g\right)\hat{\boldsymbol{k}} \tag{4.113}$$

$$\boldsymbol{v}_{O'}^- = \left(\dot{x}_g + \dot{x}_s^-\right)\hat{\boldsymbol{i}} + \left(\dot{z}_g\right)\hat{\boldsymbol{k}} \tag{4.114}$$

$$\boldsymbol{\omega}^- = \dot{\theta}^-\hat{\boldsymbol{j}} \tag{4.115}$$

$$\boldsymbol{r}_{C/O'} = r\sin\left(a-\theta\right)\hat{\boldsymbol{i}} + r\cos\left(a-\theta\right)\hat{\boldsymbol{k}} \tag{4.116}$$

At impact, the angular velocity of the block becomes zero $\left(\theta = 0\right)$ and the position vector of the mass center relative to point O' can be rewritten as

$$\boldsymbol{r}_{C/O'} = \left(r\sin a\right)\hat{\boldsymbol{i}} + \left(r\cos a\right)\hat{\boldsymbol{k}} = b\hat{\boldsymbol{i}} + h\hat{\boldsymbol{k}} \tag{4.117}$$

On substituting Equations (4.113) through (4.117) into Equation (4.112), the pre-impact translational velocity therefore becomes

$$\boldsymbol{v}^- \equiv \left(\dot{x}_g + \dot{x}_{rot}^- + \dot{x}_s^-\right)\hat{\boldsymbol{i}} + \left(\dot{z}_{rot}^- + \dot{z}_g\right)\hat{\boldsymbol{k}} = \left(\dot{x}_g + \dot{x}_s^-\right)\hat{\boldsymbol{i}} + \left(\dot{z}_g\right)\hat{\boldsymbol{k}} + \left(\dot{\theta}^-\hat{\boldsymbol{j}}\right)\times\left(b\hat{\boldsymbol{i}} + h\hat{\boldsymbol{k}}\right) \tag{4.118}$$

which reduces to

$$\dot{x}_{rot}^-\hat{\boldsymbol{i}} + \dot{z}_{rot}^-\hat{\boldsymbol{k}} = \left(-b\dot{\theta}^-\right)\hat{\boldsymbol{k}} + \left(h\dot{\theta}^-\right)\hat{\boldsymbol{i}} \tag{4.119}$$

from which the pre-impact horizontal and vertical components of $\boldsymbol{v}^-$ can be retrieved as

$$\dot{x}_{rot}^- = h\dot{\theta}^- \tag{4.120}$$

$$\dot{z}_{rot}^- = -b\dot{\theta}^- \tag{4.121}$$

For the post-impact state, the translational velocity vector of the mass center can be expressed as

$$\boldsymbol{v}^{+} = \boldsymbol{v}_{O}^{+} + \boldsymbol{\omega}^{+} \times \boldsymbol{r}_{C/O} \tag{4.122}$$

where $\boldsymbol{v}^{+}$ is post-impact translational velocity vector of center-of-mass, $\boldsymbol{v}_{O}^{+}$ is post-impact translational velocity vector of point O, $\boldsymbol{\omega}^{+}$ is post-impact angular velocity vector of the block, and $\boldsymbol{r}_{C/O}$ is position vector of the mass center relative to point O.

Expressions for these vector quantities are given below:

$$\boldsymbol{v}^{+} = \dot{X}^{+}\hat{\boldsymbol{i}} + \dot{Z}^{+}\hat{\boldsymbol{k}} = \left(\dot{x}_g + \dot{x}_{rot}^{+} + \dot{x}_s^{+}\right)\hat{\boldsymbol{i}} + \left(\dot{z}_{rot}^{+} + \dot{z}_g\right)\hat{\boldsymbol{k}} \tag{4.123}$$

$$\boldsymbol{v}_{O}^{+} = \left(\dot{x}_g + \dot{x}_s^{+}\right)\hat{\boldsymbol{i}} + \left(\dot{z}_g\right)\hat{\boldsymbol{k}} \tag{4.124}$$

$$\boldsymbol{\omega}^{+} = \dot{\theta}^{+}\hat{\boldsymbol{j}} = 0\hat{\boldsymbol{j}} \tag{4.125}$$

$$\boldsymbol{r}_{C/O} = -r\sin\left(a-\theta\right)\hat{\boldsymbol{i}} + r\cos\left(a-\theta\right)\hat{\boldsymbol{k}} \tag{4.126}$$

At impact $\theta = 0$, the position vector of the mass center relative to point O becomes

$$\boldsymbol{r}_{C/O} = -\left(r\sin a\right)\hat{\boldsymbol{i}} + \left(r\cos a\right)\hat{\boldsymbol{k}} = -b\hat{\boldsymbol{i}} + h\hat{\boldsymbol{k}} \tag{4.127}$$

On substituting Equations (4.123) through (4.127) into Equation(4.122), the post-impact translational velocity therefore becomes

$$\boldsymbol{v}^{+} \equiv \left(\dot{x}_g + \dot{x}_{rot}^{+} + \dot{x}_s^{+}\right)\hat{\boldsymbol{i}} + \left(\dot{z}_{rot}^{+} + \dot{z}_g\right)\hat{\boldsymbol{k}} = \left(\dot{x}_g + \dot{x}_s^{+}\right)\hat{\boldsymbol{i}} + \left(\dot{z}_g\right)\hat{\boldsymbol{k}} + \left(0\hat{\boldsymbol{j}}\right)\times\left(-b\hat{\boldsymbol{i}} + h\hat{\boldsymbol{k}}\right) \tag{4.128}$$

which simplifies to

$$\dot{x}_{rot}^{+}\hat{\boldsymbol{i}} + \dot{z}_{rot}^{+}\hat{\boldsymbol{k}} = 0\hat{\boldsymbol{k}} + 0\hat{\boldsymbol{i}} \tag{4.129}$$

from which the post-impact horizontal and vertical components of $\boldsymbol{v}^{+}$ can be retrieved as

$$\dot{x}_{rot}^{+} = 0 \tag{4.130}$$

$$\dot{z}_{rot}^{+} = 0 \tag{4.131}$$

Substitution of Equations (4.120) through (4.131) into Equations (4.110) and (4.111) yields

$$\int F_x dt = m\dot{x}_s^{+} - m\left(h\dot{\theta}^{-}\right) - m\dot{x}_s^{-} \tag{4.132}$$

$$\int F_z dt = mb\dot{\theta}^{-} \tag{4.133}$$

which constitutes one equation with two unknowns: $\int F_x dt$, $\dot{x}_s^{+}$.

One additional equation is therefore required to uniquely determine the post-impact velocity $\dot{x}_s^{+}$.

With regard to the block, the principle of frictional impulse in the x and z directions states that

$$\int F_x dt = -\operatorname{sgn}\left(\dot{x}_s^{+}\right)\mu_k \left|\int F_z dt\right| \tag{4.134}$$

Substituting Equations (4.132) and (4.133) in Equation (4.134) gives

$$m\dot{x}_s^{+} - m\left(h\dot{\theta}^{-}\right) - m\dot{x}_s^{-} = -\operatorname{sgn}\left(\dot{x}_s^{+}\right)\mu_k \left|mb\dot{\theta}^{-}\right| \tag{4.135}$$

Assuming that $\operatorname{sgn}\left(\dot{x}_s^{+}\right) > 0$, Equation (4.135) can be rewritten as

$$\dot{x}_s^{+} = -\mu_k \left|b\dot{\theta}^{-}\right| + h\dot{\theta}^{-} + \dot{x}_s^{-} \tag{4.136}$$

Once Equation (4.136) is solved and $\dot{x}_s^{+}$ is calculated positive, then the assumption and Equation (4.136) are correct, else a second assumption must be computed, $\operatorname{sgn}\left(\dot{x}_s^{+}\right) < 0$ and Equation (4.135) can be rewritten as

$$\dot{x}_s^{+} = \mu_k \left|b\dot{\theta}^{-}\right| + h\dot{\theta}^{-} + \dot{x}_s^{-} \tag{4.137}$$

The absolute value in Equations (4.136) and (4.137) can be dropped since the impulse in the z direction must be positive.

4.4.2.3 Slide-rocking continues after impact

In this case, the system continues slide-rocking regime after impact and the impact analysis is reduced to the computation of the initial conditions for the post-impact motion, $\dot{x}_s^+$, and $\dot{\theta}^+$, given the position and the pre-impact velocities, $\dot{x}_s^-$, and $\dot{\theta}^-$.

Derivation for the case of impact during rocking about point O

Consider the system at the instant when the block hits the moving base from rocking about O.

With regard to the block, the principle of linear impulse and momentum in the x and z direction states that

$$\int F_x dt = \left(\Delta L\right)_x = L_x^+ - L_x^- : \quad \int F_x dt = m\dot{X}^+ - m\dot{X}^- \tag{4.138}$$

$$\int F_z dt = \left(\Delta L\right)_z = L_z^+ - L_z^- : \quad \int F_z dt = m\dot{Z}^+ - m\dot{Z}^- \tag{4.139}$$

in which $\int F_x dt$ and $\int F_z dt$ are the horizontal and vertical impulses (assumed to act at O'); $\dot{X}^- = \dot{x}_g + \dot{x}_s^- + \dot{x}_{rot}^-$, $\dot{X}^+ = \dot{x}_g + \dot{x}_s^+ + \dot{x}_{rot}^+$ and $\dot{Z}^- = \left(\dot{z}_{rot}^- + \dot{z}_g\right)$, $\dot{Z}^+ = \left(\dot{z}_{rot}^+ + \dot{z}_g\right)$ are the absolute pre- and post-impact horizontal and vertical velocities of the mass center of the block, respectively; $\dot{x}_{rot}^-$, $\dot{x}_{rot}^+$ and $\dot{z}_{rot}^-$, $\dot{z}_{rot}^+$ are the relative pre- and post-impact horizontal and vertical velocities of the mass center of the block due to the rocking, relative to the foundation; $\dot{x}_s^-$ and $\dot{x}_s^+$ are the relative pre- and post-impact horizontal velocities of the mass center of the block due to the sliding, relative to the foundation; L_x^-, L_x^+, L_z^- and L_z^+ are the pre- and post-impact horizontal and vertical linear momentum, respectively; $\left(\Delta L\right)_x$ and $\left(\Delta L\right)_z$ are the changes in horizontal and vertical linear momentum, respectively.

Substituting these expressions into Equations (4.138) and (4.139), we obtain

$$\int F_x dt = m\dot{x}_s^+ + m\dot{x}_{rot}^+ - m\dot{x}_s^- - m\dot{x}_{rot}^- \tag{4.140}$$

$$\int F_z dt = m\dot{z}_{rot}^{+} - m\dot{z}_{rot}^{-} \tag{4.141}$$

In addition, the principle of angular impulse and momentum states that

$$\int M_C dt = \Delta H_C = H_C^{+} - H_C^{-}: \;\; b\left(\int F_z dt\right) - h\left(\int F_x dt\right) = I\dot{\theta}^{+} - I\dot{\theta}^{-} \tag{4.142}$$

in which $\int M_C dt$ is the angular impulse; H_C^{-} and H_C^{+} are the pre- and post-impact angular momentum about the mass center, respectively; ΔH_C is the change in the angular momentum about the mass center.

In Equations (4.140) and (4.141), the pre- and post-impact horizontal and vertical components of the relative translational velocity of the mass center can be expressed in terms of the pre- and post-impact angular velocity of the block, $\dot{\theta}^{-}$ and $\dot{\theta}^{+}$ as follows.

For the pre-impact state, the translational velocity vector of the mass center (Figure 4-8) can be expressed as

$$\boldsymbol{v}^{-} = \boldsymbol{v}_O^{-} + \boldsymbol{\omega}^{-} \times \boldsymbol{r}_{C/O} \tag{4.143}$$

where $\boldsymbol{v}^{-}$ is pre-impact translational velocity vector of center-of-mass, $\boldsymbol{v}_O^{-}$ is pre-impact translational velocity vector of point O, $\boldsymbol{\omega}^{-}$ is pre-impact angular velocity vector of the block, and $\boldsymbol{r}_{C/O}$ is position vector of mass center relative to point O.

Expressions for these vector quantities are given below:

$$\boldsymbol{v}^{-} = \dot{X}^{-}\hat{\boldsymbol{i}} + \dot{Z}^{-}\hat{\boldsymbol{k}} = \left(\dot{x}_g + \dot{x}_s^{-} + \dot{x}_{rot}^{-}\right)\hat{\boldsymbol{i}} + \left(\dot{z}_{rot}^{-} + \dot{z}_g\right)\hat{\boldsymbol{k}} \tag{4.144}$$

$$\boldsymbol{v}_O^{-} = \left(\dot{x}_g + \dot{x}_s^{-}\right)\hat{\boldsymbol{i}} + \left(\dot{z}_g\right)\hat{\boldsymbol{k}} \tag{4.145}$$

$$\boldsymbol{\omega}^{-} = \dot{\theta}^{-}\hat{\boldsymbol{j}} \tag{4.146}$$

$$\boldsymbol{r}_{C/O} = -r\sin\left(a-\theta\right)\hat{\boldsymbol{i}} + r\cos\left(a-\theta\right)\hat{\boldsymbol{k}} \tag{4.147}$$

At impact, the angular rotation of the block becomes zero $\left(\theta = 0\right)$ and the position vector of

mass center relative to point O, $\boldsymbol{r}_{C/O}$, can be rewritten as

$$\boldsymbol{r}_{C/O} = -\left(r\sin a\right)\hat{\boldsymbol{i}} + \left(r\cos a\right)\hat{\boldsymbol{k}} = -b\hat{\boldsymbol{i}} + h\hat{\boldsymbol{k}} \tag{4.148}$$

in which $\hat{\boldsymbol{i}}$ and $\hat{\boldsymbol{k}}$ are the horizontal and vertical unit vectors respectively.

On substituting Equations (4.144) through (4.148) into Equation (4.143), the pre-impact translational velocity therefore becomes

$$\boldsymbol{v}^{-} \equiv \left(\dot{x}_g + \dot{x}_s^{-} + \dot{x}_{rot}^{-}\right)\hat{\boldsymbol{i}} + \left(\dot{z}_{rot}^{-} + \dot{z}_g\right)\hat{\boldsymbol{k}} = \left(\dot{x}_g + \dot{x}_s^{-}\right)\hat{\boldsymbol{i}} + \left(\dot{z}_g\right)\hat{\boldsymbol{k}} + \left(\dot{\theta}^{-}\hat{\boldsymbol{j}}\right)\times\left(-b\hat{\boldsymbol{i}} + h\hat{\boldsymbol{k}}\right) \tag{4.149}$$

which reduces to

$$\dot{x}_{rot}^{-}\hat{\boldsymbol{i}} + \dot{z}_{rot}^{-}\hat{\boldsymbol{k}} = \left(b\dot{\theta}^{-}\right)\hat{\boldsymbol{k}} + \left(h\dot{\theta}^{-}\right)\hat{\boldsymbol{i}} \tag{4.150}$$

from which the pre-impact horizontal and vertical components of $\boldsymbol{v}^{-}$ can be retrieved as

$$\dot{x}_{rot}^{-} = h\dot{\theta}^{-} \tag{4.151}$$

$$\dot{z}_{rot}^{-} = b\dot{\theta}^{-} \tag{4.152}$$

For the post-impact state, the translational velocity vector of the mass center (Figure 4-10) can be expressed as

$$\boldsymbol{v}^{+} = \boldsymbol{v}_{O'}^{+} + \boldsymbol{\omega}^{+}\times\boldsymbol{r}_{C/O'} \tag{4.153}$$

where $\boldsymbol{v}^{+}$ is post-impact translational velocity vector of center-of-mass, $\boldsymbol{v}_{O'}^{+}$ is post-impact translational velocity vector of point O', $\boldsymbol{\omega}^{+}$ is post-impact angular velocity vector of the block, and $\boldsymbol{r}_{C/O'}$ is position vector of the mass center relative to point O'.

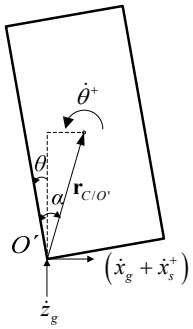

Figure 4-10: Components of post-impact translational velocity of the non-isolated block for the case of impact during slide-rocking about point *O'*.

Expressions for these vector quantities are given below:

$$\boldsymbol{v}^+ = \dot{X}^+\hat{\boldsymbol{i}} + \dot{Z}^+\hat{\boldsymbol{k}} = \left(\dot{x}_g + \dot{x}_s^+ + \dot{x}_{rot}^+\right)\hat{\boldsymbol{i}} + \left(\dot{z}_{rot}^+ + \dot{z}_g\right)\hat{\boldsymbol{k}} \tag{4.154}$$

$$\boldsymbol{v}_{O'}^+ = \left(\dot{x}_g + \dot{x}_s^+\right)\hat{\boldsymbol{i}} + \left(\dot{z}_g\right)\hat{\boldsymbol{k}} \tag{4.155}$$

$$\boldsymbol{\omega}^+ = \dot{\theta}^+\hat{\boldsymbol{j}} \tag{4.156}$$

$$\boldsymbol{r}_{C/O'} = r\sin\left(a-\theta\right)\hat{\boldsymbol{i}} + r\cos\left(a-\theta\right)\hat{\boldsymbol{k}} \tag{4.157}$$

At impact $\left(\theta = 0\right)$ the position vector of mass center relative to point O', $\boldsymbol{r}_{C/O'}$, becomes

$$\boldsymbol{r}_{C/O'} = \left(r\sin a\right)\hat{\boldsymbol{i}} + \left(r\cos a\right)\hat{\boldsymbol{k}} = b\hat{\boldsymbol{i}} + h\hat{\boldsymbol{k}} \tag{4.158}$$

On substituting Equations (4.154) through (4.158) into Equation (4.153), the post-impact translational velocity therefore becomes

$$\boldsymbol{v}^+ \equiv \left(\dot{x}_g + \dot{x}_{rot}^+ + \dot{x}_s^+\right)\hat{\boldsymbol{i}} + \left(\dot{z}_{rot}^+ + \dot{z}_g\right)\hat{\boldsymbol{k}} = \left(\dot{x}_g + \dot{x}_s^+\right)\hat{\boldsymbol{i}} + \left(\dot{z}_g\right)\hat{\boldsymbol{k}} + \left(\dot{\theta}^+\hat{\boldsymbol{j}}\right)\times\left(b\hat{\boldsymbol{i}} + h\hat{\boldsymbol{k}}\right) \tag{4.159}$$

which reduces to

$$\dot{x}_{rot}^+\hat{\boldsymbol{i}} + \dot{z}_{rot}^+\hat{\boldsymbol{k}} = \left(-b\dot{\theta}^+\right)\hat{\boldsymbol{k}} + \left(h\dot{\theta}^+\right)\hat{\boldsymbol{i}} \tag{4.160}$$

from which the post-impact horizontal and vertical components of $\boldsymbol{v}^+$ can be retrieved as

$$\dot{x}_{rot}^+ = h\dot{\theta}^+ \tag{4.161}$$

$$\dot{z}_{rot}^+ = -b\dot{\theta}^+ \tag{4.162}$$

Substituting Equations (4.151) through (4.162) into Equations (4.140) through (4.142) yields

$$\int F_x dt = m\left(h\dot{\theta}^+\right) + m\dot{x}_s^+ - m\dot{x}_s^- - m\left(h\dot{\theta}^-\right) \tag{4.163}$$

$$\int F_z dt = m\left(-b\dot{\theta}^+\right) - m\left(b\dot{\theta}^-\right) \tag{4.164}$$

$$b\left(\int F_z dt\right) - h\left(\int F_x dt\right) = I\left(\dot{\theta}^+\right) - I\left(\dot{\theta}^-\right) \tag{4.165}$$

in which the centroid mass moment of inertia for the rectangular block is given by

$$I = \frac{m}{3}r^2 = \frac{m}{3}\left(b^2 + h^2\right) \tag{4.166}$$

Equations (4.163), (4.164) and (4.165) constitute a set of three equations with four unknowns, namely $\int F_x dt$, $\int F_z dt$, $\dot{\theta}^+$, $\dot{x}_s^+$.

Equivalently, the three Equations (4.163), (4.164) and (4.165) can be combined in one (by eliminating the two impulses) with two unknowns:

$$\left(4b^2 + 4h^2\right)\dot{\theta}^+ + 3h\dot{x}_s^+ = \left(4h^2 - 2b^2\right)\dot{\theta}^- + 3h\dot{x}_s^- \tag{4.167}$$

which upon rearranging terms becomes

$$\dot{\theta}^+ = \frac{\left(4h^2 - 2b^2\right)\dot{\theta}^- + 3h\dot{x}_s^- - 3h\dot{x}_s^+}{\left(4b^2 + 4h^2\right)} \tag{4.168}$$

One additional equation is therefore required to uniquely determine the post-impact velocity $\dot{x}_s^+$.

With regard to the block, the principle of frictional impulse in the x and z direction states that

$$\int F_x dt = -\text{sgn}\left(\dot{x}_s^+\right)\mu_k \left|\int F_z dt\right| \tag{4.169}$$

Substituting Equations (4.163) and (4.164) in Equation (4.169) gives

$$m\left(h\dot{\theta}^+\right) + m\dot{x}_s^+ - m\dot{x}_s^- - m\left(h\dot{\theta}^-\right) = -\text{sgn}\left(\dot{x}_s^+\right)\mu_k \left|m\left(-b\dot{\theta}^+\right) - m\left(b\dot{\theta}^-\right)\right| \tag{4.170}$$

Assuming that $\text{sgn}\left(\dot{x}_s^+\right) > 0$, Equation (4.170) can be rewritten as

$$\dot{x}_s^+ = -\mu_k \left|\left(-b\dot{\theta}^+\right) - \left(b\dot{\theta}^-\right)\right| - h\dot{\theta}^+ + \dot{x}_s^- + h\dot{\theta}^- \tag{4.171}$$

Once Equation (4.171) is solved and $\dot{x}_s^+$ is calculated positive, then the assumption and Equation (4.171) are correct, else a second assumption must be computed, $\text{sgn}\left(\dot{x}_s^+\right) < 0$ and Equation (4.170) can be rewritten as

$$\dot{x}_s^+ = \mu_k \left|\left(-b\dot{\theta}^+\right) - \left(b\dot{\theta}^-\right)\right| - h\dot{\theta}^+ + \dot{x}_s^- + h\dot{\theta}^- \tag{4.172}$$

The absolute value in Equations (4.171) and (4.172) can be dropped since the impulse in the z direction must be positive.

Derivation for the case of impact during rocking about point O'

Consider the system at the instant when the block hits the moving base from rocking about O'.

With regard to the block, the principle of linear impulse and momentum in the x and z directions states that

$$\int F_x dt = \left(\Delta L\right)_x = L_x^+ - L_x^- : \quad \int F_x dt = m\dot{X}^+ - m\dot{X}^- \tag{4.173}$$

$$\int F_z dt = \left(\Delta L\right)_z = L_z^+ - L_z^- : \quad \int F_z dt = m\dot{Z}^+ - m\dot{Z}^- \tag{4.174}$$

in which $\int F_x dt$ and $\int F_z dt$ are the horizontal and vertical impulses (assumed to act at O'); $\dot{X}^- = \dot{x}_g + \dot{x}_s^- + \dot{x}_{rot}^-$, $\dot{X}^+ = \dot{x}_g + \dot{x}_s^+ + \dot{x}_{rot}^+$ and $\dot{Z}^- = \left(\dot{z}_{rot}^- + \dot{z}_g\right)$, $\dot{Z}^+ = \left(\dot{z}_{rot}^+ + \dot{z}_g\right)$ are the absolute pre- and post-impact horizontal and vertical velocities of the mass center of the block, respectively; $\dot{x}_{rot}^-$, $\dot{x}_{rot}^+$ and $\dot{z}_{rot}^-$, $\dot{z}_{rot}^+$ are the relative pre- and post-impact horizontal and vertical velocities of the mass center of the block due to the rocking, relative to the foundation; $\dot{x}_s^-$ and $\dot{x}_s^+$ are the relative pre- and post-impact horizontal velocities of the mass center of the block due to the sliding, relative to the foundation; L_x^-, L_x^+, L_z^- and L_z^+ are the pre- and post-impact horizontal and vertical linear momentum, respectively; $\left(\Delta L\right)_x$ and $\left(\Delta L\right)_z$ are the changes in horizontal and vertical linear momentum, respectively.

Substituting these expressions into Equations (4.173) and (4.174), we obtain

$$\int F_x dt = m\dot{x}_s^+ + m\dot{x}_{rot}^+ - m\dot{x}_s^- - m\dot{x}_{rot}^- \tag{4.175}$$

$$\int F_z dt = m\dot{z}_{rot}^+ - m\dot{z}_{rot}^- \tag{4.176}$$

In addition, the principle of angular impulse and momentum states that

$$\int M_C dt = \Delta H_C = H_C^+ - H_C^- : \quad -b\left(\int F_z dt\right) - h\left(\int F_x dt\right) = I\dot{\theta}^+ - I\dot{\theta}^- \tag{4.177}$$

in which $\int M_C dt$ is the angular impulse; H_C^- and H_C^+ are the pre- and post-impact angular momentum about the mass center, respectively; ΔH_C is the change in the angular momentum about the mass center.

In Equations (4.175) and (4.176), the pre- and post-impact horizontal and vertical components of the relative translational velocity of the mass center can be expressed in terms of the pre- and post-impact angular velocity of the block, $\dot{\theta}^-$ and $\dot{\theta}^+$ as follows.

For the pre-impact state, the translational velocity vector of the mass center can be expressed as

$$\boldsymbol{v}^- = \boldsymbol{v}_{O'}^- + \boldsymbol{\omega}^- \times \boldsymbol{r}_{C/O'} \tag{4.178}$$

where $\boldsymbol{v}^-$ is pre-impact translational velocity vector of center-of-mass, $\boldsymbol{v}_{O'}^-$ is pre-impact translational velocity vector of point O', $\boldsymbol{\omega}^-$ is pre-impact angular velocity vector of the block, and $\boldsymbol{r}_{C/O'}$ is position vector of the mass center relative to point O'.

Expressions for these vector quantities are given below:

$$\boldsymbol{v}^- = \dot{X}^-\hat{\boldsymbol{i}} + \dot{Z}^-\hat{\boldsymbol{k}} = \left(\dot{x}_g + \dot{x}_s^- + \dot{x}_{rot}^-\right)\hat{\boldsymbol{i}} + \left(\dot{z}_{rot}^- + \dot{z}_g\right)\hat{\boldsymbol{k}} \tag{4.179}$$

$$\boldsymbol{v}_{O'}^- = \left(\dot{x}_g + \dot{x}_s^-\right)\hat{\boldsymbol{i}} + \left(\dot{z}_g\right)\hat{\boldsymbol{k}} \tag{4.180}$$

$$\boldsymbol{\omega}^- = \dot{\theta}^-\hat{\boldsymbol{j}} \tag{4.181}$$

$$\boldsymbol{r}_{C/O'} = r\sin\left(a-\theta\right)\hat{\boldsymbol{i}} + r\cos\left(a-\theta\right)\hat{\boldsymbol{k}} \tag{4.182}$$

At impact, the angular rotation of the block becomes zero $\left(\theta = 0\right)$ and the position vector of the mass center relative to point O', $\boldsymbol{r}_{C/O'}$, can be rewritten as

$$\boldsymbol{r}_{C/O'} = \left(r\sin a\right)\hat{\boldsymbol{i}} + \left(r\cos a\right)\hat{\boldsymbol{k}} = b\hat{\boldsymbol{i}} + h\hat{\boldsymbol{k}} \tag{4.183}$$

in which $\hat{\boldsymbol{i}}$ and $\hat{\boldsymbol{k}}$ are the horizontal and vertical unit vectors respectively.

On substituting Equations (4.179) through (4.183) into Equation (4.178), the pre-impact translational velocity therefore becomes

$$\boldsymbol{v}^- \equiv \left(\dot{x}_g + \dot{x}_s^- + \dot{x}_{rot}^-\right)\hat{\boldsymbol{i}} + \left(\dot{z}_{rot}^- + \dot{z}_g\right)\hat{\boldsymbol{k}} = \left(\dot{x}_g + \dot{x}_s^-\right)\hat{\boldsymbol{i}} + \left(\dot{z}_g\right)\hat{\boldsymbol{k}} + \left(\dot{\theta}^-\hat{\boldsymbol{j}}\right)\times\left(b\hat{\boldsymbol{i}} + h\hat{\boldsymbol{k}}\right) \tag{4.184}$$

which reduces to

$$\dot{x}_{rot}^-\hat{\boldsymbol{i}} + \dot{z}_{rot}^-\hat{\boldsymbol{k}} = \left(-b\dot{\theta}^-\right)\hat{\boldsymbol{k}} + \left(h\dot{\theta}^-\right)\hat{\boldsymbol{i}} \tag{4.185}$$

from which the pre-impact horizontal and vertical components of $\boldsymbol{v}^-$ can be retrieved as

$$\dot{x}_{rot}^- = h\dot{\theta}^- \tag{4.186}$$

$$\dot{z}_{rot}^{-} = -b\dot{\theta}^{-} \tag{4.187}$$

For the post-impact state, the translational velocity vector of the mass center can be expressed as

$$\boldsymbol{v}^{+} = \boldsymbol{v}_{O}^{+} + \boldsymbol{\omega}^{+} \times \boldsymbol{r}_{C/O} \tag{4.188}$$

where $\boldsymbol{v}^{+}$ is post-impact translational velocity vector of center-of-mass, $\boldsymbol{v}_{O}^{+}$ is post-impact translational velocity vector of point O, $\boldsymbol{\omega}^{+}$ is post-impact angular velocity vector of the block, and $\boldsymbol{r}_{C/O}$ is position vector of the mass center relative to point O.

Expressions for these vector quantities are given below:

$$\boldsymbol{v}^{+} = \dot{X}^{+}\hat{\boldsymbol{i}} + \dot{Z}^{+}\hat{\boldsymbol{k}} = \left(\dot{x}_g + \dot{x}_s^{+} + \dot{x}_{rot}^{+}\right)\hat{\boldsymbol{i}} + \left(\dot{z}_{rot}^{+} + \dot{z}_g\right)\hat{\boldsymbol{k}} \tag{4.189}$$

$$\boldsymbol{v}_{O}^{+} = \left(\dot{x}_g + \dot{x}_s^{+}\right)\hat{\boldsymbol{i}} + \left(\dot{z}_g\right)\hat{\boldsymbol{k}} \tag{4.190}$$

$$\boldsymbol{\omega}^{+} = \dot{\theta}^{+}\hat{\boldsymbol{j}} \tag{4.191}$$

$$\boldsymbol{r}_{C/O} = -r\sin\left(a-\theta\right)\hat{\boldsymbol{i}} + r\cos\left(a-\theta\right)\hat{\boldsymbol{k}} \tag{4.192}$$

At impact $\left(\theta = 0\right)$ the position vector of the mass center relative to point O, $\boldsymbol{r}_{C/O}$, becomes

$$\boldsymbol{r}_{C/O} = -\left(r\sin a\right)\hat{\boldsymbol{i}} + \left(r\cos a\right)\hat{\boldsymbol{k}} = -b\hat{\boldsymbol{i}} + h\hat{\boldsymbol{k}} \tag{4.193}$$

On substituting Equations (4.189) through (4.193) into Equation(4.188), the post-impact translational velocity therefore becomes

$$\boldsymbol{v}^{+} \equiv \left(\dot{x}_g + \dot{x}_{rot}^{+} + \dot{x}_s^{+}\right)\hat{\boldsymbol{i}} + \left(\dot{z}_{rot}^{+} + \dot{z}_g\right)\hat{\boldsymbol{k}} = \left(\dot{x}_g + \dot{x}_s^{+}\right)\hat{\boldsymbol{i}} + \left(\dot{z}_g\right)\hat{\boldsymbol{k}} + \left(\dot{\theta}^{+}\hat{\boldsymbol{j}}\right)\times\left(-b\hat{\boldsymbol{i}} + h\hat{\boldsymbol{k}}\right) \tag{4.194}$$

which simplifies to

$$\dot{x}_{rot}^{+}\hat{\boldsymbol{i}} + \dot{z}_{rot}^{+}\hat{\boldsymbol{k}} = \left(b\dot{\theta}^{+}\right)\hat{\boldsymbol{k}} + \left(h\dot{\theta}^{+}\right)\hat{\boldsymbol{i}} \tag{4.195}$$

from which the post-impact horizontal and vertical components of $\boldsymbol{v}^+$ can be retrieved as

$$\dot{x}_{rot}^+ = h\dot{\theta}^+ \tag{4.196}$$

$$\dot{z}_{rot}^+ = b\dot{\theta}^+ \tag{4.197}$$

Substituting Equations (4.186), (4.187), (4.196) and (4.197) into Equations (4.175) through (4.177) yields

$$\int F_x dt = m\left(h\dot{\theta}^+\right) + m\dot{x}_s^+ - m\dot{x}_s^- - m\left(h\dot{\theta}^-\right) \tag{4.198}$$

$$\int F_z dt = m\left(b\dot{\theta}^+\right) + m\left(b\dot{\theta}^-\right) \tag{4.199}$$

$$-b\left(\int F_z dt\right) - h\left(\int F_x dt\right) = I\left(\dot{\theta}^+\right) - I\left(\dot{\theta}^-\right) \tag{4.200}$$

in which the centroid mass moment of inertia for the rectangular block is given by

$$I = \frac{m}{3}r^2 = \frac{m}{3}\left(b^2 + h^2\right) \tag{4.201}$$

Equations (4.198), (4.199) and (4.200) constitute a set of three equations with four unknowns, namely $\int F_x dt$, $\int F_z dt$, $\dot{\theta}^+$, $\dot{x}_s^+$.

Equivalently, the three Equations (4.198), (4.199) and (4.200) can be combined in one (by eliminating the two impulses) with two unknowns:

$$\left(4b^2 + 4h^2\right)\dot{\theta}^+ + 3h\dot{x}_s^+ = \left(4h^2 - 2b^2\right)\dot{\theta}^- + 3h\dot{x}_s^- \tag{4.202}$$

which upon rearranging terms becomes

$$\dot{\theta}^+ = \frac{\left(4h^2 - 2b^2\right)\dot{\theta}^- + 3h\dot{x}_s^- - 3h\dot{x}_s^+}{\left(4b^2 + 4h^2\right)} \tag{4.203}$$

One additional equation is therefore required to uniquely determine the post-impact velocity $\dot{x}_s^+$.

With regard to the block, the principle of frictional impulse in the x and z directions states that

$$\int F_x dt = -\text{sgn}\left(\dot{x}_s^+\right)\mu_k \left|\int F_z dt\right| \tag{4.204}$$

Substituting Equations (4.198) and (4.199) in Equation (4.204) gives

$$m\left(h\dot{\theta}^+\right) + m\dot{x}_s^+ - m\dot{x}_s^- - m\left(h\dot{\theta}^-\right) = -\text{sgn}\left(\dot{x}_s^+\right)\mu_k \left|m\left(b\dot{\theta}^+\right) + m\left(b\dot{\theta}^-\right)\right| \tag{4.205}$$

Assuming that $\text{sgn}\left(\dot{x}_s^+\right) > 0$, Equation (4.205) can be rewritten as

$$\dot{x}_s^+ = -\mu_k \left|\left(b\dot{\theta}^+\right) + \left(b\dot{\theta}^-\right)\right| - h\dot{\theta}^+ + \dot{x}_s^- + h\dot{\theta}^- \tag{4.206}$$

Once Equation (4.206) is solved and $\dot{x}_s^+$ is calculated positive, then the assumption and Equation (4.206) are correct, else a second assumption must be computed, $\text{sgn}\left(\dot{x}_s^+\right) < 0$ and Equation (4.205) can be rewritten as

$$\dot{x}_s^+ = \mu_k \left|\left(b\dot{\theta}^+\right) + \left(b\dot{\theta}^-\right)\right| - h\dot{\theta}^+ + \dot{x}_s^- + h\dot{\theta}^- \tag{4.207}$$

The absolute value in Equations (4.206) and (4.207) can be dropped since the impulse in the z direction must be positive.

CHAPTER 5

Dynamic Analysis of Base Isolated Rigid Block

5.1 Introduction

This dissertation presents a comprehensive mathematical formulation on the dynamic response of base-isolated rigid blocks subjected to horizontal and vertical ground motions. The system to be analyzed consists of a free-standing rigid block supported on a seismically-isolated rigid base. The dynamic response of the system is realized through four distinct oscillation regimes: (a) pure *system translation* (T), in which the block and base remain in full contact at all time as the system oscillates horizontally, (b) *sliding* (S/T), in which the block slides relative to the supporting base, which translates horizontally, (c) *rocking* (R/T), in which the rigid block pivots on its edges as the supporting base translates horizontally and (d) *slide-rocking* (SR/T), in which the block simultaneously slides and pivots on its edges, as the supporting base translates horizontally. Two models for the isolation system are considered; a linear model with viscoelastic behavior and a nonlinear model with bilinear hysteretic behavior.

Despite the apparent geometric simplicity of the problem, the mathematical description of the system dynamics is profoundly complex, primarily due to the inherent nonlinear nature of the impact phenomenon, which may occur during *rocking* and *slide-rocking* response. A rigorous formulation of the impact problem is presented in this dissertation based on the classical impact theory. Derived from first principles, the impact model assumes point-impact and perfectly-inelastic impact (i.e. zero coefficient of restitution). Evidently, apart from the nonlinear nature of the governing equations, the dynamic behavior of the system is highly complex due to the potential transition from one oscillation regime to another following impact. Transition criteria that specify the conditions under which switching between the various oscillation regimes are derived.

5.2 Model Description

The system considered consists of a symmetric rigid block of mass m and centroid mass-moment of inertia I_C, standing free on a seismically-isolated rigid base of mass m_b (Figure 5-1a). The block of height $H = 2h$ and width $B = 2b$ is assumed to rotate about the corners O

and O'. A measure of the size of the block is given by the half-diagonal $R = \sqrt{b^2 + h^2}$ of the rectangle, while a measure of its slenderness is given by the characteristic angle $\alpha = \tan^{-1}(b/h)$ or equivalently (but inversely proportionally) by the height-to-width ratio $\lambda = h/b$.

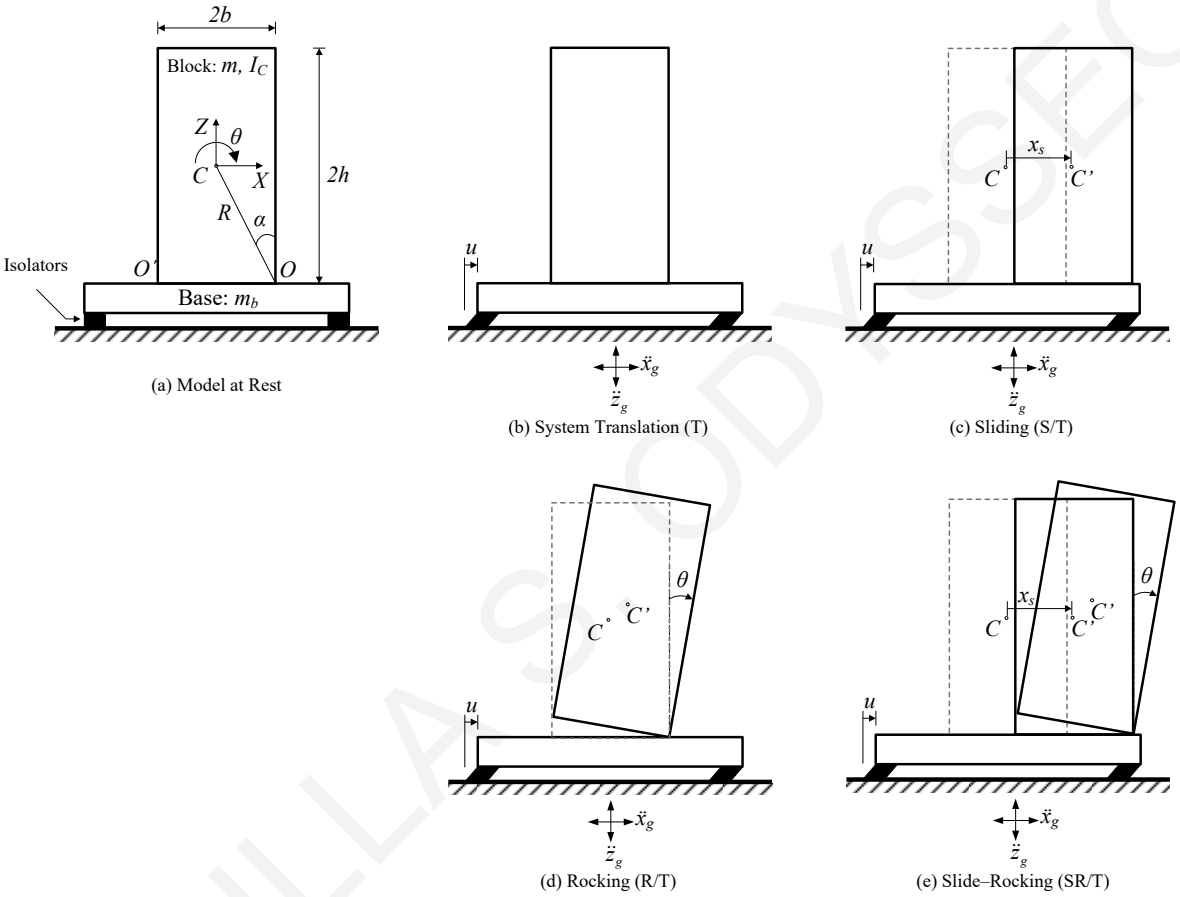

Figure 5-1: Model considered and oscillation regimes.

The dynamic response of the system is realized through four distinct oscillation regimes: (a) pure *system translation* (T), in which the block/base system in its entirety oscillates horizontally with displacement $u(t)$—1DOF response (Figure 5-1b); (b) *sliding* (S/T), in which the block slides with displacement $x_s(t)$ relative to the supporting base, which translates horizontally with $u(t)$—2DOF response (Figure 5-1c); (c) *rocking* (R/T), in which the rigid block pivots on its edges with rotation angle $\theta(t)$ as the supporting base translates horizontally with $u(t)$—2DOF response (Figure 5-1d); and (d) *slide-rocking* (SR/T), in which

the block simultaneously slides with $x_s(t)$ and pivots on its edges with $\theta(t)$, as the supporting base translates horizontally with $u(t)$—3DOF response (Figure 5-1e).

The rotation angle of the block is denoted by $\theta(t)$, positive in the clockwise direction. The horizontal displacement of the base relative to the foundation is denoted by $u(t)$, the horizontal displacement of the block relative to the base due to sliding is denoted by $x_s(t)$. The ground motion is prescribed by a horizontal acceleration, $\ddot{x}_g(t)$, and vertical acceleration, $\ddot{z}_g(t)$.

5.3 Formulation of the Equations of Motion

The governing equations for each regime of motion is formulated by means of the Lagrange method, which permits the derivation of the equations of motion from three scalar quantities; namely, the kinetic energy, the potential energy, and the virtual work due to non-conservative forces. The application of the Lagrange method for the formulation of the equations of motion is beneficial compared to the application of the Newtonian method, especially for systems composed of a number of components, as it considers the system as a whole rather than the individual components of the system separately, a process that excludes the reaction and constraint forces (Meirovitch (2001)). Lagrange's equations are derived using the extended Hamilton's principle:

$$\int_{t_1}^{t_2}\left(\delta T-\delta V+\overline{\delta W}_{nc}\right)dt=0,\quad \delta q_i=0,\quad i=1,2,3,...,n,\quad t=t_1,t_2 \tag{5.1}$$

where q_i denotes the generalized coordinate, T the kinetic energy of the system, V the potential energy of the system, and $\overline{\delta W}_{nc}$ the virtual work of the non-conservative forces.

The generalized coordinates are defined as any set of i independent quantities that are sufficient to completely specify the position of every point within an $i-\text{DOF}$ system. The kinetic energy of the system, T, can be expressed in terms of the generalized coordinates and their first derivatives. That is,

$$T=T\left(q_1,q_2,...,q_n,\dot{q}_1,\dot{q}_2,...,\dot{q}_n,t\right) \tag{5.2}$$

so that the variation in the kinetic energy is simply

$$\delta T = \sum_{i=1}^{n}\left(\frac{\partial T}{\partial q_i}\delta q_i + \frac{\partial T}{\partial \dot{q}_i}\delta \dot{q}_i\right) \tag{5.3}$$

The potential energy, V, can be expressed in terms of the generalized coordinates alone. That is,

$$V = V\left(q_1, q_2, ..., q_n, t\right) \tag{5.4}$$

so that the variation in the potential energy is

$$\delta V = \sum_{i=1}^{n}\frac{\partial V}{\partial q_i}\delta q_i \tag{5.5}$$

The virtual work of non-conservative forces, as they act through virtual displacements caused by arbitrary variations in the generalized coordinates, is given by

$$\overline{\delta W}_{nc} = \sum_{i=1}^{n} Q_i \delta q_i \tag{5.6}$$

where $Q_1, Q_2, ..., Q_n$ are the generalized forces. The symbol δ denotes the virtual character of the instantaneous variations, as opposed to the symbol d, which denotes actual differentials of position coordinates taking place in the time interval dt, during which time interval forces can change.

Substituting Equations (5.3), (5.5) and (5.6) into the extended Hamilton's principle yields

$$\begin{gathered}\int_{t_1}^{t_2}\left(\delta T - \delta V + \overline{\delta W}_{nc}\right)dt = \int_{t_1}^{t_2}\sum_{i=1}^{n}\left[\left(\frac{\partial T}{\partial q_i} - \frac{\partial V}{\partial q_i} + Q_i\right)\delta q_i + \frac{\partial T}{\partial \dot{q}_i}\delta \dot{q}_i\right]dt = 0, \\ \delta q_i = 0, \quad i = 1, 2, 3, ..., n, \quad t = t_1, t_2\end{gathered} \tag{5.7}$$

Then, the integration of the last term is given by

$$\int_{t_1}^{t_2}\frac{\partial T}{\partial \dot{q}_i}\delta\dot{q}_i dt=\int_{t_1}^{t_2}\frac{\partial T}{\partial \dot{q}_i}\frac{d}{dt}\delta q_i dt=\frac{\partial T}{\partial \dot{q}_i}\delta q_i\Big|_{t_1}^{t_2}-\int_{t_1}^{t_2}\frac{d}{dt}\left(\frac{\partial t}{\partial \dot{q}_i}\right)\delta q_i dt$$
$$=-\int_{t_1}^{t_2}\frac{d}{dt}\left(\frac{\partial T}{\partial \dot{q}_i}\right)\delta q_i dt,\quad i=1,2,3,...,n \tag{5.8}$$

in which the auxiliary conditions, δq_i=0 ($i=1,2,3,...,n$), are zero at $t=t_1$ and $t=t_2$. Substituting Equation (5.8) into Equation (5.7) yields

$$\int_{t_1}^{t_2}\sum_{i=1}^{n}\left[\frac{\partial T}{\partial q_i}-\frac{\partial V}{\partial q_i}+Q_i-\frac{d}{dt}\left(\frac{\partial T}{\partial \dot{q}_i}\right)\right]\delta q_i dt=0 \tag{5.9}$$

Assigning arbitrary values to δq_1 while setting $\delta q_i=0$ ($i=2,3,...,n$), Equation (5.9) can be satisfied only if the coefficient of δq_1 is zero. Using the same argument but with $\delta q_2,\delta q_3,...,\delta q_n$ playing the role of δq_1, the coefficient of every virtual generalized displacement δq_i ($i=1,2,3,...,n$) must be zero, which yield Lagrange's equations

$$\frac{d}{dt}\left(\frac{\partial T}{\partial \dot{q}_i}\right)-\frac{\partial T}{\partial q_i}+\frac{\partial V}{\partial q_i}=Q_i,\quad i=1,2,3,...,n \tag{5.10}$$

Equations (5.10) represent the most general form of Lagrange's equations.

5.3.1 System-translation regime (T)

The supporting base will oscillate in the horizontal direction with a displacement $u(t)$ relative to the foundation, "system translation" regime (T), (Figure 5-1b) when

$$\left|\ddot{x}_g\right|>0 \tag{5.11}$$

Linear isolation system

Consider first the block isolated with a linear isolation system composed of a linear spring with stiffness k_b and a linear viscous damper with coefficient c_b, by interposing a rigid base of mass m_b, (Section 3.4.1). In the pure-translation regime the system possesses one degree of freedom. Using as generalized coordinate the horizontal translation of the base relative to the ground, $q_1\equiv u$, Lagrange's equation takes the form

$$\frac{d}{dt}\left(\frac{\partial T}{\partial \dot{u}}\right)-\frac{\partial T}{\partial u}+\frac{\partial V}{\partial u}=Q_u \tag{5.12}$$

in which T denotes the kinetic energy of the system, V the potential energy of the system, and Q_u the generalized non-conservative forces.

The kinetic energy due to the translation of the system is obtained as

$$T=\frac{1}{2}\left(m_b+m\right)\left[\left(\dot{u}+\dot{x}_g\right)^2+\left(\dot{z}_g\right)^2\right] \tag{5.13}$$

in which $\left(m_b+m\right)$ is the total mass of the system, $\dot{u}$ is the horizontal velocity of the base relative to the foundation, $\dot{x}_g$ and $\dot{z}_g$ is the horizontal and vertical velocity of the ground.

The derivatives of the kinetic-energy function required in formulating Lagrange's equations are:

$$\frac{\partial T}{\partial u}=0 \tag{5.14}$$

$$\frac{\partial T}{\partial \dot{u}}=\left(m_b+m\right)\left(\dot{u}+\dot{x}_g\right) \tag{5.15}$$

$$\frac{d}{dt}\left(\frac{\partial T}{\partial \dot{u}}\right)=\left(m_b+m\right)\left(\ddot{u}+\ddot{x}_g\right) \tag{5.16}$$

The potential energy of the system is obtained by

$$V=V_{el}+V_{gr} \tag{5.17}$$

where V_{el} is the potential energy due to elastic deformation of spring given by

$$V_{el}=\frac{1}{2}k_b u^2 \tag{5.18}$$

and V_{gr} is the potential energy due to gravity given by

$$V_{gr}=mgZ=0 \tag{5.19}$$

so that

$$V = \frac{1}{2} k_b u^2 \tag{5.20}$$

The derivative of the potential-energy function required in formulating Lagrange's equations is:

$$\frac{\partial V}{\partial u} = k_b u \tag{5.21}$$

The generalized force Q_u is derived via the virtual work of the non-conservative forces. In particular, to find Q_u, consider a virtual displacement δu and compute the work done by the non-conservative forces of the system, i.e. the damping force f_D, Figure 5-2. The latter is given by

$$\delta W_u^{nc} = -f_D \delta u = -c_b \dot{u} \delta u \equiv Q_u \delta u \tag{5.22}$$

so that

$$Q_u = \frac{\delta W}{\delta u} = -c_b \dot{u} \tag{5.23}$$

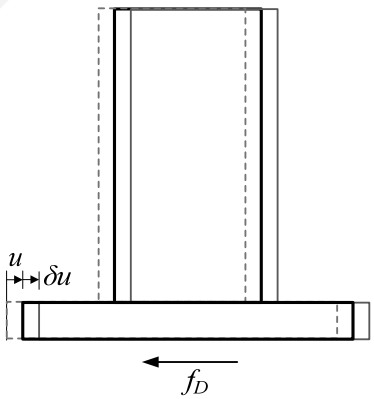

Figure 5-2: Displacement u, virtual displacement δu and non-conservative damping force.

Substituting Equations (5.14), (5.16), (5.21) and (5.23) in Lagrange's equation (Equation (5.12)) yields

$$\left(m+m_b\right)\left(\ddot{u}+\ddot{x}_g\right)+k_b u=-c_b\dot{u} \tag{5.24}$$

which upon rearranging terms Equation (5.24) becomes

$$\left(m+m_b\right)\ddot{u}+c_b\dot{u}+k_b u=-\left(m+m_b\right)\ddot{x}_g \tag{5.25}$$

Equation (5.25) is the classical linear second-order differential equation governing the response of a single-degree-of-freedom system to ground excitation (Chopra (2001)).

Nonlinear isolation system

Consider now the bilinear hysteretic model which represents the mechanical behavior of friction-pendulum-type isolation system, (Section 3.4.2). The kinetic energy of such system is given by Equation (5.13), while the potential energy of the system can be obtained by

$$V=\frac{1}{2}\left(m+m_b\right)\left(\frac{g+\ddot{z}_g}{R_b}\right)u^2 \tag{5.26}$$

The derivative of the potential-energy function required in formulating Lagrange's equations is:

$$\frac{\partial V}{\partial u}=\left(m+m_b\right)\left(\frac{g+\ddot{z}_g}{R_b}\right)u \tag{5.27}$$

The generalized force Q_u is derived via the virtual work of the non-conservative forces. In particular, to find Q_u, consider a virtual displacement δu and compute the work done by the non-conservative forces of the system. The latter is given by

$$\delta W_u^{nc}=-f_D\delta u=-\mu_b\left(m+m_b\right)\left(g+\ddot{z}_g\right)\boldsymbol{Z}\delta u\equiv Q_u\delta u \tag{5.28}$$

so that

$$Q_u=\frac{\delta W}{\delta u}=-\mu_b\left(m+m_b\right)\left(g+\ddot{z}_g\right)\boldsymbol{Z} \tag{5.29}$$

where $\boldsymbol{Z}$ is a dimensionless variable describing the rigid-plastic behavior, being governed by the following differential equation

$$Y\dot{\boldsymbol{Z}} + \gamma\left|\dot{u}\right|\boldsymbol{Z}\left|\boldsymbol{Z}\right| + \beta\dot{u}\boldsymbol{Z}^2 - \dot{u} = 0 \tag{5.30}$$

in which Y is the yield displacement, and β, γ are dimensionless parameters that control the shape of the hysteresis loop, with assigned values: $\beta = 0.1$, $\gamma = 0.9$ and $Y = 0.3\text{mm}$ (Constantinou et al. (1990)).

Substituting Equations (5.14), (5.16), (5.27) and (5.29) in Lagrange's equation (Equation (5.12)) yields

$$\left(m + m_b\right)\left(\ddot{u} + \ddot{x}_g\right) + \left(m + m_b\right)\left(\frac{g + \ddot{z}_g}{R_b}\right)u = -\mu_b\left(m + m_b\right)\left(g + \ddot{z}_g\right)\boldsymbol{Z} \tag{5.31}$$

which upon rearranging terms becomes

$$\left(m + m_b\right)\ddot{u} + \mu_b\left(m + m_b\right)\left(g + \ddot{z}_g\right)\boldsymbol{Z} + \left(m + m_b\right)\left(\frac{g + \ddot{z}_g}{R_b}\right)u = -\left(m + m_b\right)\ddot{x}_g \tag{5.32}$$

5.3.2 Sliding regime (S/T)

When subjected to ground acceleration $\ddot{x}_g$, the supporting base will oscillate in the horizontal direction with a displacement $u(t)$ relative to the foundation, (Figure 5-1c). The rigid block will initiate sliding in the horizontal direction with displacement $x_s(t)$ relative to the supporting base, once the inertia force of the mass exceeds the resistance provided by friction, $F_f = \mu_s N = \mu_s m\left(\ddot{z}_g + g\right)$, namely

$$\left|\ddot{u} + \ddot{x}_g\right| > \mu_s\left(\ddot{z}_g + g\right) \tag{5.33}$$

in which μ_s is the coefficient of static friction between the block and the supporting base, $\ddot{x}_g$ and $\ddot{z}_g$ are the horizontal and vertical components of ground acceleration respectively, and g is the gravitational acceleration.

Linear isolation system

Firstly, consider the block isolated with a linear isolation system composed of a linear spring with stiffness k_b and a linear viscous damper with coefficient c_b, by interposing a rigid base

of mass m_b, (Section 3.4.1). In the sliding regime, the system possesses two degrees of freedom. Using as generalized coordinates $q_1 \equiv u$, the horizontal translation of the base relative to the ground, and $q_2 \equiv x_s$, the horizontal translation of the block relative to the supporting base, Lagrange's equations take the form

$$\frac{d}{dt}\left(\frac{\partial T}{\partial \dot{u}}\right)-\frac{\partial T}{\partial u}+\frac{\partial V}{\partial u}=Q_u \tag{5.34}$$

$$\frac{d}{dt}\left(\frac{\partial T}{\partial \dot{x}_s}\right)-\frac{\partial T}{\partial x_s}+\frac{\partial V}{\partial x_s}=Q_{x_s} \tag{5.35}$$

in which T denotes the kinetic energy of the system, V the potential energy of the system, and Q_u, Q_x the generalized non-conservative forces.

The kinetic energy due to the translation of the system is obtained as

$$T=\frac{1}{2}m_b\left[\left(\dot{u}+\dot{x}_g\right)^2+\left(\dot{z}_g\right)^2\right]+\frac{1}{2}m\left[\left(\dot{u}+\dot{x}_s+\dot{x}_g\right)^2+\left(\dot{z}_g\right)^2\right] \tag{5.36}$$

in which m is the mass of the block, m_b is the mass of the supporting base, $\dot{u}$ is the horizontal velocity of the base relative to the foundation, $\dot{x}_s$ is the horizontal velocity of the block relative to the supporting base, and $\dot{x}_g$ is the horizontal velocity of the ground.

The derivatives of the kinetic-energy function required in formulating Lagrange's equations are:

$$\frac{\partial T}{\partial u}=0 \tag{5.37}$$

$$\frac{\partial T}{\partial x_s}=0 \tag{5.38}$$

$$\frac{\partial T}{\partial \dot{u}}=\left(m+m_b\right)\left(\dot{u}+\dot{x}_g\right)+m\dot{x}_s \tag{5.39}$$

$$\frac{\partial T}{\partial \dot{x}_s} = m\left(\dot{u} + \dot{x}_s + \dot{x}_g\right) \tag{5.40}$$

$$\frac{d}{dt}\left(\frac{\partial T}{\partial \dot{u}}\right) = \left(m + m_b\right)\left(\ddot{u} + \ddot{x}_g\right) + m\ddot{x}_s \tag{5.41}$$

$$\frac{d}{dt}\left(\frac{\partial T}{\partial \dot{x}_s}\right) = m\left(\ddot{u} + \ddot{x}_s + \ddot{x}_g\right) \tag{5.42}$$

The potential energy of the system is obtained as

$$V = V_{el} + V_{gr} \tag{5.43}$$

where V_{el} is the potential energy due to elastic deformation of spring, given by

$$V_{el} = \frac{1}{2}k_b u^2 \tag{5.44}$$

and V_{gr} is the potential energy due to gravity, given by

$$V_{gr} = mgZ = 0 \tag{5.45}$$

so that

$$V = \frac{1}{2}k_b u^2 \tag{5.46}$$

The derivatives of the potential-energy function required in formulating Lagrange's equations are:

$$\frac{\partial V}{\partial u} = k_b u \tag{5.47}$$

$$\frac{\partial V}{\partial x_s} = 0 \tag{5.48}$$

The generalized forces, Q, are derived via the virtual work of the non-conservative forces.

To find Q_u, consider a virtual displacement δu (keeping the other generalized coordinate zero, $\delta x_s = 0$) and compute the work done by the non-conservative forces of the system, Figure 5-2. The latter is given by

$$\delta W_u^{nc} = -f_D \delta u = -c_b \dot{u} \delta u \equiv Q_u \delta u \tag{5.49}$$

so that

$$Q_u = \frac{\delta W}{\delta u} = -c_b \dot{u} \tag{5.50}$$

To find Q_{x_s}, consider a virtual displacement δx_s (keeping the other generalized coordinate zero, $\delta u = 0$) and compute the work done by the non-conservative forces of the system. In this case

$$\delta W_{x_s}^{nc} = -f_f \delta x_s = -\mu_k m\left(g + \ddot{z}_g\right)\delta x_s \equiv Q_{x_s} \delta x_s \tag{5.51}$$

so that

$$Q_u = \frac{\delta W}{\delta x_s} = -\mu_k m\left(g + \ddot{z}_g\right) \tag{5.52}$$

in which μ_k is the coefficient of kinetic friction between the block and the supporting base.

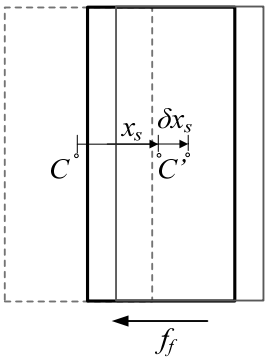

Figure 5-3: Displacement x_s, virtual displacement δx_s and non-conservative friction force.

Substituting Equations (5.37), (5.38), (5.41), (5.42), (5.47), (5.48), (5.50) and (5.52) in Lagrange's equations (Equations (5.34) and (5.35)) yield

$$\left(m+m_b\right)\left(\ddot{u}+\ddot{x}_g\right)+m\ddot{x}_s+k_b u=-c_b\dot{u} \tag{5.53}$$

$$m\left(\ddot{u}+\ddot{x}_s+\ddot{x}_g\right)=-\mu_k m\left(g+\ddot{z}_g\right) \tag{5.54}$$

The specify equations are valid for $\dot{x}>0$. In the case of, $\dot{x}<0$ the governing equations of motion are similarly derived and written in the form

$$\left(m+m_b\right)\left(\ddot{u}+\ddot{x}_g\right)+m\ddot{x}_s+k_b u=-c_b\dot{u} \tag{5.55}$$

$$m\left(\ddot{u}+\ddot{x}_s+\ddot{x}_g\right)=\mu_k m\left(g+\ddot{z}_g\right) \tag{5.56}$$

Combining Equations (5.53) through (5.56) leads to a compact set of equations for the sliding regime, namely

$$\left(m+m_b\right)\ddot{u}+m\ddot{x}_s+c_b\dot{u}+k_b u=-\left(m+m_b\right)\ddot{x}_g \tag{5.57}$$

$$m\ddot{u}+m\ddot{x}_s+\operatorname{sgn}\left(\dot{x}_s\right)m\mu_k\left(g+\ddot{z}_g\right)=-m\ddot{x}_g \tag{5.58}$$

where $\operatorname{sgn}\dot{x}_s$ denotes the signum function in $\dot{x}_s$, defined by

$$\operatorname{sgn}\dot{x}_s=\begin{cases}1 & \dot{x}_s>0\\ -1 & \dot{x}_s<0\end{cases} \tag{5.59}$$

Nonlinear isolation system

Consider now the bilinear hysteretic model which represents the mechanical behavior of friction-pendulum-type isolation system, (Section 3.4.2), the kinetic energy of the system is given by Equation (5.36). The potential energy of the system is obtained as

$$V=\frac{1}{2}\left(m+m_b\right)\left(\frac{g+\ddot{z}_g}{R_b}\right)u^2 \tag{5.60}$$

The derivatives of the potential-energy function required in formulating Lagrange's equations are:

$$\frac{\partial V}{\partial u} = \left(m + m_b\right)\left(\frac{g + \ddot{z}_g}{R_b}\right)u \tag{5.61}$$

$$\frac{\partial V}{\partial x_s} = 0 \tag{5.62}$$

The generalized forces, Q, are derived via the virtual work of the non-conservative forces. To find Q_u, consider a virtual displacement δu (keeping the other generalized coordinate zero, $\delta x_s = 0$) and compute the work done by the non-conservative forces of the system. The latter is given by

$$\delta W_u^{nc} = -f_D \delta u = -\mu_b \left(m + m_b\right)\left(g + \ddot{z}_g\right)\boldsymbol{Z}\delta u \equiv Q_u \delta u \tag{5.63}$$

so that

$$Q_u = \frac{\delta W}{\delta u} = -\mu_b \left(m + m_b\right)\left(g + \ddot{z}_g\right)\boldsymbol{Z} \tag{5.64}$$

where $\boldsymbol{Z}$ is a dimensionless variable describing the rigid-plastic behavior, being governed by the differential equation (5.30).

To find Q_{x_s}, consider a virtual displacement δx_s (keeping the other generalized coordinate zero, $\delta u = 0$) and compute the work done by the non-conservative forces of the system. In this case

$$\delta W_{x_s}^{nc} = -f_f \delta x = -\mu_k m\left(g + \ddot{z}_g\right)\delta x_s \equiv Q_{x_s}\delta x_s \tag{5.65}$$

so that

$$Q_u = \frac{\delta W}{\delta x} = -\mu_k m\left(g + \ddot{z}_g\right) \tag{5.66}$$

in which μ_k is the coefficient of kinetic friction between the block and the supporting base.

Substituting Equations (5.37), (5.38), (5.41), (5.42), (5.61), (5.62), (5.64) and (5.66) in Lagrange's equations (Equations (5.34) and (5.35)) yields

$$\left(m+m_b\right)\left(\ddot{u}+\ddot{x}_g\right)+m\ddot{x}_s+\left(m+m_b\right)\left(\frac{g+\ddot{z}_g}{R_b}\right)u=-\mu_b\left(m+m_b\right)\left(g+\ddot{z}_g\right)\boldsymbol{Z} \tag{5.67}$$

$$m\left(\ddot{u}+\ddot{x}_s+\ddot{x}_g\right)=-\mu_k m\left(g+\ddot{z}_g\right) \tag{5.68}$$

The specify equations are valid for $\dot{x}_s>0$. In the case of, $\dot{x}_s<0$ the governing equations of motion are similarly derived and written in the form

$$\left(m+m_b\right)\left(\ddot{u}+\ddot{x}_g\right)+m\ddot{x}_s+\left(m+m_b\right)\left(\frac{g+\ddot{z}_g}{R_b}\right)u=-\mu_b\left(m+m_b\right)\left(g+\ddot{z}_g\right)\boldsymbol{Z} \tag{5.69}$$

$$m\left(\ddot{u}+\ddot{x}_s+\ddot{x}_g\right)=\mu_k m\left(g+\ddot{z}_g\right) \tag{5.70}$$

Combining Equations (5.67) through (5.70) leads to a compact set of equations for the sliding regime, namely

$$\left(m+m_b\right)\ddot{u}+m\ddot{x}_s+\mu_b\left(m+m_b\right)\left(g+\ddot{z}_g\right)\boldsymbol{Z}+\left(m+m_b\right)\left(\frac{g+\ddot{z}_g}{R_b}\right)u=-\left(m+m_b\right)\ddot{x}_g \tag{5.71}$$

$$m\ddot{u}+m\ddot{x}_s+\operatorname{sgn}(\dot{x}_s)\mu_k m\left(g+\ddot{z}_g\right)=-m\ddot{x}_g \tag{5.72}$$

5.3.3 Rocking regime (R/T)

The rigid block is set into rocking on top of the moving base, (Figure 5-1d), when the overturning moment due to external loads, $M_{over}=m\left(\ddot{u}+\ddot{x}_g\right)h$, exceeds the available resisting moment due to gravity and vertical inertia force, $M_{res}=mb\left(g+\ddot{z}_g\right)$, yielding

$$\left|\ddot{u}+\ddot{x}_g\right|>\frac{b}{h}\left(g+\ddot{z}_g\right) \tag{5.73}$$

If the acceleration of the block, $(\ddot{u}+\ddot{x}_g)$, is positive, then rocking takes place about the corner O', or else if it is negative rocking takes place about the corner O.

Linear isolation system

Firstly, consider the block isolated with a linear isolation system composed of a linear spring

with stiffness k_b and a linear viscous damper with coefficient c_b, by interposing a rigid base of mass m_b, (Section 3.4.1). In the rocking regime, the system possesses two degrees of freedom. Using as generalized coordinates $q_1 \equiv u$, the horizontal translation of the base relative to the ground, and $q_2 \equiv \theta$, the rotation angle of the block about a base corner, Lagrange's equations take the form

$$\frac{d}{dt}\left(\frac{\partial T}{\partial \dot{u}}\right) - \frac{\partial T}{\partial u} + \frac{\partial V}{\partial u} = Q_u \tag{5.74}$$

$$\frac{d}{dt}\left(\frac{\partial T}{\partial \dot{\theta}}\right) - \frac{\partial T}{\partial \theta} + \frac{\partial V}{\partial \theta} = Q_\theta \tag{5.75}$$

in which T denotes the kinetic energy of the system, V the potential energy of the system, and Q_u, Q_θ the generalized non-conservative forces.

The kinetic energy due to the translation of the system and rotation of the block is obtained as

$$T = \frac{1}{2} m_b \left[\left(\dot{u} + \dot{x}_g \right)^2 + \dot{z}_g^2 \right] + \frac{1}{2} m v^2 + \frac{1}{2} I \dot{\theta}^2 \tag{5.76}$$

in which m is the mass of the block, m_b is the mass of the supporting base, I is the centroid mass moment of inertia, $\dot{u}$ is the horizontal velocity of the base relative to the foundation, $\dot{x}_g$ is the horizontal velocity of the ground, $\dot{z}_g$ is the vertical velocity of the ground, v is the velocity of the center-of-mass of the block, and $\dot{\theta}$ is the angular velocity of the block.

In Equation (5.76), the first term is associated with pure translation of the base, and the second and third term are associated with general planar motion of the block (which may be considered equivalent of pure translation of the center-of-mass plus pure rotation about the center-of-mass). The problem then reduces to computing the (magnitude of) velocity of the center-of-mass of the block.

The magnitude squared of the velocity vector of the block's center-of-mass, v, is given by

$$v^2 = \dot{X}^2 + \dot{Z}^2 \tag{5.77}$$

With reference to Figure 5-1d, the position of the center-of-mass of the block is given by

$$X = u + x_g + x_{\text{rot}} \tag{5.78}$$

$$Z = z_g + z_{\text{rot}} \tag{5.79}$$

in which x_g and z_g are the horizontal and vertical ground displacements respectively; x_{rot} is the horizontal relative displacement of the block due to rocking by an angle θ,

$$x_{\text{rot}} = x_1 + x_2 = \left(b - b\cos\theta\right) + h\sin\theta = h\sin\theta + b\left(1 - \cos\theta\right) \tag{5.80}$$

and z_{rot} is the vertical relative displacement of the block as it rotates by an angle θ, given by

$$z_{\text{rot}} = \left(z_1 + z_2\right) - h = \left(b\sin\theta + h\cos\theta\right) - h \tag{5.81}$$

so that

$$X = u + x_g + h\sin\theta + b\left(1 - \cos\theta\right) \tag{5.82}$$

$$Z = z_g + b\sin\theta - h\left(1 - \cos\theta\right) \tag{5.83}$$

The quantities x_1, x_2, z_1 and z_2 used in the calculation of x_{rot} and z_{rot} are shown in Figure 5-4.

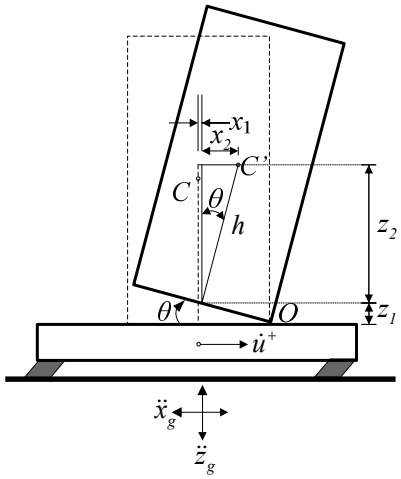

Figure 5-4: Schematic of isolated block in rocking regime.

The velocity of the center-of-mass is derived by differentiating Equations (5.78) and (5.79) with respect to time:

$$\dot{X} = \dot{u} + \dot{x}_g + h\dot{\theta}\cos\theta + b\dot{\theta}\sin\theta \tag{5.84}$$

$$\dot{Z} = \dot{z}_g + b\dot{\theta}\cos\theta - h\dot{\theta}\sin\theta \tag{5.85}$$

Thus, the kinetic energy of the system takes the form

$$\begin{aligned} T = \frac{1}{2}m_b\left[\left(\dot{u}+\dot{x}_g\right)^2 + \dot{z}_g^2\right] + \frac{1}{2}m\left[\left(\dot{u}+\dot{x}_g + h\dot{\theta}\cos\theta + b\dot{\theta}\sin\theta\right)^2\right. \\ \left. + \left(\dot{z}_g + b\dot{\theta}\cos\theta - h\dot{\theta}\sin\theta\right)^2\right] + \frac{1}{2}I\dot{\theta}^2 \end{aligned} \tag{5.86}$$

The derivatives of the kinetic-energy function required in formulating Lagrange's equations are:

$$\frac{\partial T}{\partial u} = 0 \tag{5.87}$$

$$\begin{aligned} \frac{\partial T}{\partial \theta} &= m\left(\dot{u}+\dot{x}_g + h\dot{\theta}\cos\theta + b\dot{\theta}\sin\theta\right)\left(b\dot{\theta}\cos\theta - h\dot{\theta}\sin\theta\right) \\ &\quad + m\left(\dot{z}_g + b\dot{\theta}\cos\theta - h\dot{\theta}\sin\theta\right)\left(-b\dot{\theta}\sin\theta - h\dot{\theta}\cos\theta\right) \\ &= m\left(\dot{u}+\dot{x}_g\right)\left(b\dot{\theta}\cos\theta - h\dot{\theta}\sin\theta\right) + m\dot{z}_g\left(-b\dot{\theta}\sin\theta - h\dot{\theta}\cos\theta\right) \end{aligned} \tag{5.88}$$

$$\frac{\partial T}{\partial \dot{u}} = m_b\left(\dot{u}+\dot{x}_g\right)+m\left(\dot{u}+\dot{x}_g+h\dot{\theta}\cos\theta+b\dot{\theta}\sin\theta\right) \tag{5.89}$$

$$\begin{aligned}\frac{\partial T}{\partial \dot{\theta}} &= m\left(\dot{u}+\dot{x}_g+h\dot{\theta}\cos\theta+b\dot{\theta}\sin\theta\right)\left(h\cos\theta+b\sin\theta\right)\\ &\quad +m\left(\dot{z}_g+b\dot{\theta}\cos\theta-h\dot{\theta}\sin\theta\right)\left(b\cos\theta-h\sin\theta\right)+I\dot{\theta}\\ &= m\left(\dot{u}+\dot{x}_g\right)\left(h\cos\theta+b\sin\theta\right)+m\dot{z}_g\left(b\cos\theta-h\sin\theta\right)+mR^2\dot{\theta}+I\dot{\theta}\end{aligned} \tag{5.90}$$

$$\begin{aligned}\frac{d}{dt}\left(\frac{\partial T}{\partial \dot{u}}\right) &= m_b\left(\ddot{u}+\ddot{x}_g\right)+m\left(\ddot{u}+\ddot{x}_g+h\ddot{\theta}\cos\theta-h\dot{\theta}^2\sin\theta+b\ddot{\theta}\sin\theta+b\dot{\theta}^2\cos\theta\right)\\ &= \left(m+m_b\right)\left(\ddot{u}+\ddot{x}_g\right)+m\left(h\cos\theta+b\sin\theta\right)\ddot{\theta}+m\left(b\cos\theta-h\sin\theta\right)\dot{\theta}^2\end{aligned} \tag{5.91}$$

$$\begin{aligned}\frac{d}{dt}\left(\frac{\partial T}{\partial \dot{\theta}}\right) &= m\left(\ddot{u}+\ddot{x}_g\right)\left(h\cos\theta+b\sin\theta\right)+m\left(\dot{u}+\dot{x}_g\right)\left(-h\dot{\theta}\sin\theta+b\dot{\theta}\cos\theta\right)\\ &\quad +m\ddot{z}_g\left(b\cos\theta-h\sin\theta\right)+m\dot{z}_g\left(-b\dot{\theta}\sin\theta-h\dot{\theta}\cos\theta\right)+mR^2\ddot{\theta}+I\ddot{\theta}\end{aligned} \tag{5.92}$$

The potential energy of the system is obtained as

$$V = V_{el}+V_{gr} \tag{5.93}$$

where V_{el} is the potential energy due to elastic deformation of spring, given by

$$V_{el} = \frac{1}{2}k_b u^2 \tag{5.94}$$

and V_{gr} is the potential energy due to gravity, given by

$$V_{gr} = mgZ = mg\left[b\sin\theta-h\left(1-\cos\theta\right)\right] \tag{5.95}$$

so that

$$V = \frac{1}{2}k_b u^2+mg\left[b\sin\theta-h\left(1-\cos\theta\right)\right] \tag{5.96}$$

The derivatives of the potential-energy function required in formulating Lagrange's equations are:

$$\frac{\partial V}{\partial u} = k_b u \tag{5.97}$$

$$\frac{\partial V}{\partial \theta} = mg\left(b\cos\theta - h\sin\theta\right) \tag{5.98}$$

The generalized forces, Q, are derived via the virtual work of the non-conservative forces.

To find Q_u, consider a virtual displacement δu (keeping the other generalized coordinate zero, $\delta\theta = 0$) and compute the work done by the non-conservative forces of the system, Figure 5-2. The latter is given by

$$\delta W_u^{nc} = -f_D \delta u = -c_b \dot{u} \delta u \equiv Q_u \delta u \tag{5.99}$$

so that

$$Q_u = \frac{\delta W}{\delta u} = -c_b \dot{u} \tag{5.100}$$

To find Q_θ, consider a virtual rotation $\delta\theta$ (keeping the other generalized coordinate zero, $\delta u = 0$) and compute the work done by the non-conservative forces of the system. In this case

$$\delta W_\theta^{nc} = 0 \equiv Q_\theta \delta\theta \tag{5.101}$$

so that

$$Q_\theta = 0 \tag{5.102}$$

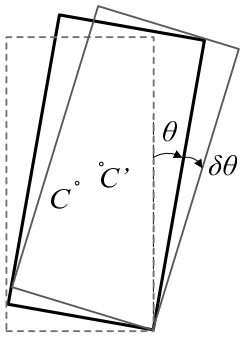

Figure 5-5: Displacement θ and virtual displacement $\delta\theta$.

Substituting Equations (5.87), (5.88), (5.91), (5.92), (5.97), (5.98), (5.100) and (5.102) in Lagrange's equations (Equations (5.74) and (5.75)) yields

$$\left(m+m_b\right)\left(\ddot{u}+\ddot{x}_g\right)+m\left(h\cos\theta+b\sin\theta\right)\ddot{\theta}+m\left(b\cos\theta-h\sin\theta\right)\dot{\theta}^2+k_b u=-c_b\dot{u} \tag{5.103}$$

$$\begin{aligned}&m\left(\ddot{u}+\ddot{x}_g\right)\left(h\cos\theta+b\sin\theta\right)+m\left(\dot{u}+\dot{x}_g\right)\left(-h\dot{\theta}\sin\theta+b\dot{\theta}\cos\theta\right)\\&+m\ddot{z}_g\left(b\cos\theta-h\sin\theta\right)+m\dot{z}_g\left(-b\dot{\theta}\sin\theta-h\dot{\theta}\cos\theta\right)+mR^2\ddot{\theta}+I\ddot{\theta}\\&-\left[m\left(\dot{u}+\dot{x}_g\right)\left(b\dot{\theta}\cos\theta-h\dot{\theta}\sin\theta\right)+m\dot{z}_g\left(-b\dot{\theta}\sin\theta-h\dot{\theta}\cos\theta\right)\right]\\&+mg\left(b\cos\theta-h\sin\theta\right)=0\end{aligned} \tag{5.104}$$

which upon rearranging terms become

$$\left(m+m_b\right)\ddot{u}+c_b\dot{u}+k_b u+m\left(h\cos\theta+b\sin\theta\right)\ddot{\theta}+m\left(b\cos\theta-h\sin\theta\right)\dot{\theta}^2=-\left(m+m_b\right)\ddot{x}_g \tag{5.105}$$

$$\begin{aligned}&\left(mR^2+I\right)\ddot{\theta}+m\ddot{u}\left(h\cos\theta+b\sin\theta\right)+mg\left(b\cos\theta-h\sin\theta\right)\\&=-m\left(h\cos\theta+b\sin\theta\right)\ddot{x}_g-m\left(b\cos\theta-h\sin\theta\right)\ddot{z}_g\end{aligned} \tag{5.106}$$

The specify equations are valid for $\theta>0$, i.e. in the case of rocking about the corner O. In the case of $\theta<0$, i.e. rocking about the corner O', the governing equations of motion are similarly derived and written in the form

$$\begin{aligned}&\left(m+m_b\right)\ddot{u}+c_b\dot{u}+k_b u+m\left(h\cos\theta-b\sin\theta\right)\ddot{\theta}+m\left(-b\cos\theta-h\sin\theta\right)\dot{\theta}^2\\&=-\left(m+m_b\right)\ddot{x}_g\end{aligned} \tag{5.107}$$

$$\begin{aligned}&\left(mR^2+I\right)\ddot{\theta}+m\ddot{u}\left(h\cos\theta-b\sin\theta\right)+mg\left(-b\cos\theta-h\sin\theta\right)\\&=-m\left(h\cos\theta-b\sin\theta\right)\ddot{x}_g-m\left(-b\cos\theta-h\sin\theta\right)\ddot{z}_g\end{aligned} \tag{5.108}$$

Combining Equations (5.105) through (5.108) leads to a compact set of equations for the rocking regime, namely

$$\begin{aligned}&\left(m+m_b\right)\ddot{u}+c_b\dot{u}+k_b u+m\left[h\cos\theta+\operatorname{sgn}\theta\left(b\sin\theta\right)\right]\ddot{\theta}\\&+m\left[\operatorname{sgn}\theta\left(b\cos\theta\right)-h\sin\theta\right]\dot{\theta}^2=-\left(m+m_b\right)\ddot{x}_g\end{aligned} \tag{5.109}$$

$$\begin{aligned}&\left(mR^2+I\right)\ddot{\theta}+m\ddot{u}\left[h\cos\theta+\operatorname{sgn}\theta\left(b\sin\theta\right)\right]+mg\left(\operatorname{sgn}\theta\left(b\cos\theta\right)-h\sin\theta\right)\\&=-m\left[h\cos\theta+\operatorname{sgn}\theta\left(b\sin\theta\right)\right]\ddot{x}_g-m\left(\operatorname{sgn}\theta\left(b\cos\theta\right)-h\sin\theta\right)\ddot{z}_g\end{aligned}\tag{5.110}$$

where $\operatorname{sgn}\theta$ denotes the signum function in θ, defined by

$$\operatorname{sgn}\theta=\begin{cases}1 & \theta>0\\-1 & \theta<0\end{cases}\tag{5.111}$$

Evidently, the mutually coupled equations governing the rocking regime are highly nonlinear and not amenable to closed-form solution, even for the simplest form of ground excitation.

Note that Equations (5.109) and (5.110) are only valid in the absence of impact ($\theta\neq 0$). At that instant, both corner points O and O' are in contact with the base, rendering the above formulation invalid. The impact problem is addressed separately in Chapter 6.

Nonlinear isolation system

Consider now the bilinear hysteretic model which represents the mechanical behavior of the friction-pendulum-type isolation system, (Section 3.4.2), the kinetic energy of the system is given by Equation (5.86). The potential energy of the system is obtained as

$$V=\frac{1}{2}\left(m+m_b\right)\left(\frac{g+\ddot{z}_g}{R_b}\right)u^2+mg\left[b\sin\theta-h\left(1-\cos\theta\right)\right]\tag{5.112}$$

The derivatives of the potential-energy function required in formulating Lagrange's equations are:

$$\frac{\partial V}{\partial u}=\left(m+m_b\right)\left(\frac{g+\ddot{z}_g}{R_b}\right)u\tag{5.113}$$

$$\frac{\partial V}{\partial\theta}=mg\left(b\cos\theta-h\sin\theta\right)\tag{5.114}$$

The generalized forces, Q, are derived via the virtual work of the non-conservative forces.

To find Q_u, consider a virtual displacement δu (keeping the other generalized coordinate zero, $\delta\theta=0$) and compute the work done by the non-conservative forces of the system. The

latter is given by

$$\delta W_u^{nc} = -f_D \delta u = -\mu_b \left(m + m_b\right)\left(g + \ddot{z}_g\right) \boldsymbol{Z} \delta u \equiv Q_u \delta u \tag{5.115}$$

so that

$$Q_u = \frac{\delta W}{\delta u} = -\mu_b \left(m + m_b\right)\left(g + \ddot{z}_g\right) \boldsymbol{Z} \tag{5.116}$$

where $\boldsymbol{Z}$ is a dimensionless variable describing the rigid-plastic behavior, being governed by the differential equation (5.30).

To find Q_θ, consider a virtual rotation $\delta\theta$ (keeping the other generalized coordinate zero, $\delta u = 0$) and compute the work done by the non-conservative forces of the system. In this case

$$\delta W_\theta^{nc} = 0 \equiv Q_\theta \delta\theta \tag{5.117}$$

so that

$$Q_\theta = 0 \tag{5.118}$$

Substituting Equations (5.87), (5.88), (5.91), (5.92), (5.113), (5.114), (5.116) and (5.118) in Lagrange's equations (Equations (5.74) and (5.75)) yields

$$\begin{aligned} &\left(m + m_b\right)\left(\ddot{u} + \ddot{x}_g\right) + m\left(h\cos\theta + b\sin\theta\right)\ddot{\theta} + m\left(b\cos\theta - h\sin\theta\right)\dot{\theta}^2 \\ &+\left(m + m_b\right)\left(\frac{g + \ddot{z}_g}{R_b}\right)u = -\mu_b \left(m + m_b\right)\left(g + \ddot{z}_g\right)\boldsymbol{Z} \end{aligned} \tag{5.119}$$

which upon rearranging terms become

$$\begin{aligned} &\left(m + m_b\right)\ddot{u} + \left(m + m_b\right)\left(\frac{g + \ddot{z}_g}{R_b}\right)u + \mu_b \left(m + m_b\right)\left(g + \ddot{z}_g\right)\boldsymbol{Z} + m\left(h\cos\theta + b\sin\theta\right)\ddot{\theta} \\ &+m\left(b\cos\theta - h\sin\theta\right)\dot{\theta}^2 = -\left(m + m_b\right)\ddot{x}_g \end{aligned} \tag{5.120}$$

$$\begin{aligned} &\left(mR^2 + I\right)\ddot{\theta} + m\ddot{u}\left(h\cos\theta + b\sin\theta\right) + mg\left(b\cos\theta - h\sin\theta\right) \\ &= -m\left(h\cos\theta + b\sin\theta\right)\ddot{x}_g - m\left(b\cos\theta - h\sin\theta\right)\ddot{z}_g \end{aligned} \tag{5.121}$$

The specify equations are valid for $\theta > 0$, i.e. in the case of rocking about the corner O. In the

case of $\theta<0$, i.e. rocking about the corner O', the governing equations of motion are similarly derived and written in the form

$$\begin{aligned}&\left(m+m_b\right)\ddot{u}+\left(m+m_b\right)\left(\frac{g+\ddot{z}_g}{R_b}\right)u+\mu_b\left(m+m_b\right)\left(g+\ddot{z}_g\right)\boldsymbol{Z}+m\left(h\cos\theta-b\sin\theta\right)\ddot{\theta}\\&+m\left(-b\cos\theta-h\sin\theta\right)\dot{\theta}^2=-\left(m+m_b\right)\ddot{x}_g\end{aligned}\tag{5.122}$$

$$\begin{aligned}&\left(mR^2+I\right)\ddot{\theta}+m\ddot{u}\left(h\cos\theta-b\sin\theta\right)+mg\left(-b\cos\theta-h\sin\theta\right)\\&=-m\left(h\cos\theta-b\sin\theta\right)\ddot{x}_g-m\left(-b\cos\theta-h\sin\theta\right)\ddot{z}_g\end{aligned}\tag{5.123}$$

Combining Equations (5.105) through (5.108) leads to a compact set of equations for the rocking regime, namely

$$\begin{aligned}&\left(m+m_b\right)\ddot{u}+\left(m+m_b\right)\left(\frac{g+\ddot{z}_g}{R_b}\right)u+\mu_b\left(m+m_b\right)\left(g+\ddot{z}_g\right)\boldsymbol{Z}\\&+m\left[h\cos\theta+\operatorname{sgn}\theta\left(b\sin\theta\right)\right]\ddot{\theta}+m\left[\operatorname{sgn}\theta\left(b\cos\theta\right)-h\sin\theta\right]\dot{\theta}^2=-\left(m+m_b\right)\ddot{x}_g\end{aligned}\tag{5.124}$$

$$\begin{aligned}&\left(mR^2+I\right)\ddot{\theta}+m\ddot{u}\left[h\cos\theta+\operatorname{sgn}\theta\left(b\sin\theta\right)\right]+mg\left(\operatorname{sgn}\theta\left(b\cos\theta\right)-h\sin\theta\right)\\&=-m\left[h\cos\theta+\operatorname{sgn}\theta\left(b\sin\theta\right)\right]\ddot{x}_g-m\left(\operatorname{sgn}\theta\left(b\cos\theta\right)-h\sin\theta\right)\ddot{z}_g\end{aligned}\tag{5.125}$$

5.3.4 Slide-rocking regime (SR/T)

Slide-rocking, (Figure 5-1e), is initiated from rest or from the system-translation regime in the singular case when the sliding-regime and rocking-regime conditions are satisfied simultaneously (Shenton III and Jones (1991)), yielding

$$\left|\ddot{u}+\ddot{x}_g\right|>\left[\mu_s\left(g+\ddot{z}_g\right),\frac{b}{h}\left(g+\ddot{z}_g\right)\right]\tag{5.126}$$

Linear isolation system

Firstly, consider the block isolated with a linear isolation system composed of a linear spring with stiffness k_b and a linear viscous damper with coefficient c_b, by interposing a rigid base of mass m_b, (Section 3.4.1). In the slide-rocking regime, the system possesses three degrees of freedom. Using as generalized coordinates $q_1\equiv u$, the horizontal translation of the base

relative to the ground, $q_2 \equiv x_s$, the horizontal translation of the block relative to the supporting base, and $q_3 \equiv \theta$, the rotation angle of the block about a base corner, Lagrange's equations take the form

$$\frac{d}{dt}\left(\frac{\partial T}{\partial \dot{u}}\right) - \frac{\partial T}{\partial u} + \frac{\partial V}{\partial u} = Q_u \tag{5.127}$$

$$\frac{d}{dt}\left(\frac{\partial T}{\partial \dot{x}_s}\right) - \frac{\partial T}{\partial x_s} + \frac{\partial V}{\partial x_s} = Q_{x_s} \tag{5.128}$$

$$\frac{d}{dt}\left(\frac{\partial T}{\partial \dot{\theta}}\right) - \frac{\partial T}{\partial \theta} + \frac{\partial V}{\partial \theta} = Q_\theta \tag{5.129}$$

in which T denotes the kinetic energy of the system, V the potential energy of the system, and Q_u, Q_x and Q_θ the generalized non-conservative forces.

The kinetic energy due to the translation of the system and rotation of the block is obtained as

$$T = \frac{1}{2} m_b \left[\left(\dot{u} + \dot{x}_g \right)^2 + \dot{z}_g^2 \right] + \frac{1}{2} m v^2 + \frac{1}{2} I \dot{\theta}^2 \tag{5.130}$$

in which m is the mass of the block, m_b is the mass of the supporting base, I is the centroid mass moment of inertia, $\dot{u}$ is the horizontal velocity of the base relative to the foundation, $\dot{x}$ is the horizontal velocity of the block relative to the supporting base, $\dot{x}_g$ is the horizontal velocity of the ground, v is the velocity of the center-of-mass of the block, and $\dot{\theta}$ is the angular velocity of the block.

In Equation (5.76), the first term is associated with the pure translation of the base, while the second and third term is associated with general planar motion of the block. The problem then reduces to computing the (magnitude of) velocity of the center-of-mass of the block.

The magnitude squared of the velocity vector of the block's center-of-mass, v, is given by

$$v^2 = \dot{X}^2 + \dot{Z}^2 \tag{5.131}$$

With reference to Figure 5-1e, the position of the center-of-mass of the block is given by

$$X = u + x_g + x_s + x_{\text{rot}} \tag{5.132}$$

$$Z = z_g + z_{\text{rot}} \tag{5.133}$$

in which x_g and z_g are the horizontal and vertical ground displacements respectively; x_s is the horizontal relative displacement of the block as it slides on the base, x_{rot} is the horizontal relative displacement of the block as it rotates by an angle θ, given by

$$x_{\text{rot}} = x_1 + x_2 = \left(b - b\cos\theta\right) + h\sin\theta = h\sin\theta + b\left(1 - \cos\theta\right) \tag{5.134}$$

and z_{rot} is the vertical relative displacement of the block as it rotates by an angle θ, given by

$$z_{\text{rot}} = \left(z_1 + z_2\right) - h = \left(b\sin\theta + h\cos\theta\right) - h \tag{5.135}$$

so that

$$X = u + x_g + x_s + h\sin\theta + b\left(1 - \cos\theta\right) \tag{5.136}$$

$$Z = z_g + b\sin\theta - h\left(1 - \cos\theta\right) \tag{5.137}$$

The quantities x_1, x_2, z_1 and z_2 used in the calculation of x_{rot} and z_{rot} are shown in Figure 5-6.

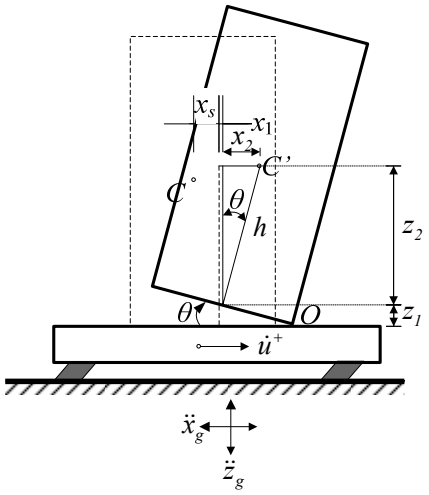

Figure 5-6: Schematic of isolated block in slide-rocking regime.

The velocity of the center-of-mass is derived by differentiating Equations (5.132) and (5.133) with respect to time:

$$\dot{X} = \dot{u} + \dot{x}_g + \dot{x}_s + h\dot{\theta}\cos\theta + b\dot{\theta}\sin\theta \tag{5.138}$$

$$\dot{Z} = \dot{z}_g + b\dot{\theta}\cos\theta - h\dot{\theta}\sin\theta \tag{5.139}$$

Therefore, the squared magnitude of the velocity vector of the block's center-of-mass can also be retrieved as

$$v^2 = \dot{X}^2 + \dot{Z}^2 = \left[\dot{u} + \dot{x}_g + \dot{x}_s + h\dot{\theta}\cos\theta + b\dot{\theta}\sin\theta\right]^2 + \left[\dot{z}_g + b\dot{\theta}\cos\theta - h\dot{\theta}\sin\theta\right]^2 \tag{5.140}$$

Thus, the kinetic energy of the system takes the form

$$\begin{aligned} T = \frac{1}{2}m_b\left(\dot{u} + \dot{x}_g\right)^2 + \frac{1}{2}m\Big[&\left(\dot{u} + \dot{x}_g + \dot{x}_s + h\dot{\theta}\cos\theta + b\dot{\theta}\sin\theta\right)^2 \\ &+ \left(\dot{z}_g + b\dot{\theta}\cos\theta - h\dot{\theta}\sin\theta\right)^2\Big] + \frac{1}{2}I\dot{\theta}^2 \end{aligned} \tag{5.141}$$

The derivatives of the kinetic-energy function required in formulating Lagrange's equations are:

$$\frac{\partial T}{\partial u} = 0 \tag{5.142}$$

$$\frac{\partial T}{\partial x_s} = 0 \tag{5.143}$$

$$\begin{aligned}\frac{\partial T}{\partial \theta} &= m\left(\dot{u} + \dot{x}_g + \dot{x}_s + h\dot{\theta}\cos\theta + b\dot{\theta}\sin\theta\right)\left(b\dot{\theta}\cos\theta - h\dot{\theta}\sin\theta\right) \\ &\quad + m\left(\dot{z}_g + b\dot{\theta}\cos\theta - h\dot{\theta}\sin\theta\right)\left(-b\dot{\theta}\sin\theta - h\dot{\theta}\cos\theta\right) \\ &= m\left(\dot{u} + \dot{x}_g + \dot{x}_s\right)\left(b\dot{\theta}\cos\theta - h\dot{\theta}\sin\theta\right) + m\dot{z}_g\left(-b\dot{\theta}\sin\theta - h\dot{\theta}\cos\theta\right)\end{aligned} \tag{5.144}$$

$$\frac{\partial T}{\partial \dot{u}} = m_b\left(\dot{u} + \dot{x}_g\right) + m\left(\dot{u} + \dot{x}_g + \dot{x}_s + h\dot{\theta}\cos\theta + b\dot{\theta}\sin\theta\right) \tag{5.145}$$

$$\frac{\partial T}{\partial \dot{x}_s} = m\left(\dot{u} + \dot{x}_g + \dot{x}_s + h\dot{\theta}\cos\theta + b\dot{\theta}\sin\theta\right) \tag{5.146}$$

$$\begin{aligned}\frac{\partial T}{\partial \dot{\theta}} &= m\left(\dot{u} + \dot{x}_g + \dot{x}_s + h\dot{\theta}\cos\theta + b\dot{\theta}\sin\theta\right)\left(h\cos\theta + b\sin\theta\right) \\ &\quad + m\left(\dot{z}_g + b\dot{\theta}\cos\theta - h\dot{\theta}\sin\theta\right)\left(b\cos\theta - h\sin\theta\right) + I\dot{\theta} \\ &= m\left(\dot{u} + \dot{x}_g + \dot{x}_s\right)\left(h\cos\theta + b\sin\theta\right) + m\dot{z}_g\left(b\cos\theta - h\sin\theta\right) + mR^2\dot{\theta} + I\dot{\theta}\end{aligned} \tag{5.147}$$

$$\begin{aligned}\frac{d}{dt}\left(\frac{\partial T}{\partial \dot{u}}\right) &= m_b\left(\ddot{u} + \ddot{x}_g\right) \\ &\quad + m\left(\ddot{u} + \ddot{x}_g + \ddot{x}_s + h\ddot{\theta}\cos\theta - h\dot{\theta}^2\sin\theta + b\ddot{\theta}\sin\theta + b\dot{\theta}^2\cos\theta\right) \\ &= \left(m + m_b\right)\left(\ddot{u} + \ddot{x}_g\right) + m\ddot{x}_s \\ &\quad + m\left(h\cos\theta + b\sin\theta\right)\ddot{\theta} + m\left(b\cos\theta - h\sin\theta\right)\dot{\theta}^2\end{aligned} \tag{5.148}$$

$$\frac{d}{dt}\left(\frac{\partial T}{\partial \dot{x}_s}\right) = m\left(\ddot{u} + \ddot{x}_g + \ddot{x}_s + h\ddot{\theta}\cos\theta - h\dot{\theta}^2\sin\theta + b\ddot{\theta}\sin\theta + b\dot{\theta}^2\cos\theta\right) \tag{5.149}$$

$$\begin{aligned}\frac{d}{dt}\left(\frac{\partial T}{\partial \dot{\theta}}\right) &= m\left(\ddot{u}+\ddot{x}_g+\ddot{x}_s\right)\left(h\cos\theta+b\sin\theta\right)\\ &+m\left(\dot{u}+\dot{x}_g+\dot{x}_s\right)\left(-h\dot{\theta}\sin\theta+b\dot{\theta}\cos\theta\right)\\ &+m\ddot{z}_g\left(b\cos\theta-h\sin\theta\right)\\ &+m\dot{z}_g\left(-b\dot{\theta}\sin\theta-h\dot{\theta}\cos\theta\right)+mR^2\ddot{\theta}+I\ddot{\theta}\end{aligned} \tag{5.150}$$

The potential energy of the system is obtained as

$$V = V_{el} + V_{gr} \tag{5.151}$$

where V_{el} is the potential energy due to elastic deformation of spring, given by

$$V_{el} = \frac{1}{2}k_b u^2 \tag{5.152}$$

and V_{gr} is the potential energy due to gravity, given by

$$V_{gr} = mgZ = mg\left[b\sin\theta - h\left(1-\cos\theta\right)\right] \tag{5.153}$$

so that

$$V = \frac{1}{2}k_b u^2 + mg\left[b\sin\theta - h\left(1-\cos\theta\right)\right] \tag{5.154}$$

The derivatives of the potential-energy function required in formulating Lagrange's equations are:

$$\frac{\partial V}{\partial u} = k_b u \tag{5.155}$$

$$\frac{\partial V}{\partial x_s} = 0 \tag{5.156}$$

$$\frac{\partial V}{\partial \theta} = mg\left(b\cos\theta - h\sin\theta\right) \tag{5.157}$$

The generalized forces, Q, are derived via the virtual work of the non-conservative forces.

To find Q_u, consider a virtual displacement δu (keeping the other generalized coordinates zero, $\delta x = 0$, $\delta\theta = 0$) and compute the work done by the non-conservative forces of the system, Figure 5-2. The latter is given by

$$\delta W_u^{nc} = -f_D \delta u = -c_b \dot{u} \delta u \equiv Q_u \delta u \tag{5.158}$$

so that

$$Q_u = \frac{\delta W}{\delta u} = -c_b \dot{u} \tag{5.159}$$

To find Q_x, consider a virtual displacement δx_s (keeping the other generalized coordinates zero, $\delta u = 0$, $\delta\theta = 0$) and compute the work done by the non-conservative forces of the system, Figure 5-3. In this case

$$\delta W_{x_s}^{nc} = -f_f \delta x_s = -\mu_k m\left(g + \ddot{Z}\right)\delta x_s \equiv Q_{x_s} \delta x_s \tag{5.160}$$

where,

$$\ddot{Z} = \ddot{z}_g + b\ddot{\theta}\cos\theta - b\dot{\theta}^2 \sin\theta - h\ddot{\theta}\sin\theta - h\dot{\theta}^2\cos\theta \tag{5.161}$$

so that

$$Q_{x_s} = \frac{\delta W}{\delta x_s} = -\mu_k m\left(g + \ddot{z}_g + b\ddot{\theta}\cos\theta - b\dot{\theta}^2 \sin\theta - h\ddot{\theta}\sin\theta - h\dot{\theta}^2\cos\theta\right) \tag{5.162}$$

in which μ_k is the coefficient of kinetic friction between the block and the supporting base.

To find Q_θ, consider a virtual rotation $\delta\theta$ (keeping the other generalized coordinates zero, $\delta u = 0$, $\delta x_s = 0$) and compute the work done by the non-conservative forces of the system, Figure 5-5. In this case

$$\delta W_\theta^{nc} = 0 \tag{5.163}$$

so that

$$Q_\theta = \frac{\delta W}{\delta\theta} = 0 \tag{5.164}$$

Substituting Equations (5.142), (5.143), (5.144), (5.148), (5.149), (5.150), (5.155),

(5.156), (5.157), (5.159), (5.162), (5.164) in Lagrange's equations (Equations (5.127), (5.128) and (5.129)) yields

$$\left(m+m_b\right)\left(\ddot{u}+\ddot{x}_g\right)+m\ddot{x}_s+m\left(h\cos\theta+b\sin\theta\right)\ddot{\theta}+m\left(b\cos\theta-h\sin\theta\right)\dot{\theta}^2+k_bu=-c_b\dot{u} \quad (5.165)$$

$$\begin{aligned}&m\left(\ddot{u}+\ddot{x}_g+\ddot{x}_s+h\ddot{\theta}\cos\theta-h\dot{\theta}^2\sin\theta+b\ddot{\theta}\sin\theta+b\dot{\theta}^2\cos\theta\right)\\&=-\operatorname{sgn}(\dot{x}_s)\mu_km\left(g+\ddot{z}_g+b\ddot{\theta}\cos\theta-b\dot{\theta}^2\sin\theta-h\ddot{\theta}\sin\theta-h\dot{\theta}^2\cos\theta\right)\end{aligned} \quad (5.166)$$

$$\begin{aligned}&\left(mR^2+I\right)\ddot{\theta}+m\left(\ddot{u}+\ddot{x}_s\right)\left(h\cos\theta+b\sin\theta\right)+mg\left(b\cos\theta-h\sin\theta\right)\\&=-m\left(h\cos\theta+b\sin\theta\right)\ddot{x}_g-m\left(b\cos\theta-h\sin\theta\right)\ddot{z}_g\end{aligned} \quad (5.167)$$

which upon rearranging terms become

$$\begin{aligned}&\left(m+m_b\right)\ddot{u}+m\ddot{x}_s+c_b\dot{u}+k_bu+m\left(h\cos\theta+b\sin\theta\right)\ddot{\theta}+m\left(b\cos\theta-h\sin\theta\right)\dot{\theta}^2\\&=-\left(m+m_b\right)\ddot{x}_g\end{aligned} \quad (5.168)$$

.. (5.169)

$$\begin{aligned}&\left(mR^2+I\right)\ddot{\theta}+m\left(\ddot{u}+\ddot{x}_s\right)\left(h\cos\theta-b\sin\theta\right)+mg\left(-b\cos\theta-h\sin\theta\right)\\&=-m\left(h\cos\theta+b\sin\theta\right)\ddot{x}_g-m\left(b\cos\theta-h\sin\theta\right)\ddot{z}_g\end{aligned} \quad (5.170)$$

The specify equations are valid for $\theta>0$, i.e. in the case of rocking about the corner O. In the case of $\theta<0$, i.e. rocking about the corner O', the governing equations of motion are similarly derived and written in the form

$$\begin{aligned}&\left(m+m_b\right)\ddot{u}+m\ddot{x}_s+c_b\dot{u}+k_bu+m\left(h\cos\theta-b\sin\theta\right)\ddot{\theta}+m\left(-b\cos\theta-h\sin\theta\right)\dot{\theta}^2\\&=-\left(m+m_b\right)\ddot{x}_g\end{aligned} \quad (5.171)$$

$$\begin{aligned}&m\left(\ddot{u}+\ddot{x}_s\right)+m\left(h\cos\theta-b\sin\theta\right)\ddot{\theta}+m\left(-b\cos\theta-h\sin\theta\right)\dot{\theta}^2\\&+\operatorname{sgn}(\dot{x}_s)\mu_km\left(g+\ddot{z}_g-b\ddot{\theta}\cos\theta+b\dot{\theta}^2\sin\theta-h\ddot{\theta}\sin\theta-h\dot{\theta}^2\cos\theta\right)=-m\ddot{x}_g\end{aligned} \quad (5.172)$$

$$\begin{aligned}&\left(mR^2+I\right)\ddot{\theta}+m\left(\ddot{u}+\ddot{x}_s\right)\left(h\cos\theta-b\sin\theta\right)+mg\left(-b\cos\theta-h\sin\theta\right)\\&=-m\left(h\cos\theta-b\sin\theta\right)\ddot{x}_g-m\left(-b\cos\theta-h\sin\theta\right)\ddot{z}_g\end{aligned} \quad (5.173)$$

Combining Equations (5.168) through (5.173) leads to a compact set of equations for the

rocking regime, namely

$$\begin{aligned}&\left(m+m_b\right)\ddot{u}+m\ddot{x}_s+c_b\dot{u}+k_bu+m\left[h\cos\theta+\operatorname{sgn}\theta\left(b\sin\theta\right)\right]\ddot{\theta}\\&+m\left[\operatorname{sgn}\theta\left(b\cos\theta\right)-h\sin\theta\right]\dot{\theta}^2=-\left(m+m_b\right)\ddot{x}_g\end{aligned}\tag{5.174}$$

$$\begin{aligned}&m\left(\ddot{u}+\ddot{x}_s\right)+m\left[h\cos\theta+\operatorname{sgn}\theta\left(b\sin\theta\right)\right]\ddot{\theta}+m\left[\operatorname{sgn}\theta\left(b\cos\theta\right)-h\sin\theta\right]\dot{\theta}^2\\&+\operatorname{sgn}(\dot{x}_s)\mu_km\left\{g+\ddot{z}_g+\left[\operatorname{sgn}\theta\left(b\cos\theta\right)-h\sin\theta\right]\ddot{\theta}\right.\\&\left.-\left[h\cos\theta+\operatorname{sgn}\theta\left(b\sin\theta\right)\right]\dot{\theta}^2\right\}=-m\ddot{x}_g\end{aligned}\tag{5.175}$$

$$\begin{aligned}&\left(mR^2+I\right)\ddot{\theta}+m\left(\ddot{u}+\ddot{x}_s\right)\left[h\cos\theta+\operatorname{sgn}\theta\left(b\sin\theta\right)\right]+mg\left[\operatorname{sgn}\theta\left(b\cos\theta\right)-h\sin\theta\right]\\&=-m\left[h\cos\theta+\operatorname{sgn}\theta\left(b\sin\theta\right)\right]\ddot{x}_g-m\left[\operatorname{sgn}\theta\left(b\cos\theta\right)-h\sin\theta\right]\ddot{z}_g\end{aligned}\tag{5.176}$$

where $\operatorname{sgn}\dot{x}_s$ denotes the signum function in $\dot{x}_s$, defined by Equation (5.59), and $\operatorname{sgn}\theta$ denotes the signum function in θ, defined by Equation (5.111).

Note that Equations (5.174)-(5.176) hold only in the absence of impact ($\theta\neq0$). At that instant, both corner points O and O' are in contact with the base, rendering the above formulation invalid. The impact problem is addressed separately in Chapter 6.

Nonlinear isolation system

Consider now the bilinear hysteretic model which represents the mechanical behavior of friction-pendulum-type isolation system, (Section 3.4.2), the kinetic energy of the system is given by Equation (5.141). The potential energy of the system is obtained as

$$V=\frac{1}{2}\left(m+m_b\right)\left(\frac{g+\ddot{z}_g}{R_b}\right)u^2+mg\left[b\sin\theta-h\left(1-\cos\theta\right)\right]\tag{5.177}$$

The derivatives of the potential-energy function required in formulating Lagrange's equations are:

$$\frac{\partial V}{\partial u}=\left(m+m_b\right)\left(\frac{g+\ddot{z}_g}{R_b}\right)u\tag{5.178}$$

$$\frac{\partial V}{\partial x_s}=0\tag{5.179}$$

$$\frac{\partial V}{\partial \theta} = mg\left(b\cos\theta - h\sin\theta\right) \tag{5.180}$$

The generalized forces, Q, are derived via the virtual work of the non-conservative forces.

To find Q_u, consider a virtual displacement δu (keeping the other generalized coordinate zero, $\delta\theta = 0$) and compute the work done by the non-conservative forces of the system. The latter is given by

$$\delta W_u^{nc} = -f_D \delta u = -\mu_b \left(m + m_b\right)\left(g + \ddot{z}_g\right)\boldsymbol{Z}\delta u \equiv Q_u \delta u \tag{5.181}$$

so that

$$Q_u = \frac{\delta W}{\delta u} = -\mu_b \left(m + m_b\right)\left(g + \ddot{z}_g\right)\boldsymbol{Z} \tag{5.182}$$

where $\boldsymbol{Z}$ is a dimensionless variable describing the rigid-plastic behavior, being governed by the differential equation (5.30).

To find Q_x, consider a virtual displacement δx_s (keeping the other generalized coordinates zero, $\delta u = 0$, $\delta\theta = 0$) and compute the work done by the non-conservative forces of the system. In this case

$$\delta W_{x_s}^{nc} = -f_f \delta x_s = -\mu_k m\left(g + \ddot{Z}\right)\delta x_s \equiv Q_{x_s}\delta x_s \tag{5.183}$$

Where,

$$\ddot{Z} = \ddot{z}_g + b\ddot{\theta}\cos\theta - b\dot{\theta}^2\sin\theta - h\ddot{\theta}\sin\theta - h\dot{\theta}^2\cos\theta \tag{5.184}$$

so that

$$Q_{x_s} = \frac{\delta W}{\delta x_s} = -\mu_k m\left(g + \ddot{z}_g + b\ddot{\theta}\cos\theta - b\dot{\theta}^2\sin\theta - h\ddot{\theta}\sin\theta - h\dot{\theta}^2\cos\theta\right) \tag{5.185}$$

in which μ_k is the coefficient of kinetic friction between the block and the supporting base.

To find Q_θ, consider a virtual rotation $\delta\theta$ (keeping the other generalized coordinate zero, $\delta u = 0$) and compute the work done by the non-conservative forces of the system. In this case

$$\delta W_{\theta}^{nc} = 0 \equiv Q_{\theta}\delta\theta \tag{5.186}$$

so that

$$Q_{\theta} = 0 \tag{5.187}$$

Substituting Equations (5.142), (5.143), (5.144), (5.148), (5.149), (5.150), (5.178), (5.179), (5.180), (5.182), (5.185), (5.187) in Lagrange's equations (Equations (5.127), (5.128) and (5.129)) yields

$$\begin{aligned}&\left(m+m_b\right)\left(\ddot{u}+\ddot{x}_g\right)+m\ddot{x}_s+m\left(h\cos\theta+b\sin\theta\right)\ddot{\theta}+m\left(b\cos\theta-h\sin\theta\right)\dot{\theta}^2\\&+\left(m+m_b\right)\left(\frac{g+\ddot{z}_g}{R_b}\right)u=-\mu_b\left(m+m_b\right)\left(g+\ddot{z}_g\right)\boldsymbol{Z}\end{aligned} \tag{5.188}$$

$$\begin{aligned}&m\left(\ddot{u}+\ddot{x}_g+\ddot{x}_s+h\ddot{\theta}\cos\theta-h\dot{\theta}^2\sin\theta+b\ddot{\theta}\sin\theta+b\dot{\theta}^2\cos\theta\right)\\&=-\operatorname{sgn}(\dot{x}_s)\mu_k m\left(g+\ddot{z}_g+b\ddot{\theta}\cos\theta-b\dot{\theta}^2\sin\theta-h\ddot{\theta}\sin\theta-h\dot{\theta}^2\cos\theta\right)\end{aligned} \tag{5.189}$$

$$\begin{aligned}&\left(mR^2+I\right)\ddot{\theta}+m\left(\ddot{u}+\ddot{x}_s\right)\left(h\cos\theta+b\sin\theta\right)+mg\left(b\cos\theta-h\sin\theta\right)\\&=-m\left(h\cos\theta+b\sin\theta\right)\ddot{x}_g-m\left(b\cos\theta-h\sin\theta\right)\ddot{z}_g\end{aligned} \tag{5.190}$$

which upon rearranging terms become

$$\begin{aligned}&\left(m+m_b\right)\ddot{u}+m\ddot{x}_s+\left(m+m_b\right)\left(\frac{g+\ddot{z}_g}{R_b}\right)u+\mu_b\left(m+m_b\right)\left(g+\ddot{z}_g\right)\boldsymbol{Z}\\&+m\left(h\cos\theta+b\sin\theta\right)\ddot{\theta}+m\left(b\cos\theta-h\sin\theta\right)\dot{\theta}^2=-\left(m+m_b\right)\ddot{x}_g\end{aligned} \tag{5.191}$$

$$\begin{aligned}&m\left(\ddot{u}+\ddot{x}_s\right)+m\left(h\cos\theta+b\sin\theta\right)\ddot{\theta}+m\left(b\cos\theta-h\sin\theta\right)\dot{\theta}^2\\&+\operatorname{sgn}(\dot{x}_s)\mu_k m\left(g+\ddot{z}_g+b\ddot{\theta}\cos\theta-b\dot{\theta}^2\sin\theta-h\ddot{\theta}\sin\theta-h\dot{\theta}^2\cos\theta\right)=-m\ddot{x}_g\end{aligned} \tag{5.192}$$

$$\begin{aligned}&\left(mR^2+I\right)\ddot{\theta}+m\left(\ddot{u}+\ddot{x}_s\right)\left(h\cos\theta-b\sin\theta\right)+mg\left(-b\cos\theta-h\sin\theta\right)\\&=-m\left(h\cos\theta+b\sin\theta\right)\ddot{x}_g-m\left(b\cos\theta-h\sin\theta\right)\ddot{z}_g\end{aligned} \tag{5.193}$$

The specify equations are valid for $\theta > 0$, i.e. in the case of rocking about the corner O. In the case of $\theta < 0$, i.e. rocking about the corner O', the governing equations of motion are similarly derived and written in the form

$$\begin{aligned}&\left(m+m_b\right)\ddot{u}+m\ddot{x}_s+\left(m+m_b\right)\left(\frac{g+\ddot{z}_g}{R_b}\right)u+\mu_b\left(m+m_b\right)\left(g+\ddot{z}_g\right)\boldsymbol{Z}\\&+m\left(h\cos\theta-b\sin\theta\right)\ddot{\theta}+m\left(-b\cos\theta-h\sin\theta\right)\dot{\theta}^2=-\left(m+m_b\right)\ddot{x}_g\end{aligned}\tag{5.194}$$

$$\begin{aligned}&m\left(\ddot{u}+\ddot{x}_s\right)+m\left(h\cos\theta-b\sin\theta\right)\ddot{\theta}+m\left(-b\cos\theta-h\sin\theta\right)\dot{\theta}^2\\&+\operatorname{sgn}(\dot{x}_s)\mu_k m\left(g+\ddot{z}_g-b\ddot{\theta}\cos\theta+b\dot{\theta}^2\sin\theta-h\ddot{\theta}\sin\theta-h\dot{\theta}^2\cos\theta\right)=-m\ddot{x}_g\end{aligned}\tag{5.195}$$

$$\begin{aligned}&\left(mR^2+I\right)\ddot{\theta}+m\left(\ddot{u}+\ddot{x}_s\right)\left(h\cos\theta-b\sin\theta\right)+mg\left(-b\cos\theta-h\sin\theta\right)\\&=-m\left(h\cos\theta-b\sin\theta\right)\ddot{x}_g-m\left(-b\cos\theta-h\sin\theta\right)\ddot{z}_g\end{aligned}\tag{5.196}$$

Combining Equations (5.191) through (5.196) leads to a compact set of equations for the rocking regime, namely

$$\begin{aligned}&\left(m+m_b\right)\ddot{u}+m\ddot{x}_s+\left(m+m_b\right)\left(\frac{g+\ddot{z}_g}{R_b}\right)u+\mu_b\left(m+m_b\right)\left(g+\ddot{z}_g\right)\boldsymbol{Z}\\&+m\left[h\cos\theta+\operatorname{sgn}\theta\left(b\sin\theta\right)\right]\ddot{\theta}+m\left[\operatorname{sgn}\theta\left(b\cos\theta\right)-h\sin\theta\right]\dot{\theta}^2=-\left(m+m_b\right)\ddot{x}_g\end{aligned}\tag{5.197}$$

$$\begin{aligned}&m\left(\ddot{u}+\ddot{x}_s\right)+m\left[h\cos\theta+\operatorname{sgn}\theta\left(b\sin\theta\right)\right]\ddot{\theta}+m\left[\operatorname{sgn}\theta\left(b\cos\theta\right)-h\sin\theta\right]\dot{\theta}^2\\&+\operatorname{sgn}(\dot{x}_s)\mu_k m\left\{g+\ddot{z}_g+\left[\operatorname{sgn}\theta\left(b\cos\theta\right)-h\sin\theta\right]\ddot{\theta}\right.\\&\left.-\left[h\cos\theta+\operatorname{sgn}\theta\left(b\sin\theta\right)\right]\dot{\theta}\right\}=-m\ddot{x}_g\end{aligned}\tag{5.198}$$

$$\begin{aligned}&\left(mR^2+I\right)\ddot{\theta}+m\left(\ddot{u}+\ddot{x}_s\right)\left[h\cos\theta+\operatorname{sgn}\theta\left(b\sin\theta\right)\right]+mg\left[\operatorname{sgn}\theta\left(b\cos\theta\right)-h\sin\theta\right]\\&=-m\left[h\cos\theta+\operatorname{sgn}\theta\left(b\sin\theta\right)\right]\ddot{x}_g-m\left[\operatorname{sgn}\theta\left(b\cos\theta\right)-h\sin\theta\right]\ddot{z}_g\end{aligned}\tag{5.199}$$

5.4 Transition Criteria between Oscillation Regimes

The dynamic behavior of the system is highly complex primarily due to the potential transition from one oscillation regime to another, each one governed by different equations of motion. This transition is governed by certain criteria, which are established by balancing the acting forces on the system for a specific time and state. A state diagram indicating the different response regimes together with the associated transition criteria is shown in Figure 5-7.

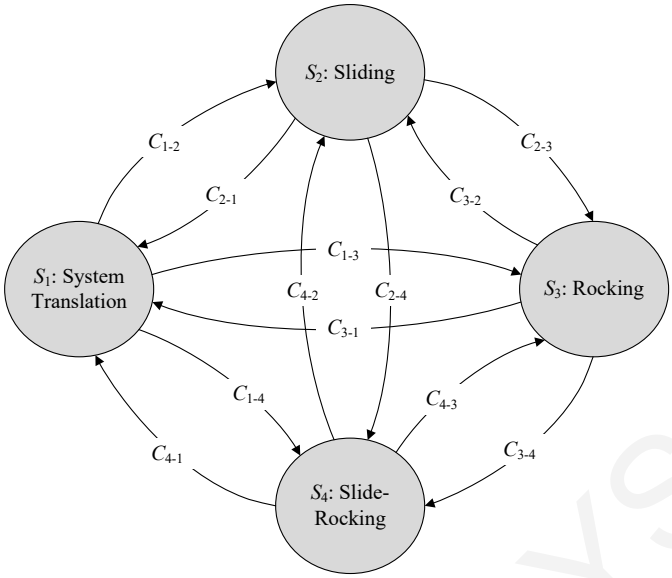

Figure 5-7: State diagram and transition criteria among different oscillation regimes.

The transition from the system-translation regime (S_1) to other oscillation regimes is governed by the following criteria:

- To sliding regime (S_2):

$$C_{1-2}: \quad \left|\ddot{u}+\ddot{x}_g\right| > \mu_s\left(g+\ddot{z}_g\right) \text{ and } \left|\ddot{u}+\ddot{x}_g\right| \le \frac{b}{h}\left(g+\ddot{z}_g\right) \tag{5.200}$$

- To rocking regime (S_3):

$$C_{1-3}: \quad \left|\ddot{u}+\ddot{x}_g\right| > \frac{b}{h}\left(g+\ddot{z}_g\right) \text{ and } \left|\ddot{u}+\ddot{x}_g\right| \le \mu_s\left(g+\ddot{z}_g\right) \tag{5.201}$$

- To slide-rocking regime (S_4):

$$C_{1-4}: \quad \left|\ddot{u}+\ddot{x}_g\right| > \frac{b}{h}\left(g+\ddot{z}_g\right) \text{ and } \left|\ddot{u}+\ddot{x}_g\right| > \mu_s\left(g+\ddot{z}_g\right) \tag{5.202}$$

The criteria (5.200), (5.201) and (5.202) are based on the initiation criteria of each oscillation pattern that are given analytically in Section 4.3.

The transition from the sliding regime (S_2) to other oscillation regimes is governed by the following criteria:

- To system-translation regime (S_1):

$$C_{2-1}: \quad \left|\dot{x}_s\right| = 0 \tag{5.203}$$

- To rocking regime (S_3):

$$C_{2-3}: \quad \left|\dot{x}_s\right| = 0 \ \text{ and } \ \left|\ddot{u} + \ddot{x}_g\right| > \frac{b}{h}\left(g + \ddot{z}_g\right) \tag{5.204}$$

- To slide-rocking regime (S_4):

$$C_{2-4}: \quad \left|\ddot{u} + \ddot{x}_g + \ddot{x}_s\right| > \mu_k\left(g + \ddot{z}_g\right) \ \text{ and } \ \left|\ddot{u} + \ddot{x}_g + \ddot{x}_s\right| > \frac{b}{h}\left(g + \ddot{z}_g\right) \tag{5.205}$$

The criteria (5.203) and (5.204) state that the transition from sliding regime to system translation or rocking regimes will be accomplished when the horizontal translation velocity of the block, $\dot{x}_s$, equals zero (sliding ceases). In addition, the initiation criterion of rocking, Section 4.3, must be satisfied. During sliding regime, the slide-rocking will be initiated once the inertia force of the mass exceeds the resistance provided by friction, $F_f = \mu_s N = \mu_s m\left(\ddot{z}_g + g\right)$ and at the same time when the overturning moment due to external loads, $M_{over} = m\left(\ddot{u} + \ddot{x}_g + \ddot{x}_s\right)h$, exceeds the available resisting moment due to gravity and vertical inertia force, $M_{res} = mb\left(g + \ddot{z}_g\right)$, criterion (5.205).

The transition from the rocking regime (S_3) to other oscillation regimes is governed by the following criteria:

- To system-translation regime (S_1):

$$C_{3-1}: \quad \left|\theta\right| = 0 \ \text{ and } \ \left|\dot{\theta}\right| = 0 \tag{5.206}$$

- To sliding regime (S_2):

$$C_{3-2}: \quad \left|\theta\right| = 0 \ \text{ and } \ \left|\dot{\theta}\right| = 0 \ \text{ and } \ \left|\ddot{u} + \ddot{x}_g\right| > \mu_s\left(g + \ddot{z}_g\right) \tag{5.207}$$

- To slide-rocking regime (S_4):

$$C_{3-4}: \quad \left|\theta\right| > 0 \ \text{ and } \ \left|\dot{\theta}\right| > 0 \ \text{ and } \ \left|\frac{f_x}{f_z}\right| > \mu_s \tag{5.208}$$

The criteria (5.206) and (5.207) state that the transition from rocking regime to system

translation and sliding regimes will be accomplished when the rotational velocity, $\dot{\theta}$, and the rotation angle, θ, of the block equal zero (rocking ceases). In addition, the initiation criterion of sliding, Section 4.3, must be satisfied. During rocking regime, the slide-rocking will be initiated once the rotational velocity, $\dot{\theta}$, and rotation angle, θ, of the block are nonzero (rocking continues) and the absolute ratio of horizontal, f_x, and vertical, f_z, reactions of the base, at points O or O', exceeds the coefficient of static friction, μ_s, criterion (5.208). The criterion (5.208) can be expressed as:

$$\left|\frac{m\left(\ddot{u}+\ddot{x}_g\right)+mA_1\ddot{\theta}+mA_2\dot{\theta}^2}{m\left(g+\ddot{z}_g\right)+mA_2\ddot{\theta}-mA_1\dot{\theta}^2}\right|>\mu_s \tag{5.209}$$

where, $A_1=h\cos\theta+\operatorname{sgn}\theta\left(b\sin\theta\right)$ and $A_2=\operatorname{sgn}\theta\left(b\cos\theta\right)-h\sin\theta$

Note that if slide-rocking regimes initiates after impact, then f_x and f_z are the horizontal and vertical impulses forces acting at the impacting corner, see Section 6.3.1.

The transition from the slide-rocking regime (S_4) to other oscillation regimes is governed by the following criteria:

- To system-translation regime (S_1):

$$C_{4-1}:\ \ |\theta|=0\ \text{ and }\ |\dot{\theta}|=0\ \text{ and }\ |\dot{x}_s|=0 \tag{5.210}$$

- To sliding regime (S_2):

$$C_{4-2}:\ \ |\theta|=0\ \text{ and }\ |\dot{\theta}|=0\ \text{ and }\ |\ddot{u}+\ddot{x}_g+\ddot{x}_s|>\mu_k\left(g+\ddot{z}_g\right) \tag{5.211}$$

- To rocking regime (S_3):

$$C_{4-3}:\ \ \left|\frac{f_x}{f_z}\right|\le\mu_k\ \text{ and }\ |\dot{\theta}|>0 \tag{5.212}$$

The criterion (5.210) states that the transition from slide-rocking regime to system translation regime will be accomplished when the rotational velocity, $\dot{\theta}$, the rotation angle, θ, and the horizontal translation velocity of the block, $\dot{x}_s$, equal zero (rocking and sliding cease). During slide-rocking regime, the rocking will cease and the sliding will continue once the rotational

velocity, $\dot{\theta}$, and the rotation angle, θ, of the block equal to zero (rocking ceases) and the inertia force of the mass continue to exceeds the resistance provided by friction, $F_f = \mu_s N = \mu_s m\left(\ddot{z}_g + g\right)$, criterion (5.211). The rocking regime will continue when sliding ceases. This will be accomplished when the ratio of horizontal, f_x, and vertical, f_z, reactions of the base, at points O or O', becomes smaller than the coefficient of static friction, μ_s, and the rotational velocity, $\dot{\theta}$, of the block remains nonzero, criterion (5.212). The criterion (5.212) can be expressed as:

$$\left|\frac{m\left(\ddot{u} + \ddot{x}_g + \ddot{x}_s\right) + mA_1\ddot{\theta} + mA_2\dot{\theta}^2}{m\left(g + \ddot{z}_g\right) + mA_2\ddot{\theta} - mA_1\dot{\theta}^2}\right| \le \mu_k \tag{5.213}$$

where, $A_1 = h\cos\theta + \operatorname{sgn}\theta\left(b\sin\theta\right)$ and $A_2 = \operatorname{sgn}\theta\left(b\cos\theta\right) - h\sin\theta$

Note that if rocking regime continues after impact, then f_x and f_z are the horizontal and vertical impulses forces acting at the impacting corner, see Section 6.4.2.

CHAPTER 6

Formulation of Impact Model

6.1 Introduction

The dynamic response of the system is strongly affected by the occurrence of impact(s) between the block and the horizontally-moving base, during "rocking" and "slide-rocking" oscillation regime. In fact, impact affects the system response on many different levels. On one level, it renders the problem highly nonlinear (aside from the nonlinear nature of the equations themselves) by virtue of the discontinuity introduced in the response (i.e. the governing equations of motion cease to be valid at $\theta = 0$). As a result, impact causes the system to switch from one oscillation regime to another (potentially modifying the degrees of freedom), each one governed by a different set of differential equations. This in turn entails that the integration of equations of motion governing the post-impact response must account for the ensuing instantaneous change of the system velocity regime. In this regard, the dynamic response is critically influenced by impact, in that impact contributes (exclusively) to the energy dissipation in the system, manifested through the reduction of the post-impact velocities.

Therefore, the critical role of impact in the dynamics of the system necessitates a rigorous formulation of the impact problem. In this dissertation, a model governing impact is derived from first principles using classical impact theory. According to the principle of impulse and momentum, the duration of impact is assumed short and the impulsive forces are assumed large relative to other forces in the system. Changes in position and orientation are neglected, and changes in velocity are considered instantaneous. Moreover, this model assumes point-impact, perfectly inelastic impact (i.e. zero coefficient of restitution) and impulses acting only at the impacting corner (i.e. impulses at the rotating corner are small compared to those at the impacting corner and are neglected).

It is worth noting that the coefficient of restitution, e, as defined in classical impact theory, relates pre- to post-impact *translational* velocities normal to the impact surface ($v_n^+ = -ev_n^-$), and hence it must not be confused (as often encountered in the literature) with the coefficient of "angular restitution" ε, which relates the pre- to post-impact *angular* velocities of the body

($\dot{\theta}^{+} = \varepsilon\dot{\theta}^{-}$). In this dissertation, the coefficient of restitution e enters in the expression $\dot{z}_{O'}^{+} = -e\dot{z}_{O'}^{-}$ which relates pre- to post-impact vertical relative velocities of the impacting corner (O'). According to the classical impact theory, the value $e = 1$ means that the capacity of the two particles to recover equals their tendency to deform. This condition is one of elastic impact with no energy loss. The value $e = 0$, on the other hand, describes inelastic or plastic impact where the particles cling together after collision and the loss of energy is maximum. In this dissertation, under the assumption of perfectly inelastic impact, the coefficient of restitution is then justified by considering $e = 0$.

6.2 Theoretical Background

In this section a review of the principles of linear impulse, linear momentum, angular impulse and angular momentum are presented, mainly based on Meriam and Kraige (2009).

6.2.1 Linear impulse and linear momentum

Based on Newton's second law, when a particle of mass m is subjected to the action of concurrent forces $\boldsymbol{F}_1, \boldsymbol{F}_2, \boldsymbol{F}_3, \ldots$, the vector sum $\Sigma\boldsymbol{F}$ equals with

$$\Sigma\boldsymbol{F} = m\dot{\boldsymbol{v}} = \frac{d}{dt}(m\boldsymbol{v}) \tag{6.1}$$

where $\dot{\boldsymbol{v}}$ and $\boldsymbol{v}$ is the acceleration and velocity of the particle, respectively.

The product of mass and velocity, $\boldsymbol{L} = m\boldsymbol{v}$, is defined as the linear momentum of the particle. Equation (6.1) states that the resultant of all forces acting on a particle equals its time of change of linear momentum. The direction of the resultant force coincides with the direction of the rate of change in linear momentum, which is the direction of the rate of change in velocity. Equation (6.1) is one of the most useful and important relationships in dynamics, and is valid as long as the mass m of the particle is not changing with time.

The effect of the resultant force $\Sigma\boldsymbol{F}$ on the linear momentum of the particle over a finite period of time can be calculated simply by integrating equation (6.1) with respect to the time t. Multiplying the equation by dt gives $\Sigma\boldsymbol{F}dt = d\boldsymbol{L}$. Integrating equation from time t_1 to time t_2 yields

$$\int_{t_1}^{t_2} \Sigma \boldsymbol{F}\, dt = \boldsymbol{L}_2 - \boldsymbol{L}_1 \tag{6.2}$$

where $\boldsymbol{L}_2$ is the linear momentum at time t_2, $\boldsymbol{L}_2 = m\boldsymbol{v}_2$, and $\boldsymbol{L}_1$ is the linear momentum at time t_1, $\boldsymbol{L}_1 = m\boldsymbol{v}_1$. The product of force and time is defined as the linear impulse of the force. Equation (6.2) states that the total linear impulse on m equals the corresponding change in linear momentum of m.

If the resultant force on a particle is zero during an interval of time, then Equation (6.1) requires that its linear momentum $\boldsymbol{L}$ remain constant and can be written as

$$\Delta \boldsymbol{L} = 0 \quad \text{or} \quad \boldsymbol{L}_1 = \boldsymbol{L}_2 \tag{6.3}$$

In such a case, the linear momentum of the particle is said to be conserved. Linear momentum may be conserved in one coordinate direction, such as x, but not necessarily in the y- or z-direction. This relation expresses the principle of conservation of linear momentum.

6.2.2 Angular impulse and angular momentum

Analogous to the equations of linear impulse and linear momentum, there exists a parallel set of equations for angular impulse and angular momentum.

Consider a single particle, P, of mass m travelling along a curve in space with a velocity $\boldsymbol{v}$, Figure 6-1(a). The particle is located by its position vector $\boldsymbol{r}$ with respect to a convenient origin O of fixed coordinates x-y-z. The linear momentum of the particle is $\boldsymbol{L} = m\boldsymbol{v}$. The moment of the linear momentum vector $m\boldsymbol{\dot{u}}$ about the origin O is defined as the angular momentum, $\boldsymbol{H}_O$, of P about O and is given by the cross-product relation for the moment of a vector:

$$\boldsymbol{H}_O = \boldsymbol{r} \times m\boldsymbol{v} \tag{6.4}$$

Figure 6-1(b) shows a two-dimensional representation of the vectors involved in Equation (6.4).

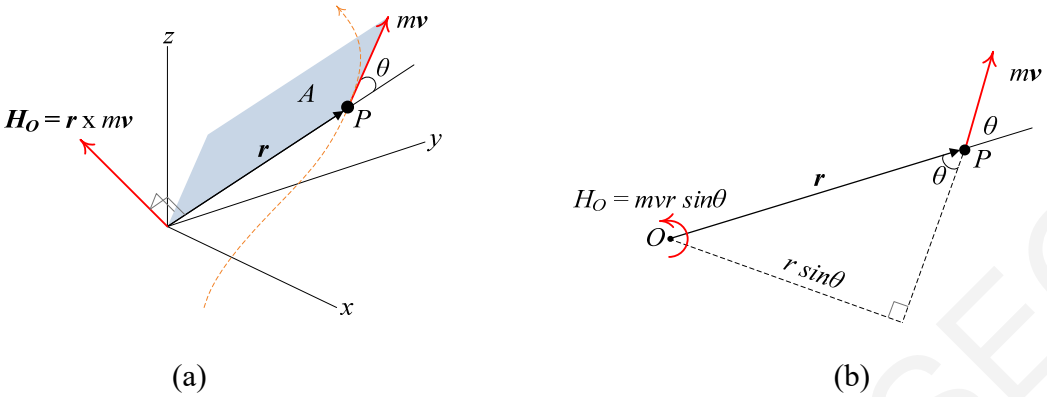

Figure 6-1: Three-dimensional (a) and two-dimensional (b) representation of the angular momentum, $\boldsymbol{H}_O$, of P about O.

For planar motion, the angular momentum vector has fixed direction (normal to the plane of motion), thus vector notation may be dropped. The magnitude of angular momentum is given by

$$H_O = mvr\sin\theta \tag{6.5}$$

Note that angular momentum is defined and measured relative to the origin chosen. This choice is arbitrary, and our origin can be chosen to correspond to the most convenient calculation.

Meaningful is that the moment of the forces, $\Sigma\boldsymbol{F}$, acting on the particle P, is related to its angular momentum. If $\Sigma\boldsymbol{F}$ represents the resultant of all forces acting on the particle, P, of Figure 6-1, the moment $\boldsymbol{M}_O$ about the origin O is the product

$$\Sigma\boldsymbol{M}_O = \boldsymbol{r}\times\Sigma\boldsymbol{F} = \boldsymbol{r}\times m\dot{\boldsymbol{v}} \tag{6.6}$$

where Newton's second law, Equation (6.1), has been substituted. Differentiating Equation (6.6) with time, using the rule for the differentiation of cross product we obtain

$$\dot{\boldsymbol{H}}_O = \dot{\boldsymbol{r}}\times m\boldsymbol{v} + \boldsymbol{r}\times m\dot{\boldsymbol{v}} = \boldsymbol{v}\times m\boldsymbol{v} + \boldsymbol{r}\times m\dot{\boldsymbol{v}} \tag{6.7}$$

The term $\boldsymbol{v}\times m\boldsymbol{v}$ is zero since the cross product of parallel vectors is identically zero. Substituting Equation (6.7) into Equation (6.6) yields

$$\Sigma\boldsymbol{M}_O = \dot{\boldsymbol{H}}_O \tag{6.8}$$

Equation (6.8) states that the moment of all forces acting on m about the fixed point O equals the time rate of change of angular momentum of m about O.

In addition, Equation (6.8) gives the instantaneous relation between the moment and the time-rate of change of angular momentum. The effect of the moment $\Sigma \boldsymbol{M}_O$ on the angular momentum of the particle over a finite period of time, is obtained by integrating Equation (6.8) from time t_1 to time t_2. Multiplying this equation by dt, gives

$$\Sigma \boldsymbol{M}_O dt = d\boldsymbol{H}_O \tag{6.9}$$

which by integrating we obtain

$$\int_{t_1}^{t_2} \Sigma \boldsymbol{M}_O dt = \left(\boldsymbol{H}_O\right)_2 - \left(\boldsymbol{H}_O\right)_1 = \Delta \boldsymbol{H}_O \tag{6.10}$$

where $\left(\boldsymbol{H}_O\right)_2 = \boldsymbol{r}_2 \times m\boldsymbol{v}_2$ and $\left(\boldsymbol{H}_O\right)_1 = \boldsymbol{r}_1 \times m\boldsymbol{v}_1$. The product of moment and time is defined as angular impulse. Equation (6.10) states that the total angular impulse on m about the fixed point O equals the corresponding change in angular momentum of m about O.

Similar with the principle of conversation of linear momentum, if the resultant moment about a fixed point O of all forces acting on a particle is zero during a particular interval of time, then

$$\Delta \boldsymbol{H}_O = 0 \quad \text{or} \quad \left(\boldsymbol{H}_O\right)_1 = \left(\boldsymbol{H}_O\right)_2 \tag{6.11}$$

This relation expresses the principle of conversation of angular momentum for a general mass system in the absence of an angular impulse.

6.2.3 Impulse-momentum principles on rigid bodies

In Section 6.2.1 and 6.2.2 the impulse-momentum principles covers any defined system of mass particles without restriction as to the connections between the particles of the system. These extended relations all apply to the motion of a rigid body, which is merely a special case of a general system mass.

Linear momentum

The linear momentum of a mass system is the vector sum of the linear momentum of all its particles

$$\boldsymbol{L} = \Sigma m_i \boldsymbol{v}_i \tag{6.12}$$

With $\boldsymbol{r}_i$ representing the position vector to m_i then, $\boldsymbol{v}_i = \dot{\boldsymbol{r}}_i$ and Equation (6.12) can be rewritten as

$$\boldsymbol{L} = \Sigma m_i \dot{\boldsymbol{r}}_i \tag{6.13}$$

For a system whose total mass is constant, Equation (6.13) can be rewritten as

$$\boldsymbol{L} = d\left(\Sigma m_i \dot{\boldsymbol{r}}_i\right)/dt \tag{6.14}$$

Substituting the principle of moments, $m\bar{\boldsymbol{r}} = \Sigma m_i \dot{\boldsymbol{r}}_i$, to locate the mass center, the momentum becomes

$$\boldsymbol{L} = d\left(m\bar{\boldsymbol{r}}\right)/dt = m\dot{\bar{\boldsymbol{r}}} \tag{6.15}$$

where $\dot{\bar{\boldsymbol{r}}}$ is the velocity $\bar{\boldsymbol{v}}$ of the mass center, Figure 6-2. Therefore, the linear momentum of any mass system, rigid or non-rigid, is

$$\boldsymbol{L} = m\bar{\boldsymbol{v}} \tag{6.16}$$

Note that it was unnecessary to employ the kinematic condition for a rigid block, Figure 6-2, which is

$$\boldsymbol{v}_i = \bar{\boldsymbol{v}} + \boldsymbol{\omega} \times \boldsymbol{\rho}_i \tag{6.17}$$

The time derivative of $\boldsymbol{L}$ is $m\dot{\bar{\boldsymbol{v}}} = m\bar{\boldsymbol{a}}$, where $\bar{\boldsymbol{a}}$ is the acceleration of the center of mass of the system, is the resultant external force acting on the system. Thus, we have

$$\Sigma \boldsymbol{F} = \dot{\boldsymbol{L}} \tag{6.18}$$

Integrating Equation (6.18) from time t_1 to time t_2 yields

$$\boldsymbol{L}_1 + \int_{t_1}^{t_2} \Sigma \boldsymbol{F} dt = \boldsymbol{L}_2 \tag{6.19}$$

In words, Equation (6.18) states that the resultant force equals the time rate of change of momentum and Equation (6.19) states that the initial linear momentum plus the linear impulse acting on the body equals the final linear momentum.

Angular momentum

Angular momentum is defined as the moment of linear momentum. The angular momentum about the mass center, G, of any prescribed system of mass equals with

$$\boldsymbol{H}_G = \sum \boldsymbol{\rho}_i \times m_i \boldsymbol{v}_i \tag{6.20}$$

which is the merely the vector sum of the moments about G of the linear momentum of all particles. With $\boldsymbol{r}_i$ representing the position vector to m_i then, $\boldsymbol{v}_i = \dot{\boldsymbol{r}}_i$ and Equation (6.20) can be rewritten as

$$\boldsymbol{H}_G = \sum \boldsymbol{\rho}_i \times m_i \dot{\boldsymbol{r}}_i \tag{6.21}$$

Referring to Figure 6-2, velocity $\dot{\boldsymbol{r}}_i$ can be rewritten as $\left(\dot{\bar{\boldsymbol{r}}} + \dot{\boldsymbol{\rho}}_i\right)$ and Equation (6.21) becomes

$$\boldsymbol{H}_G = \sum \boldsymbol{\rho}_i \times m_i \left(\dot{\bar{\boldsymbol{r}}} + \dot{\boldsymbol{\rho}}_i\right) = \sum \boldsymbol{\rho}_i \times m_i \dot{\bar{\boldsymbol{r}}} + \sum \boldsymbol{\rho}_i \times m_i \dot{\boldsymbol{\rho}}_i \tag{6.22}$$

The first term on the right side of this equation may be rewritten as $-\dot{\bar{\boldsymbol{r}}} \times \Sigma m_i \boldsymbol{\rho}_i$, which is zero because $\Sigma m_i \boldsymbol{\rho}_i = 0$ by definition of the mass center. Thus, Equation (6.21) can be rewritten as

$$\boldsymbol{H}_G = \sum \boldsymbol{\rho}_i \times m_i \dot{\boldsymbol{\rho}}_i \tag{6.23}$$

where $\dot{\boldsymbol{\rho}}_i$ is the velocity of m_i with respect to G.

The relative velocity equals with

$$\dot{\boldsymbol{\rho}}_i = \boldsymbol{\omega} \times \boldsymbol{\rho}_i \tag{6.24}$$

Where the angular velocity of the body is $\boldsymbol{\omega} = \omega \boldsymbol{k}$. The unit vector $\boldsymbol{k}$ is directed into the expression for the sense of $\boldsymbol{\omega}$ shown. Since $\dot{\boldsymbol{\rho}}_i$, $\boldsymbol{\rho}_i$, and $\boldsymbol{\omega}$ are at right angles to one another, the magnitude of $\dot{\boldsymbol{\rho}}_i$ is $\rho_i \omega$ and the magnitude of $\boldsymbol{\rho}_i \times m_i \dot{\boldsymbol{\rho}}_i$ is $\rho_i^2 \omega m_i$. Hence, Equation (6.23) can be rewritten as

$$\boldsymbol{H}_G = \sum \rho_i^2 m_i \omega \boldsymbol{k} = I \omega \boldsymbol{k} \tag{6.25}$$

where $I = \Sigma m_i \rho_i^2$ is the mass moment of inertia of the body about its mass center.

For planar motion, the angular-momentum vector is always normal to the plane of motion, vector notation is generally unnecessary, and the angular momentum about the mass center can be written as

$$H_G = I \omega \tag{6.26}$$

The moment-angular-momentum relation, see Section 6.2.2, which is scalar notation for plane motion, equals with

$$\Sigma M_G = \dot{H}_G \tag{6.27}$$

Integrating Equation (6.27) from time t_1 to time t_2 yields

$$\left(H_G\right)_1 + \int_{t_1}^{t_2} \Sigma M_G dt = \left(H_G\right)_2 \tag{6.28}$$

In words, Equation (6.27) states that the sum of the moments about the mass center of all forces acting on the body equals the time rate of change of angular momentum about the mass center. Equation (6.28) states that the initial angular momentum about the mass center G plus the external angular impulse about G equals the final angular momentum about G.

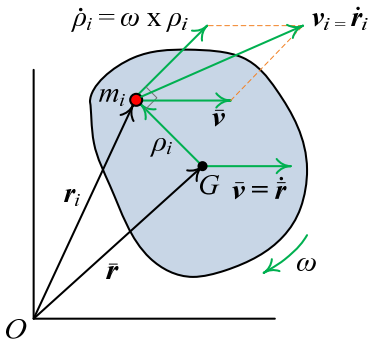

Figure 6-2: Impulse-momentum principles on rigid block.

6.3 Impact in Rocking Regime

This section is based on previous work done by Roussis et al. (2008). During the rocking oscillation regime, the dynamic response of the system is strongly affected by the occurrence of impact(s) between the block and the horizontally-moving base. Based on the assumption of perfectly inelastic impact, the block can exhibit two possible response mechanisms following impact: (a) rocking about the impacting corner, when the block re-uplifts (no bouncing), and (b) pure translation in full-contact with the base, when the block's rocking motion ceases after impact. The formulation of impact is divided into three phases: pre-impact, impact, and post-impact, as illustrated schematically in Figure 6-3 and Figure 6-6. In the following, a superscript "-" refers to a pre-impact quantity and a superscript "+" to a post-impact quantity.

6.3.1 Pure rocking continues after impact

Derivation for the case of impact during rocking about point O

Consider the system at the instant when the block hits the moving base from rocking about O and re-uplifts pivoting about the impacting corner, O' (Figure 6-3a). As mentioned before, impact is accompanied by an instantaneous change in velocities, with the system displacements being unchanged. Therefore, the impact analysis is reduced to the computation of the initial conditions for the post-impact motion, $\dot{u}^+$ and $\dot{\theta}^+$, given the position and the pre-impact velocities, $\dot{u}^-$ and $\dot{\theta}^-$.

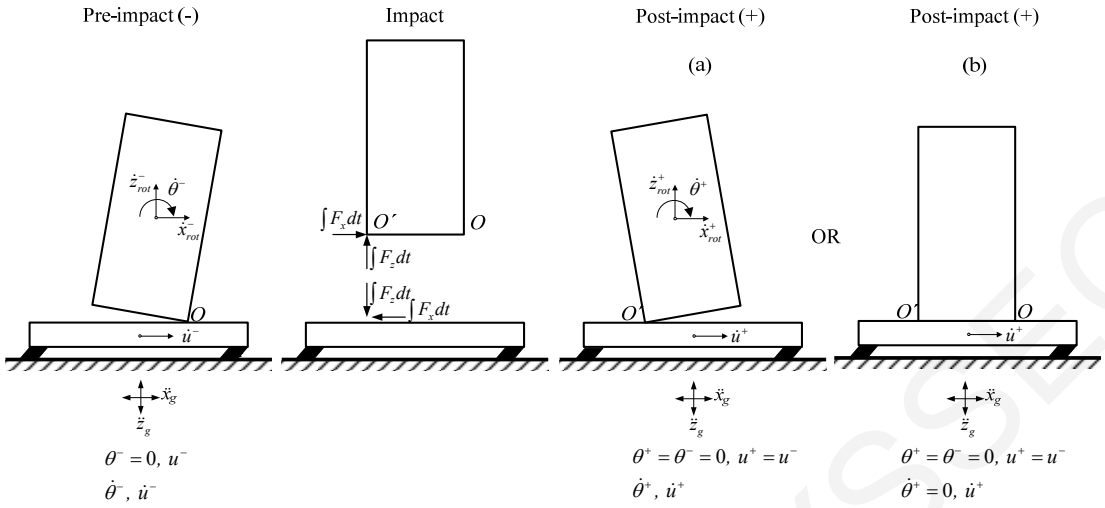

Figure 6-3: Impact from rocking about O followed by
(a) re-uplift about O' and (b) termination of rocking.

With regard to the block, the principle of linear impulse and momentum in the x and z direction requires that

$$\int F_x dt = \left(\Delta L\right)_x = L_x^+ - L_x^- : \quad \int F_x dt = m\dot{X}^+ - m\dot{X}^- \tag{6.29}$$

$$\int F_z dt = \left(\Delta L\right)_z = L_z^+ - L_z^- : \quad \int F_z dt = m\dot{Z}^+ - m\dot{Z}^- \tag{6.30}$$

in which $\int F_x dt$ and $\int F_z dt$ are the horizontal and vertical impulses (assumed to act at O'); $\dot{X}^- = \left(\dot{u}^- + \dot{x}_g\right) + \dot{x}_{rot}^-$, $\dot{X}^+ = \left(\dot{u}^+ + \dot{x}_g\right) + \dot{x}_{rot}^+$ and $\dot{Z}^- = \left(\dot{z}_{rot}^- + \dot{z}_g\right)$, $\dot{Z}^+ = \left(\dot{z}_{rot}^+ + \dot{z}_g\right)$ are the absolute pre- and post-impact horizontal and vertical velocities of the mass center of the block, respectively; $\dot{x}_{rot}^-$, $\dot{x}_{rot}^+$ and $\dot{z}_{rot}^-$, $\dot{z}_{rot}^+$ are the relative pre- and post-impact horizontal and vertical velocities of the mass center of the block due to the rocking, relative to the rigid base; L_x^-, L_x^+, L_z^- and L_z^+ are the pre- and post-impact horizontal and vertical linear momentum, respectively; $\left(\Delta L\right)_x$ and $\left(\Delta L\right)_z$ are the changes in horizontal and vertical linear momentum, respectively.

Substituting these expressions into Equations (6.29) and (6.30), we obtain

$$\int F_x dt = m\dot{u}^+ + m\dot{x}_{rot}^+ - m\dot{u}^- - m\dot{x}_{rot}^- \tag{6.31}$$

$$\int F_z dt = m\dot{z}_{rot}^{+} - m\dot{z}_{rot}^{-} \tag{6.32}$$

In addition, the principle of angular impulse and momentum states that

$$\int M_C dt = \Delta H_C = H_C^{+} - H_C^{-}: \; b\left(\int F_z dt\right) - h\left(\int F_x dt\right) = I\dot{\theta}^{+} - I\dot{\theta}^{-} \tag{6.33}$$

in which $\int M_C dt$ is the angular impulse; H_C^{-} and H_C^{+} are the pre- and post-impact angular momentum about the mass center, respectively; ΔH_C is the change in the angular momentum about the mass center.

In Equations (6.31) and (6.32), the pre- and post-impact horizontal and vertical components of the relative translational velocity of the mass center can be expressed in terms of the pre- and post-impact angular velocity of the block, $\dot{\theta}^{-}$ and $\dot{\theta}^{+}$ as follows.

For the pre-impact state, the translational velocity vector of the mass center (Figure 6-4) can be expresses as

$$\boldsymbol{v}^{-} = \boldsymbol{v}_O^{-} + \boldsymbol{\omega}^{-} \times \boldsymbol{r}_{C/O} \tag{6.34}$$

where $\boldsymbol{v}^{-}$ is pre-impact translational velocity vector of center-of-mass, $\boldsymbol{v}_O^{-}$ is pre-impact translational velocity vector of point O, $\boldsymbol{\omega}^{-}$ is pre-impact angular velocity vector of the block, and $\boldsymbol{r}_{C/O}$ is position vector of the mass center relative to point O.

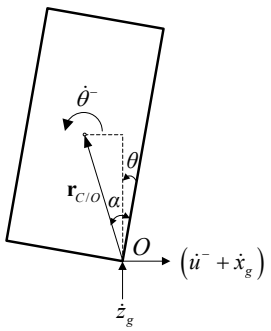

Figure 6-4: Components of pre-impact translational velocity of the isolated block for the case of impact during rocking about point *O*.

Expressions for these vector quantities are given below:

$$\boldsymbol{v}^{-} = \dot{X}^{-}\hat{\boldsymbol{i}} + \dot{Z}^{-}\hat{\boldsymbol{k}} = \left(\dot{u}^{-} + \dot{x}_g + \dot{x}_{rot}^{-}\right)\hat{\boldsymbol{i}} + \left(\dot{z}_{rot}^{-} + \dot{z}_g\right)\hat{\boldsymbol{k}} \tag{6.35}$$

$$\boldsymbol{v}_O^{-} = \left(\dot{u}^{-} + \dot{x}_g\right)\hat{\boldsymbol{i}} + \left(\dot{z}_g\right)\hat{\boldsymbol{k}} \tag{6.36}$$

$$\boldsymbol{\omega}^{-} = \dot{\theta}^{-}\hat{\boldsymbol{j}} \tag{6.37}$$

$$\boldsymbol{r}_{C/O} = -r\sin\left(a-\theta\right)\hat{\boldsymbol{i}} + r\cos\left(a-\theta\right)\hat{\boldsymbol{k}} \tag{6.38}$$

At impact, the angular rotation of the block becomes zero $\left(\theta = 0\right)$ and the position vector of the mass center relative to point O, $\boldsymbol{r}_{C/O}$, can be rewritten as

$$\boldsymbol{r}_{C/O} = -\left(r\sin a\right)\hat{\boldsymbol{i}} + \left(r\cos a\right)\hat{\boldsymbol{k}} = -b\hat{\boldsymbol{i}} + h\hat{\boldsymbol{k}} \tag{6.39}$$

in which $\hat{\boldsymbol{i}}$ and $\hat{\boldsymbol{k}}$ are the horizontal and vertical unit vectors respectively.

On substituting Equations (6.35) through (6.39) into Equation (6.34), the pre-impact translational velocity becomes

$$\boldsymbol{v}^{-} \equiv \left(\dot{u}^{-} + \dot{x}_g + \dot{x}_{rot}^{-}\right)\hat{\boldsymbol{i}} + \left(\dot{z}_{rot}^{-} + \dot{z}_g\right)\hat{\boldsymbol{k}} = \left(\dot{u}^{-} + \dot{x}_g\right)\hat{\boldsymbol{i}} + \left(\dot{z}_g\right)\hat{\boldsymbol{k}} + \left(\dot{\theta}^{-}\hat{\boldsymbol{j}}\right)\times\left(-b\hat{\boldsymbol{i}} + h\hat{\boldsymbol{k}}\right) \tag{6.40}$$

which reduces to

$$\dot{x}_{rot}^{-}\hat{\boldsymbol{i}} + \dot{z}_{rot}^{-}\hat{\boldsymbol{k}} = \left(b\dot{\theta}^{-}\right)\hat{\boldsymbol{k}} + \left(h\dot{\theta}^{-}\right)\hat{\boldsymbol{i}} \tag{6.41}$$

from which the pre-impact horizontal and vertical components of $\boldsymbol{v}^{-}$ can be retrieved as

$$\dot{x}_{rot}^{-} = h\dot{\theta}^{-} \tag{6.42}$$

$$\dot{z}_{rot}^{-} = b\dot{\theta}^{-} \tag{6.43}$$

For the post-impact state, the translational velocity vector of the mass center (Figure 6-5) can be expresses as

$$\boldsymbol{v}^{+} = \boldsymbol{v}_{O'}^{+} + \boldsymbol{\omega}^{+}\times\boldsymbol{r}_{C/O'} \tag{6.44}$$

where $\boldsymbol{v}^+$ is post-impact translational velocity vector of center-of-mass, $\boldsymbol{v}_{O'}^+$ is post-impact translational velocity vector of point O', $\boldsymbol{\omega}^+$ is post-impact angular velocity vector of the block, and $\boldsymbol{r}_{C/O'}$ is position vector of the mass center relative to point O'.

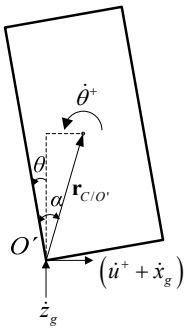

Figure 6-5: Components of post-impact translational velocity of the isolated block for the case of impact during rocking about point *O*.

Expressions for these vector quantities are given below:

$$\boldsymbol{v}^+ = \dot{X}^+\hat{\boldsymbol{i}} + \dot{Z}^+\hat{\boldsymbol{k}} = \left(\dot{u}^+ + \dot{x}_g + \dot{x}_{rot}^+\right)\hat{\boldsymbol{i}} + \left(\dot{z}_{rot}^+ + \dot{z}_g\right)\hat{\boldsymbol{k}} \tag{6.45}$$

$$\boldsymbol{v}_{O'}^+ = \left(\dot{u}^+ + \dot{x}_g\right)\hat{\boldsymbol{i}} + \left(\dot{z}_g\right)\hat{\boldsymbol{k}} \tag{6.46}$$

$$\boldsymbol{\omega}^+ = \dot{\theta}^+\hat{\boldsymbol{j}} \tag{6.47}$$

$$\boldsymbol{r}_{C/O'} = r\sin\left(a-\theta\right)\hat{\boldsymbol{i}} + r\cos\left(a-\theta\right)\hat{\boldsymbol{k}} \tag{6.48}$$

At impact the position vector of the mass center relative to point O', $\boldsymbol{r}_{C/O'}$, becomes

$$\boldsymbol{r}_{C/O'} = \left(r\sin a\right)\hat{\boldsymbol{i}} + \left(r\cos a\right)\hat{\boldsymbol{k}} = b\hat{\boldsymbol{i}} + h\hat{\boldsymbol{k}} \tag{6.49}$$

On substituting Equations (6.45) through (6.49) into Equation (6.44), the post-impact translational velocity becomes

$$\boldsymbol{v}^+ \equiv \left(\dot{u}^+ + \dot{x}_g + \dot{x}_{rot}^+\right)\hat{\boldsymbol{i}} + \left(\dot{z}_{rot}^+ + \dot{z}_g\right)\hat{\boldsymbol{k}} = \left(\dot{u}^+ + \dot{x}_g\right)\hat{\boldsymbol{i}} + \left(\dot{z}_g\right)\hat{\boldsymbol{k}} + \left(\dot{\theta}^+\hat{\boldsymbol{j}}\right)\times\left(b\hat{\boldsymbol{i}} + h\hat{\boldsymbol{k}}\right) \tag{6.50}$$

which simplifies to

$$\dot{x}_{rot}^{+}\hat{\boldsymbol{i}} + \dot{z}_{rot}^{+}\hat{\boldsymbol{k}} = \left(-b\dot{\theta}^{+}\right)\hat{\boldsymbol{k}} + \left(h\dot{\theta}^{+}\right)\hat{\boldsymbol{i}} \tag{6.51}$$

from which the post-impact horizontal and vertical components of $\boldsymbol{v}^{+}$ can be retrieved as

$$\dot{x}_{rot}^{+} = h\dot{\theta}^{+} \tag{6.52}$$

$$\dot{z}_{rot}^{+} = -b\dot{\theta}^{+} \tag{6.53}$$

Substitution of Equations (6.42) through (6.53) into Equations (6.31) through (6.33) yields

$$\int F_x dt = m\dot{u}^{+} + m\left(h\dot{\theta}^{+}\right) - m\dot{u}^{-} - m\left(h\dot{\theta}^{-}\right) \tag{6.54}$$

$$\int F_z dt = m\left(-b\dot{\theta}^{+}\right) - m\left(b\dot{\theta}^{-}\right) \tag{6.55}$$

$$b\left(\int F_z dt\right) - h\left(\int F_x dt\right) = I\left(\dot{\theta}^{+}\right) - I\left(\dot{\theta}^{-}\right) \tag{6.56}$$

in which for rectangular block the centroid mass moment of inertia for the rectangular block is given by

$$I = \frac{m}{3}r^2 = \frac{m}{3}\left(b^2 + h^2\right) \tag{6.57}$$

Equations (6.54), (6.55) and (6.56) constitute a set of three equations in four unknowns, namely $\int F_x dt$, $\int F_z dt$, $\dot{\theta}^{+}$, $\dot{u}^{+}$.

Equivalently, the three Equations (6.54), (6.55) and (6.56) can be combined in one (by eliminating the two impulses) in two unknowns:

$$\left(4b^2 + 4h^2\right)\dot{\theta}^{+} + 3h\dot{u}^{+} = \left(4h^2 - 2b^2\right)\dot{\theta}^{-} + 3h\dot{u}^{-} \tag{6.58}$$

One additional equation is therefore required to uniquely determine the post-impact velocities $\dot{\theta}^{+}$ and $\dot{u}^{+}$. By considering the system in its entirety during the impact, it can be stated that the horizontal impulse on the system is zero, resulting in the conservation of the system's linear momentum in the horizontal direction. That is,

$$\begin{aligned}\left(\Delta L_{sys}\right)_x = \left(L_{sys}\right)_x^+ - \left(L_{sys}\right)_x^- = 0: \quad \left[\left(L_{base}\right)_x^+ + \left(L_{obj}\right)_x^+\right] - \left[\left(L_{base}\right)_x^- + \left(L_{obj}\right)_x^-\right] = 0 \\ \Rightarrow \left[m_b\left(\dot{u}^+ + \dot{x}_g\right) + m\left(\dot{u}^+ + \dot{x}_g + \dot{x}_{rot}^+\right)\right] = \left[m_b\left(\dot{u}^- + \dot{x}_g\right) + m\left(\dot{u}^- + \dot{x}_g + \dot{x}_{rot}^-\right)\right]\end{aligned} \tag{6.59}$$

in which $\left(L_{sys}\right)_x^-$ and $\left(L_{sys}\right)_x^+$ are the pre- and post-impact horizontal linear momentum of the system respectively; $\left(\Delta L_{sys}\right)_x$ is the change in horizontal linear momentum of the system.

Substituting Equations (6.42) and (6.52) in Equation (6.59) gives

$$m_b\dot{u}^+ + m\dot{u}^+ + mh\dot{\theta}^+ = m_b\dot{u}^- + m\dot{u}^- + mh\dot{\theta}^- \tag{6.60}$$

which upon rearranging terms becomes

$$\dot{u}^+ = \frac{1}{m_b + m}\left[\left(m_b + m\right)\dot{u}^- - mh\dot{\theta}^+ + mh\dot{\theta}^-\right] \tag{6.61}$$

Substituting Equation (6.61) in (6.58) gives

$$\left(4b^2 + 4h^2\right)\dot{\theta}^+ + \frac{3h}{m_b + m}\left[\left(m_b + m\right)\dot{u}^- - mh\dot{\theta}^+ + mh\dot{\theta}^-\right] = \left(4h^2 - 2b^2\right)\dot{\theta}^- + 3h\dot{u}^- \tag{6.62}$$

which yields the post-impact angular velocity of the block as a function of the pre-impact angular velocity as

$$\dot{\theta}^+ = \frac{\left(4m_bh^2 - 2m_bb^2 + mh^2 - 2mb^2\right)}{\left(4m_bh^2 + 4m_bb^2 + mh^2 + 4mb^2\right)}\dot{\theta}^- \tag{6.63}$$

Substituting the expression for $\dot{\theta}^+$ in Equation (6.61) gives the post-impact translational velocity as a function of the pre-impact translational and angular velocity as

$$\dot{u}^+ = \dot{u}^- + \frac{6mhb^2}{m_b + m}\left(\frac{m_b + m}{4m_bh^2 + 4m_bb^2 + mh^2 + 4mb^2}\right)\dot{\theta}^- \tag{6.64}$$

Equations (6.63) and (6.64) can be written as

$$\dot{\theta}^{+} = \frac{\lambda^2(\rho+4)-2(\rho+1)}{\lambda^2(\rho+4)+4(\rho+1)}\dot{\theta}^{-} \equiv \varepsilon\dot{\theta}^{-} \tag{6.65}$$

$$\dot{u}^{+} = \dot{u}^{-} + \frac{6\rho h}{\lambda^2(\rho+4)+4(\rho+1)}\dot{\theta}^{-} \equiv \dot{u}^{-} + \beta_1\dot{\theta}^{-} \tag{6.66}$$

in which $\lambda = h/b$ is the geometric aspect ratio and $\rho = m/m_b$ is the mass ratio.

Alternatively, instead of considering the conservation of the linear momentum (in the horizontal direction) of the entire system, one can apply the principle of linear impulse and momentum (in the horizontal direction) of the base alone, which states that

$$-\int F_x dt = \left(\Delta L_{base}\right)_x = \left(L_{base}\right)_x^{+} - \left(L_{base}\right)_x^{-} \tag{6.67}$$

in which $\left(\Delta L_{base}\right)_x$ is the change in horizontal linear momentum of the base; $\left(L_{base}\right)_x^{-} = m_b\left(\dot{u}^{-} + \dot{x}_g\right)$ and $\left(L_{base}\right)_x^{+} = m_b\left(\dot{u}^{+} + \dot{x}_g\right)$ are the pre- and post-impact horizontal linear momentum of the base respectively. Equation (6.67) can be rewritten in the form

$$\int F_x dt = m_b\dot{u}^{-} - m_b\dot{u}^{+} \tag{6.68}$$

Substituting Equation (6.68) into Equation (6.54) gives

$$m_b\dot{u}^{-} - m_b\dot{u}^{+} = m\dot{u}^{+} - m\dot{u}^{-} + mh\dot{\theta}^{+} - mh\dot{\theta}^{-} \tag{6.69}$$

which yields

$$\dot{u}^{+} = \frac{1}{m_b+m}\left[\left(m_b+m\right)\dot{u}^{-} - mh\dot{\theta}^{+} + mh\dot{\theta}^{-}\right] \tag{6.70}$$

Substituting Equation (6.70) in Equation (6.58) gives

$$\dot{\theta}^{+} = \frac{\left(4m_bh^2 - 2m_bb^2 + mh^2 - 2mb^2\right)}{\left(4m_bh^2 + 4m_bb^2 + mh^2 + 4mb^2\right)}\dot{\theta}^{-} \tag{6.71}$$

which is identical to the result derived by considering the conservation of the system's linear momentum in the horizontal direction.

Derivation for the case of impact during rocking about point O′

Consider the system at the instant when the block hits the moving base from rocking about O' and re-uplifts pivoting about the impacting corner, O (Figure 6-6a). As mentioned before, impact is accompanied by an instantaneous change in velocities, with the system displacements being unchanged. Therefore, the impact analysis is reduced to the computation of the initial conditions for the post-impact motion, $\dot{u}^+$ and $\dot{\theta}^+$, given the position and the pre-impact velocities, $\dot{u}^-$ and $\dot{\theta}^-$.

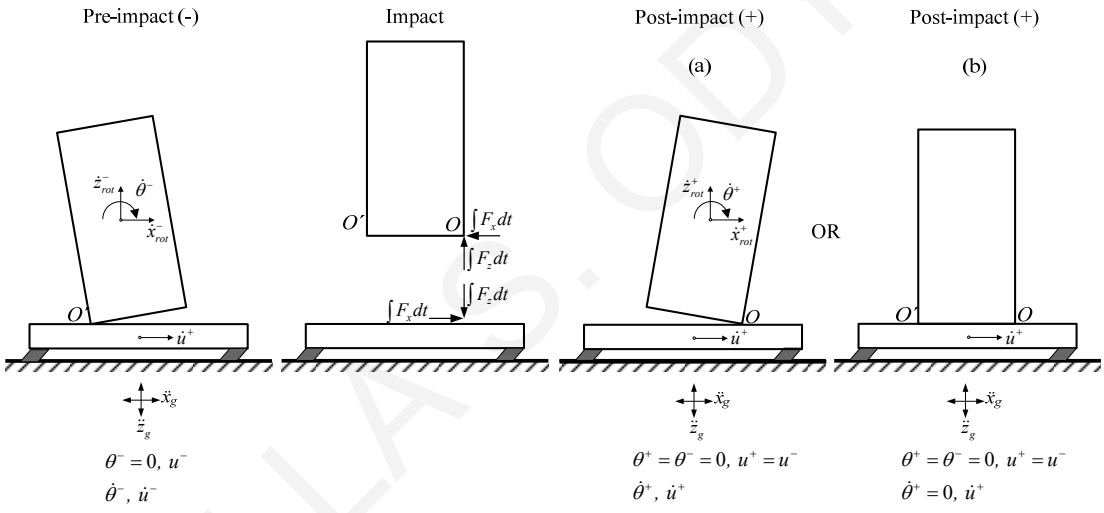

Figure 6-6: Impact from rocking about O' followed by (a) re-uplift about O and (b) termination of rocking.

With regard to the block, the principle of linear impulse and momentum in the x and z direction states that

$$\int F_x dt = \left(\Delta L\right)_x = L_x^+ - L_x^- : \quad \int F_x dt = m\dot{X}^+ - m\dot{X}^- \tag{6.72}$$

$$\int F_z dt = \left(\Delta L\right)_z = L_z^+ - L_z^- : \quad \int F_z dt = m\dot{Z}^+ - m\dot{Z}^- \tag{6.73}$$

in which $\int F_x dt$ and $\int F_z dt$ are the horizontal and vertical impulses (assumed to act at O); $\dot{X}^- = \left(\dot{u}^- + \dot{x}_g\right) + \dot{x}_{rot}^-$, $\dot{X}^+ = \left(\dot{u}^+ + \dot{x}_g\right) + \dot{x}_{rot}^+$ and $\dot{Z}^- = \left(\dot{z}_{rot}^- + \dot{z}_g\right)$, $\dot{Z}^+ = \left(\dot{z}_{rot}^+ + \dot{z}_g\right)$ are the absolute pre- and post-impact horizontal and vertical velocities of the mass center of the block, respectively; $\dot{x}_{rot}^-$, $\dot{x}_{rot}^+$ and $\dot{z}_{rot}^-$, $\dot{z}_{rot}^+$ are the relative pre- and post-impact horizontal and vertical velocities of the mass center of the block due to the rocking, relative to the rigid base; L_x^-, L_x^+, L_z^- and L_z^+ are the pre- and post-impact horizontal and vertical linear momentum, respectively; $\left(\Delta L\right)_x$ and $\left(\Delta L\right)_z$ are the changes in horizontal and vertical linear momentum, respectively.

Substituting these expressions into Equations (6.72) and (6.73), we obtain

$$\int F_x dt = m\dot{u}^+ + m\dot{x}_{rot}^+ - m\dot{u}^- - m\dot{x}_{rot}^- \tag{6.74}$$

$$\int F_z dt = m\dot{z}_{rot}^+ - m\dot{z}_{rot}^- \tag{6.75}$$

In addition, the principle of angular impulse and momentum states that

$$\int M_C dt = \Delta H_C = H_C^+ - H_C^- : \quad -b\left(\int F_z dt\right) - h\left(\int F_x dt\right) = I\dot{\theta}^+ - I\dot{\theta}^- \tag{6.76}$$

in which $\int M_C dt$ is the angular impulse; H_C^- and H_C^+ are the pre- and post-impact angular momentum about the mass center, respectively; ΔH_C is the change in the angular momentum about the mass center.

In Equations (6.74) and (6.75), the horizontal and vertical components of relative translational velocity of the center-of-mass can be expressed in terms of the pre- and post-impact angular velocity of the block, $\dot{\theta}^-$ and $\dot{\theta}^+$ as follows.

For the pre-impact state, the translational velocity vector of the mass center (Figure 6-7) can be expressed as

$$\boldsymbol{v}^- = \boldsymbol{v}_{O'}^- + \boldsymbol{\omega}^- \times \boldsymbol{r}_{C/O'} \tag{6.77}$$

where $\boldsymbol{v}^-$ is pre-impact translational velocity vector of center-of-mass, $\boldsymbol{v}_O^-$ is pre-impact translational velocity vector of point O', $\boldsymbol{\omega}^-$ is pre-impact angular velocity vector of the block, and $\boldsymbol{r}_{C/O}$ is position vector of the mass center relative to point O'.

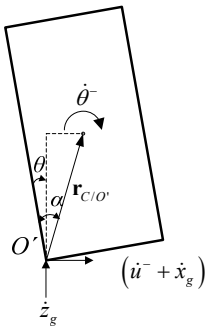

Figure 6-7: Components of pre-impact translational velocity of the isolated block for the case of impact during rocking about point O'.

Expressions for these vector quantities are given below:

$$\boldsymbol{v}^- = \dot{X}^-\hat{\boldsymbol{i}} + \dot{Z}^-\hat{\boldsymbol{k}} = \left(\dot{u}^- + \dot{x}_g + \dot{x}_{rot}^-\right)\hat{\boldsymbol{i}} + \left(\dot{z}_{rot}^- + \dot{z}_g\right)\hat{\boldsymbol{k}} \tag{6.78}$$

$$\boldsymbol{v}_{O'}^- = \left(\dot{u}^- + \dot{x}_g\right)\hat{\boldsymbol{i}} + \left(\dot{z}_g\right)\hat{\boldsymbol{k}} \tag{6.79}$$

$$\boldsymbol{\omega}^- = \dot{\theta}^-\hat{\boldsymbol{j}} \tag{6.80}$$

$$\boldsymbol{r}_{C/O'} = r\sin\left(a-\theta\right)\hat{\boldsymbol{i}} + r\cos\left(a-\theta\right)\hat{\boldsymbol{k}} \tag{6.81}$$

At impact, the angular rotation of the block is zero $\left(\theta = 0\right)$ and the position vector of the mass center relative to point O' can be rewritten as

$$\boldsymbol{r}_{C/O'} = \left(r\sin a\right)\hat{\boldsymbol{i}} + \left(r\cos a\right)\hat{\boldsymbol{k}} = b\hat{\boldsymbol{i}} + h\hat{\boldsymbol{k}} \tag{6.82}$$

On substituting Equations (6.78) through (6.82) into Equation (6.77), the post-impact translational velocity becomes

$$\boldsymbol{v}^- \equiv \left(\dot{u}^- + \dot{x}_g + \dot{x}_{rot}^-\right)\hat{\boldsymbol{i}} + \left(\dot{z}_{rot}^- + \dot{z}_g\right)\hat{\boldsymbol{k}} = \left(\dot{u}^- + \dot{x}_g\right)\hat{\boldsymbol{i}} + \left(\dot{z}_g\right)\hat{\boldsymbol{k}} + \left(\dot{\theta}^-\hat{\boldsymbol{j}}\right)\times\left(b\hat{\boldsymbol{i}} + h\hat{\boldsymbol{k}}\right) \tag{6.83}$$

which reduces to

$$\dot{x}_{rot}^{-}\hat{\boldsymbol{i}} + \dot{z}_{rot}^{-}\hat{\boldsymbol{k}} = \left(-b\dot{\theta}^{-}\right)\hat{\boldsymbol{k}} + \left(h\dot{\theta}^{-}\right)\hat{\boldsymbol{i}} \tag{6.84}$$

from which the pre-impact horizontal and vertical components of $\boldsymbol{v}^{-}$ can be retrieved as

$$\dot{x}_{rot}^{-} = h\dot{\theta}^{-} \tag{6.85}$$

$$\dot{z}_{rot}^{-} = -b\dot{\theta}^{-} \tag{6.86}$$

For the post-impact state, the translational velocity vector of the mass center (Figure 6-8) can be expressed as

$$\boldsymbol{v}^{+} = \boldsymbol{v}_{O}^{+} + \boldsymbol{\omega}^{+} \times \boldsymbol{r}_{C/O} \tag{6.87}$$

where $\boldsymbol{v}^{+}$ is post-impact translational velocity vector of center-of-mass, $\boldsymbol{v}_{O}^{+}$ is post-impact translational velocity vector of point O, $\boldsymbol{\omega}^{+}$ is post-impact angular velocity vector of the block, and $\boldsymbol{r}_{C/O}$ is position vector of the mass center relative to point O.

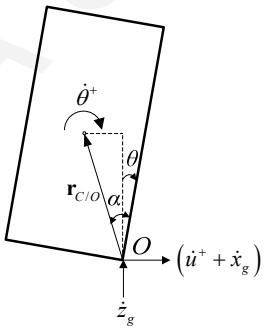

Figure 6-8: Components of post-impact translational velocity of the isolated block for the case of impact during rocking about point O'.

Expressions for these vector quantities are given below:

$$\boldsymbol{v}^{+} = \dot{X}^{+}\hat{\boldsymbol{i}} + \dot{Z}^{+}\hat{\boldsymbol{k}} = \left(\dot{u}^{+} + \dot{x}_{g} + \dot{x}_{rot}^{+}\right)\hat{\boldsymbol{i}} + \left(\dot{z}_{rot}^{+} + \dot{z}_{g}\right)\hat{\boldsymbol{k}} \tag{6.88}$$

$$\boldsymbol{v}_{O}^{+} = \left(\dot{u}^{+} + \dot{x}_{g}\right)\hat{\boldsymbol{i}} + \left(\dot{z}_{g}\right)\hat{\boldsymbol{k}} \tag{6.89}$$

$$\boldsymbol{\omega}^{+} = \theta^{+}\hat{\boldsymbol{j}} \tag{6.90}$$

$$\boldsymbol{r}_{C/O} = -r\sin\left(a-\theta\right)\hat{\boldsymbol{i}} + r\cos\left(a-\theta\right)\hat{\boldsymbol{k}} \tag{6.91}$$

At impact $\left(\theta = 0\right)$ the position vector of the mass center relative to point O becomes

$$\boldsymbol{r}_{C/O} = -\left(r\sin a\right)\hat{\boldsymbol{i}} + \left(r\cos a\right)\hat{\boldsymbol{k}} = -b\hat{\boldsymbol{i}} + h\hat{\boldsymbol{k}} \tag{6.92}$$

On substituting Equations (6.88) through (6.92) into Equation (6.87), the post-impact translational velocity becomes

$$\boldsymbol{v}^{+} \equiv \left(\dot{u}^{+} + \dot{x}_g + \dot{x}_{rot}^{+}\right)\hat{\boldsymbol{i}} + \left(\dot{z}_{rot}^{+} + \dot{z}_g\right)\hat{\boldsymbol{k}} = \left(\dot{u}^{+} + \dot{x}_g\right)\hat{\boldsymbol{i}} + \left(\dot{z}_g\right)\hat{\boldsymbol{k}} + \left(\dot{\theta}^{+}\hat{\boldsymbol{j}}\right)\times\left(-b\hat{\boldsymbol{i}} + h\hat{\boldsymbol{k}}\right) \tag{6.93}$$

which simplifies to

$$\dot{x}_{rot}^{+}\hat{\boldsymbol{i}} + \dot{z}_{rot}^{+}\hat{\boldsymbol{k}} = \left(b\dot{\theta}^{+}\right)\hat{\boldsymbol{k}} + \left(h\dot{\theta}^{+}\right)\hat{\boldsymbol{i}} \tag{6.94}$$

from which the post-impact horizontal and vertical components of $\boldsymbol{v}^{+}$ can be retrieved as

$$\dot{x}_{rot}^{+} = h\dot{\theta}^{+} \tag{6.95}$$

$$\dot{z}_{rot}^{+} = b\dot{\theta}^{+} \tag{6.96}$$

Substitution of Equations (6.85) through (6.96) into Equations (6.74) through (6.76) yields

$$\int F_x dt = m\dot{u}^{+} + m\left(h\dot{\theta}^{+}\right) - m\dot{u}^{-} - m\left(h\dot{\theta}^{-}\right) \tag{6.97}$$

$$\int F_z dt = m\left(b\dot{\theta}^{+}\right) - m\left(-b\dot{\theta}^{-}\right) \tag{6.98}$$

$$-b\left(\int F_z dt\right) - h\left(\int F_x dt\right) = I\left(\dot{\theta}^{+}\right) - I\left(\dot{\theta}^{-}\right) \tag{6.99}$$

in which the centroid mass moment of inertia for the rectangular block is given by Equation (6.57).

Equations (6.97), (6.98) and (6.99) constitute a set of three equations in four unknowns: $\int F_x dt$, $\int F_z dt$, $\dot{\theta}^+$, $\dot{u}^+$.

Equivalently, the three equations can be combined in one (by eliminating the two impulses) in two unknowns:

$$\left(4b^2+4h^2\right)\dot{\theta}^+ + 3h\dot{u}^+ = \left(4h^2-2b^2\right)\dot{\theta}^- + 3h\dot{u}^- \tag{6.100}$$

One additional equation is therefore required to uniquely determine the post-impact velocities $\dot{\theta}^+$ and $\dot{u}^+$. By considering the system in its entirety during the impact, it can be stated that the horizontal impulse on the system is zero, resulting in the conservation of the system's linear momentum in the horizontal direction. That is,

$$\begin{aligned} &\left(\Delta L_{sys}\right)_x = \left(L_{sys}\right)_x^+ - \left(L_{sys}\right)_x^- = 0: \quad \left[\left(L_{base}\right)_x^+ + \left(L_{obj}\right)_x^+\right] - \left[\left(L_{base}\right)_x^- + \left(L_{obj}\right)_x^-\right] = 0 \\ &\Rightarrow \left[m_b\left(\dot{u}^+ + \dot{x}_g\right) + m\left(\dot{u}^+ + \dot{x}_g + \dot{x}_{rot}^+\right)\right] = \left[m_b\left(\dot{u}^- + \dot{x}_g\right) + m\left(\dot{u}^- + \dot{x}_g + \dot{x}_{rot}^-\right)\right] \end{aligned} \tag{6.101}$$

in which $\left(L_{sys}\right)_x^-$ and $\left(L_{sys}\right)_x^+$ are the pre- and post-impact horizontal linear momentum of the system respectively; $\left(\Delta L_{sys}\right)_x$ is the change in horizontal linear momentum of the system.

Substituting Equations (6.85) and (6.95) in Equation (6.101)

$$m_b\dot{u}^+ + m\dot{u}^+ + mh\dot{\theta}^+ = m_b\dot{u}^- + m\dot{u}^- + mh\dot{\theta}^- \tag{6.102}$$

which yields

$$\dot{u}^+ = \frac{1}{m_b+m}\left[\left(m_b+m\right)\dot{u}^- - mh\dot{\theta}^+ + mh\dot{\theta}^-\right] \tag{6.103}$$

Substituting in (6.100) gives

$$\left(4b^2+4h^2\right)\dot{\theta}^+ + \frac{3h}{m_b+m}\left[\left(m_b+m\right)\dot{u}^- - mh\dot{\theta}^+ + mh\dot{\theta}^-\right] = \left(4h^2-2b^2\right)\dot{\theta}^- + 3h\dot{u}^- \tag{6.104}$$

which upon rearranging terms becomes

$$\dot{\theta}^{+}=\frac{\left(4m_b h^2-2m_b b^2+mh^2-2mb^2\right)}{\left(4m_b h^2+4m_b b^2+mh^2+4mb^2\right)}\dot{\theta}^{-} \tag{6.105}$$

Substituting the expression for $\dot{\theta}^{+}$ in Equation (6.102) gives

$$\dot{u}^{+}=\dot{u}^{-}+\left(\frac{6mhb^2}{4m_b h^2+4m_b b^2+mh^2+4mb^2}\right)\dot{\theta}^{-} \tag{6.106}$$

Equations (6.104) and (6.106) can be written as

$$\dot{\theta}^{+}=\frac{\lambda^2(\rho+4)-2(\rho+1)}{\lambda^2(\rho+4)+4(\rho+1)}\dot{\theta}^{-}\equiv\varepsilon\dot{\theta}^{-} \tag{6.107}$$

$$\dot{u}^{+}=\dot{u}^{-}+\frac{6\rho h}{\lambda^2(\rho+4)+4(\rho+1)}\dot{\theta}^{-}\equiv\dot{u}^{-}+\beta_1\dot{\theta}^{-} \tag{6.108}$$

in which $\lambda=h/b$ is the geometric aspect ratio and $\rho=m/m_b$ is the mass ratio.

Alternatively, instead of considering the conservation of the linear momentum (in the horizontal direction) of the entire system, one can apply the principle of linear impulse and momentum (in the horizontal direction) of the base alone, which states that

$$\begin{gathered}-\int F_x dt=\left(\Delta L_{base}\right)_x=\left(L_{base}\right)_x^{+}-\left(L_{base}\right)_x^{-}:\ -\int F_x dt=m_b\left(\dot{u}^{+}+\dot{x}_g\right)-m_b\left(\dot{u}^{-}+\dot{x}_g\right)\\ \Rightarrow\int F_x dt=m_b\dot{u}^{-}-m_b\dot{u}^{+}\end{gathered} \tag{6.109}$$

in which $\left(L_{base}\right)_x^{-}$ and $\left(L_{base}\right)_x^{+}$ are the pre- and post-impact horizontal linear momentum of the base respectively; $\left(\Delta L_{base}\right)_x$ is the change in horizontal linear momentum of the base.

Substitute (6.109) into (6.97):

$$m_b\dot{u}^{-}-m_b\dot{u}^{+}=m\dot{u}^{+}-m\dot{u}^{-}+mh\dot{\theta}^{+}-mh\dot{\theta}^{-} \tag{6.110}$$

which yields

$$\dot{u}^{+} = \frac{1}{m_b + m}\left[\left(m_b + m\right)\dot{u}^{-} - mh\dot{\theta}^{+} + mh\dot{\theta}^{-}\right] \tag{6.111}$$

Substituting in (6.100) gives

$$\dot{\theta}^{+} = \frac{\left(4m_b h^2 - 2m_b b^2 + mh^2 - 2mb^2\right)}{\left(4m_b h^2 + 4m_b b^2 + mh^2 + 4mb^2\right)}\dot{\theta}^{-} \tag{6.112}$$

which is identical to the result derived by considering the conservation of the system's linear momentum in the horizontal direction.

Observe that Equations (6.107) and (6.108) giving the post-impact velocities for impact from rocking about O' (realized when $\dot{\theta} > 0$) are identical to the Equations (6.65) and (6.66) giving the post-impact velocities for impact from rocking about O (realized when $\dot{\theta} < 0$).

The coefficient of "angular restitution" ε in Equation (6.107), associated with the reduction of the post-impact angular velocity of the block, is defined by

$$\varepsilon \doteq \frac{\lambda^2\left(\rho+4\right) - 2\left(\rho+1\right)}{\lambda^2\left(\rho+4\right) + 4\left(\rho+1\right)}, \tag{6.113}$$

and the coefficient of "linear restitution" β_1 in Equation (6.108), associated with the reduction of the post-impact linear velocity of the rigid base, is defined by

$$\beta_1 \doteq \frac{6\rho h}{\lambda^2\left(\rho+4\right) + 4\left(\rho+1\right)} \tag{6.114}$$

Equation (6.113) reveals that the coefficient of angular restitution ε depends both on the slenderness ratio λ and the mass ratio ρ. An upper bound for the coefficient of angular restitution is obtained by taking the limit as $\lambda \to \infty$, yielding

$$\varepsilon_{\max} = \lim_{\lambda\to\infty} \frac{\lambda^2\left(\rho+4\right) - 2\left(\rho+1\right)}{\lambda^2\left(\rho+4\right) + 4\left(\rho+1\right)} = 1 \tag{6.115}$$

The value $\varepsilon = 1$, implying preservation of the magnitude of the angular velocity after impact, is associated with an energy-lossless impact.

For the assumption of *no-bouncing* to be satisfied, the coefficient of angular restitution ε should have a positive value. In such a case, the angular velocity of the block will maintain sign upon impact, implying switching pole of rotation from one corner to the other. This requires that

$$\lambda > \sqrt{\frac{2(\rho+1)}{\rho+4}} \tag{6.116}$$

The variation of the coefficient of restitution ε with the slenderness ratio λ is shown in Figure 6-9a for different values of the mass ratio ρ. The strong effect of λ on the coefficient of angular restitution, and hence on the energy dissipated during impact, is evident from this figure. This effect is more pronounced in the lower λ-range (stocky blocks). Similarly, the dependency of coefficient ε on the mass ratio ρ is seen to be weak for very slender blocks, practically diminishing for $\lambda > 8$.

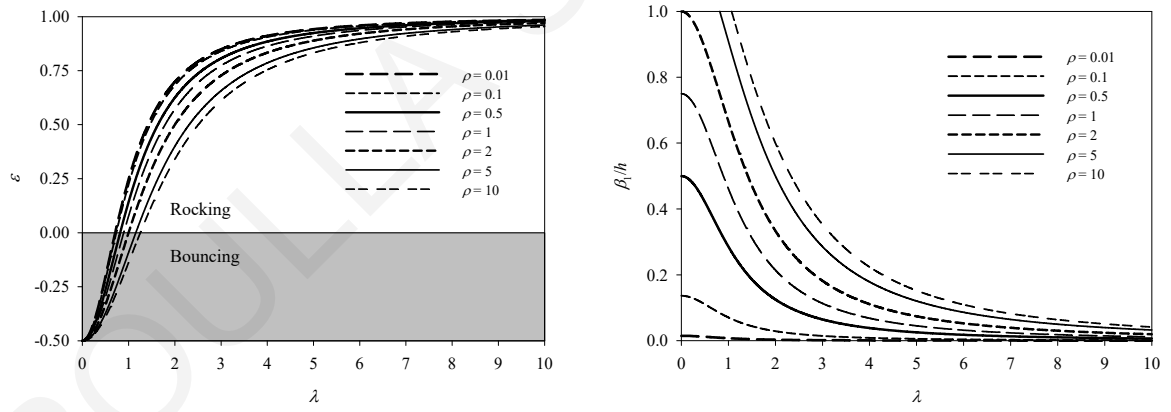

(a) (b)

Figure 6-9: Variation of (a) coefficient of angular restitution ε, and (b) coefficient $\bar{\beta}_1$ with slenderness ratio λ.

The coefficient β_1 in Equation (6.114), which is associated with the reduction of the post-impact linear velocity of the rigid base, depends not only on the parameters λ and ρ, but also

on the absolute size of the block (in terms of its height). The normalized coefficient $\bar{\beta}_1 \equiv \beta_1 / h$ is plotted against the slenderness ratio λ for different values of the mass ratio ρ in Figure 6-9b. Observe that the value of the coefficient $\bar{\beta}_1$ decays rapidly with the slenderness ratio λ. As follows from the comparison of Figure 6-9a and Figure 6-9b, the influence of the mass ratio ρ on the coefficient $\bar{\beta}_1$ is much greater than that on the coefficient ε.

Equation (6.108) elucidates the character of base-block dynamic interaction realized upon impact. In effect, the response of the "structure" (rocking block) modifies the input motion of the "foundation" (translating base). This inherent response feature stands in contrast to the dynamic behavior of the Housner-type model, in which the foundation mass is infinite. This interaction ceases to exist when coefficient β_1 becomes zero, which by virtue of Equation (6.114) occurs when $\lambda \to \infty$ or $\rho \to 0$. That is to say, the horizontal velocity of base will remain practically unchanged upon impact either in the case of extremely slender block (independently of the block size and value of the mass ratio) or in the case of extremely small block mass relative to the base mass (independently of the block size and slenderness). This observation is demonstrated in Figure 6-10 using different mass ratios, $\rho = 0.003$, $\rho = 0.5$, $\rho = 2$ and $\rho = 300$. As can be seen, the horizontal velocity of the base remains practically unchanged upon impact, $\theta / \alpha = 0$ (dot vertical lines), as the mass ratio, ρ, is getting smaller.

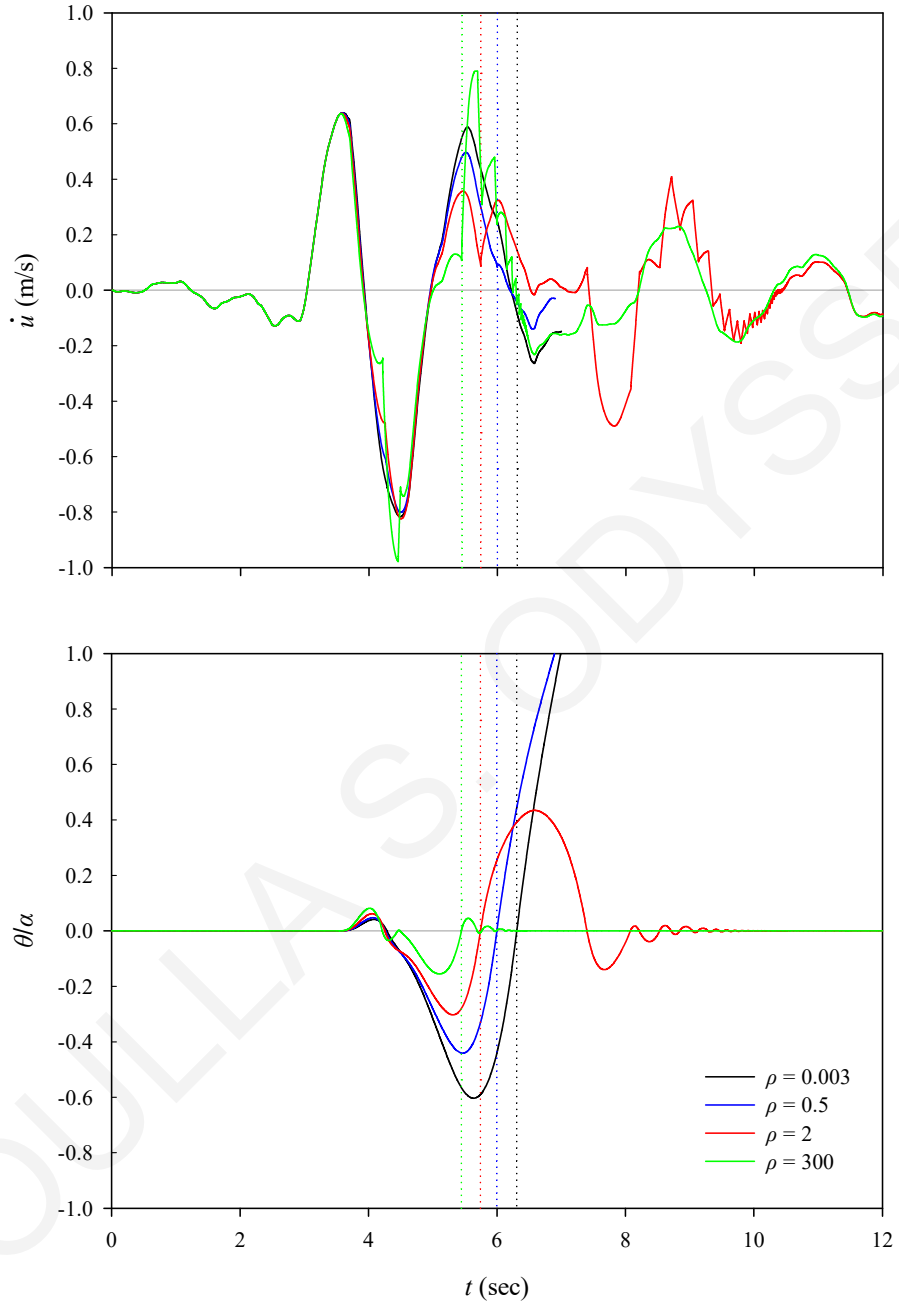

Figure 6-10: Influence of mass ratio on base-block dynamic interaction.

6.3.2 Pure system translation occurs after impact

When rocking of the block on top of the moving base ceases, the system will attain a pure-translation regime (Figure 6-3b and Figure 6-6b). In this case, the impact analysis is reduced to the computation of the post-impact translational velocity of the system, $\dot{u}^+$, given the position and the pre-impact velocities, $\dot{u}^-$ and $\dot{\theta}^-$.

Derivation for the case of impact during rocking about point O

Consider the system at the instant when the block hits the moving base from rocking about O (Figure 6-3b).

With regard to the block, the principle of linear impulse in the x direction states that

$$\int F_x dt = \left(\Delta L\right)_x = L_x^+ - L_x^- : \quad \int F_x dt = m\dot{X}^+ - m\dot{X}^- \tag{6.117}$$

in which $\int F_x dt$ is the horizontal impulse (assumed to act at O'); $\dot{X}^- = \left(\dot{u}^- + \dot{x}_g\right) + \dot{x}_{rot}^-$ and $\dot{X}^+ = \left(\dot{u}^+ + \dot{x}_g\right) + \dot{x}_{rot}^+$ are the absolute pre- and post-impact horizontal velocities of the mass center of the block, respectively; $\dot{x}_{rot}^-$ and $\dot{x}_{rot}^+$ are the relative pre- and post-impact horizontal velocities of the mass center of the block due to the rocking, relative to the rigid base; L_x^- and L_x^+ are the pre- and post-impact horizontal linear momentum, respectively; $\left(\Delta L\right)_x$ is the change in horizontal linear momentum.

Substituting this expression into Equation (6.117), we obtain

$$\int F_x dt = m\dot{u}^+ + m\dot{x}_{rot}^+ - m\dot{u}^- - m\dot{x}_{rot}^- \tag{6.118}$$

In Equation (6.118), the pre- and post-impact horizontal components of the relative translational velocity of the mass center can be expressed in terms of the pre-impact angular velocity of the block, $\dot{\theta}^-$ as follows.

For the pre-impact state, the translational velocity vector of the mass center (Figure 6-4) can be expressed as

$$\boldsymbol{v}^- = \boldsymbol{v}_O^- + \boldsymbol{\omega}^- \times \boldsymbol{r}_{C/O} \tag{6.119}$$

where $\boldsymbol{v}^-$ is pre-impact translational velocity vector of center-of-mass, $\boldsymbol{v}_O^-$ is pre-impact translational velocity vector of point O, $\boldsymbol{\omega}^-$ is pre-impact angular velocity vector of the block, and $\boldsymbol{r}_{C/O}$ is position vector of the mass center relative to point O.

Expressions for these vector quantities are given below:

$$\boldsymbol{v}^- = \dot{X}^-\hat{\boldsymbol{i}} + \dot{Z}^-\hat{\boldsymbol{k}} = \left(\dot{u}^- + \dot{x}_g + \dot{x}_{rot}^-\right)\hat{\boldsymbol{i}} + \left(\dot{z}_{rot}^- + \dot{z}_g\right)\hat{\boldsymbol{k}} \tag{6.120}$$

$$\boldsymbol{v}_O^- = \left(\dot{u}^- + \dot{x}_g\right)\hat{\boldsymbol{i}} + \left(\dot{z}_g\right)\hat{\boldsymbol{k}} \tag{6.121}$$

$$\boldsymbol{\omega}^- = \dot{\theta}^-\hat{\boldsymbol{j}} \tag{6.122}$$

$$\boldsymbol{r}_{C/O} = -r\sin\left(a-\theta\right)\hat{\boldsymbol{i}} + r\cos\left(a-\theta\right)\hat{\boldsymbol{k}} \tag{6.123}$$

At impact, the angular velocity of the block becomes zero $\left(\theta = 0\right)$ and the position vector of the mass center relative to point O can be rewritten as

$$\boldsymbol{r}_{C/O} = -\left(r\sin a\right)\hat{\boldsymbol{i}} + \left(r\cos a\right)\hat{\boldsymbol{k}} = -b\hat{\boldsymbol{i}} + h\hat{\boldsymbol{k}} \tag{6.124}$$

On substituting Equations (6.120) through (6.124) into Equation (6.119), the pre-impact translational velocity becomes

$$\boldsymbol{v}^- \equiv \left(\dot{u}^- + \dot{x}_g + \dot{x}_{rot}^-\right)\hat{\boldsymbol{i}} + \left(\dot{z}_{rot}^- + \dot{z}_g\right)\hat{\boldsymbol{k}} = \left(\dot{u}^- + \dot{x}_g\right)\hat{\boldsymbol{i}} + \left(\dot{z}_g\right)\hat{\boldsymbol{k}} + \left(\dot{\theta}^-\hat{\boldsymbol{j}}\right)\times\left(-b\hat{\boldsymbol{i}} + h\hat{\boldsymbol{k}}\right) \tag{6.125}$$

which reduces to

$$\dot{x}_{rot}^-\hat{\boldsymbol{i}} + \dot{z}_{rot}^-\hat{\boldsymbol{k}} = \left(b\dot{\theta}^-\right)\hat{\boldsymbol{k}} + \left(h\dot{\theta}^-\right)\hat{\boldsymbol{i}} \tag{6.126}$$

from which the pre-impact horizontal and vertical components of $\boldsymbol{v}^-$ can be retrieved as

$$\dot{x}_{rot}^- = h\dot{\theta}^- \tag{6.127}$$

$$\dot{z}_{rot}^- = b\dot{\theta}^- \tag{6.128}$$

For the post-impact state, the translational velocity vector of the mass center can be expressed as

$$\boldsymbol{v}^{+} = \boldsymbol{v}_{O'}^{+} + \boldsymbol{\omega}^{+} \times \boldsymbol{r}_{C/O'} \tag{6.129}$$

where $\boldsymbol{v}^{+}$ is post-impact translational velocity vector of center-of-mass, $\boldsymbol{v}_{O'}^{+}$ is post-impact translational velocity vector of point O', $\boldsymbol{\omega}^{+}$ is post-impact angular velocity vector of the block, and $\boldsymbol{r}_{C/O'}$ is position vector of the mass center relative to point O'.

Expressions for these vector quantities are given below:

$$\boldsymbol{v}^{+} = \dot{X}^{+}\hat{\boldsymbol{i}} + \dot{Z}^{+}\hat{\boldsymbol{k}} = \left(\dot{u}^{+} + \dot{x}_g + \dot{x}_{rot}^{+}\right)\hat{\boldsymbol{i}} + \left(\dot{z}_{rot}^{+} + \dot{z}_g\right)\hat{\boldsymbol{k}} \tag{6.130}$$

$$\boldsymbol{v}_{O'}^{+} = \left(\dot{u}^{+} + \dot{x}_g\right)\hat{\boldsymbol{i}} + \left(\dot{z}_g\right)\hat{\boldsymbol{k}} \tag{6.131}$$

$$\boldsymbol{\omega}^{+} = \dot{\theta}^{+}\hat{\boldsymbol{j}} = 0\,\hat{\boldsymbol{j}} \tag{6.132}$$

$$\boldsymbol{r}_{C/O'} = r\sin\left(a-\theta\right)\hat{\boldsymbol{i}} + r\cos\left(a-\theta\right)\hat{\boldsymbol{k}} \tag{6.133}$$

At impact $\theta = 0$, the position vector of the mass center relative to point O' becomes

$$\boldsymbol{r}_{C/O'} = \left(r\sin a\right)\hat{\boldsymbol{i}} + \left(r\cos a\right)\hat{\boldsymbol{k}} = b\hat{\boldsymbol{i}} + h\hat{\boldsymbol{k}} \tag{6.134}$$

On substituting Equations (6.130) through (6.134) into Equation (6.129), the post-impact translational velocity becomes

$$\boldsymbol{v}^{+} \equiv \left(\dot{u}^{+} + \dot{x}_g + \dot{x}_{rot}^{+}\right)\hat{\boldsymbol{i}} + \left(\dot{z}_{rot}^{+} + \dot{z}_g\right)\hat{\boldsymbol{k}} = \left(\dot{u}^{+} + \dot{x}_g\right)\hat{\boldsymbol{i}} + \left(\dot{z}_g\right)\hat{\boldsymbol{k}} + \left(0\,\hat{\boldsymbol{j}}\right)\times\left(b\hat{\boldsymbol{i}} + h\hat{\boldsymbol{k}}\right) \tag{6.135}$$

which simplifies to

$$\dot{x}_{rot}^{+}\hat{\boldsymbol{i}} + \dot{z}_{rot}^{+}\hat{\boldsymbol{k}} = 0\hat{\boldsymbol{k}} + 0\hat{\boldsymbol{i}} \tag{6.136}$$

from which the post-impact horizontal and vertical components of $\boldsymbol{v}^{+}$ can be retrieved as

$$\dot{x}_{rot}^{+} = 0 \tag{6.137}$$

$$\dot{z}_{rot}^{+} = 0 \tag{6.138}$$

Substitution of Equations (6.127) through (6.138) into Equation (6.118) yields

$$\int F_x dt = m\dot{u}^{+} - m\dot{u}^{-} - m\left(h\dot{\theta}^{-}\right) \tag{6.139}$$

which constitutes one equation in two unknowns: $\int F_x dt$, $\dot{u}^{+}$.

One additional equation is therefore required to uniquely determine the post-impact velocity $\dot{u}^{+}$. By considering the system in its entirety during the impact, it can be stated that the horizontal impulse on the system is zero, resulting in the conservation of the system's linear momentum in the horizontal direction. That is,

$$\begin{aligned} &\left(\Delta L_{sys}\right)_x = \left(L_{sys}\right)_x^{+} - \left(L_{sys}\right)_x^{-} = 0: \quad \left[\left(L_{base}\right)_x^{+} + \left(L_{obj}\right)_x^{+}\right] - \left[\left(L_{base}\right)_x^{-} + \left(L_{obj}\right)_x^{-}\right] = 0 \\ &\Rightarrow \left[m_b\left(\dot{u}^{+} + \dot{x}_g\right) + m\left(\dot{u}^{+} + \dot{x}_g + \dot{x}_{rot}^{+}\right)\right] = \left[m_b\left(\dot{u}^{-} + \dot{x}_g\right) + m\left(\dot{u}^{-} + \dot{x}_g + \dot{x}_{rot}^{-}\right)\right] \end{aligned} \tag{6.140}$$

Substituting Equations (6.127) and (6.137) in Equation (6.140) gives

$$m_b\dot{u}^{+} + m\dot{u}^{+} = m_b\dot{u}^{-} + m\dot{u}^{-} + mh\dot{\theta}^{-} \tag{6.141}$$

which upon rearranging terms becomes

$$\dot{u}^{+} = \frac{1}{m_b + m}\left[\left(m_b + m\right)\dot{u}^{-} + mh\dot{\theta}^{-}\right] \tag{6.142}$$

Equation (6.141) can be written as

$$\dot{u}^{+} = \dot{u}^{-} + \frac{\rho h}{\left(\rho + 1\right)}\dot{\theta}^{-} \equiv \dot{u}^{-} + \beta_2\dot{\theta}^{-} \tag{6.143}$$

in which $\rho = m / m_b$ is the mass ratio.

Alternatively, instead of considering the conservation of the linear momentum (in the horizontal direction) of the entire system, one can apply the principle of linear impulse and momentum (in the horizontal direction) of the base alone, which states that

$$-\int F_x dt = \left(\Delta L_{base}\right)_x = \left(L_{base}\right)_x^+ - \left(L_{base}\right)_x^- : \; -\int F_x dt = m_b\left(\dot{u}^+ + \dot{x}_g\right) - m_b\left(\dot{u}^- + \dot{x}_g\right)$$
$$\Rightarrow \int F_x dt = m_b\dot{u}^- - m_b\dot{u}^+ \tag{6.144}$$

Substitute (6.144) into (6.139):

$$\dot{u}^+ = \frac{1}{m_b + m}\left[\left(m_b + m\right)\dot{u}^- + mh\dot{\theta}^-\right] \tag{6.145}$$

which is identical to the result derived by considering the conservation of the system's linear momentum in the horizontal direction.

Derivation for the case of impact during rocking about point O′

Consider the system at the instant when the block hits the moving base from rocking about O' (Figure 6-6b).

With regard to the block, the principle of linear impulse in the x direction states that

$$\int F_x dt = \left(\Delta L\right)_x = \; L_x^+ - L_x^- : \; \int F_x dt = m\dot{X}^+ - m\dot{X}^- \tag{6.146}$$

in which $\int F_x dt$ is the horizontal impulse (assumed to act at O); $\dot{X}^- = \left(\dot{u}^- + \dot{x}_g\right) + \dot{x}_{rot}^-$ and $\dot{X}^+ = \left(\dot{u}^+ + \dot{x}_g\right) + \dot{x}_{rot}^+$ are the absolute pre- and post-impact horizontal velocities of the mass center of the block, respectively; $\dot{x}_{rot}^-$ and $\dot{x}_{rot}^+$ are the relative pre- and post-impact horizontal velocities of the mass center of the block due to the rocking, relative to the rigid base; L_x^- and L_x^+ are the pre- and post-impact horizontal linear momentum, respectively; $\left(\Delta L\right)_x$ is the change in horizontal linear momentum.

Substituting this expression into Equation(6.146), we obtain

$$\int F_x dt = m\dot{u}^+ + m\dot{x}_{rot}^+ - m\dot{u}^- - m\dot{x}_{rot}^- \tag{6.147}$$

In Equation (6.147), the horizontal component of relative translational velocity of the center-of-mass can be expressed in terms of the pre-impact angular velocity of the block, $\dot{\theta}^-$ as follows.

For the pre-impact state, the translational velocity vector of the mass center (Figure 6-7) can be expressed as

$$\boldsymbol{v}^{-} = \boldsymbol{v}_{O'}^{-} + \boldsymbol{\omega}^{-} \times \boldsymbol{r}_{C/O'} \tag{6.148}$$

where $\boldsymbol{v}^{-}$ is pre-impact translational velocity vector of center-of-mass, $\boldsymbol{v}_{O'}^{-}$ is pre-impact translational velocity vector of point O', $\boldsymbol{\omega}^{-}$ is pre-impact angular velocity vector of the block, and $\boldsymbol{r}_{C/O'}$ is position vector of the mass center relative to point O'.

Expressions for these vector quantities are given below:

$$\boldsymbol{v}^{-} = \dot{X}^{-}\hat{\boldsymbol{i}} + \dot{Z}^{-}\hat{\boldsymbol{k}} = \left(\dot{u}^{-} + \dot{x}_g + \dot{x}_{rot}^{-}\right)\hat{\boldsymbol{i}} + \left(\dot{z}_{rot}^{-} + \dot{z}_g\right)\hat{\boldsymbol{k}} \tag{6.149}$$

$$\boldsymbol{v}_{O'}^{-} = \left(\dot{u}^{-} + \dot{x}_g\right)\hat{\boldsymbol{i}} + \left(\dot{z}_g\right)\hat{\boldsymbol{k}} \tag{6.150}$$

$$\boldsymbol{\omega}^{-} = \dot{\theta}^{-}\hat{\boldsymbol{j}} \tag{6.151}$$

$$\boldsymbol{r}_{C/O'} = r\sin\left(a-\theta\right)\hat{\boldsymbol{i}} + r\cos\left(a-\theta\right)\hat{\boldsymbol{k}} \tag{6.152}$$

At impact, the angular rotation of the block becomes zero $\left(\theta = 0\right)$ and the position vector of center-of-mass relative to point O' can be rewritten as

$$\boldsymbol{r}_{C/O'} = \left(r\sin a\right)\hat{\boldsymbol{i}} + \left(r\cos a\right)\hat{\boldsymbol{k}} = b\hat{\boldsymbol{i}} + h\hat{\boldsymbol{k}} \tag{6.153}$$

On substituting Equations (6.149) through (6.153) into Equation (6.148), the pre-impact translational velocity becomes

$$\boldsymbol{v}^{-} \equiv \left(\dot{u}^{-} + \dot{x}_g + \dot{x}_{rot}^{-}\right)\hat{\boldsymbol{i}} + \left(\dot{z}_{rot}^{-} + \dot{z}_g\right)\hat{\boldsymbol{k}} = \left(\dot{u}^{-} + \dot{x}_g\right)\hat{\boldsymbol{i}} + \left(\dot{z}_g\right)\hat{\boldsymbol{k}} + \left(\dot{\theta}^{-}\hat{\boldsymbol{j}}\right)\times\left(b\hat{\boldsymbol{i}} + h\hat{\boldsymbol{k}}\right) \tag{6.154}$$

which reduces to

$$\dot{x}_{rot}^{-}\hat{\boldsymbol{i}} + \dot{z}_{rot}^{-}\hat{\boldsymbol{k}} = \left(-b\dot{\theta}^{-}\right)\hat{\boldsymbol{k}} + \left(h\dot{\theta}^{-}\right)\hat{\boldsymbol{i}} \tag{6.155}$$

from which the pre-impact horizontal and vertical components of $\boldsymbol{v}^{-}$ can be retrieved as

$$\dot{x}_{rot}^{-} = h\dot{\theta}^{-} \tag{6.156}$$

$$\dot{z}_{rot}^{-} = -b\dot{\theta}^{-} \tag{6.157}$$

For the post-impact state, the translational velocity vector of the mass center can be expressed as

$$\boldsymbol{v}^{+} = \boldsymbol{v}_{O}^{+} + \boldsymbol{\omega}^{+} \times \boldsymbol{r}_{C/O} \tag{6.158}$$

where $\boldsymbol{v}^{+}$ is post-impact translational velocity vector of center-of-mass, $\boldsymbol{v}_{O}^{+}$ is post-impact translational velocity vector of point O, $\boldsymbol{\omega}^{+}$ is post-impact angular velocity vector of the block, and $\boldsymbol{r}_{C/O}$ is position vector of the mass center relative to point O.

Expressions for these vector quantities are given below:

$$\boldsymbol{v}^{+} = \dot{X}^{+}\hat{\boldsymbol{i}} + \dot{Z}^{+}\hat{\boldsymbol{k}} = \left(\dot{u}^{+} + \dot{x}_{g} + \dot{x}_{rot}^{+}\right)\hat{\boldsymbol{i}} + \left(\dot{z}_{rot}^{+} + \dot{z}_{g}\right)\hat{\boldsymbol{k}} \tag{6.159}$$

$$\boldsymbol{v}_{O}^{+} = \left(\dot{u}^{+} + \dot{x}_{g}\right)\hat{\boldsymbol{i}} + \left(\dot{z}_{g}\right)\hat{\boldsymbol{k}} \tag{6.160}$$

$$\boldsymbol{\omega}^{+} = \dot{\theta}^{+}\hat{\boldsymbol{j}} = 0\,\hat{\boldsymbol{j}} \tag{6.161}$$

$$\boldsymbol{r}_{C/O} = -r\sin\left(a-\theta\right)\hat{\boldsymbol{i}} + r\cos\left(a-\theta\right)\hat{\boldsymbol{k}} \tag{6.162}$$

At impact $\left(\theta = 0\right)$ the position vector of the mass center relative to point O becomes

$$\boldsymbol{r}_{C/O} = -\left(r\sin a\right)\hat{\boldsymbol{i}} + \left(r\cos a\right)\hat{\boldsymbol{k}} = -b\hat{\boldsymbol{i}} + h\hat{\boldsymbol{k}} \tag{6.163}$$

On substituting Equations (6.159) through (6.163) into Equation (6.158), the post-impact translational velocity becomes

$$\boldsymbol{v}^{+} \equiv \left(\dot{u}^{+} + \dot{x}_{g} + \dot{x}_{rot}^{+}\right)\hat{\boldsymbol{i}} + \left(\dot{z}_{rot}^{+} + \dot{z}_{g}\right)\hat{\boldsymbol{k}} = \left(\dot{u}^{+} + \dot{x}_{g}\right)\hat{\boldsymbol{i}} + \left(\dot{z}_{g}\right)\hat{\boldsymbol{k}} + \left(0\,\hat{\boldsymbol{j}}\right)\times\left(-b\hat{\boldsymbol{i}} + h\hat{\boldsymbol{k}}\right) \tag{6.164}$$

which simplifies to

$$\dot{x}_{rot}^{+}\hat{\boldsymbol{i}} + \dot{z}_{rot}^{+}\hat{\boldsymbol{k}} = 0\hat{\boldsymbol{k}} + 0\hat{\boldsymbol{i}} \tag{6.165}$$

from which the post-impact horizontal and vertical components of $\boldsymbol{v}^+$ can be retrieved as

$$\dot{x}_{rot}^+ = 0 \tag{6.166}$$

$$\dot{z}_{rot}^+ = 0 \tag{6.167}$$

Substitution of Equations (6.156) through (6.167) into Equation (6.147) yields

$$\int F_x dt = m\dot{u}^+ - m\dot{u}^- - m\left(h\dot{\theta}^-\right) \tag{6.168}$$

which constitutes one equation in two unknowns: $\int F_x dt$, $\dot{u}^+$.

One additional equation is therefore required to uniquely determine the post-impact velocity $\dot{u}^+$. By considering the system in its entirety during the impact, it can be stated that the horizontal impulse on the system is zero, resulting in the conservation of the system's linear momentum in the horizontal direction. That is,

$$\begin{aligned} &\left(\Delta L_{sys}\right)_x = \left(L_{sys}\right)_x^+ - \left(L_{sys}\right)_x^- = 0: \quad \left[\left(L_{base}\right)_x^+ + \left(L_{obj}\right)_x^+\right] - \left[\left(L_{base}\right)_x^- + \left(L_{obj}\right)_x^-\right] = 0 \\ &\Rightarrow \left[m_b\left(\dot{u}^+ + \dot{x}_g\right) + m\left(\dot{u}^+ + \dot{x}_g + \dot{x}_{rot}^+\right)\right] = \left[m_b\left(\dot{u}^- + \dot{x}_g\right) + m\left(\dot{u}^- + \dot{x}_g + \dot{x}_{rot}^-\right)\right] \end{aligned} \tag{6.169}$$

Substitution of Equations (6.156) and (6.166) in Equation (6.169) gives

$$m_b\dot{u}^+ + m\dot{u}^+ = m_b\dot{u}^- + m\dot{u}^- + mh\dot{\theta}^- \tag{6.170}$$

which yields

$$\dot{u}^+ = \frac{1}{m_b + m}\left[\left(m_b + m\right)\dot{u}^- + mh\dot{\theta}^-\right] \tag{6.171}$$

Equation (6.170) can be written as

$$\dot{u}^+ = \dot{u}^- + \frac{\rho h}{\rho + 1}\dot{\theta}^- \equiv \dot{u}^- + \beta_2\dot{\theta}^- \tag{6.172}$$

in which $\rho = m / m_b$ is the mass ratio.

Alternatively, instead of considering the conservation of the linear momentum (in the horizontal direction) of the entire system, one can apply the principle of linear impulse and momentum (in the horizontal direction) of the base alone, which states that

$$-\int F_x dt = \left(\Delta L_{base}\right)_x = \left(L_{base}\right)_x^+ - \left(L_{base}\right)_x^- : \; -\int F_x dt = m_b\left(\dot{u}^+ + \dot{x}_g\right) - m_b\left(\dot{u}^- + \dot{x}_g\right)$$
$$\Rightarrow \int F_x dt = m_b\dot{u}^- - m_b\dot{u}^+ \tag{6.173}$$

Substituting Equation (6.173) into Equation (6.168) gives

$$\dot{u}^+ = \frac{1}{m_b + m}\left[\left(m_b + m\right)\dot{u}^- - mh\dot{\theta}^+ + mh\dot{\theta}^-\right] \tag{6.174}$$

which is identical to the result derived by considering the conservation of the system's linear momentum in the horizontal direction.

As it can be seen the Equation (6.174) giving the post-impact horizontal velocity for impact from rocking about O' (realized when $\dot{\theta} > 0$) is identical to the Equation (6.142) giving the post-impact horizontal velocity for impact from rocking about O (realized when $\dot{\theta} < 0$).

6.4 Impact in Slide-Rocking Regime

During slide-rocking regime, the response of the system can be drastically affected by the occurrence of impact(s) between the block and the horizontally-moving base. Under the assumption of perfectly inelastic impact, there are four possible response mechanisms following impact: (a) system translation when rocking and sliding motions cease after impact, Figure 6-11, (b) rocking about the impacting corner when the block re-uplifts (no bouncing), sliding motion ceases after impact, Figure 6-12, (c) sliding only when the rocking ceases after impact, Figure 6-13, or (d) sliding and rocking about the impacting corner when the block re-uplifts (no bouncing), Figure 6-14. In the following, a superscript "-" refers to a pre-impact quantity and a superscript "+" to a post-impact quantity.

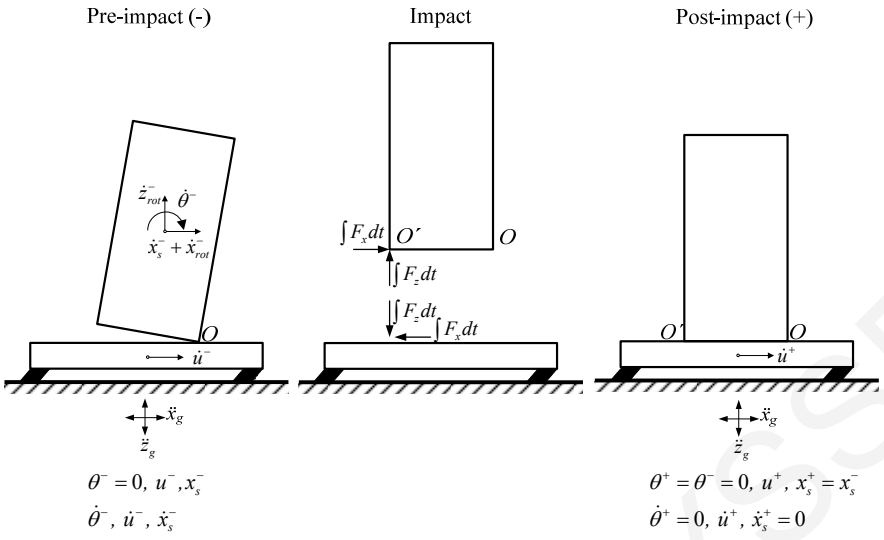

Figure 6-11: Impact from slide-rocking about *O* followed by pure system translation.

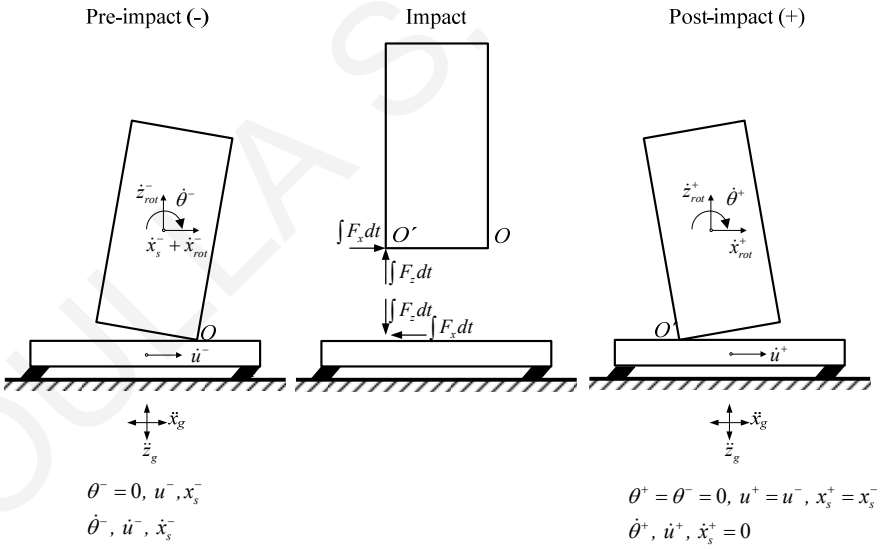

Figure 6-12: Impact from slide-rocking about *O* followed by pure rocking about *O′* (sliding ceases).

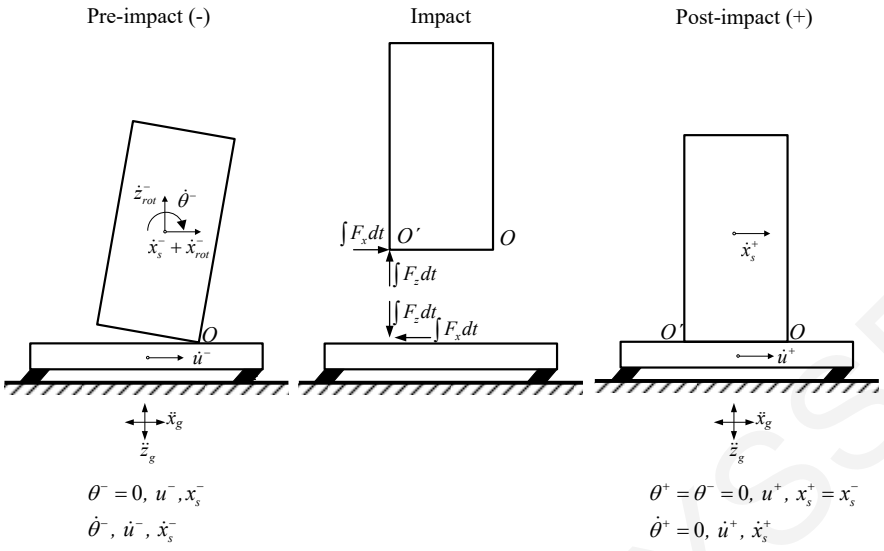

Figure 6-13: Impact from slide-rocking about *O* followed by pure sliding (rocking ceases).

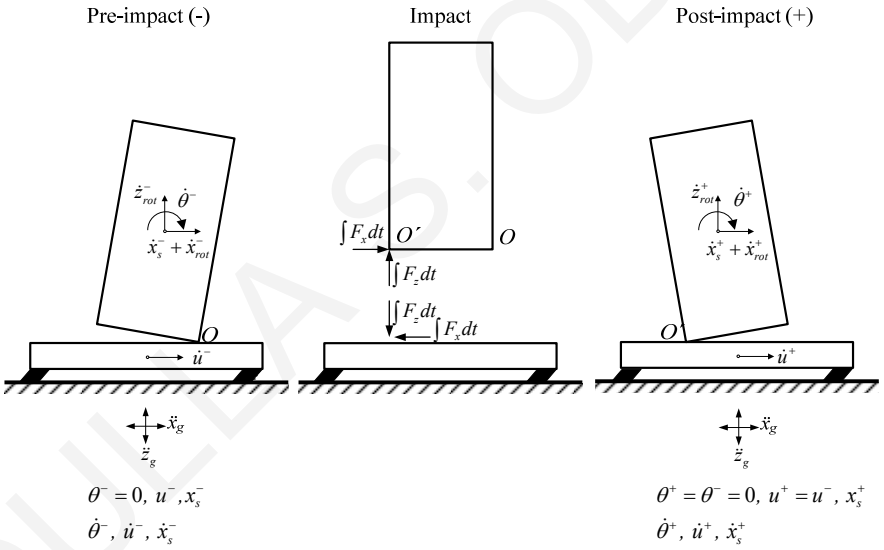

Figure 6-14: Impact from slide-rocking about *O* followed by slide-rocking about *O′*.

6.4.1 Pure system translation occurs after impact

When rocking and sliding of the block on top of the moving base ceases, the system will attain a pure-translation regime. In this case, the impact analysis is reduced to the computation of the post-impact translational velocity of the system, $\dot u^+$, given the position and the pre-impact velocities, $\dot u^-$, $\dot x_s^-$, and $\dot\theta^-$.

Derivation for the case of impact during rocking about point O

Consider the system at the instant when the block hits the moving base from rocking about O.

With regard to the block, the principle of linear impulse in the x direction states that

$$\int F_x dt = (\Delta L)_x = L_x^+ - L_x^- : \int F_x dt = m\dot{X}^+ - m\dot{X}^- \tag{6.175}$$

in which $\int F_x dt$ is the horizontal impulse (assumed to act at O'); $\dot{X}^- = (\dot{u}^- + \dot{x}_g) + \dot{x}_{rot}^- + \dot{x}_s^-$ and $\dot{X}^+ = (\dot{u}^+ + \dot{x}_g) + \dot{x}_{rot}^+ + \dot{x}_s^+$ are the absolute pre- and post-impact horizontal velocities of the mass center of the block, respectively; $\dot{x}_{rot}^-$ and $\dot{x}_{rot}^+$ are the relative pre- and post-impact horizontal velocities of the mass center of the block due to the rocking, relative to the rigid base; $\dot{x}_s^-$ and $\dot{x}_s^+$ are the relative pre- and post-impact horizontal velocities of the mass center of the block due to the sliding, relative to the rigid base; L_x^- and L_x^+ are the pre- and post-impact horizontal linear momentum, respectively; $(\Delta L)_x$ is the change in horizontal linear momentum.

Substituting this expression into Equation (6.175) we obtain

$$\int F_x dt = m\dot{u}^+ + m\dot{x}_{rot}^+ + m\dot{x}_s^+ - m\dot{u}^- - m\dot{x}_{rot}^- - m\dot{x}_s^- \tag{6.176}$$

In Equation (6.176), the pre- and post-impact horizontal components of the relative translational velocity of the mass center can be expressed in terms of the pre-impact angular velocity of the block, $\dot{\theta}^-$ as follows.

For the pre-impact state, the translational velocity vector of the mass center (Figure 6-15) can be expressed as

$$\boldsymbol{v}^- = \boldsymbol{v}_O^- + \boldsymbol{\omega}^- \times \boldsymbol{r}_{C/O} \tag{6.177}$$

where $\boldsymbol{v}^-$ is pre-impact translational velocity vector of center-of-mass, $\boldsymbol{v}_O^-$ is pre-impact translational velocity vector of point O, $\boldsymbol{\omega}^-$ is pre-impact angular velocity vector of the block, and $\boldsymbol{r}_{C/O}$ is position vector of the mass center relative to point O.

Expressions for these vector quantities are given below:

$$\boldsymbol{v}^{-} = \dot{X}^{-}\hat{\boldsymbol{i}} + \dot{Z}^{-}\hat{\boldsymbol{k}} = \left(\dot{u}^{-} + \dot{x}_g + \dot{x}_{rot}^{-} + \dot{x}_s^{-}\right)\hat{\boldsymbol{i}} + \left(\dot{z}_{rot}^{-} + \dot{z}_g\right)\hat{\boldsymbol{k}} \tag{6.178}$$

$$\boldsymbol{v}_O^{-} = \left(\dot{u}^{-} + \dot{x}_g + \dot{x}_s^{-}\right)\hat{\boldsymbol{i}} + \left(\dot{z}_g\right)\hat{\boldsymbol{k}} \tag{6.179}$$

$$\boldsymbol{\omega}^{-} = \dot{\theta}^{-}\hat{\boldsymbol{j}} \tag{6.180}$$

$$\boldsymbol{r}_{C/O} = -r\sin\left(a-\theta\right)\hat{\boldsymbol{i}} + r\cos\left(a-\theta\right)\hat{\boldsymbol{k}} \tag{6.181}$$

At impact, the angular velocity of the block becomes zero $\left(\theta = 0\right)$ and the position vector of center-of-mass relative to point O can be written as

$$\boldsymbol{r}_{C/O} = -\left(r\sin a\right)\hat{\boldsymbol{i}} + \left(r\cos a\right)\hat{\boldsymbol{k}} = -b\hat{\boldsymbol{i}} + h\hat{\boldsymbol{k}} \tag{6.182}$$

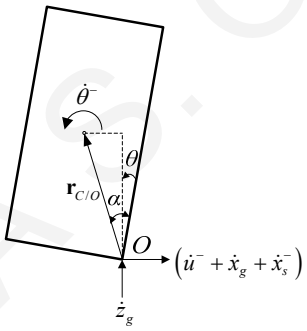

Figure 6-15: Components of pre-impact translational velocities of the isolated block for the case of impact during slide-rocking about point *O*.

On substituting Equations (6.178) through (6.182) into Equation (6.177), the pre-impact translational velocity becomes

$$\boldsymbol{v}^{-} \equiv \left(\dot{u}^{-} + \dot{x}_g + \dot{x}_{rot}^{-} + \dot{x}_s^{-}\right)\hat{\boldsymbol{i}} + \left(\dot{z}_{rot}^{-} + \dot{z}_g\right)\hat{\boldsymbol{k}} = \left(\dot{u}^{-} + \dot{x}_g + \dot{x}_s^{-}\right)\hat{\boldsymbol{i}} + \left(\dot{z}_g\right)\hat{\boldsymbol{k}} + \left(\dot{\theta}^{-}\hat{\boldsymbol{j}}\right)\times\left(-b\hat{\boldsymbol{i}} + h\hat{\boldsymbol{k}}\right) \tag{6.183}$$

which reduces to

$$\dot{x}_{rot}^{-}\hat{\boldsymbol{i}} + \dot{z}_{rot}^{-}\hat{\boldsymbol{k}} = \left(b\dot{\theta}^{-}\right)\hat{\boldsymbol{k}} + \left(h\dot{\theta}^{-}\right)\hat{\boldsymbol{i}} \tag{6.184}$$

from which the pre-impact horizontal and vertical components of $\boldsymbol{v}^-$ can be retrieved as

$$\dot{x}_{rot}^- = h\dot{\theta}^- \tag{6.185}$$

$$\dot{z}_{rot}^- = b\dot{\theta}^- \tag{6.186}$$

For the post-impact state, the translational velocity vector of the mass center can be expressed as

$$\boldsymbol{v}^+ = \boldsymbol{v}_{O'}^+ + \boldsymbol{\omega}^+ \times \boldsymbol{r}_{C/O'} \tag{6.187}$$

where $\boldsymbol{v}^+$ is post-impact translational velocity vector of center-of-mass, $\boldsymbol{v}_{O'}^+$ is post-impact translational velocity vector of point O', $\boldsymbol{\omega}^+$ is post-impact angular velocity vector of the block, and $\boldsymbol{r}_{C/O'}$ is position vector of the mass center relative to point O'.

Expressions for these vector quantities are given below:

$$\boldsymbol{v}^+ = \dot{X}^+\hat{\boldsymbol{i}} + \dot{Z}^+\hat{\boldsymbol{k}} = \left(\dot{u}^+ + \dot{x}_g + \dot{x}_{rot}^+\right)\hat{\boldsymbol{i}} + \left(\dot{z}_{rot}^+ + \dot{z}_g\right)\hat{\boldsymbol{k}} \tag{6.188}$$

$$\boldsymbol{v}_{O'}^+ = \left(\dot{u}^+ + \dot{x}_g\right)\hat{\boldsymbol{i}} + \left(\dot{z}_g\right)\hat{\boldsymbol{k}} \tag{6.189}$$

$$\boldsymbol{\omega}^+ = \dot{\theta}^+\hat{\boldsymbol{j}} = 0\,\hat{\boldsymbol{j}} \tag{6.190}$$

$$\boldsymbol{r}_{C/O'} = r\sin\left(a-\theta\right)\hat{\boldsymbol{i}} + r\cos\left(a-\theta\right)\hat{\boldsymbol{k}} \tag{6.191}$$

At impact $\theta = 0$, the position vector of the mass center relative to point O' becomes

$$\boldsymbol{r}_{C/O'} = \left(r\sin a\right)\hat{\boldsymbol{i}} + \left(r\cos a\right)\hat{\boldsymbol{k}} = b\hat{\boldsymbol{i}} + h\hat{\boldsymbol{k}} \tag{6.192}$$

On substituting Equations (6.188) through (6.192) into Equation (6.187), the post-impact translational velocity becomes

$$\boldsymbol{v}^+ \equiv \left(\dot{u}^+ + \dot{x}_g + \dot{x}_{rot}^+\right)\hat{\boldsymbol{i}} + \left(\dot{z}_{rot}^+ + \dot{z}_g\right)\hat{\boldsymbol{k}} = \left(\dot{u}^+ + \dot{x}_g\right)\hat{\boldsymbol{i}} + \left(\dot{z}_g\right)\hat{\boldsymbol{k}} + \left(0\,\hat{\boldsymbol{j}}\right)\times\left(b\hat{\boldsymbol{i}} + h\hat{\boldsymbol{k}}\right) \tag{6.193}$$

which reduces to

$$\dot{x}_{rot}^{+}\hat{\boldsymbol{i}} + \dot{z}_{rot}^{+}\hat{\boldsymbol{k}} = 0\hat{\boldsymbol{k}} + 0\hat{\boldsymbol{i}} \tag{6.194}$$

from which the post-impact horizontal and vertical components of $\boldsymbol{v}^{+}$ can be retrieved as

$$\dot{x}_{rot}^{+} = 0 \tag{6.195}$$

$$\dot{z}_{rot}^{+} = 0 \tag{6.196}$$

Substitution of Equations (6.185), (6.186), (6.195), (6.196) into Equation (6.176) yields

$$\int F_x dt = m\dot{u}^{+} - m\dot{u}^{-} - m\left(h\dot{\theta}^{-}\right) - m\dot{x}_s^{-} \tag{6.197}$$

which constitutes one equation in two unknowns: $\int F_x dt$, $\dot{u}^{+}$.

One additional equation is therefore required to uniquely determine the post-impact velocity $\dot{u}^{+}$. By considering the system in its entirety during the impact, it can be stated that the horizontal impulse on the system is zero, resulting in the conservation of the system's linear momentum in the horizontal direction. That is,

$$\begin{aligned} &\left(\Delta L_{sys}\right)_x = \left(L_{sys}\right)_x^{+} - \left(L_{sys}\right)_x^{-} = 0: \quad \left[\left(L_{base}\right)_x^{+} + \left(L_{obj}\right)_x^{+}\right] - \left[\left(L_{base}\right)_x^{-} + \left(L_{obj}\right)_x^{-}\right] = 0 \\ &\Rightarrow \left[m_b\left(\dot{u}^{+} + \dot{x}_g\right) + m\left(\dot{u}^{+} + \dot{x}_g + \dot{x}_s^{+} + \dot{x}_{rot}^{+}\right)\right] = \left[m_b\left(\dot{u}^{-} + \dot{x}_g\right) + m\left(\dot{u}^{-} + \dot{x}_g + \dot{x}^{-} + \dot{x}_s^{-} + \dot{x}_{rot}^{-}\right)\right] \end{aligned} \tag{6.198}$$

Substituting Equations (6.185), (6.186), (6.195), (6.196) in Equation (6.198) gives

$$m_b\dot{u}^{+} + m\dot{u}^{+} = m_b\dot{u}^{-} + m\dot{u}^{-} + mh\dot{\theta}^{-} + m\dot{x}_s^{-} \tag{6.199}$$

which upon rearranging terms becomes

$$\dot{u}^{+} = \frac{1}{m_b + m}\left[\left(m_b + m\right)\dot{u}^{-} + mh\dot{\theta}^{-} + m\dot{x}_s^{-}\right] \tag{6.200}$$

Equation (6.200) can be written as

$$\dot{u}^{+} = \dot{u}^{-} + \frac{\rho h}{\left(\rho+1\right)}\dot{\theta}^{-} + \frac{\rho}{\left(\rho+1\right)}\dot{x}_s^{-} \equiv \dot{u}^{-} + \beta_3\dot{\theta}^{-} + \frac{\beta_3}{h}\dot{x}_s^{-} \tag{6.201}$$

in which $\rho = m / m_b$ is the mass ratio.

Alternatively, instead of considering the conservation of the linear momentum (in the horizontal direction) of the entire system, one can apply the principle of linear impulse and momentum (in the horizontal direction) of the base alone, which states that

$$-\int F_x dt = \left(\Delta L_{base}\right)_x = \left(L_{base}\right)_x^+ - \left(L_{base}\right)_x^- : \; -\int F_x dt = m_b\left(\dot{u}^+ + \dot{x}_g\right) - m_b\left(\dot{u}^- + \dot{x}_g\right)$$
$$\Rightarrow \int F_x dt = m_b\dot{u}^- - m_b\dot{u}^+ \tag{6.202}$$

Substitute (6.197) into (6.202):

$$\dot{u}^+ = \frac{1}{m_b + m}\left[\left(m_b + m\right)\dot{u}^- + mh\dot{\theta}^- + m\dot{x}_s^-\right] \tag{6.203}$$

which is identical to the result derived by considering the conservation of the system's linear momentum in the horizontal direction.

Derivation for the case of impact during rocking about point O'

Consider the system at the instant when the block hits the moving base from rocking about O'.

With regard to the block, the principle of linear impulse in the x direction states that

$$\int F_x dt = \left(\Delta L\right)_x = L_x^+ - L_x^- : \; \int F_x dt = m\dot{X}^+ - m\dot{X}^- \tag{6.204}$$

in which $\int F_x dt$ is the horizontal impulse (assumed to act at O); $\dot{X}^- = \left(\dot{u}^- + \dot{x}_g\right) + \dot{x}_{rot}^- + \dot{x}_s^-$ and $\dot{X}^+ = \left(\dot{u}^+ + \dot{x}_g\right) + \dot{x}_{rot}^+ + \dot{x}_s^+$ are the absolute pre- and post-impact horizontal velocities of the mass center of the block, respectively; $\dot{x}_{rot}^-$ and $\dot{x}_{rot}^+$ are the relative pre- and post-impact horizontal velocities of the mass center of the block due to the rocking, relative to the rigid base; $\dot{x}_s^-$ and $\dot{x}_s^+$ are the relative pre- and post-impact horizontal velocities of the mass center of the block due to the sliding, relative to the rigid base; L_x^- and L_x^+ are the pre- and post-impact horizontal linear momentum, respectively; $\left(\Delta L\right)_x$ is the change in horizontal linear momentum.

Substituting this expression into Equation (6.204) we obtain

$$\int F_x dt = m\dot{u}^+ + m\dot{x}_{rot}^+ + m\dot{x}_s^+ - m\dot{u}^- - m\dot{x}_{rot}^- - m\dot{x}_s^- \tag{6.205}$$

In Equation (6.176), the pre- and post-impact horizontal components of the relative translational velocity of the mass center can be expressed in terms of the pre-impact angular velocity of the block, $\dot{\theta}^-$ as follows.

For the pre-impact state, the translational velocity vector of the mass center (Figure 6-16) can be expressed as

$$\boldsymbol{v}^- = \boldsymbol{v}_{O'}^- + \boldsymbol{\omega}^- \times \boldsymbol{r}_{C/O'} \tag{6.206}$$

where $\boldsymbol{v}^-$ is pre-impact translational velocity vector of center-of-mass, $\boldsymbol{v}_{O'}^-$ is pre -impact translational velocity vector of point O', $\boldsymbol{\omega}^-$ is pre-impact angular velocity vector of the block, and $\boldsymbol{r}_{C/O'}$ is position vector of the mass center relative to point O'.

Expressions for these vector quantities are given below:

$$\boldsymbol{v}^- = \dot{X}^-\hat{\boldsymbol{i}} + \dot{Z}^-\hat{\boldsymbol{k}} = \left(\dot{u}^- + \dot{x}_g + \dot{x}_{rot}^- + \dot{x}_s^-\right)\hat{\boldsymbol{i}} + \left(\dot{z}_{rot}^- + \dot{z}_g\right)\hat{\boldsymbol{k}} \tag{6.207}$$

$$\boldsymbol{v}_{O'}^- = \left(\dot{u}^- + \dot{x}_g + \dot{x}_s^-\right)\hat{\boldsymbol{i}} + \left(\dot{z}_g\right)\hat{\boldsymbol{k}} \tag{6.208}$$

$$\boldsymbol{\omega}^- = \dot{\theta}^-\hat{\boldsymbol{j}} \tag{6.209}$$

$$\boldsymbol{r}_{C/O'} = -r\sin\left(a-\theta\right)\hat{\boldsymbol{i}} + r\cos\left(a-\theta\right)\hat{\boldsymbol{k}} \tag{6.210}$$

At impact, the angular velocity of the block becomes zero $\left(\theta = 0\right)$ and the position vector of the mass center relative to point O' can be rewritten as

$$\boldsymbol{r}_{C/O'} = -\left(r\sin a\right)\hat{\boldsymbol{i}} + \left(r\cos a\right)\hat{\boldsymbol{k}} = -b\hat{\boldsymbol{i}} + h\hat{\boldsymbol{k}} \tag{6.211}$$

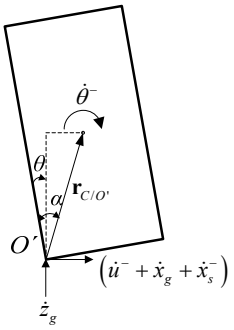

Figure 6-16: Components of pre-impact translational velocity of the isolated block for the case of impact during slide-rocking about point O'.

On substituting Equations (6.207) through (6.211) into Equation (6.206), the pre-impact translational velocity becomes

$$\boldsymbol{v}^- \equiv \left(\dot{u}^- + \dot{x}_g + \dot{x}_{rot}^- + \dot{x}_s^-\right)\hat{\boldsymbol{i}} + \left(\dot{z}_{rot}^- + \dot{z}_g\right)\hat{\boldsymbol{k}} = \left(\dot{u}^- + \dot{x}_g + \dot{x}_s^-\right)\hat{\boldsymbol{i}} + \left(\dot{z}_g\right)\hat{\boldsymbol{k}} + \left(\dot{\theta}^-\hat{\boldsymbol{j}}\right)\times\left(-b\hat{\boldsymbol{i}} + h\hat{\boldsymbol{k}}\right) \quad (6.212)$$

which reduces to

$$\dot{x}_{rot}^-\hat{\boldsymbol{i}} + \dot{z}_{rot}^-\hat{\boldsymbol{k}} = \left(b\dot{\theta}^-\right)\hat{\boldsymbol{k}} + \left(h\dot{\theta}^-\right)\hat{\boldsymbol{i}} \quad (6.213)$$

from which the pre-impact horizontal and vertical components of $\boldsymbol{v}^-$ can be retrieved as

$$\dot{x}_{rot}^- = h\dot{\theta}^- \quad (6.214)$$

$$\dot{z}_{rot}^- = b\dot{\theta}^- \quad (6.215)$$

For the post-impact state, the translational velocity vector of the mass center can be expressed as

$$\boldsymbol{v}^+ = \boldsymbol{v}_O^+ + \boldsymbol{\omega}^+ \times \boldsymbol{r}_{C/O} \quad (6.216)$$

where $\boldsymbol{v}^+$ is post-impact translational velocity vector of center-of-mass, $\boldsymbol{v}_O^+$ is post-impact translational velocity vector of point O, $\boldsymbol{\omega}^+$ is post-impact angular velocity vector of the block, and $\boldsymbol{r}_{C/O}$ is position vector of the mass center relative to point O.

Expressions for these vector quantities are given below:

$$\boldsymbol{v}^{+} = \dot{X}^{+}\hat{\boldsymbol{i}} + \dot{Z}^{+}\hat{\boldsymbol{k}} = \left(\dot{u}^{+} + \dot{x}_g + \dot{x}_{rot}^{+}\right)\hat{\boldsymbol{i}} + \left(\dot{z}_{rot}^{+} + \dot{z}_g\right)\hat{\boldsymbol{k}} \tag{6.217}$$

$$\boldsymbol{v}_O^{+} = \left(\dot{u}^{+} + \dot{x}_g\right)\hat{\boldsymbol{i}} + \left(\dot{z}_g\right)\hat{\boldsymbol{k}} \tag{6.218}$$

$$\boldsymbol{\omega}^{+} = \dot{\theta}^{+}\hat{\boldsymbol{j}} = 0\,\hat{\boldsymbol{j}} \tag{6.219}$$

$$\boldsymbol{r}_{C/O} = r\sin\left(a-\theta\right)\hat{\boldsymbol{i}} + r\cos\left(a-\theta\right)\hat{\boldsymbol{k}} \tag{6.220}$$

At impact $\left(\theta = 0\right)$, the position vector of the mass center relative to point O becomes

$$\boldsymbol{r}_{C/O} = \left(r\sin a\right)\hat{\boldsymbol{i}} + \left(r\cos a\right)\hat{\boldsymbol{k}} = b\hat{\boldsymbol{i}} + h\hat{\boldsymbol{k}} \tag{6.221}$$

On substituting Equations (6.217) through (6.221) into Equation (6.216), the post-impact translational velocity becomes

$$\boldsymbol{v}^{+} \equiv \left(\dot{u}^{+} + \dot{x}_g + \dot{x}_{rot}^{+}\right)\hat{\boldsymbol{i}} + \left(\dot{z}_{rot}^{+} + \dot{z}_g\right)\hat{\boldsymbol{k}} = \left(\dot{u}^{+} + \dot{x}_g\right)\hat{\boldsymbol{i}} + \left(\dot{z}_g\right)\hat{\boldsymbol{k}} + \left(0\hat{\boldsymbol{j}}\right)\times\left(b\hat{\boldsymbol{i}} + h\hat{\boldsymbol{k}}\right) \tag{6.222}$$

which reduces to

$$\dot{x}_{rot}^{+}\hat{\boldsymbol{i}} + \dot{z}_{rot}^{+}\hat{\boldsymbol{k}} = 0\hat{\boldsymbol{k}} + 0\hat{\boldsymbol{i}} \tag{6.223}$$

from which the post-impact horizontal and vertical components of $\boldsymbol{v}^{+}$ can be retrieved as

$$\dot{x}_{rot}^{+} = 0 \tag{6.224}$$

$$\dot{z}_{rot}^{+} = 0 \tag{6.225}$$

Substitution of Equations (6.185), (6.186), (6.195), (6.196) into Equation (6.176) yields

$$\int F_x dt = m\dot{u}^{+} - m\dot{u}^{-} - m\left(h\dot{\theta}^{-}\right) - m\dot{x}_s^{-} \tag{6.226}$$

which constitutes one equation in two unknowns: $\int F_x dt$, $\dot{u}^{+}$.

One additional equation is therefore required to uniquely determine the post-impact velocity $\dot{u}^{+}$. By considering the system in its entirety during the impact, it can be stated that the

horizontal impulse on the system is zero, resulting in the conservation of the system's linear momentum in the horizontal direction. That is,

$$\begin{aligned}\left(\Delta L_{sys}\right)_x = \left(L_{sys}\right)_x^+ - \left(L_{sys}\right)_x^- = 0: \quad \left[\left(L_{base}\right)_x^+ + \left(L_{obj}\right)_x^+\right] - \left[\left(L_{base}\right)_x^- + \left(L_{obj}\right)_x^-\right] = 0 \\ \Rightarrow \left[m_b\left(\dot{u}^+ + \dot{x}_g\right) + m\left(\dot{u}^+ + \dot{x}_g + \dot{x}_s^+ + \dot{x}_{rot}^+\right)\right] = \left[m_b\left(\dot{u}^- + \dot{x}_g\right) + m\left(\dot{u}^- + \dot{x}_g + \dot{x}^- + \dot{x}_s^- + \dot{x}_{rot}^-\right)\right]\end{aligned} \tag{6.227}$$

Substituting Equations (6.185), (6.186), (6.195), (6.196) in Equation (6.198) gives

$$m_b\dot{u}^+ + m\dot{u}^+ = m_b\dot{u}^- + m\dot{u}^- + mh\dot{\theta}^- + m\dot{x}_s^- \tag{6.228}$$

which upon rearranging terms becomes

$$\dot{u}^+ = \frac{1}{m_b + m}\left[\left(m_b + m\right)\dot{u}^- + mh\dot{\theta}^- + m\dot{x}_s^-\right] \tag{6.229}$$

Equation (6.200) can be written as

$$\dot{u}^+ = \dot{u}^- + \frac{\rho h}{\left(\rho + 1\right)}\dot{\theta}^- + \frac{\rho}{\left(\rho + 1\right)}\dot{x}_s^- \equiv \dot{u}^- + \beta_3\dot{\theta}^- + \frac{\beta_3}{h}\dot{x}_s^- \tag{6.230}$$

in which $\rho = m / m_b$ is the mass ratio.

Alternatively, instead of considering the conservation of the linear momentum (in the horizontal direction) of the entire system, one can apply the principle of linear impulse and momentum (in the horizontal direction) of the base alone, which states that

$$\begin{aligned}-\int F_x dt = \left(\Delta L_{base}\right)_x = \left(L_{base}\right)_x^+ - \left(L_{base}\right)_x^-: \quad -\int F_x dt = m_b\left(\dot{u}^+ + \dot{x}_g\right) - m_b\left(\dot{u}^- + \dot{x}_g\right) \\ \Rightarrow \int F_x dt = m_b\dot{u}^- - m_b\dot{u}^+\end{aligned} \tag{6.231}$$

Substitute (6.226) into (6.231):

$$\dot{u}^+ = \frac{1}{m_b + m}\left[\left(m_b + m\right)\dot{u}^- + mh\dot{\theta}^- + m\dot{x}_s^-\right] \tag{6.232}$$

which is identical to the result derived by considering the conservation of the system's linear momentum in the horizontal direction.

As it can be seen the Equation (6.232) giving the post-impact horizontal velocity for impact from slide-rocking about O' (realized when $\dot{\theta} > 0$) is identical to the Equation (6.203) giving the post-impact horizontal velocity for impact from slide-rocking about O (realized when $\dot{\theta} < 0$).

6.4.2 Pure rocking occurs after impact

Derivation for the case of impact during rocking about point O

Consider the system at the instant when the block hits the moving base from rocking about O and re-uplifts pivoting about the impacting corner, O'. As mentioned before, impact is accompanied by an instantaneous change in velocities, with the system displacements being unchanged. Therefore, the impact analysis is reduced to the computation of the initial conditions for the post-impact motion, $\dot{u}^+$, and $\dot{\theta}^+$, given the position and the pre-impact velocities, $\dot{u}^-$, $\dot{x}_s^-$, and $\dot{\theta}^-$.

With regard to the block, the principle of linear impulse and momentum in the x and z direction states that

$$\int F_x dt = \left(\Delta L\right)_x = L_x^+ - L_x^- : \quad \int F_x dt = m\dot{X}^+ - m\dot{X}^- \tag{6.233}$$

$$\int F_z dt = \left(\Delta L\right)_z = L_z^+ - L_z^- : \quad \int F_z dt = m\dot{Z}^+ - m\dot{Z}^- \tag{6.234}$$

in which $\int F_x dt$ and $\int F_z dt$ are the horizontal and vertical impulses (assumed to act at O'); $\dot{X}^- = \left(\dot{u}^- + \dot{x}_g\right) + \dot{x}_s^- + \dot{x}_{rot}^-$, $\dot{X}^+ = \left(\dot{u}^+ + \dot{x}_g\right) + \dot{x}_s^+ + \dot{x}_{rot}^+$ and $\dot{Z}^- = \left(\dot{z}_{rot}^- + \dot{z}_g\right)$, $\dot{Z}^+ = \left(\dot{z}_{rot}^+ + \dot{z}_g\right)$ are the absolute pre- and post-impact horizontal and vertical velocities of the mass center of the block, respectively; $\dot{x}_{rot}^-$, $\dot{x}_{rot}^+$ and $\dot{z}_{rot}^-$, $\dot{z}_{rot}^+$ are the relative pre- and post-impact horizontal and vertical velocities of the mass center of the block due to the rocking, relative to the rigid base; $\dot{x}_s^-$ and $\dot{x}_s^+$ are the relative pre- and post-impact horizontal velocities of the mass center of the block due to the sliding, relative to the rigid base; L_x^-, L_x^+, L_z^- and L_z^+ are the pre- and post-impact horizontal and vertical linear momentum, respectively; $\left(\Delta L\right)_x$ and $\left(\Delta L\right)_z$ are the changes in horizontal and vertical linear momentum, respectively.

Substituting these expressions into Equations (6.233) and (6.234) we obtain

$$\int F_x dt = m\dot{u}^+ + m\dot{x}_s^+ + m\dot{x}_{rot}^+ - m\dot{u}^- - m\dot{x}_s^- - m\dot{x}_{rot}^- \tag{6.235}$$

$$\int F_z dt = m\dot{z}_{rot}^+ - m\dot{z}_{rot}^- \tag{6.236}$$

In addition, the principle of angular impulse and momentum states that

$$\int M_C dt = \Delta H_C = H_C^+ - H_C^- : \; b\left(\int F_z dt\right) - h\left(\int F_x dt\right) = I\dot{\theta}^+ - I\dot{\theta}^- \tag{6.237}$$

in which $\int M_C dt$ is the angular impulse; H_C^- and H_C^+ are the pre- and post-impact angular momentum about the mass center, respectively; ΔH_C is the change in the angular momentum about the mass center.

In Equations (6.235) and (6.236), the pre- and post-impact horizontal and vertical components of the relative translational velocity of the mass center can be expressed in terms of the pre- and post-impact angular velocity of the block, $\dot{\theta}^-$ and $\dot{\theta}^+$ as follows.

For the pre-impact state, the translational velocity vector of the mass center (Figure 6-15) can be expressed as

$$\boldsymbol{v}^- = \boldsymbol{v}_O^- + \boldsymbol{\omega}^- \times \boldsymbol{r}_{C/O} \tag{6.238}$$

where $\boldsymbol{v}^-$ is pre-impact translational velocity vector of center-of-mass, $\boldsymbol{v}_O^-$ is pre-impact translational velocity vector of point O, $\boldsymbol{\omega}^-$ is pre-impact angular velocity vector of the block, and $\boldsymbol{r}_{C/O}$ is position vector of the mass center relative to point O.

Expressions for these vector quantities are given below:

$$\boldsymbol{v}^- = \dot{X}^-\hat{\boldsymbol{i}} + \dot{Z}^-\hat{\boldsymbol{k}} = \left(\dot{u}^- + \dot{x}_g + \dot{x}_s^- + \dot{x}_{rot}^-\right)\hat{\boldsymbol{i}} + \left(\dot{z}_{rot}^- + \dot{z}_g\right)\hat{\boldsymbol{k}} \tag{6.239}$$

$$\boldsymbol{v}_O^- = \left(\dot{u}^- + \dot{x}_g + \dot{x}_s^-\right)\hat{\boldsymbol{i}} + \left(\dot{z}_g\right)\hat{\boldsymbol{k}} \tag{6.240}$$

$$\boldsymbol{\omega}^- = \dot{\theta}^-\hat{\boldsymbol{j}} \tag{6.241}$$

$$\boldsymbol{r}_{C/O} = -r\sin\left(a-\theta\right)\hat{\boldsymbol{i}} + r\cos\left(a-\theta\right)\hat{\boldsymbol{k}} \tag{6.242}$$

At impact, the angular rotation of the block becomes zero $\left(\theta = 0\right)$ and the position vector of center-of-mass relative to point O, $\boldsymbol{r}_{C/O}$, can be rewritten as

$$\boldsymbol{r}_{C/O} = -\left(r\sin a\right)\hat{\boldsymbol{i}} + \left(r\cos a\right)\hat{\boldsymbol{k}} = -b\hat{\boldsymbol{i}} + h\hat{\boldsymbol{k}} \tag{6.243}$$

in which $\hat{\boldsymbol{i}}$ and $\hat{\boldsymbol{k}}$ are the horizontal and vertical unit vectors respectively.

On substituting Equations (6.239) through (6.243) into Equation (6.238), the pre-impact translational velocity becomes

$$\boldsymbol{v}^{-} \equiv \left(\dot{u}^{-} + \dot{x}_g + \dot{x}_s^{-} + \dot{x}_{rot}^{-}\right)\hat{\boldsymbol{i}} + \left(\dot{z}_{rot}^{-} + \dot{z}_g\right)\hat{\boldsymbol{k}} = \left(\dot{u}^{-} + \dot{x}_g + \dot{x}_s^{-}\right)\hat{\boldsymbol{i}} + \left(\dot{z}_g\right)\hat{\boldsymbol{k}} + \left(\dot{\theta}^{-}\hat{\boldsymbol{j}}\right)\times\left(-b\hat{\boldsymbol{i}} + h\hat{\boldsymbol{k}}\right) \tag{6.244}$$

which simplifies to

$$\dot{x}_{rot}^{-}\hat{\boldsymbol{i}} + \dot{z}_{rot}^{-}\hat{\boldsymbol{k}} = \left(b\dot{\theta}^{-}\right)\hat{\boldsymbol{k}} + \left(h\dot{\theta}^{-}\right)\hat{\boldsymbol{i}} \tag{6.245}$$

from which the pre-impact horizontal and vertical components of $\boldsymbol{v}^{-}$ can be retrieved as

$$\dot{x}_{rot}^{-} = h\dot{\theta}^{-} \tag{6.246}$$

$$\dot{z}_{rot}^{-} = b\dot{\theta}^{-} \tag{6.247}$$

For the post-impact state, the translational velocity vector of the mass center (Figure 6-17) can be expressed as

$$\boldsymbol{v}^{+} = \boldsymbol{v}_{O'}^{+} + \boldsymbol{\omega}^{+}\times\boldsymbol{r}_{C/O'} \tag{6.248}$$

where $\boldsymbol{v}^{+}$ is post-impact translational velocity vector of center-of-mass, $\boldsymbol{v}_{O'}^{+}$ is post-impact translational velocity vector of point O', $\boldsymbol{\omega}^{+}$ is post-impact angular velocity vector of the block, and $\boldsymbol{r}_{C/O'}$ is position vector of the mass center relative to point O'.

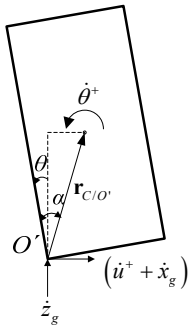

Figure 6-17: Components of post-impact translational velocity of the isolated block for the case of impact during slide-rocking about point *O*.

Expressions for these vector quantities are given below:

$$\boldsymbol{v}^+ = \dot{X}^+\hat{\boldsymbol{i}} + \dot{Z}^+\hat{\boldsymbol{k}} = \left(\dot{u}^+ + \dot{x}_g + \dot{x}_{rot}^+\right)\hat{\boldsymbol{i}} + \left(\dot{z}_{rot}^+ + \dot{z}_g\right)\hat{\boldsymbol{k}} \tag{6.249}$$

$$\boldsymbol{v}_{O'}^+ = \left(\dot{u}^+ + \dot{x}_g\right)\hat{\boldsymbol{i}} + \left(\dot{z}_g\right)\hat{\boldsymbol{k}} \tag{6.250}$$

$$\boldsymbol{\omega}^+ = \dot{\theta}^+\hat{\boldsymbol{j}} \tag{6.251}$$

$$\boldsymbol{r}_{C/O'} = r\sin\left(a-\theta\right)\hat{\boldsymbol{i}} + r\cos\left(a-\theta\right)\hat{\boldsymbol{k}} \tag{6.252}$$

At impact $\left(\theta = 0\right)$ the position vector of the mass center relative to point O', $\boldsymbol{r}_{C/O'}$, becomes

$$\boldsymbol{r}_{C/O'} = \left(r\sin a\right)\hat{\boldsymbol{i}} + \left(r\cos a\right)\hat{\boldsymbol{k}} = b\hat{\boldsymbol{i}} + h\hat{\boldsymbol{k}} \tag{6.253}$$

On substituting Equations (6.249) through (6.253) into Equation (6.248), the post-impact translational velocity becomes

$$\boldsymbol{v}^+ \equiv \left(\dot{u}^+ + \dot{x}_g + \dot{x}_{rot}^+\right)\hat{\boldsymbol{i}} + \left(\dot{z}_{rot}^+ + \dot{z}_g\right)\hat{\boldsymbol{k}} = \left(\dot{u}^+ + \dot{x}_g\right)\hat{\boldsymbol{i}} + \left(\dot{z}_g\right)\hat{\boldsymbol{k}} + \left(\dot{\theta}^+\hat{\boldsymbol{j}}\right)\times\left(b\hat{\boldsymbol{i}} + h\hat{\boldsymbol{k}}\right) \tag{6.254}$$

which reduces to

$$\dot{x}_{rot}^+\hat{\boldsymbol{i}} + \dot{z}_{rot}^+\hat{\boldsymbol{k}} = \left(-b\dot{\theta}^+\right)\hat{\boldsymbol{k}} + \left(h\dot{\theta}^+\right)\hat{\boldsymbol{i}} \tag{6.255}$$

from which the post-impact horizontal and vertical components of $\boldsymbol{v}^+$ can be retrieved as

$$\dot{x}_{rot}^{+} = h\dot{\theta}^{+} \tag{6.256}$$

$$\dot{z}_{rot}^{+} = -b\dot{\theta}^{+} \tag{6.257}$$

Substitution of Equations (6.246) through (6.257) into Equations (6.235) through (6.237) yields

$$\int F_x dt = m\dot{u}^{+} + m\left(h\dot{\theta}^{+}\right) - m\dot{u}^{-} - m\dot{x}_s^{-} - m\left(h\dot{\theta}^{-}\right) \tag{6.258}$$

$$\int F_z dt = m\left(-b\dot{\theta}^{+}\right) - m\left(b\dot{\theta}^{-}\right) \tag{6.259}$$

$$b\left(\int F_z dt\right) - h\left(\int F_x dt\right) = I\left(\dot{\theta}^{+}\right) - I\left(\dot{\theta}^{-}\right) \tag{6.260}$$

in which the centroid mass moment of inertia for the rectangular block is given by

$$I = \frac{m}{3}r^2 = \frac{m}{3}\left(b^2 + h^2\right) \tag{6.261}$$

Equations (6.258), (6.259) and (6.260) constitute a set of three equations in four unknowns, namely $\int F_x dt$, $\int F_z dt$, $\dot{\theta}^{+}$, $\dot{u}^{+}$.

Equivalently, the three Equations (6.258), (6.259) and (6.260) can be combined in one (by eliminating the two impulses) in two unknowns:

$$\left(4b^2 + 4h^2\right)\dot{\theta}^{+} + 3h\dot{u}^{+} = \left(4h^2 - 2b^2\right)\dot{\theta}^{-} + 3h\dot{u}^{-} + 3h\dot{x}_s^{-} \tag{6.262}$$

One additional equation is therefore required to uniquely determine the post-impact velocities $\dot{\theta}^{+}$, $\dot{u}^{+}$. By considering the system in its entirety during the impact, it can be stated that the horizontal impulse on the system is zero, resulting in the conservation of the system's linear momentum in the horizontal direction. That is,

$$\begin{aligned} &\left(\Delta L_{sys}\right)_x = \left(L_{sys}\right)_x^{+} - \left(L_{sys}\right)_x^{-} = 0: \quad \left[\left(L_{base}\right)_x^{+} + \left(L_{obj}\right)_x^{+}\right] - \left[\left(L_{base}\right)_x^{-} + \left(L_{obj}\right)_x^{-}\right] = 0 \\ &\Rightarrow \left[m_b\left(\dot{u}^{+} + \dot{x}_g\right) + m\left(\dot{u}^{+} + \dot{x}_g + \dot{x}_{rot}^{+}\right)\right] = \left[m_b\left(\dot{u}^{-} + \dot{x}_g\right) + m\left(\dot{u}^{-} + \dot{x}_g + \dot{x}_s^{-} + \dot{x}_{rot}^{-}\right)\right] \end{aligned} \tag{6.263}$$

in which $\left(L_{sys}\right)_x^-$ and $\left(L_{sys}\right)_x^+$ are the pre- and post-impact horizontal linear momentum of the system respectively; $\left(\Delta L_{sys}\right)_x$ is the change in horizontal linear momentum of the system.

Substituting Equations (6.246) and (6.256) in Equation (6.263) gives

$$m_b\dot{u}^+ + m\dot{u}^+ + mh\dot{\theta}^+ = m_b\dot{u}^- + m\dot{u}^- + m\dot{x}_s^- + mh\dot{\theta}^- \tag{6.264}$$

which upon rearranging terms becomes

$$\dot{u}^+ = \frac{1}{m_b+m}\left[\left(m_b+m\right)\dot{u}^- + m\dot{x}_s^- - mh\dot{\theta}^+ + mh\dot{\theta}^-\right] \tag{6.265}$$

Substituting Equation (6.265) in (6.262) gives

$$\begin{aligned}&\left(4b^2+4h^2\right)\dot{\theta}^+ + \frac{3h}{m_b+m}\left[\left(m_b+m\right)\dot{u}^- + m\dot{x}_s^- - mh\dot{\theta}^+ + mh\dot{\theta}^-\right]\\ &=\left(4h^2-2b^2\right)\dot{\theta}^- + 3h\dot{u}^- + 3h\dot{x}_s^-\end{aligned} \tag{6.266}$$

which yields

$$\dot{\theta}^+ = \frac{\left(4m_bh^2 - 2m_bb^2 + mh^2 - 2mb^2\right)\dot{\theta}^- + 3hm_b\dot{x}_s^-}{\left(4m_bh^2 + 4m_bb^2 + mh^2 + 4mb^2\right)} \tag{6.267}$$

Alternatively, instead of considering the conservation of the linear momentum (in the horizontal direction) of the entire system, one can apply the principle of linear impulse and momentum (in the horizontal direction) of the base alone, which states that

$$\begin{aligned}-\int F_x dt = \left(\Delta L_{base}\right)_x = \left(L_{base}\right)_x^+ - \left(L_{base}\right)_x^- :\ -\int F_x dt &= m_b\left(\dot{u}^+ + \dot{x}_g\right) - m_b\left(\dot{u}^- + \dot{x}_g\right)\\ \Rightarrow \int F_x dt &= m_b\dot{u}^- - m_b\dot{u}^+\end{aligned} \tag{6.268}$$

in which $\left(L_{base}\right)_x^-$ and $\left(L_{base}\right)_x^+$ are the pre- and post-impact horizontal linear momentum of the base respectively; $\left(\Delta L_{base}\right)_x$ is the change in horizontal linear momentum of the base.

Substituting Equation (6.268) into Equation (6.258) gives

$$m_b\dot{u}^- - m_b\dot{u}^+ = m\dot{u}^+ + m\left(h\dot{\theta}^+\right) - m\dot{u}^- - m\dot{x}_s^- - m\left(h\dot{\theta}^-\right) \tag{6.269}$$

which yields

$$\dot{u}^+ = \frac{1}{m_b + m}\left[\left(m_b + m\right)\dot{u}^- + m\dot{x}_s^- - mh\dot{\theta}^+ + mh\dot{\theta}^-\right] \tag{6.270}$$

Substituting Equation (6.270) in Equation (6.262) gives

$$\dot{\theta}^+ = \frac{\left(4m_bh^2 - 2m_bb^2 + mh^2 - 2mb^2\right)\dot{\theta}^- + 3hm_b\dot{x}_s^-}{\left(4m_bh^2 + 4m_bb^2 + mh^2 + 4mb^2\right)} \tag{6.271}$$

which is identical to the result derived by considering the conservation of the system's linear momentum in the horizontal direction.

Derivation for the case of impact during rocking about point O′

With regard to the block, the principle of linear impulse and momentum in the x and z direction states that

$$\int F_x dt = \left(\Delta L\right)_x = L_x^+ - L_x^- : \quad \int F_x dt = m\dot{X}^+ - m\dot{X}^- \tag{6.272}$$

$$\int F_z dt = \left(\Delta L\right)_z = L_z^+ - L_z^- : \quad \int F_z dt = m\dot{Z}^+ - m\dot{Z}^- \tag{6.273}$$

in which $\int F_x dt$ and $\int F_z dt$ are the horizontal and vertical impulses (assumed to act at O); $\dot{X}^- = \left(\dot{u}^- + \dot{x}_g\right) + \dot{x}_s^- + \dot{x}_{rot}^-$, $\dot{X}^+ = \left(\dot{u}^+ + \dot{x}_g\right) + \dot{x}_s^+ + \dot{x}_{rot}^+$ and $\dot{Z}^- = \left(\dot{z}_{rot}^- + \dot{z}_g\right)$, $\dot{Z}^+ = \left(\dot{z}_{rot}^+ + \dot{z}_g\right)$ are the absolute pre- and post-impact horizontal and vertical velocities of the mass center of the block, respectively; $\dot{x}_{rot}^-$, $\dot{x}_{rot}^+$ and $\dot{z}_{rot}^-$, $\dot{z}_{rot}^+$ are the relative pre- and post-impact horizontal and vertical velocities of the mass center of the block due to the rocking, relative to the rigid base; $\dot{x}_s^-$ and $\dot{x}_s^+$ are the relative pre- and post-impact horizontal velocities of the mass center of the block due to the sliding, relative to the rigid base; L_x^-, L_x^+, L_z^- and L_z^+ are the pre- and post-impact horizontal and vertical linear momentum, respectively; $\left(\Delta L\right)_x$ and $\left(\Delta L\right)_z$ are the changes in horizontal and vertical linear momentum, respectively.

Substituting these expressions into Equations (6.272) and (6.273) we obtain

$$\int F_x dt = m\dot{u}^+ + m\dot{x}_s^+ + m\dot{x}_{rot}^+ - m\dot{u}^- - m\dot{x}_s^- - m\dot{x}_{rot}^- \tag{6.274}$$

$$\int F_z dt = m\dot{z}_{rot}^+ - m\dot{z}_{rot}^- \tag{6.275}$$

In addition, the principle of angular impulse and momentum states that

$$\int M_C dt = \Delta H_C = H_C^+ - H_C^- : \; b\left(\int F_z dt\right) - h\left(\int F_x dt\right) = I\dot{\theta}^+ - I\dot{\theta}^- \tag{6.276}$$

in which $\int M_C dt$ is the angular impulse; H_C^- and H_C^+ are the pre- and post-impact angular momentum about the mass center, respectively; ΔH_C is the change in the angular momentum about the mass center.

In Equations (6.235) and (6.236), the pre- and post-impact horizontal and vertical components of the relative translational velocity of the mass center can be expressed in terms of the pre- and post-impact angular velocity of the block, $\dot{\theta}^-$ and $\dot{\theta}^+$ as follows.

For the pre-impact state, the translational velocity vector of the mass center (Figure 6-16) can be expressed as

$$\boldsymbol{v}^- = \boldsymbol{v}_{O'}^- + \boldsymbol{\omega}^- \times \boldsymbol{r}_{C/O'} \tag{6.277}$$

where $\boldsymbol{v}^-$ is pre-impact translational velocity vector of center-of-mass, $\boldsymbol{v}_{O'}^-$ is pre -impact translational velocity vector of point O', $\boldsymbol{\omega}^-$ is pre-impact angular velocity vector of the block, and $\boldsymbol{r}_{C/O'}$ is position vector of the mass center relative to point O'.

Expressions for these vector quantities are given below:

$$\boldsymbol{v}^- = \dot{X}^-\hat{\boldsymbol{i}} + \dot{Z}^-\hat{\boldsymbol{k}} = \left(\dot{u}^- + \dot{x}_g + \dot{x}_s^- + \dot{x}_{rot}^-\right)\hat{\boldsymbol{i}} + \left(\dot{z}_{rot}^- + \dot{z}_g\right)\hat{\boldsymbol{k}} \tag{6.278}$$

$$\boldsymbol{v}_{O'}^- = \left(\dot{u}^- + \dot{x}_g + \dot{x}_s^-\right)\hat{\boldsymbol{i}} + \left(\dot{z}_g\right)\hat{\boldsymbol{k}} \tag{6.279}$$

$$\boldsymbol{\omega}^- = \dot{\theta}^-\hat{\boldsymbol{j}} \tag{6.280}$$

$$\boldsymbol{r}_{C/O'} = -r\sin\left(a-\theta\right)\hat{\boldsymbol{i}} + r\cos\left(a-\theta\right)\hat{\boldsymbol{k}} \tag{6.281}$$

At impact, the angular rotation of the block becomes zero $\left(\theta = 0\right)$ and the position vector of the mass center relative to point O', $\boldsymbol{r}_{C/O'}$, can be rewritten as

$$\boldsymbol{r}_{C/O'} = -\left(r\sin a\right)\hat{\boldsymbol{i}} + \left(r\cos a\right)\hat{\boldsymbol{k}} = -b\hat{\boldsymbol{i}} + h\hat{\boldsymbol{k}} \tag{6.282}$$

in which $\hat{\boldsymbol{i}}$ and $\hat{\boldsymbol{k}}$ are the horizontal and vertical unit vectors respectively.

On substituting Equations (6.278) through (6.282) into Equation (6.277), the pre-impact translational velocity becomes

$$\boldsymbol{v}^{-} \equiv \left(\dot{u}^{-} + \dot{x}_g + \dot{x}_s^{-} + \dot{x}_{rot}^{-}\right)\hat{\boldsymbol{i}} + \left(\dot{z}_{rot}^{-} + \dot{z}_g\right)\hat{\boldsymbol{k}} = \left(\dot{u}^{-} + \dot{x}_g + \dot{x}_s^{-}\right)\hat{\boldsymbol{i}} + \left(\dot{z}_g\right)\hat{\boldsymbol{k}} + \left(\dot{\theta}^{-}\hat{\boldsymbol{j}}\right)\times\left(-b\hat{\boldsymbol{i}} + h\hat{\boldsymbol{k}}\right) \tag{6.283}$$

which reduces to

$$\dot{x}_{rot}^{-}\hat{\boldsymbol{i}} + \dot{z}_{rot}^{-}\hat{\boldsymbol{k}} = \left(b\dot{\theta}^{-}\right)\hat{\boldsymbol{k}} + \left(h\dot{\theta}^{-}\right)\hat{\boldsymbol{i}} \tag{6.284}$$

from which the pre-impact horizontal and vertical components of $\boldsymbol{v}^{-}$ can be retrieved as

$$\dot{x}_{rot}^{-} = h\dot{\theta}^{-} \tag{6.285}$$

$$\dot{z}_{rot}^{-} = b\dot{\theta}^{-} \tag{6.286}$$

For the post-impact state, the translational velocity vector of the mass center (Figure 6-18) can be expressed as

$$\boldsymbol{v}^{+} = \boldsymbol{v}_O^{+} + \boldsymbol{\omega}^{+}\times\boldsymbol{r}_{C/O} \tag{6.287}$$

where $\boldsymbol{v}^{+}$ is post-impact translational velocity vector of center-of-mass, $\boldsymbol{v}_O^{+}$ is post-impact translational velocity vector of point O, $\boldsymbol{\omega}^{+}$ is post-impact angular velocity vector of the block, and $\boldsymbol{r}_{C/O}$ is position vector of the mass center relative to point O.

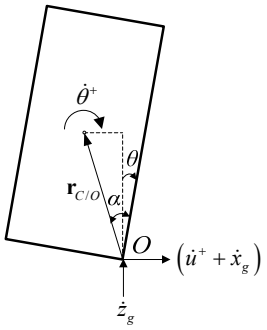

Figure 6-18: Components of post-impact translational velocity of the isolated block for the case of impact during slide-rocking about point O'.

Expressions for these vector quantities are given below:

$$\boldsymbol{v}^+ = \dot{X}^+\hat{\boldsymbol{i}} + \dot{Z}^+\hat{\boldsymbol{k}} = \left(\dot{u}^+ + \dot{x}_g + \dot{x}_{rot}^+\right)\hat{\boldsymbol{i}} + \left(\dot{z}_{rot}^+ + \dot{z}_g\right)\hat{\boldsymbol{k}} \tag{6.288}$$

$$\boldsymbol{v}_O^+ = \left(\dot{u}^+ + \dot{x}_g\right)\hat{\boldsymbol{i}} + \left(\dot{z}_g\right)\hat{\boldsymbol{k}} \tag{6.289}$$

$$\boldsymbol{\omega}^+ = \dot{\theta}^+\hat{\boldsymbol{j}} \tag{6.290}$$

$$\boldsymbol{r}_{C/O} = r\sin\left(a-\theta\right)\hat{\boldsymbol{i}} + r\cos\left(a-\theta\right)\hat{\boldsymbol{k}} \tag{6.291}$$

At impact $\left(\theta = 0\right)$ the position vector of the mass center relative to point O, $\boldsymbol{r}_{C/O}$, becomes

$$\boldsymbol{r}_{C/O} = \left(r\sin a\right)\hat{\boldsymbol{i}} + \left(r\cos a\right)\hat{\boldsymbol{k}} = b\hat{\boldsymbol{i}} + h\hat{\boldsymbol{k}} \tag{6.292}$$

On substituting Equations (6.288) through (6.292) into Equation (6.287), the post-impact translational velocity becomes

$$\boldsymbol{v}^+ \equiv \left(\dot{u}^+ + \dot{x}_g + \dot{x}_{rot}^+\right)\hat{\boldsymbol{i}} + \left(\dot{z}_{rot}^+ + \dot{z}_g\right)\hat{\boldsymbol{k}} = \left(\dot{u}^+ + \dot{x}_g\right)\hat{\boldsymbol{i}} + \left(\dot{z}_g\right)\hat{\boldsymbol{k}} + \left(\dot{\theta}^+\hat{\boldsymbol{j}}\right)\times\left(b\hat{\boldsymbol{i}} + h\hat{\boldsymbol{k}}\right) \tag{6.293}$$

which simplifies to

$$\dot{x}_{rot}^+\hat{\boldsymbol{i}} + \dot{z}_{rot}^+\hat{\boldsymbol{k}} = \left(-b\dot{\theta}^+\right)\hat{\boldsymbol{k}} + \left(h\dot{\theta}^+\right)\hat{\boldsymbol{i}} \tag{6.294}$$

from which the post-impact horizontal and vertical components of $\boldsymbol{v}^+$ can be retrieved as

$$\dot{x}_{rot}^{+} = h\dot{\theta}^{+} \tag{6.295}$$

$$\dot{z}_{rot}^{+} = -b\dot{\theta}^{+} \tag{6.296}$$

Substitution of Equations (6.246) through (6.257) into Equations (6.235) through (6.237) yields

$$\int F_x dt = m\dot{u}^{+} + m\left(h\dot{\theta}^{+}\right) - m\dot{u}^{-} - m\dot{x}_s^{-} - m\left(h\dot{\theta}^{-}\right) \tag{6.297}$$

$$\int F_z dt = m\left(-b\dot{\theta}^{+}\right) - m\left(b\dot{\theta}^{-}\right) \tag{6.298}$$

$$b\left(\int F_z dt\right) - h\left(\int F_x dt\right) = I\left(\dot{\theta}^{+}\right) - I\left(\dot{\theta}^{-}\right) \tag{6.299}$$

in which the centroid mass moment of inertia for the rectangular block is given by

$$I = \frac{m}{3}r^2 = \frac{m}{3}\left(b^2 + h^2\right) \tag{6.300}$$

Equations (6.258), (6.259) and (6.260) constitute a set of three equations in four unknowns, namely $\int F_x dt$, $\int F_z dt$, $\dot{\theta}^{+}$, $\dot{u}^{+}$.

Equivalently, the three Equations (6.258), (6.259) and (6.260) can be combined in one (by eliminating the two impulses) in two unknowns:

$$\left(4b^2 + 4h^2\right)\dot{\theta}^{+} + 3h\dot{u}^{+} = \left(4h^2 - 2b^2\right)\dot{\theta}^{-} + 3h\dot{u}^{-} + 3h\dot{x}_s^{-} \tag{6.301}$$

One additional equation is therefore required to uniquely determine the post-impact velocities $\dot{\theta}^{+}$, $\dot{u}^{+}$. By considering the system in its entirety during the impact, it can be stated that the horizontal impulse on the system is zero, resulting in the conservation of the system's linear momentum in the horizontal direction. That is,

$$\begin{aligned} &\left(\Delta L_{sys}\right)_x = \left(L_{sys}\right)_x^{+} - \left(L_{sys}\right)_x^{-} = 0: \ \left[\left(L_{base}\right)_x^{+} + \left(L_{obj}\right)_x^{+}\right] - \left[\left(L_{base}\right)_x^{-} + \left(L_{obj}\right)_x^{-}\right] = 0 \\ &\Rightarrow \left[m_b\left(\dot{u}^{+} + \dot{x}_g\right) + m\left(\dot{u}^{+} + \dot{x}_g + \dot{x}_{rot}^{+}\right)\right] = \left[m_b\left(\dot{u}^{-} + \dot{x}_g\right) + m\left(\dot{u}^{-} + \dot{x}_g + \dot{x}_s^{-} + \dot{x}_{rot}^{-}\right)\right] \end{aligned} \tag{6.302}$$

in which $\left(L_{sys}\right)_x^-$ and $\left(L_{sys}\right)_x^+$ are the pre- and post-impact horizontal linear momentum of the system respectively; $\left(\Delta L_{sys}\right)_x$ is the change in horizontal linear momentum of the system.

Substituting Equations (6.246) and (6.256) in Equation (6.263) gives

$$m_b\dot{u}^+ + m\dot{u}^+ + mh\dot{\theta}^+ = m_b\dot{u}^- + m\dot{u}^- + m\dot{x}_s^- + mh\dot{\theta}^- \tag{6.303}$$

which upon rearranging terms becomes

$$\dot{u}^+ = \frac{1}{m_b+m}\left[\left(m_b+m\right)\dot{u}^- + m\dot{x}_s^- - mh\dot{\theta}^+ + mh\dot{\theta}^-\right] \tag{6.304}$$

Substituting Equation (6.265) in (6.262) gives

$$\begin{aligned}&\left(4b^2+4h^2\right)\dot{\theta}^+ + \frac{3h}{m_b+m}\left[\left(m_b+m\right)\dot{u}^- + m\dot{x}_s^- - mh\dot{\theta}^+ + mh\dot{\theta}^-\right]\\ &= \left(4h^2-2b^2\right)\dot{\theta}^- + 3h\dot{u}^- + 3h\dot{x}_s^-\end{aligned} \tag{6.305}$$

which yields

$$\dot{\theta}^+ = \frac{\left(4m_bh^2 - 2m_bb^2 + mh^2 - 2mb^2\right)\dot{\theta}^- + 3hm_b\dot{x}_s^-}{\left(4m_bh^2 + 4m_bb^2 + mh^2 + 4mb^2\right)} \tag{6.306}$$

Alternatively, instead of considering the conservation of the linear momentum (in the horizontal direction) of the entire system, one can apply the principle of linear impulse and momentum (in the horizontal direction) of the base alone, which states that

$$\begin{aligned}-\int F_x dt = \left(\Delta L_{base}\right)_x = \left(L_{base}\right)_x^+ - \left(L_{base}\right)_x^- :\ -\int F_x dt &= m_b\left(\dot{u}^+ + \dot{x}_g\right) - m_b\left(\dot{u}^- + \dot{x}_g\right)\\ \Rightarrow \int F_x dt &= m_b\dot{u}^- - m_b\dot{u}^+\end{aligned} \tag{6.307}$$

in which $\left(L_{base}\right)_x^-$ and $\left(L_{base}\right)_x^+$ are the pre- and post-impact horizontal linear momentum of the base respectively; $\left(\Delta L_{base}\right)_x$ is the change in horizontal linear momentum of the base.

Substituting Equation (6.268) into Equation (6.258) gives

$$m_b\dot{u}^- - m_b\dot{u}^+ = m\dot{u}^+ + m\left(h\dot{\theta}^+\right) - m\dot{u}^- - m\dot{x}_s^- - m\left(h\dot{\theta}^-\right) \tag{6.308}$$

which yields

$$\dot{u}^+ = \frac{1}{m_b + m}\left[\left(m_b + m\right)\dot{u}^- + m\dot{x}_s^- - mh\dot{\theta}^+ + mh\dot{\theta}^-\right] \tag{6.309}$$

Substituting Equation (6.270) in Equation (6.262) gives

$$\dot{\theta}^+ = \frac{\left(4m_b h^2 - 2m_b b^2 + mh^2 - 2mb^2\right)\dot{\theta}^- + 3hm_b\dot{x}_s^-}{\left(4m_b h^2 + 4m_b b^2 + mh^2 + 4mb^2\right)} \tag{6.310}$$

which is identical to the result derived by considering the conservation of the system's linear momentum in the horizontal direction.

Substituting the expression for $\dot{\theta}^+$ in Equation (6.309), Equations (6.309) and (6.311) can be written as

$$\dot{u}^+ = \dot{u}^- + \frac{\rho\left(\lambda^2 + 4\right)}{\lambda^2\left(\rho + 4\right) + 4\left(\rho + 1\right)}\dot{x}_s^- + \frac{6\rho h}{\lambda^2\left(\rho + 4\right) + 4\left(\rho + 1\right)}\dot{\theta}^- \equiv \dot{u}^- + \beta_4\dot{x}_s^- + \beta_1\dot{\theta}^- \tag{6.312}$$

$$\dot{\theta}^+ = \frac{3\lambda}{b\left[\lambda^2\left(\rho + 4\right) + 4\left(\rho + 1\right)\right]}\dot{x}_s^- + \frac{\lambda^2\left(\rho + 4\right) - 2\left(\rho + 1\right)}{\lambda^2\left(\rho + 4\right) + 4\left(\rho + 1\right)}\dot{\theta}^- \equiv \beta_5\dot{x}_s^- + \varepsilon\dot{\theta}^- \tag{6.313}$$

where $\lambda = h / b$ and $\rho = m / m_b$.

As it can be seen the Equations (6.270) and (6.271) giving the post-impact horizontal velocity for impact from slide-rocking about O' (realized when $\dot{\theta} > 0$) is identical to the Equations (6.309) and (6.310) giving the post-impact horizontal velocity for impact from slide-rocking about O (realized when $\dot{\theta} < 0$).

The coefficients of "linear restitution" β_1 and β_4 in Equation (6.312), associated with the reduction of the post-impact linear velocity of the rigid base, is defined by

$$\beta_1 \doteq \frac{6\rho h}{\lambda^2\left(\rho + 4\right) + 4\left(\rho + 1\right)} \tag{6.314}$$

$$\beta_4 \doteq \frac{\rho\left(\lambda^2+4\right)}{\lambda^2\left(\rho+4\right)+4\left(\rho+1\right)} \tag{6.315}$$

and the coefficients of "angular restitution" ε and "linear restitution" β_5 in Equation (6.313), associated with the reduction of the post-impact angular velocity of the block, is defined by

$$\varepsilon \doteq \frac{\lambda^2\left(\rho+4\right)-2\left(\rho+1\right)}{\lambda^2\left(\rho+4\right)+4\left(\rho+1\right)} \tag{6.316}$$

$$\beta_5 \doteq \frac{3\lambda}{b\left[\lambda^2\left(\rho+4\right)+4\left(\rho+1\right)\right]} \tag{6.317}$$

Equation (6.316) reveals that the coefficient of angular restitution ε depends both on the slenderness ratio λ and the mass ratio ρ. The coefficient β_1 in Equation (6.314), which is associated with the reduction of the post-impact linear velocity of the rigid base, depends not only on the parameters λ and ρ, but also on the absolute size of the block (in terms of its height). The variation of coefficient of angular restitution ε, and coefficient $\overline{\beta}_1$ with slenderness ratio λ is shown in Figure 6-9.

The coefficient β_4 in Equation (6.315), which is associated with the reduction of the post-impact linear velocity of the rigid base, depends on the parameters λ and ρ. The variation of the coefficient β_4 is plotted against the slenderness ratio λ for different values of the mass ratio ρ, Figure 6-19a. Observe that value of the coefficient β_4 reduces faster for lower values of slenderness ratio λ (stocky blocks) in comparison with larger values of λ which the coefficient β_4 is almost steady. In contrast, the coefficient β_4 is seen to be dependent on the mass ratio ρ, regardless of slenderness ratio λ. As follows from the comparison of Figure 6-9 and Figure 6-19, the post-impact linear velocity of the rigid base is strongly dependent on the mass ratio ρ and on small values of slenderness ratio λ (stocky blocks).

The coefficient β_5 in Equation (6.317), which is associated with the reduction of the post-impact angular velocity of the rigid base, depends not only on the parameters λ and ρ, but also on the absolute size of the block (in terms of its width). The normalized coefficient

$\bar{\beta}_5 \equiv \beta_5 b$ is plotted against the slenderness ratio λ for different values of the mass ratio ρ in Figure 6-19b. Observe that the value of the coefficient $\bar{\beta}_5$ increases rapidly with the slenderness ratio λ, until $\lambda \approx 1$ and then it decreases more slowly as the slenderness ratio is getting larger. Similarly, the dependency of coefficient ε on the mass ratio ρ is seen to be weak for very slender blocks, practically diminishing for $\lambda > 8$. As follows from the comparison of Figure 6-9 and Figure 6-19, the post-impact angular velocity of the rigid base is strongly dependent on the slenderness ratio λ and the influence of the mass ratio ρ on the coefficients $\bar{\beta}_1$ and β_4 is much greater than that on the coefficients ε and $\bar{\beta}_5 \equiv \beta_5 b$.

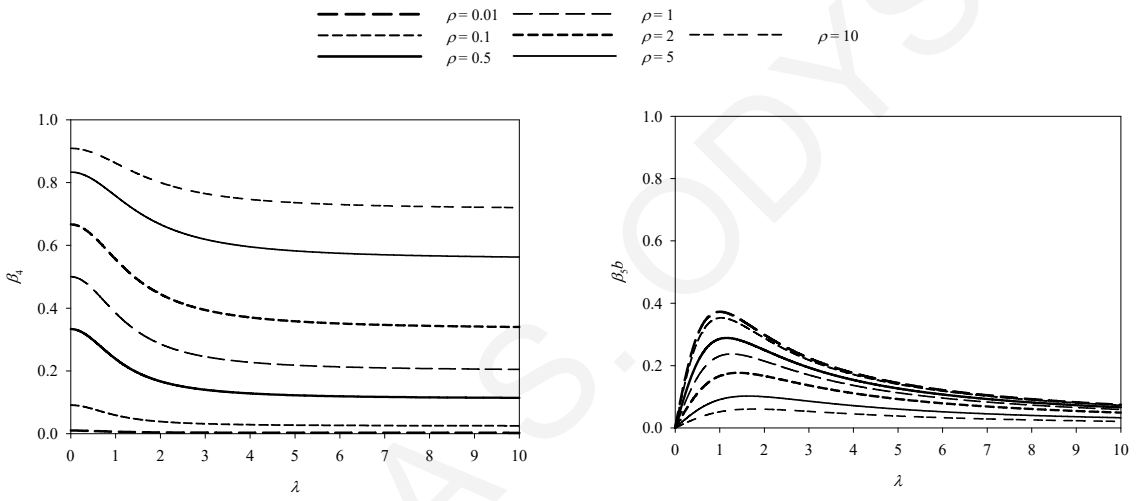

(a) (b)

Figure 6-19: Variation of (a) coefficient β_4, and (b) coefficient $\bar{\beta}_5$ with slenderness ratio λ.

6.4.3 Pure Sliding occurs after impact

When rocking of the block on top of the moving base ceases, the system will attain a sliding regime. In this case, the impact analysis is reduced to the computation of the post-impact translational velocity of the system, $\dot{u}^+$, $\dot{x}_s^+$, given the position and the pre-impact velocities, $\dot{u}^-$, $\dot{x}_s^-$, and $\dot{\theta}^-$.

Derivation for the case of impact during rocking about point O

Consider the system at the instant when the block hits the moving base from rocking about O.

With regard to the block, the principle of linear impulse and momentum in the x and z direction states that

$$\int F_x dt = \left(\Delta L\right)_x = L_x^+ - L_x^- : \quad \int F_x dt = m\dot{X}^+ - m\dot{X}^- \tag{6.318}$$

$$\int F_z dt = \left(\Delta L\right)_z = L_z^+ - L_z^- : \quad \int F_z dt = m\dot{Z}^+ - m\dot{Z}^- \tag{6.319}$$

in which $\int F_x dt$ and $\int F_z dt$ are the horizontal and vertical impulses (assumed to act at O'); $\dot{X}^- = \left(\dot{u}^- + \dot{x}_g\right) + \dot{x}_s^- + \dot{x}_{rot}^-$, $\dot{X}^+ = \left(\dot{u}^+ + \dot{x}_g\right) + \dot{x}_s^+ + \dot{x}_{rot}^+$ and $\dot{Z}^- = \left(\dot{z}_{rot}^- + \dot{z}_g\right)$, $\dot{Z}^+ = \left(\dot{z}_{rot}^+ + \dot{z}_g\right)$ are the absolute pre- and post-impact horizontal and vertical velocities of the mass center of the block, respectively; $\dot{x}_{rot}^-$, $\dot{x}_{rot}^+$ and $\dot{z}_{rot}^-$, $\dot{z}_{rot}^+$ are the relative pre- and post-impact horizontal and vertical velocities of the mass center of the block due to the rocking, relative to the rigid base; $\dot{x}_s^-$ and $\dot{x}_s^+$ are the relative pre- and post-impact horizontal velocities of the mass center of the block due to the sliding, relative to the rigid base; L_x^-, L_x^+, L_z^- and L_z^+ are the pre- and post-impact horizontal and vertical linear momentum, respectively; $\left(\Delta L\right)_x$ and $\left(\Delta L\right)_z$ are the changes in horizontal and vertical linear momentum, respectively.

Substituting these expressions into Equations (6.318) and (6.319) we obtain

$$\int F_x dt = m\dot{u}^+ + m\dot{x}_s^+ + m\dot{x}_{rot}^+ - m\dot{u}^- - m\dot{x}_s^- - m\dot{x}_{rot}^- \tag{6.320}$$

$$\int F_z dt = m\dot{z}_{rot}^+ - m\dot{z}_{rot}^- \tag{6.321}$$

In Equations (6.320) and (6.321), the pre- and post-impact horizontal components of the relative translational velocity of the mass center can be expressed in terms of the pre-impact angular velocity of the block, $\dot{\theta}^-$ as follows.

For the pre-impact state, the translational velocity vector of the mass center (Figure 6-15) can be expressed as

$$\boldsymbol{v}^- = \boldsymbol{v}_O^- + \boldsymbol{\omega}^- \times \boldsymbol{r}_{C/O} \tag{6.322}$$

where $\boldsymbol{v}^-$ is pre-impact translational velocity vector of center-of-mass, $\boldsymbol{v}_O^-$ is pre-impact translational velocity vector of point O, $\boldsymbol{\omega}^-$ is pre-impact angular velocity vector of the block, and $\boldsymbol{r}_{C/O}$ is position vector of the mass center relative to point O.

Expressions for these vector quantities are given below:

$$\boldsymbol{v}^- = \dot{X}^-\hat{\boldsymbol{i}} + \dot{Z}^-\hat{\boldsymbol{k}} = \left(\dot{u}^- + \dot{x}_g + \dot{x}_{rot}^- + \dot{x}_s^-\right)\hat{\boldsymbol{i}} + \left(\dot{z}_{rot}^- + \dot{z}_g\right)\hat{\boldsymbol{k}} \tag{6.323}$$

$$\boldsymbol{v}_O^- = \left(\dot{u}^- + \dot{x}_g + \dot{x}_s^-\right)\hat{\boldsymbol{i}} + \left(\dot{z}_g\right)\hat{\boldsymbol{k}} \tag{6.324}$$

$$\boldsymbol{\omega}^- = \dot{\theta}^-\hat{\boldsymbol{j}} \tag{6.325}$$

$$\boldsymbol{r}_{C/O} = -r\sin\left(a-\theta\right)\hat{\boldsymbol{i}} + r\cos\left(a-\theta\right)\hat{\boldsymbol{k}} \tag{6.326}$$

At impact, the angular velocity of the block becomes zero $\left(\theta = 0\right)$ and the position vector of center-of-mass relative to point O can be written as

$$\boldsymbol{r}_{C/O} = -\left(r\sin a\right)\hat{\boldsymbol{i}} + \left(r\cos a\right)\hat{\boldsymbol{k}} = -b\hat{\boldsymbol{i}} + h\hat{\boldsymbol{k}} \tag{6.327}$$

On substituting Equations (6.323) through (6.327) into Equation (6.322), the pre-impact translational velocity becomes

$$\boldsymbol{v}^- \equiv \left(\dot{u}^- + \dot{x}_g + \dot{x}_{rot}^- + \dot{x}_s^-\right)\hat{\boldsymbol{i}} + \left(\dot{z}_{rot}^- + \dot{z}_g\right)\hat{\boldsymbol{k}} = \left(\dot{u}^- + \dot{x}_g + \dot{x}_s^-\right)\hat{\boldsymbol{i}} + \left(\dot{z}_g\right)\hat{\boldsymbol{k}} + \left(\dot{\theta}^-\hat{\boldsymbol{j}}\right)\times\left(-b\hat{\boldsymbol{i}} + h\hat{\boldsymbol{k}}\right) \tag{6.328}$$

which reduces to

$$\dot{x}_{rot}^-\hat{\boldsymbol{i}} + \dot{z}_{rot}^-\hat{\boldsymbol{k}} = \left(b\dot{\theta}^-\right)\hat{\boldsymbol{k}} + \left(h\dot{\theta}^-\right)\hat{\boldsymbol{i}} \tag{6.329}$$

from which the pre-impact horizontal and vertical components of $\boldsymbol{v}^-$ can be retrieved as

$$\dot{x}_{rot}^- = h\dot{\theta}^- \tag{6.330}$$

$$\dot{z}_{rot}^- = b\dot{\theta}^- \tag{6.331}$$

For the post-impact state, the translational velocity vector of the mass center can be expressed as

$$\boldsymbol{v}^{+} = \boldsymbol{v}_{O'}^{+} + \boldsymbol{\omega}^{+} \times \boldsymbol{r}_{C/O'} \tag{6.332}$$

where $\boldsymbol{v}^{+}$ is post-impact translational velocity vector of center-of-mass, $\boldsymbol{v}_{O'}^{+}$ is post-impact translational velocity vector of point O', $\boldsymbol{\omega}^{+}$ is post-impact angular velocity vector of the block, and $\boldsymbol{r}_{C/O'}$ is position vector of the mass center relative to point O'.

Expressions for these vector quantities are given below:

$$\boldsymbol{v}^{+} = \dot{X}^{+}\hat{\boldsymbol{i}} + \dot{Z}^{+}\hat{\boldsymbol{k}} = \left(\dot{u}^{+} + \dot{x}_g + \dot{x}_{rot}^{+} + \dot{x}_s^{+}\right)\hat{\boldsymbol{i}} + \left(\dot{z}_{rot}^{+} + \dot{z}_g\right)\hat{\boldsymbol{k}} \tag{6.333}$$

$$\boldsymbol{v}_{O'}^{+} = \left(\dot{u}^{+} + \dot{x}_g + \dot{x}_s^{+}\right)\hat{\boldsymbol{i}} + \left(\dot{z}_g\right)\hat{\boldsymbol{k}} \tag{6.334}$$

$$\boldsymbol{\omega}^{+} = \dot{\theta}^{+}\hat{\boldsymbol{j}} = 0\,\hat{\boldsymbol{j}} \tag{6.335}$$

$$\boldsymbol{r}_{C/O'} = r\sin\left(a-\theta\right)\hat{\boldsymbol{i}} + r\cos\left(a-\theta\right)\hat{\boldsymbol{k}} \tag{6.336}$$

At impact $\left(\theta = 0\right)$, the position vector of the mass center relative to point O' becomes

$$\boldsymbol{r}_{C/O'} = \left(r\sin a\right)\hat{\boldsymbol{i}} + \left(r\cos a\right)\hat{\boldsymbol{k}} = b\hat{\boldsymbol{i}} + h\hat{\boldsymbol{k}} \tag{6.337}$$

On substituting Equations (6.333) through (6.337) into Equation (6.332), the post-impact translational velocity becomes

$$\boldsymbol{v}^{+} \equiv \left(\dot{u}^{+} + \dot{x}_g + \dot{x}_{rot}^{+} + \dot{x}_s^{+}\right)\hat{\boldsymbol{i}} + \left(\dot{z}_{rot}^{+} + \dot{z}_g\right)\hat{\boldsymbol{k}} = \left(\dot{u}^{+} + \dot{x}_g + \dot{x}_s^{+}\right)\hat{\boldsymbol{i}} + \left(\dot{z}_g\right)\hat{\boldsymbol{k}} + \left(0\,\hat{\boldsymbol{j}}\right)\times\left(b\hat{\boldsymbol{i}} + h\hat{\boldsymbol{k}}\right) \tag{6.338}$$

which simplifies to

$$\dot{x}_{rot}^{+}\hat{\boldsymbol{i}} + \dot{z}_{rot}^{+}\hat{\boldsymbol{k}} = 0\hat{\boldsymbol{k}} + 0\hat{\boldsymbol{i}} \tag{6.339}$$

from which the post-impact horizontal and vertical components of $\boldsymbol{v}^{+}$ can be retrieved as

$$\dot{x}_{rot}^{+} = 0 \tag{6.340}$$

$$\dot{z}_{rot}^{+} = 0 \tag{6.341}$$

Substitution of Equations (6.330) through (6.341) into Equations (6.320) and (6.321) yields

$$\int F_x dt = m\dot{u}^{+} + m\dot{x}_s^{+} - m\dot{u}^{-} - m\left(h\dot{\theta}^{-}\right) - m\dot{x}_s^{-} \tag{6.342}$$

$$\int F_z dt = -mb\dot{\theta}^{-} \tag{6.343}$$

which constitutes one equation in three unknowns: $\int F_x dt$, $\dot{u}^{+}$, $\dot{x}_s^{+}$.

Two additional equation is therefore required to uniquely determine the post-impact velocity $\dot{u}^{+}$ and $\dot{x}_s^{+}$.

By considering the system in its entirety during the impact, it can be stated that the horizontal impulse on the system is zero, resulting in the conservation of the system's linear momentum in the horizontal direction. That is,

$$\begin{aligned} &\left(\Delta L_{sys}\right)_x = \left(L_{sys}\right)_x^{+} - \left(L_{sys}\right)_x^{-} = 0: \quad \left[\left(L_{base}\right)_x^{+} + \left(L_{obj}\right)_x^{+}\right] - \left[\left(L_{base}\right)_x^{-} + \left(L_{obj}\right)_x^{-}\right] = 0 \\ &\Rightarrow \left[m_b\left(\dot{u}^{+} + \dot{x}_g\right) + m\left(\dot{u}^{+} + \dot{x}_g + \dot{x}_s^{+}\right)\right] = \left[m_b\left(\dot{u}^{-} + \dot{x}_g\right) + m\left(\dot{u}^{-} + \dot{x}_g + \dot{x}^{-} + \dot{x}_s^{-} + \dot{x}_{rot}^{-}\right)\right] \end{aligned} \tag{6.344}$$

Substituting Equations (6.330) and (6.331) in Equation (6.344) gives

$$m_b\dot{u}^{+} + m\dot{u}^{+} + m\dot{x}_s^{+} = m_b\dot{u}^{-} + m\dot{u}^{-} + mh\dot{\theta}^{-} + m\dot{x}_s^{-} \tag{6.345}$$

which upon rearranging terms becomes

$$\dot{u}^{+} = \frac{1}{m_b + m}\left[\left(m_b + m\right)\dot{u}^{-} + mh\dot{\theta}^{-} + m\dot{x}_s^{-} - m\dot{x}_s^{+}\right] \tag{6.346}$$

With regard to the block, the principle of frictional impulse in the x and z direction states that

$$\int F_x dt = -\operatorname{sgn}\left(\dot{x}_s^{+}\right)\mu_k \left|\int F_z dt\right| \tag{6.347}$$

Substituting Equations (6.342) and (6.343) in Equation (6.347) gives

$$m\dot{u}^{+} + m\dot{x}_s^{+} - m\dot{u}^{-} - m\left(h\dot{\theta}^{-}\right) - m\dot{x}_s^{-} = -\operatorname{sgn}\left(\dot{x}_s^{+}\right)\mu_k \left|-mb\dot{\theta}^{-}\right| \tag{6.348}$$

Assume that $\operatorname{sgn}\left(\dot{x}_s^+\right) > 0$, Equation (6.348) can be written as

$$\dot{x}_s^+ = -\mu_k \left|-b\dot{\theta}^-\right| + \dot{u}^- + h\dot{\theta}^- + \dot{x}_s^- - \dot{u}^+ \tag{6.349}$$

Substituting Equations (6.349) in Equation (6.346) gives

$$\dot{u}^+ = \frac{1}{m_b + m}\left[\left(m_b + m\right)\dot{u}^- + mh\dot{\theta}^- + m\dot{x}_s^- - m\left(-\mu_k \left|-b\dot{\theta}^-\right| + \dot{u}^- + h\dot{\theta}^- + \dot{x}_s^- - \dot{u}^+\right)\right] \tag{6.350}$$

Which upon rearranging terms become

$$\dot{u}^+ = \dot{u}^- + \frac{m}{m_b}\mu_k \left|-b\dot{\theta}^-\right| \tag{6.351}$$

Substituting Equation (6.351) in Equation (6.349) gives

$$\dot{x}_s^+ = -\left(1 + \frac{m}{m_b}\right)\mu_k \left|-b\dot{\theta}^-\right| + h\dot{\theta}^- + \dot{x}_s^- \tag{6.352}$$

Once Equation (6.352) is solved and $\dot{x}_s^+$ is calculated positive, then the assumption and Equation (6.352) are correct, else a second assumption must be computed, $\operatorname{sgn}\left(\dot{x}_s^+\right) < 0$ and Equation (6.351) can be rewritten as

$$\dot{x}_s^+ = \mu_k \left|-b\dot{\theta}^-\right| + \dot{u}^- + h\dot{\theta}^- + \dot{x}_s^- - \dot{u}^+ \tag{6.353}$$

Substituting Equations (6.353) in Equation (6.346) gives

$$\dot{u}^+ = \frac{1}{m_b + m}\left[\left(m_b + m\right)\dot{u}^- + mh\dot{\theta}^- + m\dot{x}_s^- - m\left(\mu_k \left|-b\dot{\theta}^-\right| + \dot{u}^- + h\dot{\theta}^- + \dot{x}_s^- - \dot{u}^+\right)\right] \tag{6.354}$$

Which upon rearranging terms become

$$\dot{u}^+ = \dot{u}^- - \frac{m}{m_b}\mu_k \left|-b\dot{\theta}^-\right| \tag{6.355}$$

Substituting Equation (6.355) in Equation (6.353) gives

$$\dot{x}_s^+ = \left(1+\frac{m}{m_b}\right)\mu_k\left|-b\dot{\theta}^-\right| + h\dot{\theta}^- + \dot{x}_s^- \tag{6.356}$$

The absolute value in Equations (6.351), (6.352), (6.355) and (6.356) can be dropped since the impulse in the z direction must be positive.

Equations (6.351), (6.352), (6.355) and (6.356) can be rewritten in the form

$$\dot{u}^+ = \dot{u}^- + \mathrm{sgn}\left(\dot{x}_s^+\right)\frac{m}{m_b}\mu_k\left(-b\dot{\theta}^-\right) \tag{6.357}$$

$$\dot{x}_s^+ = -\mathrm{sgn}\left(\dot{x}_s^+\right)\left(1+\frac{m}{m_b}\right)\mu_k\left(-b\dot{\theta}^-\right) + h\dot{\theta}^- + \dot{x}_s^- \tag{6.358}$$

Derivation for the case of impact during rocking about point O'

Consider the system at the instant when the block hits the moving base from rocking about O.

With regard to the block, the principle of linear impulse and momentum in the x and z direction states that

$$\int F_x dt = \left(\Delta L\right)_x = L_x^+ - L_x^- : \quad \int F_x dt = m\dot{X}^+ - m\dot{X}^- \tag{6.359}$$

$$\int F_z dt = \left(\Delta L\right)_z = L_z^+ - L_z^- : \quad \int F_z dt = m\dot{Z}^+ - m\dot{Z}^- \tag{6.360}$$

in which $\int F_x dt$ and $\int F_z dt$ are the horizontal and vertical impulses (assumed to act at O'); $\dot{X}^- = \left(\dot{u}^- + \dot{x}_g\right) + \dot{x}_s^- + \dot{x}_{rot}^-$, $\dot{X}^+ = \left(\dot{u}^+ + \dot{x}_g\right) + \dot{x}_s^+ + \dot{x}_{rot}^+$ and $\dot{Z}^- = \left(\dot{z}_{rot}^- + \dot{z}_g\right)$, $\dot{Z}^+ = \left(\dot{z}_{rot}^+ + \dot{z}_g\right)$ are the absolute pre- and post-impact horizontal and vertical velocities of the mass center of the block, respectively; $\dot{x}_{rot}^-$, $\dot{x}_{rot}^+$ and $\dot{z}_{rot}^-$, $\dot{z}_{rot}^+$ are the relative pre- and post-impact horizontal and vertical velocities of the mass center of the block due to the rocking, relative to the rigid base; $\dot{x}_s^-$ and $\dot{x}_s^+$ are the relative pre- and post-impact horizontal velocities of the mass center of the block due to the sliding, relative to the rigid base; L_x^-, L_x^+, L_z^- and L_z^+ are the pre- and post-impact horizontal and vertical linear momentum, respectively; $\left(\Delta L\right)_x$ and $\left(\Delta L\right)_z$ are the changes in horizontal and vertical linear momentum, respectively.

Substituting these expressions into Equations (6.359) and (6.360) we obtain

$$\int F_x dt = m\dot{u}^+ + m\dot{x}_s^+ + m\dot{x}_{rot}^+ - m\dot{u}^- - m\dot{x}_s^- - m\dot{x}_{rot}^- \tag{6.361}$$

$$\int F_z dt = m\dot{z}_{rot}^+ - m\dot{z}_{rot}^- \tag{6.362}$$

In Equations (6.361) and (6.362), the pre- and post-impact horizontal components of the relative translational velocity of the mass center can be expressed in terms of the pre-impact angular velocity of the block, $\dot{\theta}^-$ as follows.

For the pre-impact state, the translational velocity vector of the mass center (Figure 6-16) can be expressed as

$$\boldsymbol{v}^- = \boldsymbol{v}_{O'}^- + \boldsymbol{\omega}^- \times \boldsymbol{r}_{C/O'} \tag{6.363}$$

where $\boldsymbol{v}^-$ is pre-impact translational velocity vector of center-of-mass, $\boldsymbol{v}_{O'}^-$ is pre -impact translational velocity vector of point O', $\boldsymbol{\omega}^-$ is pre-impact angular velocity vector of the block, and $\boldsymbol{r}_{C/O'}$ is position vector of the mass center relative to point O'.

Expressions for these vector quantities are given below:

$$\boldsymbol{v}^- = \dot{X}^-\hat{\boldsymbol{i}} + \dot{Z}^-\hat{\boldsymbol{k}} = \left(\dot{u}^- + \dot{x}_g + \dot{x}_{rot}^- + \dot{x}_s^-\right)\hat{\boldsymbol{i}} + \left(\dot{z}_{rot}^- + \dot{z}_g\right)\hat{\boldsymbol{k}} \tag{6.364}$$

$$\boldsymbol{v}_{O'}^- = \left(\dot{u}^- + \dot{x}_g + \dot{x}_s^-\right)\hat{\boldsymbol{i}} + \left(\dot{z}_g\right)\hat{\boldsymbol{k}} \tag{6.365}$$

$$\boldsymbol{\omega}^- = \dot{\theta}^-\hat{\boldsymbol{j}} \tag{6.366}$$

$$\boldsymbol{r}_{C/O'} = r\sin\left(a-\theta\right)\hat{\boldsymbol{i}} + r\cos\left(a-\theta\right)\hat{\boldsymbol{k}} \tag{6.367}$$

At impact, the angular velocity of the block becomes zero $\left(\theta = 0\right)$ and the position vector of the mass center relative to point O' can be rewritten as

$$\boldsymbol{r}_{C/O'} = \left(r\sin a\right)\hat{\boldsymbol{i}} + \left(r\cos a\right)\hat{\boldsymbol{k}} = b\hat{\boldsymbol{i}} + h\hat{\boldsymbol{k}} \tag{6.368}$$

On substituting Equations (6.364) through (6.368) into Equation (6.363), the pre-impact translational velocity becomes

$$\boldsymbol{v}^{-} \equiv \left(\dot{u}^{-} + \dot{x}_g + \dot{x}_{rot}^{-} + \dot{x}_s^{-}\right)\hat{\boldsymbol{i}} + \left(\dot{z}_{rot}^{-} + \dot{z}_g\right)\hat{\boldsymbol{k}} = \left(\dot{u}^{-} + \dot{x}_g + \dot{x}_s^{-}\right)\hat{\boldsymbol{i}} + \left(\dot{z}_g\right)\hat{\boldsymbol{k}} + \left(\dot{\theta}^{-}\hat{\boldsymbol{j}}\right)\times\left(b\hat{\boldsymbol{i}} + h\hat{\boldsymbol{k}}\right) \quad (6.369)$$

which reduces to

$$\dot{x}_{rot}^{-}\hat{\boldsymbol{i}} + \dot{z}_{rot}^{-}\hat{\boldsymbol{k}} = \left(-b\dot{\theta}^{-}\right)\hat{\boldsymbol{k}} + \left(h\dot{\theta}^{-}\right)\hat{\boldsymbol{i}} \quad (6.370)$$

from which the pre-impact horizontal and vertical components of $\boldsymbol{v}^{-}$ can be retrieved as

$$\dot{x}_{rot}^{-} = h\dot{\theta}^{-} \quad (6.371)$$

$$\dot{z}_{rot}^{-} = -b\dot{\theta}^{-} \quad (6.372)$$

For the post-impact state, the translational velocity vector of the mass center can be expressed as

$$\boldsymbol{v}^{+} = \boldsymbol{v}_O^{+} + \boldsymbol{\omega}^{+} \times \boldsymbol{r}_{C/O} \quad (6.373)$$

where $\boldsymbol{v}^{+}$ is post-impact translational velocity vector of center-of-mass, $\boldsymbol{v}_O^{+}$ is post-impact translational velocity vector of point O, $\boldsymbol{\omega}^{+}$ is post-impact angular velocity vector of the block, and $\boldsymbol{r}_{C/O}$ is position vector of the mass center relative to point O.

Expressions for these vector quantities are given below:

$$\boldsymbol{v}^{+} = \dot{X}^{+}\hat{\boldsymbol{i}} + \dot{Z}^{+}\hat{\boldsymbol{k}} = \left(\dot{u}^{+} + \dot{x}_g + \dot{x}_{rot}^{+} + \dot{x}_s^{+}\right)\hat{\boldsymbol{i}} + \left(\dot{z}_{rot}^{+} + \dot{z}_g\right)\hat{\boldsymbol{k}} \quad (6.374)$$

$$\boldsymbol{v}_O^{+} = \left(\dot{u}^{+} + \dot{x}_g + \dot{x}_s^{+}\right)\hat{\boldsymbol{i}} + \left(\dot{z}_g\right)\hat{\boldsymbol{k}} \quad (6.375)$$

$$\boldsymbol{\omega}^{+} = \dot{\theta}^{+}\hat{\boldsymbol{j}} = 0\,\hat{\boldsymbol{j}} \quad (6.376)$$

$$\boldsymbol{r}_{C/O} = -r\sin\left(a-\theta\right)\hat{\boldsymbol{i}} + r\cos\left(a-\theta\right)\hat{\boldsymbol{k}} \quad (6.377)$$

At impact $\left(\theta = 0\right)$, the position vector of the mass center relative to point O becomes

$$\boldsymbol{r}_{C/O} = -\left(r\sin a\right)\hat{\boldsymbol{i}} + \left(r\cos a\right)\hat{\boldsymbol{k}} = -b\hat{\boldsymbol{i}} + h\hat{\boldsymbol{k}} \tag{6.378}$$

On substituting Equations (6.374) through (6.378) into Equation (6.373), the post-impact translational velocity becomes

$$\boldsymbol{v}^{+} \equiv \left(\dot{u}^{+} + \dot{x}_g + \dot{x}_{rot}^{+} + \dot{x}_s^{+}\right)\hat{\boldsymbol{i}} + \left(\dot{z}_{rot}^{+} + \dot{z}_g\right)\hat{\boldsymbol{k}} = \left(\dot{u}^{+} + \dot{x}_g + \dot{x}_s^{+}\right)\hat{\boldsymbol{i}} + \left(\dot{z}_g\right)\hat{\boldsymbol{k}} + \left(0\hat{\boldsymbol{j}}\right)\times\left(-b\hat{\boldsymbol{i}} + h\hat{\boldsymbol{k}}\right) \tag{6.379}$$

which simplifies to

$$\dot{x}_{rot}^{+}\hat{\boldsymbol{i}} + \dot{z}_{rot}^{+}\hat{\boldsymbol{k}} = 0\hat{\boldsymbol{k}} + 0\hat{\boldsymbol{i}} \tag{6.380}$$

from which the post-impact horizontal and vertical components of $\boldsymbol{v}^{+}$ can be retrieved as

$$\dot{x}_{rot}^{+} = 0 \tag{6.381}$$

$$\dot{z}_{rot}^{+} = 0 \tag{6.382}$$

Substitution of Equations (6.371), (6.372), (6.381) and (6.382) into Equations (6.361) and (6.362) yields

$$\int F_x dt = m\dot{u}^{+} + m\dot{x}_s^{+} - m\dot{u}^{-} - m\left(h\dot{\theta}^{-}\right) - m\dot{x}_s^{-} \tag{6.383}$$

$$\int F_z dt = mb\dot{\theta}^{-} \tag{6.384}$$

which constitutes one equation in three unknowns: $\int F_x dt$, $\dot{u}^{+}$, $\dot{x}_s^{+}$.

Two additional equation is therefore required to uniquely determine the post-impact velocity $\dot{u}^{+}$ and $\dot{x}_s^{+}$.

By considering the system in its entirety during the impact, it can be stated that the horizontal impulse on the system is zero, resulting in the conservation of the system's linear momentum in the horizontal direction. That is,

$$\begin{aligned}&\left(\Delta L_{sys}\right)_x=\left(L_{sys}\right)_x^+-\left(L_{sys}\right)_x^-=0:\ \left[\left(L_{base}\right)_x^++\left(L_{obj}\right)_x^+\right]-\left[\left(L_{base}\right)_x^-+\left(L_{obj}\right)_x^-\right]=0\\&\Rightarrow\left[m_b\left(\dot{u}^++\dot{x}_g\right)+m\left(\dot{u}^++\dot{x}_g+\dot{x}_s^+\right)\right]=\left[m_b\left(\dot{u}^-+\dot{x}_g\right)+m\left(\dot{u}^-+\dot{x}_g+\dot{x}^-+\dot{x}_s^-+\dot{x}_{rot}^-\right)\right]\end{aligned}\tag{6.385}$$

Substituting Equations (6.371) and (6.372) in Equation (6.385) gives

$$m_b\dot{u}^++m\dot{u}^++m\dot{x}_s^+=m_b\dot{u}^-+m\dot{u}^-+mh\dot{\theta}^-+m\dot{x}_s^-\tag{6.386}$$

which upon rearranging terms becomes

$$\dot{u}^+=\frac{1}{m_b+m}\left[\left(m_b+m\right)\dot{u}^-+mh\dot{\theta}^-+m\dot{x}_s^--m\dot{x}_s^+\right]\tag{6.387}$$

With regard to the block, the principle of frictional impulse in the x and z direction states that

$$\int F_x dt=-\operatorname{sgn}\left(\dot{x}_s^+\right)\mu_k\left|\int F_z dt\right|\tag{6.388}$$

Substituting Equations (6.383) and (6.384) in Equation (6.388) gives

$$m\dot{u}^++m\dot{x}_s^+-m\dot{u}^--m\left(h\dot{\theta}^-\right)-m\dot{x}_s^-=-\operatorname{sgn}\left(\dot{x}_s^+\right)\mu_k\left|mb\dot{\theta}^-\right|\tag{6.389}$$

Assume that $\operatorname{sgn}\left(\dot{x}_s^+\right)>0$, Equation (6.389) can be written as

$$\dot{x}_s^+=-\mu_k\left|b\dot{\theta}^-\right|+\dot{u}^-+h\dot{\theta}^-+\dot{x}_s^--\dot{u}^+\tag{6.390}$$

Substituting Equations (6.390) in Equation (6.387) gives

$$\dot{u}^+=\frac{1}{m_b+m}\left[\left(m_b+m\right)\dot{u}^-+mh\dot{\theta}^-+m\dot{x}_s^--m\left(-\mu_k\left|b\dot{\theta}^-\right|+\dot{u}^-+h\dot{\theta}^-+\dot{x}_s^--\dot{u}^+\right)\right]\tag{6.391}$$

Which upon rearranging terms become

$$\dot{u}^+=\dot{u}^-+\frac{m}{m_b}\mu_k\left|b\dot{\theta}^-\right|\tag{6.392}$$

Substituting Equation (6.392) in Equation (6.390) gives

$$\dot{x}_s^+ = -\left(1+\frac{m}{m_b}\right)\mu_k\left|b\dot{\theta}^-\right| + h\dot{\theta}^- + \dot{x}_s^- \tag{6.393}$$

Once Equation (6.393) is solved and $\dot{x}_s^+$ is calculated positive, then the assumption and Equation (6.393) are correct, else a second assumption must be computed, $\text{sgn}\left(\dot{x}_s^+\right) < 0$ and Equation (6.392) can be rewritten as

$$\dot{x}_s^+ = \mu_k\left|b\dot{\theta}^-\right| + \dot{u}^- + h\dot{\theta}^- + \dot{x}_s^- - \dot{u}^+ \tag{6.394}$$

Substituting Equations (6.394) in Equation (6.387) gives

$$\dot{u}^+ = \frac{1}{m_b+m}\left[\left(m_b+m\right)\dot{u}^- + mh\dot{\theta}^- + m\dot{x}_s^- - m\left(\mu_k\left|b\dot{\theta}^-\right| + \dot{u}^- + h\dot{\theta}^- + \dot{x}_s^- - \dot{u}^+\right)\right] \tag{6.395}$$

Which upon rearranging terms become

$$\dot{u}^+ = \dot{u}^- - \frac{m}{m_b}\mu_k\left|b\dot{\theta}^-\right| \tag{6.396}$$

Substituting Equation (6.396) in Equation (6.394) gives

$$\dot{x}_s^+ = \left(1+\frac{m}{m_b}\right)\mu_k\left|b\dot{\theta}^-\right| + h\dot{\theta}^- + \dot{x}_s^- \tag{6.397}$$

The absolute value in Equations (6.392), (6.393), (6.396) and (6.397) can be dropped since the impulse in the z direction must be positive.

Equations (6.392), (6.393), (6.396) and (6.397) can be rewritten in the form

$$\dot{u}^+ = \dot{u}^- + \text{sgn}\left(\dot{x}_s^+\right)\frac{m}{m_b}\mu_k\left(b\dot{\theta}^-\right) \tag{6.398}$$

$$\dot{x}_s^+ = -\text{sgn}\left(\dot{x}_s^+\right)\left(1+\frac{m}{m_b}\right)\mu_k\left(b\dot{\theta}^-\right) + h\dot{\theta}^- + \dot{x}_s^- \tag{6.399}$$

6.4.4 Slide-rocking continues after impact

Derivation for the case of impact during rocking about point O

Consider the system at the instant when the block hits the moving base from rocking about O and re-uplifts pivoting about the impacting corner, O'. As mentioned before, impact is accompanied by an instantaneous change in velocities, with the system displacements being unchanged. Therefore, the impact analysis is reduced to the computation of the initial conditions for the post-impact motion, $\dot{u}^+$, $\dot{x}_s^+$, and $\dot{\theta}^+$, given the position and the pre-impact velocities, $\dot{u}^-$, $\dot{x}_s^-$, and $\dot{\theta}^-$.

With regard to the block, the principle of linear impulse and momentum in the x and z direction states that

$$\int F_x dt = \left(\Delta L\right)_x = L_x^+ - L_x^- : \quad \int F_x dt = m\dot{X}^+ - m\dot{X}^- \tag{6.400}$$

$$\int F_z dt = \left(\Delta L\right)_z = L_z^+ - L_z^- : \quad \int F_z dt = m\dot{Z}^+ - m\dot{Z}^- \tag{6.401}$$

in which $\int F_x dt$ and $\int F_z dt$ are the horizontal and vertical impulses (assumed to act at O'); $\dot{X}^- = \left(\dot{u}^- + \dot{x}_g\right) + \dot{x}_s^- + \dot{x}_{rot}^-$, $\dot{X}^+ = \left(\dot{u}^+ + \dot{x}_g\right) + \dot{x}_s^+ + \dot{x}_{rot}^+$ and $\dot{Z}^- = \left(\dot{z}_{rot}^- + \dot{z}_g\right)$, $\dot{Z}^+ = \left(\dot{z}_{rot}^+ + \dot{z}_g\right)$ are the absolute pre- and post-impact horizontal and vertical velocities of the mass center of the block, respectively; $\dot{x}_{rot}^-$, $\dot{x}_{rot}^+$ and $\dot{z}_{rot}^-$, $\dot{z}_{rot}^+$ are the relative pre- and post-impact horizontal and vertical velocities of the mass center of the block due to the rocking, relative to the rigid base; $\dot{x}_s^-$ and $\dot{x}_s^+$ are the relative pre- and post-impact horizontal velocities of the mass center of the block due to the sliding, relative to the rigid base; L_x^-, L_x^+, L_z^- and L_z^+ are the pre- and post-impact horizontal and vertical linear momentum, respectively; $\left(\Delta L\right)_x$ and $\left(\Delta L\right)_z$ are the changes in horizontal and vertical linear momentum, respectively.

Substituting these expressions into Equations (6.400) and (6.401) we obtain

$$\int F_x dt = m\dot{u}^+ + m\dot{x}_s^+ + m\dot{x}_{rot}^+ - m\dot{u}^- - m\dot{x}_s^- - m\dot{x}_{rot}^- \tag{6.402}$$

$$\int F_z dt = m\dot{z}_{rot}^+ - m\dot{z}_{rot}^- \tag{6.403}$$

In addition, the principle of angular impulse and momentum states that

$$\int M_C dt = \Delta H_C = H_C^+ - H_C^- : \; b\left(\int F_z dt\right) - h\left(\int F_x dt\right) = I\dot{\theta}^+ - I\dot{\theta}^- \tag{6.404}$$

in which $\int M_C dt$ is the angular impulse; H_C^- and H_C^+ are the pre- and post-impact angular momentum about the mass center, respectively; ΔH_C is the change in the angular momentum about the mass center.

In Equations (6.400) and (6.401), the pre- and post-impact horizontal and vertical components of the relative translational velocity of the mass center can be expressed in terms of the pre- and post-impact angular velocity of the block, $\dot{\theta}^-$ and $\dot{\theta}^+$ as follows.

For the pre-impact state, the translational velocity vector of the mass center (Figure 6-15) can be expressed as

$$\boldsymbol{v}^- = \boldsymbol{v}_O^- + \boldsymbol{\omega}^- \times \boldsymbol{r}_{C/O} \tag{6.405}$$

where $\boldsymbol{v}^-$ is pre-impact translational velocity vector of center-of-mass, $\boldsymbol{v}_O^-$ is pre-impact translational velocity vector of point O, $\boldsymbol{\omega}^-$ is pre-impact angular velocity vector of the block, and $\boldsymbol{r}_{C/O}$ is position vector of the mass center relative to point O.

Expressions for these vector quantities are given below:

$$\boldsymbol{v}^- = \dot{X}^-\hat{\boldsymbol{i}} + \dot{Z}^-\hat{\boldsymbol{k}} = \left(\dot{u}^- + \dot{x}_g + \dot{x}_s^- + \dot{x}_{rot}^-\right)\hat{\boldsymbol{i}} + \left(\dot{z}_{rot}^- + \dot{z}_g\right)\hat{\boldsymbol{k}} \tag{6.406}$$

$$\boldsymbol{v}_O^- = \left(\dot{u}^- + \dot{x}_g + \dot{x}_s^-\right)\hat{\boldsymbol{i}} + \left(\dot{z}_g\right)\hat{\boldsymbol{k}} \tag{6.407}$$

$$\boldsymbol{\omega}^- = \dot{\theta}^-\hat{\boldsymbol{j}} \tag{6.408}$$

$$\boldsymbol{r}_{C/O} = -r\sin\left(a-\theta\right)\hat{\boldsymbol{i}} + r\cos\left(a-\theta\right)\hat{\boldsymbol{k}} \tag{6.409}$$

At impact, the angular rotation of the block becomes zero $\left(\theta = 0\right)$ and the position vector of center-of-mass relative to point O, $\boldsymbol{r}_{C/O}$, can be rewritten as

$$\boldsymbol{r}_{C/O} = -\left(r\sin a\right)\hat{\boldsymbol{i}} + \left(r\cos a\right)\hat{\boldsymbol{k}} = -b\hat{\boldsymbol{i}} + h\hat{\boldsymbol{k}} \tag{6.410}$$

in which $\hat{\boldsymbol{i}}$ and $\hat{\boldsymbol{k}}$ are the horizontal and vertical unit vectors respectively.

On substituting Equations (6.406) through (6.410) into Equation (6.405), the pre-impact translational velocity becomes

$$\boldsymbol{v}^{-} \equiv \left(\dot{u}^{-} + \dot{x}_g + \dot{x}_s^{-} + \dot{x}_{rot}^{-}\right)\hat{\boldsymbol{i}} + \left(\dot{z}_{rot}^{-} + \dot{z}_g\right)\hat{\boldsymbol{k}} = \left(\dot{u}^{-} + \dot{x}_g + \dot{x}_s^{-}\right)\hat{\boldsymbol{i}} + \left(\dot{z}_g\right)\hat{\boldsymbol{k}} + \left(\dot{\theta}^{-}\hat{\boldsymbol{j}}\right)\times\left(-b\hat{\boldsymbol{i}} + h\hat{\boldsymbol{k}}\right) \quad (6.411)$$

which reduces to

$$\dot{x}_{rot}^{-}\hat{\boldsymbol{i}} + \dot{z}_{rot}^{-}\hat{\boldsymbol{k}} = \left(b\dot{\theta}^{-}\right)\hat{\boldsymbol{k}} + \left(h\dot{\theta}^{-}\right)\hat{\boldsymbol{i}} \quad (6.412)$$

from which the pre-impact horizontal and vertical components of $\boldsymbol{v}^{-}$ can be retrieved as

$$\dot{x}_{rot}^{-} = h\dot{\theta}^{-} \quad (6.413)$$

$$\dot{z}_{rot}^{-} = b\dot{\theta}^{-} \quad (6.414)$$

For the post-impact state, the translational velocity vector of the mass center (Figure 6-20) can be expressed as

$$\boldsymbol{v}^{+} = \boldsymbol{v}_{O'}^{+} + \boldsymbol{\omega}^{+} \times \boldsymbol{r}_{C/O'} \quad (6.415)$$

where $\boldsymbol{v}^{+}$ is post-impact translational velocity vector of center-of-mass, $\boldsymbol{v}_{O'}^{+}$ is post-impact translational velocity vector of point O', $\boldsymbol{\omega}^{+}$ is post-impact angular velocity vector of the block, and $\boldsymbol{r}_{C/O'}$ is position vector of the mass center relative to point O'.

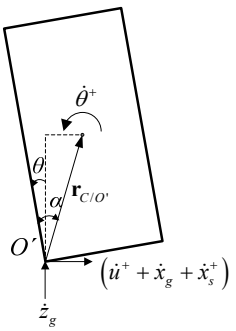

Figure 6-20: Components of post-impact translational velocity of the isolated block for the case of impact during slide-rocking about point *O*.

Expressions for these vector quantities are given below:

$$\boldsymbol{v}^{+} = \dot{X}^{+}\hat{\boldsymbol{i}} + \dot{Z}^{+}\hat{\boldsymbol{k}} = \left(\dot{u}^{+} + \dot{x}_g + \dot{x}_s^{+} + \dot{x}_{rot}^{+}\right)\hat{\boldsymbol{i}} + \left(\dot{z}_{rot}^{+} + \dot{z}_g\right)\hat{\boldsymbol{k}} \tag{6.416}$$

$$\boldsymbol{v}_{O'}^{+} = \left(\dot{u}^{+} + \dot{x}_g + \dot{x}_s^{+}\right)\hat{\boldsymbol{i}} + \left(\dot{z}_g\right)\hat{\boldsymbol{k}} \tag{6.417}$$

$$\boldsymbol{\omega}^{+} = \dot{\theta}^{+}\hat{\boldsymbol{j}} \tag{6.418}$$

$$\boldsymbol{r}_{C/O'} = r\sin\left(a-\theta\right)\hat{\boldsymbol{i}} + r\cos\left(a-\theta\right)\hat{\boldsymbol{k}} \tag{6.419}$$

At impact $\left(\theta = 0\right)$ the position vector of center-of-mass relative to point O', $\boldsymbol{r}_{C/O'}$, becomes

$$\boldsymbol{r}_{C/O'} = \left(r\sin a\right)\hat{\boldsymbol{i}} + \left(r\cos a\right)\hat{\boldsymbol{k}} = b\hat{\boldsymbol{i}} + h\hat{\boldsymbol{k}} \tag{6.420}$$

On substituting Equations (6.416) through (6.420) into Equation (6.415), the post-impact translational velocity becomes

$$\boldsymbol{v}^{+} \equiv \left(\dot{u}^{+} + \dot{x}_g + \dot{x}_{rot}^{+} + \dot{x}_s^{+}\right)\hat{\boldsymbol{i}} + \left(\dot{z}_{rot}^{+} + \dot{z}_g\right)\hat{\boldsymbol{k}} = \left(\dot{u}^{+} + \dot{x}_g + \dot{x}_s^{+}\right)\hat{\boldsymbol{i}} + \left(\dot{z}_g\right)\hat{\boldsymbol{k}} + \left(\dot{\theta}^{+}\hat{\boldsymbol{j}}\right)\times\left(b\hat{\boldsymbol{i}} + h\hat{\boldsymbol{k}}\right) \tag{6.421}$$

which simplifies to

$$\dot{x}_{rot}^{+}\hat{\boldsymbol{i}} + \dot{z}_{rot}^{+}\hat{\boldsymbol{k}} = \left(-b\dot{\theta}^{+}\right)\hat{\boldsymbol{k}} + \left(h\dot{\theta}^{+}\right)\hat{\boldsymbol{i}} \tag{6.422}$$

from which the post-impact horizontal and vertical components of $\boldsymbol{v}^{+}$ can be retrieved as

$$\dot{x}_{rot}^{+} = h\dot{\theta}^{+} \tag{6.423}$$

$$\dot{z}_{rot}^{+} = -b\dot{\theta}^{+} \tag{6.424}$$

Substitution of Equations (6.410), (6.411), (6.420) and (6.421) into Equations (6.402) through (6.404) yields

$$\int F_x dt = m\dot{u}^{+} + m\left(h\dot{\theta}^{+}\right) + m\dot{x}_s^{+} - m\dot{u}^{-} - m\dot{x}_s^{-} - m\left(h\dot{\theta}^{-}\right) \tag{6.425}$$

$$\int F_z dt = m\left(-b\dot{\theta}^+\right) - m\left(b\dot{\theta}^-\right) \tag{6.426}$$

$$b\left(\int F_z dt\right) - h\left(\int F_x dt\right) = I\left(\dot{\theta}^+\right) - I\left(\dot{\theta}^-\right) \tag{6.427}$$

in which the centroid mass moment of inertia for the rectangular block is given by

$$I = \frac{m}{3} r^2 = \frac{m}{3}\left(b^2 + h^2\right) \tag{6.428}$$

Equations (6.425), (6.426) and (6.427) constitute a set of three equations in five unknowns, namely $\int F_x dt$, $\int F_z dt$, $\dot{\theta}^+$, $\dot{u}^+$, $\dot{x}_s^+$.

Equivalently, the three Equations (6.425), (6.426) and (6.427) can be combined in one (by eliminating the two impulses) in three unknowns:

$$\left(4b^2 + 4h^2\right)\dot{\theta}^+ + 3h\dot{u}^+ + 3h\dot{x}_s^+ = \left(4h^2 - 2b^2\right)\dot{\theta}^- + 3h\dot{u}^- + 3h\dot{x}_s^- \tag{6.429}$$

Three additional equations is therefore required to uniquely determine the post-impact velocities $\dot{\theta}^+$, $\dot{u}^+$, $\dot{x}_s^+$. By considering the system in its entirety during the impact, it can be stated that the horizontal impulse on the system is zero, resulting in the conservation of the system's linear momentum in the horizontal direction. That is,

$$\begin{aligned} &\left(\Delta L_{sys}\right)_x = \left(L_{sys}\right)_x^+ - \left(L_{sys}\right)_x^- = 0: \quad \left[\left(L_{base}\right)_x^+ + \left(L_{obj}\right)_x^+\right] - \left[\left(L_{base}\right)_x^- + \left(L_{obj}\right)_x^-\right] = 0 \\ &\Rightarrow \left[m_b\left(\dot{u}^+ + \dot{x}_g\right) + m\left(\dot{u}^+ + \dot{x}_g + \dot{x}_s^+ + \dot{x}_{rot}^+\right)\right] = \left[m_b\left(\dot{u}^- + \dot{x}_g\right) + m\left(\dot{u}^- + \dot{x}_g + \dot{x}_s^- + \dot{x}_{rot}^-\right)\right] \end{aligned} \tag{6.430}$$

in which $\left(L_{sys}\right)_x^-$ and $\left(L_{sys}\right)_x^+$ are the pre- and post-impact horizontal linear momentum of the system respectively; $\left(\Delta L_{sys}\right)_x$ is the change in horizontal linear momentum of the system.

Substituting Equations (6.413), (6.414), (6.423) and (6.424) in Equation (6.430) gives

$$m_b\dot{u}^+ + m\dot{u}^+ + m\dot{x}_s^+ + mh\dot{\theta}^+ = m_b\dot{u}^- + m\dot{u}^- + m\dot{x}_s^- + mh\dot{\theta}^- \tag{6.431}$$

which upon rearranging terms becomes

$$\dot{u}^{+}=\frac{1}{m_b+m}\left[\left(m_b+m\right)\dot{u}^{-}+m\dot{x}_s^{-}-mh\dot{\theta}^{+}-m\dot{x}_s^{+}+mh\dot{\theta}^{-}\right] \tag{6.432}$$

Substituting Equation (6.432) in (6.429) gives

$$\begin{aligned}&\left(4b^2+4h^2\right)\dot{\theta}^{+}+\frac{3h}{m_b+m}\left[\left(m_b+m\right)\dot{u}^{-}+m\dot{x}_s^{-}-mh\dot{\theta}^{+}-m\dot{x}_s^{+}+mh\dot{\theta}^{-}\right]+3h\dot{x}_s^{+}\\&=\left(4h^2-2b^2\right)\dot{\theta}^{-}+3h\dot{u}^{-}+3h\dot{x}_s^{-}\end{aligned} \tag{6.433}$$

which yields

$$\dot{\theta}^{+}=\frac{\left(4m_bh^2-2m_bb^2+mh^2-2mb^2\right)\dot{\theta}^{-}+3hm_b\dot{x}_s^{-}-3hm_b\dot{x}_s^{+}}{\left(4m_bh^2+4m_bb^2+mh^2+4mb^2\right)} \tag{6.434}$$

With regard to the block, the principle of frictional impulse in the x and z direction states that

$$\int F_x dt=-\operatorname{sgn}\left(\dot{x}_s^{+}\right)\mu_k\left|\int F_z dt\right| \tag{6.435}$$

Substituting Equations (6.425) and (6.426) in Equation (6.435) gives

$$m\dot{u}^{+}+m\left(h\dot{\theta}^{+}\right)+m\dot{x}_s^{+}-m\dot{u}^{-}-m\dot{x}_s^{-}-m\left(h\dot{\theta}^{-}\right)=-\operatorname{sgn}\left(\dot{x}_s^{+}\right)\mu_k\left|m\left(-b\dot{\theta}^{+}\right)-m\left(b\dot{\theta}^{-}\right)\right| \tag{6.436}$$

Assume that $\operatorname{sgn}\left(\dot{x}_s^{+}\right)>0$, Equation (6.436) can be written as

$$\dot{x}_s^{+}=-\mu_k\left|\left(-b\dot{\theta}^{+}\right)-\left(b\dot{\theta}^{-}\right)\right|-\dot{u}^{+}-h\dot{\theta}^{+}+\dot{u}^{-}+\dot{x}_s^{-}+h\dot{\theta}^{-} \tag{6.437}$$

Once Equation (6.437) is solved and $\dot{x}_s^{+}$ is calculated positive, then the assumption and Equation (6.437) are correct, else a second assumption must be computed, $\operatorname{sgn}\left(\dot{x}_s^{+}\right)<0$ and Equation (6.436) can be rewritten as

$$\dot{x}_s^{+}=\mu_k\left|\left(-b\dot{\theta}^{+}\right)-\left(b\dot{\theta}^{-}\right)\right|-\dot{u}^{+}-h\dot{\theta}^{+}+\dot{u}^{-}+\dot{x}_s^{-}+h\dot{\theta}^{-} \tag{6.438}$$

The absolute value in Equations (6.437) and (6.438) can be dropped since the impulse in the z direction must be positive.

Equations (6.437) and (6.438) can be rewritten in the form

$$\dot{x}_s^+ = -\mathrm{sgn}\left(\dot{x}_s^+\right)\mu_k\left[\left(-b\dot{\theta}^+\right)-\left(b\dot{\theta}^-\right)\right]-\dot{u}^+ - h\dot{\theta}^+ + \dot{u}^- + \dot{x}_s^- + h\dot{\theta}^- \tag{6.439}$$

Derivation for the case of impact during rocking about point O'

With regard to the block, the principle of linear impulse and momentum in the x and z direction states that

$$\int F_x dt = \left(\Delta L\right)_x = L_x^+ - L_x^- : \quad \int F_x dt = m\dot{X}^+ - m\dot{X}^- \tag{6.440}$$

$$\int F_z dt = \left(\Delta L\right)_z = L_z^+ - L_z^- : \quad \int F_z dt = m\dot{Z}^+ - m\dot{Z}^- \tag{6.441}$$

in which $\int F_x dt$ and $\int F_z dt$ are the horizontal and vertical impulses (assumed to act at O'); $\dot{X}^- = \left(\dot{u}^- + \dot{x}_g\right) + \dot{x}_s^- + \dot{x}_{rot}^-$, $\dot{X}^+ = \left(\dot{u}^+ + \dot{x}_g\right) + \dot{x}_s^+ + \dot{x}_{rot}^+$ and $\dot{Z}^- = \left(\dot{z}_{rot}^- + \dot{z}_g\right)$, $\dot{Z}^+ = \left(\dot{z}_{rot}^+ + \dot{z}_g\right)$ are the absolute pre- and post-impact horizontal and vertical velocities of the mass center of the block, respectively; $\dot{x}_{rot}^-$, $\dot{x}_{rot}^+$ and $\dot{z}_{rot}^-$, $\dot{z}_{rot}^+$ are the relative pre- and post-impact horizontal and vertical velocities of the mass center of the block due to the rocking, relative to the rigid base; $\dot{x}_s^-$ and $\dot{x}_s^+$ are the relative pre- and post-impact horizontal velocities of the mass center of the block due to the sliding, relative to the rigid base; L_x^-, L_x^+, L_z^- and L_z^+ are the pre- and post-impact horizontal and vertical linear momentum, respectively; $\left(\Delta L\right)_x$ and $\left(\Delta L\right)_z$ are the changes in horizontal and vertical linear momentum, respectively.

Substituting these expressions into Equations (6.440) and (6.441) we obtain

$$\int F_x dt = m\dot{u}^+ + m\dot{x}_s^+ + m\dot{x}_{rot}^+ - m\dot{u}^- - m\dot{x}_s^- - m\dot{x}_{rot}^- \tag{6.442}$$

$$\int F_z dt = m\dot{z}_{rot}^+ - m\dot{z}_{rot}^- \tag{6.443}$$

In addition, the principle of angular impulse and momentum states that

$$\int M_C dt = \Delta H_C = H_C^+ - H_C^- : \quad -b\left(\int F_z dt\right) - h\left(\int F_x dt\right) = I\dot{\theta}^+ - I\dot{\theta}^- \tag{6.444}$$

in which $\int M_C dt$ is the angular impulse; H_C^- and H_C^+ are the pre- and post-impact angular momentum about the mass center, respectively; ΔH_C is the change in the angular momentum about the mass center.

In Equations (6.442) and (6.443), the pre- and post-impact horizontal and vertical components of the relative translational velocity of the mass center can be expressed in terms of the pre- and post-impact angular velocity of the block, $\dot{\theta}^-$ and $\dot{\theta}^+$ as follows.

For the pre-impact state, the translational velocity vector of the mass center (Figure 6-16) can be expressed as

$$\boldsymbol{v}^- = \boldsymbol{v}_{O'}^- + \boldsymbol{\omega}^- \times \boldsymbol{r}_{C/O'} \tag{6.445}$$

where $\boldsymbol{v}^-$ is pre-impact translational velocity vector of center-of-mass, $\boldsymbol{v}_{O'}^-$ is pre -impact translational velocity vector of point O', $\boldsymbol{\omega}^-$ is pre-impact angular velocity vector of the block, and $\boldsymbol{r}_{C/O'}$ is position vector of the mass center relative to point O'.

Expressions for these vector quantities are given below:

$$\boldsymbol{v}^- = \dot{X}^-\hat{\boldsymbol{i}} + \dot{Z}^-\hat{\boldsymbol{k}} = \left(\dot{u}^- + \dot{x}_g + \dot{x}_s^- + \dot{x}_{rot}^-\right)\hat{\boldsymbol{i}} + \left(\dot{z}_{rot}^- + \dot{z}_g\right)\hat{\boldsymbol{k}} \tag{6.446}$$

$$\boldsymbol{v}_{O'}^- = \left(\dot{u}^- + \dot{x}_g + \dot{x}_s^-\right)\hat{\boldsymbol{i}} + \left(\dot{z}_g\right)\hat{\boldsymbol{k}} \tag{6.447}$$

$$\boldsymbol{\omega}^- = \dot{\theta}^-\hat{\boldsymbol{j}} \tag{6.448}$$

$$\boldsymbol{r}_{C/O'} = r\sin\left(a-\theta\right)\hat{\boldsymbol{i}} + r\cos\left(a-\theta\right)\hat{\boldsymbol{k}} \tag{6.449}$$

At impact, the angular rotation of the block becomes zero $\left(\theta = 0\right)$ and the position vector of center-of-mass relative to point O', $\boldsymbol{r}_{C/O'}$, can be written as

$$\boldsymbol{r}_{C/O'} = \left(r\sin a\right)\hat{\boldsymbol{i}} + \left(r\cos a\right)\hat{\boldsymbol{k}} = b\hat{\boldsymbol{i}} + h\hat{\boldsymbol{k}} \tag{6.450}$$

in which $\hat{\boldsymbol{i}}$ and $\hat{\boldsymbol{k}}$ are the horizontal and vertical unit vectors respectively.

On substituting Equations (6.446) through (6.450) into Equation (6.445), the pre-impact translational velocity becomes

$$\boldsymbol{v}^{-} \equiv \left(\dot{u}^{-} + \dot{x}_g + \dot{x}_s^{-} + \dot{x}_{rot}^{-}\right)\hat{\boldsymbol{i}} + \left(\dot{z}_{rot}^{-} + \dot{z}_g\right)\hat{\boldsymbol{k}} = \left(\dot{u}^{-} + \dot{x}_g + \dot{x}_s^{-}\right)\hat{\boldsymbol{i}} + \left(\dot{z}_g\right)\hat{\boldsymbol{k}} + \left(\dot{\theta}^{-}\hat{\boldsymbol{j}}\right)\times\left(b\hat{\boldsymbol{i}} + h\hat{\boldsymbol{k}}\right) \quad (6.451)$$

which reduces to

$$\dot{x}_{rot}^{-}\hat{\boldsymbol{i}} + \dot{z}_{rot}^{-}\hat{\boldsymbol{k}} = \left(-b\dot{\theta}^{-}\right)\hat{\boldsymbol{k}} + \left(h\dot{\theta}^{-}\right)\hat{\boldsymbol{i}} \quad (6.452)$$

from which the pre-impact horizontal and vertical components of $\boldsymbol{v}^{-}$ can be retrieved as

$$\dot{x}_{rot}^{-} = h\dot{\theta}^{-} \quad (6.453)$$

$$\dot{z}_{rot}^{-} = -b\dot{\theta}^{-} \quad (6.454)$$

For the post-impact state, the translational velocity vector of the mass center (Figure 6-21) can be expressed as

$$\boldsymbol{v}^{+} = \boldsymbol{v}_O^{+} + \boldsymbol{\omega}^{+} \times \boldsymbol{r}_{C/O} \quad (6.455)$$

where $\boldsymbol{v}^{+}$ is post-impact translational velocity vector of center-of-mass, $\boldsymbol{v}_O^{+}$ is post-impact translational velocity vector of point O, $\boldsymbol{\omega}^{+}$ is post-impact angular velocity vector of the block, and $\boldsymbol{r}_{C/O}$ is position vector of the mass center relative to point O.

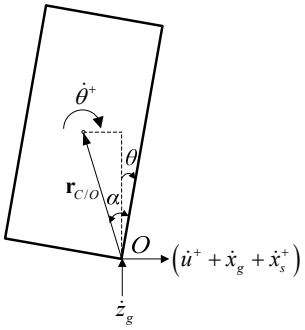

Figure 6-21: Components of post-impact translational velocity of the isolated block for the case of impact during slide-rocking about point O'.

Expressions for these vector quantities are given below:

$$\boldsymbol{v}^+ = \dot{X}^+\hat{\boldsymbol{i}} + \dot{Z}^+\hat{\boldsymbol{k}} = \left(\dot{u}^+ + \dot{x}_g + \dot{x}_s^+ + \dot{x}_{rot}^+\right)\hat{\boldsymbol{i}} + \left(\dot{z}_{rot}^+ + \dot{z}_g\right)\hat{\boldsymbol{k}} \tag{6.456}$$

$$\boldsymbol{v}_O^+ = \left(\dot{u}^+ + \dot{x}_g + \dot{x}_s^+\right)\hat{\boldsymbol{i}} + \left(\dot{z}_g\right)\hat{\boldsymbol{k}} \tag{6.457}$$

$$\boldsymbol{\omega}^+ = \dot{\theta}^+\hat{\boldsymbol{j}} \tag{6.458}$$

$$\boldsymbol{r}_{C/O} = -r\sin\left(a-\theta\right)\hat{\boldsymbol{i}} + r\cos\left(a-\theta\right)\hat{\boldsymbol{k}} \tag{6.459}$$

At impact $\left(\theta = 0\right)$ the position vector of the mass center relative to point O, $\boldsymbol{r}_{C/O}$, becomes

$$\boldsymbol{r}_{C/O} = -\left(r\sin a\right)\hat{\boldsymbol{i}} + \left(r\cos a\right)\hat{\boldsymbol{k}} = -b\hat{\boldsymbol{i}} + h\hat{\boldsymbol{k}} \tag{6.460}$$

On substituting Equations (6.456) through (6.460) into Equation(6.455), the post-impact translational velocity becomes

$$\begin{aligned}\boldsymbol{v}^+ \equiv \left(\dot{u}^+ + \dot{x}_g + \dot{x}_{rot}^+ + \dot{x}_s^+\right)\hat{\boldsymbol{i}} + \left(\dot{z}_{rot}^+ + \dot{z}_g\right)\hat{\boldsymbol{k}} &= \left(\dot{u}^+ + \dot{x}_g + \dot{x}_s^+\right)\hat{\boldsymbol{i}} + \left(\dot{z}_g\right)\hat{\boldsymbol{k}} + \left(\dot{\theta}^+\hat{\boldsymbol{j}}\right)\times\left(-b\hat{\boldsymbol{i}} + h\hat{\boldsymbol{k}}\right) \\ \Rightarrow \dot{x}_{rot}^+\hat{\boldsymbol{i}} + \dot{z}_{rot}^+\hat{\boldsymbol{k}} &= \left(b\dot{\theta}^+\right)\hat{\boldsymbol{k}} + \left(h\dot{\theta}^+\right)\hat{\boldsymbol{i}}\end{aligned} \tag{6.461}$$

from which the post-impact horizontal and vertical components of $\boldsymbol{v}^+$ can be retrieved as

$$\dot{x}_{rot}^+ = h\dot{\theta}^+ \tag{6.462}$$

$$\dot{z}_{rot}^+ = b\dot{\theta}^+ \tag{6.463}$$

Substitution of Equations (6.453), (6.454), (6.462) and (6.463) into Equations (6.442) through (6.444) yields

$$\int F_x dt = m\dot{u}^+ + m\left(h\dot{\theta}^+\right) + m\dot{x}_s^+ - m\dot{u}^- - m\dot{x}_s^- - m\left(h\dot{\theta}^-\right) \tag{6.464}$$

$$\int F_z dt = m\left(b\dot{\theta}^+\right) - m\left(-b\dot{\theta}^-\right) \tag{6.465}$$

$$-b\left(\int F_z dt\right) - h\left(\int F_x dt\right) = I\left(\dot{\theta}^+\right) - I\left(\dot{\theta}^-\right) \tag{6.466}$$

in which the centroid mass moment of inertia for the rectangular block is given by

$$I = \frac{m}{3} r^2 = \frac{m}{3}\left(b^2 + h^2\right) \tag{6.467}$$

Equations (6.464), (6.465) and (6.466) constitute a set of three equations in five unknowns, namely $\int F_x dt$, $\int F_z dt$, $\dot{\theta}^+$, $\dot{u}^+$, $\dot{x}_s^+$.

Equivalently, the three Equations (6.464), (6.465) and (6.466) can be combined in one (by eliminating the two impulses) in three unknowns:

$$\left(4b^2 + 4h^2\right)\dot{\theta}^+ + 3h\dot{u}^+ + 3h\dot{x}_s^+ = \left(4h^2 - 2b^2\right)\dot{\theta}^- + 3h\dot{u}^- + 3h\dot{x}_s^- \tag{6.468}$$

Three additional equations are therefore required to uniquely determine the post-impact velocities $\dot{\theta}^+$, $\dot{u}^+$, $\dot{x}_s^+$. By considering the system in its entirety during the impact, it can be stated that the horizontal impulse on the system is zero, resulting in the conservation of the system's linear momentum in the horizontal direction. That is,

$$\begin{aligned} &\left(\Delta L_{sys}\right)_x = \left(L_{sys}\right)_x^+ - \left(L_{sys}\right)_x^- = 0: \quad \left[\left(L_{base}\right)_x^+ + \left(L_{obj}\right)_x^+\right] - \left[\left(L_{base}\right)_x^- + \left(L_{obj}\right)_x^-\right] = 0 \\ &\Rightarrow \left[m_b\left(\dot{u}^+ + \dot{x}_g\right) + m\left(\dot{u}^+ + \dot{x}_g + \dot{x}_s^+ + \dot{x}_{rot}^+\right)\right] = \left[m_b\left(\dot{u}^- + \dot{x}_g\right) + m\left(\dot{u}^- + \dot{x}_g + \dot{x}_s^- + \dot{x}_{rot}^-\right)\right] \end{aligned} \tag{6.469}$$

in which $\left(L_{sys}\right)_x^-$ and $\left(L_{sys}\right)_x^+$ are the pre- and post-impact horizontal linear momentum of the system respectively; $\left(\Delta L_{sys}\right)_x$ is the change in horizontal linear momentum of the system.

Substituting Equations (6.453), (6.454), (6.462) and (6.463) in Equation (6.469) gives

$$m_b\dot{u}^+ + m\dot{u}^+ + m\dot{x}_s^+ + mh\dot{\theta}^+ = m_b\dot{u}^- + m\dot{u}^- + m\dot{x}_s^- + mh\dot{\theta}^- \tag{6.470}$$

which upon rearranging terms becomes

$$\dot{u}^+ = \frac{1}{m_b + m}\left[\left(m_b + m\right)\dot{u}^- + m\dot{x}_s^- - mh\dot{\theta}^+ - m\dot{x}_s^+ + mh\dot{\theta}^-\right] \tag{6.471}$$

Substituting Equation (6.471) in (6.468) gives

$$\begin{aligned}&\left(4b^2+4h^2\right)\dot{\theta}^+ + \frac{3h}{m_b+m}\left[\left(m_b+m\right)\dot{u}^- + m\dot{x}_s^- - mh\dot{\theta}^+ - m\dot{x}_s^+ + mh\dot{\theta}^-\right] + 3h\dot{x}_s^+ \\ &= \left(4h^2-2b^2\right)\dot{\theta}^- + 3h\dot{u}^- + 3h\dot{x}_s^-\end{aligned} \tag{6.472}$$

which yields

$$\dot{\theta}^+ = \frac{\left(4m_bh^2-2m_bb^2+mh^2-2mb^2\right)\dot{\theta}^- + 3hm_b\dot{x}_s^- - 3hm_b\dot{x}_s^+}{\left(4m_bh^2+4m_bb^2+mh^2+4mb^2\right)} \tag{6.473}$$

With regard to the block, the principle of frictional impulse in the x and z direction states that

$$\int F_x dt = -\operatorname{sgn}\left(\dot{x}_s^+\right)\mu_k\left|\int F_z dt\right| \tag{6.474}$$

Substituting Equations (6.464) and (6.465) in Equation (6.474) gives

$$m\dot{u}^+ + m\left(h\dot{\theta}^+\right) + m\dot{x}_s^+ - m\dot{u}^- - m\dot{x}_s^- - m\left(h\dot{\theta}^-\right) = -\operatorname{sgn}\left(\dot{x}_s^+\right)\mu_k\left|m\left(b\dot{\theta}^+\right) + m\left(b\dot{\theta}^-\right)\right| \tag{6.475}$$

Assume that $\operatorname{sgn}\left(\dot{x}_s^+\right) > 0$, Equation (6.475) can be written as

$$\dot{x}_s^+ = -\mu_k\left|\left(b\dot{\theta}^+\right) + \left(b\dot{\theta}^-\right)\right| - \dot{u}^+ - h\dot{\theta}^+ + \dot{u}^- + \dot{x}_s^- + h\dot{\theta}^- \tag{6.476}$$

Once Equation (6.476) is solved and $\dot{x}_s^+$ is calculated positive, then the assumption and Equation (6.476) are correct, else a second assumption must be computed, $\operatorname{sgn}\left(\dot{x}_s^+\right) < 0$ and Equation (6.475) can be rewritten as

$$\dot{x}_s^+ = \mu_k\left|\left(b\dot{\theta}^+\right) + \left(b\dot{\theta}^-\right)\right| - \dot{u}^+ - h\dot{\theta}^+ + \dot{u}^- + \dot{x}_s^- + h\dot{\theta}^- \tag{6.477}$$

The absolute value in Equations (6.476) and (6.477) can be dropped since the impulse in the z direction must be positive.

Equations (6.476) and (6.477) can be rewritten in the form

$$\dot{x}_s^+ = -\operatorname{sgn}\left(\dot{x}_s^+\right)\mu_k\left[\left(b\dot{\theta}^+\right) + \left(b\dot{\theta}^-\right)\right] - \dot{u}^+ - h\dot{\theta}^+ + \dot{u}^- + \dot{x}_s^- + h\dot{\theta}^- \tag{6.478}$$

CHAPTER 7

Computer Program and Numerical Solution

7.1 Introduction

A computer program was developed to numerically determine the response of the system under horizontal and vertical ground excitations. The numerical integration of the equations of motion is pursued in Matlab (MathWorks 2006) through a state-space formulation. The computer program calculates the response of a non-isolated or isolated block subjected to ground excitation under general conditions, considering the different possible oscillation regimes, impact, transition criteria and arbitrary excitation. In particular, at each time step the program determines the correct oscillation regime and integrates the corresponding exact nonlinear equations of motion. In addition, close attention is paid to the possibility of transition from one regime of motion to another and to the accurate evaluation of the initial conditions for the next regime of oscillation.

By utilizing the developed computer program, an extensive numerical investigation is performed to calculate the dynamic response of the system under simple trigonometric, idealized ground-acceleration pulses and recorded pulse-type earthquake motions, with the aim of revealing interrelations among the problem parameters and identifying potential trends in the response and stability of the system.

7.2 Structure of the Program

Figure 7-1 presents the main structure of the program through a flowchart. The program is versatile and easy to use as it gives the ability to the user to choose different variables:

- the type of model: rocking rigid block or general rigid block (sliding, rocking, slide-rocking etc.),
- the type of system: non-isolated or isolated,
- the type of isolation system: linear or nonlinear, and its characteristics,
- the characteristics of the block: mass of the block, mass of the base, block size, slenderness ratio, coefficient of static friction between the block and the base (for

general rigid block),

- the type of ground excitation: earthquake or pulse-type motion and
- the results: response histories, response-regime spectra etc.

The developed program runs an accurate and highly nonlinear analysis to determine the response of the system under horizontal and vertical ground excitations. The system may transit from one oscillation pattern to another (potentially modifying the degrees of freedom), at any time due to an impact event and when an appropriate transition criterion is satisfied.

In particular, the run analysis section is composed of a main program that is divided into several functions. Each function represents an oscillation pattern and integrates the corresponding exact nonlinear equations of motion using an ordinary-differential-equation solver. The main program calls for the first time a function when an initiation criterion is satisfied. In each time step, the function checks if any appropriate transition criterion is satisfied, if an impact event is detected ($\theta = 0$), or if the rigid block has failed (overturning, $\theta / \alpha \geq 1$). If any of the aforementioned criteria are detected, the output of the function includes the exact time that the event happened and the values of the appropriate variables (degrees-of-freedom) that were calculated using integration until this time.

Then, the main program checks which transition criterion is satisfied, or if an impact event is detected, and computes the initial conditions or the post-impact velocities for the next regime of oscillation. If the block fails (overturns) then the program stops the analysis and exports the appropriate results. The above procedure is accomplished at each time step of the excitation. Finally, the program exports the results from the analysis that can be easily processed by the user. The main structure of the aforementioned procedure for the general isolated rigid block is shown through flowcharts in Figures 7-2 through 7-5.

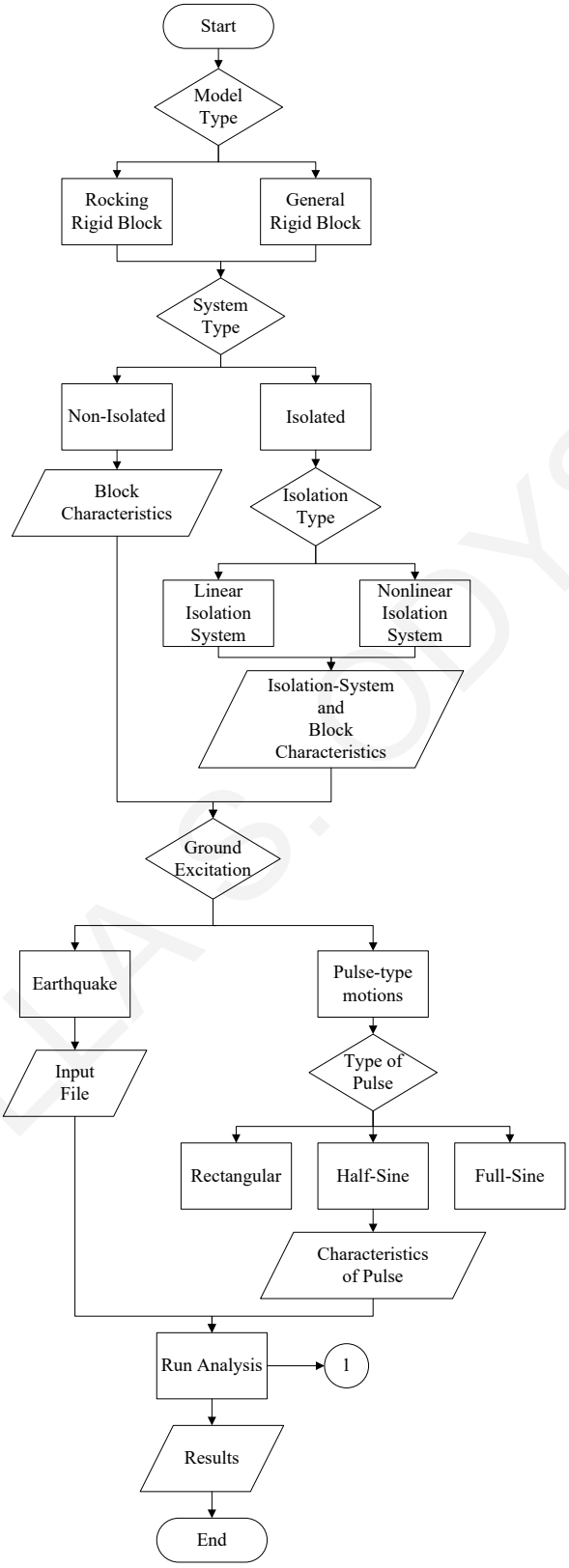

Figure 7-1: Structure of developed program.

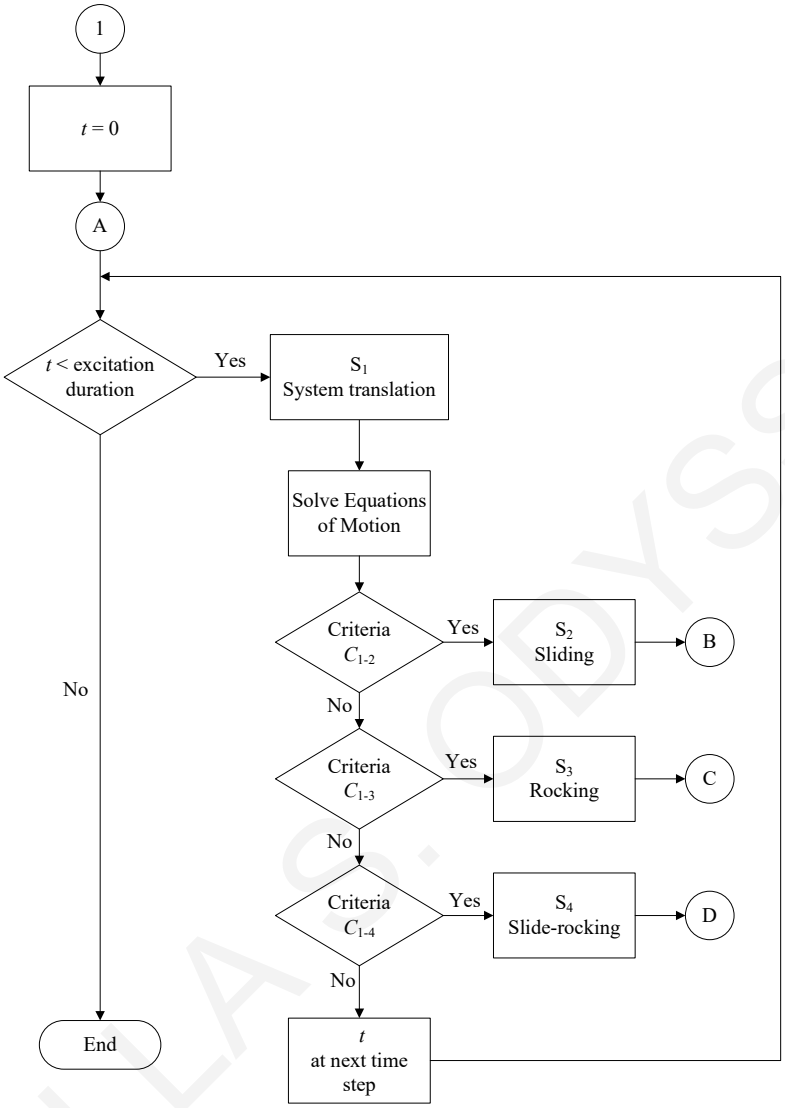

Figure 7-2: Structure of developed program: links 1 and A.

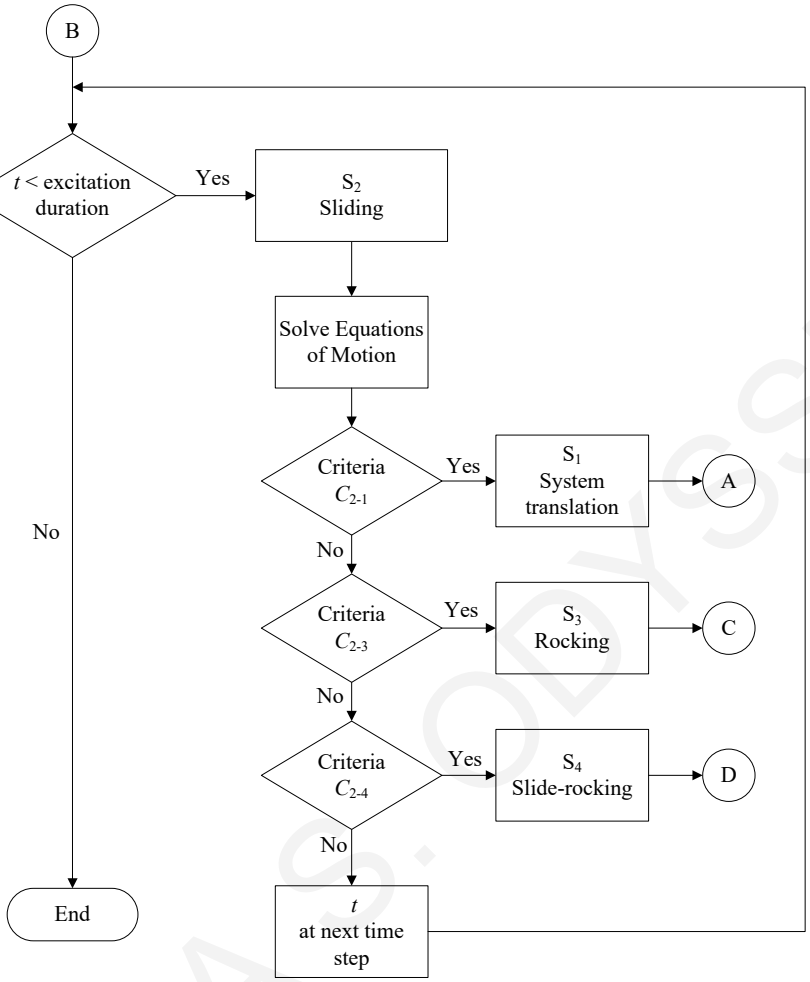

Figure 7-3: Structure of developed program: link B.

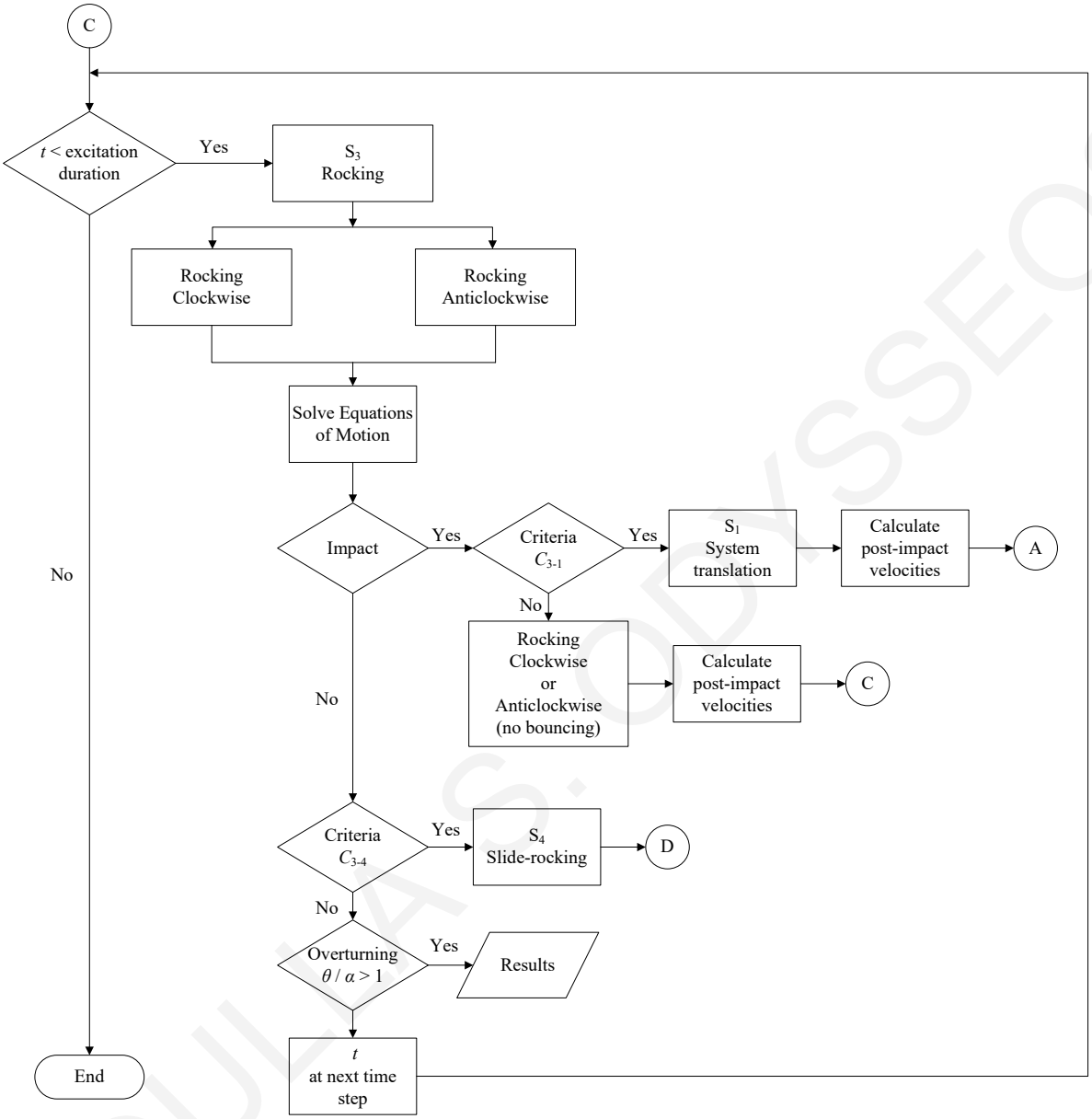

Figure 7-4: Structure of developed program: link C.

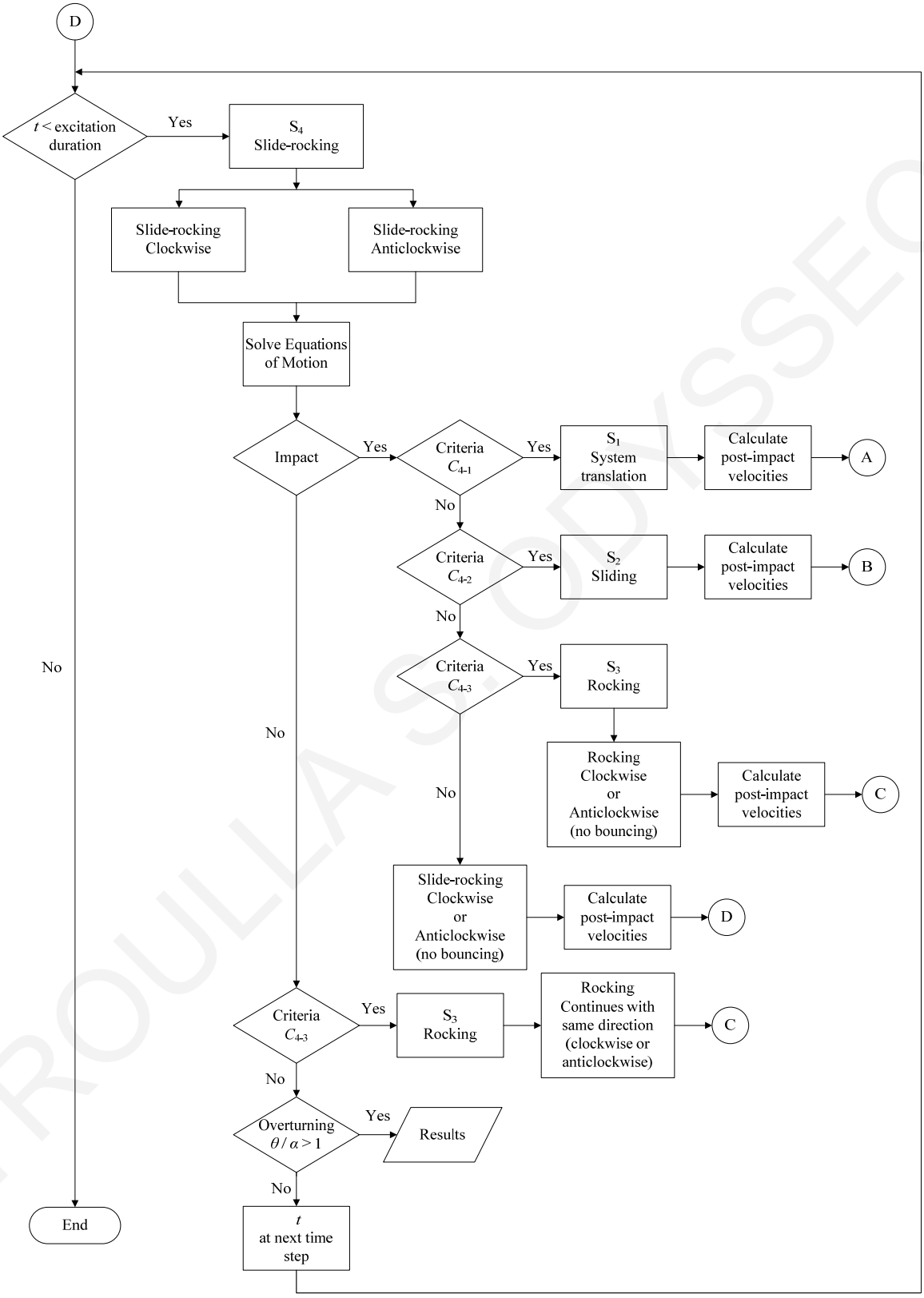

Figure 7-5: Structure of developed program: link D.

7.3 State-space formulation

The numerical integration of the governing equations of motion is accomplished using Matlab's ordinary-differential-equation solver ODE45, which is an implementation of fourth/fifth-order Runge-Kutta method (Dormand and Prince (1980)). Solving the equations of motion applying this function involves re-writing the differential equations as a set of first-order ordinary differential equations (ODEs). This involves introduction of new variables and recasting the original equations in terms of first-order ODEs in the new variables. For this reason, a state-space formulation is employed to yield a system of first-order differential equations.

7.3.1 System translation regime

Linear Isolation System

For motion in the system translation regime, the governing equation of motion is

$$M\ddot{u} + c_b\dot{u} + k_b u = -M\ddot{x}_g \tag{7.1}$$

where

$$M = m + m_b \tag{7.2}$$

The state-space formulation of a second-order differential equations is derived by setting the displacement, u, and velocity, $\dot{u}$, of the linear isolation system equal to the state variables z_1 and z_2 respectively as

$$z_1 \equiv u \tag{7.3}$$

$$z_2 \equiv \dot{u} \tag{7.4}$$

The derivatives of the state variables are expressed as

$$\dot{z}_1 = \dot{u} = z_2 \tag{7.5}$$

$$\dot{z}_2 = \ddot{u} = -\frac{1}{M}\left(c_b\dot{u} + k_b u + M\ddot{x}_g\right) \tag{7.6}$$

Finally, Equation (7.1) can be rewritten as a set of two first-order ODEs, representing the first derivative (Equation (7.5)) and the second derivative (Equation (7.6)) of the displacement of isolation system as

$$\{\dot{z}\} = \begin{Bmatrix} \dot{z}_1 \\ \dot{z}_2 \end{Bmatrix} = \begin{Bmatrix} z_2 \\ -\frac{1}{M}\left(c_b z_2 + k_b z_1\right) - \ddot{x}_g \end{Bmatrix} \tag{7.7}$$

Nonlinear Isolation System

For motion in the system translation regime, the governing equation of motion is

$$M\ddot{u} + \mu_b M g\, \boldsymbol{Z} + \left[\left(Mg + M\ddot{z}_g\right)/R\right]u = -M\ddot{x}_g \tag{7.8}$$

where

$$M = m + m_b \tag{7.9}$$

The state-space formulation of a second-order differential equations is derived by setting the displacement, u, velocity, $\dot{u}$, and dimensionless variable, $\boldsymbol{Z}$, of the nonlinear isolation system equal to the state variables z_1, z_2, and z_3 respectively as

$$z_1 \equiv u \tag{7.10}$$

$$z_2 \equiv \dot{u} \tag{7.11}$$

$$z_3 \equiv \boldsymbol{Z} \tag{7.12}$$

The derivatives of the state variables are expressed as

$$\dot{z}_1 = \dot{u} = z_2 \tag{7.13}$$

$$\dot{z}_2 = \ddot{u} = -\frac{1}{M}\left\{\left(\mu_b Mg + \mu_b M\ddot{z}_g\right)\boldsymbol{Z} + \left[\left(Mg + M\ddot{z}_g\right)/R\right]u + M\ddot{x}_g\right\} \tag{7.14}$$

$$\dot{z}_3 = \dot{\boldsymbol{Z}} = \frac{-\gamma\left|\dot{u}\right|\boldsymbol{Z}\left|\boldsymbol{Z}\right| - \beta\dot{u}\left|\boldsymbol{Z}\right|^2 + A\dot{u}}{Y} \tag{7.15}$$

Finally, Equation (7.8) can be rewritten as a set of three first-order ODEs, representing the first derivative (Equation (7.13)) and the second derivative (Equation (7.14)) of the displacement of isolation system and the first derivative (Equation (7.15)) of the dimensionless variable as

$$\left\{\dot{z}\right\}=\begin{Bmatrix}\dot{z}_1\\ \dot{z}_2\\ \dot{z}_3\end{Bmatrix}=\begin{Bmatrix} z_2 \\ -\frac{1}{M}\left\{\left(\mu_b Mg+\mu_b M\ddot{z}_g\right)z_3+\left[\left(Mg+M\ddot{z}_g\right)/R\right]z_1\right\}-\ddot{x}_g \\ \frac{-\gamma\left|z_2\right|z_3\left|z_3\right|-\beta z_2\left|z_3\right|^2+Az_2}{Y}\end{Bmatrix} \tag{7.16}$$

7.3.2 Sliding regime

Linear Isolation System

The motion of the system in the sliding regime can be described by the following set of equations

$$M\ddot{u}+m\ddot{x}_s+c_b\dot{u}+k_b u=-M\ddot{x}_g \tag{7.17}$$

$$m\ddot{u}+m\ddot{x}_s+m\,\mathrm{sgn}\left(\dot{x}_s\right)\mu_k\left(g+\ddot{z}_g\right)=-m\ddot{x}_g \tag{7.18}$$

where

$$M=m+m_b \tag{7.19}$$

Adding Equation (7.18) to Equation (7.17) gives

$$\ddot{u}=-\ddot{x}_g-\frac{c_b}{m_b}\dot{u}-\frac{k_b}{m_b}u+\frac{m}{m_b}\mathrm{sgn}\left(\dot{x}_s\right)\mu_k\left(g+\ddot{z}_g\right) \tag{7.20}$$

Multiplying Equation (7.17) by $\frac{m}{M}$ and adding to Equation (7.18) gives

$$\ddot{x}_s=\left[\frac{k_b u}{M}+\frac{c_b\dot{u}}{M}-\mathrm{sgn}\left(\dot{x}_s\right)\mu_k\left(g+\ddot{z}_g\right)\right]\Big/\left(1-\frac{m}{M}\right) \tag{7.21}$$

The state-space formulation of a second-order differential equations is derived by setting the displacement, u, velocity, $\dot{u}$, of the linear isolation system and the displacement, x_s, and velocity, $\dot{x}_s$, of the rigid block due to sliding on the rigid base equal to the state variables z_1, z_2, z_3, and z_4 respectively as

$$z_1 \equiv u \tag{7.22}$$

$$z_2 \equiv \dot{u} \tag{7.23}$$

$$z_3 \equiv x_s \tag{7.24}$$

$$z_4 \equiv \dot{x}_s \tag{7.25}$$

The derivatives of the state variables are expressed as

$$\dot{z}_1 = \dot{u} = z_2 \tag{7.26}$$

$$\dot{z}_2 = \ddot{u} \tag{7.27}$$

$$\dot{z}_3 = \dot{x}_s = z_4 \tag{7.28}$$

$$\dot{z}_4 = \ddot{x}_s \tag{7.29}$$

Finally, Equations (7.20) and (7.21) can be rewritten as a set of four first-order ODEs, representing the first derivative (Equation (7.26)) and the second derivative (Equation (7.27)) of the displacement of isolation system and the first derivative (Equation (7.28)) and the second derivative (Equation (7.29)) of the displacement of rigid block due to sliding as

$$\{\dot{z}\} = \begin{Bmatrix} \dot{z}_1 \\ \dot{z}_2 \\ \dot{z}_3 \\ \dot{z}_4 \end{Bmatrix} = \begin{Bmatrix} z_2 \\ -\ddot{x}_g - \dfrac{c_b}{m_b} z_2 - \dfrac{k_b}{m_b} z_1 + \dfrac{m}{m_b} \operatorname{sgn}(z_4)\, \mu_k \left(g + \ddot{z}_g\right) \\ z_4 \\ \left[\dfrac{k_b z_1}{M} + \dfrac{c_b z_2}{M} - \operatorname{sgn}(z_4)\, \mu_k \left(g + \ddot{z}_g\right) \right] \Big/ \left(1 - \dfrac{m}{M}\right) \end{Bmatrix} \tag{7.30}$$

Nonlinear Isolation System

The motion of the system in the sliding regime is governed by the following set of equations

$$\left(m+m_b\right)\ddot{u}+m\ddot{x}_s+\mu_b Mg\boldsymbol{Z}+\left[\left(Mg+M\ddot{z}_g\right)/R\right]u=-\left(m+m_b\right)\ddot{x}_g \tag{7.31}$$

$$m\ddot{u}+m\ddot{x}_s+\mathrm{sgn}(\dot{x}_s)\mu_k m\left(g+\ddot{z}_g\right)=-m\ddot{x}_g \tag{7.32}$$

where

$$M=m+m_b \tag{7.33}$$

Adding Equation (7.32) to Equation (7.31) gives

$$\ddot{u}=-\ddot{x}_g-\frac{\mu_b Mg\boldsymbol{Z}}{m_b}-\left[\left(Mg+M\ddot{z}_g\right)/\left(m_b R\right)\right]u+\frac{m}{m_b}\mathrm{sgn}\left(\dot{x}_s\right)\mu_k\left(g+\ddot{z}_g\right) \tag{7.34}$$

Multiplying Equation (7.31) by $\frac{m}{M}$ and adding to Equation (7.32) gives

$$\ddot{x}_s=\left\{\left[\left(Mg+M\ddot{z}_g\right)/\left(MR\right)\right]u+\frac{\mu_b Mg\boldsymbol{Z}}{M}-\mathrm{sgn}\left(\dot{x}_s\right)\mu_k\left(g+\ddot{z}_g\right)\right\}\Big/\left(1-\frac{m}{M}\right) \tag{7.35}$$

The state-space formulation of a second-order differential equations is derived by setting the displacement, u, velocity, $\dot{u}$, dimensionless variable, $\boldsymbol{Z}$, of the nonlinear isolation system and the displacement, x_s, and velocity, $\dot{x}_s$, of the rigid block due to sliding on the rigid base equal to the state variables z_1, z_2, z_3, z_4 and z_5 respectively as

$$z_1\equiv u \tag{7.36}$$

$$z_2\equiv\dot{u} \tag{7.37}$$

$$z_3\equiv\boldsymbol{Z} \tag{7.38}$$

$$z_4\equiv x_s \tag{7.39}$$

$$z_5\equiv\dot{x}_s \tag{7.40}$$

The derivatives of the state variables are expressed as

$$\dot{z}_1 = \dot{u} = z_2 \tag{7.41}$$

$$\dot{z}_2 = \ddot{u} \tag{7.42}$$

$$\dot{z}_3 = \dot{\boldsymbol{Z}} = \frac{-\gamma|\dot{u}|\boldsymbol{Z}|\boldsymbol{Z}| - \beta\dot{u}|\boldsymbol{Z}|^2 + A\dot{u}}{Y} \tag{7.43}$$

$$\dot{z}_4 = \dot{x}_s = z_5 \tag{7.44}$$

$$\dot{z}_5 = \ddot{x}_s \tag{7.45}$$

Finally, Equations (7.34) and (7.35) can be rewritten as a set of five first-order ODEs, representing the first (Equation (7.41)) and the second derivative (Equation (7.42)) of the displacement of isolation system, the first derivative (Equation (7.43)) of the dimensionless variable and the first (Equation (7.44)) and the second derivative (Equation (7.45)) of the displacement of rigid block due to sliding as

$$\{\dot{z}\} = \begin{Bmatrix} \dot{z}_1 \\ \dot{z}_2 \\ \dot{z}_3 \\ \dot{z}_4 \\ \dot{z}_5 \end{Bmatrix} = \begin{Bmatrix} z_2 \\ -\ddot{x}_g - \dfrac{\mu_b M g z_3}{m_b} - \left[\left(Mg + M\ddot{z}_g\right)/\left(m_b R\right)\right] z_1 + \dfrac{m}{m_b}\operatorname{sgn}\left(z_5\right)\mu_k\left(g + \ddot{z}_g\right) \\ \dfrac{-\gamma|z_2|z_3|z_3| - \beta z_2|z_3|^2 + A z_2}{Y} \\ z_5 \\ \left\{\left[\left(Mg + M\ddot{z}_g\right)/\left(MR\right)\right] z_1 + \dfrac{\mu_b M g z_3}{M} - \operatorname{sgn}\left(z_5\right)\mu_k\left(g + \ddot{z}_g\right)\right\} \Big/ \left(1 - \dfrac{m}{M}\right) \end{Bmatrix} \tag{7.46}$$

7.3.3 Rocking regime

Linear Isolation System

The motion of the system in the rocking regime is governed by the following set of equations

$$\begin{aligned} &M\ddot{u} + c_b\dot{u} + k_b u + m\left[h\cos\theta + \operatorname{sgn}\theta\left(b\sin\theta\right)\right]\ddot{\theta} + m\left[\operatorname{sgn}\theta\left(b\cos\theta\right) - h\sin\theta\right]\dot{\theta}^2 \\ &= -M\ddot{x}_g \end{aligned} \tag{7.47}$$

$$I_o\ddot{\theta} + m\ddot{u}\left[h\cos\theta + \operatorname{sgn}\theta\left(b\sin\theta\right)\right] + mg\left(\operatorname{sgn}\theta\left(b\cos\theta\right) - h\sin\theta\right)$$
$$= -m\left[h\cos\theta + \operatorname{sgn}\theta\left(b\sin\theta\right)\right]\ddot{x}_g - m\left[\operatorname{sgn}\theta\left(b\cos\theta\right) - h\sin\theta\right]\ddot{z}_g \tag{7.48}$$

where

$$M = m + m_b \tag{7.49}$$

$$I_o = mr^2 + I \tag{7.50}$$

Letting

$$A_1 \equiv h\cos\theta + \operatorname{sgn}\theta\left(b\sin\theta\right) \equiv A_1\left(\theta\right) \tag{7.51}$$

$$A_2 \equiv \operatorname{sgn}\theta\left(b\cos\theta\right) - h\sin\theta \equiv A_2\left(\theta\right) \tag{7.52}$$

Equations (7.47) and (7.48) can be rewritten in the form

$$M\ddot{u} + c_b\dot{u} + k_b u + mA_1\ddot{\theta} + mA_2\dot{\theta}^2 = -M\ddot{x}_g \tag{7.53}$$

$$I_o\ddot{\theta} + mA_1\ddot{u} + mgA_2 = -mA_1\ddot{x}_g - mA_2\ddot{z}_g \tag{7.54}$$

Equations (7.53) and (7.54) can be rewritten as

$$M\ddot{u} + mA_1\ddot{\theta} = -M\ddot{x}_g - c_b\dot{u} - k_b u - mA_2\dot{\theta}^2 \tag{7.55}$$

$$I_o\ddot{\theta} + mA_1\ddot{u} + mgA_2 = -mA_1\ddot{x}_g - mA_2\ddot{z}_g \tag{7.56}$$

Multiplying Equation (7.56) by $-\dfrac{mA_1}{I_o}$ and adding to Equation (7.55) gives

$$\left(M - \frac{m^2A_1^2}{I_o}\right)\ddot{u} = \left(\frac{m^2A_1^2}{I_o} - M\right)\ddot{x}_g - c_b\dot{u} - k_b u - mA_2\dot{\theta}^2 + \frac{m^2gA_1A_2}{I_o} + \frac{m^2A_1A_2}{I_o}\ddot{z}_g \tag{7.57}$$

which upon rearranging terms yields

$$\ddot{u} = -\ddot{x}_g + \frac{1}{\left(M - \frac{m^2 A_1^{\,2}}{I_o}\right)}\left[-c_b\dot{u} - k_b u - mA_2\dot{\theta}^2 + \frac{m^2 A_1 A_2}{I_o}\left(g + \ddot{z}_g\right)\right] \tag{7.58}$$

Multiplying Equation (7.55) by $-\frac{mA_1}{M}$ and adding to Equation (7.56) gives

$$\left(I_o - \frac{m^2 A_1^{\,2}}{M}\right)\ddot{\theta} = \frac{mA_1 c_b}{M}\dot{u} + \frac{mA_1 k_b}{M}u + \frac{m^2 A_1 A_2}{M}\dot{\theta}^2 - mA_2\left(g + \ddot{z}_g\right) \tag{7.59}$$

which upon rearranging terms yields

$$\ddot{\theta} = \left(\frac{1}{I_o - \frac{m^2 A_1^{\,2}}{M}}\right)\left[\frac{mA_1 c_b}{M}\dot{u} + \frac{mA_1 k_b}{M}u + \frac{m^2 A_1 A_2}{M}\dot{\theta}^2 - mA_2\left(g + \ddot{z}_g\right)\right] \tag{7.60}$$

The state-space formulation of a second-order differential equations is derived by setting the displacement, u, velocity, $\dot{u}$, of the linear isolation system and the rotation angle, θ, and rotation velocity, $\dot{\theta}$, of the rigid block due to rocking on the rigid base equal to the state variables z_1, z_2, z_3 and z_4 respectively as

$$z_1 \equiv u \tag{7.61}$$

$$z_2 \equiv \dot{u} \tag{7.62}$$

$$z_3 \equiv \theta \tag{7.63}$$

$$z_4 \equiv \dot{\theta} \tag{7.64}$$

The derivatives of the state variables are expressed as

$$\dot{z}_1 = \dot{u} = z_2 \tag{7.65}$$

$$\dot{z}_2 = \ddot{u} \tag{7.66}$$

$$\dot{z}_3 = \dot{\theta} = z_4 \tag{7.67}$$

$$\dot{z}_4 = \ddot{\theta} \tag{7.68}$$

Finally, Equations (7.58) and (7.60) can be rewritten as a set of four first-order ODEs, representing the first (Equation (7.65)) and the second derivative (Equation (7.66)) of the displacement of isolation system and the first (Equation (7.67)) and the second derivative (Equation (7.68)) of the rotation angle of rigid block due to rocking as

$$\{\dot{z}\} = \begin{Bmatrix} \dot{z}_1 \\ \dot{z}_2 \\ \dot{z}_3 \\ \dot{z}_4 \end{Bmatrix} = \begin{Bmatrix} z_2 \\ -\ddot{x}_g + \dfrac{1}{\left(M - \dfrac{m^2 A_1^{\,2}}{I_o}\right)}\left[-c_b z_2 - k_b z_1 - m A_2 z_4^{\,2} + \dfrac{m^2 A_1 A_2}{I_o}\left(g + \ddot{z}_g\right)\right] \\ z_4 \\ \left(\dfrac{1}{I_o - \dfrac{m^2 A_1^{\,2}}{M}}\right)\left[\dfrac{m A_1 c_b}{M} z_2 + \dfrac{m A_1 k_b}{M} z_1 + \dfrac{m^2 A_1 A_2}{M} z_4^{\,2} - m A_2\left(g + \ddot{z}_g\right)\right] \end{Bmatrix} \tag{7.69}$$

Nonlinear Isolation System

The motion of the system in the rocking regime is governed by the following set of equations

$$\begin{aligned} &M\ddot{u} + \mu_b\left(Mg + M\ddot{z}_g\right)\boldsymbol{Z} + \left[\left(Mg + M\ddot{z}_g\right)/R\right]u + m\left[h\cos\theta + \operatorname{sgn}\theta\left(b\sin\theta\right)\right]\ddot{\theta} \\ &+ m\left[\operatorname{sgn}\theta\left(b\cos\theta\right) - h\sin\theta\right]\dot{\theta}^2 = -M\ddot{x}_g \end{aligned} \tag{7.70}$$

$$\begin{aligned} &I_o\ddot{\theta} + m\ddot{u}\left[h\cos\theta + \operatorname{sgn}\theta\left(b\sin\theta\right)\right] + mg\left(\operatorname{sgn}\theta\left(b\cos\theta\right) - h\sin\theta\right) \\ &= -m\left[h\cos\theta + \operatorname{sgn}\theta\left(b\sin\theta\right)\right]\ddot{x}_g - m\left[\operatorname{sgn}\theta\left(b\cos\theta\right) - h\sin\theta\right]\ddot{z}_g \end{aligned} \tag{7.71}$$

where

$$M = m + m_b \tag{7.72}$$

$$I_o = mr^2 + I \tag{7.73}$$

Letting

$$A_1 \equiv h\cos\theta + \operatorname{sgn}\theta\left(b\sin\theta\right) \equiv A_1\left(\theta\right) \tag{7.74}$$

$$A_2 \equiv \operatorname{sgn}\theta\left(b\cos\theta\right) - h\sin\theta \equiv A_2\left(\theta\right) \tag{7.75}$$

Equations (7.70) and (7.71) can be rewritten in the form

$$M\ddot{u} + \mu_b\left(Mg + M\ddot{z}_g\right)\boldsymbol{Z} + \left[\left(Mg + M\ddot{z}_g\right)/R\right]u + mA_1\ddot{\theta} + mA_2\dot{\theta}^2 = -M\ddot{x}_g \tag{7.76}$$

$$I_o\ddot{\theta} + mA_1\ddot{u} + mgA_2 = -mA_1\ddot{x}_g - mA_2\ddot{z}_g \tag{7.77}$$

Equations (7.76) and (7.77) can be rewritten as

$$M\ddot{u} + mA_1\ddot{\theta} = -M\ddot{x}_g - \mu_b\left(Mg + M\ddot{z}_g\right)\boldsymbol{Z} - \left[\left(Mg + M\ddot{z}_g\right)/R\right]u - mA_2\dot{\theta}^2 \tag{7.78}$$

$$I_o\ddot{\theta} + mA_1\ddot{u} + mgA_2 = -mA_1\ddot{x}_g - mA_2\ddot{z}_g \tag{7.79}$$

Multiplying Equation (7.79) by $-\dfrac{mA_1}{I_o}$ and adding to Equation (7.78) gives

$$\begin{aligned}\left(M - \frac{m^2A_1^{\,2}}{I_o}\right)\ddot{u} = {} & \left(\frac{m^2A_1^{\,2}}{I_o} - M\right)\ddot{x}_g - \mu_b\left(Mg + M\ddot{z}_g\right)\boldsymbol{Z} - \left[\left(Mg + M\ddot{z}_g\right)/R\right]u \\ & -mA_2\dot{\theta}^2 + \frac{m^2gA_1A_2}{I_o} + \frac{m^2A_1A_2}{I_o}\ddot{z}_g\end{aligned} \tag{7.80}$$

which upon rearranging terms yields

$$\ddot{u} = -\ddot{x}_g + \frac{1}{\left(M - \dfrac{m^2A_1^{\,2}}{I_o}\right)}\left\{\begin{array}{l} -\mu_b\left(Mg + M\ddot{z}_g\right)\boldsymbol{Z} - \left[\left(Mg + M\ddot{z}_g\right)/R\right]u \\ -mA_2\dot{\theta}^2 + \dfrac{m^2A_1A_2}{I_o}\left(g + \ddot{z}_g\right)\end{array}\right\} \tag{7.81}$$

Multiplying Equation (7.78) by $-\dfrac{mA_1}{M}$ and adding to Equation (7.79) gives

$$\left(I_o-\frac{m^2A_1^{\,2}}{M}\right)\ddot{\theta}=\frac{mA_1}{M}\left(Mg+M\ddot{z}_g\right)\boldsymbol{Z}+\frac{mA_1}{M}\left[\left(Mg+M\ddot{z}_g\right)/R\right]u$$
$$+\frac{m^2A_1A_2}{M}\dot{\theta}^2-mA_2\left(g+\ddot{z}_g\right) \tag{7.82}$$

which upon rearranging terms yields

$$\ddot{\theta}=\left(\frac{1}{I_o-\frac{m^2A_1^{\,2}}{M}}\right)\left\{\begin{array}{l}\frac{mA_1}{M}\left(Mg+M\ddot{z}_g\right)\boldsymbol{Z}+\frac{mA_1}{M}\left[\left(Mg+M\ddot{z}_g\right)/R\right]u\\+\frac{m^2A_1A_2}{M}\dot{\theta}^2-mA_2\left(g+\ddot{z}_g\right)\end{array}\right\} \tag{7.83}$$

The state-space formulation of a second-order differential equations is derived by setting the displacement, u, velocity, $\dot{u}$, dimensionless variable $\boldsymbol{Z}$ of the nonlinear isolation system and the rotation angle, θ, and rotation velocity, $\dot{\theta}$, of the rigid block due to rocking on the rigid base equal to the state variables z_1, z_2, z_3, z_4 and z_5 respectively as

$$z_1\equiv u \tag{7.84}$$

$$z_2\equiv\dot{u} \tag{7.85}$$

$$z_3\equiv\boldsymbol{Z} \tag{7.86}$$

$$z_4\equiv\theta \tag{7.87}$$

$$z_5\equiv\dot{\theta} \tag{7.88}$$

The derivatives of the state variables are expressed as

$$\dot{z}_1=\dot{u}=z_2 \tag{7.89}$$

$$\dot{z}_2=\ddot{u} \tag{7.90}$$

$$\dot{z}_3=\dot{\boldsymbol{Z}}=\frac{-\gamma\left|\dot{u}\right|\boldsymbol{Z}\left|\boldsymbol{Z}\right|-\beta\dot{u}\left|\boldsymbol{Z}\right|^2+A\dot{u}}{Y} \tag{7.91}$$

$$\dot{z}_4=\dot{\theta}=z_5 \tag{7.92}$$

$$\dot{z}_5 = \ddot{\theta} \tag{7.93}$$

Finally, Equations (7.81) and (7.83) can be rewritten as a set of five first-order ODEs, representing the first (Equation (7.89)) and the second derivative (Equation (7.90)) of the displacement of isolation system, the first derivative (Equation (7.91)) of the dimensionless variable and the first (Equation (7.92)) and the second derivative (Equation (7.93)) of the rotation angle of rigid block due to rocking as

$$\{\dot{z}\} = \begin{Bmatrix} \dot{z}_1 \\ \dot{z}_2 \\ \dot{z}_3 \\ \dot{z}_4 \\ \dot{z}_5 \end{Bmatrix} = \begin{Bmatrix} z_2 \\ -\ddot{x}_g + \dfrac{1}{\left(M - \dfrac{m^2 A_1^{\,2}}{I_o}\right)} \begin{Bmatrix} -\mu_b \left(Mg + M\ddot{z}_g\right) z_3 - \left[\left(Mg + M\ddot{z}_g\right)/R\right] z_1 \\ -mA_2 z_5^2 + \dfrac{m^2 A_1 A_2}{I_o}\left(g + \ddot{z}_g\right) \end{Bmatrix} \\ \dfrac{-\gamma |z_2| z_3 |z_3| - \beta z_2 |z_3|^2 + A z_2}{Y} \\ z_5 \\ \left(\dfrac{1}{I_o - \dfrac{m^2 A_1^{\,2}}{M}}\right) \begin{Bmatrix} \dfrac{mA_1}{M}\left(Mg + M\ddot{z}_g\right) z_3 + \dfrac{mA_1}{M}\left[\left(Mg + M\ddot{z}_g\right)/R\right] z_1 \\ + \dfrac{m^2 A_1 A_2}{M} z_5^{\,2} - mA_2\left(g + \ddot{z}_g\right) \end{Bmatrix} \end{Bmatrix} \tag{7.94}$$

7.3.4 Slide-rocking regime

Linear Isolation System

The motion of the system in the slide-rocking regime is governed by the following set of equations

$$\begin{aligned} &\left(m + m_b\right)\ddot{u} + m\ddot{x}_s + c_b\dot{u} + k_b u + m\left[h\cos\theta + \operatorname{sgn}\theta\left(b\sin\theta\right)\right]\ddot{\theta} \\ &+ m\left[\operatorname{sgn}\theta\left(b\cos\theta\right) - h\sin\theta\right]\dot{\theta}^2 = -\left(m + m_b\right)\ddot{x}_g \end{aligned} \tag{7.95}$$

$$\begin{aligned} &m\left(\ddot{u} + \ddot{x}_s\right) + m\left[h\cos\theta + \operatorname{sgn}\theta\left(b\sin\theta\right)\right]\ddot{\theta} + m\left[\operatorname{sgn}\theta\left(b\cos\theta\right) - h\sin\theta\right]\dot{\theta}^2 \\ &+ \operatorname{sgn}(\dot{x}_s)\mu_k m\left\{g + \ddot{z}_g + \left[\operatorname{sgn}\theta\left(b\cos\theta\right) - h\sin\theta\right]\ddot{\theta} - \left[h\cos\theta + \operatorname{sgn}\theta\left(b\sin\theta\right)\right]\dot{\theta}^2\right\} \\ &= -m\ddot{x}_g \end{aligned} \tag{7.96}$$

$$\begin{aligned}&\left(mR^2+I\right)\ddot{\theta}+m\left(\ddot{u}+\ddot{x}_s\right)\left[h\cos\theta+\operatorname{sgn}\theta\left(b\sin\theta\right)\right]+mg\left[\operatorname{sgn}\theta\left(b\cos\theta\right)-h\sin\theta\right]\\&=-m\left[h\cos\theta+\operatorname{sgn}\theta\left(b\sin\theta\right)\right]\ddot{x}_g-m\left[\operatorname{sgn}\theta\left(b\cos\theta\right)-h\sin\theta\right]\ddot{z}_g\end{aligned}\tag{7.97}$$

where

$$M=m+m_b\tag{7.98}$$

$$I_o=mR^2+I\tag{7.99}$$

Letting

$$A_1\equiv h\cos\theta+\operatorname{sgn}\theta\left(b\sin\theta\right)\equiv A_1\left(\theta\right)\tag{7.100}$$

$$A_2\equiv \operatorname{sgn}\theta\left(b\cos\theta\right)-h\sin\theta\equiv A_2\left(\theta\right)\tag{7.101}$$

Equations (7.95), (7.96) and (7.97) can be rewritten in the form

$$M\ddot{u}+m\ddot{x}_s+c_b\dot{u}+k_bu+mA_1\ddot{\theta}+mA_2\dot{\theta}^2=-M\ddot{x}_g\tag{7.102}$$

$$m\left(\ddot{u}+\ddot{x}_s\right)+mA_1\ddot{\theta}+mA_2\dot{\theta}^2+\operatorname{sgn}(\dot{x}_s)\mu_k m\left(g+\ddot{z}_g+A_2\ddot{\theta}-A_1\dot{\theta}^2\right)=-m\ddot{x}_g\tag{7.103}$$

$$I_o\ddot{\theta}+m\left(\ddot{u}+\ddot{x}_s\right)A_1+mgA_2=-mA_1\ddot{x}_g-mA_2\ddot{z}_g\tag{7.104}$$

Adding Equation (7.103) into Equation (7.104), Equation (7.104) can be rewritten as

$$\begin{aligned}&I_o\ddot{\theta}-mA_1^2\ddot{\theta}-mA_1A_2\dot{\theta}^2-\operatorname{sgn}(\dot{x}_s)\mu_k mA_1\left(g+\ddot{z}_g+A_2\ddot{\theta}-A_1\dot{\theta}^2\right)-mA_1\ddot{x}_g\\&+mgA_2=-mA_1\ddot{x}_g-mA_2\ddot{z}_g\end{aligned}\tag{7.105}$$

which upon rearranging terms yields

$$\ddot{\theta}=\frac{1}{\left(I_o-mA_1^2-\operatorname{sgn}(\dot{x}_s)\mu_k mA_1A_2\right)}\begin{bmatrix}mA_1A_2\dot{\theta}^2-\operatorname{sgn}(\dot{x}_s)\mu_k mA_1^2\dot{\theta}^2\\+\left(\operatorname{sgn}(\dot{x}_s)\mu_k mA_1-mA_2\right)\left(g+\ddot{z}_g\right)\end{bmatrix}\tag{7.106}$$

Adding Equation (7.103) into Equation (7.102), Equation (7.102) can be rewritten as

$$\begin{aligned} &M\ddot{u} - m\ddot{u} - mA_1\ddot{\theta} - mA_2\dot{\theta}^2 - \text{sgn}(\dot{x}_s)\mu_k m\left(g + \ddot{z}_g + A_2\ddot{\theta} - A_1\dot{\theta}^2\right) \\ &-m\ddot{x}_g + c_b\dot{u} + k_b u + mA_1\ddot{\theta} + mA_2\dot{\theta}^2 = -M\ddot{x}_g \end{aligned} \tag{7.107}$$

which upon rearranging terms yields

$$\ddot{u} = -\ddot{x}_g + \frac{1}{(M-m)}\left(\text{sgn}(\dot{x}_s)\mu_k m\left(g + \ddot{z}_g + A_2\ddot{\theta} - A_1\dot{\theta}^2\right) - c_b\dot{u} - k_b u\right) \tag{7.108}$$

Equation (7.103) can be rewritten as

$$\ddot{x}_s = -\ddot{u} - A_1\ddot{\theta} - A_2\dot{\theta}^2 - \text{sgn}(\dot{x}_s)\mu_k\left(g + \ddot{z}_g + A_2\ddot{\theta} - A_1\dot{\theta}^2\right) - \ddot{x}_g \tag{7.109}$$

The state-space formulation of a second-order differential equations is derived by setting the displacement, u, velocity, $\dot{u}$, of the linear isolation system, the rotation angle, θ, and rotation velocity, $\dot{\theta}$, of the rigid block due to rocking on the rigid base and the displacement, x_s, and velocity, $\dot{x}_s$, of the rigid block due to sliding on the rigid base equal to the state variables z_1, z_2, z_3, z_4, z_5 and z_6 respectively as

$$z_1 \equiv u \tag{7.110}$$

$$z_2 \equiv \dot{u} \tag{7.111}$$

$$z_3 \equiv \theta \tag{7.112}$$

$$z_4 \equiv \dot{\theta} \tag{7.113}$$

$$z_5 \equiv x_s \tag{7.114}$$

$$z_6 \equiv \dot{x}_s \tag{7.115}$$

The derivatives of the state variables are expressed as

$$\dot{z}_1 = \dot{u} = z_2 \tag{7.116}$$

$$\dot{z}_2 = \ddot{u} \tag{7.117}$$

$$\dot{z}_3 = \dot{\theta} = z_4 \tag{7.118}$$

$$\dot{z}_4 = \ddot{\theta} \tag{7.119}$$

$$\dot{z}_5 = \dot{x}_s = z_6 \tag{7.120}$$

$$\dot{z}_6 = \ddot{x}_s \tag{7.121}$$

Finally, Equations (7.106), (7.108) and (7.109) can be rewritten as a set of six first-order ODEs, representing the first (Equation (7.116)) and the second derivative (Equation (7.117)) of the displacement of isolation system, the first (Equation (7.118)) and the second derivative (Equation (7.119)) of the rotation angle of rigid block due to rocking and the first (Equation (7.120)) and the second derivative (Equation (7.121)) of the displacement of rigid block due to sliding as

$$\left\{\dot{z}\right\} = \begin{Bmatrix} \dot{z}_1 \\ \dot{z}_2 \\ \dot{z}_3 \\ \dot{z}_4 \\ \dot{z}_5 \\ \dot{z}_6 \end{Bmatrix} = \begin{Bmatrix} z_2 \\ -\ddot{x}_g + \dfrac{1}{(M-m)}\left(\mathrm{sgn}(z_6)\mu_k m\left(g + \ddot{z}_g + A_2\dot{z}_4 - A_1 z_4^2\right) - c_b z_2 - k_b z_1\right) \\ z_4 \\ \dfrac{1}{\left(I_o - mA_1^2 - \mathrm{sgn}(z_6)\mu_k m A_1 A_2\right)}\begin{bmatrix} mA_1A_2z_4^2 - \mathrm{sgn}(z_6)\mu_k m A_1^2 z_4^2 \\ +\left(\mathrm{sgn}(z_6)\mu_k m A_1 - mA_2\right)\left(g + \ddot{z}_g\right) \end{bmatrix} \\ z_6 \\ -\dot{z}_2 - A_1\dot{z}_4 - A_2 z_4^2 - \mathrm{sgn}(z_6)\mu_k\left(g + \ddot{z}_g + A_2\dot{z}_4 - A_1 z_4^2\right) - \ddot{x}_g \end{Bmatrix} \tag{7.122}$$

Nonlinear Isolation System

The motion of the system in the slide-rocking regime is governed by the following set of equations

$$\begin{aligned} &\left(m + m_b\right)\ddot{u} + m\ddot{x}_s + \mu_b\left(Mg + M\ddot{z}_g\right)\boldsymbol{Z} + \left[\left(Mg + M\ddot{z}_g\right)/R\right]u \\ &+ m\left[h\cos\theta + \mathrm{sgn}\,\theta\left(b\sin\theta\right)\right]\ddot{\theta} + m\left[\mathrm{sgn}\,\theta\left(b\cos\theta\right) - h\sin\theta\right]\dot{\theta}^2 = -\left(m + m_b\right)\ddot{x}_g \end{aligned} \tag{7.123}$$

$$
\begin{aligned}
&m\left(\ddot{u}+\ddot{x}_s\right)+m\left(h\cos\theta+\operatorname{sgn}\theta\left(b\sin\theta\right)\right)\ddot{\theta}+m\left(\operatorname{sgn}\theta\left(b\cos\theta\right)-h\sin\theta\right)\dot{\theta}^2\\
&+\operatorname{sgn}(\dot{x}_s)\mu_k m\left\{g+\ddot{z}_g+\left[\operatorname{sgn}\theta\left(b\cos\theta\right)-h\sin\theta\right]\ddot{\theta}-\left[h\cos\theta+\operatorname{sgn}\theta\left(b\sin\theta\right)\right]\dot{\theta}^2\right\}\\
&=-m\ddot{x}_g
\end{aligned}
\tag{7.124}
$$

$$
\begin{aligned}
&\left(mR^2+I\right)\ddot{\theta}+m\left(\ddot{u}+\ddot{x}_s\right)\left[h\cos\theta+\operatorname{sgn}\theta\left(b\sin\theta\right)\right]+mg\left[\operatorname{sgn}\theta\left(b\cos\theta\right)-h\sin\theta\right]\\
&=-m\left[h\cos\theta+\operatorname{sgn}\theta\left(b\sin\theta\right)\right]\ddot{x}_g-m\left[\operatorname{sgn}\theta\left(b\cos\theta\right)-h\sin\theta\right]\ddot{z}_g
\end{aligned}
\tag{7.125}
$$

where

$$M=m+m_b \tag{7.126}$$

$$I_o=mR^2+I \tag{7.127}$$

Letting

$$A_1\equiv h\cos\theta+\operatorname{sgn}\theta\left(b\sin\theta\right)\equiv A_1\left(\theta\right) \tag{7.128}$$

$$A_2\equiv \operatorname{sgn}\theta\left(b\cos\theta\right)-h\sin\theta\equiv A_2\left(\theta\right) \tag{7.129}$$

Equations (7.123), (7.124) and (7.125) can be rewritten in the form

$$M\ddot{u}+m\ddot{x}_s+\mu_b\left(Mg+M\ddot{z}_g\right)\boldsymbol{Z}+\left[\left(Mg+M\ddot{z}_g\right)/R\right]u+mA_1\ddot{\theta}+mA_2\dot{\theta}^2=-M\ddot{x}_g \tag{7.130}$$

$$m\left(\ddot{u}+\ddot{x}_s\right)+mA_1\ddot{\theta}+mA_2\dot{\theta}^2+\operatorname{sgn}(\dot{x}_s)\mu_k m\left(g+\ddot{z}_g+A_2\ddot{\theta}-A_1\dot{\theta}^2\right)=-m\ddot{x}_g \tag{7.131}$$

$$I_o\ddot{\theta}+m\left(\ddot{u}+\ddot{x}_s\right)A_1+mgA_2=-mA_1\ddot{x}_g-mA_2\ddot{z}_g \tag{7.132}$$

Adding Equation (7.131) into Equation (7.132), Equation (7.132) can be rewritten as

$$
\begin{aligned}
&I_o\ddot{\theta}-mA_1^2\ddot{\theta}-mA_1A_2\dot{\theta}^2-\operatorname{sgn}(\dot{x}_s)\mu_k mA_1\left(g+\ddot{z}_g+A_2\ddot{\theta}-A_1\dot{\theta}^2\right)-mA_1\ddot{x}_g\\
&+mgA_2=-mA_1\ddot{x}_g-mA_2\ddot{z}_g
\end{aligned}
\tag{7.133}
$$

which upon rearranging terms yields

$$\ddot{\theta} = \frac{1}{\left(I_o - mA_1^2 - \text{sgn}(\dot{x}_s)\mu_k mA_1 A_2\right)} \begin{bmatrix} mA_1 A_2 \dot{\theta}^2 - \text{sgn}(\dot{x}_s)\mu_k mA_1^2 \dot{\theta}^2 \\ +\left(\text{sgn}(\dot{x}_s)\mu_k mA_1 - mA_2\right)\left(g + \ddot{z}_g\right) \end{bmatrix} \tag{7.134}$$

Adding Equation (7.131) into Equation (7.130), Equation (7.130) can be rewritten as

$$\begin{aligned} &M\ddot{u} - m\ddot{u} - mA_1\ddot{\theta} - mA_2\dot{\theta}^2 - \text{sgn}(\dot{x}_s)\mu_k m\left(g + \ddot{z}_g + A_2\ddot{\theta} - A_1\dot{\theta}^2\right) \\ &-m\ddot{x}_g + \mu_b\left(Mg + M\ddot{z}_g\right)\boldsymbol{Z} + \left[\left(Mg + M\ddot{z}_g\right)/R\right]u + mA_1\ddot{\theta} + mA_2\dot{\theta}^2 = -M\ddot{x}_g \end{aligned} \tag{7.135}$$

which upon rearranging terms yields

$$\ddot{u} = -\ddot{x}_g + \frac{1}{(M-m)} \begin{Bmatrix} \text{sgn}(\dot{x}_s)\mu_k m\left(g + \ddot{z}_g + A_2\ddot{\theta} - A_1\dot{\theta}^2\right) - \mu\left(Mg + M\ddot{z}_g\right)\boldsymbol{Z} \\ -\left[\left(Mg + M\ddot{z}_g\right)/R\right]u \end{Bmatrix} \tag{7.136}$$

Equation (7.131) can be rewritten as

$$\ddot{x}_s = -\ddot{u} - A_1\ddot{\theta} - A_2\dot{\theta}^2 - \text{sgn}(\dot{x}_s)\mu_k\left(g + \ddot{z}_g + A_2\ddot{\theta} - A_1\dot{\theta}^2\right) - \ddot{x}_g \tag{7.137}$$

The state-space formulation of a second-order differential equations is derived by setting the displacement, u, velocity, $\dot{u}$, the dimensionless variable, $\boldsymbol{Z}$, of the nonlinear isolation system, the rotation angle, θ, and rotation velocity, $\dot{\theta}$, of the rigid block due to rocking on the rigid base and the displacement, x_s, and velocity, $\dot{x}_s$, of the rigid block due to sliding on the rigid base equal to the state variables z_1, z_2, z_3, z_4, z_5, z_6 and z_7 respectively as

$$z_1 \equiv u \tag{7.138}$$

$$z_2 \equiv \dot{u} \tag{7.139}$$

$$z_3 \equiv \theta \tag{7.140}$$

$$z_4 \equiv \dot{\theta} \tag{7.141}$$

$$z_5 \equiv x_s \tag{7.142}$$

$$z_6 \equiv \dot{x}_s \tag{7.143}$$

$$z_7 \equiv \boldsymbol{Z} \tag{7.144}$$

The derivatives of the state variables are expressed as

$$\dot{z}_1 = \dot{u} = z_2 \tag{7.145}$$

$$\dot{z}_2 = \ddot{u} \tag{7.146}$$

$$\dot{z}_3 = \dot{\theta} = z_4 \tag{7.147}$$

$$\dot{z}_4 = \ddot{\theta} \tag{7.148}$$

$$\dot{z}_5 = \dot{x}_s = z_6 \tag{7.149}$$

$$\dot{z}_6 = \ddot{x}_s \tag{7.150}$$

$$\dot{z}_7 = \dot{\boldsymbol{Z}} = \frac{-\gamma|\dot{u}|\boldsymbol{Z}|\boldsymbol{Z}| - \beta\dot{u}|\boldsymbol{Z}|^2 + A\dot{u}}{Y} \tag{7.151}$$

Finally, Equations (7.134), (7.136) and (7.137) can be rewritten as a set of seven first-order ODEs, representing the first (Equation (7.145)) and the second derivative (Equation (7.146)) of the displacement of isolation system, the first derivative (Equation (7.151)) of the dimensionless variable, the first (Equation (7.147)) and the second derivative (Equation (7.148)) of the rotation angle of rigid block due to rocking and the first (Equation (7.149)) and the second derivative (Equation (7.150)) of the displacement of rigid block due to sliding as

$$\{\dot{z}\}=\begin{Bmatrix}\dot{z}_1\\ \dot{z}_2\\ \dot{z}_3\\ \dot{z}_4\\ \dot{z}_5\\ \dot{z}_6\\ \dot{z}_7\end{Bmatrix}=\begin{Bmatrix} z_2 \\ -\ddot{x}_g+\dfrac{1}{(M-m)}\begin{pmatrix}\operatorname{sgn}(z_6)\mu_k m\left(g+\ddot{z}_g+A_2\dot{z}_4-A_1z_4^2\right)\\ -\mu_b\left(Mg+M\ddot{z}_g\right)z_7-\left[\left(Mg+M\ddot{z}_g\right)/R\right]z_1\end{pmatrix} \\ z_4 \\ \dfrac{1}{\left(I_o-mA_1^2-\operatorname{sgn}(z_6)\mu_k mA_1A_2\right)}\begin{bmatrix} mA_1A_2z_4^2-\operatorname{sgn}(z_6)\mu_k mA_1^2z_4^2\\ +\left(\operatorname{sgn}(z_6)\mu_k mA_1-mA_2\right)\left(g+\ddot{z}_g\right)\end{bmatrix} \\ z_6 \\ -\dot{z}_2-A_1\dot{z}_4-A_2z_4^2-\operatorname{sgn}(z_6)\mu_k\left(g+\ddot{z}_g+A_2\dot{z}_4-A_1z_4^2\right)-\ddot{x}_g \\ \dfrac{-\gamma|z_2|z_7|z_7|-\beta z_2|z_7|^2+Az_2}{Y}\end{Bmatrix} \quad (7.152)$$

CHAPTER 8

Rocking Response to Dynamic Base Excitation

The dynamic response of the system is investigated herein by assuming sufficient friction between the block and the supporting base under simple half- and full-cycle horizontal acceleration pulses, horizontal near-fault ground motions, and idealized pulse-type motions. Under the assumption of sufficient friction to prevent sliding, the response of the isolated system can be described in terms of two oscillation regimes: system translation, in which the base-block system translates as a whole; and rocking, in which the block pivot on its edges with respect to the horizontally-moving base. The investigation aims to identify potential trends in the response and stability of the system.

8.1 Response to Simple Base-Acceleration Pulses

The response of the system is investigated under simple half- and full-cycle horizontal acceleration pulses. In particular, the analysis considers a half-cycle rectangular pulse, a half-cycle sinusoidal pulse, and a full-cycle sinusoidal pulse, characterized by amplitude A_{g0} and half-cycle duration t_d (corresponding to frequency $\omega_p = \pi / t_d$), expressed mathematically as follows

$$\ddot{x}_g(t) = \begin{cases} A_{g0}, & \text{if } 0 \le t \le t_d \\ 0, & \text{if } t > t_d \end{cases} \qquad \text{half-cycle rectangular pulse} \tag{8.1}$$

$$\ddot{x}_g(t) = \begin{cases} A_{g0} \sin(\pi t / t_d), & \text{if } 0 \le t \le t_d \\ 0, & \text{if } t > t_d \end{cases} \qquad \text{half-cycle sinusoidal pulse} \tag{8.2}$$

$$\ddot{x}_g(t) = \begin{cases} A_{g0} \sin(\pi t / t_d), & \text{if } 0 \le t \le 2t_d \\ 0, & \text{if } t > 2t_d \end{cases} \qquad \text{full-cycle sinusoidal pulse} \tag{8.3}$$

The stability of the isolated block is examined in terms of the minimum amplitude of ground acceleration required to overturn the block ($\theta / \alpha \ge 1$), by considering the influence of input-motion characteristics, the geometric parameters of the block, the inertia parameters of the base/block system, and the constitutive parameters of the isolation system.

Figure 8-1 plots the normalized minimum overturning ground acceleration as a function of block size R for different values of t_d (left), and as a function of the excitation frequency ω_p for different values of R (right) for the simple acceleration pulses used in the analysis. A linear isolation system with $\xi_b = 0.35$, $T_b = 3\text{s}$ is considered in this analysis. As demonstrated from the left-half of Figure 8-1, for the one-sided (rectangular and half-sine) pulses, the isolation has a positive effect on the stability of the block for $t_d < 0.5\text{s}$ or equivalently excitation period $T_p < 1\text{s}$. For the two-sided (full-sine) pulse, this holds true for short-period pulses with $t_d < 0.25\text{s}$ ($T_p < 0.5\text{s}$), while the effectiveness of isolation in the range $0.25 < t_d < 0.6\text{s}$ ($0.5 < T_p < 1.2\text{s}$) is conditional on the size of the block R. That is, the isolation ceases to improve the stability of the block (compared with the non-isolated case) when subjected to such intermediate-period full-sine pulses with increasing block size. Nevertheless, the range of R-values for which the isolation is effective increases as the pulse duration increases. It should be noted however that, regardless of pulse type, the use of isolation is not practically beneficial (with respect to the stability of the block) for long-period excitations (i.e. $T_p > 1\text{s}$ for half-cycle pulses and $T_p > 1.2\text{s}$ for full-sine pulses). With reference to the right-half of Figure 8-1, the use of isolation results in enhanced behavior with decreasing block size, unless the system is subjected to long-period acceleration pulses.

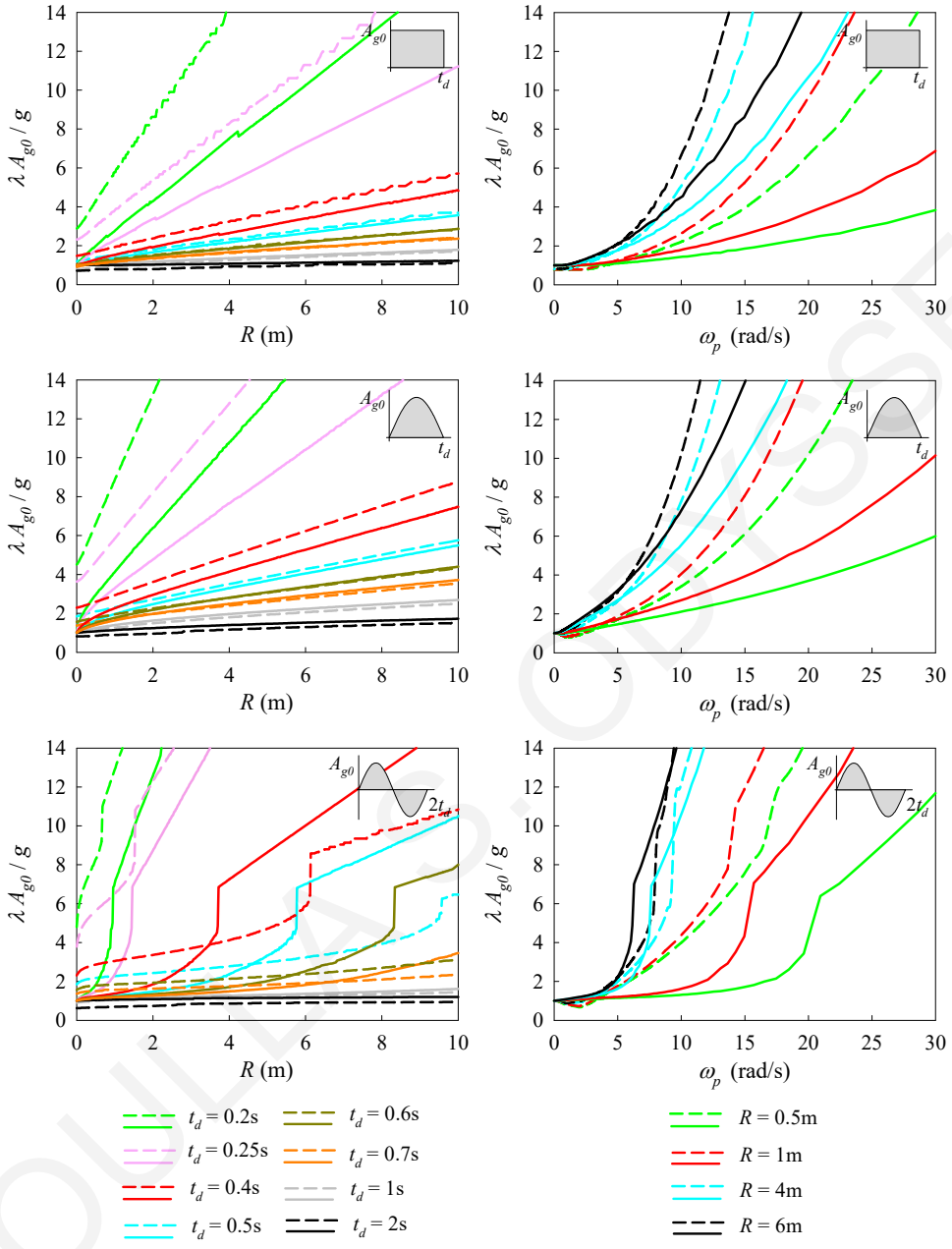

Solid Line: Non-isolated, Dashed Line: Isolated

Figure 8-1: Minimum overturning acceleration as a function of R (left) and ω_p (right) for simple ground-acceleration pulses ($\lambda = 4$, $\rho = 0.5$, $\xi_b = 0.35$, $T_b = 3\text{s}$).

Figures 8-2 through 8-4 illustrate the influence of linear isolation-system parameters (T_b, ξ_b) and mass ratio $\rho = m / m_b$ on the stability of the isolated block, for different values of R (left)

and for different values of t_d (right) for simple half- and full-cycle horizontal acceleration pulses. As can be seen from these figures, the most influential parameter on the block stability is the isolation-system period T_b. That is, the minimum overturning ground acceleration increases with increasing isolation-system period, regardless of block size R, provided that the pulse duration does not exceed a certain value (roughly less than 1s). Observe also that the influence of each parameter on the stability is amplified as the pulse duration decreases.

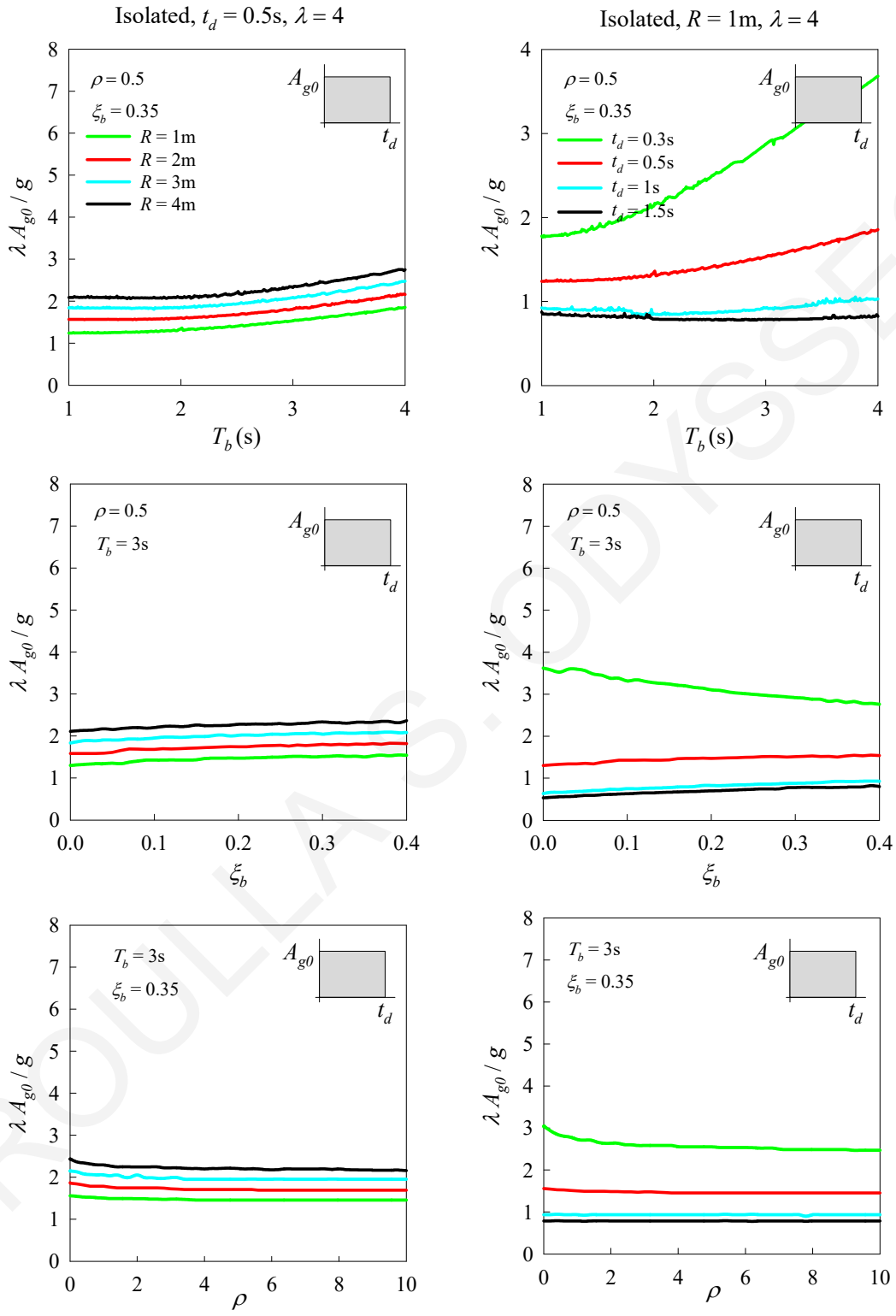

Figure 8-2: Minimum overturning acceleration as a function of T_b, ξ_b and ρ for half-cycle rectangular pulse.

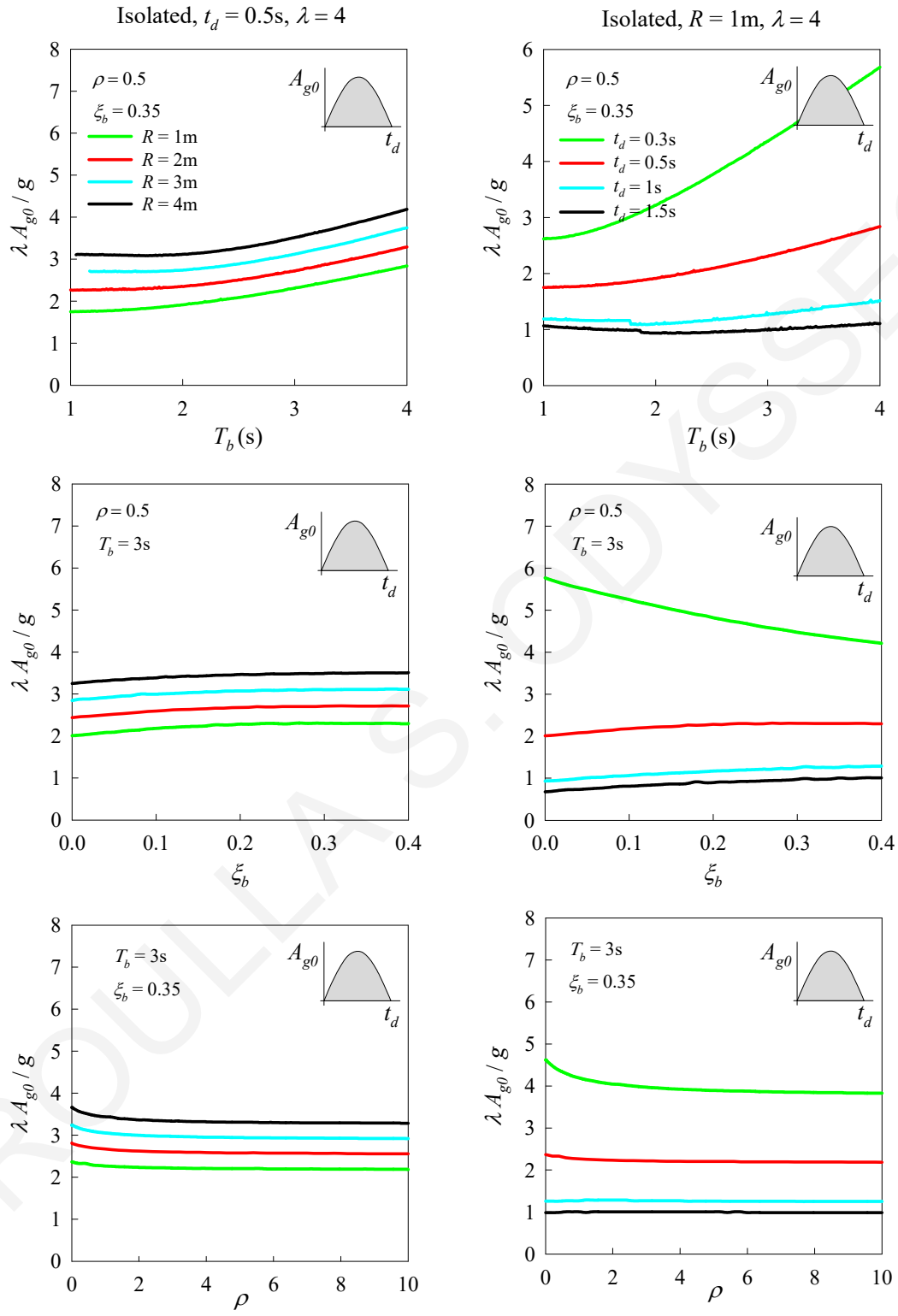

Figure 8-3: Minimum overturning acceleration as a function of T_b, ξ_b and ρ for half-cycle sinusoidal pulse.

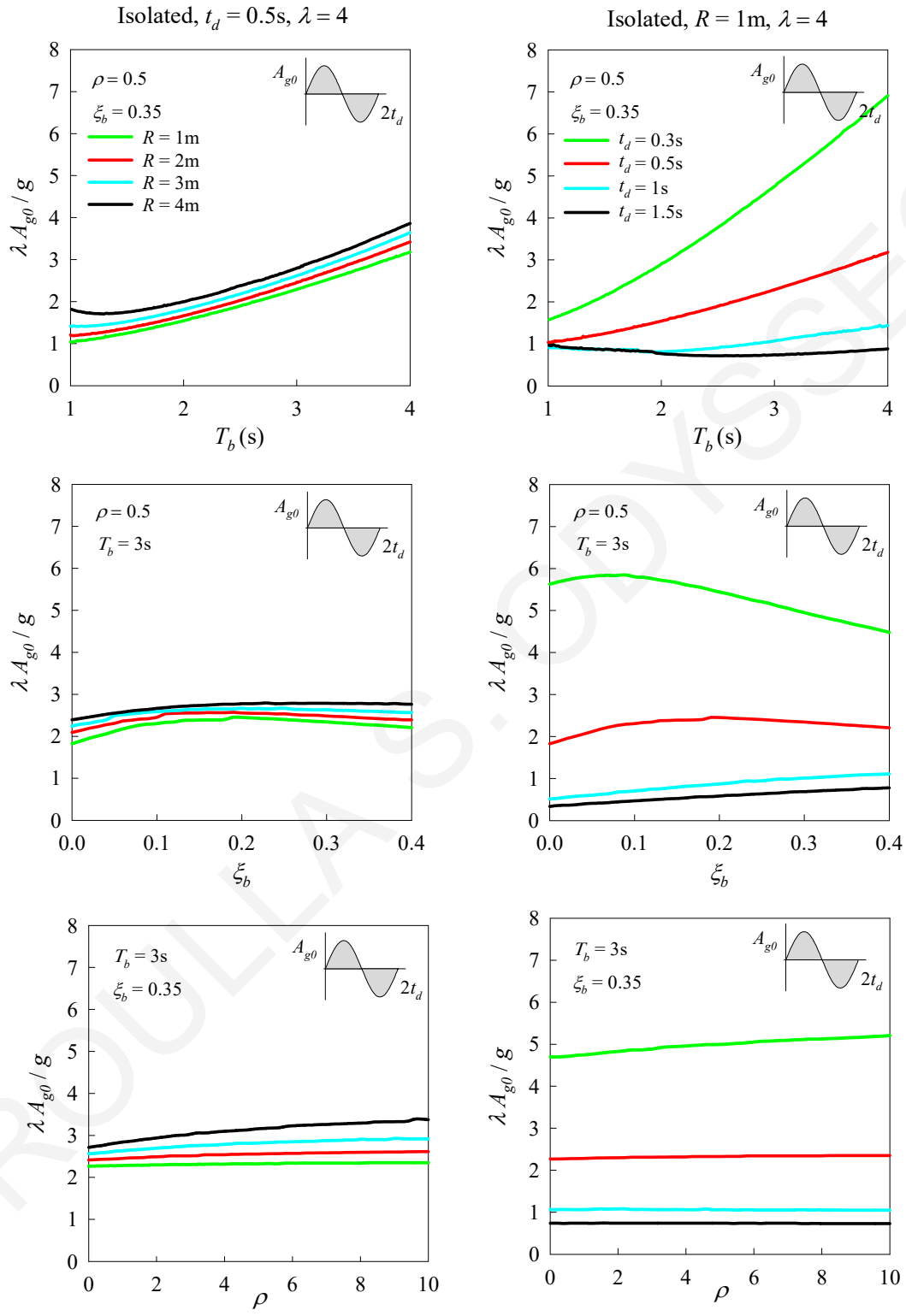

Figure 8-4: Minimum overturning acceleration as a function of T_b, ξ_b and ρ for full-cycle sinusoidal pulse.

Figure 8-5 presents response-regime spectra in the $\lambda - R$ space for non-isolated and isolated blocks of varying geometric characteristics, for half- and full-cycle pulses with duration $t_d = 0.2\text{s}$ and 0.5s. A linear isolation system is considered in these analyses with $T_b = 3\text{s}$ and $\xi_b = 0.35$. These spectra depict in a clear way the distinct regimes of block response, with the cyan area indicating "No Uplift", the green area "Rocking", and the red area "Overturning" of the block. A total of 6,000 nonlinear dynamic analyses were performed in constructing each behavior map. Each dot in these maps represents the outcome of a single analysis. As illustrated in Figure 8-5, the use of isolation results in an increase in the acceleration required to initiate rocking. In addition, the spectra plotted in Figure 8-5 elucidate a counterintuitive trend observed for bilateral excitations (not observed for unilateral excitations), in terms of the overturning potential of a given input-acceleration amplitude. That is to say, for a given block size, overturning occurring for certain slenderness does not necessarily imply overturning of the block with increasing λ. In mathematical terms, this is equivalent to stating that the (stability) curve defining the boundary between rocking and overturning is not single-valued. By and large, the use of isolation results in better system performance, with respect to the initiation of rocking and overturning, for short-period pulses. On the contrary, for long-period pulses, the use of isolation is not beneficial in improving the stability of the block (compared with the non-isolated case). Nevertheless, the use of isolation results in an increase in the acceleration required to initiate rocking, regardless the pulse-period.

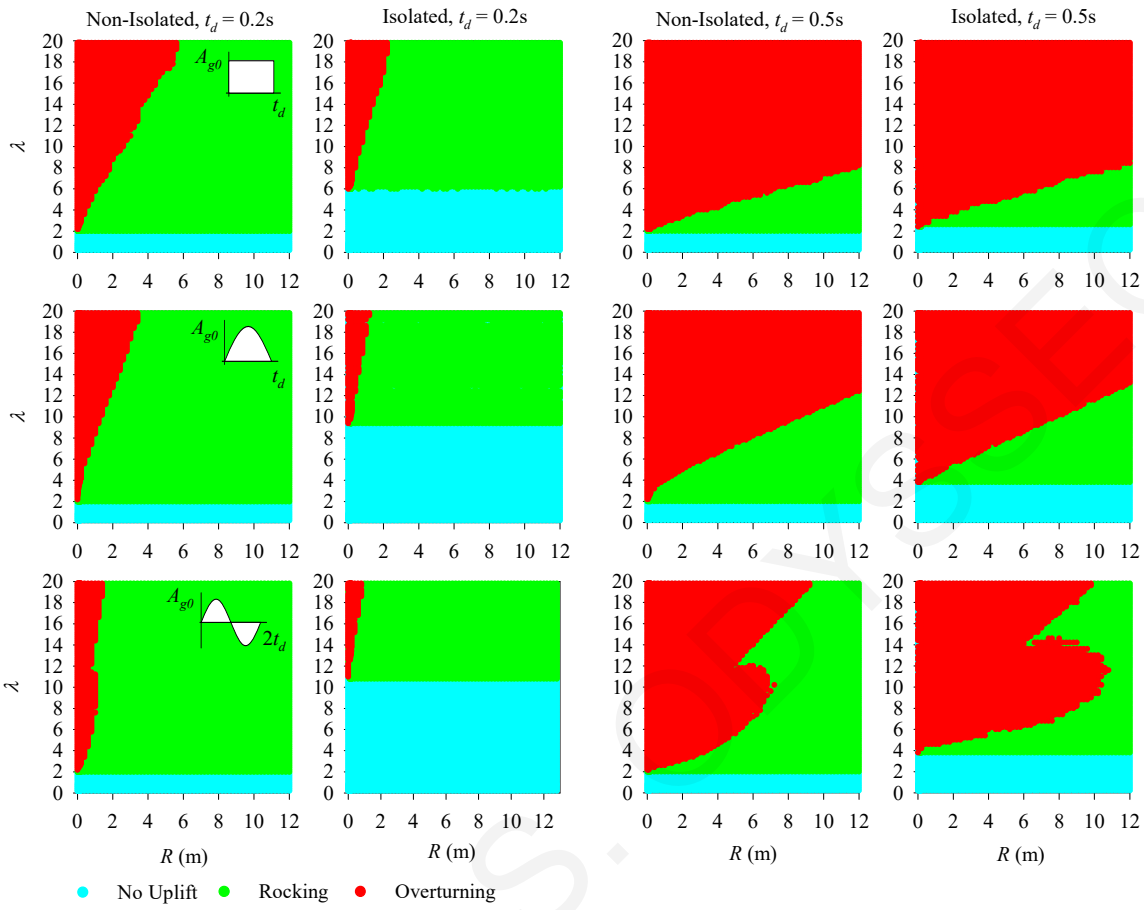

Figure 8-5: Response-regime spectra in the $\lambda - R$ space for a non-isolated and isolated block of varying geometric characteristics for simple ground-acceleration pulses with $A_{g0} = 0.5g$, $t_d = 0.2$s (left), $t_d = 0.5$s (right) and mass ratio $\rho = 0.5$.

Figure 8-6 compares the response of the block when isolated considering a linear viscoelastic model with $T_b = 3$s and $\xi_b = 0.35$, and a bilinear hysteretic model (typified by friction-pendulum isolator) with parameters $\mu_b = 0.11$ and $R_b = 2.24$s (corresponding to $T_b = 3$s). In particular, Figure 8-6 plots the normalized minimum overturning ground acceleration as a function of block size R (left), and as a function of the excitation frequency ω_p (right). As can be seen from this figure, the calculated response of the block is comparable for the two isolation-system models. The small discrepancy observed for large R (>10m), does not affect (qualitatively or quantitatively) the conclusions drawn above on the basis of a linear isolation model regarding the stability and the rocking incipient condition of the block.

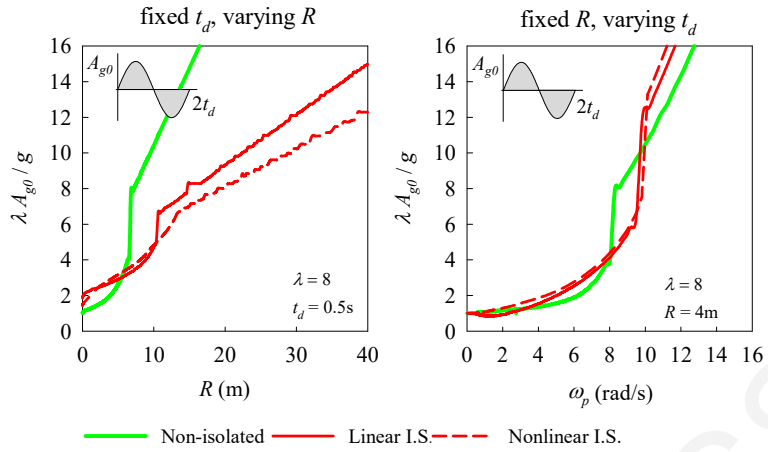

Figure 8-6: Minimum overturning acceleration for linear and bilinear hysteretic isolation model as a function of R (left) and ω_p (right) for full-cycle sinusoidal pulse.

Figures 8-7 and 8-8 present time histories of the dynamic response of the isolated and non-isolated rigid blocks under full-sine pulses. Two types of isolation system are considered in the analysis: (a) a nonlinear isolation system with a bilinear hysteretic model (typified by friction-pendulum isolator) with parameters $\mu_b = 0.11$ and $R_b = 2.24$m (corresponding to $T_b = 3$s), and (b) a linear isolation system with viscoelastic model ($T_b = 3$s). These figures plot the ground acceleration, $\ddot{x}_g$, the normalized angular displacement, θ/α, (with the overturning of the block indicated when $\theta/\alpha \geq 1$), the angular velocity of the block, $\dot{\theta}$ and the horizontal displacement of the isolation system, u.

Figure 8-7 shows the response of a rigid block with size-parameter $R = 2$m and slenderness ratio $\lambda = 6$ under a short-period pulse ($t_d = 0.2$s), with a peak amplitude of 0.5g. The isolated block oscillates in the system-translation regime only. Using the linear isolation system, the maximum horizontal system translation is approximately 95mm and using the nonlinear isolation system it is approximately 70mm. In contrast, the non-isolated block oscillates in the rocking motion and an impact event between the block and the foundation causes the system to switch from anti-clockwise ($\theta < 0$) rocking motion to clockwise, ($\theta > 0$).Attention should also be drawn to the fact that the maximum response of the non-isolated block does not immediately follow the peak amplitude in the ground acceleration but it happens after the end of the full-sine pulse, in free vibration.

The response of the same block using a long-period pulse ($t_d = 0.5\text{s}$) is shown in Figure 8-8. The isolation system ceases to improve the stability of the system and both blocks (isolated and non-isolated) oscillate with rocking motion and finally overturn. The isolated block translates horizontally with a maximum displacement of approximately 350mm using both isolation systems. It appears that the use of isolation system delays the initiation of rocking but in this case it cannot prevent the overturning of the block. It is worth mentioning, that both blocks (isolated and non-isolated) overturn after the end of the earthquake record. The comparison between two figures verifies the observation made from Figure 8-5 that the use of isolation system is beneficial for short-period pulses.

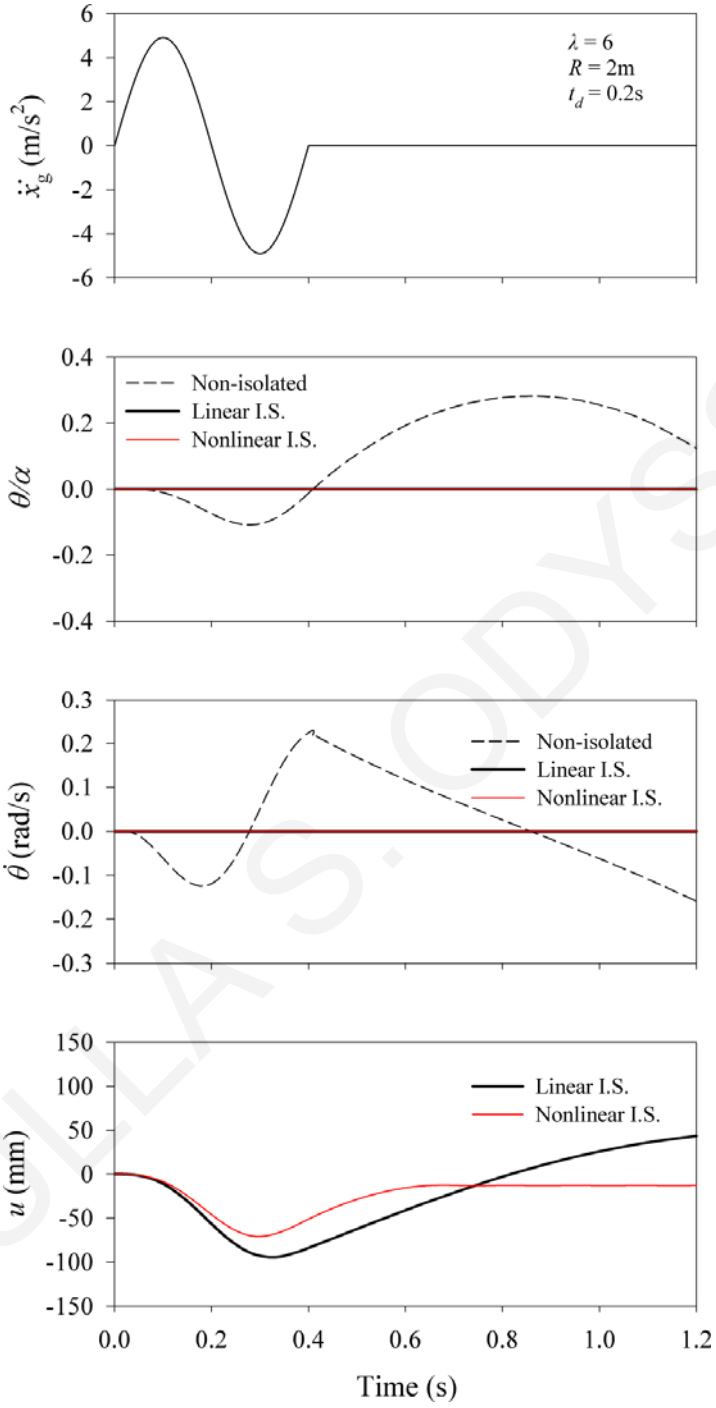

Figure 8-7: Response histories for non-isolated and isolated rigid block under full-sine pulse with $A_{g0} = 0.5g$ and $t_d = 0.2\text{s}$ ($\rho = 0.5$, $\lambda = 6$, $R = 2\text{m}$).

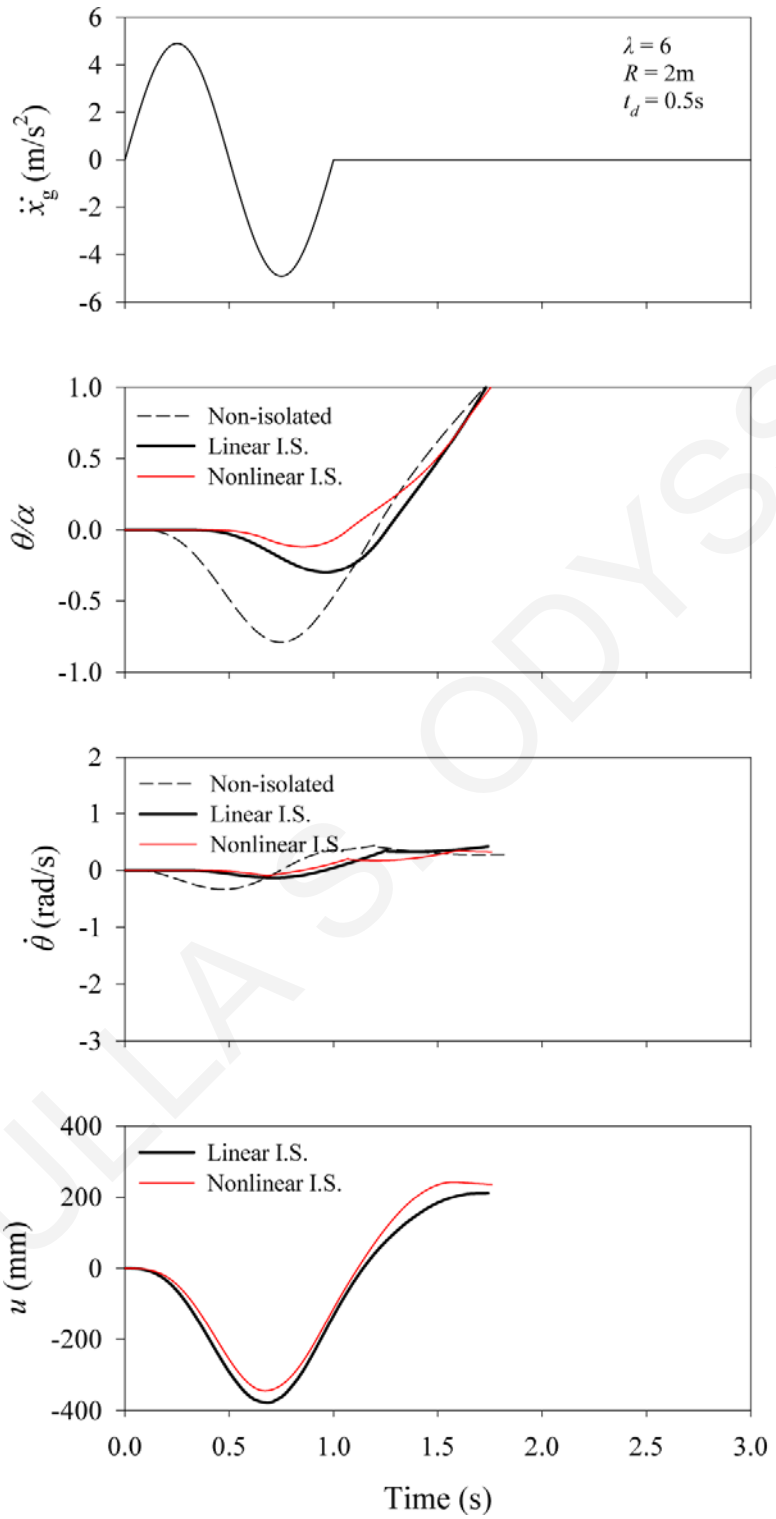

Figure 8-8: Response histories for non-isolated and isolated rigid block under full-sine pulse with $A_{g0} = 0.5g$ and $t_d = 0.5\text{s}$ ($\rho = 0.5$, $\lambda = 6$, $R = 2\text{m}$).

8.2 Response to Earthquake Motions

In this section, the stability of the isolated block is investigated using a wide range of near-fault seismic ground motions. Near-fault ground motions are typically characterized by intense velocity and displacement pulses of relatively long periods that clearly distinguish them from typical far-field ground motions. Table 8-1 lists the characteristics of the motions used for the dynamic analysis.

Table 8-1: Ground motions used for the dynamic analysis

Earthquake	Station / Component	Magnitude (M_w)	Distance (km)	PGA (g)	PGV (m/s)	T_p (s)
1966 Parkfield, CA, USA	C02/SN	6.20	0.1	0.48	0.75	2.00
1971 San Fernando, CA, USA	PCD/SN	6.55	3.0	1.29	1.20	1.47
1978 Tabas, Iran	TAB/SP	7.11	1.2	0.85	1.22	5.26
1979 Imperial Valley, CA, USA	E04/SN	6.50	6.0	0.36	0.78	4.44
	E05/SN	6.50	2.7	0.38	0.92	3.92
	E06/SN	6.50	0.3	0.44	1.12	3.85
	E07/SN	6.50	1.8	0.46	1.09	3.64
	EMO / SN	6.50	1.2	0.38	1.15	2.94
1994 Northridge, CA, USA	JFA/SN	6.70	5.2	0.39	1.05	3.03
	RRS/SN	6.70	6.0	0.89	1.73	1.25
	SCG/SN	6.70	5.1	0.59	1.34	2.94
	SCH/SN	6.70	5.0	0.89	1.22	3.03
	NWS/SN	6.70	5.3	0.41	1.17	2.70
1995 Aigion, Greece	AEG/Long	6.33	6.0	0.50	0.41	0.71
	AEG/Tran	6.33	6.0	0.55	0.52	0.68
1999 Izmit, Turkey	ARC/SN	7.40	14.0	0.13	0.44	7.14
	SKR/SP	7.40	3.1	0.41	0.80	9.52
	GBZ/SN	7.40	11.0	0.26	0.41	4.76
	GBZ/SP	7.40	11.0	0.03	0.29	6.06
1977 Bucharest, Romania	BRI / SN	7.3	190	0.21	0.75	2.13
1994 Northridge, CA, USA	Pacoima / PKC090	6.7	8.2	0.30	0.31	0.61
2004 Parkfield	Cholame 3W / 360	6.0	8	0.57	0.38	0.52

The stability of the isolated block is examined in terms of the minimum amplitude of ground acceleration required to overturn the block ($\theta / \alpha \geq 1$), by considering the influence of input-motion characteristics, the geometric parameters of the block, the inertia parameters of the base/block system, and the constitutive parameters of the isolation system.

Representative results are shown in Figure 8-9 for the SN-component of the BRI record from the 1977 Bucharest earthquake, and the SN-component of the EMO record from the 1977

Imperial Valley motion (long-period records with prevailing period $T_p = 2.13\text{s}$ and $T_p = 2.94\text{s}$ respectively, based on Mavroeidis and Papageorgiou (2003)), as well as the 90-component of the Pacoima Dam record from the 1994 Northridge earthquake and the 360-component of the Cholame-3W record from the 2004 Parkfield event (short-period records with prevailing period $T_p = 0.61\text{s}$ and $T_p = 0.52\text{s}$ respectively, based on Bray and Rodriguez-Marek (2004). In particular, Figure 8-9 plots the minimum ground acceleration needed to overturn the block as a function of block size R, for both the non-isolated and isolated case (with isolation-system periods $T_b = 2\text{s}$ and $T_b = 3\text{s}$). As indicated in this figure, for the short-period Parkfield, Cholame-3W record (with $T_p = 0.52\text{s}$), the isolation system has a positive effect on the stability of the block, regardless of block size R, provided that the isolation system is designed to have sufficiently large period (case of $T_b = 3\text{s}$). Note that for the case of the Northridge, Pacoima-Dam record (with $T_p = 0.61\text{s}$), the effectiveness of isolation is conditional on the size of the block R. On the contrary, for the long-period Bucharest, BRI record and Imperial Valley, EMO record ($T_p > 2\text{s}$), the use of isolation is not beneficial in improving the stability of the block (compared with the non-isolated case). It is worthy of noting that these response trends, with respect to the excitation period, are in line with the observed trends for the case of simple full-cycle acceleration pulses.

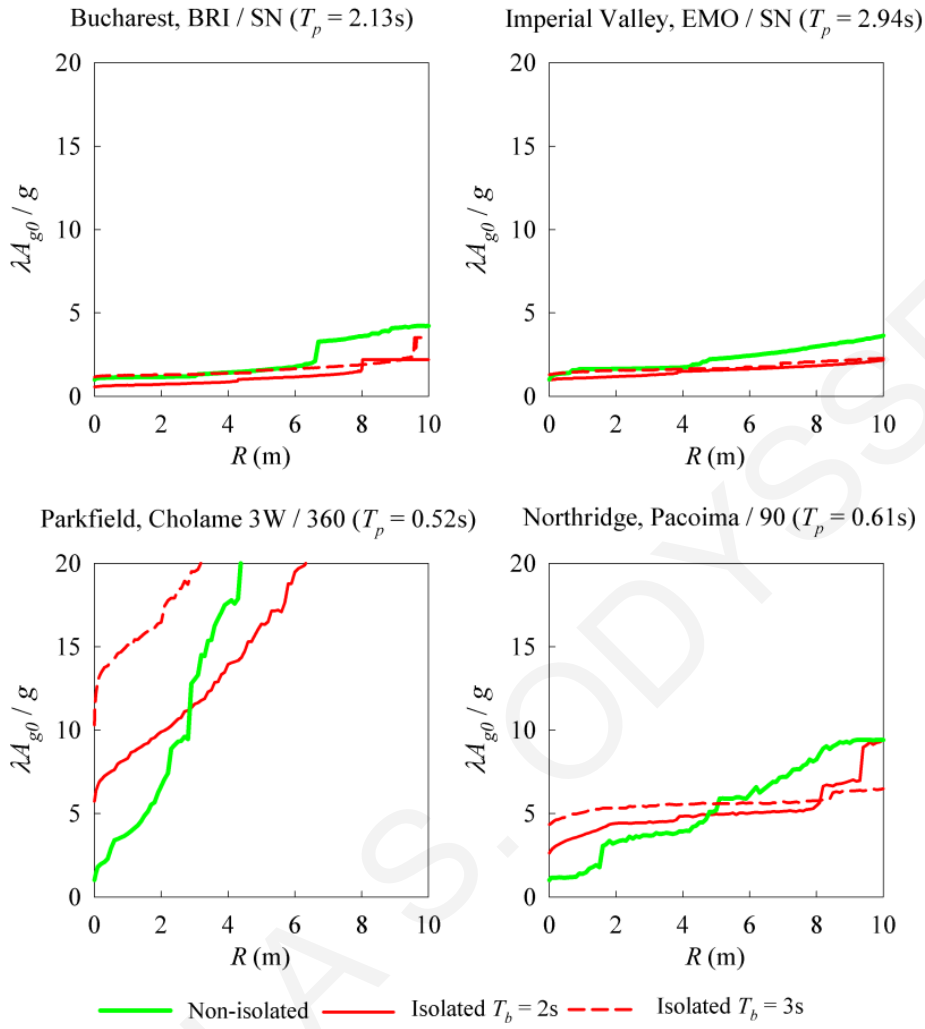

Figure 8-9: Minimum overturning acceleration for short- and long-period pulse-like earthquake motions. ($\lambda = 4$, $\rho = 0.5$, $\xi_b = 0.2$).

Figures 8-10 and 8-11 depict response-regime spectra in the $\lambda - R$ space for non-isolated and isolated blocks of varying geometric characteristics, for the considered long- and short-period earthquake records. These spectra suggest that, for the short-period earthquake motions the use of isolation results in an increase in the acceleration required to initiate rocking, a benefit that increases as the isolation period increases. The effectiveness of isolation in increasing the stability of the block is evident in the case of short- to intermediate-range period excitations, i.e. the Parkfield, Cholame-3W record (with $T_p = 0.52\text{s}$), the Aigion, AEG record (with $T_p = 0.71\text{s}$), and the Aigion, AEG record (with $T_p = 0.68\text{s}$). This is also true for the case of the Northridge, Pacoima-Dam record (with $T_p = 0.61\text{s}$), with the exception of very slender blocks

(large λ) where the effectiveness of isolation depends on the size of the block R. On the contrary, for long-period excitations, i.e. the Bucharest, BRI record, the Imperial Valley, EMO record, the Parkfield, C02 record and the Northridge, NWS record (with $T_p > 2\text{s}$), the use of isolation is not beneficial in improving the stability of the block. Similar observations have been made from analysis results with simple full-cycle acceleration pulses. It is also interesting to observe that the use of isolation improves the performance of the block, with respect to the initiation of rocking, regardless of the excitation period. The only exception to this, was the case of an isolation system with $T_b = 2\text{s}$ under Bucharest, BRI record. However, with an appropriate selection of the isolation-system period ($T_b > 2.5\text{s}$), the aforementioned observation is still valid. Appendix A contains comparisons of experimental and analytical results for non-isolated and isolated rigid blocks through response-regime spectra in the $\lambda - R$ space. A representative sample of results from Appendix A is presented in Figures 8-10 and 8-11.

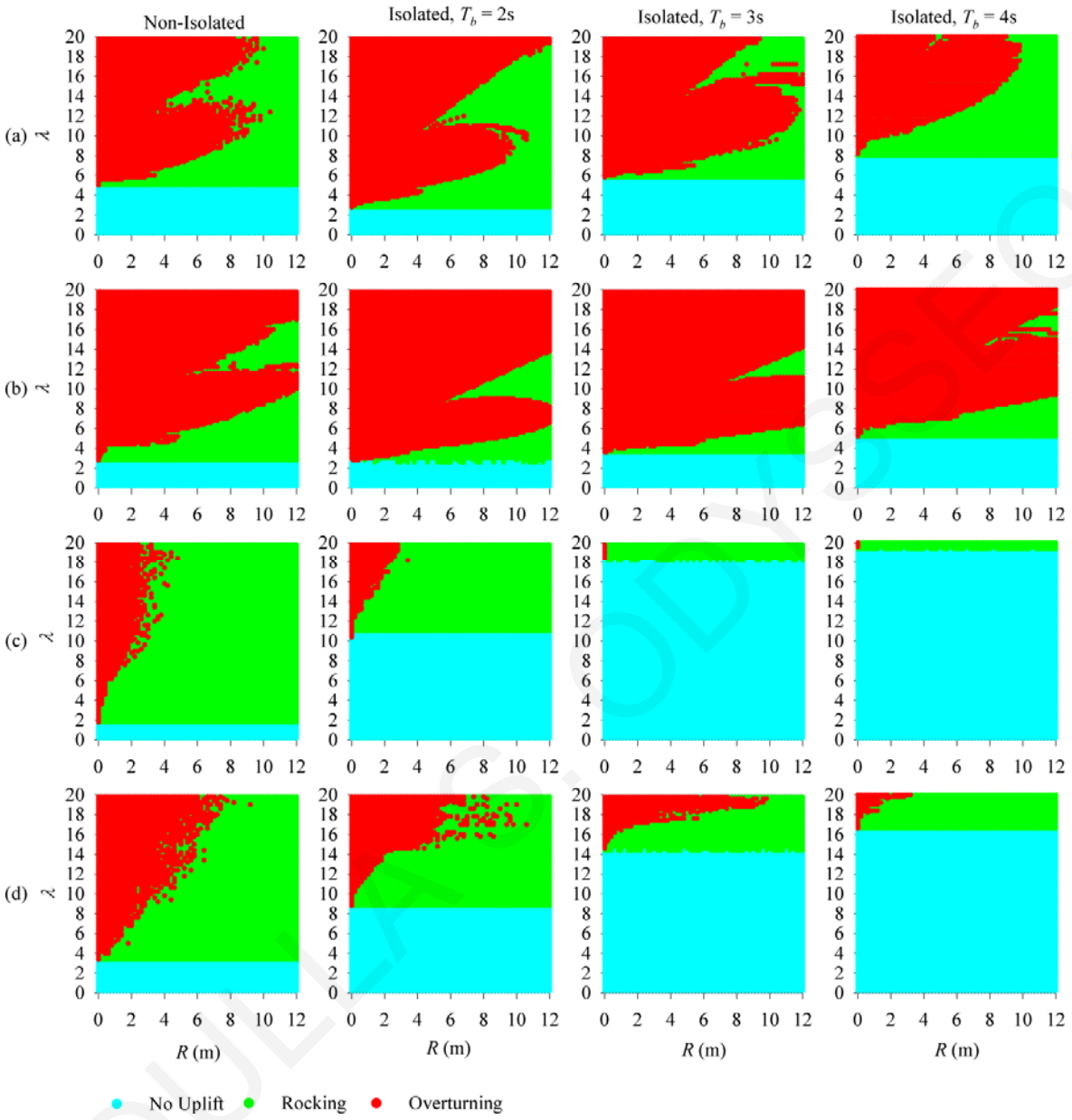

Figure 8-10: Response-regime spectra in the $\lambda - R$ space for a non-isolated and isolated block of varying geometric characteristics under (a) Bucharest, BRI / SN (T_p = 2.13s), (b) Imperial Valley, EMO / SN (T_p = 2.94s), (c) Parkfield, Cholame 3W / 360 (T_p = 0.52s), and (d) Northridge, Pacoima / 90 (T_p = 0.61s) records.

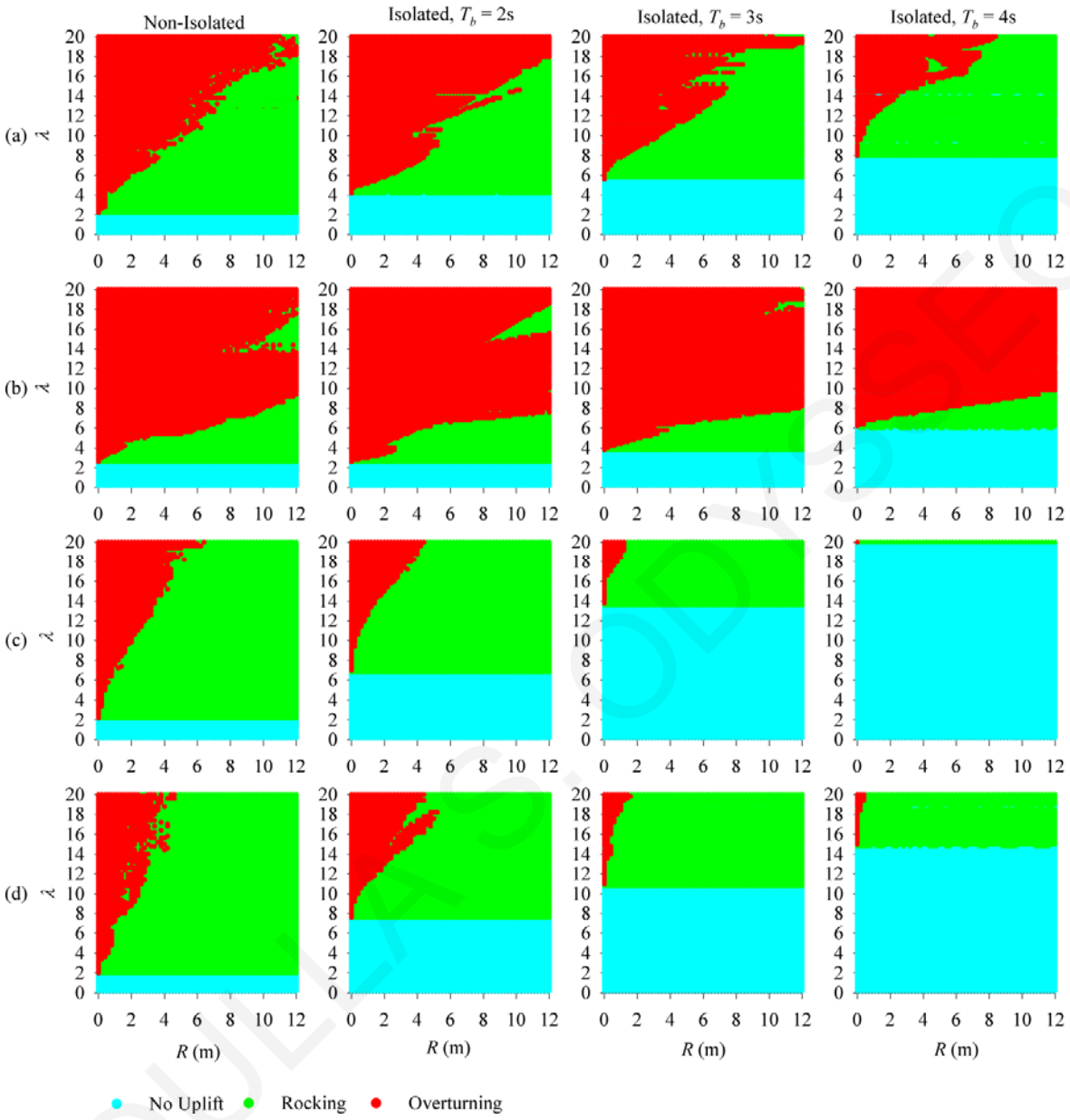

Figure 8-11: Response-regime spectra in the $\lambda - R$ space for a non-isolated and isolated block of varying geometric characteristics under (a) Parkfield, C02 / SN (T_p = 2.00s), (b) Northridge, NWS / SN (T_p = 2.70s), (c) Aigion, AEG / Long (T_p = 0.71s), and (d) Aigion, AEG / Tran (T_p = 0.68s) records.

The effect of linear isolation-system parameters on the block behavior is illustrated in Figure 8-12 through response-regime spectra in the T_b-ξ_b space for the considered earthquake records. These spectra specify the values of the constitutive parameters of the isolation system that provide improved performance of the analyzed block subjected to the specific pulse-type

ground excitations. As seen from Figure 8-12, the range of T_b, ξ_b values corresponding to enhanced system performance are considerably larger for the case of short-period records. The effect of block size R is shown in the T_b-ξ_b spectra of Figures 8-13 and 8-14 for the Bucharest, BRI and Northridge, Pacoima record, respectively, for a given block slenderness λ. Observe that the boundary between no-uplift and rocking regimes (cyan and green areas, respectively) is invariant to the change of block size R, justifying that the initiation of rocking is not dependent on the absolute size of the block (but rather on the height-to-width ratio λ, as Equation (5.73) suggests). Moreover, the unfavourable (red) region in the T_b-ξ_b space entailing overturning of the block is reduced as the block size R increases. Similar observation has been made from analysis results with simple acceleration pulses (Figure 8-5). Evidently, the damping ratio, ξ_b, has a significant influence on the effectiveness of isolation. In particular, the effectiveness of isolation is reduced as the damping ratio decreases.

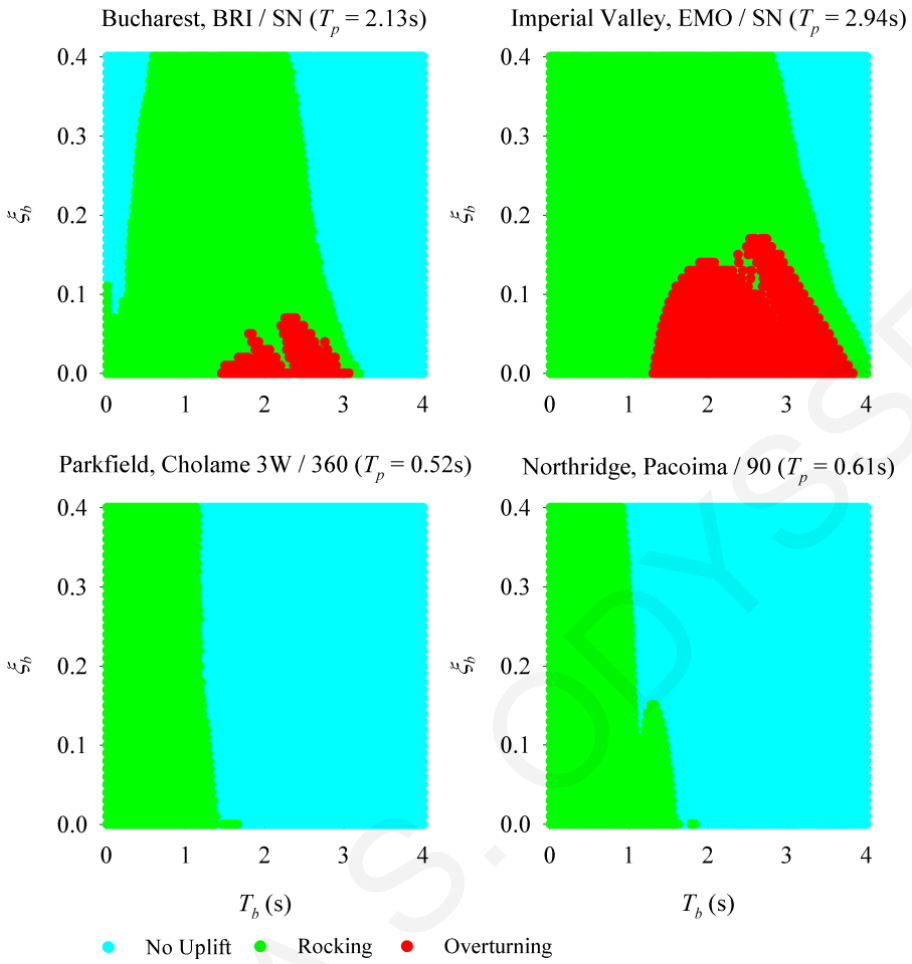

Figure 8-12: Response-regime spectra in the T_b-ξ_b space for isolated block under Bucharest, BRI / SN, Imperial Valley, EMO / SN, Parkfield, Cholame 3W / 360 and Northridge, Pacoima / 90 records ($\lambda = 4$, $\rho = 0.5$, $R = 6\text{m}$).

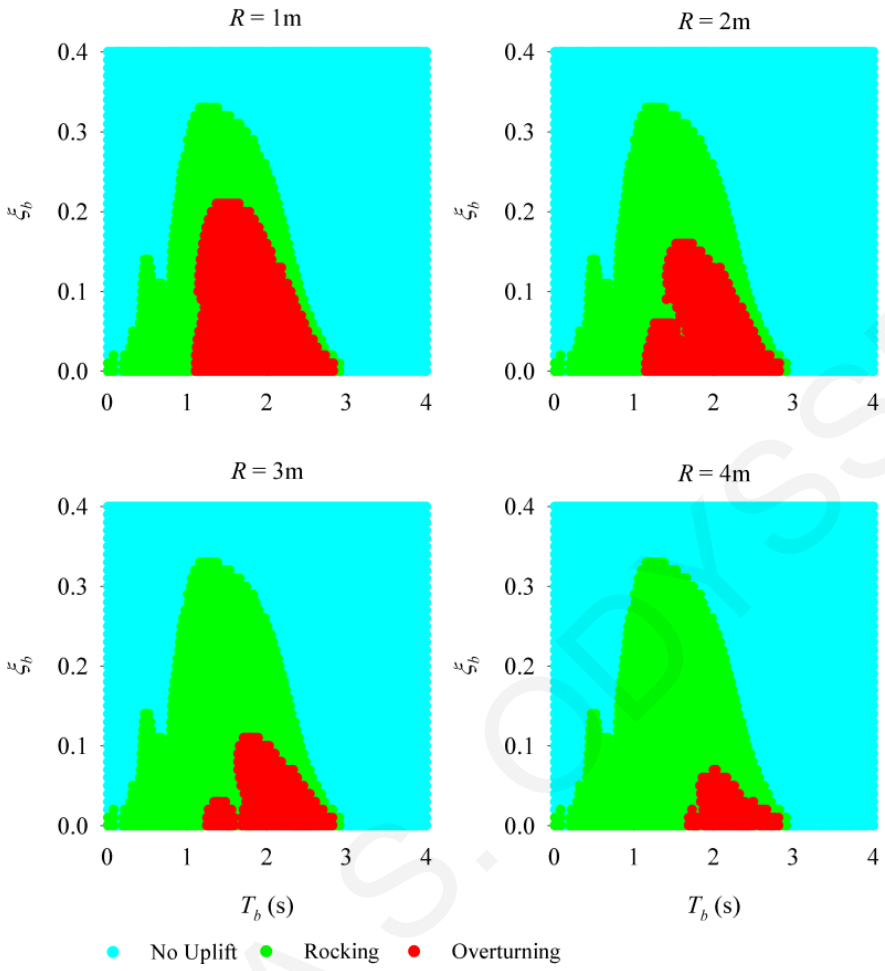

Figure 8-13: Response-regime spectra in the T_b-ξ_b space for isolated block of varying size R under Bucharest, BRI / SN record ($T_p = 2.13$s, $\lambda = 3$).

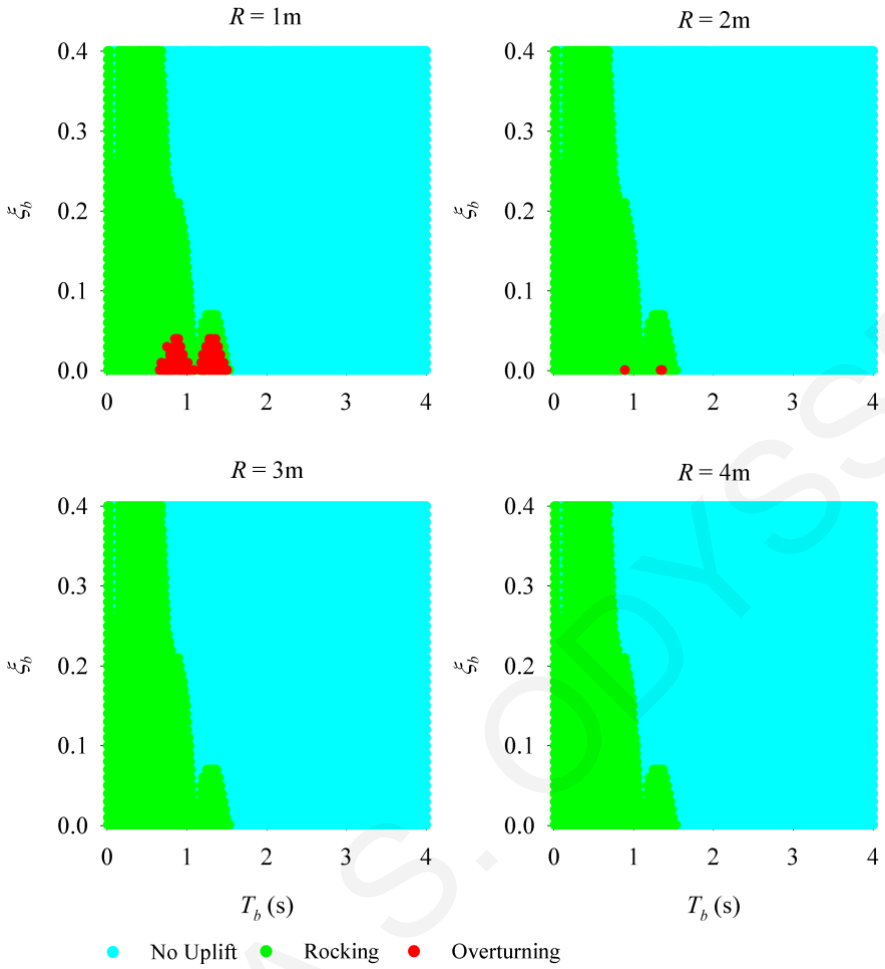

Figure 8-14: Response-regime spectra in the T_b-ξ_b space for isolated block of varying size R under Northridge, Pacoima / 90 record ($T_p = 0.61$s, $\lambda = 3$).

Figure 8-15 depicts response-regime spectra in the $\lambda - R$ space for a wide range of rigid blocks under recorded near-fault ground motions using a bilinear hysteretic model with parameters $\mu_b = 0.11$ and $R_b = 2.24$s (corresponding to $T_b = 3$s), and a viscoelastic model with $T_b = 3$s and $\xi_b = 0.35$. As shown in these figures, the dynamic behavior of the block for the two types of seismic isolation is similar while the initiation of rocking (boundary between cyan and green areas) is not drastically affected. Appendix B presents comparisons of experimental and analytical results for isolated rigid blocks using linear and nonlinear isolation system through response-regime spectra in the $\lambda - R$ space. A representative sample of results from Appendix B is presented in Figure 8-15.

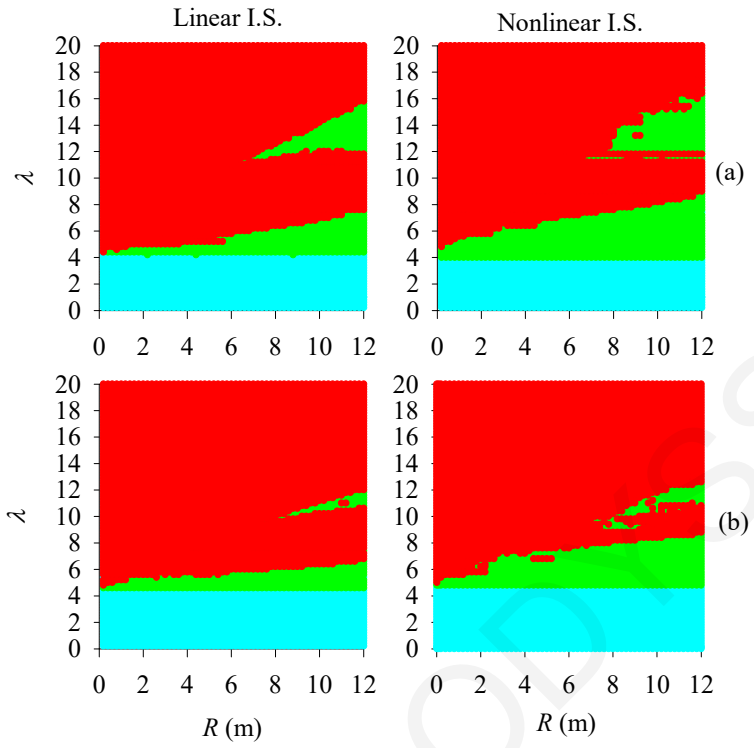

Figure 8-15: Response-regime spectra in the $\lambda - R$ space for a class of isolated rigid blocks under (a) the SN component of 1979 Imperial Valley, CA, USA earthquake (EMO station) and (b) the SN component of 1979 Imperial Valley E05 earthquake ($\rho = 0.5$, $\mu_b = 0.11$, $R_b = 2.24\text{m}$, $T_b = 3\text{s}$).

Figures 8-16 through 8-18 present time histories of the dynamic response of isolated and non-isolated rigid blocks under the SN component of 1977 Bucharest, Romania earthquake with a peak amplitude of 0.21g. Two types of isolation systems are considered in the analysis: (a) a nonlinear isolation system with a bilinear hysteretic model (typified by friction-pendulum isolator) with parameters $\mu_b = 0.11$ and $R_b = 2.24\text{m}$ (corresponding to $T_b = 3\text{s}$), and (b) a linear isolation system with viscoelastic model with $T_b = 3\text{s}$. These figures plot the ground acceleration, $\ddot{x}_g$, the normalized angular displacement, θ/α, (with the overturning of the block indicated when $\theta/\alpha \geq 1$), the angular velocity of the block, $\dot{\theta}$ and the horizontal displacement of the isolation system, u.

Figure 8-16 shows the response of a block with size-parameter $R = 8\text{m}$, slenderness ratio $\lambda = 8$, and mass ratio $\rho = 0.5$. The block (non-isolated or isolated) oscillates in the rocking

regime. This estimation can also be made from Figure 8-10, but the response history reveals that the angular velocity and rotation angle of an isolated block using linear-isolation system is reduced drastically with time (rocking regime ceases) and the system finally oscillates in the system-translation regime. It is also observed that, the initiation of rocking for isolated and non-isolated block follows the peak amplitude of the ground acceleration. Using a linear isolation system the maximum horizontal system translation is approximately 250mm. Finally, the system comes to rest before the end of the earthquake record. Using the nonlinear isolation system the maximum horizontal system translation is approximately the same with the permanent displacement (100mm).

Figure 8-17 shows that both blocks (isolated and non-isolated) with $R = 2\text{m}$ and $\lambda = 10$, oscillate with rocking motion and finally overturn. In particular, the non-isolated block overturns immediately after the initiation of rocking clockwise. The isolated block enters clockwise rocking regime and after an impact event it finally overturns.

Figure 8-18 depicts response histories of system with $R = 0.8\text{m}$ and $\lambda = 5.6$. The non-isolated block initially oscillates with clockwise rocking and upon impact the oscillation pattern switches to anti-clockwise rocking motion and finally overturns. In contrast, the isolated block switches between anticlockwise and clockwise rocking motions, and after a few seconds the system switches to system-translation regime. For further response histories for non-isolated and isolated rigid blocks under near-fault ground motions, refer to Appendix C.

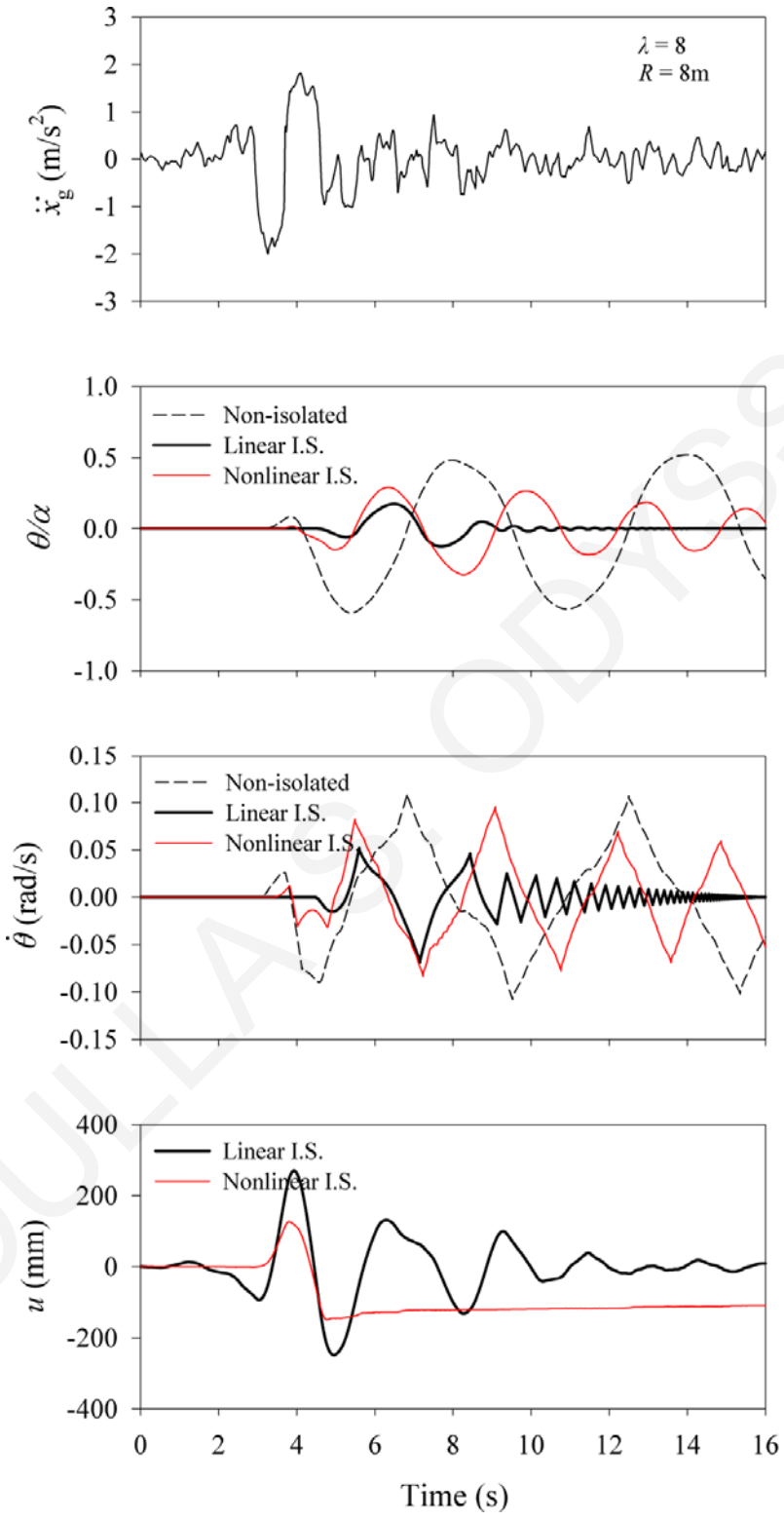

Figure 8-16: Response histories for non-isolated and isolated rigid block under the SN component of 1977 Bucharest, Romania earthquake ($\rho = 0.5$, $\lambda = 8$, $R = 8\text{m}$).

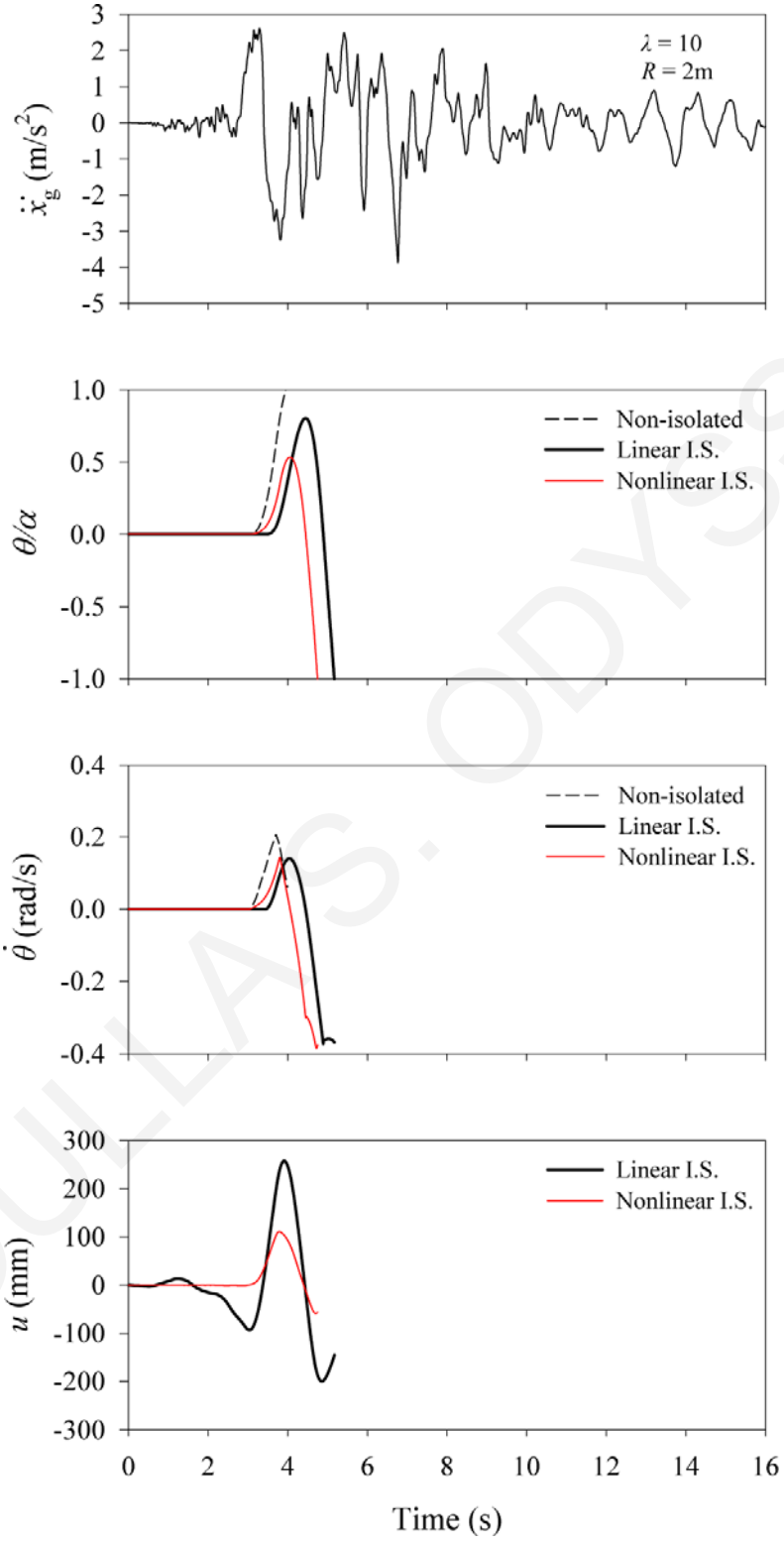

Figure 8-17: Response histories for non-isolated and isolated rigid block under the SN component of 1977 Bucharest, Romania earthquake ($\rho = 0.5$, $\lambda = 10$, $R = 2\text{m}$).

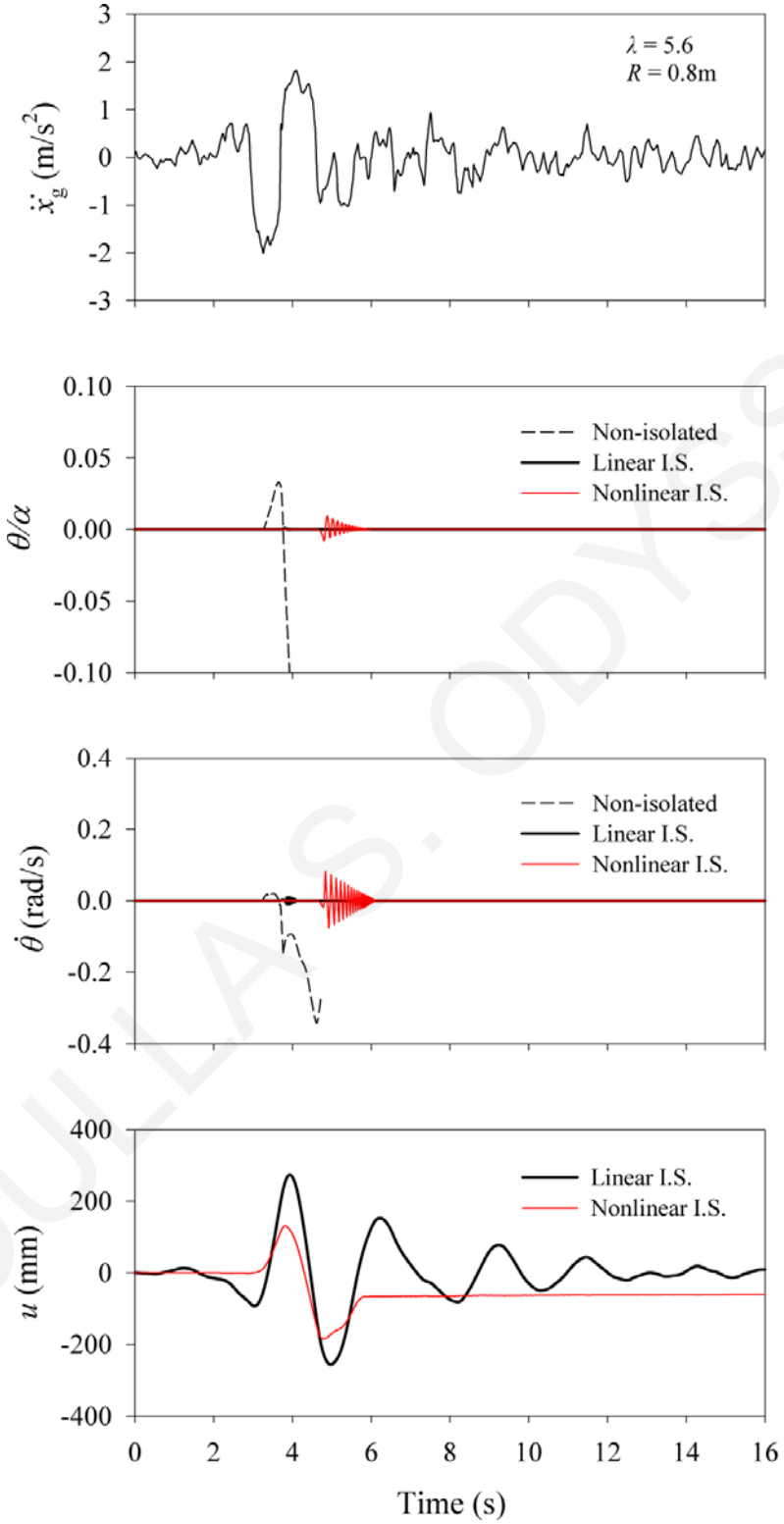

Figure 8-18: Response histories for non-isolated and isolated rigid block under the SN component of 1977 Bucharest, Romania earthquake ($\rho = 0.5$, $\lambda = 5.6$, $R = 0.8\text{m}$).

8.3 Response to Idealized Pulse-Type Motions

In this section, a comparison between the dynamic response of the system using idealized pulse-type motions and recorded near-fault ground motions is presented. The aim is to investigate whether the dynamic response of such systems can be estimated accurately using the idealized pulse-type motions instead of the actual ground motions. The sophisticated analytical model of Mavroeidis and Papageorgiou (2003) is used for the representation of near-fault ground motions as idealized pulse-type motions.

The mathematical representation of ground acceleration for near-fault ground motions, as proposed by Mavroeidis and Papageorgiou (2003), is

$$a(t)=\begin{cases}-\dfrac{A\pi f_p}{\gamma}\left[\begin{array}{l}\sin\left(\dfrac{2\pi f_p}{\gamma}\left(t-t_0\right)\right)\cos\left[2\pi f_p\left(t-t_0\right)+\nu\right]\\ +\gamma\sin\left[2\pi f_p\left(t-t_0\right)+\nu\right]\left[1+\cos\left(\dfrac{2\pi f_p}{\gamma}\left(t-t_0\right)\right)\right]\end{array}\right], & t_0-\dfrac{\gamma}{2f_p}\le t\le t_0+\dfrac{\gamma}{2f_p},\ \gamma>1\\ 0\end{cases} \quad (8.4)$$

where, T_p is the pulse duration, equal to the inverse of the prevailing frequency (f_p); γ is a parameter that defines the oscillatory character; A controls the amplitude of the signal; v is the phase of the amplitude-modulated harmonic; and t_0 specifies the epoch of the envelope's peak.

Table 8-2 lists the characteristics of the recorded near-fault ground motions, together with the model input parameters associated with the idealized pulse-type motions, used for the dynamic analysis.

Table 8-2: Characteristics of recorded near-fault ground motions and model input parameters for the idealized pulse-type motions (Mavroeidis and Papageorgiou (2003)).

Earthquake	Station / Component	Magnitude (M_w)	Distance (km)	PGA (g)	PGV (m/s)	A	γ	$\nu(^o)$	f_p (Hz)
1966 Parkfield, CA, USA	C02/SN	6.20	0.1	0.48	0.75	60.0	1.700	100.0	0.500
1971 San Fernando, CA, USA	PCD/SN	6.55	3.0	1.29	1.20	115.0	1.600	180.0	0.680
1978 Tabas, Iran	TAB/SP	7.11	1.2	0.85	1.22	104.0	2.200	180.0	0.190
1979 Imperial Valley, CA, USA	E04/SN	6.50	6.0	0.36	0.78	71.0	1.900	305.0	0.225
	E05/SN	6.50	2.7	0.38	0.92	84.0	1.900	300.0	0.255
	E06/SN	6.50	0.3	0.44	1.12	96.0	2.100	265.0	0.260
	E07/SN	6.50	1.8	0.46	1.09	79.0	2.100	25.0	0.275
	EMO / SN	6.50	1.2	0.38	1.15	78.0	2.300	0.0	0.340
1994 Northridge, CA, USA	JFA/SN	6.70	5.2	0.39	1.05	87.0	2.300	100.0	0.330
	RRS/SN	6.70	6.0	0.89	1.73	142.0	1.700	20.0	0.800
	SCG/SN	6.70	5.1	0.59	1.34	93.0	2.500	0.0	0.340
	SCH/SN	6.70	5.0	0.89	1.22	80.0	2.300	0.0	0.330
	NWS/SN	6.70	5.3	0.41	1.17	94.0	1.700	200.0	0.370
1995 Aigion, Greece	AEG/Long	6.33	6.0	0.50	0.41	44.5	1.450	75.0	1.400
	AEG/Tran	6.33	6.0	0.55	0.52	61.0	1.200	205.0	1.480
1999 Izmit, Turkey	ARC/SN	7.40	14.0	0.13	0.44	41.0	1.380	225.0	0.140
	SKR/SP	7.40	3.1	0.41	0.80	67.0	1.023	5.0	0.105
	GBZ/SN	7.40	11.0	0.26	0.41	34.5	2.200	220.0	0.210
	GBZ/SP	7.40	11.0	0.03	0.29	28.0	1.800	85.0	0.165
1977 Bucharest, Romania	BRI / SN	7.3	190	0.21	0.75	62.0	2.400	200.0	0.470

Figures 8-19 through 8-24 present results from the dynamic behavior of isolated rigid blocks under near-fault ground motions and their pulse-type idealization based on Mavroeidis and Papageorgiou (2003). A linear isolation system is considered in these analyses with $T_b = 3\text{s}$, $\xi_b = 0.35$. The response history, located at the top of each figure, illustrates the recorded ground motion and its idealized pulse-type motion. The dynamic response of the system is presented using response-regime spectra in the $\lambda - R$ space, located at the bottom of each figure. As seen from this figure, the system response when subjected to the recorded near-field motion and its simulated representation is similar. The initiation of rocking (boundary between cyan and green areas) is not drastically affected and the rocking (green area) and overturning areas (red area) are comparable. It is evident, that the dynamic response of the isolated system can be estimated properly using the idealized pulse-type motion (Mavroeidis and Papageorgiou (2003)) instead of the actual ground motion.

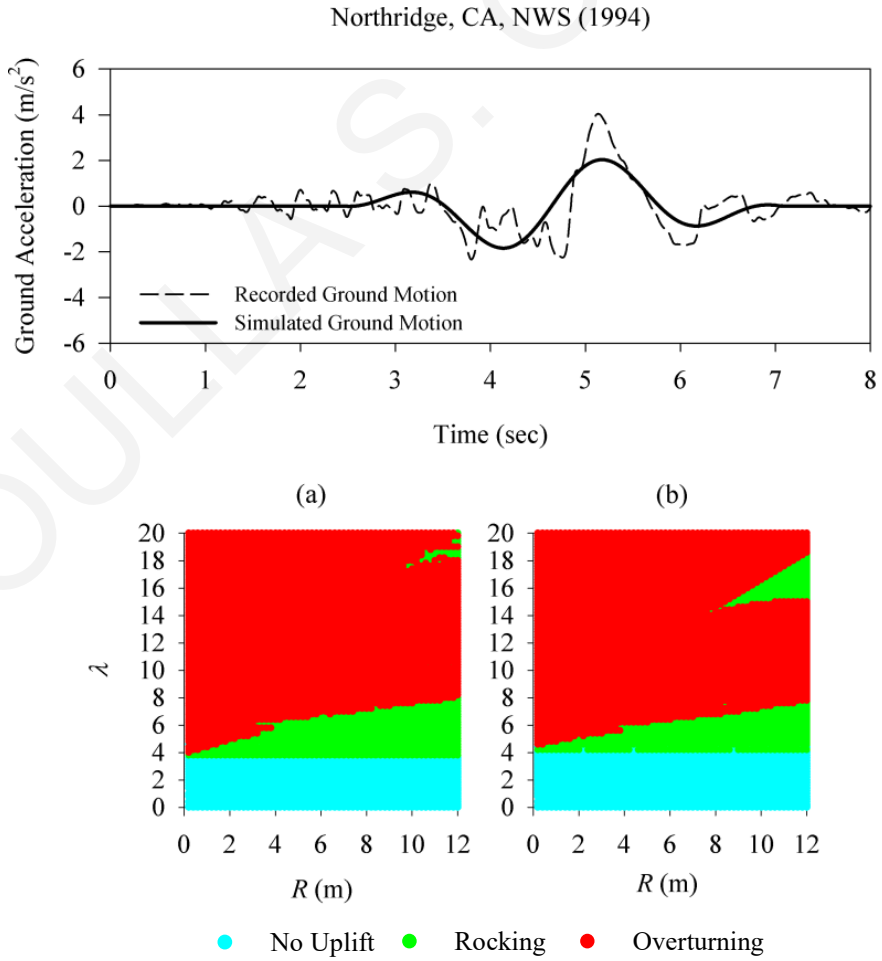

Figure 8-19: Response-regime spectra in the $\lambda - R$ space for an isolated block of varying geometric characteristics under (a) the SN component of 1994 Northridge, CA, NWS earthquake and (b) its pulse-type representation.

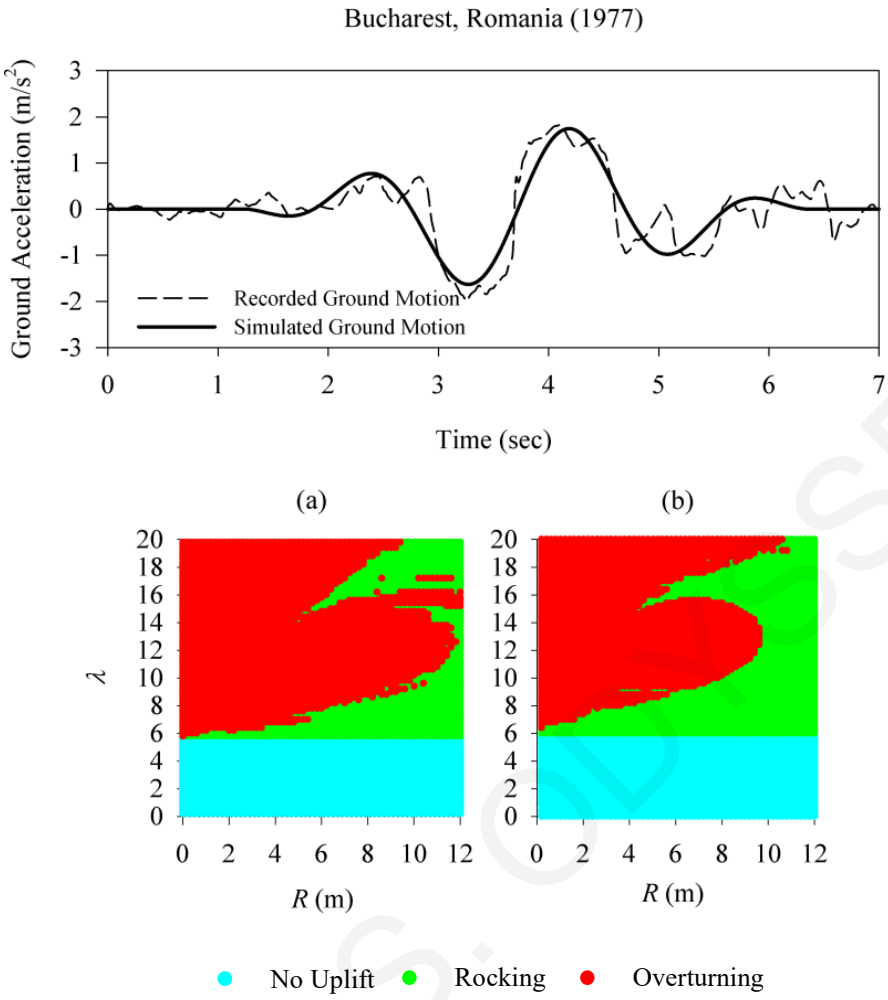

Figure 8-20: Response-regime spectra in the $\lambda - R$ space for an isolated block of varying geometric characteristics under (a) the SN component of 1977 Bucharest, Romania earthquake and (b) its pulse-type representation.

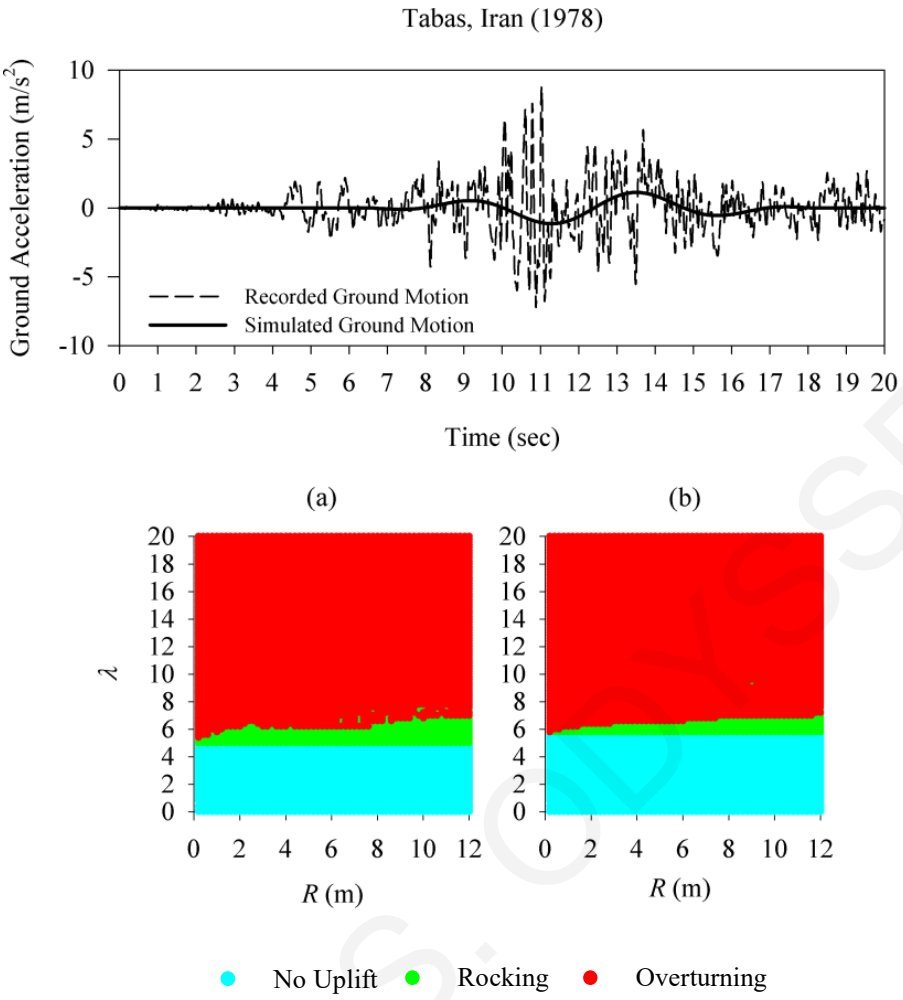

Figure 8-21: Response-regime spectra in the $\lambda - R$ space for an isolated block of varying geometric characteristics under (a) the SP component of 1978 Tabas, Iran earthquake and (b) its pulse-type representation.

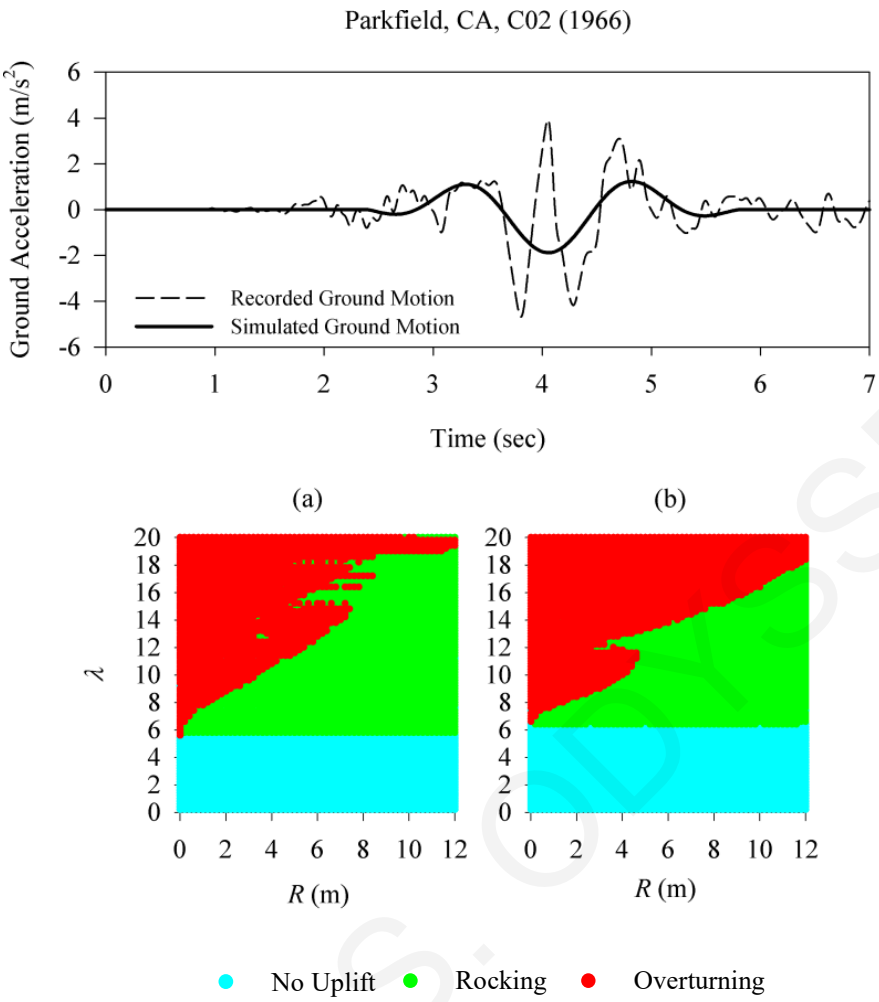

Figure 8-22: Response-regime spectra in the $\lambda - R$ space for an isolated block of varying geometric characteristics under (a) the SN component of 1966 Parkfield, CA earthquake and (b) its pulse-type representation.

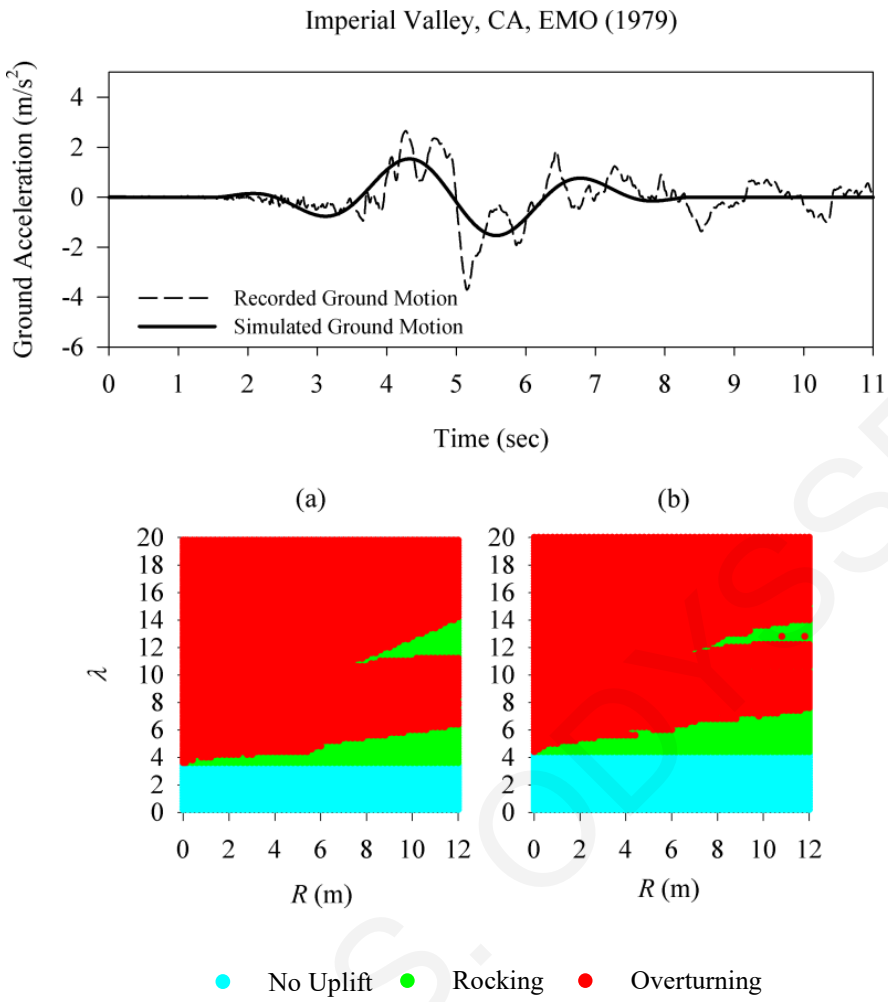

Figure 8-23: Response-regime spectra in the $\lambda - R$ space for an isolated block of varying geometric characteristics under (a) the SN component of 1979 Imperial Valley, CA, EMO earthquake and (b) its pulse-type representation.

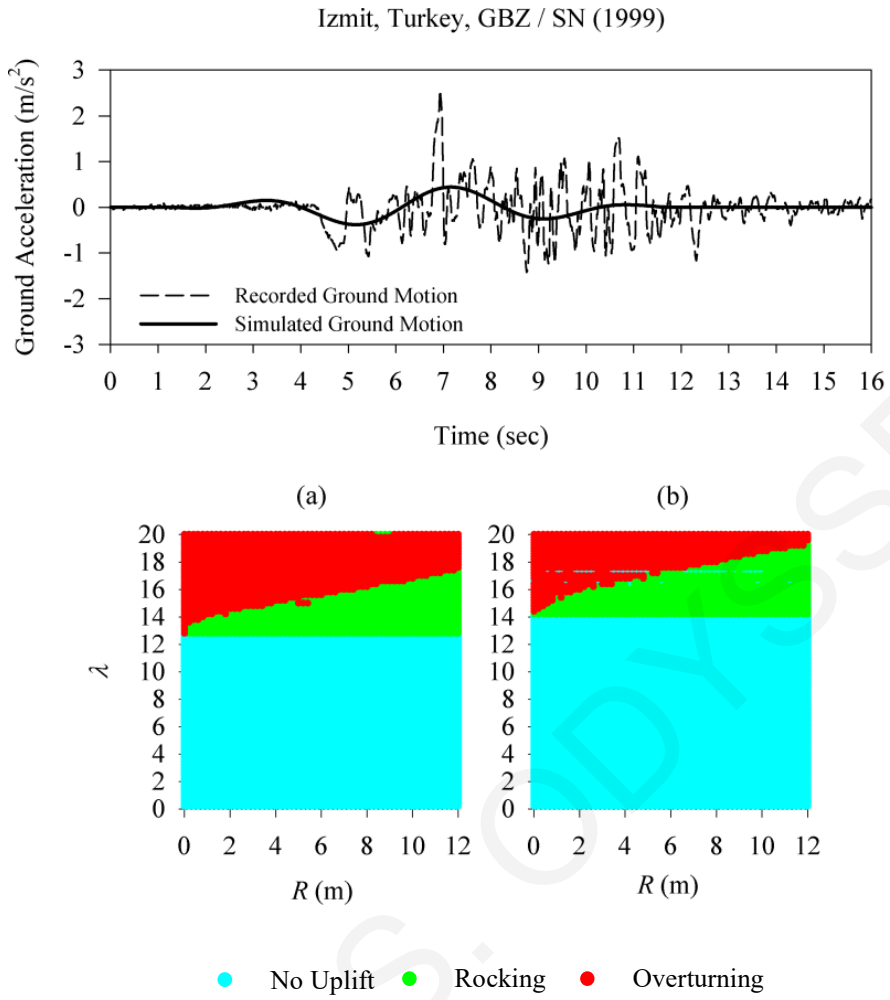

Figure 8-24: Response-regime spectra in the $\lambda - R$ space for an isolated block of varying geometric characteristics under (a) the SN component of 1999 Izmit, Turkey, GBZ earthquake and (b) its pulse-type representation.

The effect of isolation-system parameters on the block behavior using the actual ground motion and the idealized pulse-type motion of Bucharest, BRI record is illustrated in Figure 8-25 through response-regime spectra in the T_b-ξ_b space. These spectra specify the values of the constitutive parameters of the isolation system that provide improved performance of the analyzed block subjected to the specific pulse-type ground excitation. The analysis has been accomplished for different size, R, of the block. As seen from this figure, for the idealized pulse-type motion, the boundary between no-uplift and rocking regime (cyan and green areas, respectively) is different from that of the actual record especially for $T_p < 1\text{s}$. In general, the use of idealized pulse motions yields to more conservative results, regarding the initiation of rocking (larger cyan area). On the other hand, the overturning region (red area) is approximately the same using actual and idealized pulse-type motions.

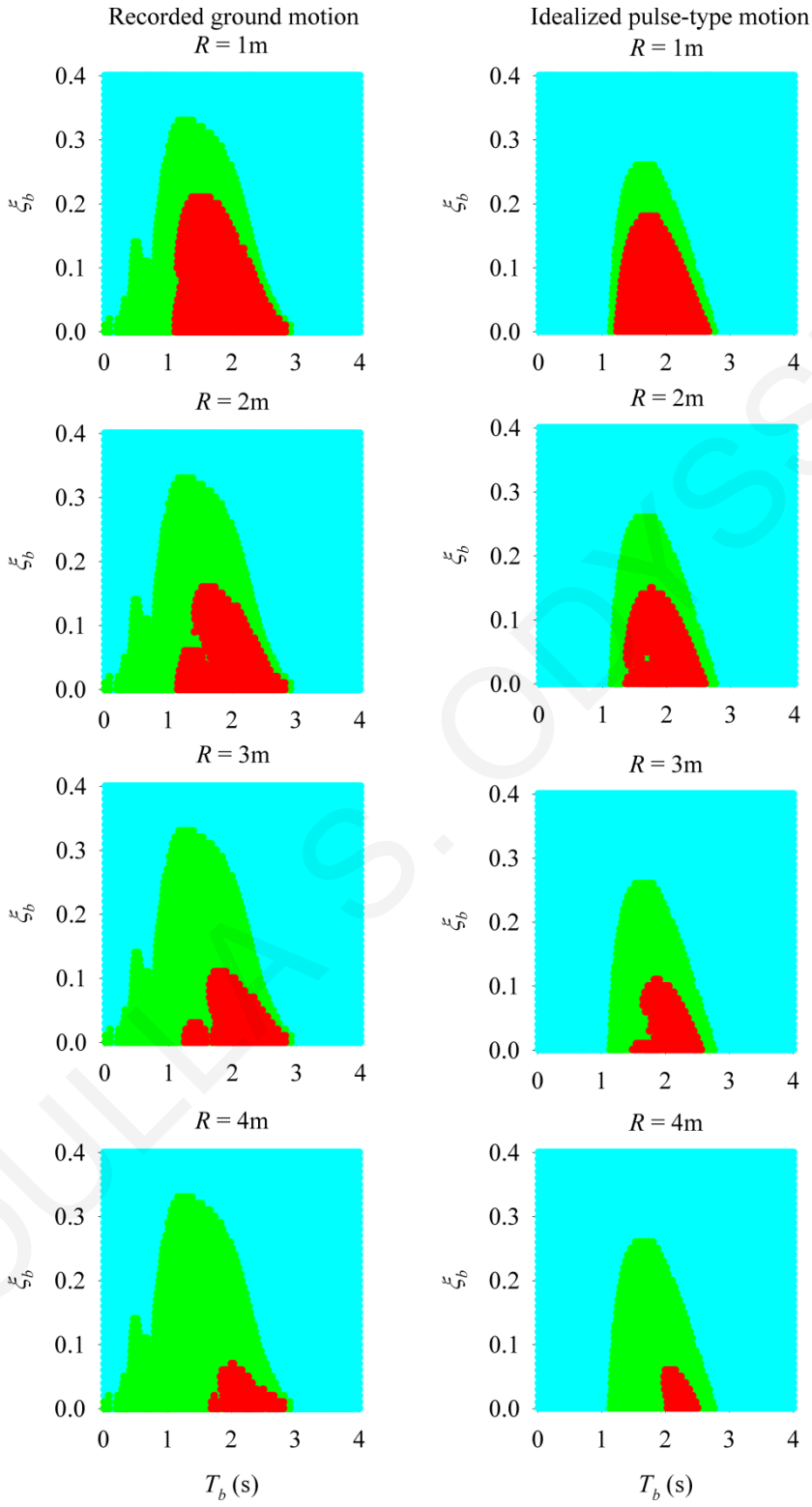

Figure 8-25: Response-regime spectra in the T_b-ξ_b space for isolated block of varying size R under Bucharest, BRI / SN record (first column) and its pulse-type idealization (second column) ($\lambda = 3$).

CHAPTER 9

Multi-Pattern Response to Dynamic Base Excitation

In this chapter, the multi-pattern response of the isolated rigid block subjected to full-cycle sinusoidal pulses and horizontal near-fault ground motions is investigated, assuming sliding between the block and the supporting base. The complexity of the problem increases in comparison with the previous chapter as the system is realized through pure system translation, sliding, rocking, and slide-rocking oscillation regimes. This investigation gives a more realistic approximation for the dynamic response of the system and reveals the general treatment of the problem.

9.1 Response to Simple Acceleration Pulses

The general planar motion response of the isolated and non-isolated rigid block is investigated first using full-cycle sinusoidal pulses. The horizontal full-cycle sinusoidal pulse is characterized by amplitude A_{g0} and half-cycle duration t_d (corresponding to frequency $\omega_p = \pi / t_d$), expressed mathematically as follows

$$\ddot{x}_g(t) = \begin{cases} A_{g0} \sin\left(\pi t / t_d\right), & \text{if } \ 0 \le t \le 2t_d \\ 0, & \text{if } \ t > 2t_d \end{cases} \tag{9.1}$$

The stability of the isolated block is examined in terms of the minimum amplitude of ground acceleration required to initiate each oscillation pattern and overturn the block ($\theta / \alpha \ge 1$), by considering the influence of input-motion characteristics, the friction coefficient between the block and the base, and the constitutive parameters of the isolation system.

Figures 9-1 through 9-5 present the general response of non-isolated (left) and isolated (right) rigid blocks with different block size R under full-cycle sinusoidal pulses. These figures plot the minimum acceleration amplitude, A_{g0} / g, required for the system to enter into different oscillation regimes, as a function of the static-friction coefficient, μ_s, and duration of pulse, t_d. The isolation-system parameters used in the analysis are elastic stiffness $k_b = 40\text{kN/m}$, period $T_b = 3\text{s}$, and damping ratio $\xi_b = 0.35$. Each figure is divided into five areas: (a) S: pure sliding occurs (grey area), (b) R: pure rocking occurs (green area), (c) SR: slide-rocking occurs (blue area), (d) SA: safe area and (e) CA: critical

area. It is worth mentioning that pure sliding or pure rocking may preceded the slide-rocking motion. The safe area indicates that the system is at rest (non-isolated) or at system translation regime (isolated). The critical area corresponds to system failure through overturning of the block (when the normalized rotation angle $\theta / \alpha \geq 1$).

As seen from Figure 9-1 the sliding motions are more intensive for small values of coefficient of static friction, while rocking motion predominates for higher values of the static-friction coefficient. For small values of the coefficient of friction, the block oscillates in the sliding regime while as the acceleration increases the system undergoes slide-rocking and finally overturns. As expected, the minimum ground acceleration needed to initiate sliding is increased linearly with the coefficient of static friction, Equation (5.33). For pulse duration $t_d = 0.3\text{s}$, the minimum ground acceleration required to initiate pure sliding or pure rocking is larger in the case of the isolated block. As a result, the safe area is extended in comparison with the non-isolated block. In addition, the overturning failure is associated with larger ground accelerations for the isolated block. It is also observed that, for small values of the coefficient of friction, the minimum overturning ground acceleration for isolated block is markedly greater than that for large values of friction. Evidently, the value of the coefficient of friction plays an important role in the performance of the isolated block. Note that the system is highly nonlinear and very sensitive to the variation of the parameters; the minimum overturning ground acceleration differs for each coefficient of static friction.

The effect of pulse duration on the rocking response (green area) of the system is investigated in detail in Section 8.1. Herein, the investigation focuses mostly on the effect of pulse duration on sliding (grey area) and slide-rocking (blue area). Figures 9-1 through 9-5 show that the isolation system has a positive effect on the stability of the block in comparison to the non-isolated block for period pulses with $t_d < 0.7\text{s}$ or equivalently excitation period $T_p < 1.4\text{s}$. As the pulse duration decreases the safe area increases in comparison to the non-isolated block. However, it should also be noted that as the pulse duration increases, the minimum overturning ground acceleration decreases rapidly in comparison to the non-isolated block. Consequently, the use of isolation may not be beneficial for excitation periods $T_p > 1.4\text{s}$ $(t_d > 0.7\text{s})$.

It is also observed that, as the size of the block, R, increases, the minimum ground acceleration needed to overturn the block (be it non-isolated or isolated) increases. Note

that the safe area is invariant to the change of the block size R, justifying that the initiation of rocking and sliding in not dependent on the absolute size of the block (but rather to the height-to-width ratio λ).

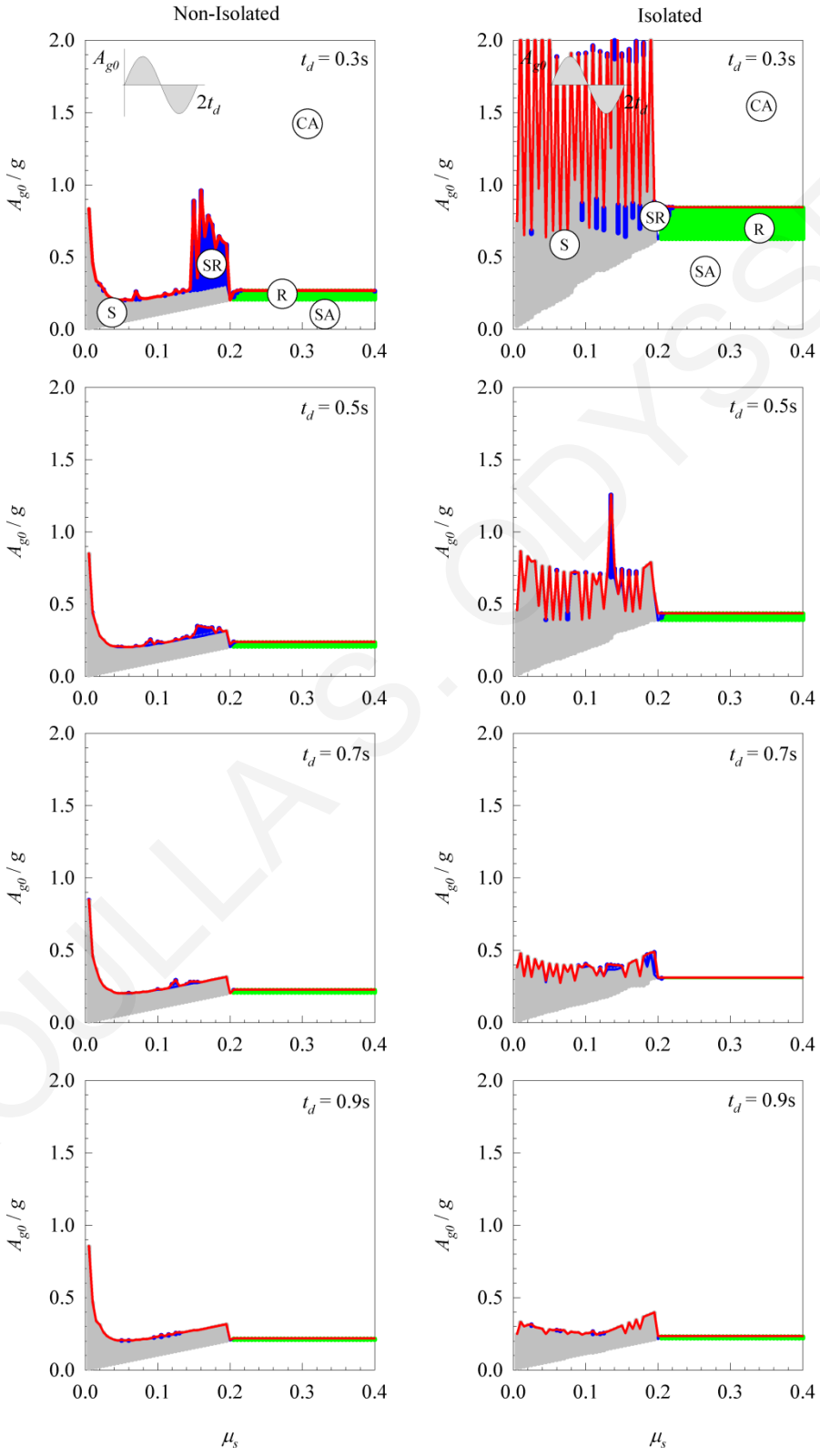

Figure 9-1: Minimum ground acceleration as a function of coefficient of static friction for

simple full-sine ground-acceleration pulse ($\lambda = 5$, $R = 0.5\text{m}$, $\rho = 0.5$).

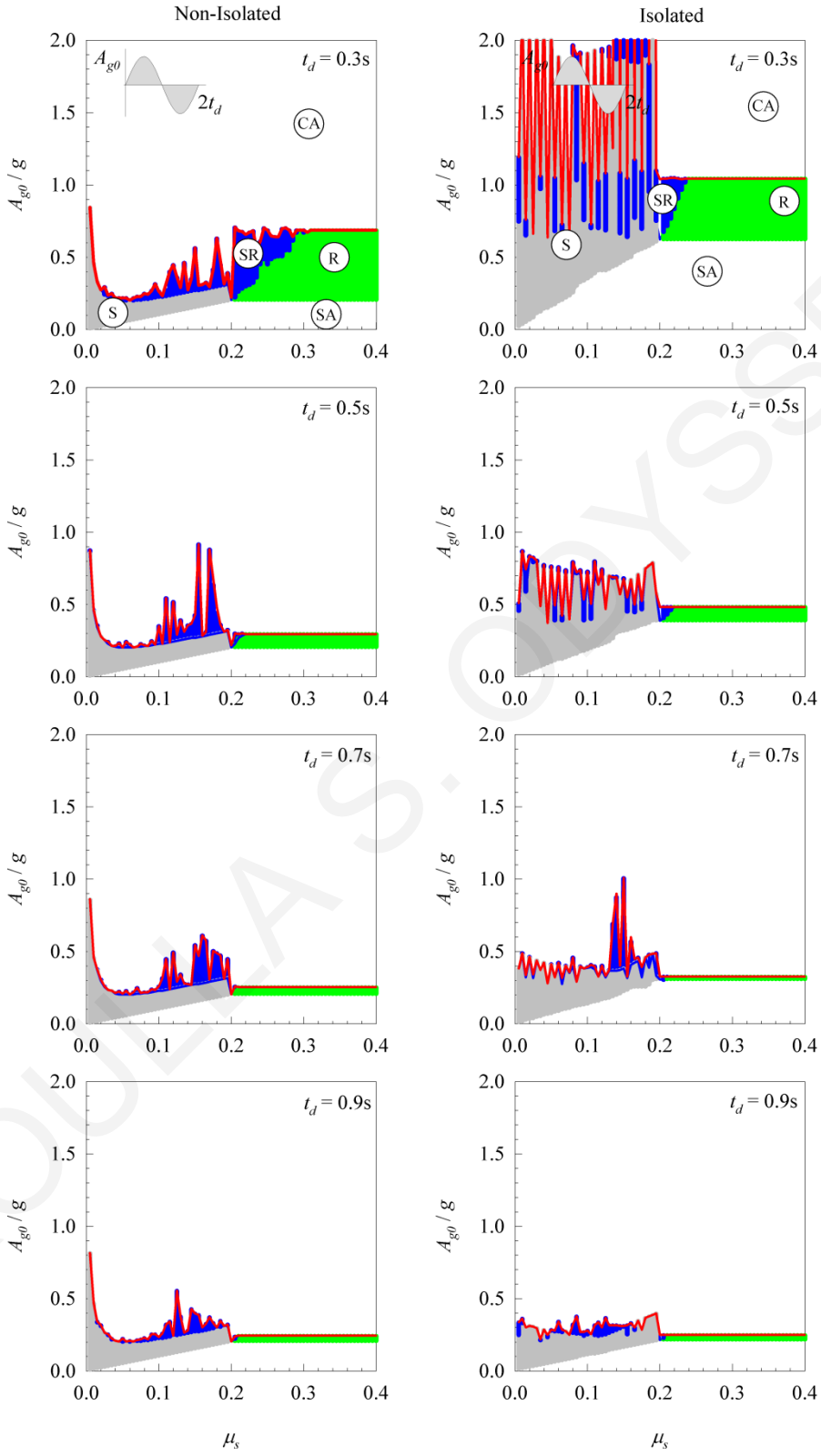

Figure 9-2: Minimum ground acceleration as a function of coefficient of static friction for simple full-sine ground-acceleration pulse ($\lambda = 5$, $R = 2\text{m}$, $\rho = 0.5$).

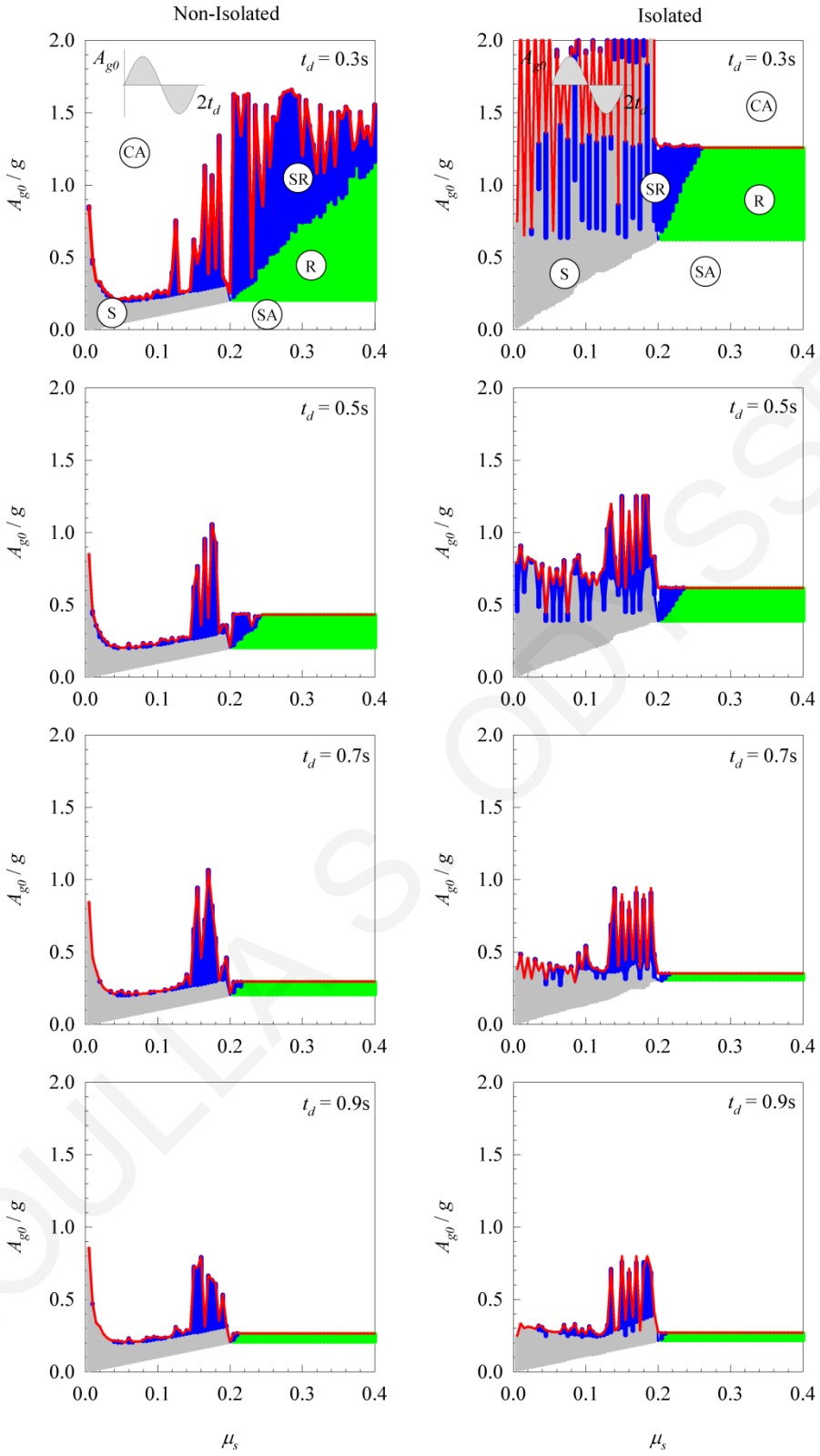

Figure 9-3: Minimum ground acceleration as a function of coefficient of static friction for simple full-sine ground-acceleration pulse ($\lambda = 5$, $R = 4\text{m}$, $\rho = 0.5$).

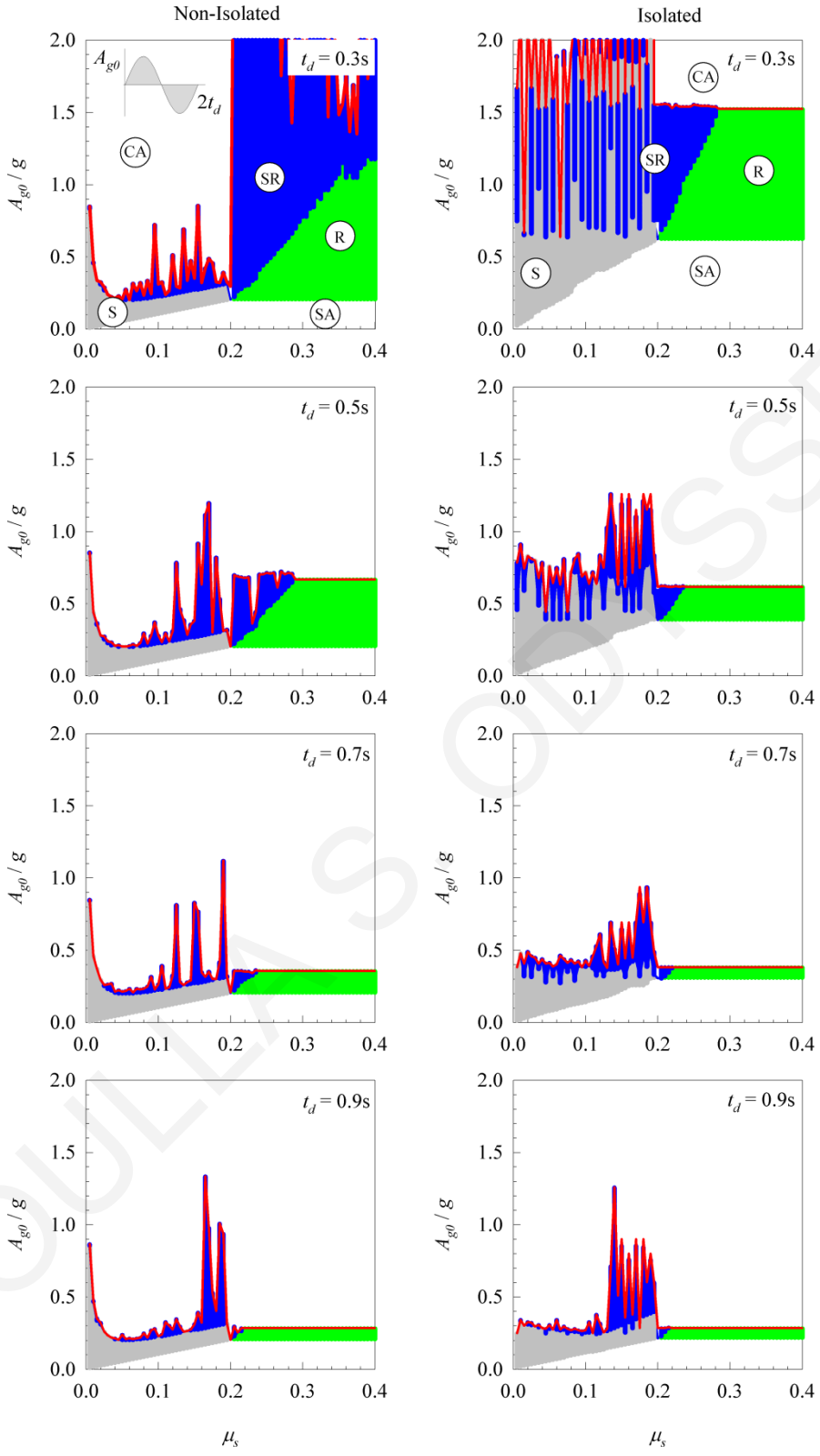

Figure 9-4: Minimum ground acceleration as a function of coefficient of static friction for simple full-sine ground-acceleration pulse ($\lambda = 5$, $R = 6\text{m}$, $\rho = 0.5$).

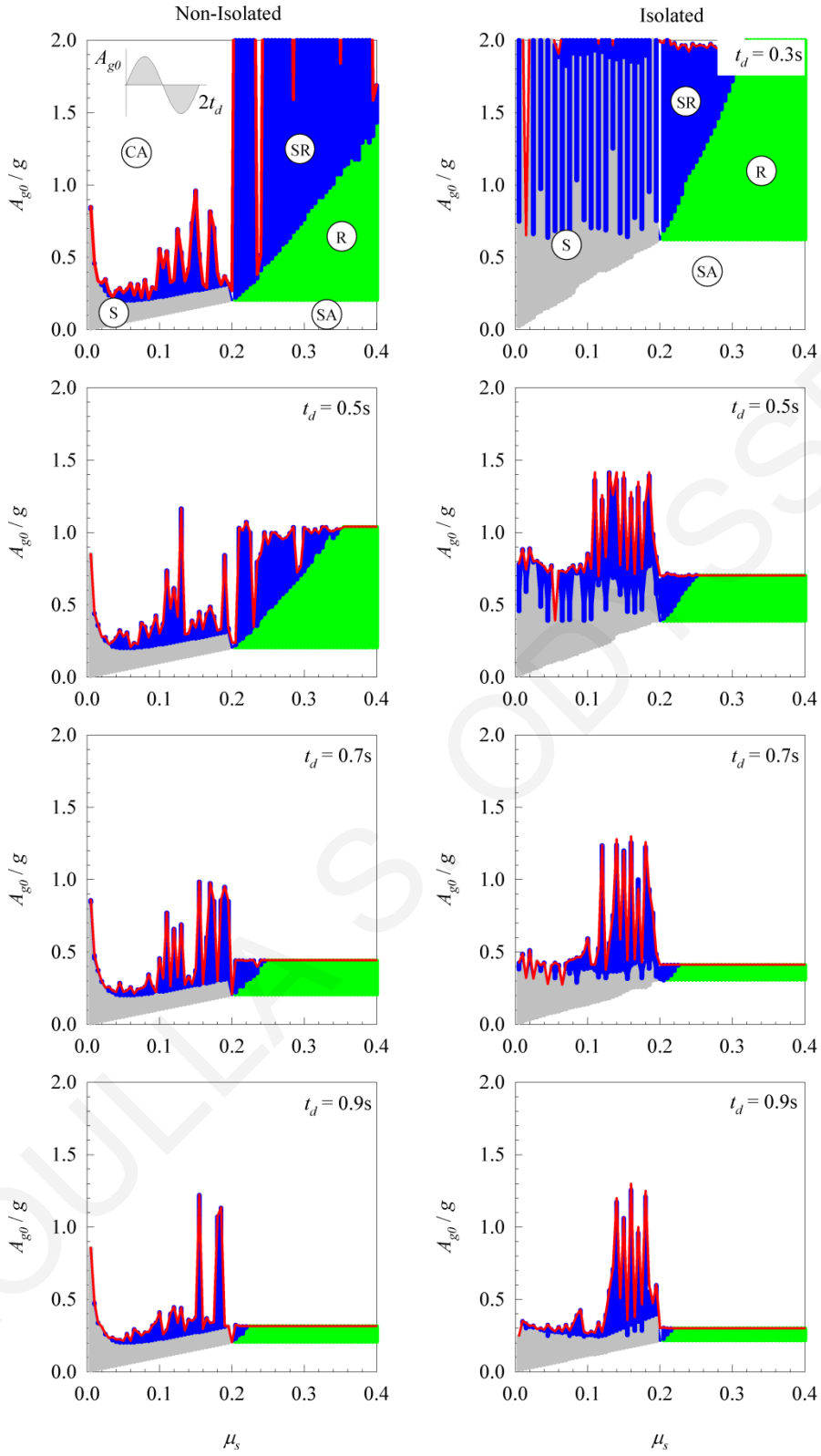

Figure 9-5: Minimum ground acceleration as a function of coefficient of static friction for simple full-sine ground-acceleration pulse ($\lambda = 5$, $R = 8\text{m}$, $\rho = 0.5$).

Figure 9-6 illustrates the influence of the linear isolation-system period, T_b, on the performance of the isolated block, for different values of the coefficient of static friction,

μ_s, for full-cycle sinusoidal pulses. As demonstrated in this figure, the minimum ground acceleration, for all areas, increases with increasing isolation-system period and the safe area is extended. Nevertheless, as shown in Figure 8-13 (Section 8.2), the values of isolation system parameters (ξ_b, T_b) have a significant influence on the response of the system.

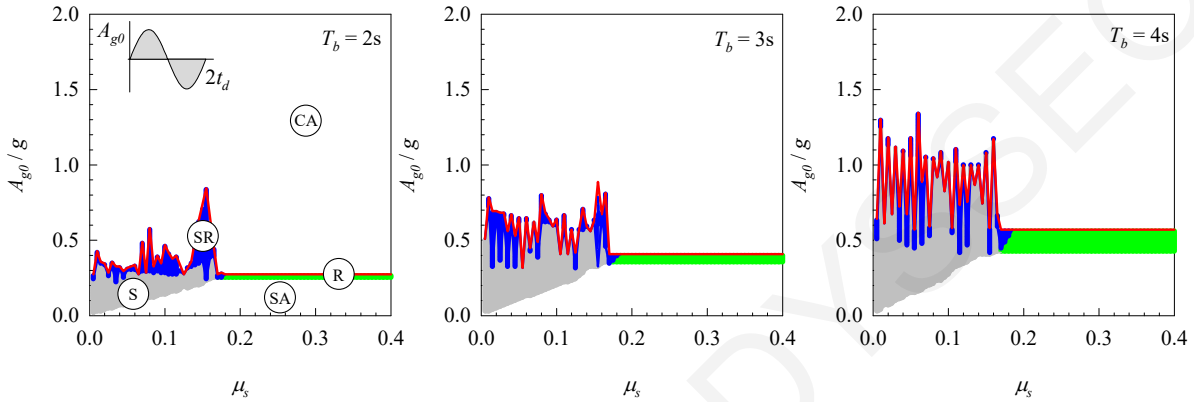

Figure 9-6: Minimum ground acceleration as a function of isolation-system period and coefficient of static friction for full-cycle sinusoidal pulse ($\lambda = 6$, $R = 2$m, $\rho = 0.5$, $t_d = 0.5$s, $\xi_b = 0.35$).

Figure 9-7 presents response-regime spectra in the $\lambda - R$ space for non-isolated and isolated blocks of varying geometric characteristics, for full-cycle pulses with duration $t_d = 0.2$s and 0.5s. These spectra depict in a clear way the distinct regimes of block response, with the cyan area indicating "No Uplift/No Sliding", the grey area "Pure Sliding", the green area "Pure Rocking", the blue area "Slide-rocking" and the red area "Overturning" of the block. In these figures, the analysis is concentrated in the case where the coefficient of static friction, μ_s, it equal to 0.20. As illustrated in Figure 9-7, the use of isolation for pulse duration $t_d = 0.2$s prevents the occurrence of sliding motions and the response-regime spectrum is the same as that of the pure-rocking block. For pulse duration $t_d = 0.5$s, it is observed that for isolated rigid blocks with slenderness ratio $\lambda < 1/\mu_s$, pure sliding motion is more intensive regardless of block size R. In contrast, rocking motions predominates for $\lambda > 1/\mu_s$ and the effect of isolation system is not beneficial to the dynamic response of the system.

By and large, the use of isolation results in better system performance, with respect to overturning and initiation of rocking and slide-rocking, for short-period pulses. On the contrary, for long period pulses, the response does not adhere to an observable trend,

regarding the stability of the system, inasmuch as there exist combinations of (λ, R) values for which the isolation is either effective or ineffective.

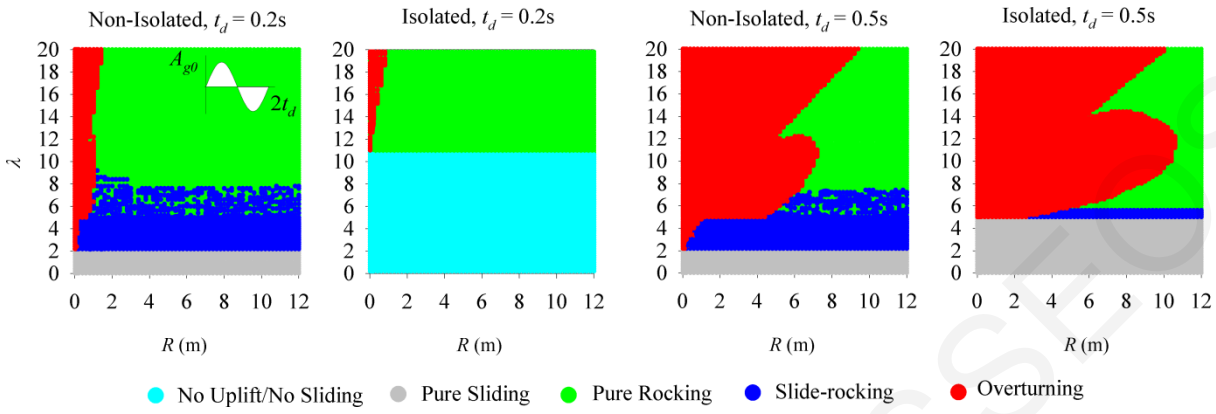

Figure 9-7: Response-regime spectra in the $\lambda - R$ space for non-isolated and isolated block of varying geometric characteristics for full-sine ground-acceleration pulses with $t_d = 0.2$s (left) and $t_d = 0.5$s (right) ($A_{g0} = 0.5g$, $\rho = 0.5$, $\mu_s = 0.2$, $T_b = 3$s, $\xi_b = 0.35$).

Figure 9-8 presents the response-regime spectra in the $\lambda - R$ space for non-isolated and isolated blocks of varying geometric characteristics, for full-cycle pulse with duration $t_d = 0.5$s using different values of the coefficient of friction μ_s. It is observed that for small values of the coefficient of friction, the sliding motions are dominating, while as the coefficient of friction increases the rocking motions predominate. In addition, an isolated block with $\lambda < 1/\mu_s$ has better performance with respect to the initiation of rocking, slide-rocking and overturning of the block, in comparison with the non-isolated block. Pure sliding is suppressed for blocks with $\lambda > 1/\mu_s$ and slide-rocking and pure rocking motions occur. The coefficient of static friction appears to improve the stability of the system. Note that a wrong estimation of the value of the coefficient of friction may result in a conservative and incorrect solution.

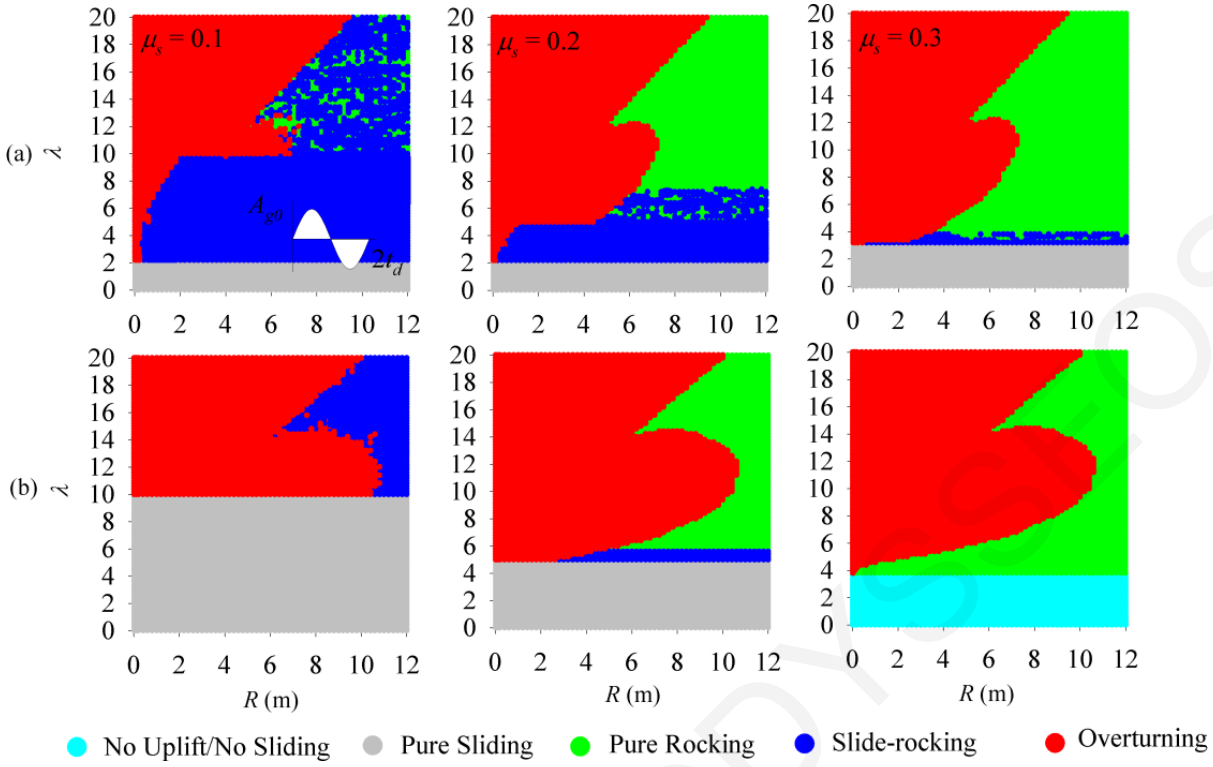

Figure 9-8: Response-regime spectra in the $\lambda - R$ space for (a) non-isolated and (b) isolated block of varying geometric characteristics for full-sine ground-acceleration pulses with $t_d = 0.5\text{s}$ for different coefficients of static friction ($A_{g0} = 0.5g$, $\rho = 0.5$, $T_b = 3\text{s}$, $\xi_b = 0.35$).

Figures 9-9 and 9-10 present time histories of the dynamic response of isolated and non-isolated rigid blocks under full-sine pulses. The general dynamic response is calculated for specific geometric characteristics of the block and using a linear isolation system with $T_b = 3\text{s}$ and $\xi_b = 0.35$. The plots illustrate the ground acceleration, $\ddot{x}_g$, the horizontal displacement and velocity of the isolation system, u and $\dot{u}$, the normalized angular displacement, θ/α, (with the overturning of the block indicated when $\theta/\alpha \geq 1$), the angular velocity of the block, $\dot{\theta}$ and the horizontal displacement and velocity of the block due to sliding, x_s and $\dot{x}_s$. Note that the block enters a slide-rocking regime when sliding and pivoting on its edges at the same time.

Figure 9-9 shows the response of a rigid block with size-parameter $R = 4\text{m}$, slenderness ratio $\lambda = 4$, mass ratio $\rho = 0.5$ and coefficient of friction between the block and the base $\mu_s = 0.2$ under short-period pulse, $t_d = 0.2\text{s}$ with a peak amplitude of 0.5g. The isolated block oscillates only with system-translation regime. The maximum horizontal displacement is approximately 100mm and the permanent displacement 50mm. In contrast,

the non-isolated block oscillates in the slide-rocking regime which leads to several impact events between the block and the supporting base and permanent displacement due to sliding $x_s = 40\text{mm}$. It appears that, the sliding between the block and the base prevented the initiation of rocking for a small duration of time.

Figure 9-10 depicts response histories of a system with the same characteristics under a long-period pulse $t_d = 0.5\text{s}$. The isolated block oscillates in the system-translation and sliding regimes. The isolated block translates horizontally with the isolation system approximately 350mm. In contrast, the non-isolated block oscillates in the sliding and slide-rocking regimes. Finally, both blocks (non-isolated/isolated) have a permanent displacement due to sliding. The non-isolated block has $x_s = 305\text{mm}$ and the isolated block $x_s = 125\text{mm}$. Note that non-isolated block faced impact event several times during rocking motion.

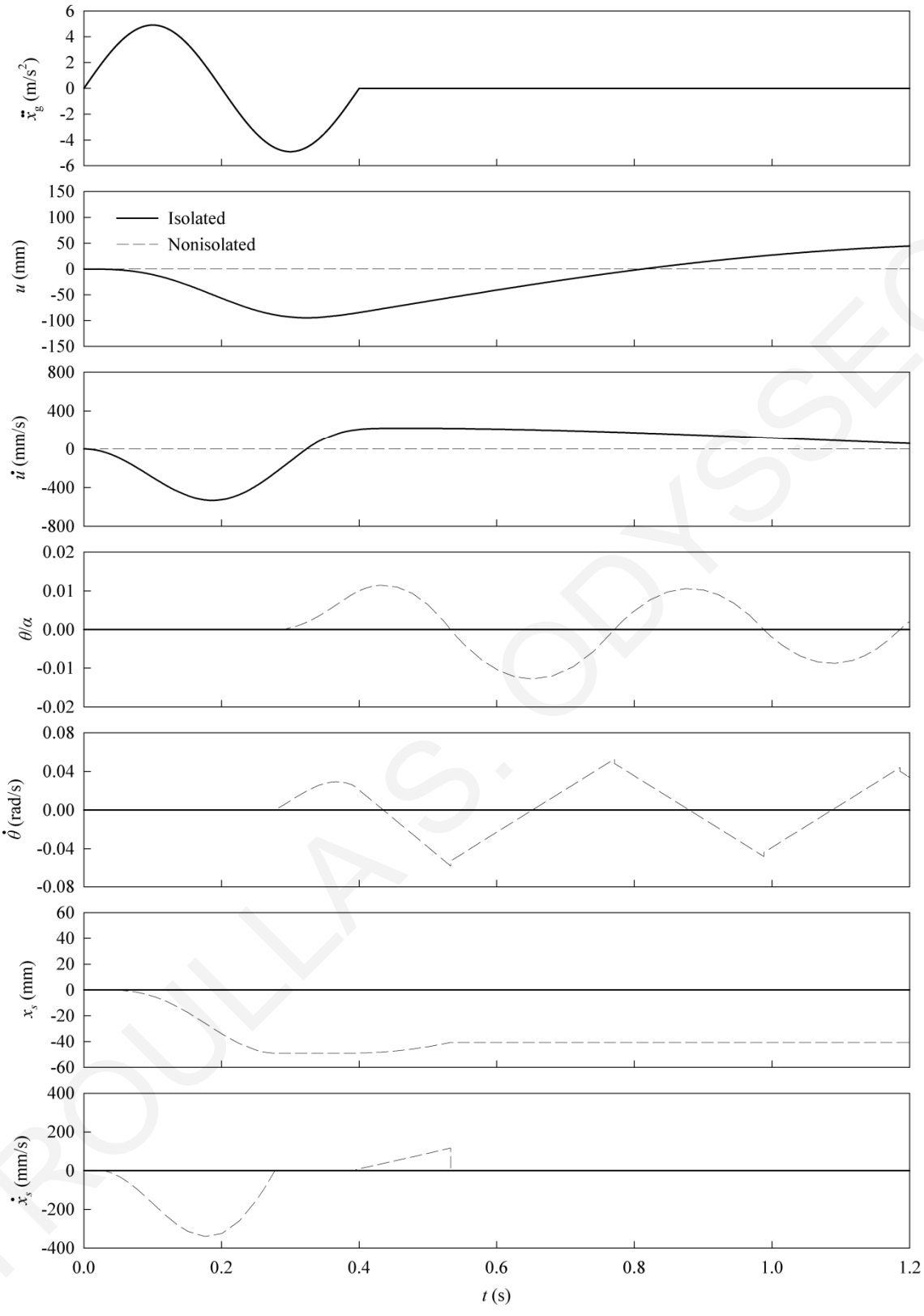

Figure 9-9: Response histories for non-isolated and isolated rigid block under full-sine pulse with $A_{g0} = 0.5g$ and $t_d = 0.2$s ($\lambda = 4$, $R = 4$m, $\mu_s = 0.2$, $\rho = 0.5$).

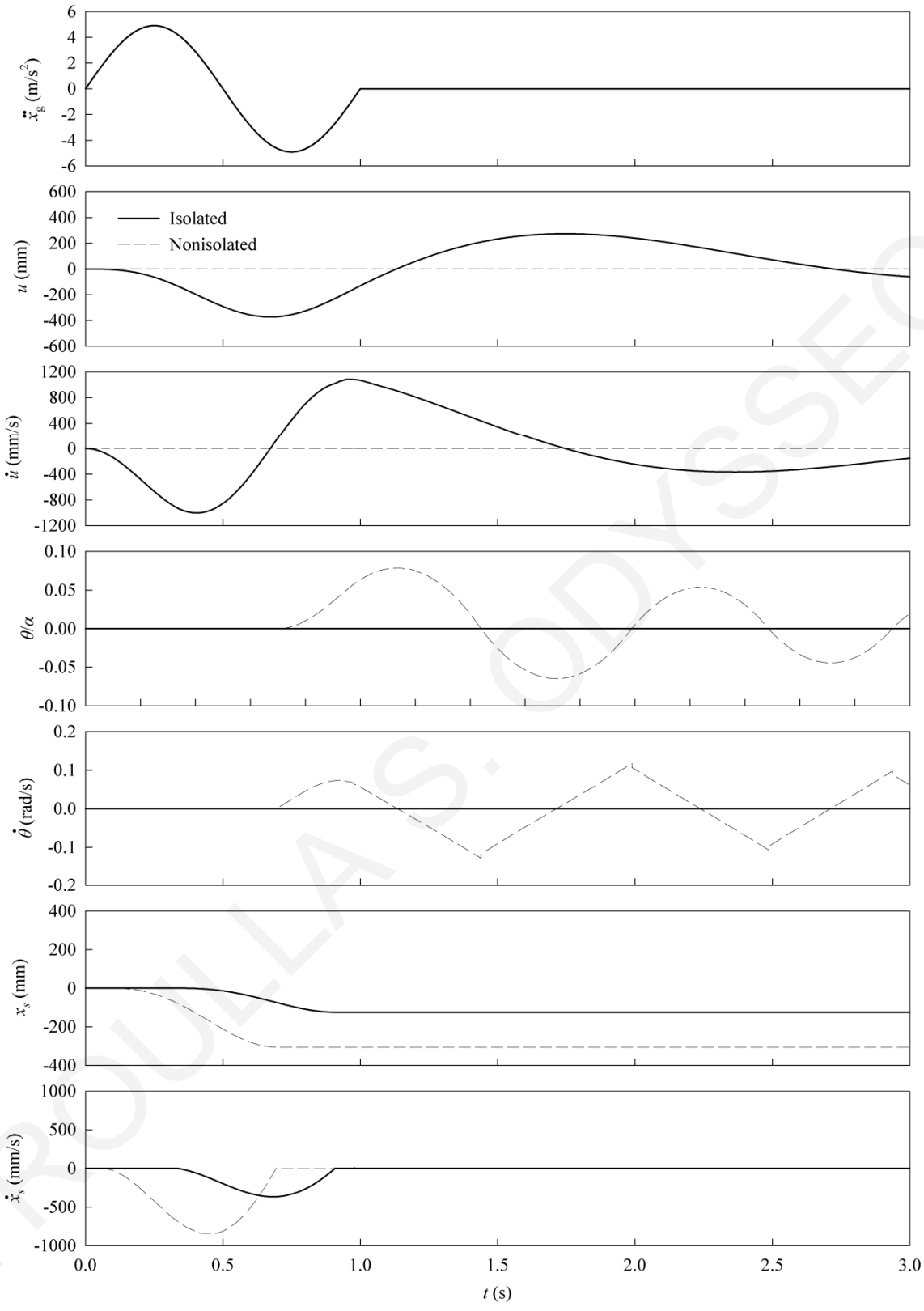

Figure 9-10: Response histories for non-isolated and isolated rigid block under full-sine pulse with $A_{g0} = 0.5g$ and $t_d = 0.5\text{s}$ ($\lambda = 4$, $R = 4\text{m}$, $\mu_s = 0.2$, $\rho = 0.5$).

9.2 Response to Earthquake Motions

In this section, the general-planar motion dynamic response of the isolated and non-isolated rigid block is calculated using near-fault seismic ground motions. Near- fault ground motions are typically characterized by intense velocity and displacement pulses of relatively long period that clearly distinguish them from typical far-field ground motions. Table 8-1 lists the characteristics of the motions used for the dynamic analysis.

Representative results are shown in Figure 9-11 for SN component of 1977 Bucharest, Romania earthquake, SN component of 1979 Imperial Valley E05, California, USA earthquake and SN component of 1966 Parkfield C02, California, USA earthquake. This figure plots the minimum acceleration amplitude required for the system to enter into different oscillation regimes, as a function of the static-friction coefficient. The isolation-system parameters used in the analysis are: elastic stiffness $k_b = 40\text{kN/m}$, period $T_b = 3\text{s}$, and damping ratio $\xi_b = 0.35$. Each figure is divided into five areas: (a) S: pure sliding occurs (grey area), (b) R: pure rocking occurs (green area), (c) SR: slide-rocking occurs (blue area), (d) SA: safe area and (e) CA: critical area. It is worth mentioning that pure sliding or pure rocking may have preceded the slide-rocking motion. The safe area indicates that the system is at rest (non-isolated) or in system translation regime (isolated). The critical area corresponds to system failure through overturning of the block ($\theta / \alpha \geq 1$).

Figure 9-11 reveals that, for a system with geometric characteristics $\lambda = 5$, $R = 2\text{m}$, and $\rho = 0.5$, the use of isolation results in improved performance in comparison with non-isolated block. The minimum ground acceleration required to initiate sliding or rocking is larger in the case of the isolated block. As a result, the safe area is extended in comparison to the non-isolated block. In addition, overturning (boundary of critical area) is associated with larger ground accelerations for the isolated block. As expected, sliding motions are dominating for small values of the coefficient of static friction, while rocking motion predominates for higher values of the static-friction coefficient. It is also observed that, for small values of the coefficient of friction the minimum overturning ground acceleration is noticeably greater than that for large values of friction. Evidently, the value of the coefficient of friction has a significant impact on the performance of the isolated block. Using a small for the coefficient of friction, the initiation of slide-rocking regime and the overturning of the block occur at larger values of ground acceleration.

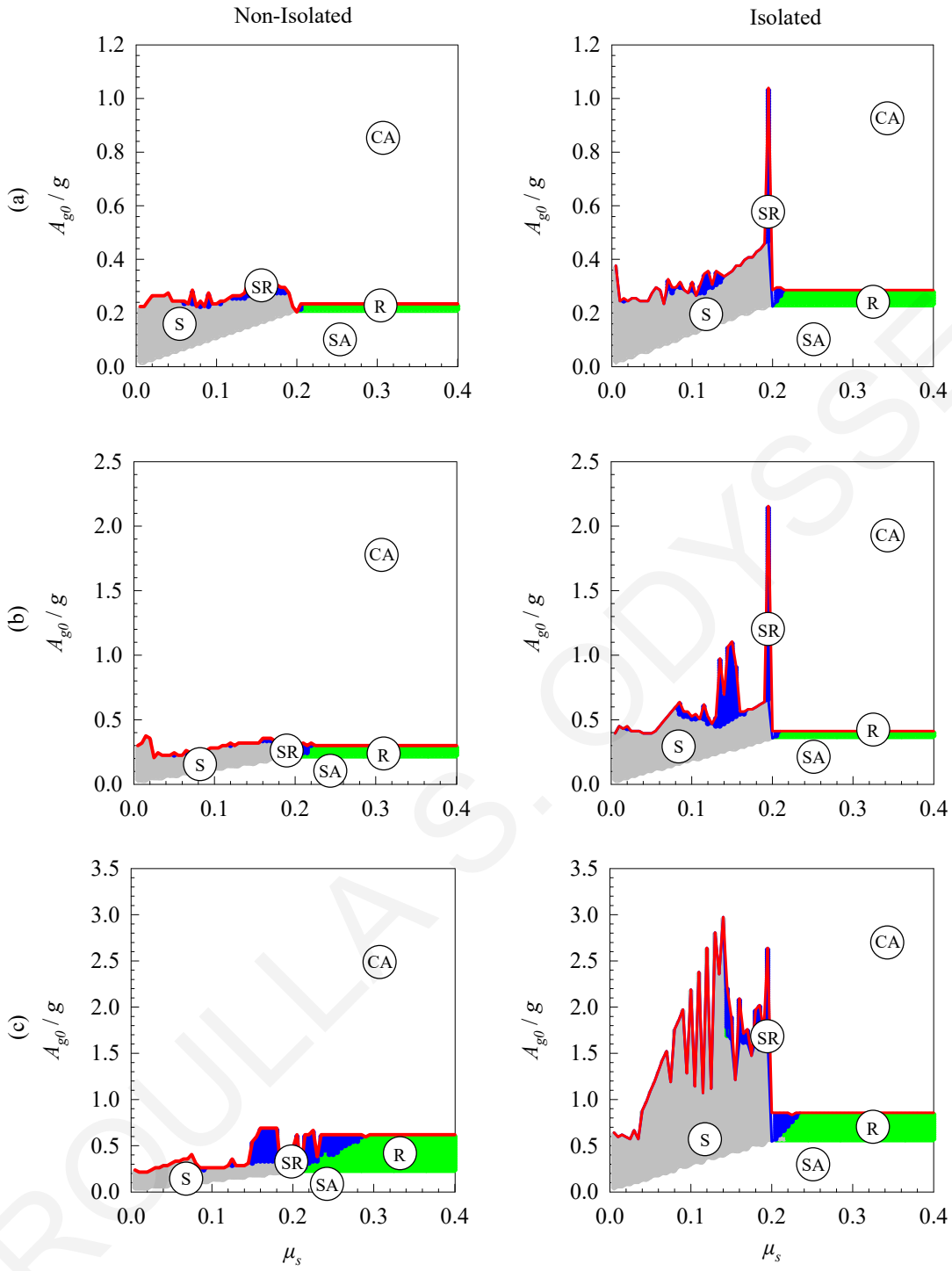

Figure 9-11: Minimum ground-acceleration amplitude required for the system to enter into different oscillation regimes under (a) SN component of 1977 Bucharest, Romania earthquake, (b) SN component of 1979 Imperial Valley E05, California, USA earthquake and (c) SN component of 1966 Parkfield C02, California, USA earthquake ($\lambda = 5$, $R = 2\text{m}$, $\rho = 0.5$).

Figure 9-12 illustrates the influence of isolation-system period, T_b, on the stability of the

isolated block, for different values of the coefficient of static friction, μ_s, for near-fault ground motions. The minimum ground acceleration needed to initiate each motion is extended to larger values with increasing isolation-system period. In addition, overturning (boundary of critical area) is associated with larger ground accelerations. A similar observation has been made for the analysis with simple full-cycle acceleration pulses, Figure 9-6.

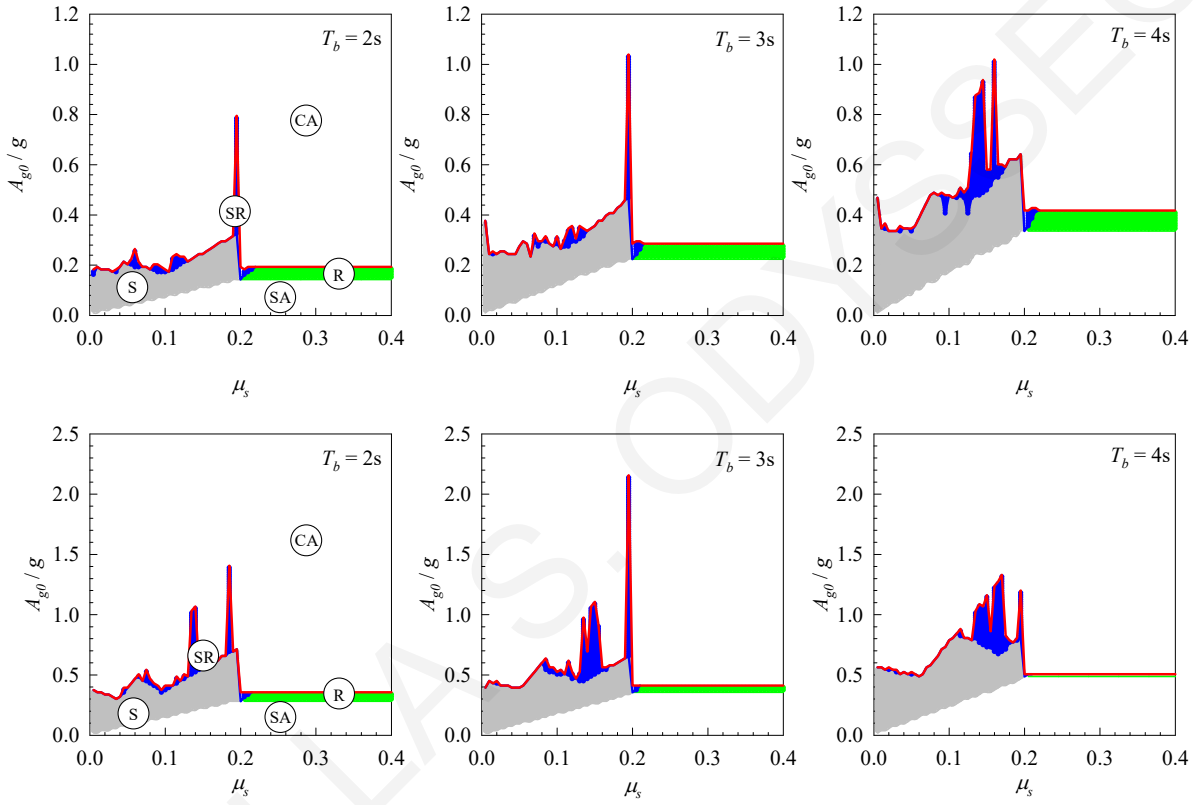

Figure 9-12: Minimum ground acceleration as a function of isolation-system period and coefficient of static friction under the SN component of 1977 Bucharest, Romania earthquake (top) and the SN component of 1979 Imperial Valley E05, California, USA earthquake (bottom) ($\lambda = 5$, $R = 2$m, $\rho = 0.5$).

Figures 9-13 and 9-14 present response-regime spectra in the $\lambda - R$ space for non-isolated and isolated blocks of varying geometric characteristics, for near-fault ground motions using different values of the coefficient of friction μ_s. As expected, for small values of the coefficient of friction, the sliding motions are dominating and as the coefficient of friction increases the sliding motions are suppressed and the rocking motions occur. The investigation has shown that an isolated block with $\lambda < 1/\mu_s$ eliminates the possibility of failure in comparison with the non-isolated block. The initiation of rocking motion and

potential overturning of the block appear in blocks with $\lambda > 1/\mu_s$. Based on this observation, knowing the value of the coefficient of friction and the slenderness ratio of the rigid block, a proper estimation of the effectiveness of isolation can be carried out. Note that a wrong estimation of the value of the coefficient of friction may result in a conservative and incorrect solution. Similar observations have been made for the analysis with simple full-cycle acceleration pulses, Figure 9-8. Appendix D contains comparisons of experimental and analytical results for non-isolated and isolated rigid blocks through response-regime spectra in $\lambda - R$ space. A representative sample of results from Appendix D is presented in Figures 9-13 and 9-14.

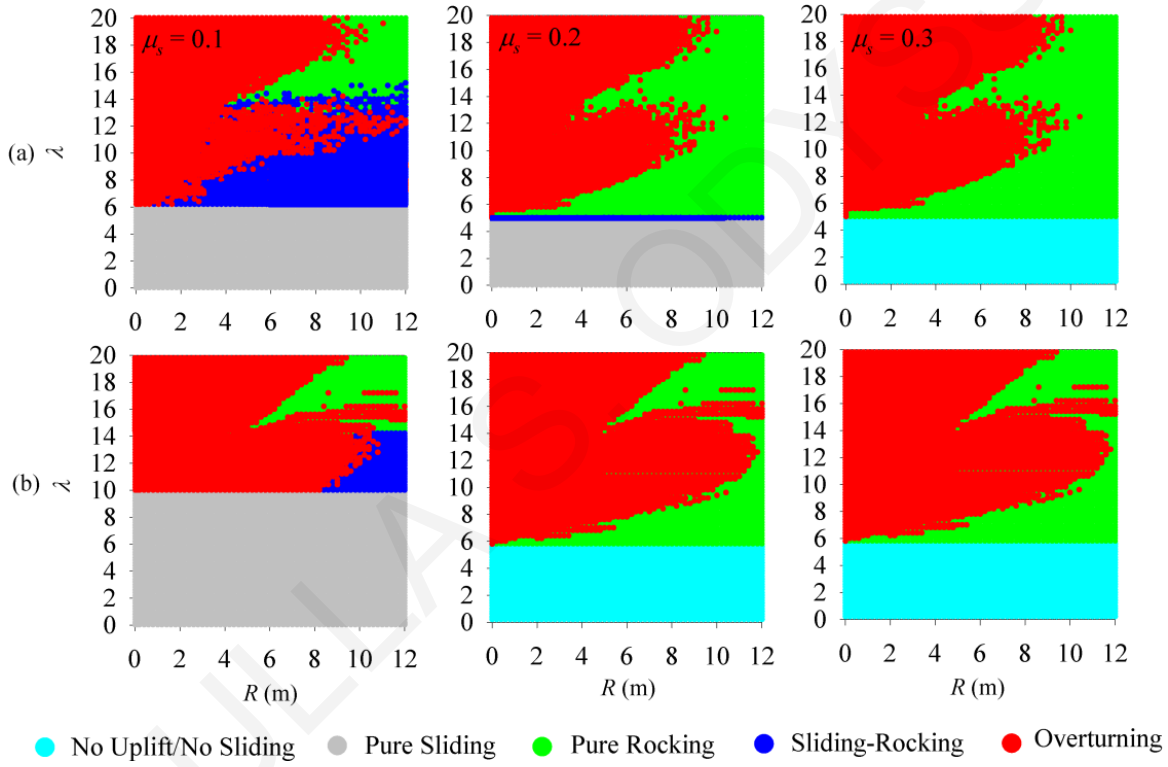

Figure 9-13: Response-regime spectra in the $\lambda - R$ space for (a) non-isolated and (b) isolated block of varying geometric characteristics under the SN component of 1977 Bucharest, Romania earthquake for different coefficients of static friction ($\rho = 0.5$, $T_b = 3\text{s}$, $\xi_b = 0.35$).

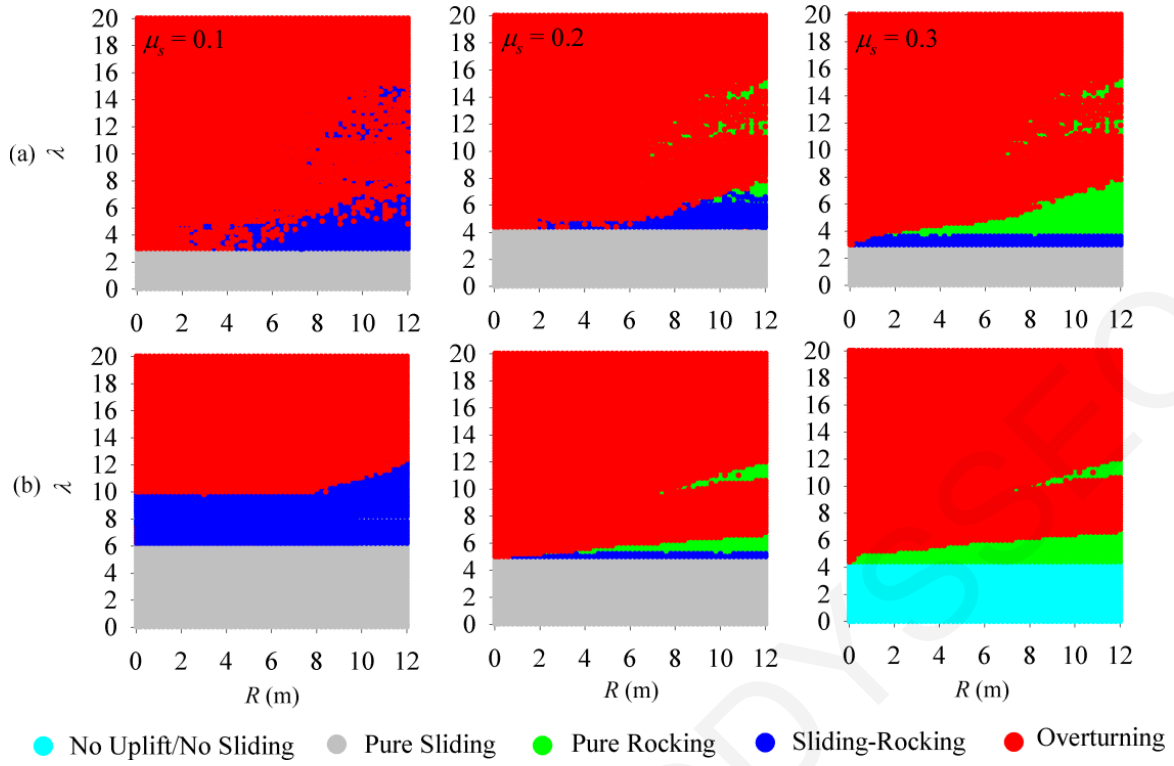

Figure 9-14: Response-regime spectra in the $\lambda - R$ space for (a) non-isolated and (b) isolated block of varying geometric characteristics under the SN component of 1979 Imperial Valley E05, California, USA earthquake for different coefficients of static friction ($\rho = 0.5$, $T_b = 3\text{s}$, $\xi_b = 0.35$).

Figures 9-15 and 9-16 depict response-regime spectra in the $\lambda - R$ space for a wide range of rigid blocks under recorded near-fault ground motions using a bilinear hysteretic model with parameters $\mu_b = 0.11$ and $R_b = 2.24\text{s}$ (corresponding to $T_b = 3\text{s}$), and a viscoelastic model with $T_b = 3\text{s}$ and $\xi_b = 0.35$. Two different values of coefficient of static friction, μ_s, are considered in the analysis 0.2 and 0.3. As can be seen from these figures, the dynamic response of the system is comparable using either small or large values of the coefficient of static friction between the block and the base, with the initiation of slide-rocking, rocking and overturning of the block are not drastically affected. In particular, for small value of the coefficient of static friction and slenderness ratio $\lambda < 1/\mu_s$, both systems oscillate in the pure sliding regime. As the slenderness ratio increases, both systems oscillate in the slide-rocking and pure rocking regimes which may result in overturning failure. For large values of the coefficient of friction, sliding motions are suppressed and rocking motions predominate. Appendix E contains comparisons of experimental and analytical results for isolated rigid blocks using linear and nonlinear isolation system through response-regime

spectra in the $\lambda - R$ space. A representative sample of results from Appendix E is presented in Figures 9-15 and 9-16.

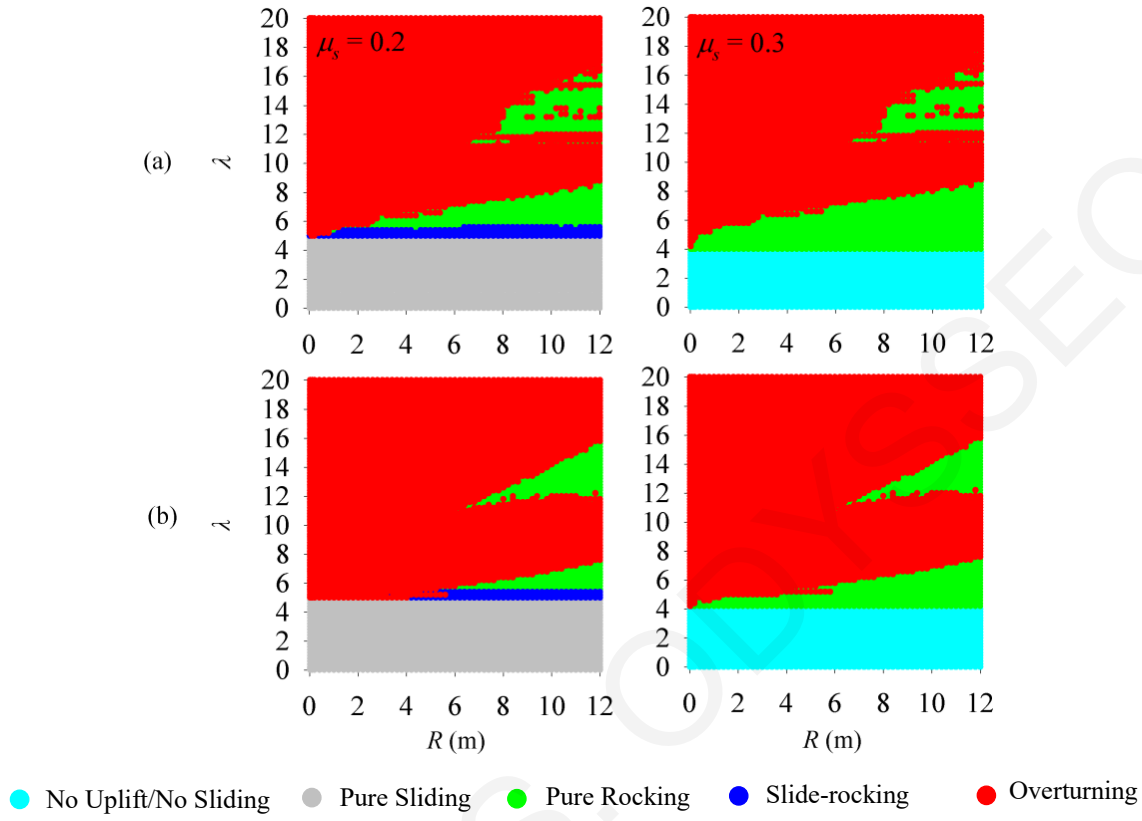

Figure 9-15: Response-regime spectra in the $\lambda - R$ space for isolated rigid block of varying geometric characteristics using (a) Nonlinear I.S. and (b) Linear I.S under the SN component of 1979 Imperial Valley, CA, USA earthquake (EMO station) for different coefficients of static friction ($\rho = 0.5$, $\mu_b = 0.11$, $R_b = 2.24\text{m}$, $T_b = 3\text{s}$).

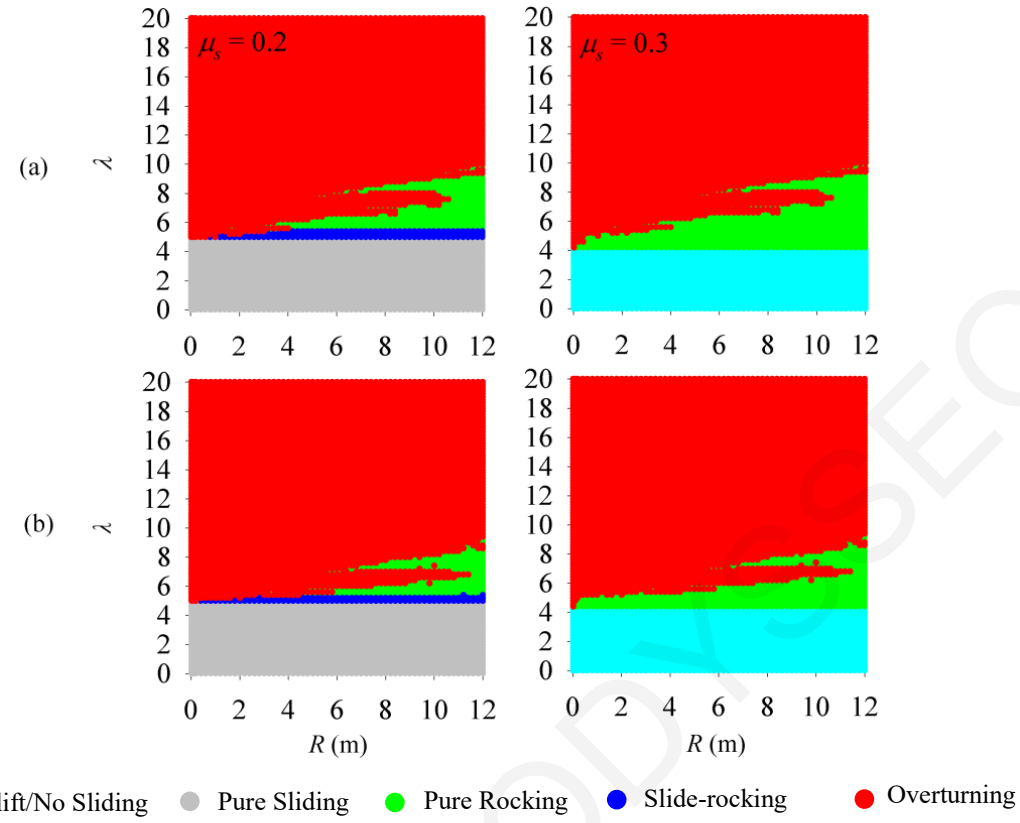

Figure 9-16: Response-regime spectra in the $\lambda - R$ space for isolated rigid block of varying geometric characteristics using (a) Nonlinear I.S. and (b) Linear I.S under the SN component of 1994 Northridge JFA, CA, USA earthquake for different coefficients of static friction ($\rho = 0.5$).

Figures 9-17 through 9-19 present time histories of the dynamic response of the isolated and non-isolated rigid blocks under horizontal ground excitations. The general dynamic response is calculated for specific geometric characteristics of the block and using a linear isolation system with $T_b = 3\text{s}$ and $\xi_b = 0.35$. The plots illustrate the ground acceleration, $\ddot{x}_g$, the horizontal displacement and velocity of the isolation system, u and $\dot{u}$, the normalized angular displacement, θ/α, (with the overturning of the block indicated when $\theta/\alpha \geq 1$), the angular velocity of the block, $\dot{\theta}$ and the horizontal displacement and velocity of the block due to sliding, x_s and $\dot{x}_s$. Note that the block enters slide-rocking regime when sliding and pivoting on its edges at the same time.

Figure 9-17 shows the response of a block with size-parameter $R = 11\text{m}$, slenderness ratio $\lambda = 11$, mass ratio $\rho = 0.5$, and coefficient of friction between the block and the base $\mu_s = 0.1$ under the SN component of 1977 Bucharest, Romania earthquake. The non-isolated block oscillates in the rocking and slide-rocking regimes. In contrast, the isolated

block oscillates in the system translation and rocking regimes. The maximum horizontal displacement due to system translation is approximately 250mm. For this case, the system-translation regime prevents sliding of the block on the rigid base. Neither of the blocks (non-isolated/isolated) overturn, yet the non-isolated block has a small permanent displacement due to sliding $x_s \approx 6\text{mm}$.

Figure 9-18 plots the response of a system with $R = 2\text{m}$, $\lambda = 12$, $\rho = 0.5$, and $\mu_s = 0.1$ under the SN component of 1977 Bucharest, Romania earthquake. The block gets though slide-rocking motion and finally overturns. It appears that, the system-translation response caused a small delay to the overturning of the block, in comparison with the non-isolated case. The displacement attained due to sliding is very small for both systems.

Figure 9-19 depicts response histories of a system with $R = 4\text{m}$, $\lambda = 8$, $\rho = 0.5$, and $\mu_s = 0.2$, under the SN component of 1979 Imperial Valley E05 earthquake. The block oscillates in the rocking motion and finally overturns. It is possible that the system-translation response delayed the initiation of rocking in comparison with the non-isolated system.

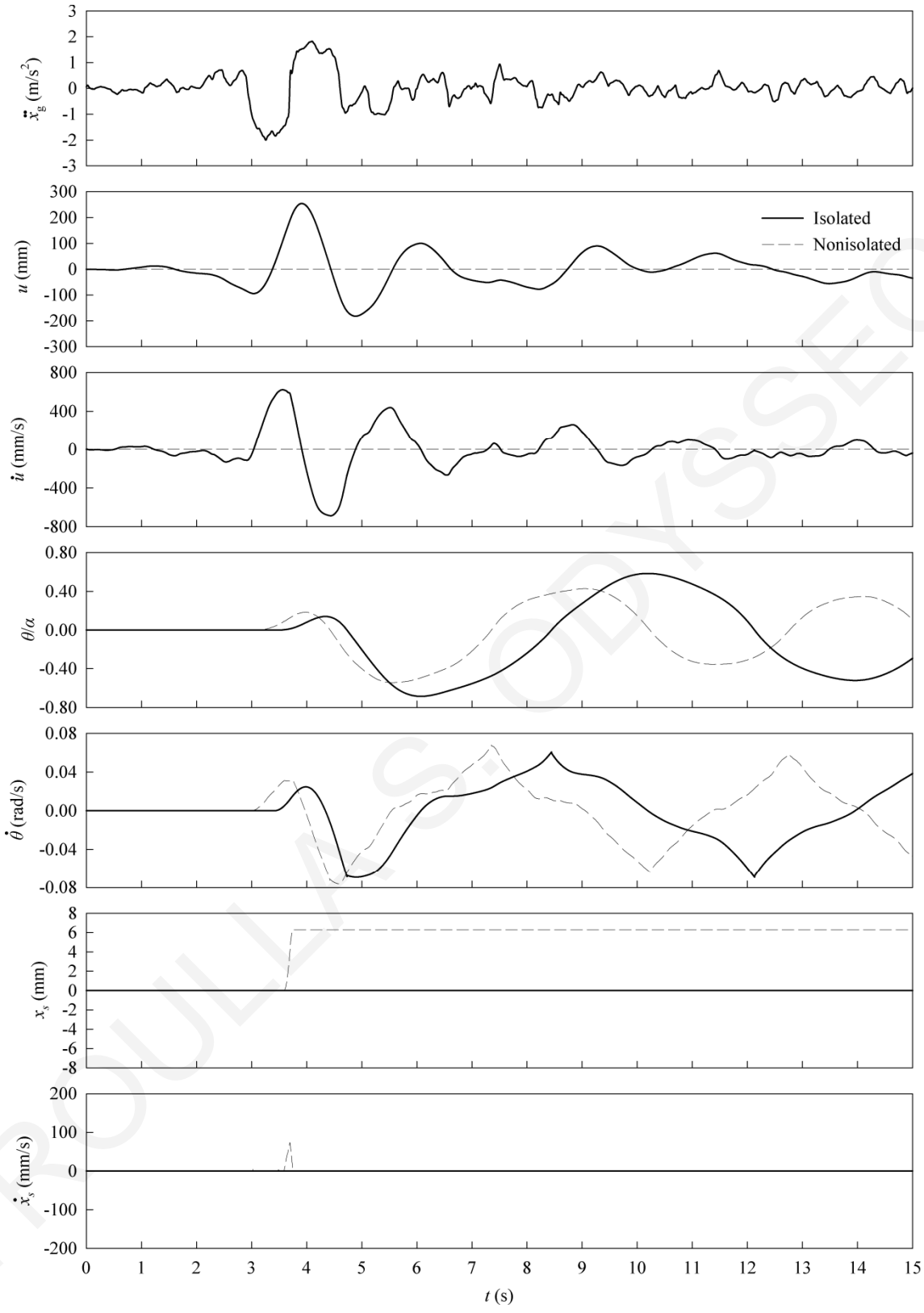

Figure 9-17: Response histories for non-isolated and isolated rigid block under the SN component of 1977 Bucharest, Romania earthquake ($\lambda = 11$, $R = 11\text{m}$, $\mu_s = 0.1$, $\rho = 0.5$).

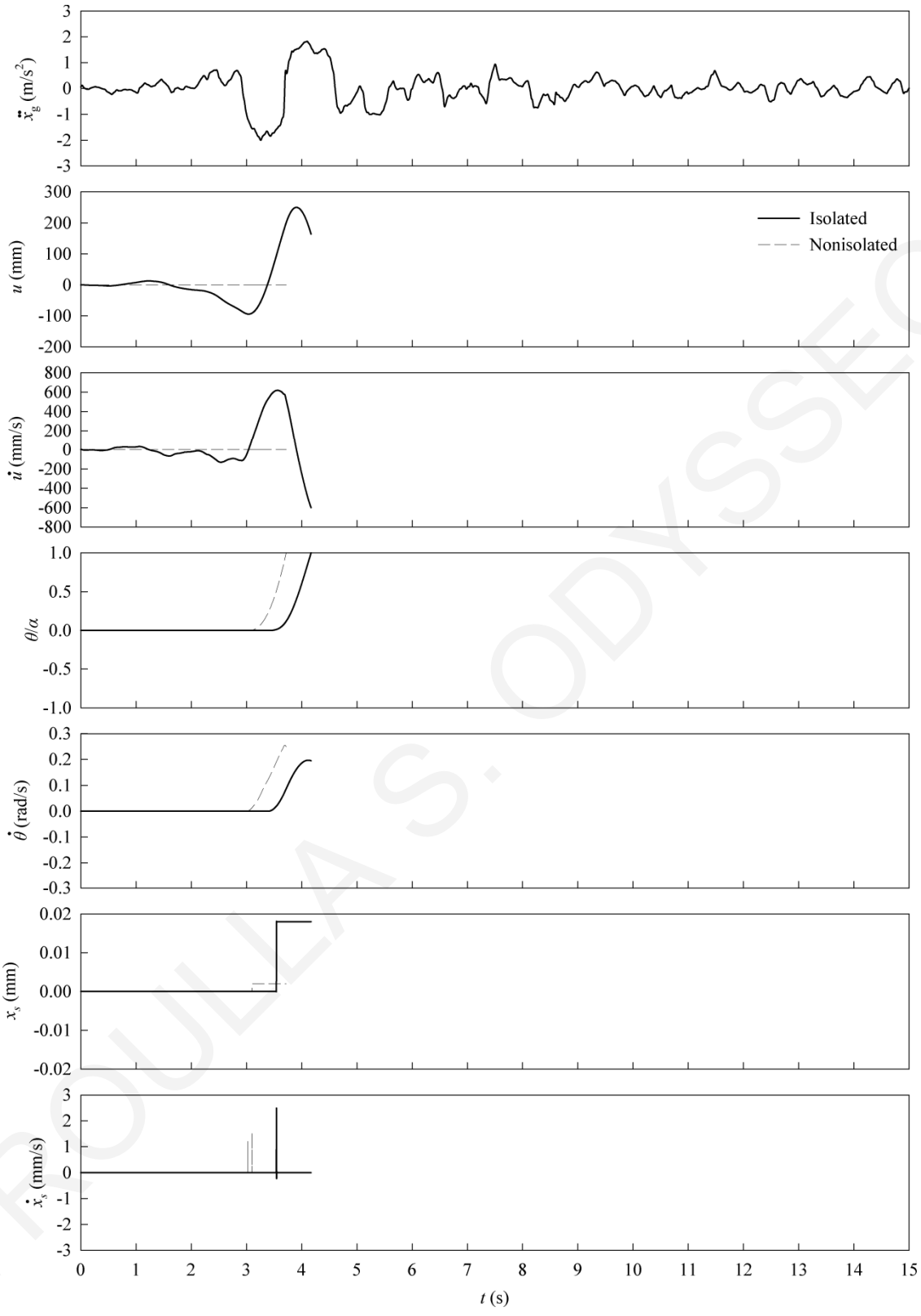

Figure 9-18: Response histories for non-isolated and isolated rigid block under the SN component of 1977 Bucharest, Romania earthquake ($\lambda = 12$, $R = 2\text{m}$, $\mu_s = 0.1$, $\rho = 0.5$).

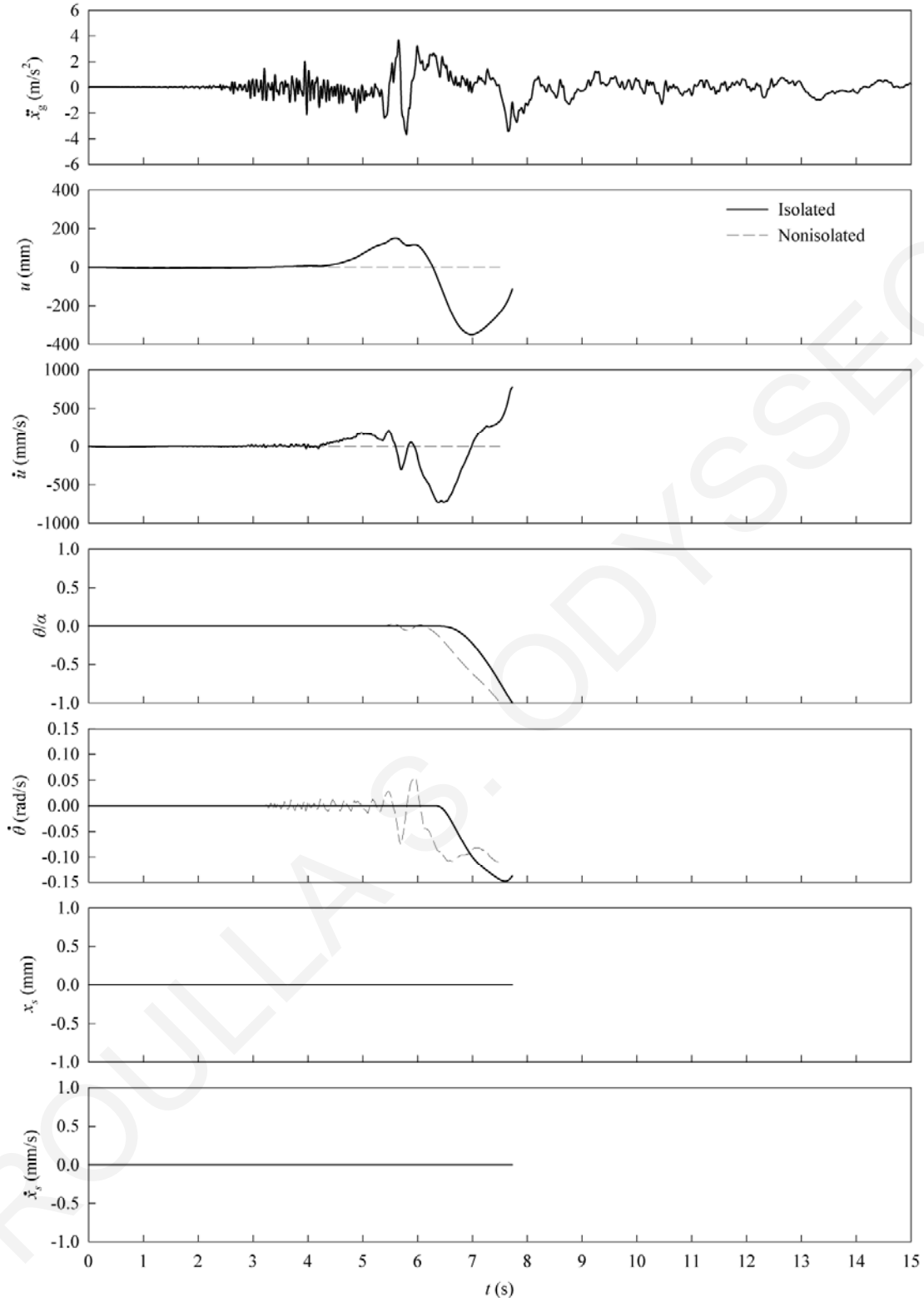

Figure 9-19: Response histories for non-isolated and isolated rigid block under the SN component of 1977 Bucharest, Romania earthquake ($\lambda = 8$, $R = 4\text{m}$, $\mu_s = 0.2$, $\rho = 0.5$).

CHAPTER 10
Conclusions

10.1 Summary and Conclusions

Most seismic design codes permit heavy damages to buildings in case of large earthquakes, provided that the building is protected against collapse. Conventional seismic design practice ties buildings rigidly to their foundations and makes them strong enough to resist forces produced by earthquakes. But experience has revealed that this approach generates large forces in structures during a seismic event. Even if the structural system survives, damage to nonstructural components and contents can affect the operation of the building. Loss of function is unacceptable for high-importance individual elements, such as high-value building contents, mechanical or electrical equipment, computer servers, and irreplaceable museum artifacts.

To minimize these large earthquake forces, seismic engineers have been using a new technology over the last three decades as a practical method of protecting buildings from earthquake shaking, known as base or seismic isolation. In contrast with the conventional design, seismic isolators decouple the structure from the foundation while permitting large horizontal displacements. In effect, seismic isolation lengthens the natural period of a structure away from the predominant frequency of the ground motion. The effectiveness of base-isolation technology in safeguarding engineering structures paved the way for extending the concept to individual elements of high-importance. The aforementioned elements often exhibit rigid-body behavior under seismic excitation, and their study should be performed within the context of rigid-body dynamics.

This dissertation concentrates on the general multi-pattern dynamic response of base-isolated rigid blocks subjected to ground excitation, through the development of a comprehensive mathematical formulation, including a rigorous model governing impact. The study examines in depth the motion of the system with a large-displacement formulation that combines the exact (nonlinear) equations of motion together with a rigorous model governing impact. The system considered consists of a symmetric rigid block standing free on a seismically isolated rigid base. The response of the system is described in terms of four oscillation regimes: system translation, in which the base-block system translates as a whole (one-degree-of-freedom response); sliding, in which the block slides relative to the horizontally-moving base (two-degree-of-freedom response); rocking,

in which the block pivots on its edges with respect to the horizontally-moving base (two-degree-of-freedom response); and slide-rocking, in which the block simultaneously slides and pivots on its edges with respect to the horizontally-moving base (three-degree-of-freedom response). Two models for the isolation system are considered, a linear model with viscoelastic behavior and a nonlinear model with bilinear hysteretic behavior. The governing equations of motion are obtained for each oscillation regime using the Lagrange method. The mathematical treatment of the problem is broad in scope in that it is neither restricted to small rotations nor slender blocks.

The mathematical description of the system dynamics is profoundly complex primarily due to the inherent nonlinear nature of the impact phenomenon and the potential (alternating) transition from one oscillation pattern to another, each one governed by a different set of differential equations. A rigorous mathematical model governing impact from rocking and slide-rocking regimes has been formulated using classical impact theory. The model assumes point-impact, perfectly-inelastic impact (i.e. zero coefficient of restitution), and impulses forces acting only at the impacting corner (i.e. impulses at the rotating corner are small compared to those at the impacting corner and are neglected).

On the basis of the proposed analytical model, a computer program has been developed to determine numerically the dynamic response of the system by considering the different possible oscillation regimes, impact occurrence(s), transition criteria, and arbitrary excitation. An extensive numerical investigation has been carried out for varying block geometric characteristics and isolation-system parameters, under idealized base-acceleration pulses and recorded pulse-type earthquake motions with a wide range of amplitude and frequency content, with the aim of identifying potential trends in the response and stability of the system.

Assuming no sliding of the block relative to the supporting base, entailing a pure rocking response, the investigation has shown that the use of isolation results in better system performance, with respect to the initiation of rocking and overturning, for short-period pulses. In particular, the use of isolation improves the stability of blocks with decreasing block size, provided that the system is not subjected to long-period acceleration pulses. On the contrary, for long-period pulses, the use of isolation is not beneficial in improving the stability of the block, in comparison with the non-isolated case. Nevertheless, in general, the use of isolation results in an increase in the acceleration required to initiate rocking in comparison with the non-isolated block, regardless of the block size and pulse-period.

In addition, this investigation has shown that the variance of the isolation-system parameters (T_b, ξ_b) has a significant impact on the effectiveness of the isolation system. The isolated block has better performance as the period of the isolation system increases. In addition, the damping ratio, ξ_b, has significant influence on the effectiveness of the isolation, with the latter reduced as the damping ratio decreases.

The response of the system has been calculated considering two seismic-isolation models, a linear model with viscoelastic behavior and a nonlinear model with bilinear hysteretic behavior. The analysis has demonstrated that the calculated responses on the basis of the two isolation-system models are in good agreement.

Furthermore, an analysis using idealized pulse-type motions instead of actual ground motions has revealed that the use of idealized pulse-type motions yields to more conservative results, regarding the initiation of rocking. On the other hand, the stability of the isolated system can be estimated relatively accurately using the idealized pulse-type motions.

Assuming sliding between the block and the supporting base, entailing a multi-pattern response, the investigation has shown that the value of the coefficient of friction between the block and the supporting base plays an important role on the performance of the isolated block. In particular, an isolated block with $\lambda < 1/\mu_s$ eliminates the possibility of failure in comparison with the non-isolated block. The initiation of rocking motion and potential overturning of the block appear in blocks with $\lambda > 1/\mu_s$. Based on this observation, knowing the value of the coefficient of friction and the slenderness ratio of the rigid block, a proper estimation of the effectiveness of isolation can be carried out. Note that a wrong estimation of the value of the coefficient of friction may result in a conservative and incorrect solution.

It is also observed that, sliding response is dominating for small values of the coefficient of static friction, while rocking motion predominates for higher values of the static-friction coefficient. For small values of the coefficient of friction, the block oscillates in the sliding regime and as the acceleration increases the system undergoes slide-rocking regime and finally overturns. As expected, the minimum ground acceleration needed to initiate sliding increases linearly with the coefficient of static friction. In addition, as the size of the block increases, the minimum ground acceleration needed to overturn the block increases.

Moreover, the analysis has shown that the use of isolation results in better system

performance, with respect to overturning and initiation of rocking and slide-rocking, for short-period pulses. On the contrary, for long period pulses, the response does not adhere to an observable trend, regarding the stability of the system, inasmuch as there exist combinations of (λ, R) values for which the isolation is either effective or ineffective.

In conclusion, the scientific contribution of this dissertation lies in (a) the development of a comprehensive mathematical formulation, including a rigorous model governing impact, for calculating the general multi-pattern dynamic response of base-isolated systems that exhibit rigid-body behavior under seismic excitation; (b) the development of a computer program to determine numerically the dynamic response of the system; (c) the undertaken of an extensive numerical investigation under idealized base-acceleration pulses and recorded pulse-type earthquake motions with the aim of identifying potential trends in the response and stability of the system.

10.2 Recommendations for Future Research

This work could be extended in a number of ways. In particular, future research could consider: (a) supporting the system on a different type of foundation; (b) investigating the response of systems consisting of multiple (stacked) rigid blocks; (c) studying the possibility of bouncing and diversifying the model governing impact (i.e. uplifting by rotating about the corner of rotation); (d) examining the effect of vertical ground excitation on the response of the system; (e) investigating the effect of a non-constant coefficient of friction between the block and the rigid base (e.g. due to temperature change); and (g) verifying the findings of this dissertation through experimental investigations.

References

Agbabian, M.S., Masri, S.F., Nigbor, R.L., and Ginell, W.S., 1988, Seismic damage mitigation concepts for art objects in museums, *Ninth World Conference on Earthquake Engineering*.

Apostolou, M., Gazetas, G., and Garini, E., 2007, Seismic response of slender rigid structures with foundation uplifting, *Soil Dynamics and Earthquake Engineering,* 27(7): 642–654.

Aslam, M., Godden, W.G., and Scalise, D.T., 1980, Earthquake rocking response of rigid bodies, *Journal of the Structural Division (ASCE),* 106(2): 377–392.

Augusti, G., Ciampoli, M., and Airoldi, L., 1992, Mitigation of seismic risk for museum contents: An introductory investigation, *Proceedings of the Tenth World Conference on Earthquake Engineering*.

Augusti, G., Ciampoli, M., and Sepe, V., 1995, Further studies on seismic behavior and risk reduction for museum contents, *Proceedings of the Tenth European Conference on Earthquake Engineering*.

Bray, J.D. and Rodriguez-Marek, A., 2004, Characterization of forward-directivity ground motions in the near-fault region, *Soil Dynamics and Earthquake Engineering,* 24(11): 815–828.

Caliò, I. and Marletta, M., 2003, Passive control of the seismic rocking response of art objects, *Engineering Structures,* 25: 1009–1018.

Caliò, I. and Marletta, M., 2004, On the mitigation of the seismic risk of art objects: Case-studies, *13th World Conference on Earthquake Engineering*.

Chatzis, M. and Smyth, A., 2012, Robust Modeling of the Rocking Problem, *Journal of Engineering Mechanics,* 138(3): 247–262.

Chopra, A.K., 2001, Dynamics of structures: Theory and applications to earthquake engineering, New Jersey.

Christopoulos, C. and Filiatrault, A., 2006, Principles of passive supplemental damping and seismic isolation, Pavia - Italy.

Constantinou, M.C., 2004, *Friction pendulum double concave bearing,* Technical Report, University at Buffalo, New York.

Constantinou, M.C., Mokha, A., and Reinhorn, A.M., 1990, Teflon bearings in base isolation II: Modeling, *Journal of Structural Engineering,* 116(2): 455–474.

Dimitrakopoulos, E. and DeJong, M., 2012, Overturning of Retrofitted Rocking Structures under Pulse-Type Excitations, *Journal of Engineering Mechanics,* 138(8): 963–972.

Di Egidio, A. and Contento, A., 2009, Base isolation of slide-rocking non-symmetric rigid blocks under impulsive and seismic excitations, *Engineering Structures,* 31: 2723–2734.

Fenz, D.M. and Constantinou, M.C., 2006, Behaviour of the double concave friction pendulum bearing, *Earthquake Engineering and Structural Dynamics,* 35: 1403–1424.

Fenz, D.M. and Constantinou, M.C., 2008a, Spherical sliding isolation bearings with adaptive behavior: Theory, *Earthquake Engineering and Structural Dynamics,* 37(2): 163–183.

Fenz, D.M. and Constantinou, M.C., 2008b, Spherical sliding isolation bearings with adaptive behavior: Experimental verification, *Earthquake Engineering and Structural Dynamics,* 37(2): 185–205.

Housner, G.W., 1963, The behavior of inverted pendulum structures during earthquakes, *GSW Bulletin of the Seismological Society of America,* 53(2): 403–417.

Al-Hussaini, T.M., Zayas, V.A., and Constantinou, M.C., 1994, *Seismic isolation of multi-story frame structures using spherical sliding isolation system,* MCEER Technical Reports.

Ishiyama, Y., 1982, Motions of rigid bodies and criteria for overturning by earthquake excitations, *Earthquake Engineering and Structural Dynamics,* 10: 635–650.

Makris, N. and Roussos, Y.S., 2000, Rocking response of rigid blocks under near-source ground motions, *Géotechnique,* 50(3): 243–262.

MathWorks, 2006, Matlab: The language of technical computing.

Mavroeidis, G.P. and Papageorgiou, A.S., 2003, A Mathematical Representation of Near-Fault Ground Motions, *Bulletin of the Seismological Society of America,* 93(3): 1099–1131.

Meirovitch, L., 2001, Fundamentals of vibrations, Boston.

Meriam, J.L. and Kraige, L.G., 2008, Engineering Mechanics: Statics, Hoboken, NJ.

Meriam, J.L. and Kraige, L.G., 2009, Engineering Mechanics: Dynamics, Hoboken, NJ.

Mokha, A.S., Constantinou, M.C., and Reinhorn, A.M., 1990, *Experimental study and analytical prediction of earthquake response of a sliding isolation system with spherical surface,* MCEER Technical Reports.

Morgan, T.A. and Mahin, S.A., 2007, Enhancing the performance of seismically isolated buildings using multi-stage friction pendulum sliding bearings, *Proceedings World Forum on Smart Materials and Smart Structures Technology.*

Morgan, T.A. and Mahin, S.A., 2008, The optimization of multi-stage friction pendulum isolators for loss mitigation considering a range of seismic hazard, *The 14th World Conference on Earthquake Engineering*.

Myslimaj, B., Gamble, S., Chin-Quee, D., Davies, A., and Breukelman, B., 2003, Base isolation technologies for seismic protection of museum artifacts, *The 2003 IAMFA Annual Conference*.

Naeim, F. and Kelly, J.M., 1999, Design of seismic isolated structures: From theory to practice, NY.

Psycharis, I.N., 1990, Dynamic behaviour of rocking two-block assemblies, *Earthquake Engineering and Structural Dynamics,* 19: 555–575.

Robinson, W.H. and Tucker, A.G., 1977, A Lead-Rubber Shear Damper, *Bulletin of the New Zealand National Society Earthquake Engineering,* 10(3): 151–153.

Robinson, W.H. and Tucker, A.G., 1983, Test results for lead-rubber bearing for the William M. Clayton Building, Toe Toe Bridge and Waiotukupuna Bridge, *Bulletin of the New Zealand National Society Earthquake Engineering,* 14(1): 21–23.

Roussis, P.C. and Constantinou, M.C., 2006, Uplift-restraining friction pendulum seismic isolation system, *Earthquake Engineering and Structural Dynamics,* 35(5): 577–593.

Roussis, P.C., Pavlou, E.A., and Pisiara, E.C., 2008, Base-isolation technology for earthquake protection of art objects, *The 14th World Conference on Earthquake Engineering*.

Shenton III, H.W. and Jones, N.P., 1991, Base excitation of rigid bodies. I: Formulation, *Journal of Engineering Mechanics (ASCE),* 117(10): 2286–2306.

Skinner, R.I., Robinson, W.H., and McVerry, G.H., 1993, An introduction to seismic isolation, NY.

Soong, T.T. and Constantinou, M.C., 1994, Passive and active structural vibration control in civil engineering, Wien.

Spanos, P.D. and Koh, A.-S., 1984, Rocking of rigid blocks due to harmonic shaking, *Journal of Engineering Mechanics (ASCE),* 110(11): 1627–1642.

Spanos, P.D., Roussis, P.C., and Politis, N.P.A., 2001, Dynamic analysis of stacked rigid blocks, *Soil Dynamics and Earthquake Engineering,* (21): 559–578.

Taniguchi, T., 2002, Non-linear response analyses of rectangular rigid bodies subjected to horizontal and vertical ground motion, *Earthquake Engineering and Structural Dynamics,* 31: 1481–1500.

Tsai, C.S., Chiang, T.C., and Chen, B.J., 2003a, Seismic behavior of MFPS isolated structure under near-fault earthquakes and strong ground motions with long predominant periods, *Proceedings, 2003 ASME Pressure Vessels and Piping Conference*, p.p. 73–79.

Tsai, C.S., Chiang, T.C., and Chen, B.J., 2003b, Shaking table tests of a full scale steel structure isolated with MFPS, *Proceedings, 2003 ASME Pressure Vessels and Piping Conference*, p.p. 41–47.

Tsai, C.S., Chiang, T.C., and Chen, B.J., 2004, Experimental study for multiple Friction Pendulum system, *13th World Conference on Earthquake Engineering*, Paper 669.

Tsai, C.S., Chiang, T.C., and Chen, B.J., 2005, Experimental evaluation of piecewise exact solution for predicting seismic responses of spherical sliding type isolated structures, *Earthquake Engineering and Structural Dynamics,* 34(9): 1027–1046.

Tsopelas, P.C., Constantinou, M.C., and Reinhorn, A.M., 1994, *3D-BASIS-ME: Computer program for nonlinear dynamic analysis of seismically isolated single and multiple structures and liquid storage tanks,* MCEER Technical Reports..

Vassiliou, M.F. and Makris, N., 2012, Analysis of the rocking response of rigid blocks standing free on a seismically isolated base, *Earthquake Engineering & Structural Dynamics,* 41(2): 177–196.

Vestroni, F. and Di Cintio, S., 2000, Base isolation for seismic protection of statues, *12th World Conference on Earthquake Engineering*.

Voyagaki, E., Psycharis, I.N., and Mylonakis, G., 2013, Rocking response and overturning criteria for free standing rigid blocks to single—lobe pulses, *Soil Dynamics and Earthquake Engineering,* 46: 85–95.

Yang, Y.B., Hung, H.-H., and He, M.-J., 2000, Sliding and rocking response of rigid blocks due to horizontal excitations, *Structural Engineering and Mechanics,* 9(1): 1–16.

Yim, C.-S., Chopra, A.K., and Penzien, J., 1980, Rocking response of rigid blocks to earthquakes, *Earthquake Engineering and Structural Dynamics,* 8(6): 565–587.

Zayas, V., Low, S., and Mahin, S., 1990, A simple pendulum technique for achieving seismic isolation, *Earthquake Spectra,* 6(2): 317–333.

Zhang, J. and Makris, N., 2001, Rocking response of free-standing blocks under cycloidal pulses, *Journal of Engineering Mechanics (ASCE),* 127(5): 473–483.

APPENDIX A

Rocking Response-Regime Spectra for Non-Isolated and Isolated Blocks Using Linear Isolation System

Assuming no sliding of the block relative to the supporting base, entailing a pure rocking response, this appendix presents a numerous response-regime spectra in the $\lambda - R$ space for a class of non-isolated and isolated rigid blocks under near-fault ground motions.

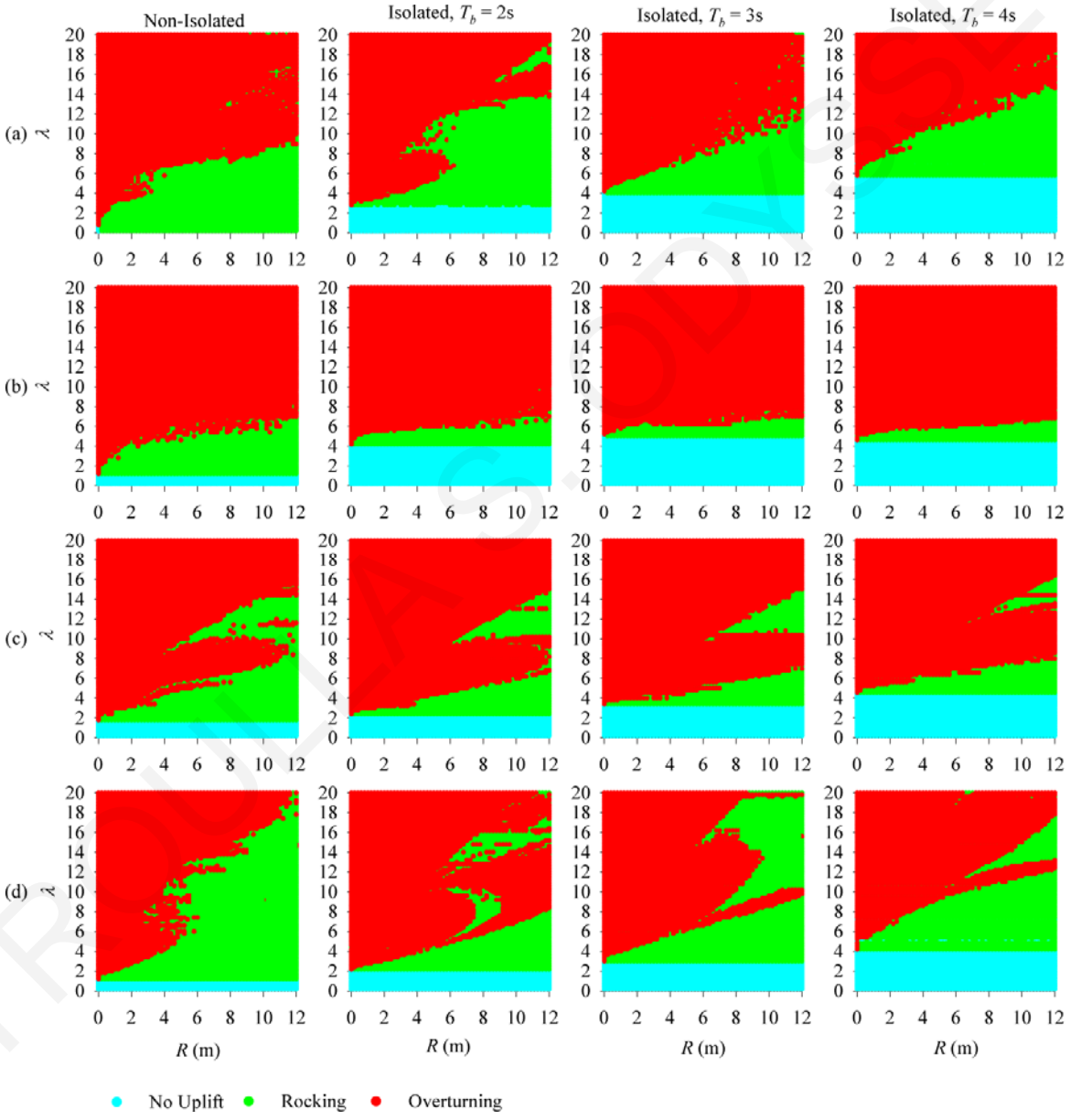

Figure A-1: Response-regime spectra in the $\lambda - R$ space for a non-isolated and isolated block of varying geometric characteristics under (a) San Fernando, PCD / SN (T_p = 1.47s), (b) Tabas, TAB / SP (T_p = 5.26s), (c) Northridge, SCG / SN (T_p = 2.94s), (d) Northridge, RRS / SN (T_p = 1.25s) records.

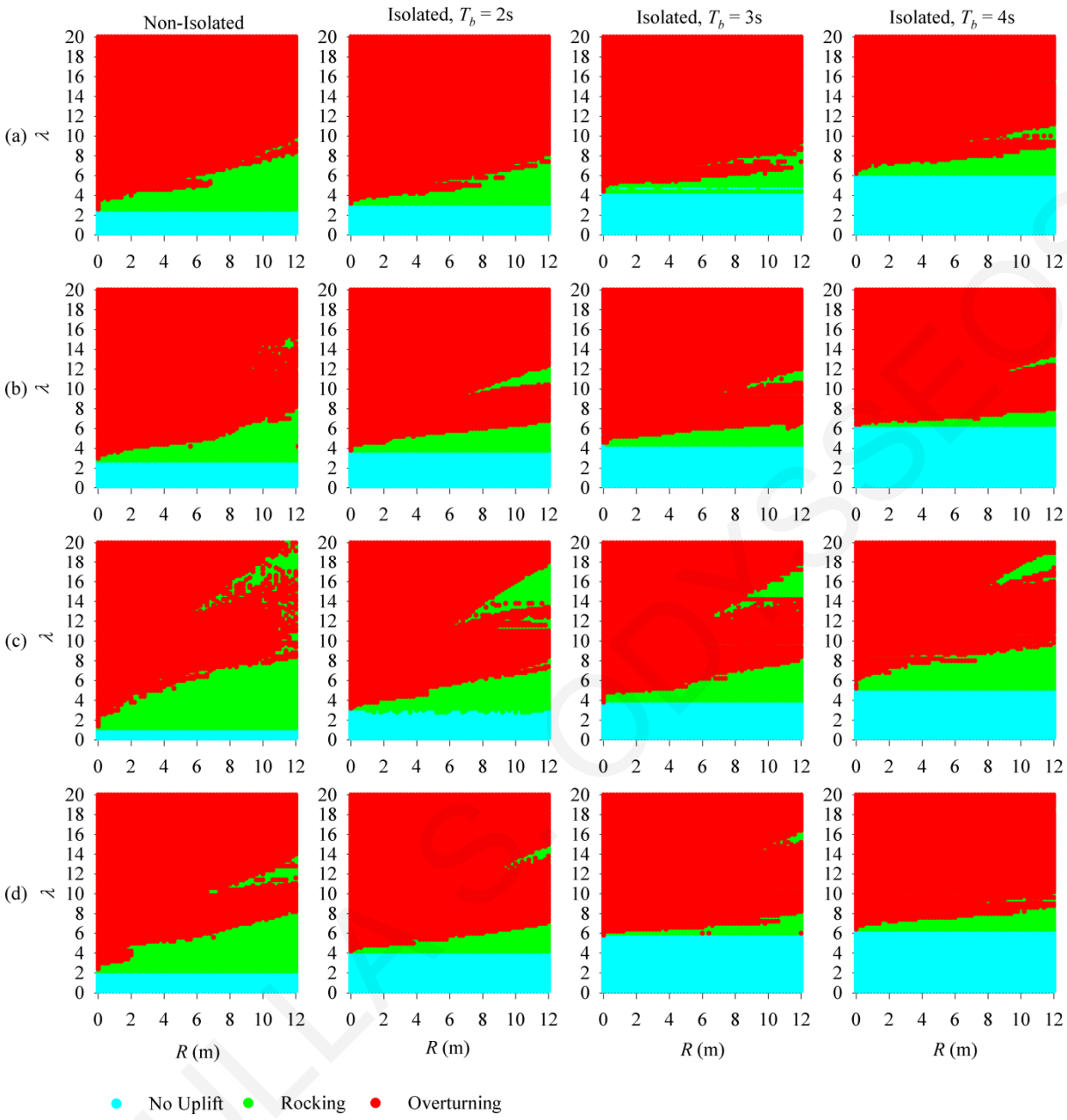

Figure A-2: Response-regime spectra in the $\lambda - R$ space for a non-isolated and isolated block of varying geometric characteristics under (a) Northridge, JFA / SN (T_p = 3.03s), (b) Imperial Valley, E05 / SN (T_p = 3.92s), (c) Northridge, SCH / SN (T_p = 3.03s), (d) Imperial Valley, E07 / SN (T_p = 3.64s) records.

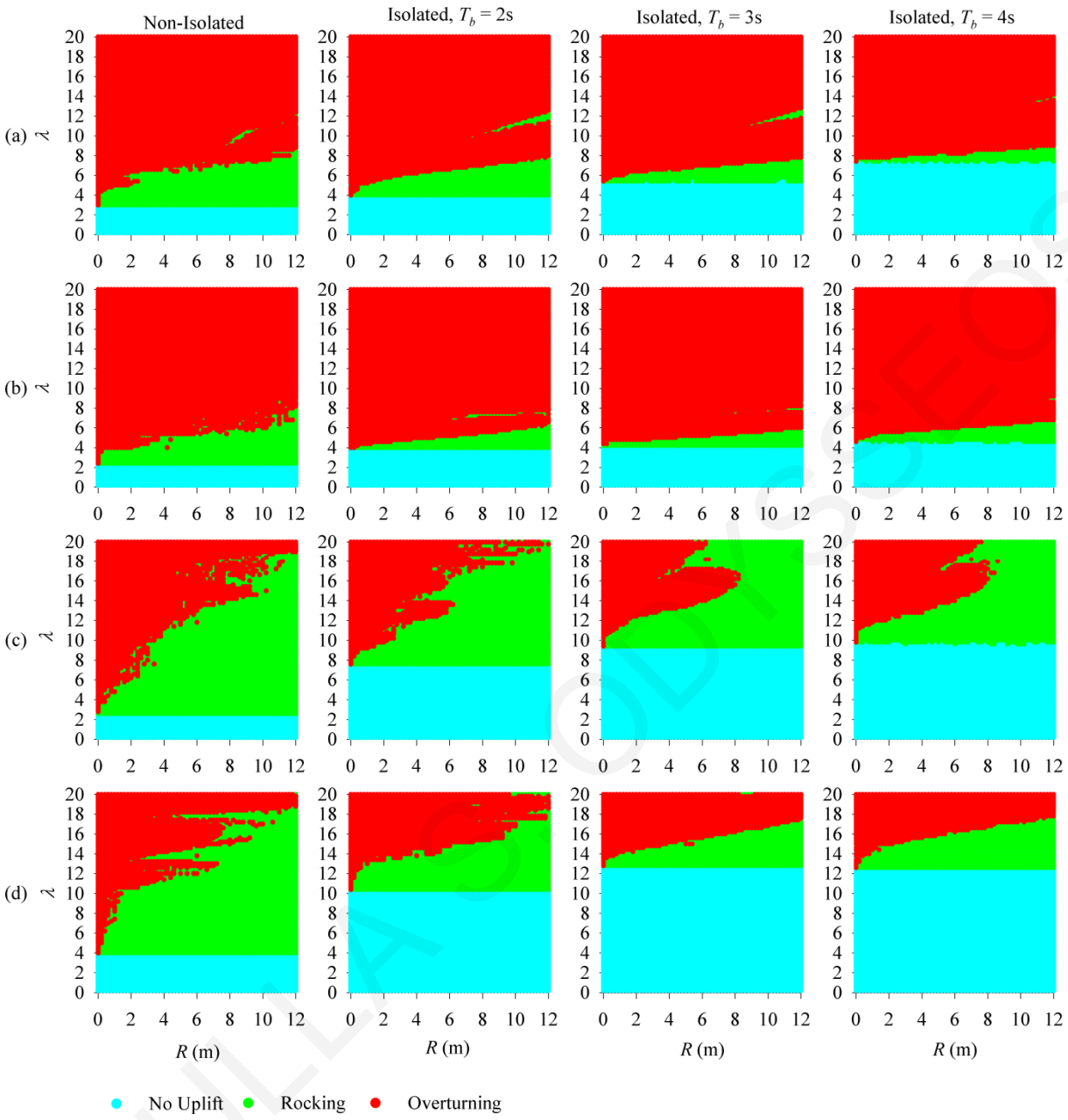

Figure A-3: Response-regime spectra in the $\lambda - R$ space for a non-isolated and isolated block of varying geometric characteristics under (a) Imperial Valley, E04 / SN (T_p = 4.44s), (b) Imperial Valley, E06 / SN (T_p = 3.85s), (c) Izmit, SKR / SP (T_p = 9.52s), (d) Izmit, GBZ / SN (T_p = 4.76s) records.

APPENDIX B

Rocking Response-Regime Spectra for Non-Isolated and Isolated Blocks Using Linear and Nonlinear Isolation Systems

Assuming no sliding of the block relative to the supporting base, entailing a pure rocking response, this appendix presents a numerous response-regime spectra in the $\lambda - R$ space for a class of non-isolated and isolated rigid blocks under near-fault ground motions . Two types of isolation system are considered in the analysis: (a) a Nonlinear I.S. with a bilinear hysteretic model (typified by friction-pendulum isolator) with parameters $\mu_b = 0.11$ and $R_b = 2.24\text{m}$ (corresponding to $T_b = 3\text{s}$) and (b) a Linear I.S. with viscoelastic model with $T_b = 3\text{s}$.

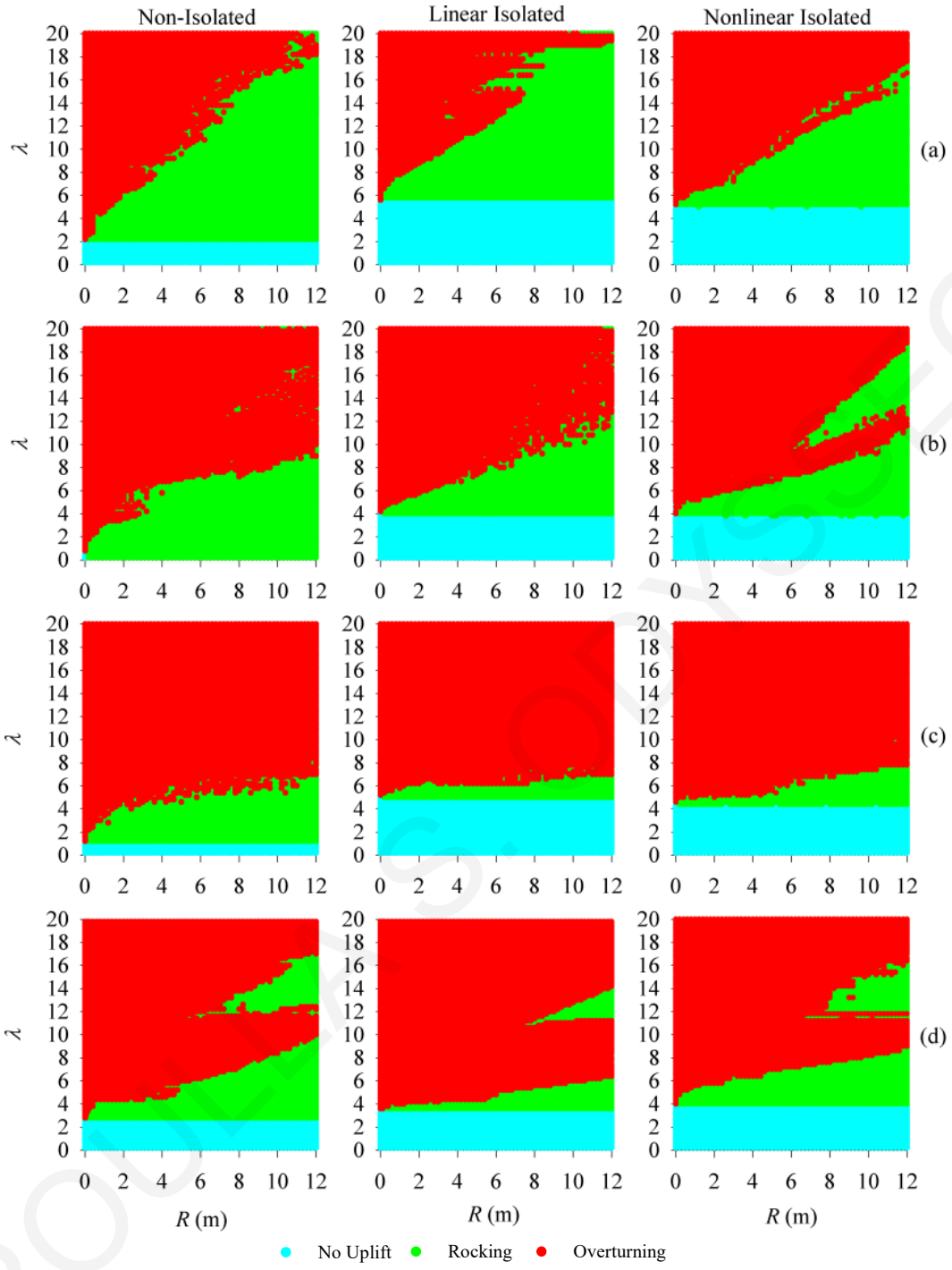

Figure B-1: Response-regime spectra in the $\lambda - R$ space for a non-isolated and isolated block of varying geometric characteristics under (a) the SN component of 1966 Parkfield, CA, USA earthquake, (b) the SN component of 1971 San Fernando, CA, USA earthquake, (c) the SP component of 1978 Tabas, Iran earthquake and (d) the SN component of 1979 Imperial Valley, CA, USA earthquake (EMO station).

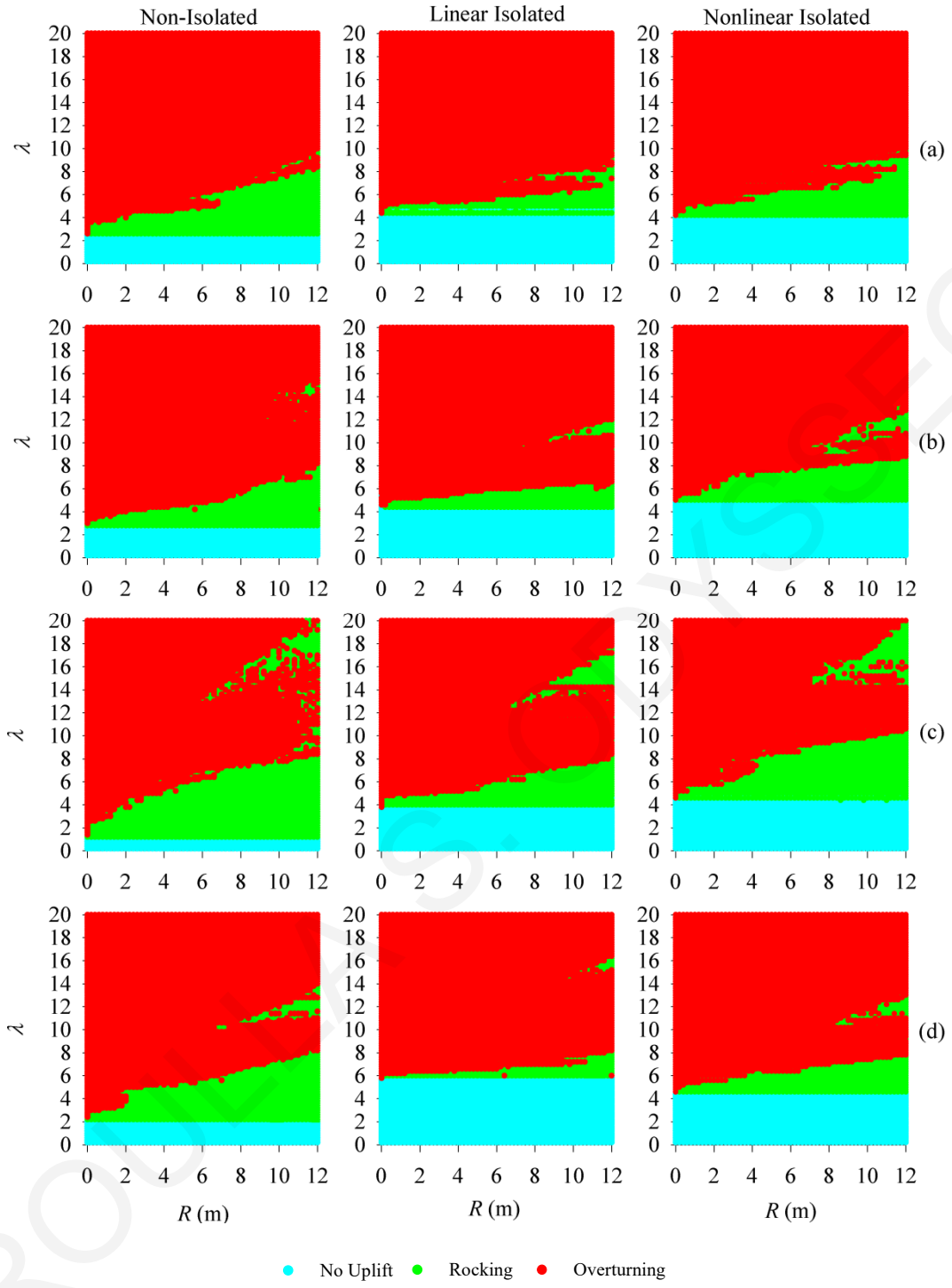

Figure B-2: Response-regime spectra in the $\lambda - R$ space for a non-isolated and isolated block of varying geometric characteristics under (a) the SN component of 1994 Northridge, CA, USA earthquake (JFA station), (b) the SN component of 1979 Imperial Valley, CA, USA earthquake (E05 station), (c) the SN component of 1994 Northridge, CA, USA earthquake (SCH station) and (d) the SN component of 1979 Imperial Valley, CA, USA earthquake (E07 station).

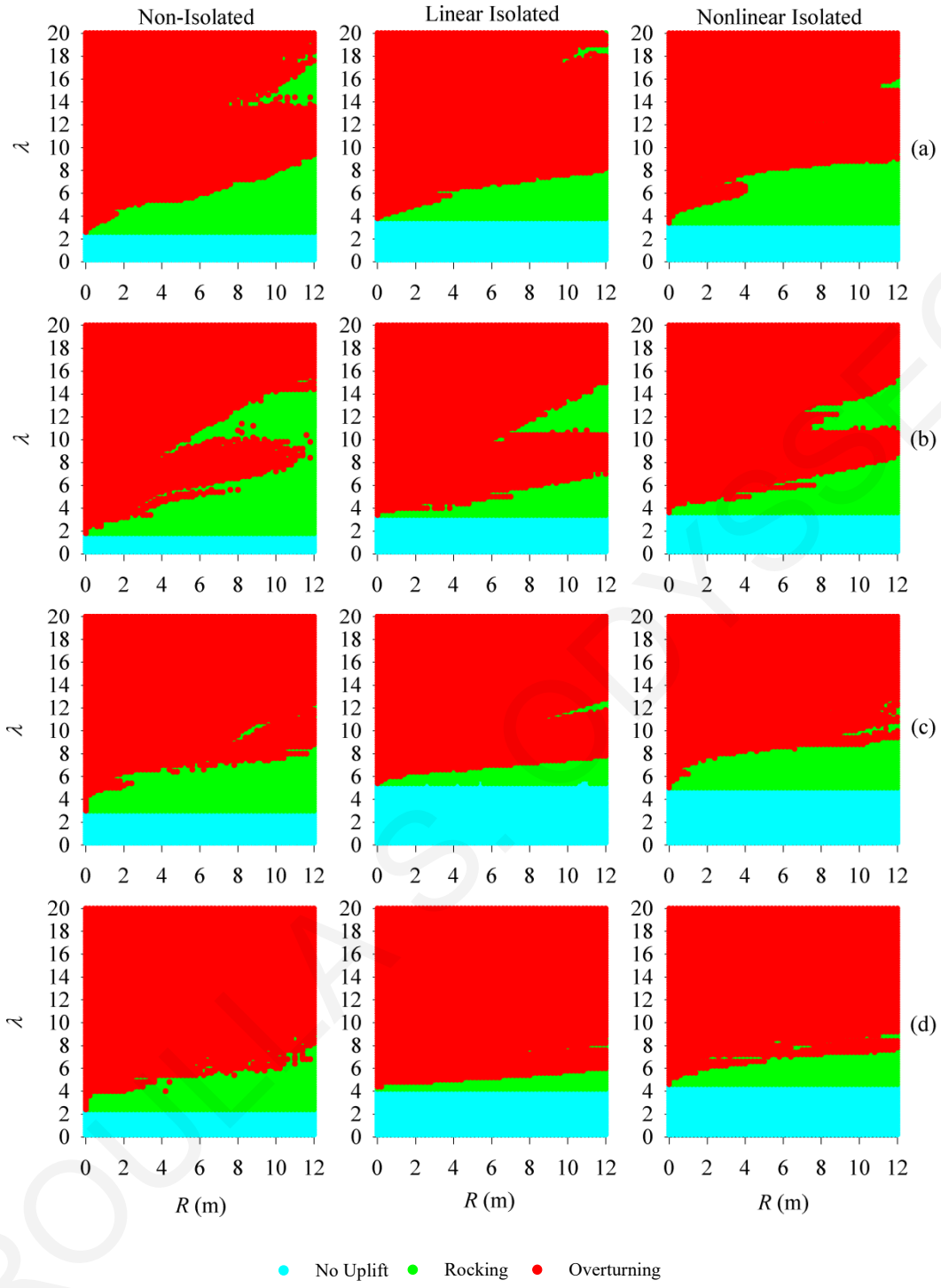

Figure B-3: Response-regime spectra in the $\lambda - R$ space for a non-isolated and isolated block of varying geometric characteristics under (a) the SN component of 1994 Northridge, CA, USA earthquake (NWS station), (b) the SN component of 1994 Northridge, CA, USA earthquake (SCG station), (c) the SN component of 1979 Imperial Valley, CA, USA earthquake (E04 station), and (d) the SN component of 1979 Imperial Valley, CA, USA earthquake (E06 station).

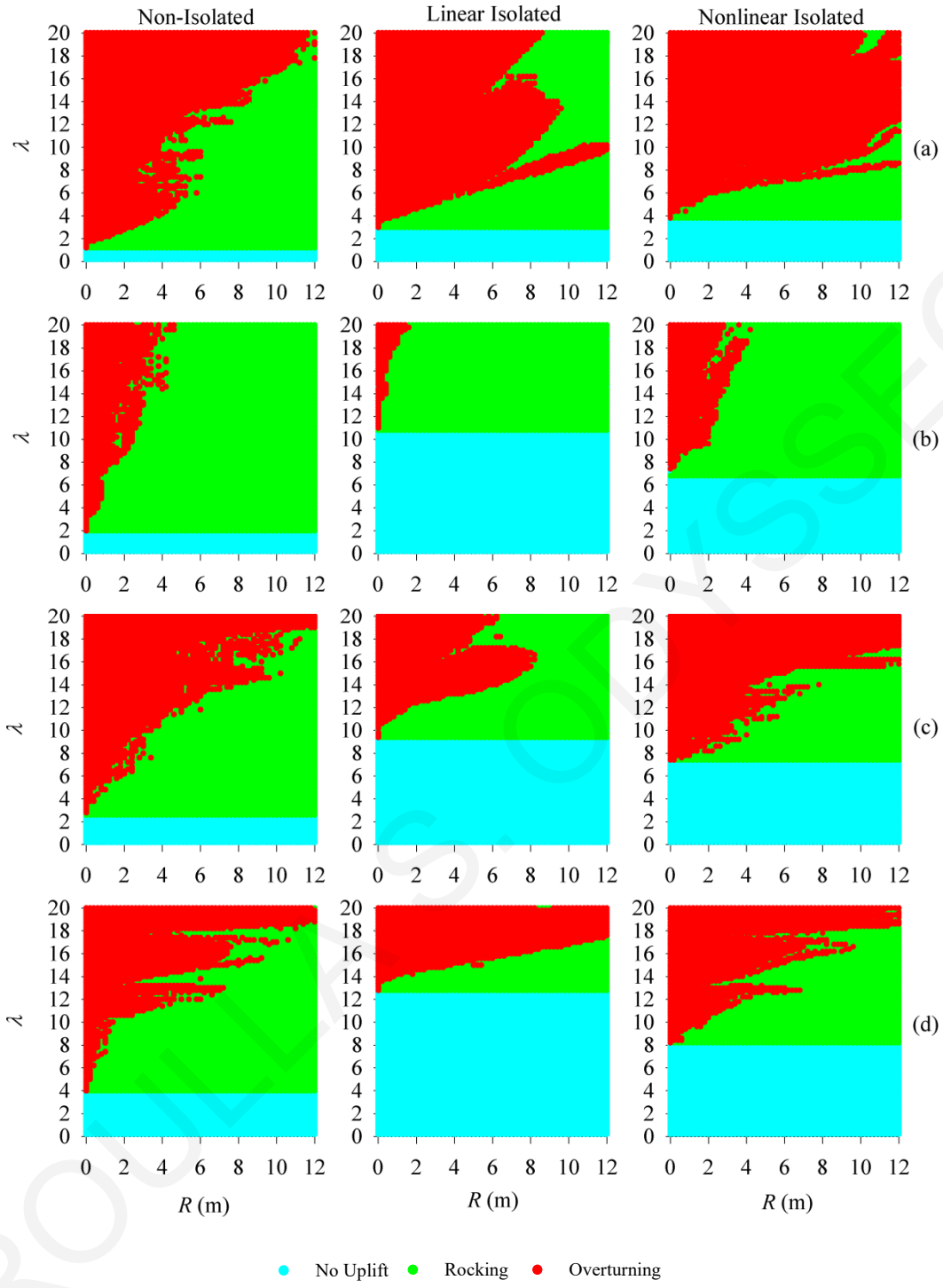

Figure B-4: Response-regime spectra in the $\lambda - R$ space for a non-isolated and isolated block of varying geometric characteristics under (a) the SN component of 1994 Northridge, CA, USA earthquake (RRS station), (b) the Tran component of 1995 Aigion, Greece earthquake, (c) the SP component of 1999 Izmit, Turkey earthquake (SKR station), and (d) the SN component of 1999 Izmit, Turkey earthquake (GBZ station).

APPENDIX C

Rocking Response Histories

Assuming no sliding of the block relative to the supporting base, entailing a pure rocking response, this appendix presents response histories for non-isolated and isolated rigid blocks under recorded ground excitations. Two types of isolation system are considered in the analysis: (a) a Nonlinear I.S. with a bilinear hysteretic model (typified by friction-pendulum isolator) with parameters $\mu_b = 0.11$ and $R_b = 2.24\text{m}$ (corresponding to $T_b = 3\text{s}$) and (b) a Linear I.S. with viscoelastic model with $T_b = 3\text{s}$.

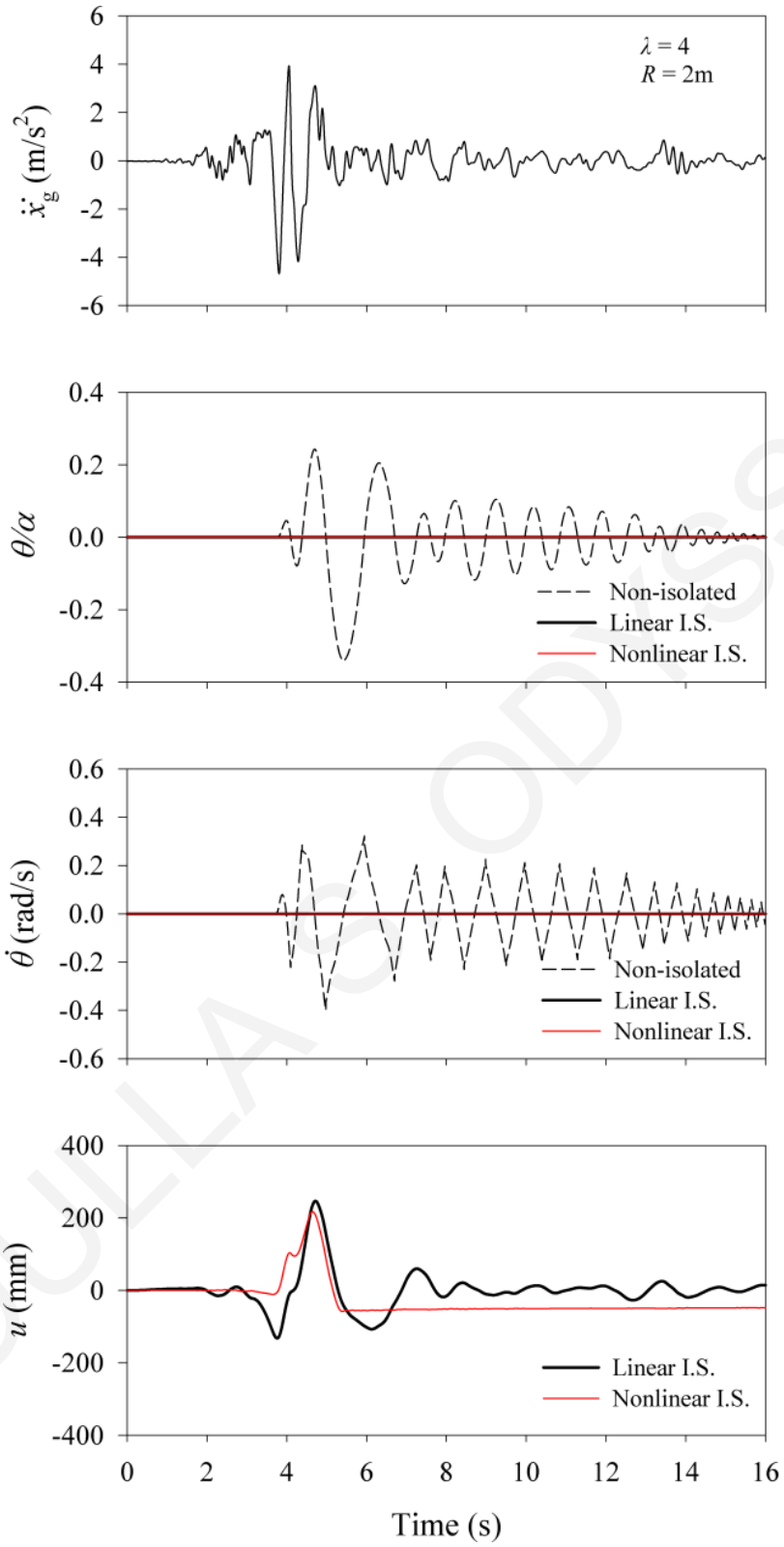

Figure C-1: Response histories for non-isolated and isolated rigid block under the SN component of 1966 Parkfield, CA, USA earthquake ($\rho = 0.5$, $\lambda = 4$, $R = 2$m).

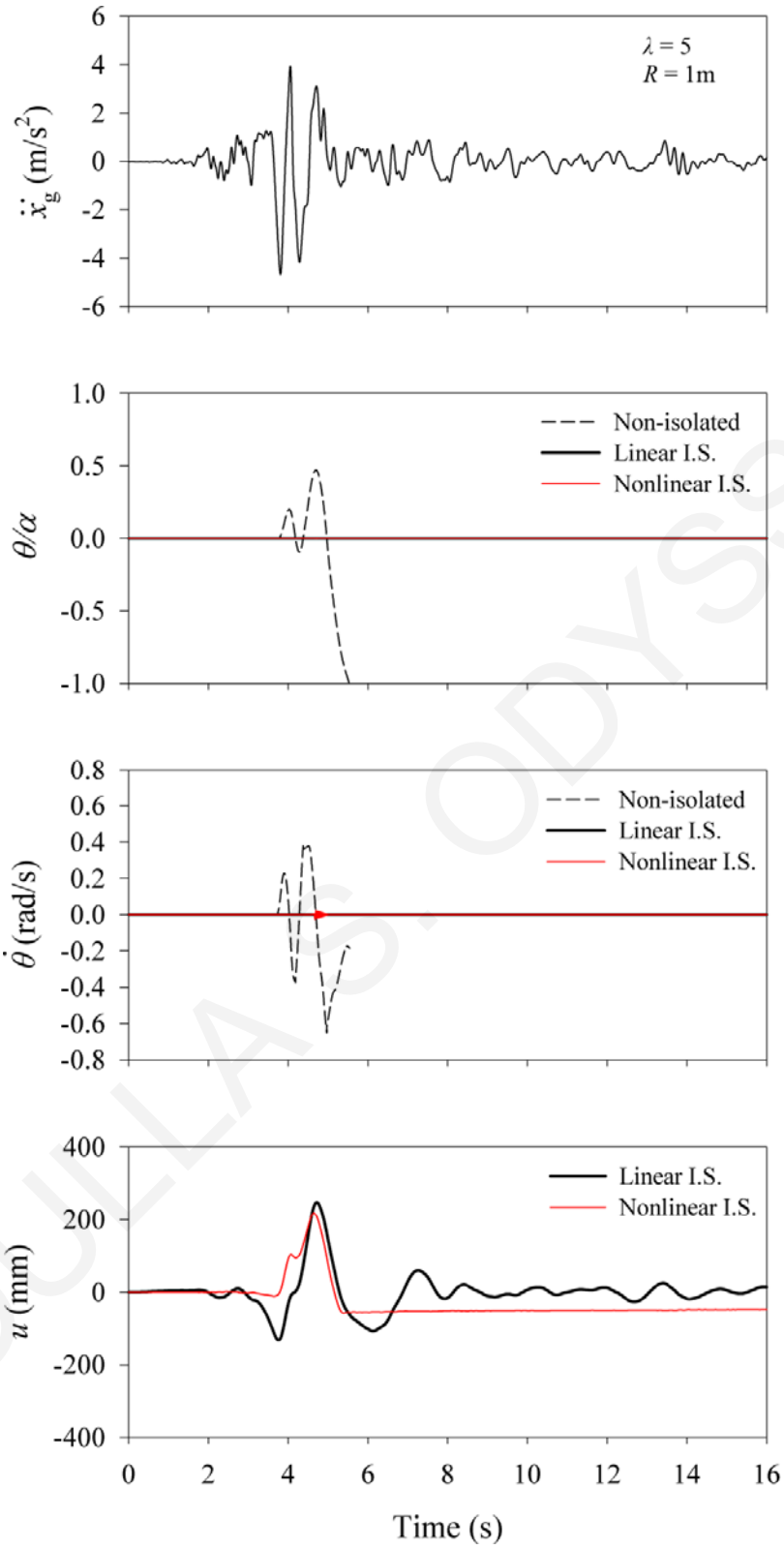

Figure C-2: Response histories for non-isolated and isolated rigid block under the SN component of 1966 Parkfield, CA, USA earthquake ($\rho = 0.5$, $\lambda = 5$, $R = 1$m).

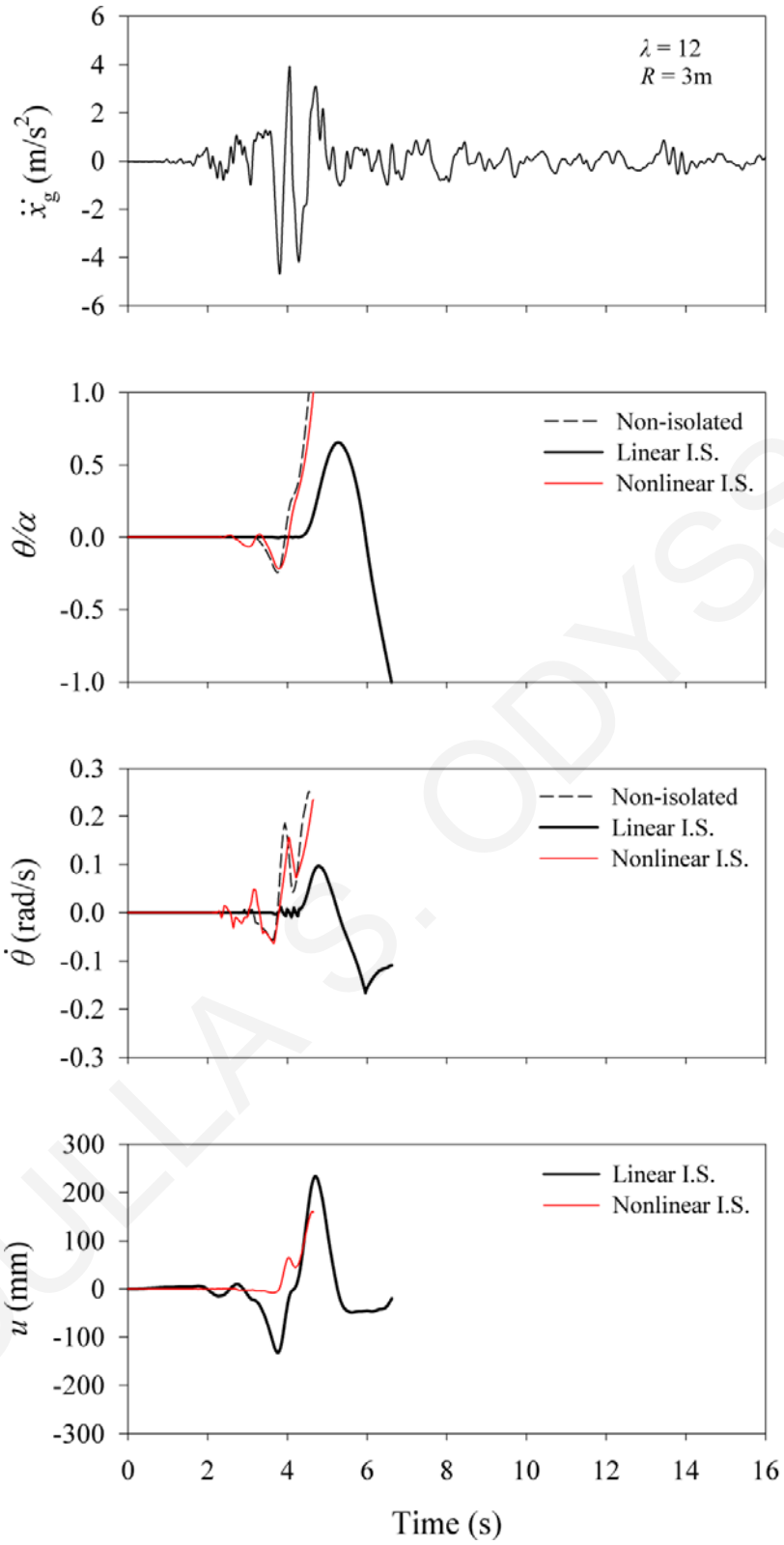

Figure C-3: Response histories for non-isolated and isolated rigid block under the SN component of 1966 Parkfield, CA, USA earthquake ($\rho = 0.5$, $\lambda = 12$, $R = 3$m).

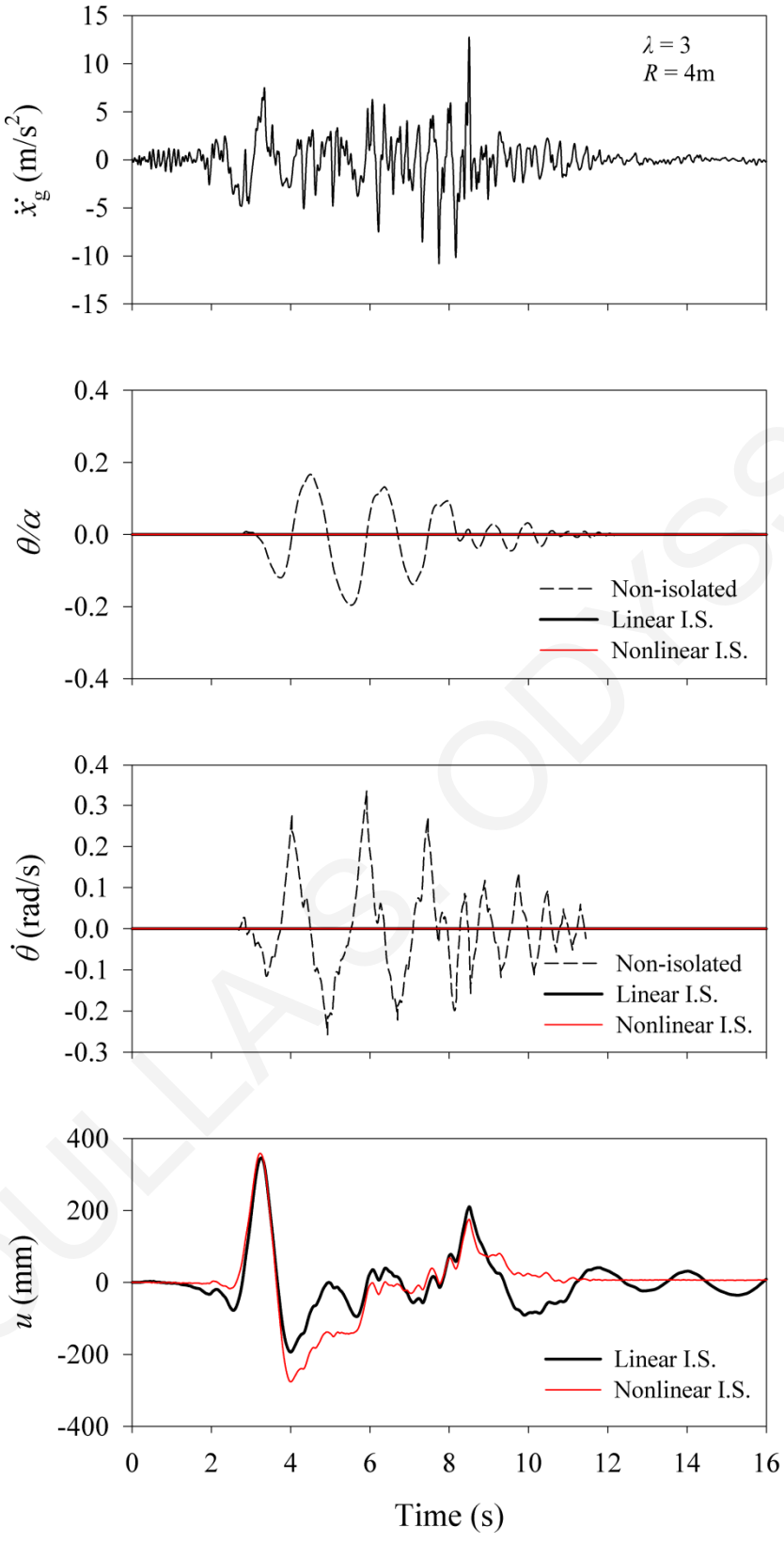

Figure C-4: Response histories for non-isolated and isolated rigid block under the SN component of 1971 San Fernando, CA, USA earthquake ($\rho = 0.5$, $\lambda = 3$, $R = 4$m).

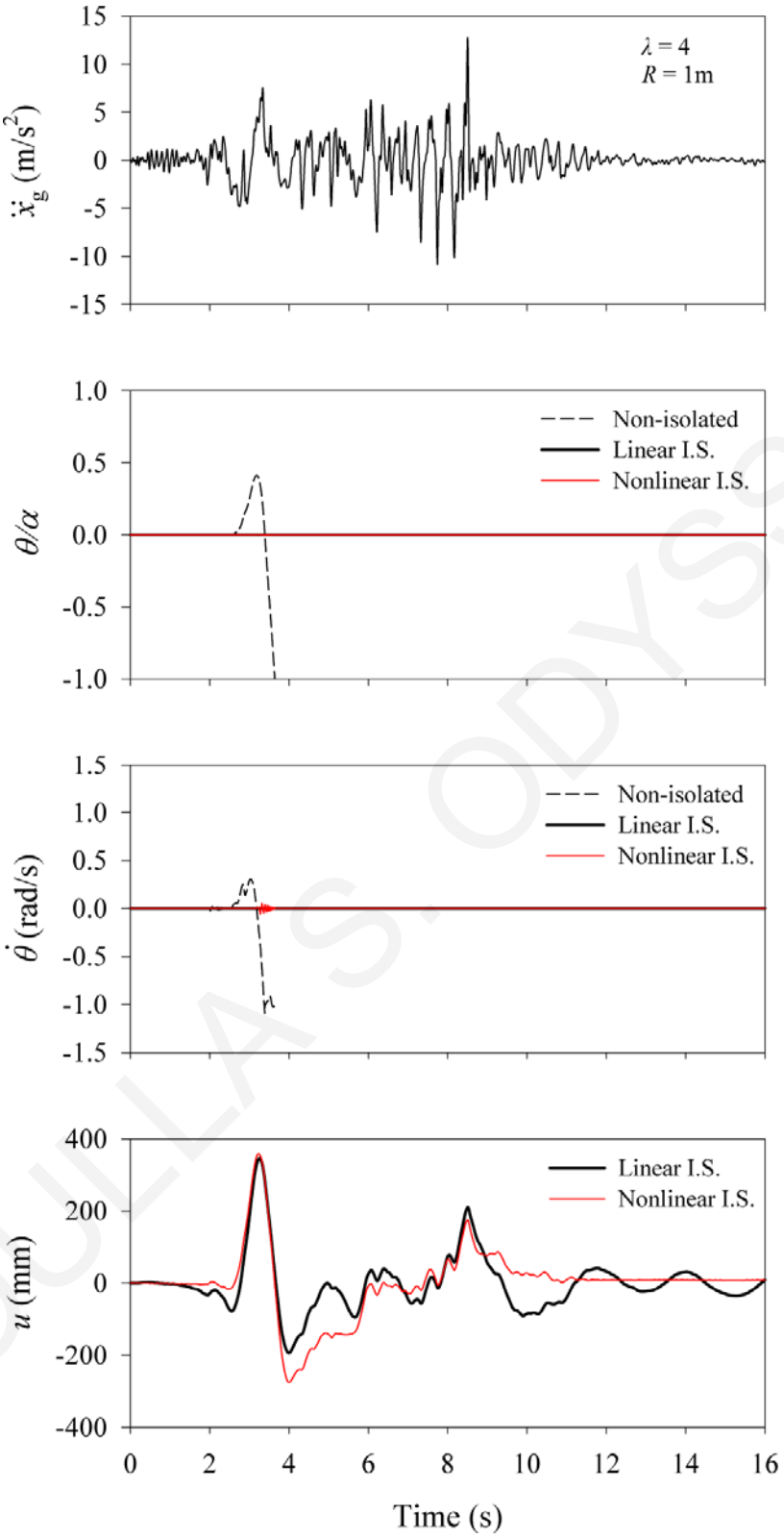

Figure C-5: Response histories for non-isolated and isolated rigid block under the SN component of 1971 San Fernando, CA, USA earthquake ($\rho = 0.5$, $\lambda = 4$, $R = 1$m).

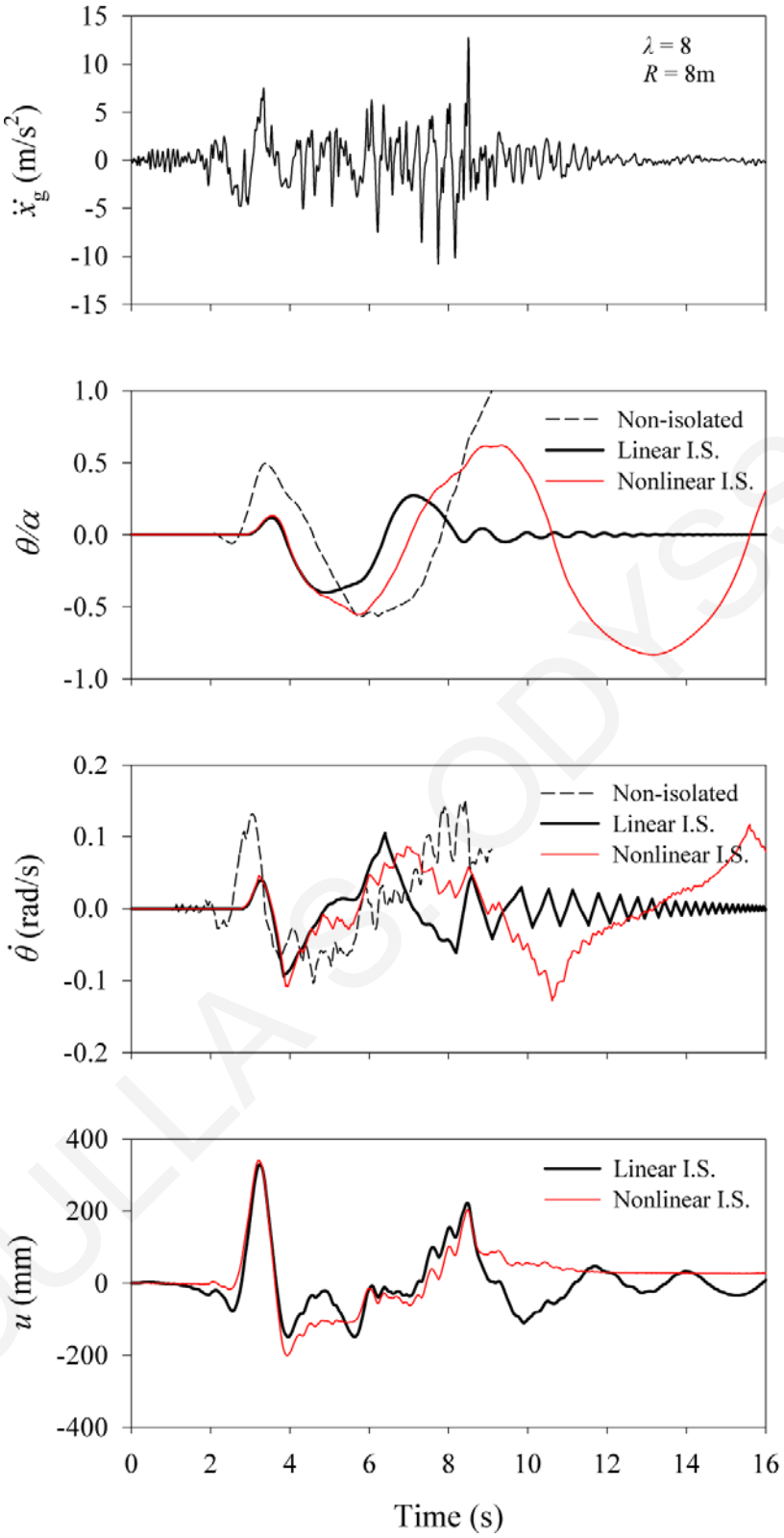

Figure C-6: Response histories for non-isolated and isolated rigid block under the SN component of 1971 San Fernando, CA, USA earthquake ($\rho = 0.5$, $\lambda = 8$, $R = 8$m).

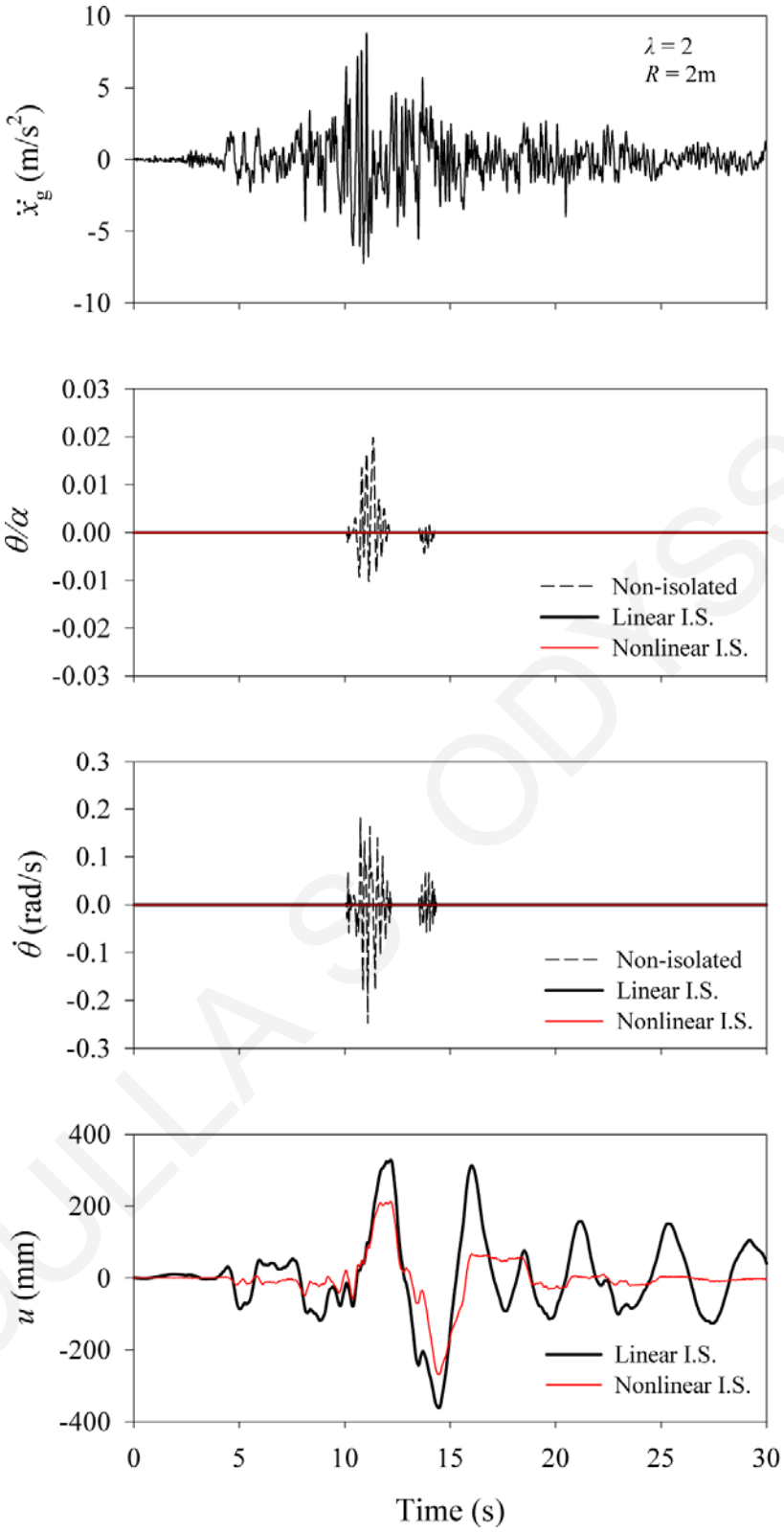

Figure C-7: Response histories for non-isolated and isolated rigid block under the SP component of 1978 Tabas, Iran earthquake ($\rho = 0.5$, $\lambda = 2$, $R = 2$m).

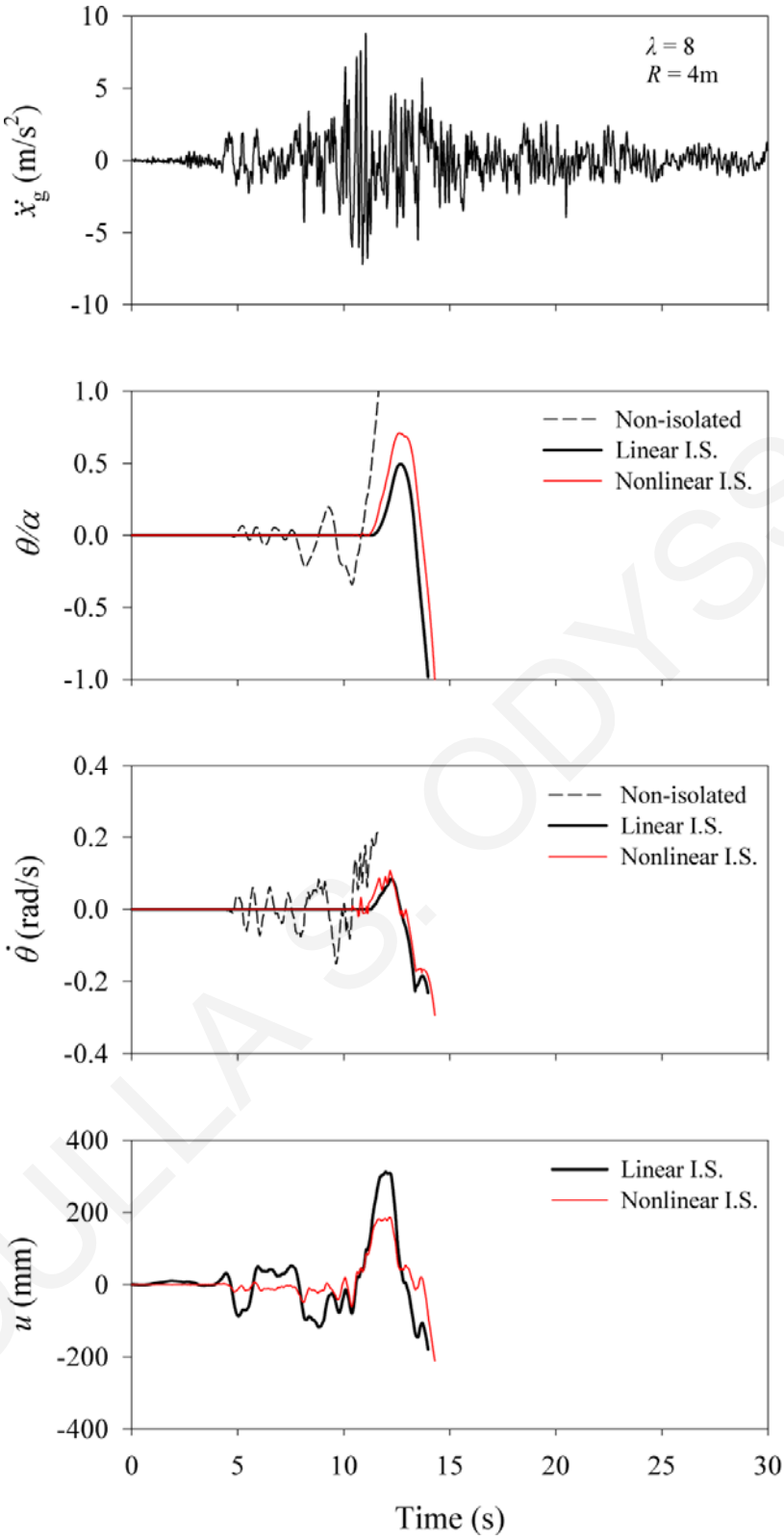

Figure C-8: Response histories for non-isolated and isolated rigid block under the SP component of 1978 Tabas, Iran earthquake ($\rho = 0.5$, $\lambda = 8$, $R = 4$m).

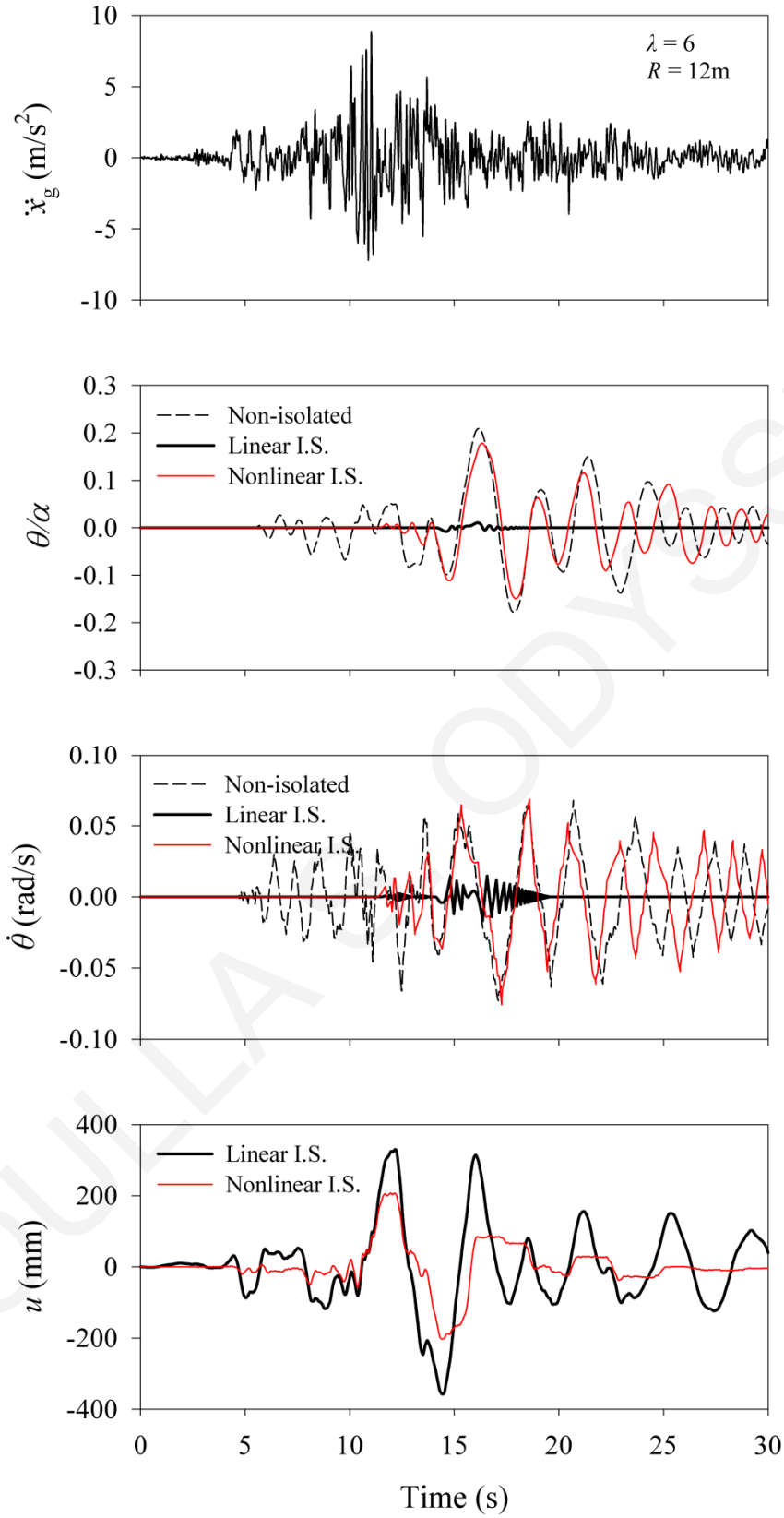

Figure C-9: Response histories for non-isolated and isolated rigid block under the SP component of 1978 Tabas, Iran earthquake ($\rho = 0.5$, $\lambda = 6$, $R = 12$m).

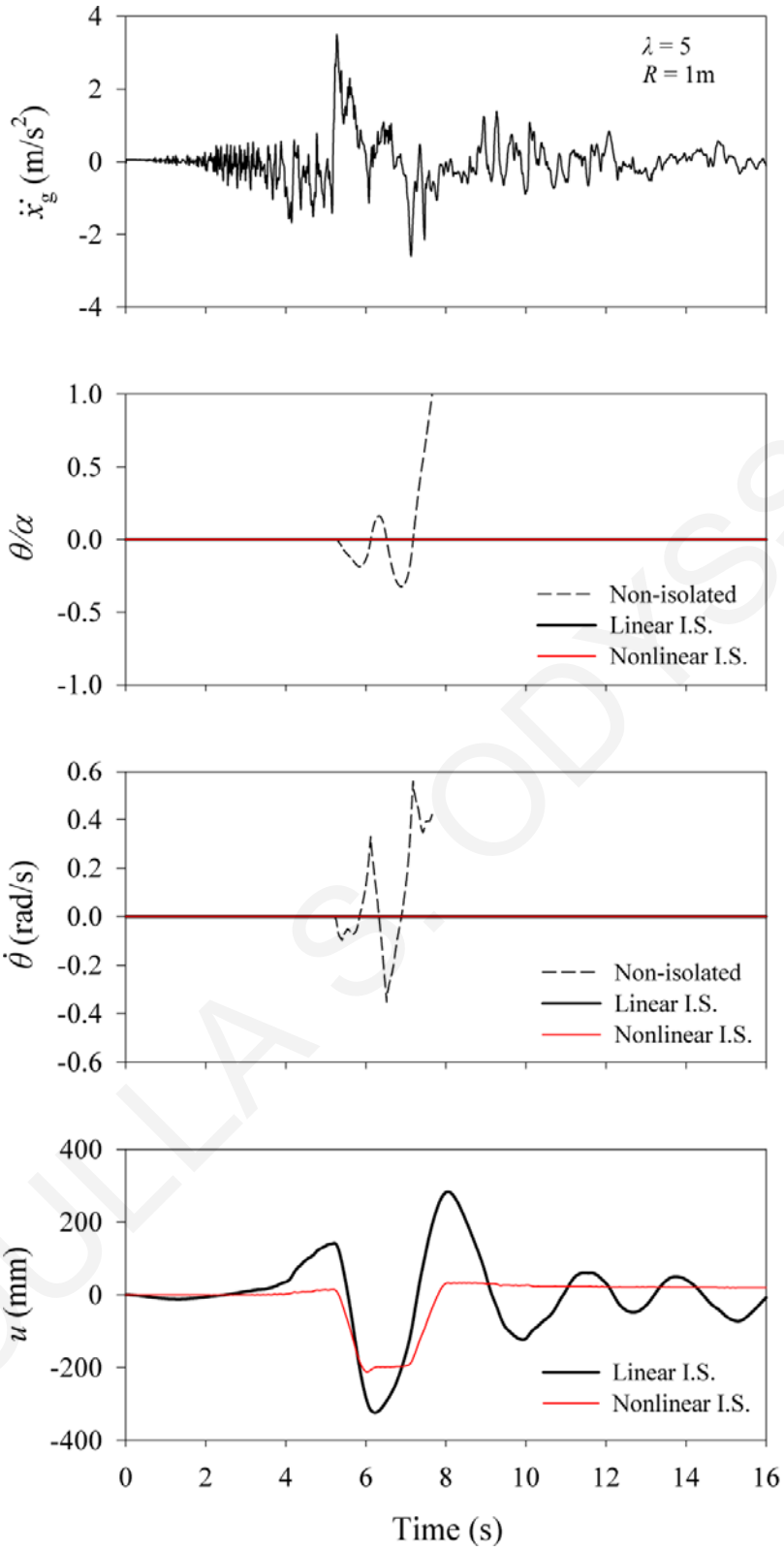

Figure C-10: Response histories for non-isolated and isolated rigid block under the SN component of 1979 Imperial Valley (E04 station), CA, USA earthquake ($\rho = 0.5$, $\lambda = 5$, $R = 1$m).

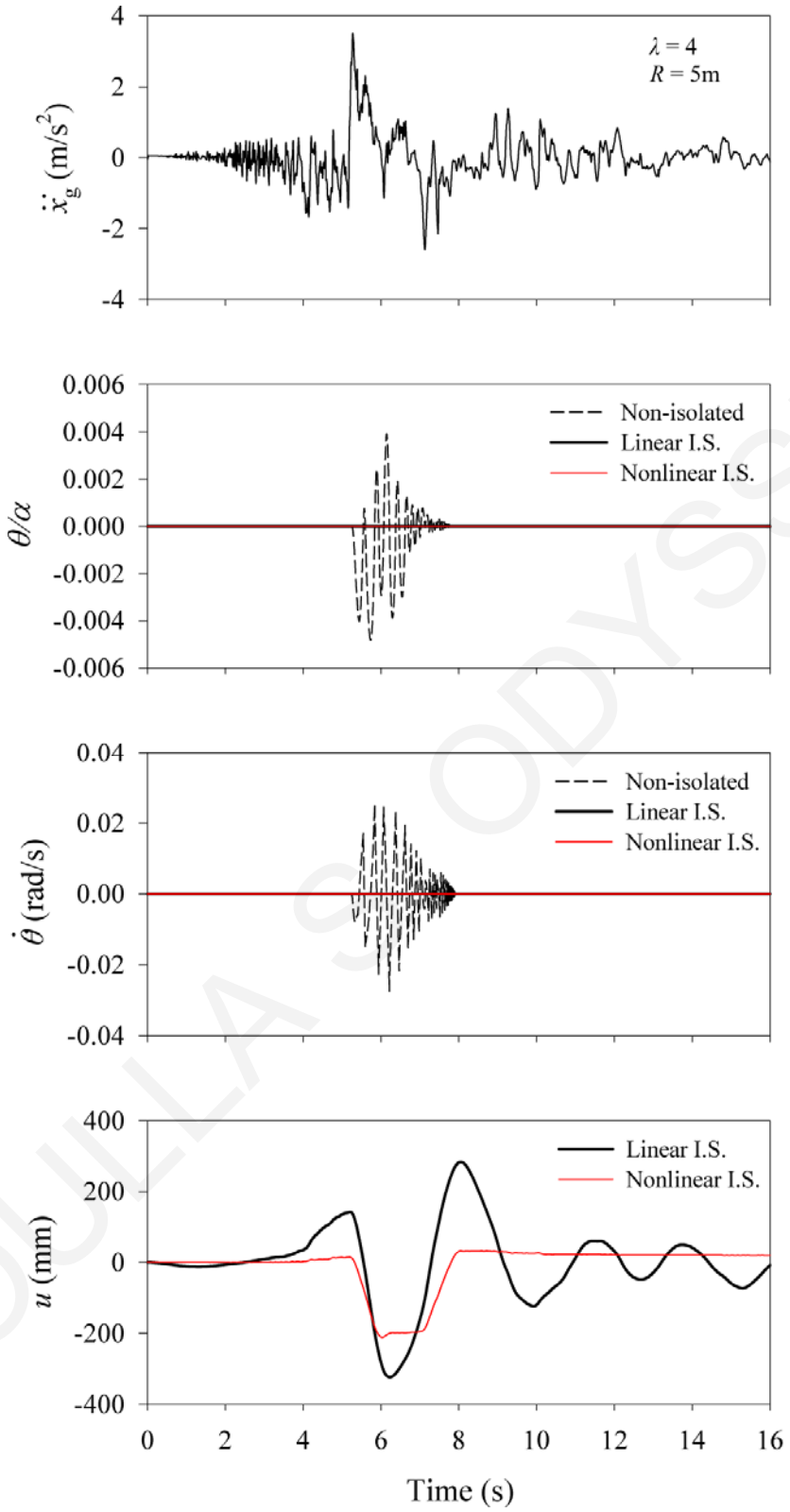

Figure C-11: Response histories for non-isolated and isolated rigid block under the SN component of 1979 Imperial Valley (E04 station), CA, USA earthquake ($\rho = 0.5$, $\lambda = 4$, $R = 5$m).

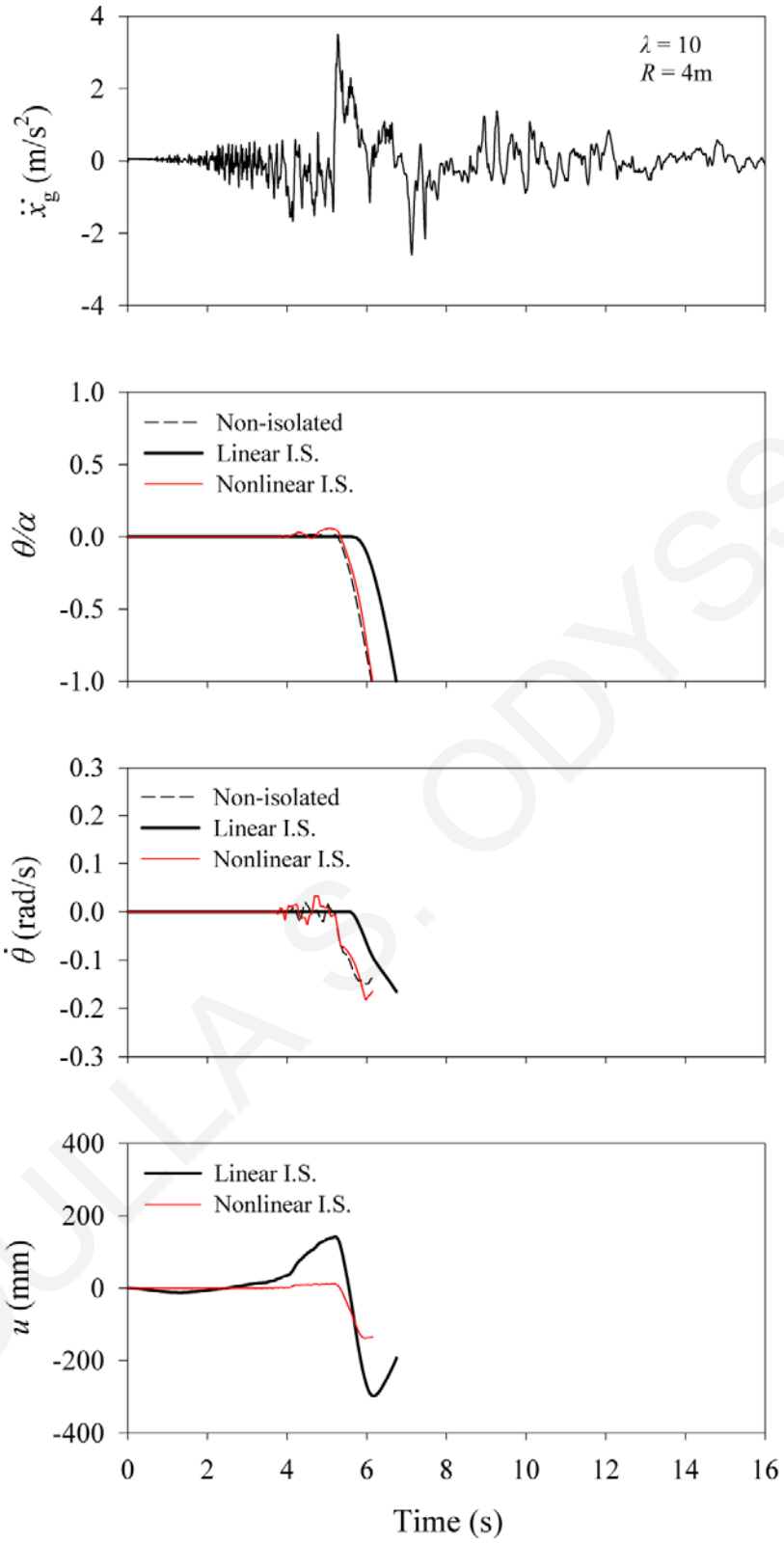

Figure C-12: Response histories for non-isolated and isolated rigid block under the SN component of 1979 Imperial Valley (E04 station), CA, USA earthquake ($\rho = 0.5$, $\lambda = 10$, $R = 4$m).

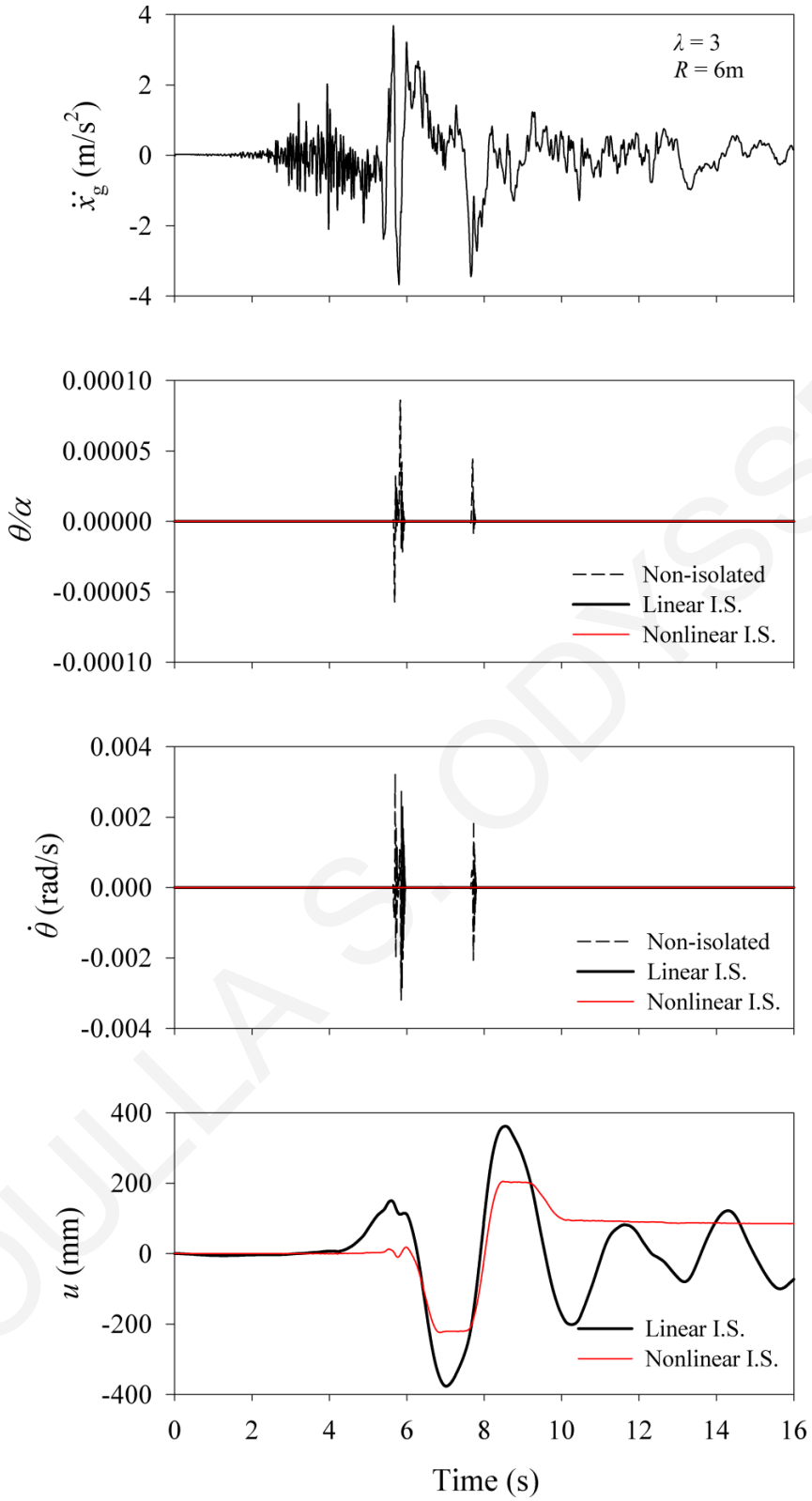

Figure C-13: Response histories for non-isolated and isolated rigid block under the SN component of 1979 Imperial Valley (E05 station), CA, USA earthquake ($\rho = 0.5$, $\lambda = 3$, $R = 6$m).

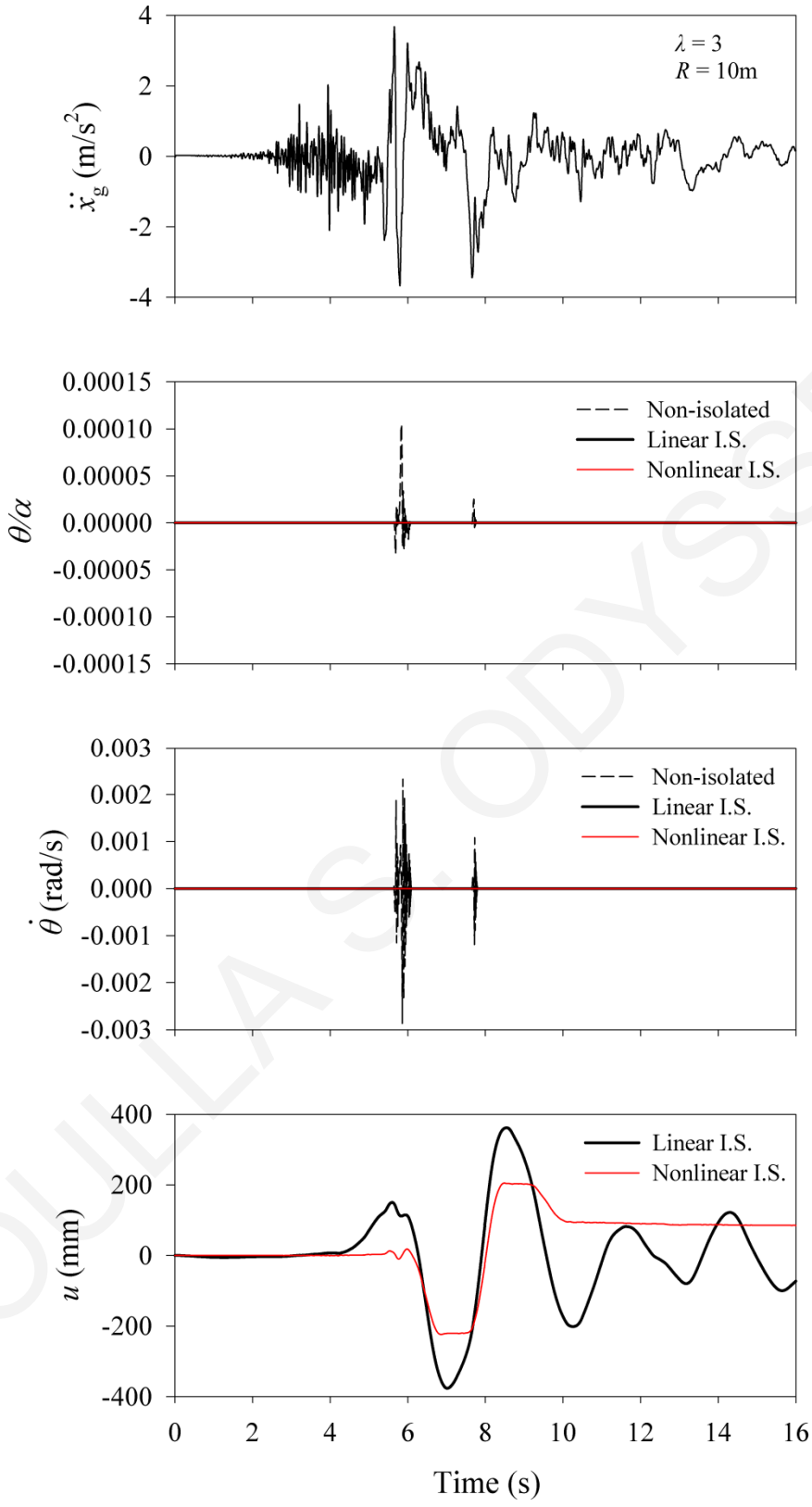

Figure C-14: Response histories for non-isolated and isolated rigid block under the SN component of 1979 Imperial Valley (E05 station), CA, USA earthquake ($\rho = 0.5$, $\lambda = 3$, $R = 10$ m).

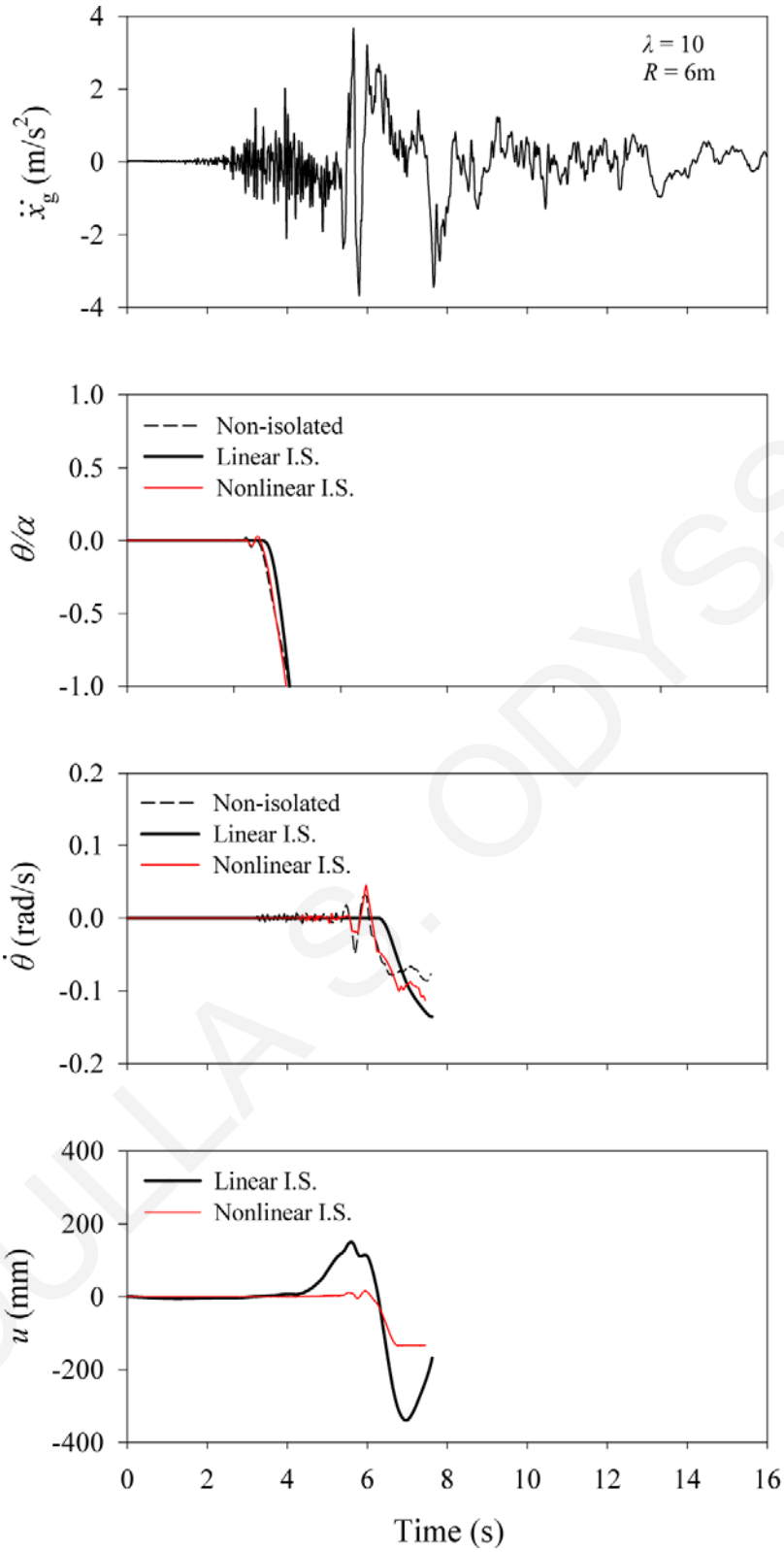

Figure C-15: Response histories for non-isolated and isolated rigid block under the SN component of 1979 Imperial Valley (E05 station), CA, USA earthquake ($\rho = 0.5$, $\lambda = 10$, $R = 6$m).

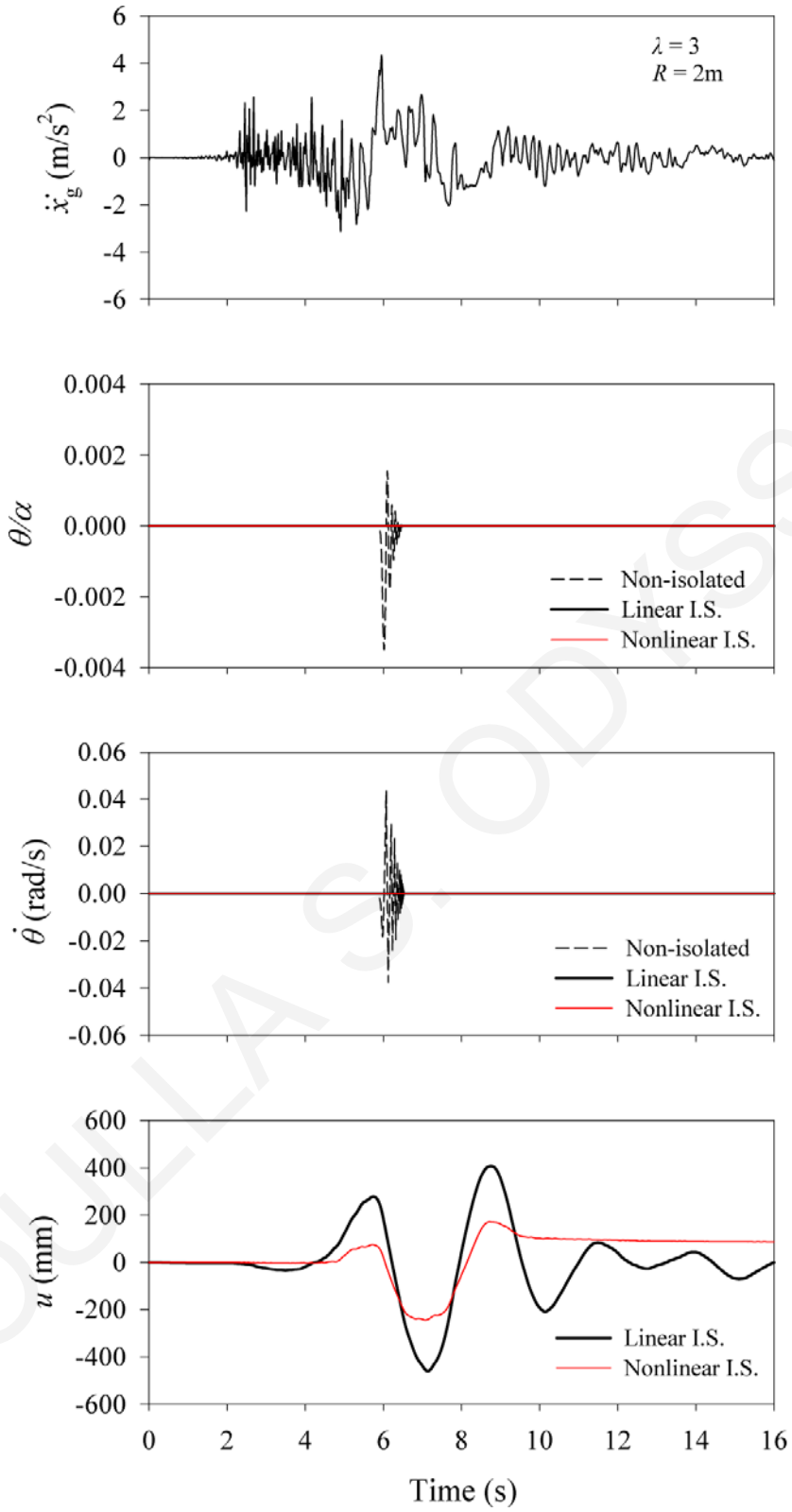

Figure C-16: Response histories for non-isolated and isolated rigid block under the SN component of 1979 Imperial Valley (E06 station), CA, USA earthquake ($\rho = 0.5$, $\lambda = 3$, $R = 2$m).

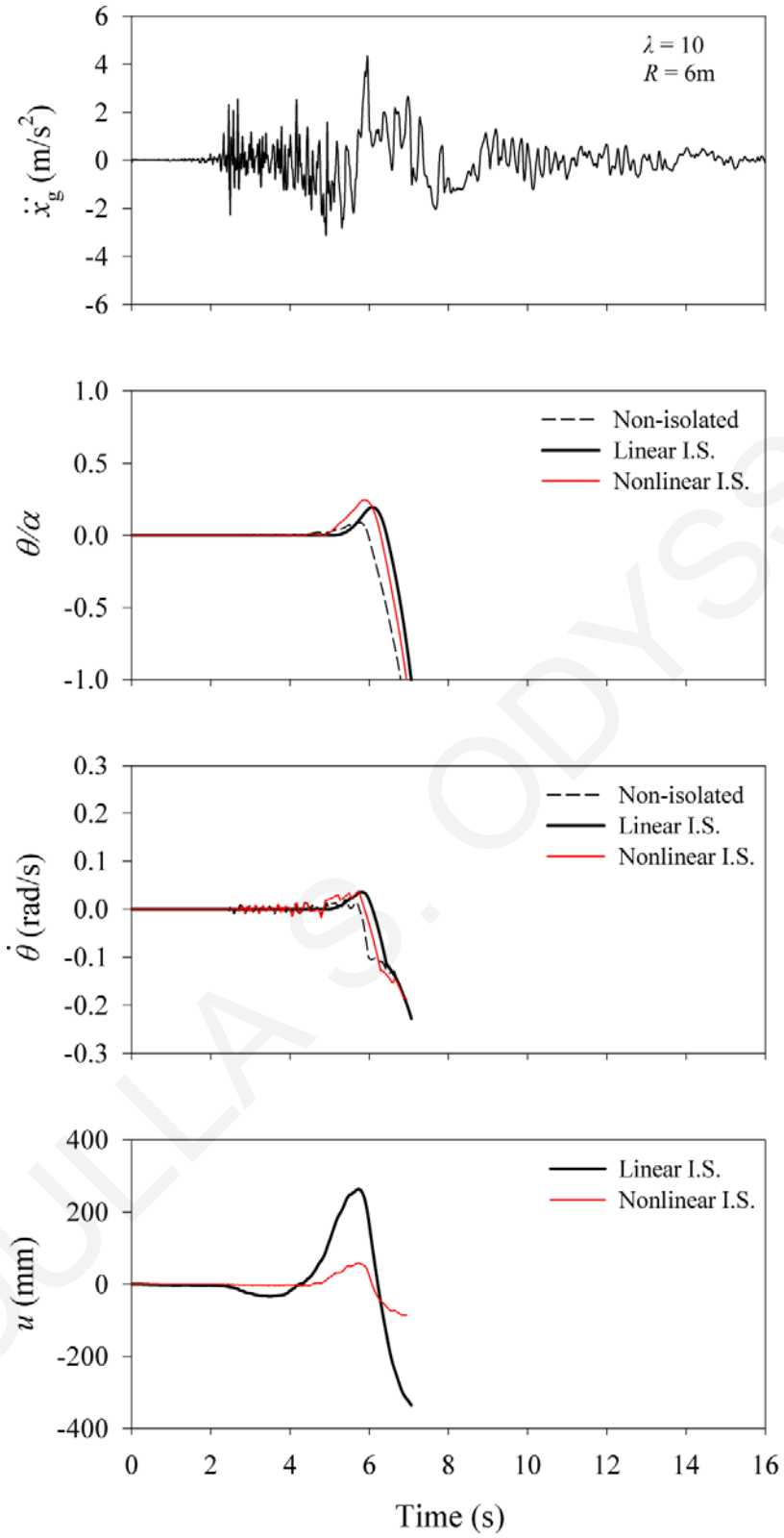

Figure C-17: Response histories for non-isolated and isolated rigid block under the SN component of 1979 Imperial Valley (E06 station), CA, USA earthquake ($\rho = 0.5$, $\lambda = 10$, $R = 6$m).

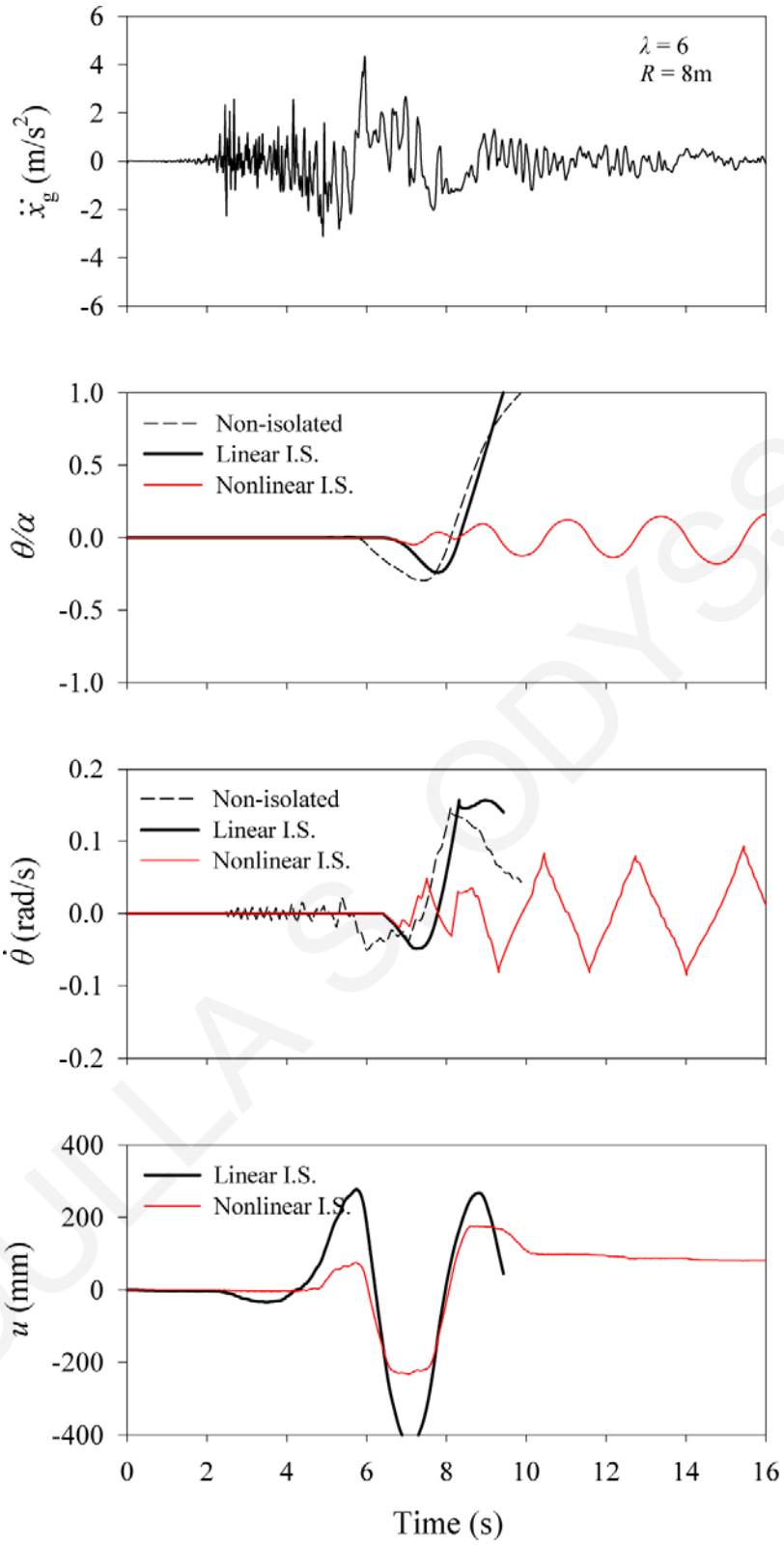

Figure C-18: Response histories for non-isolated and isolated rigid block under the SN component of 1979 Imperial Valley (E06 station), CA, USA earthquake ($\rho = 0.5$, $\lambda = 6$, $R = 8$m).

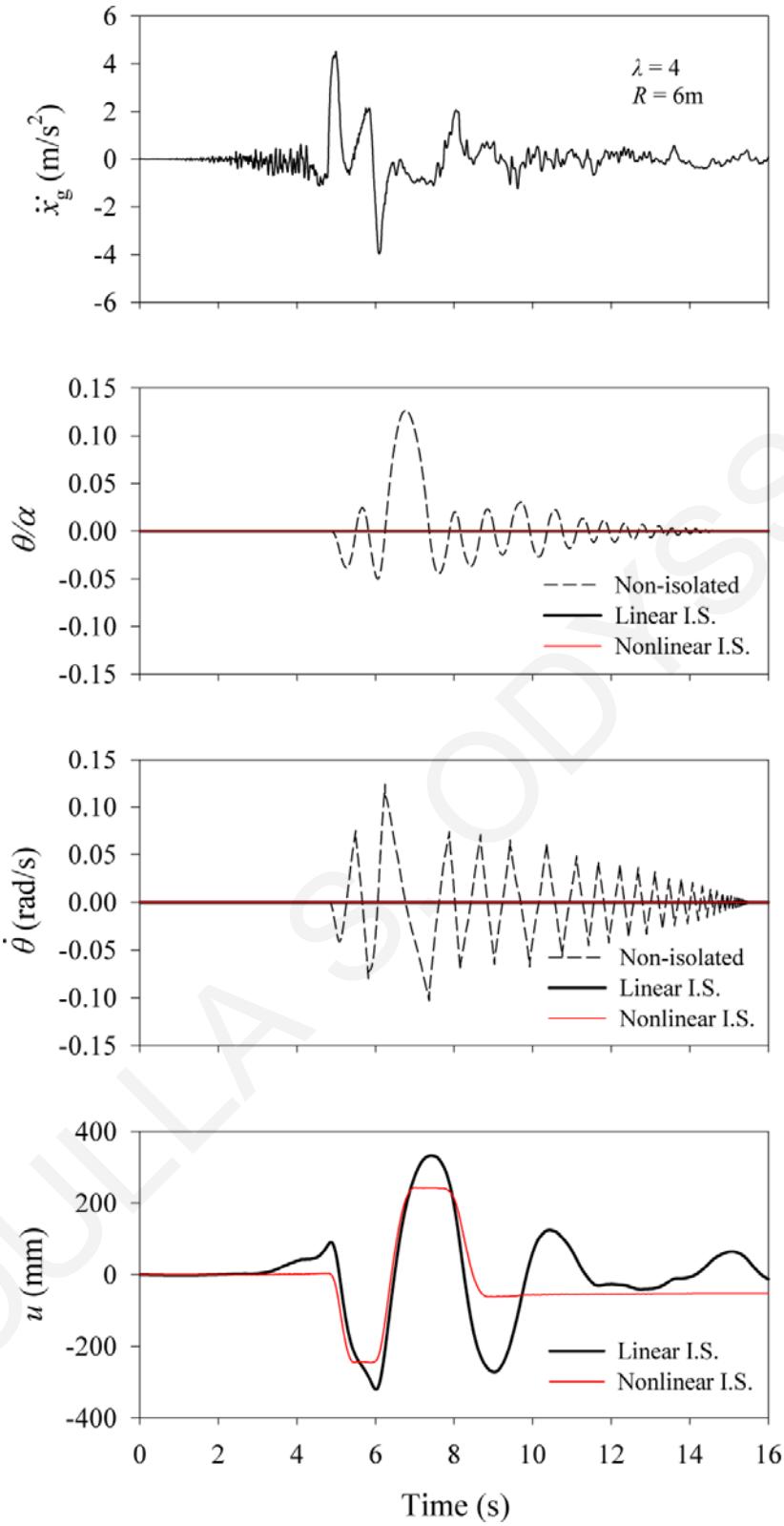

Figure C-19: Response histories for non-isolated and isolated rigid block under the SN component of 1979 Imperial Valley (E07 station), CA, USA earthquake ($\rho = 0.5$, $\lambda = 4$, $R = 6$m).

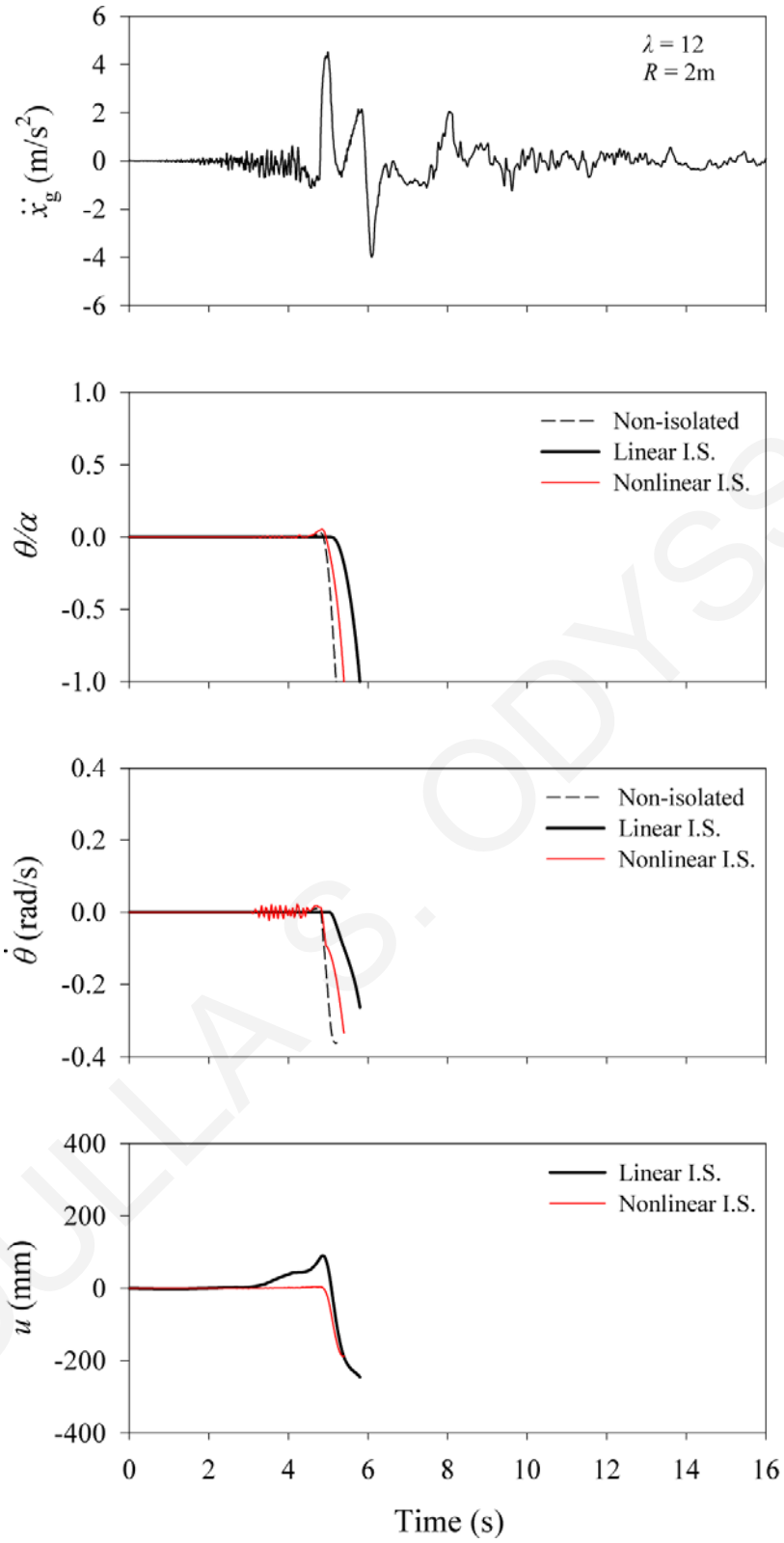

Figure C-20: Response histories for non-isolated and isolated rigid block under the SN component of 1979 Imperial Valley (E07 station), CA, USA earthquake ($\rho = 0.5$, $\lambda = 12$, $R = 2$m).

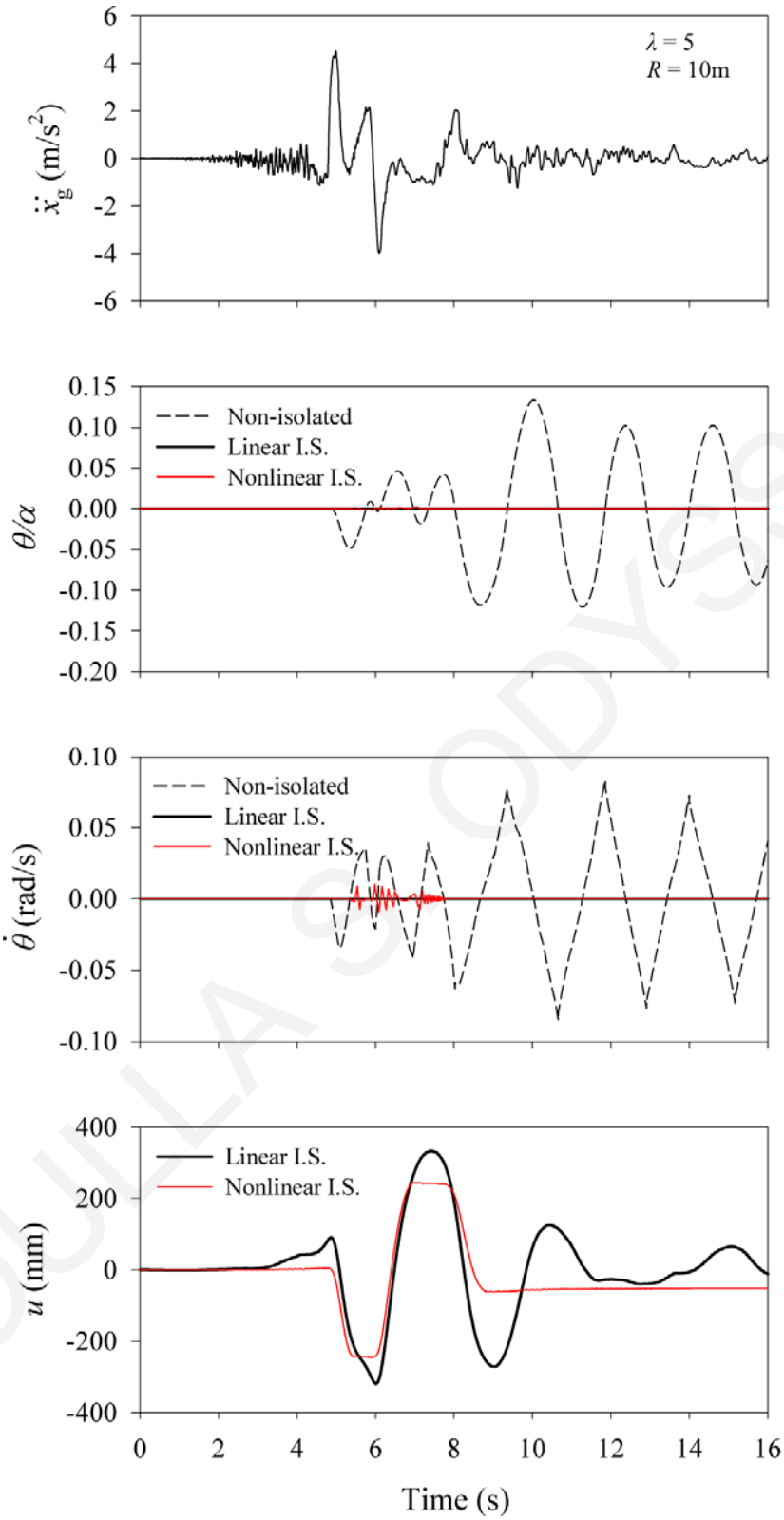

Figure C-21: Response histories for non-isolated and isolated rigid block under the SN component of 1979 Imperial Valley (E07 station), CA, USA earthquake ($\rho = 0.5$, $\lambda = 5$, $R = 10$m).

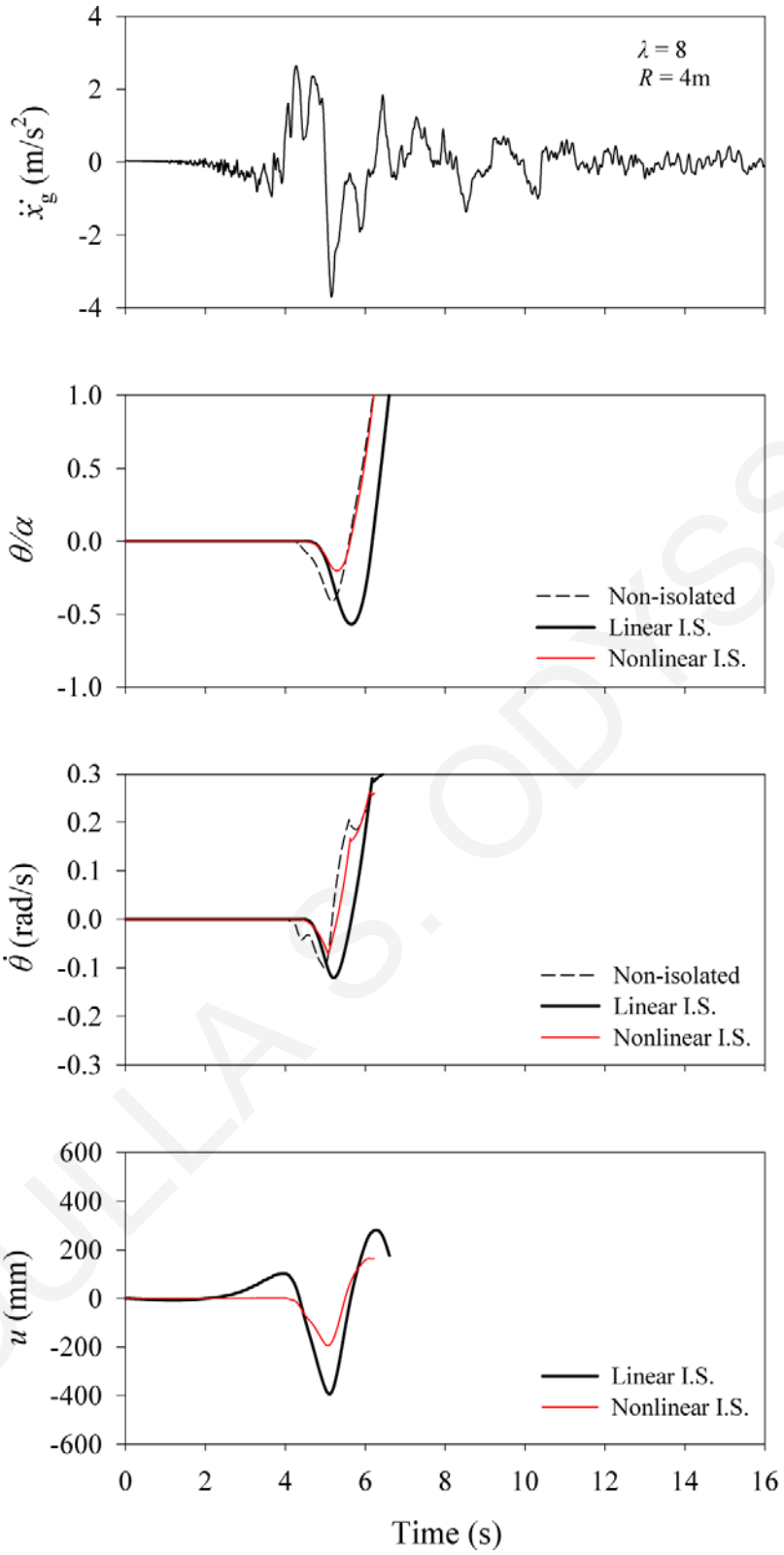

Figure C-22: Response histories for non-isolated and isolated rigid block under the SN component of 1979 Imperial Valley (EMO station), CA, USA earthquake ($\rho = 0.5$, $\lambda = 8$, $R = 4$m).

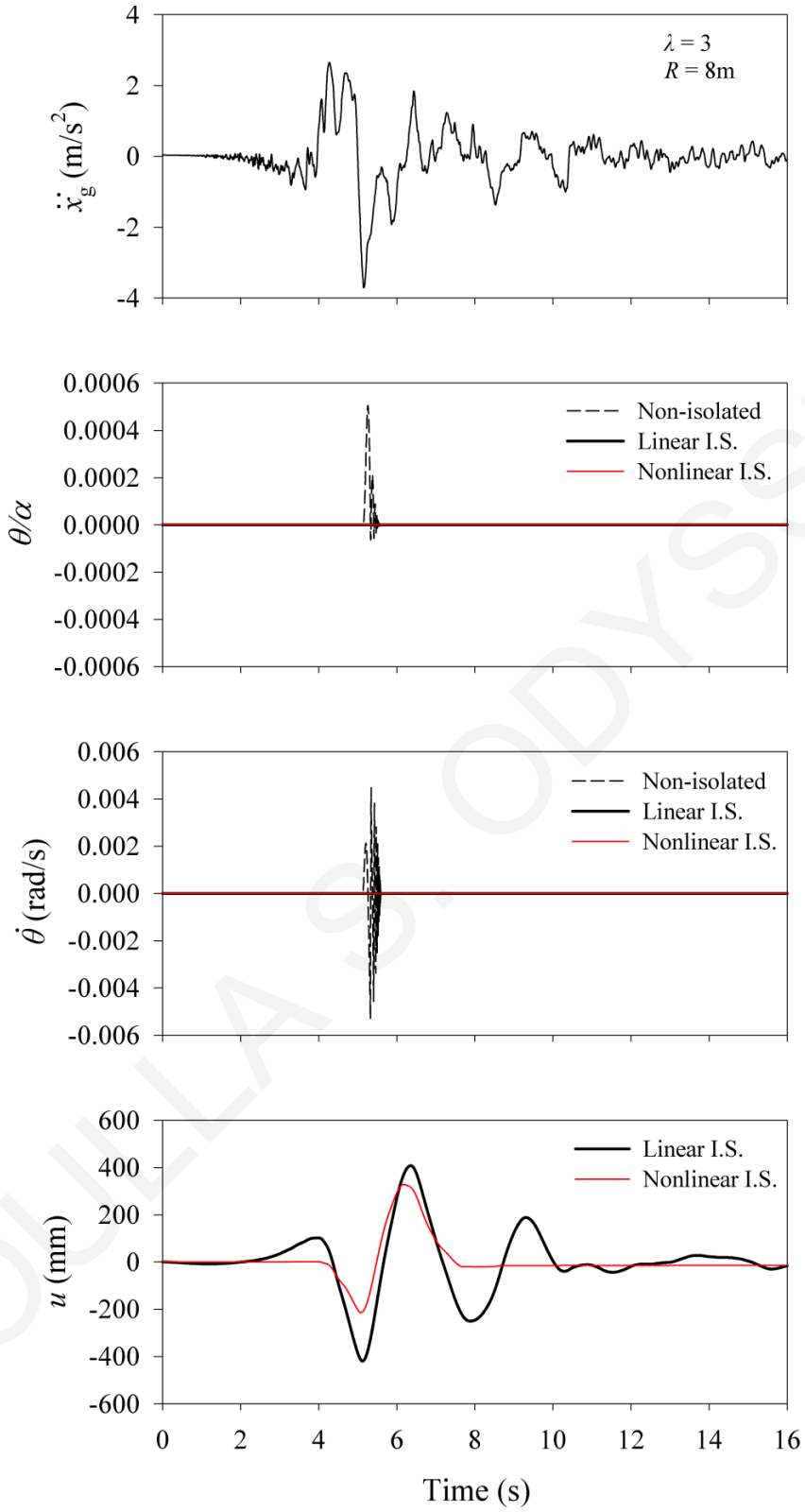

Figure C-23: Response histories for non-isolated and isolated rigid block under the SN component of 1979 Imperial Valley (EMO station), CA, USA earthquake ($\rho = 0.5$, $\lambda = 3$, $R = 8$m).

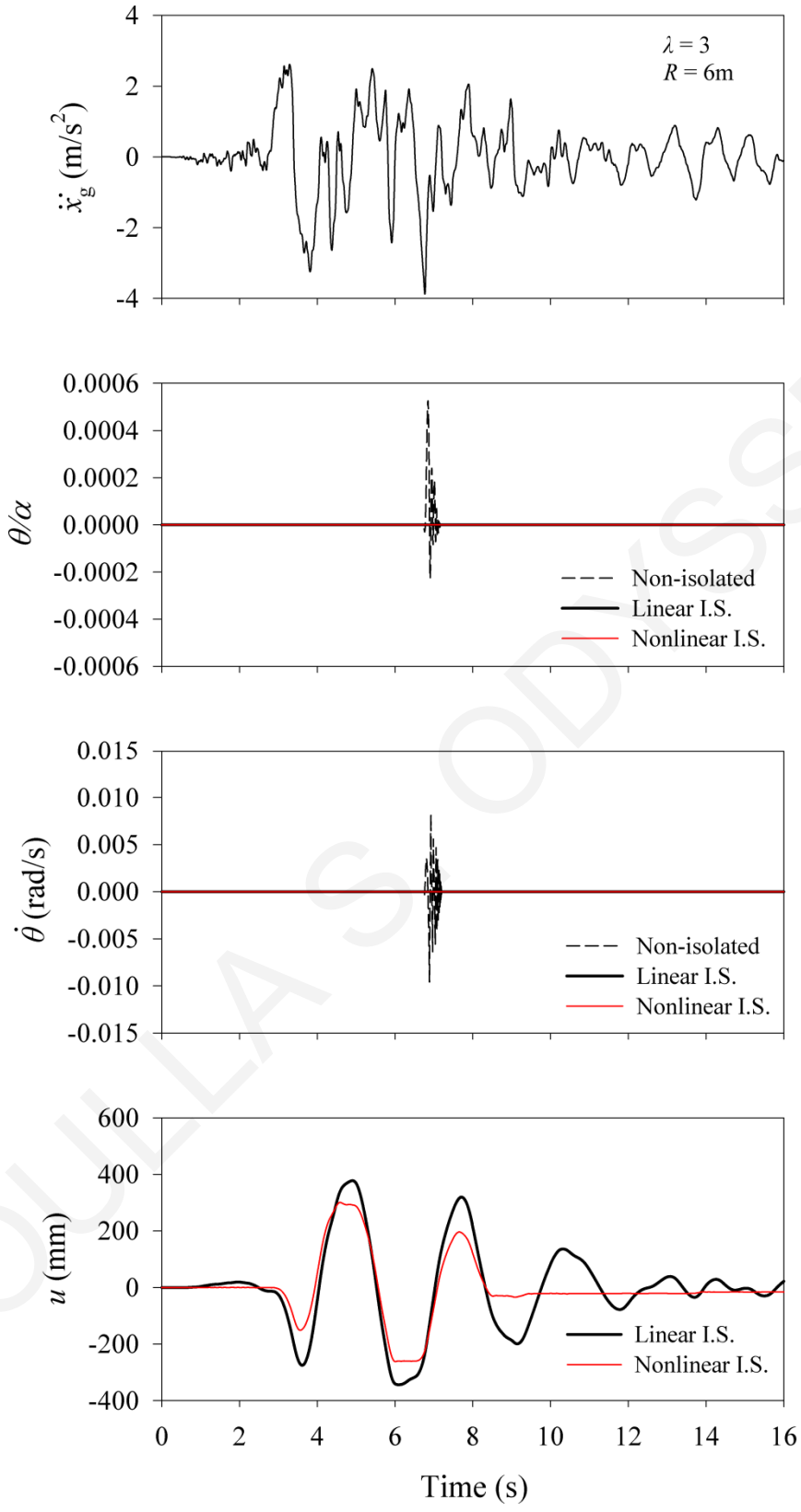

Figure C-24: Response histories for non-isolated and isolated rigid block under the SN component of 1994 Northridge (JFA station), CA, USA earthquake (ρ = 0.5, λ = 3, R = 6m).

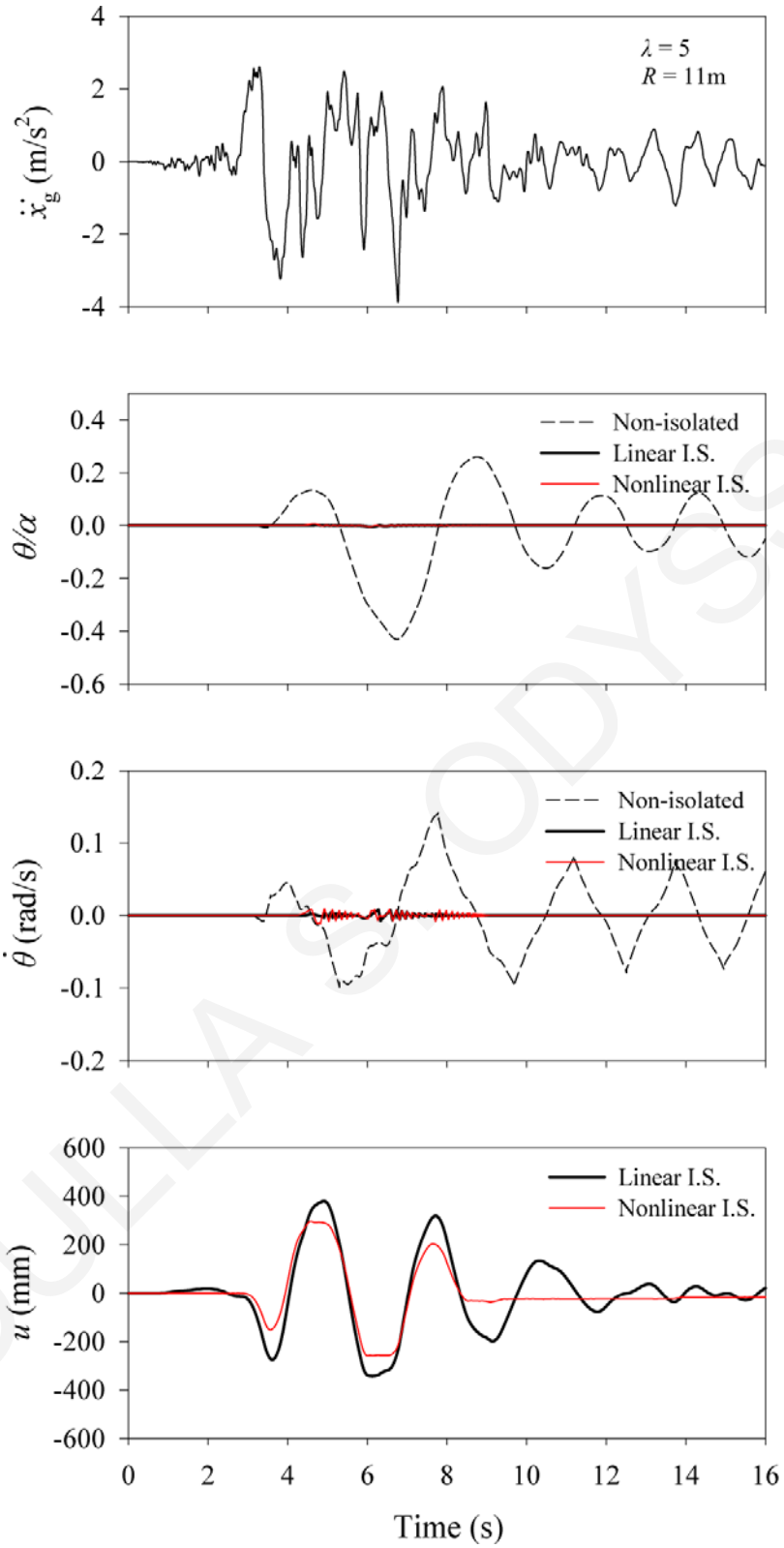

Figure C-25: Response histories for non-isolated and isolated rigid block under the SN component of 1994 Northridge (JFA station), CA, USA earthquake ($\rho = 0.5$, $\lambda = 5$, $R = 11$m).

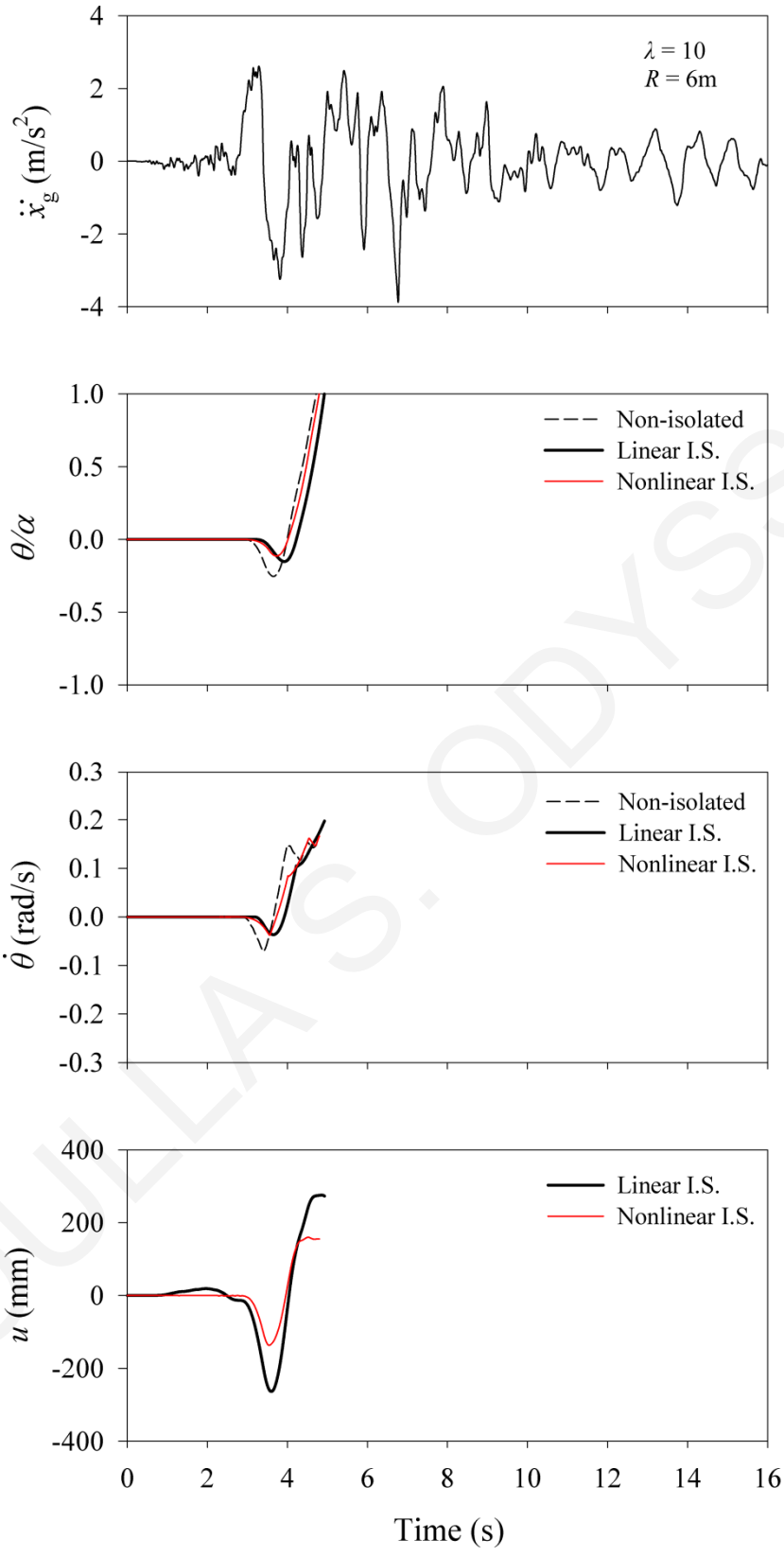

Figure C-26: Response histories for non-isolated and isolated rigid block under the SN component of 1994 Northridge (JFA station), CA, USA earthquake ($\rho = 0.5$, $\lambda = 10$, $R = 6$m).

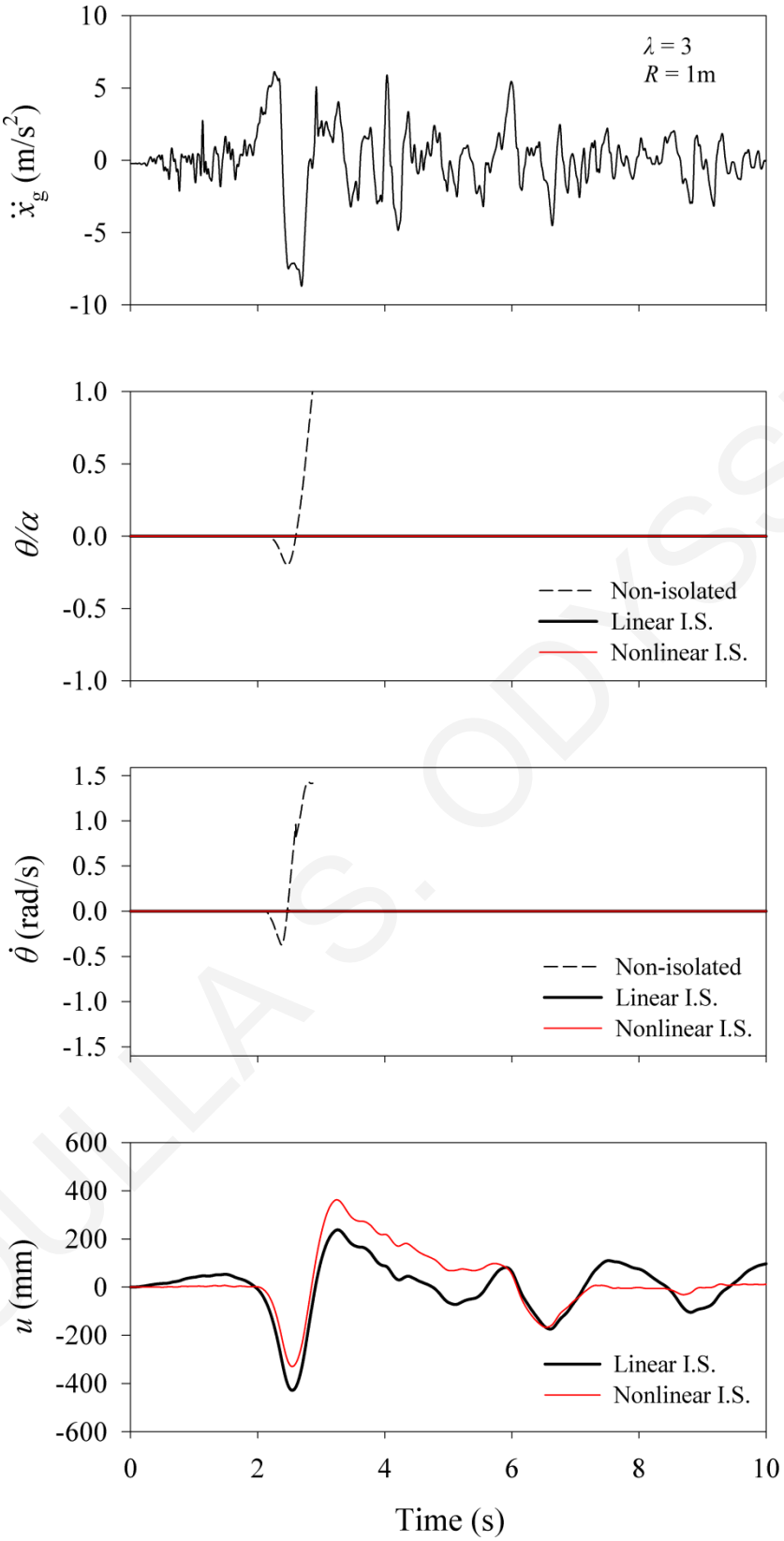

Figure C-27: Response histories for non-isolated and isolated rigid block under the SN component of 1994 Northridge (RRS station), CA, USA earthquake ($\rho = 0.5$, $\lambda = 3$, $R = 1$m).

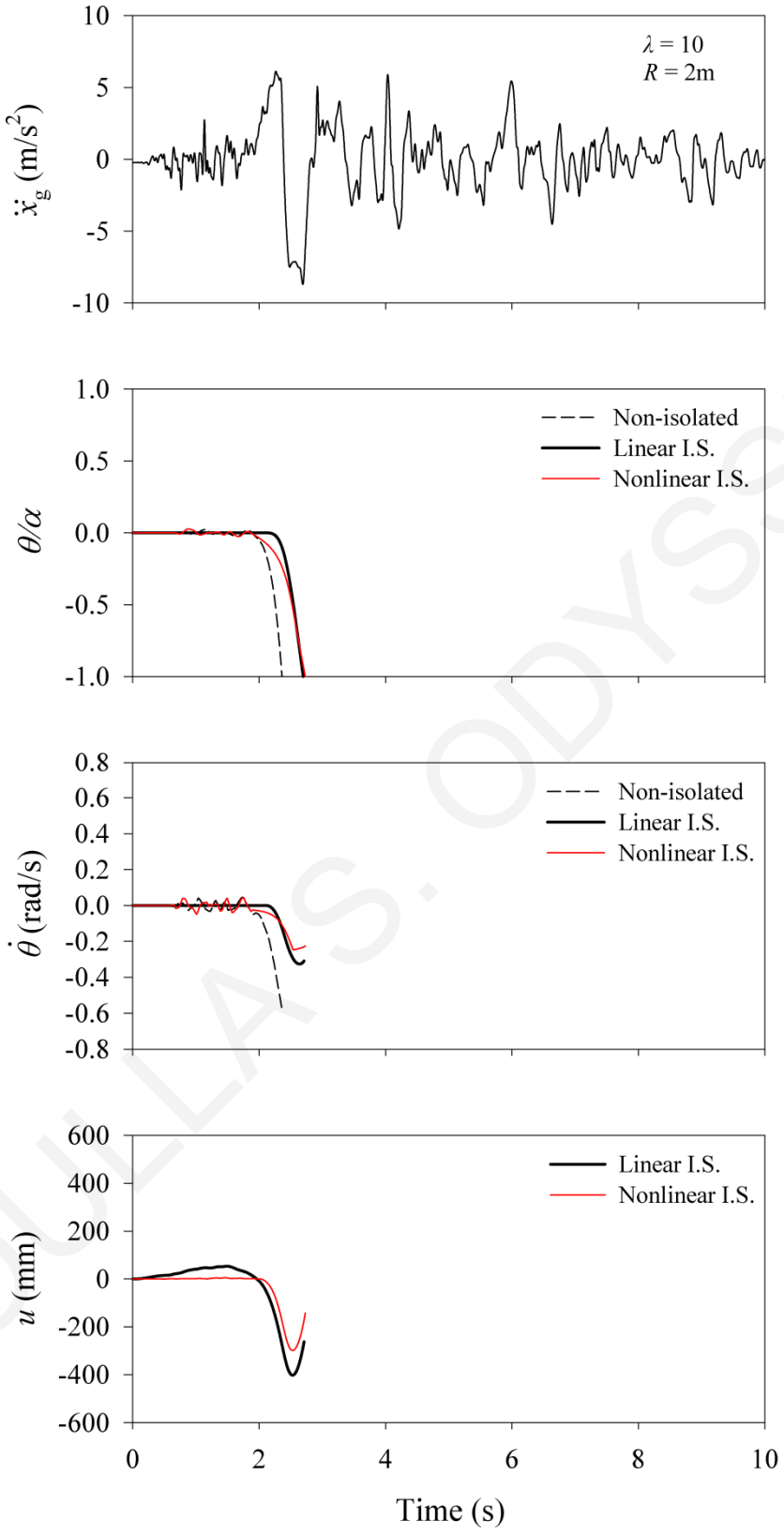

Figure C-28: Response histories for non-isolated and isolated rigid block under the SN component of 1994 Northridge (RRS station), CA, USA earthquake ($\rho = 0.5$, $\lambda = 10$, $R = 2$m).

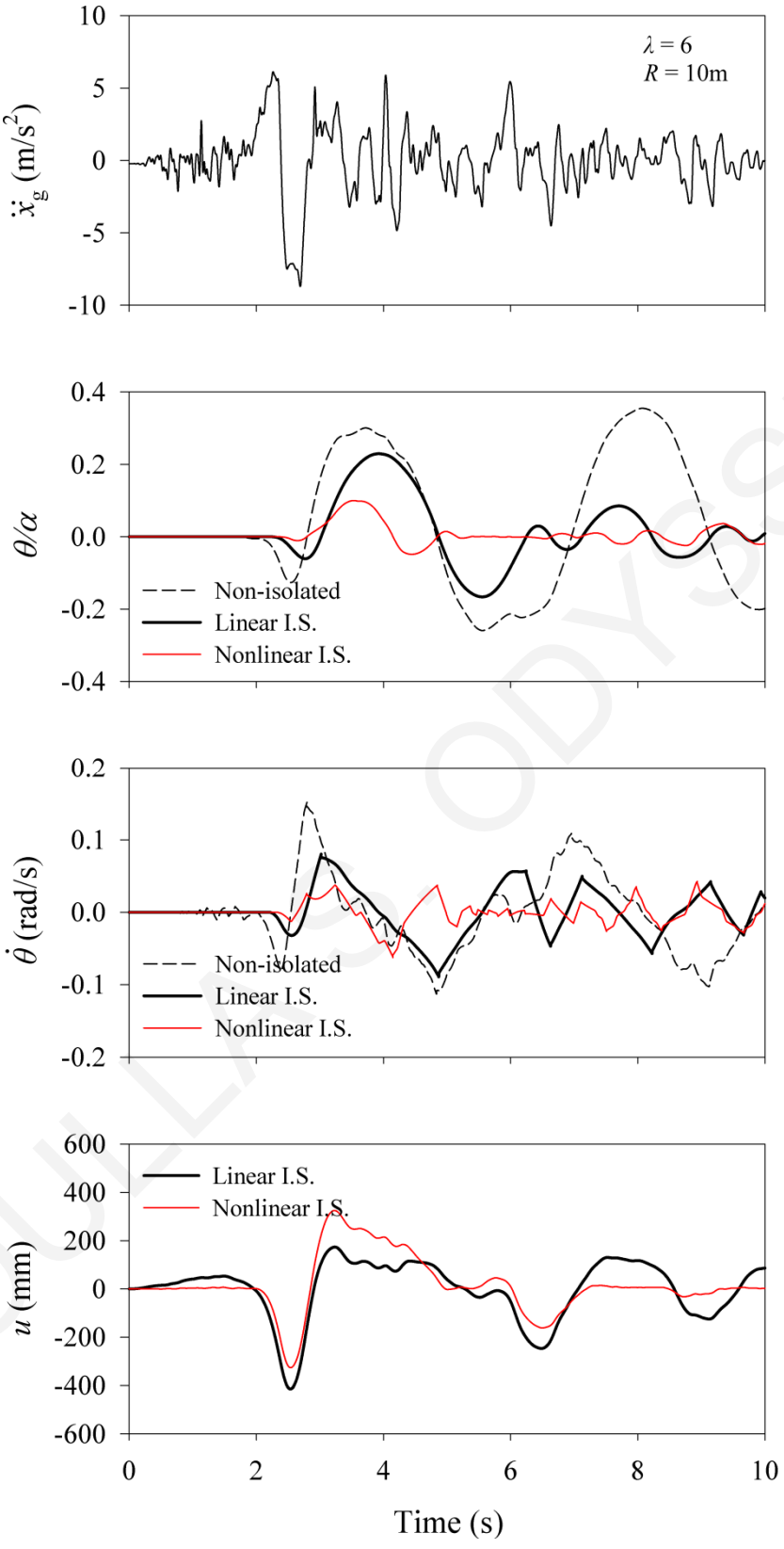

Figure C-29: Response histories for non-isolated and isolated rigid block under the SN component of 1994 Northridge (RRS station), CA, USA earthquake ($\rho = 0.5$, $\lambda = 6$, $R = 10$m).

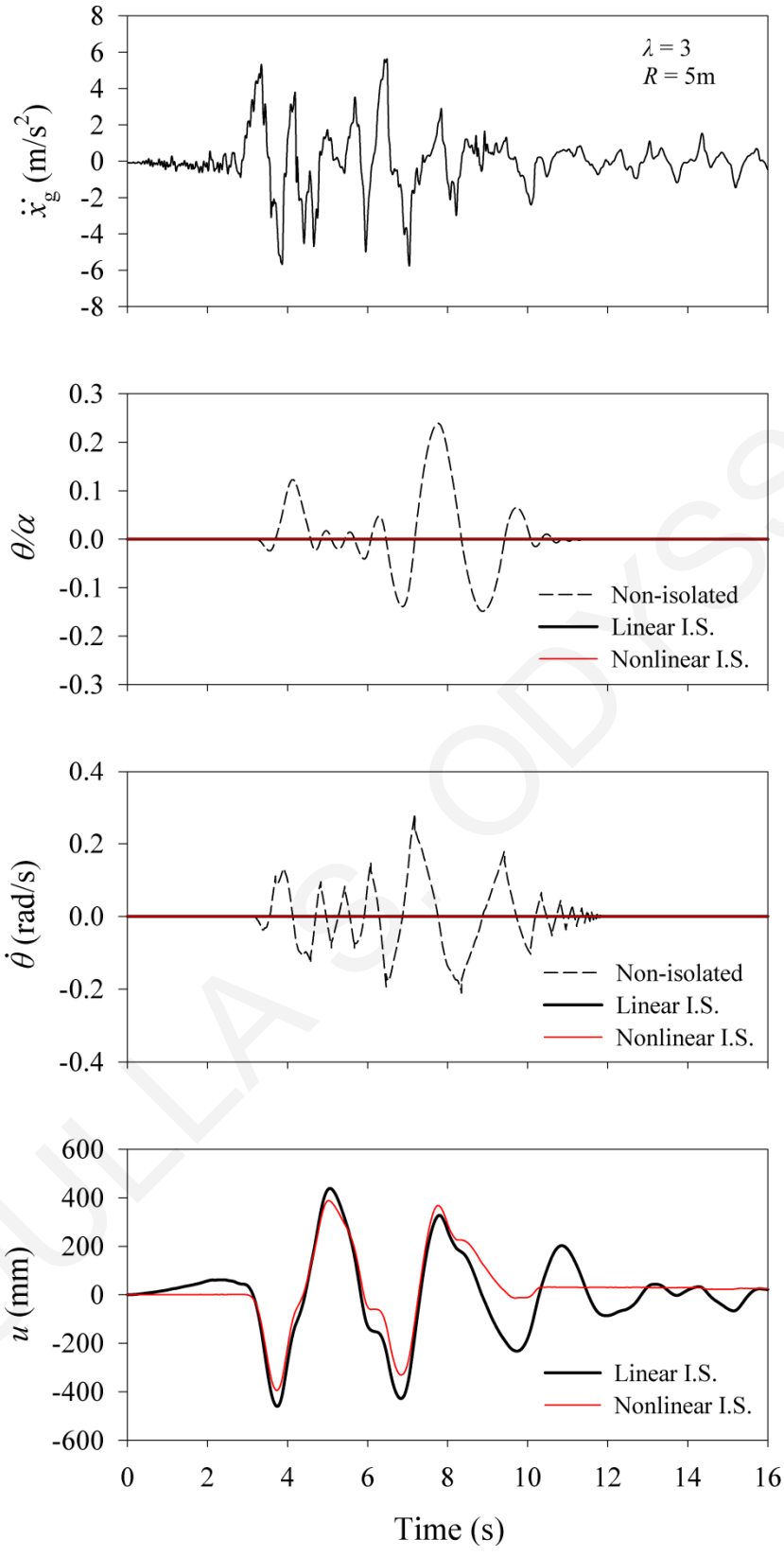

Figure C-30: Response histories for non-isolated and isolated rigid block under the SN component of 1994 Northridge (SCG station), CA, USA earthquake ($\rho = 0.5$, $\lambda = 3$, $R = 5$m).

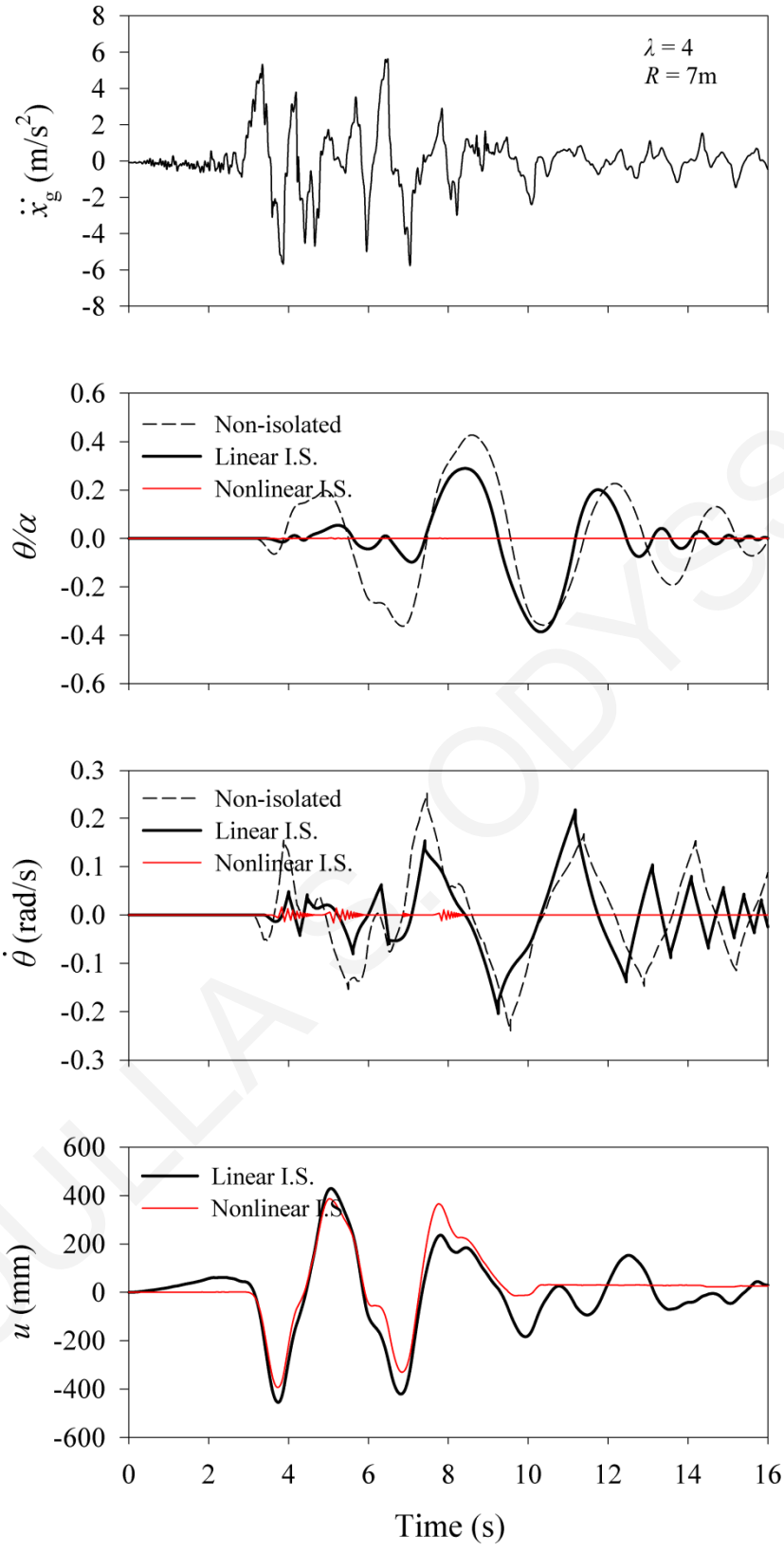

Figure C-31: Response histories for non-isolated and isolated rigid block under the SN component of 1994 Northridge (SCG station), CA, USA earthquake ($\rho = 0.5$, $\lambda = 4$, $R = 7$m).

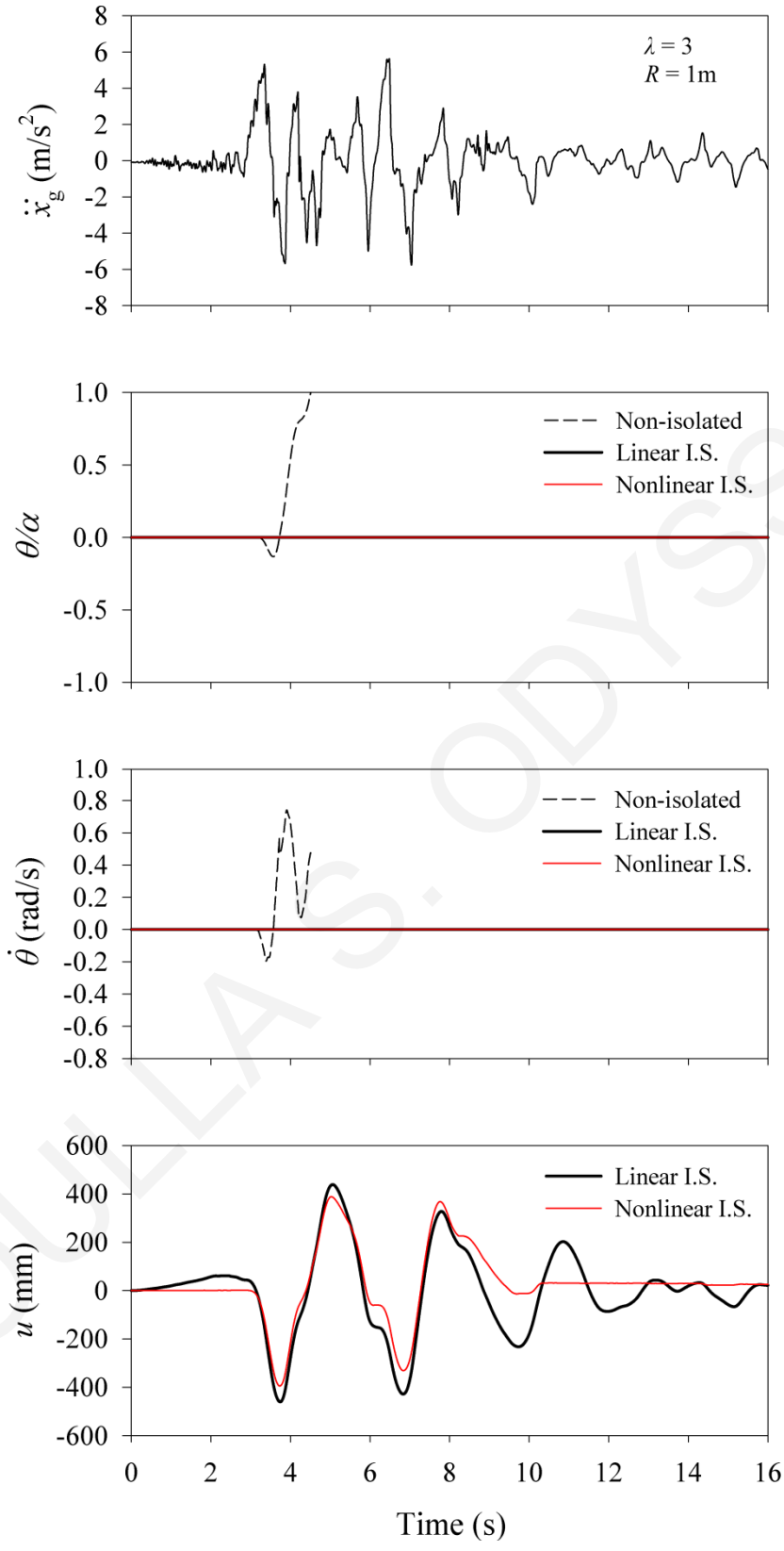

Figure C-32: Response histories for non-isolated and isolated rigid block under the SN component of 1994 Northridge (SCG station), CA, USA earthquake ($\rho = 0.5$, $\lambda = 3$, $R = 1$m).

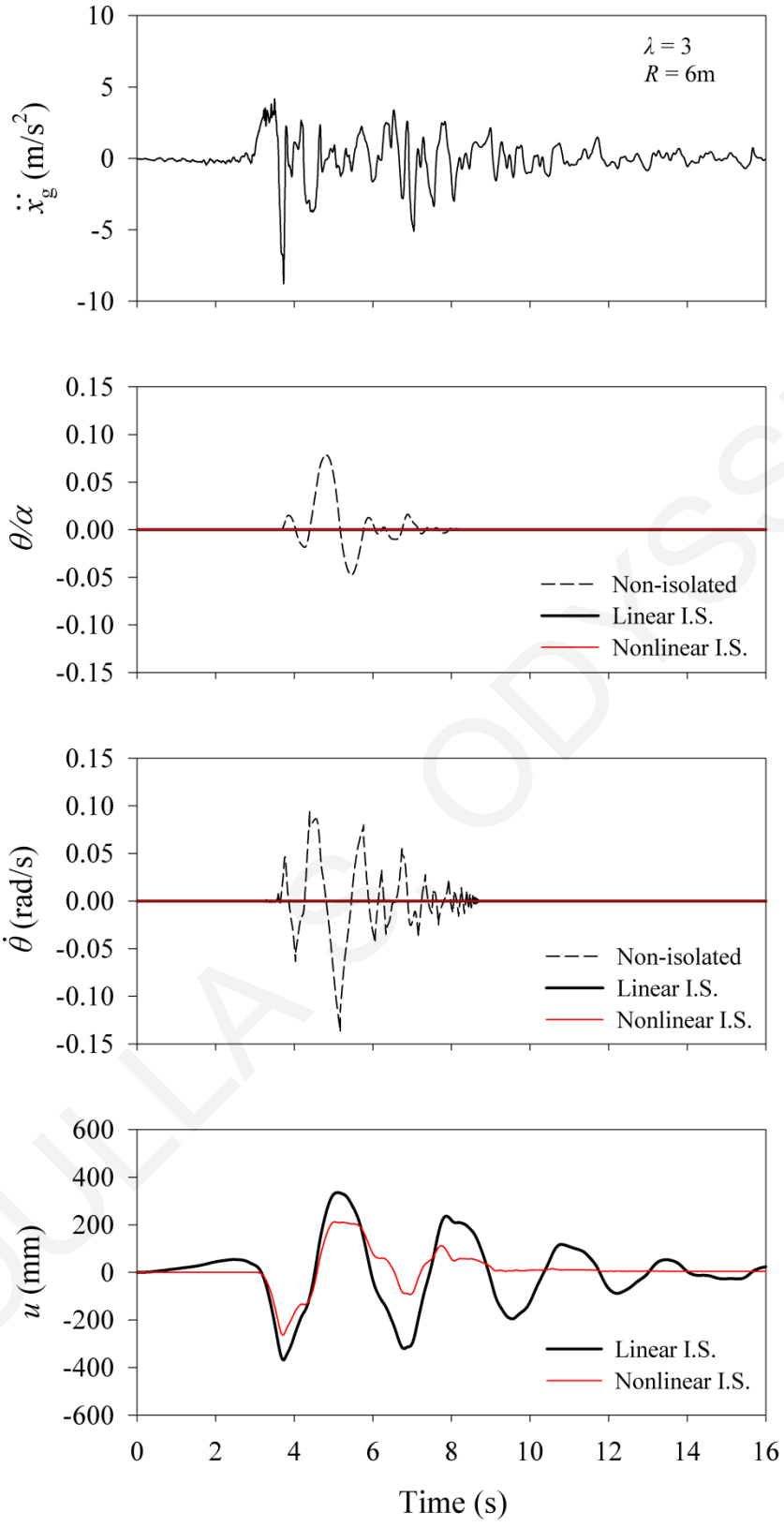

Figure C-33: Response histories for non-isolated and isolated rigid block under the SN component of 1994 Northridge (SCH station), CA, USA earthquake ($\rho = 0.5$, $\lambda = 3$, $R = 6$m).

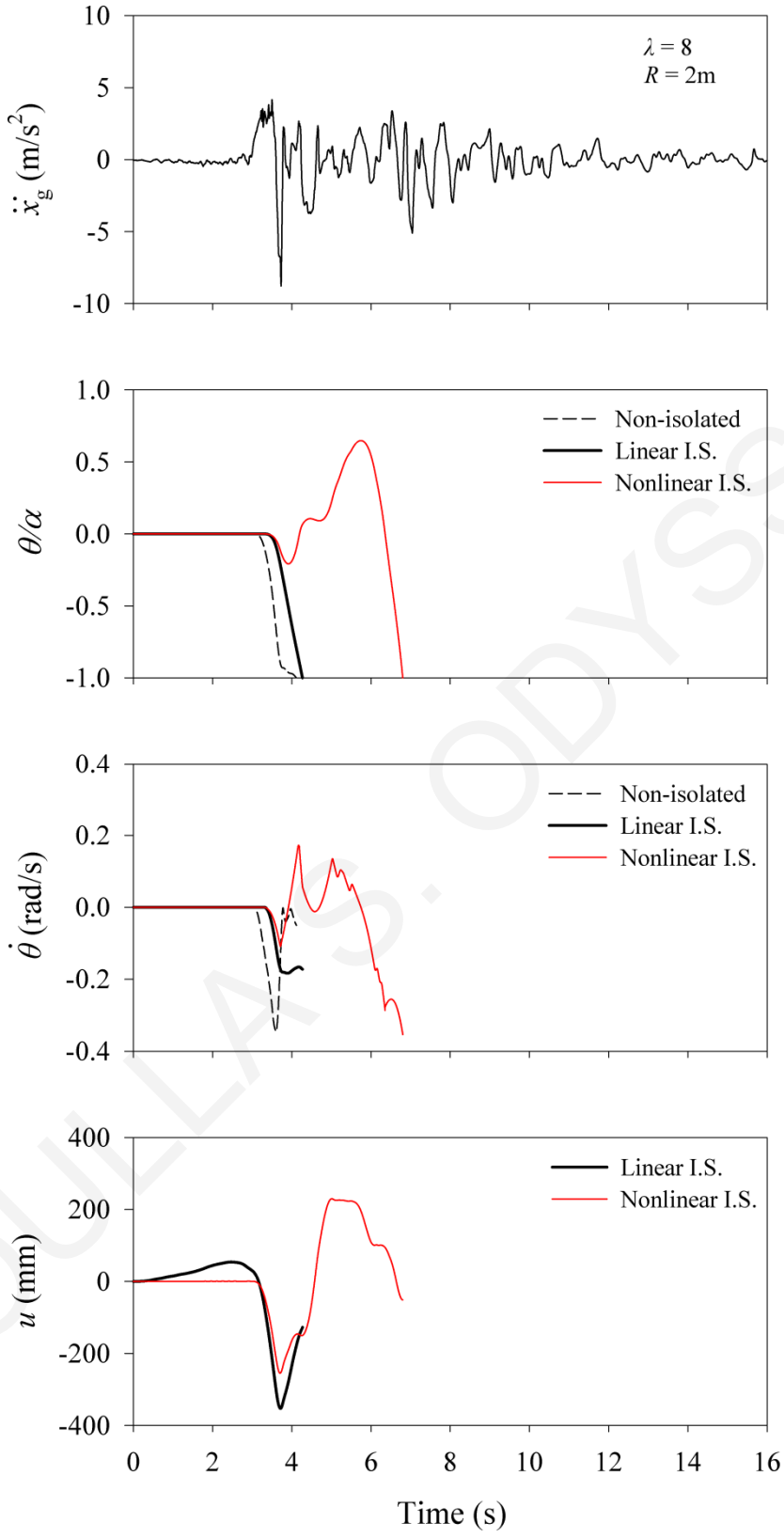

Figure C-34: Response histories for non-isolated and isolated rigid block under the SN component of 1994 Northridge (SCH station), CA, USA earthquake ($\rho = 0.5$, $\lambda = 8$, $R = 2$m).

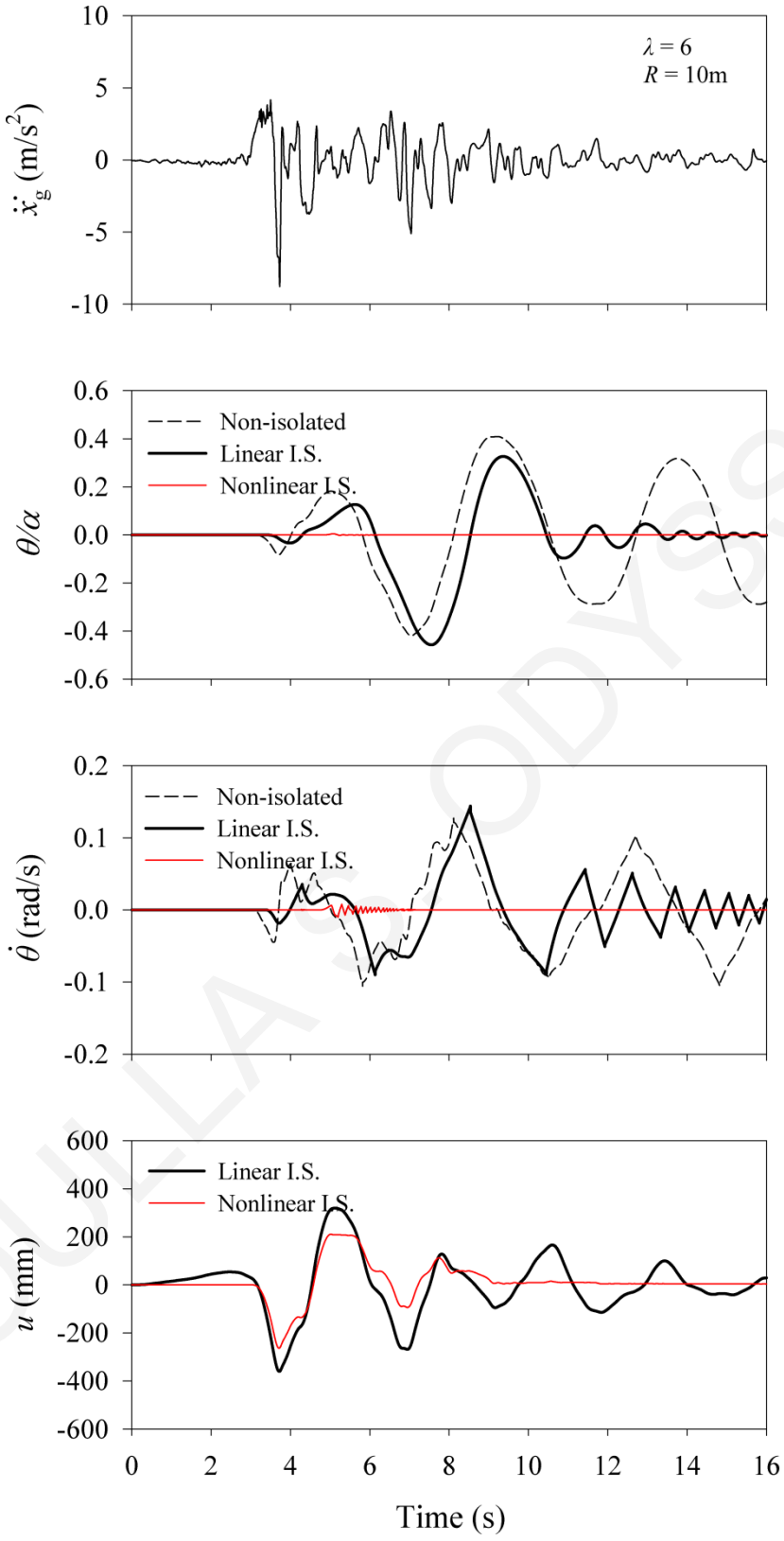

Figure C-35: Response histories for non-isolated and isolated rigid block under the SN component of 1994 Northridge (SCH station), CA, USA earthquake ($\rho = 0.5$, $\lambda = 6$, $R = 10$m).

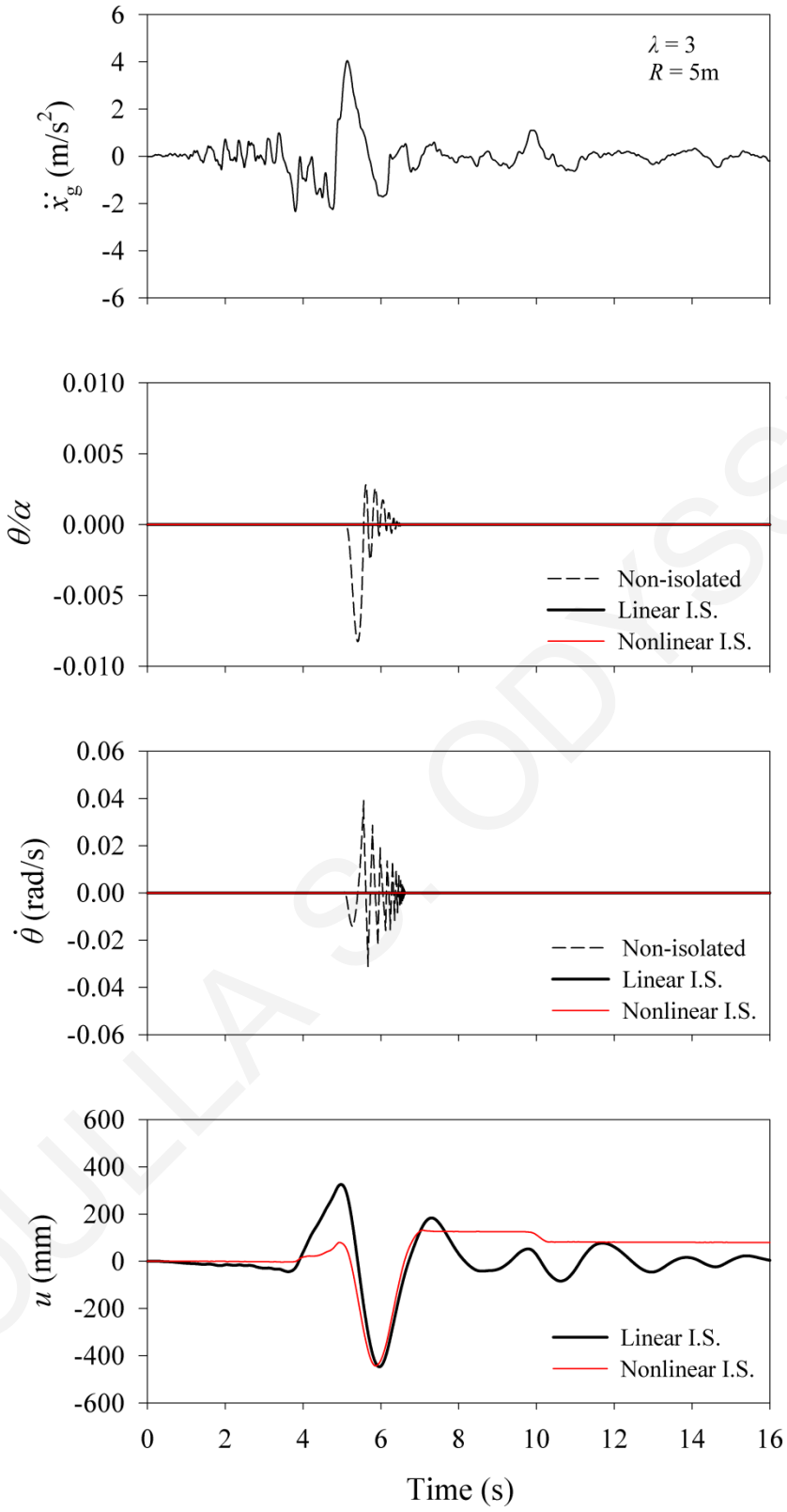

Figure C-36: Response histories for non-isolated and isolated rigid block under the SN component of 1994 Northridge (NWS station), CA, USA earthquake ($\rho = 0.5$, $\lambda = 3$, $R = 5$m).

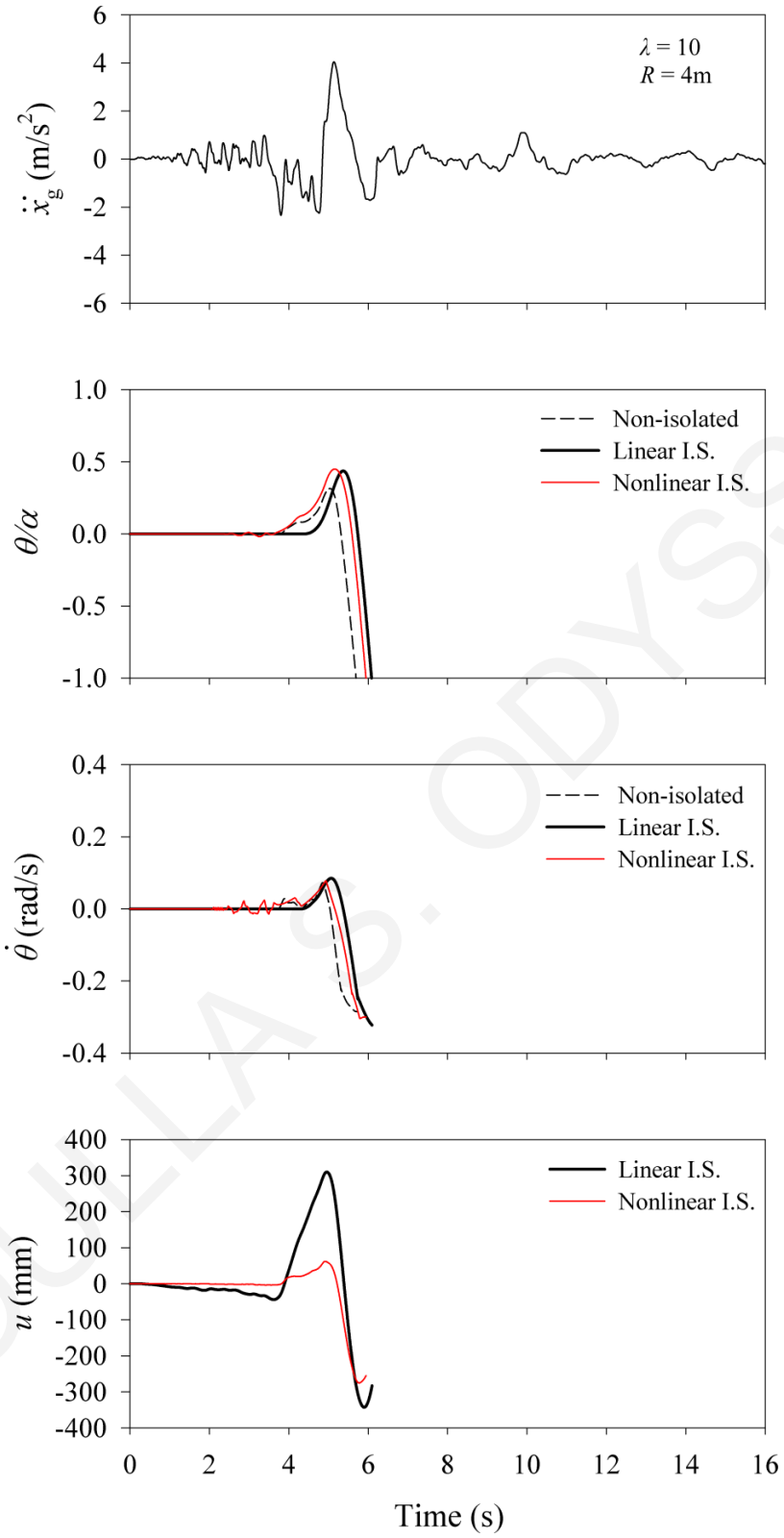

Figure C-37: Response histories for non-isolated and isolated rigid block under the SN component of 1994 Northridge (NWS station), CA, USA earthquake ($\rho = 0.5$, $\lambda = 10$, $R = 4$m).

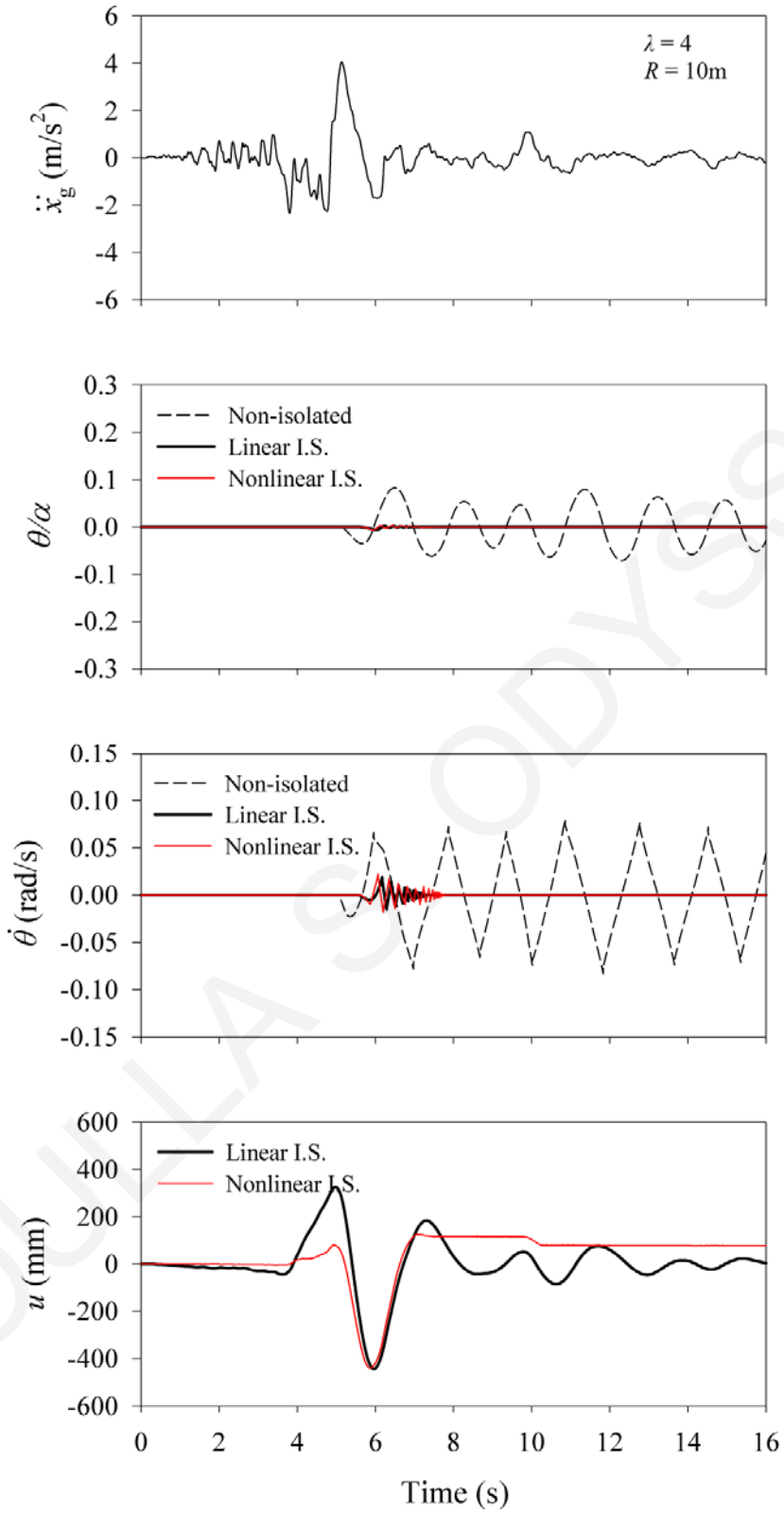

Figure C-38: Response histories for non-isolated and isolated rigid block under the SN component of 1994 Northridge (NWS station), CA, USA earthquake ($\rho = 0.5$, $\lambda = 4$, $R = 10$m).

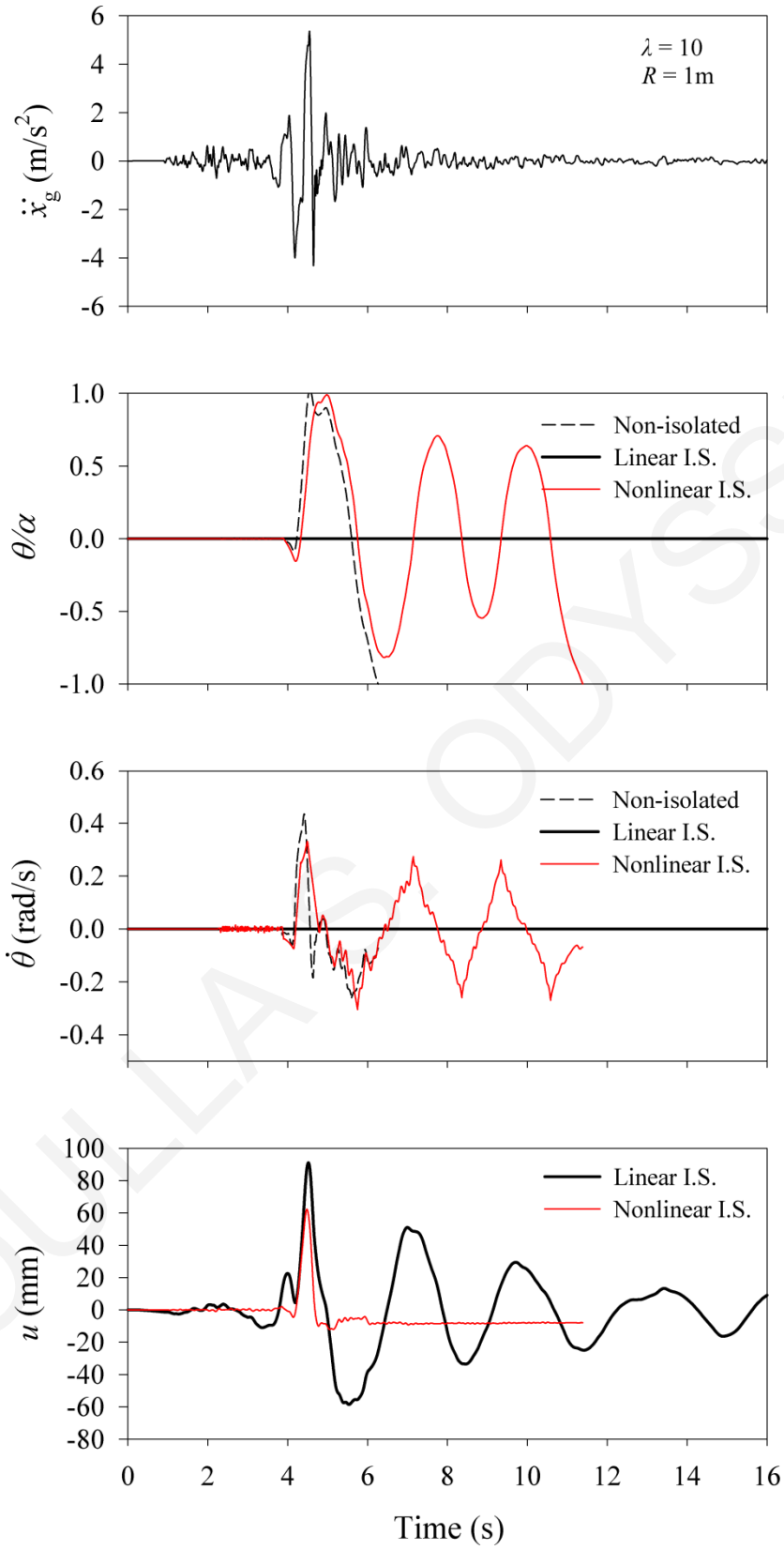

Figure C-39: Response histories for non-isolated and isolated rigid block under the Tran component of 1995 Aigion (AEG station), Greece earthquake ($\rho = 0.5$, $\lambda = 10$, $R = 1$m).

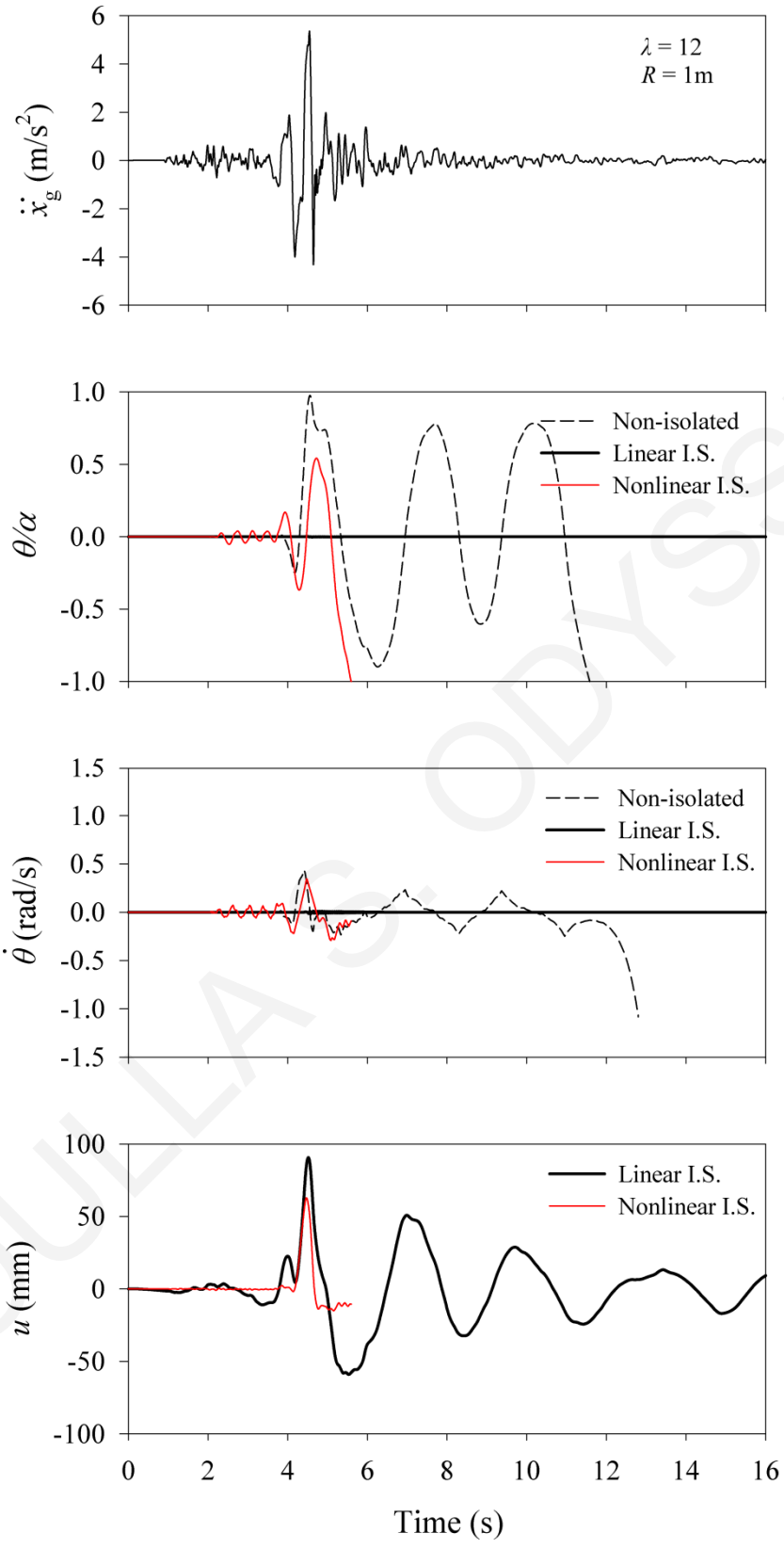

Figure C-40: Response histories for non-isolated and isolated rigid block under the Tran component of 1995 Aigion (AEG station), Greece earthquake (ρ = 0.5, λ = 12, R = 1m).

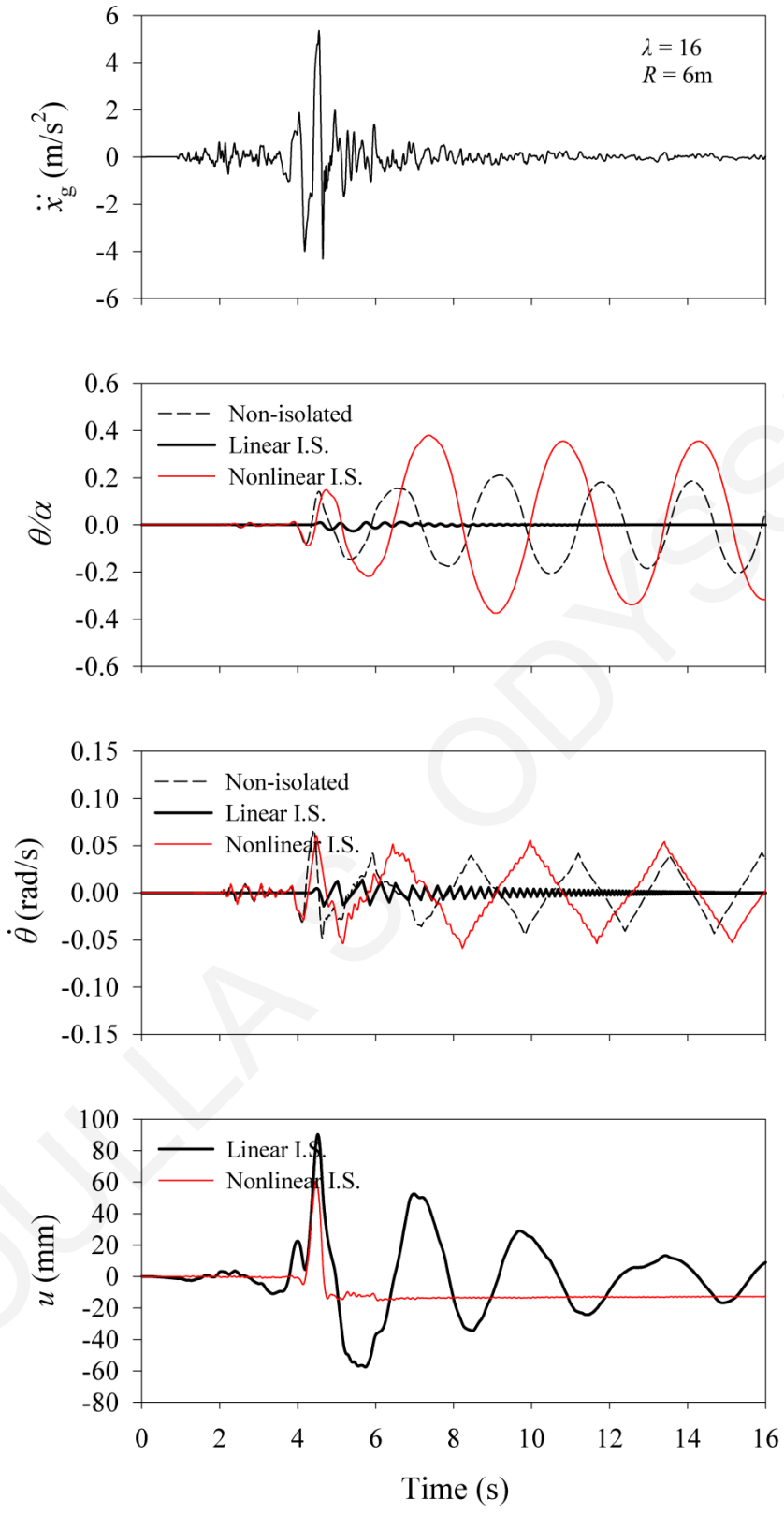

Figure C-41: Response histories for non-isolated and isolated rigid block under the Tran component of 1995 Aigion (AEG station), Greece earthquake (ρ = 0.5, λ = 16, R = 6m).

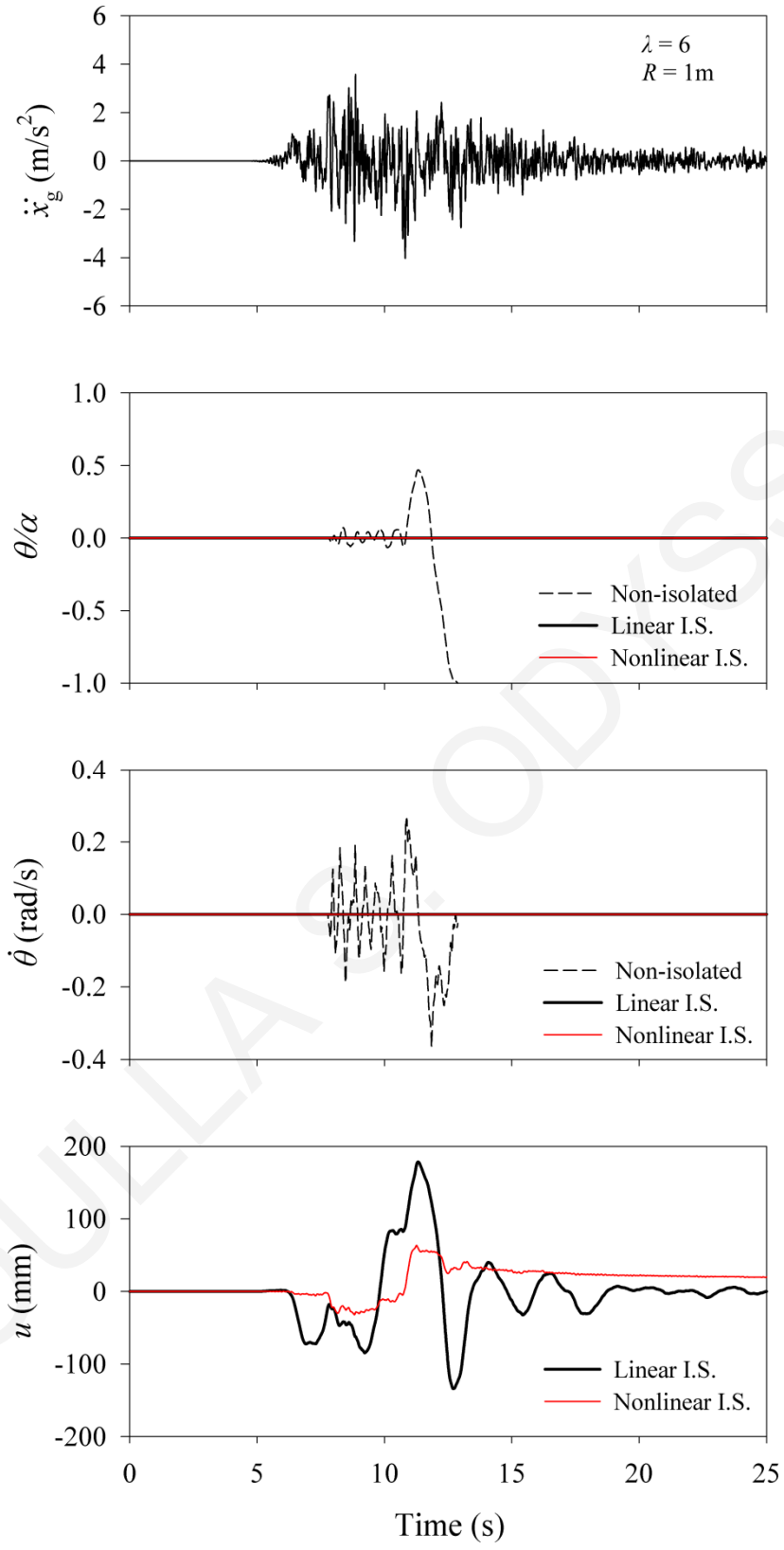

Figure C-42: Response histories for non-isolated and isolated rigid block under the SP component of 1999 Izmit (SKR station), Turkey earthquake (ρ = 0.5, λ = 6, R = 1m).

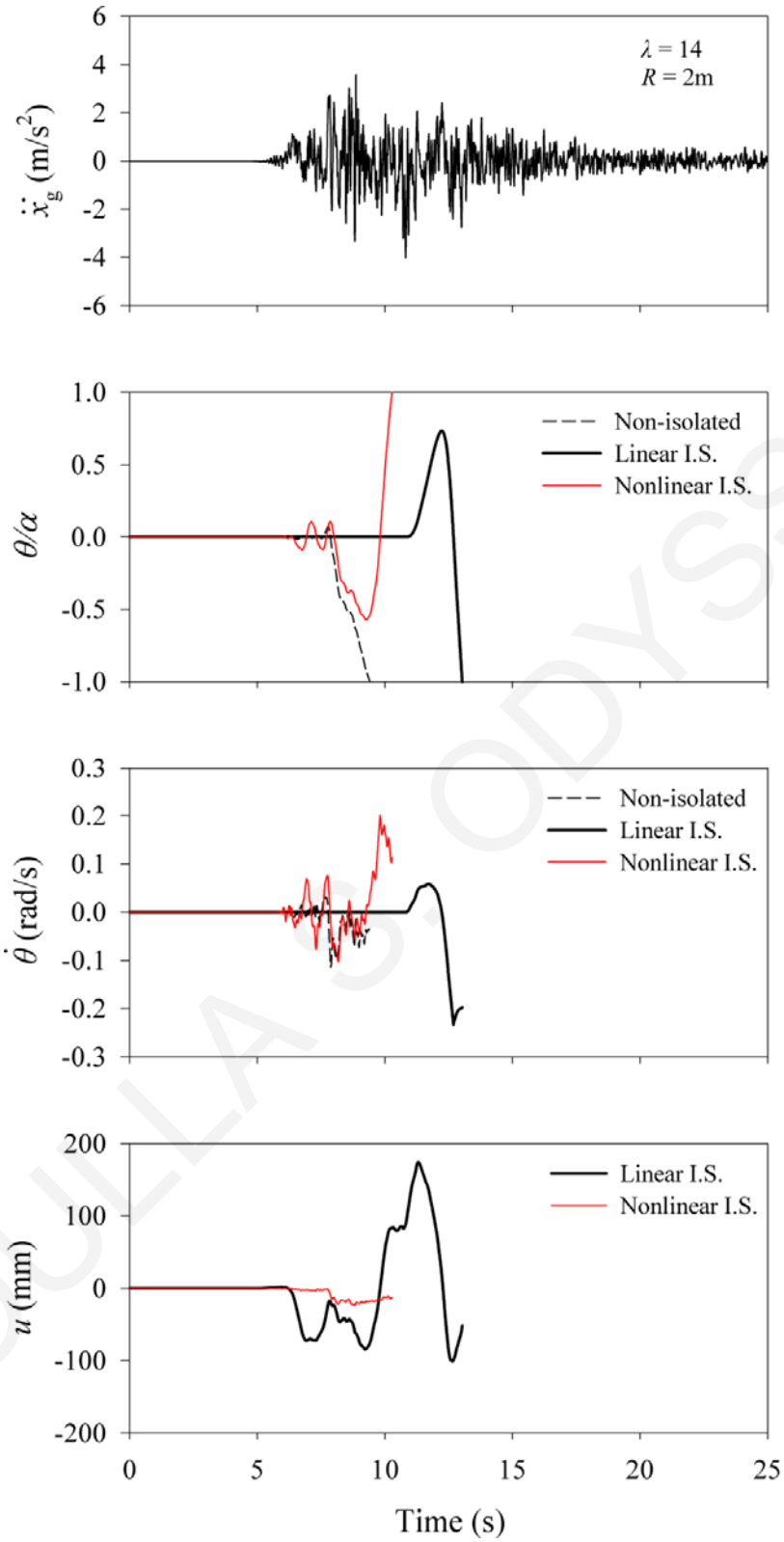

Figure C-43: Response histories for non-isolated and isolated rigid block under the SP component of 1999 Izmit (SKR station), Turkey earthquake ($\rho = 0.5$, $\lambda = 14$, $R = 2$m).

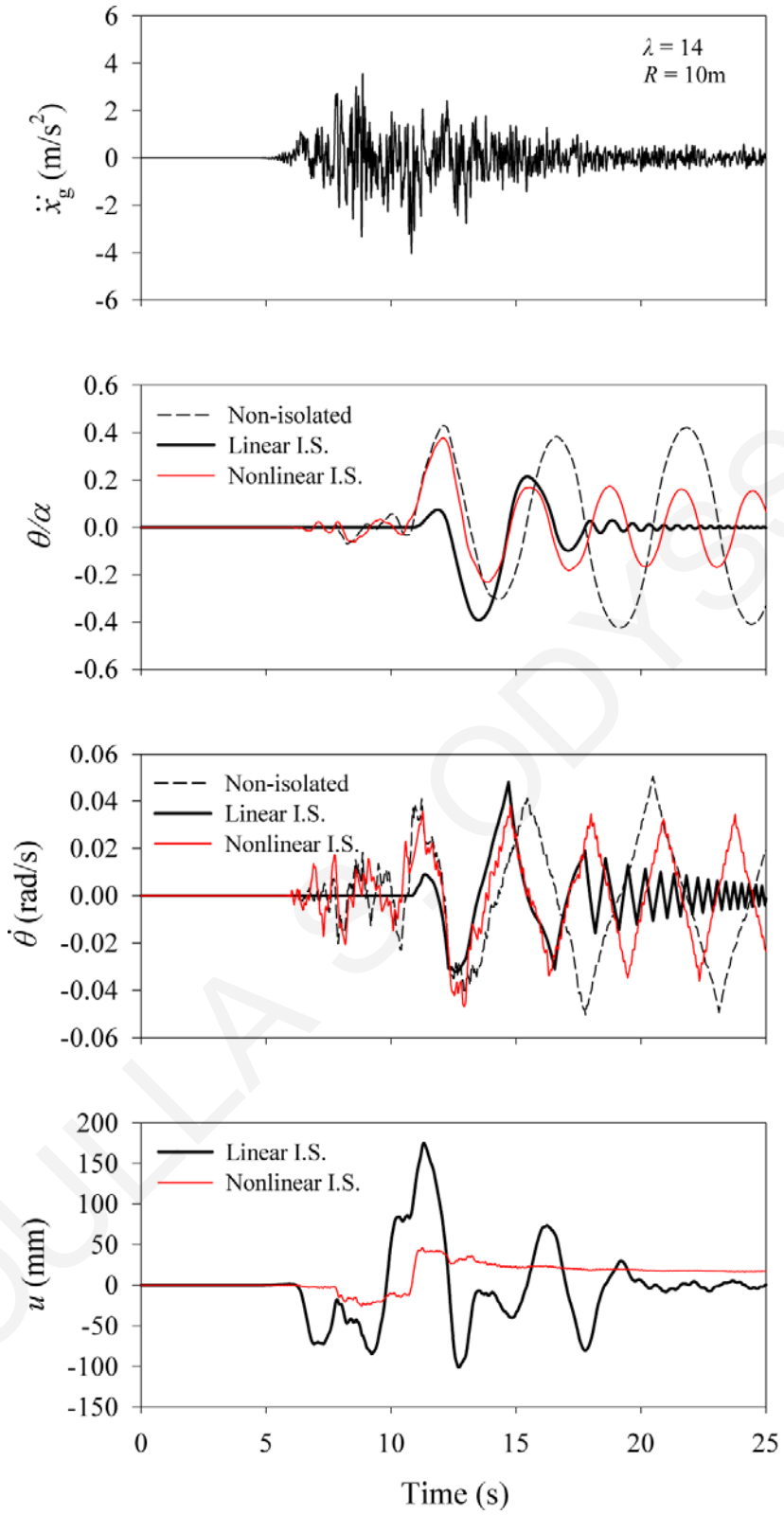

Figure C-44: Response histories for non-isolated and isolated rigid block under the SP component of 1999 Izmit (SKR station), Turkey earthquake ($\rho = 0.5$, $\lambda = 14$, $R = 10$m).

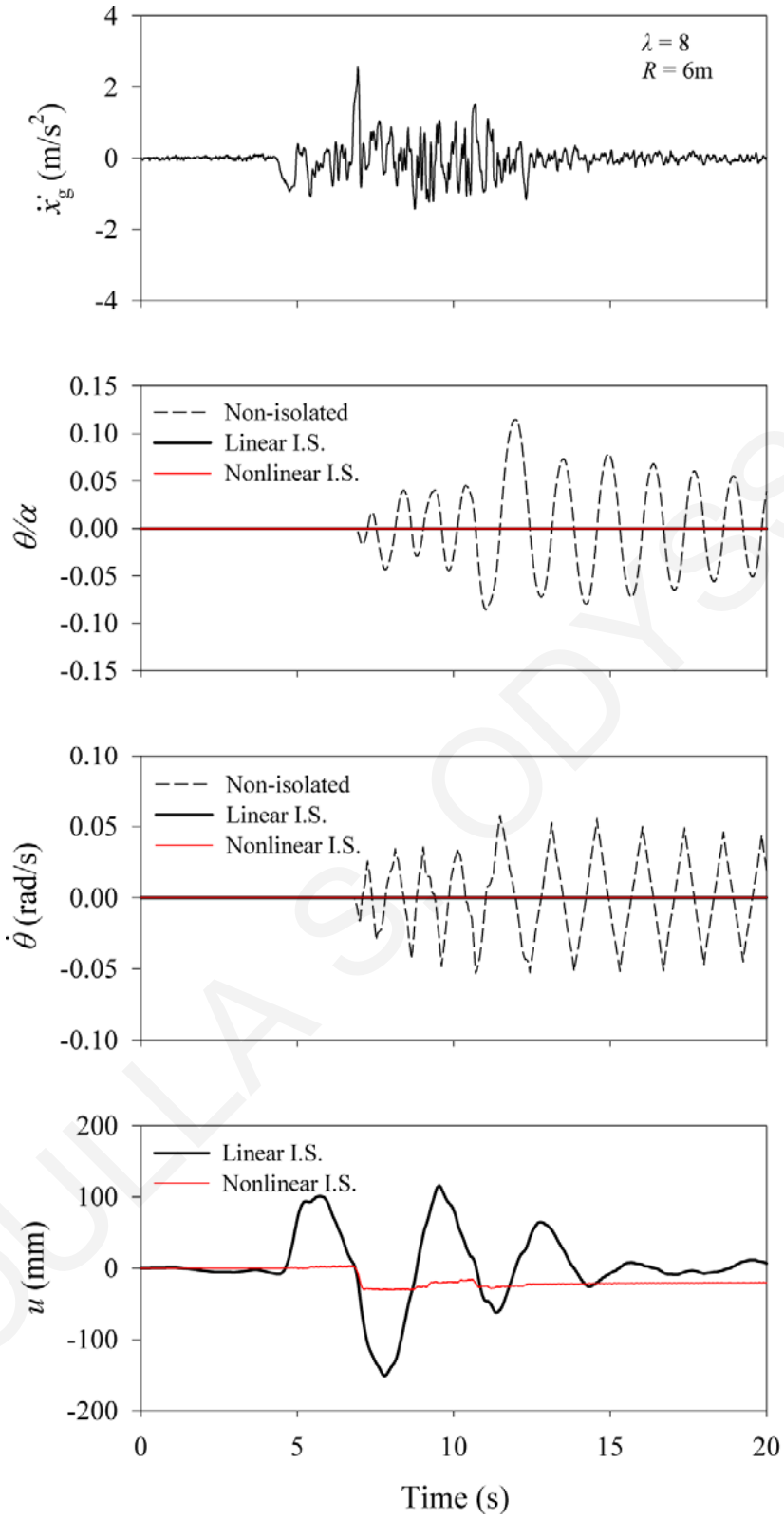

Figure C-45: Response histories for non-isolated and isolated rigid block under the SN component of 1999 Izmit (GBZ station), Turkey earthquake (ρ = 0.5, λ = 8, R = 6m).

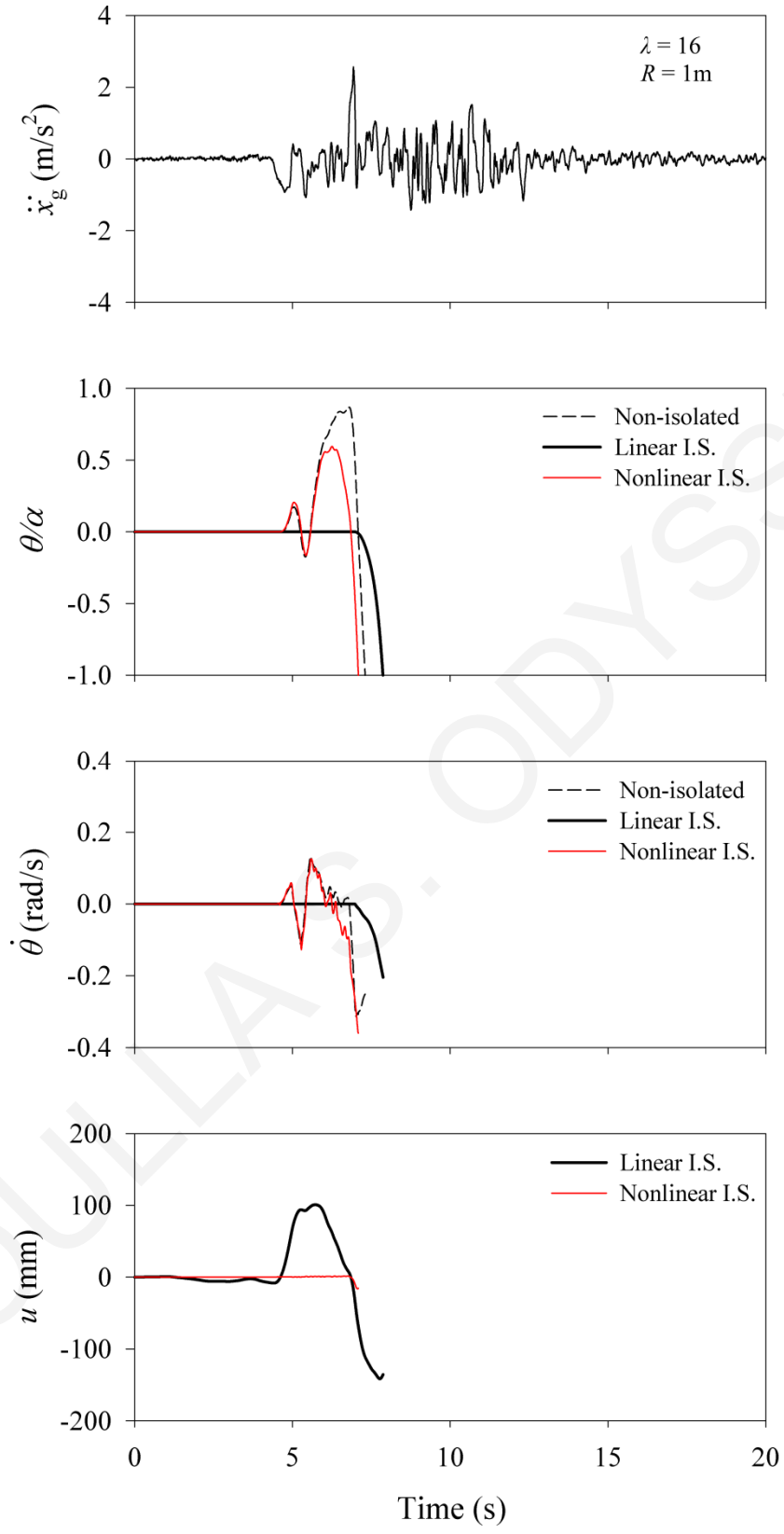

Figure C-46: Response histories for non-isolated and isolated rigid block under the SN component of 1999 Izmit (GBZ station), Turkey earthquake ($\rho = 0.5$, $\lambda = 16$, $R = 1$m).

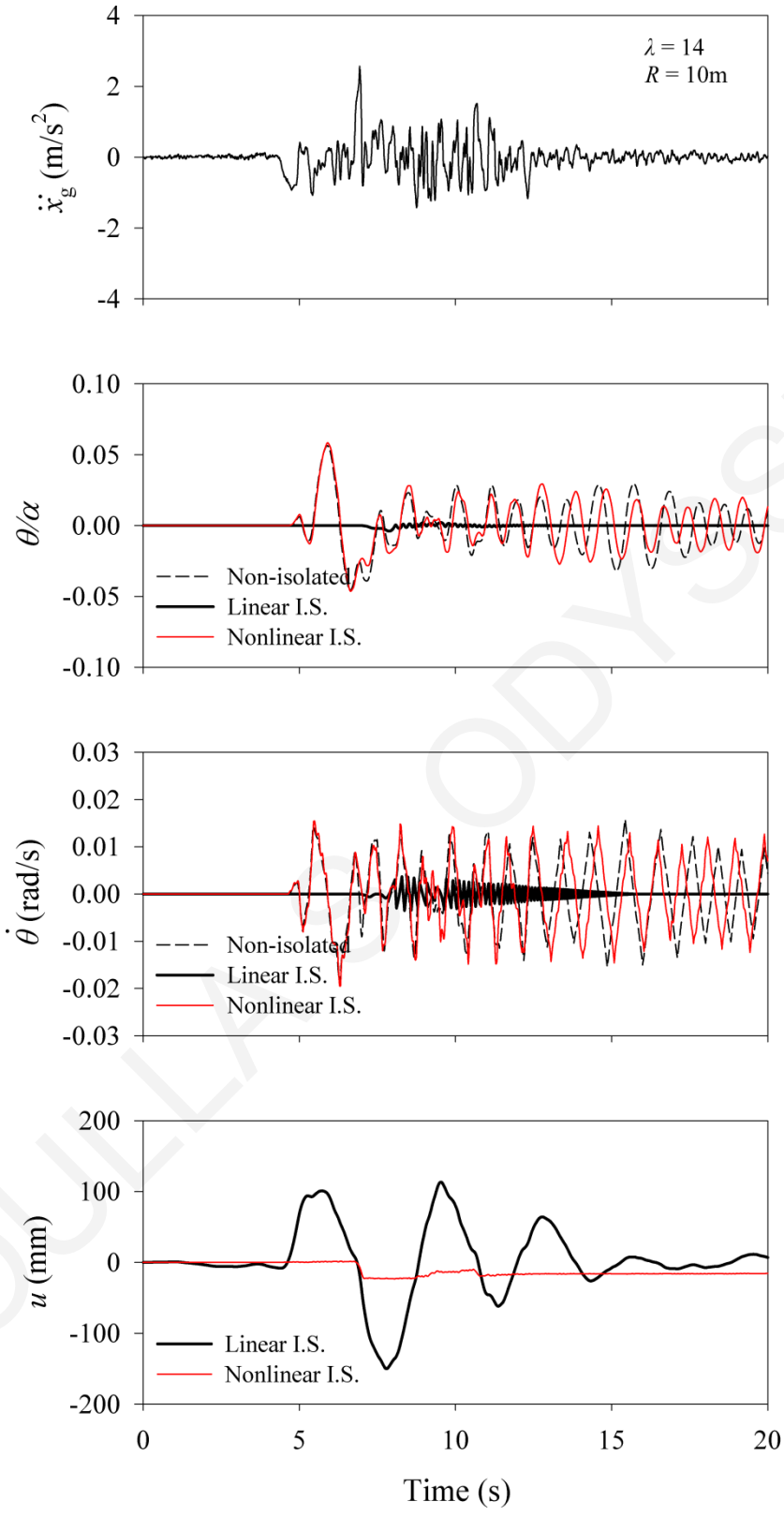

Figure C-47: Response histories for non-isolated and isolated rigid block under the SP component of 1999 Izmit (GBZ station), Turkey earthquake (ρ = 0.5, λ = 14, R = 10m).

APPENDIX D

Multi-Pattern Response-Regime Spectra for Non-Isolated and Isolated Blocks Using Linear Isolation System

Assuming sliding between the block and the supporting base, entailing a multi-pattern response, this appendix presents a numerous response-regime spectra in the $\lambda - R$ space for (a) non-isolated and (b) isolated blocks of varying geometric characteristics under earthquake excitations.

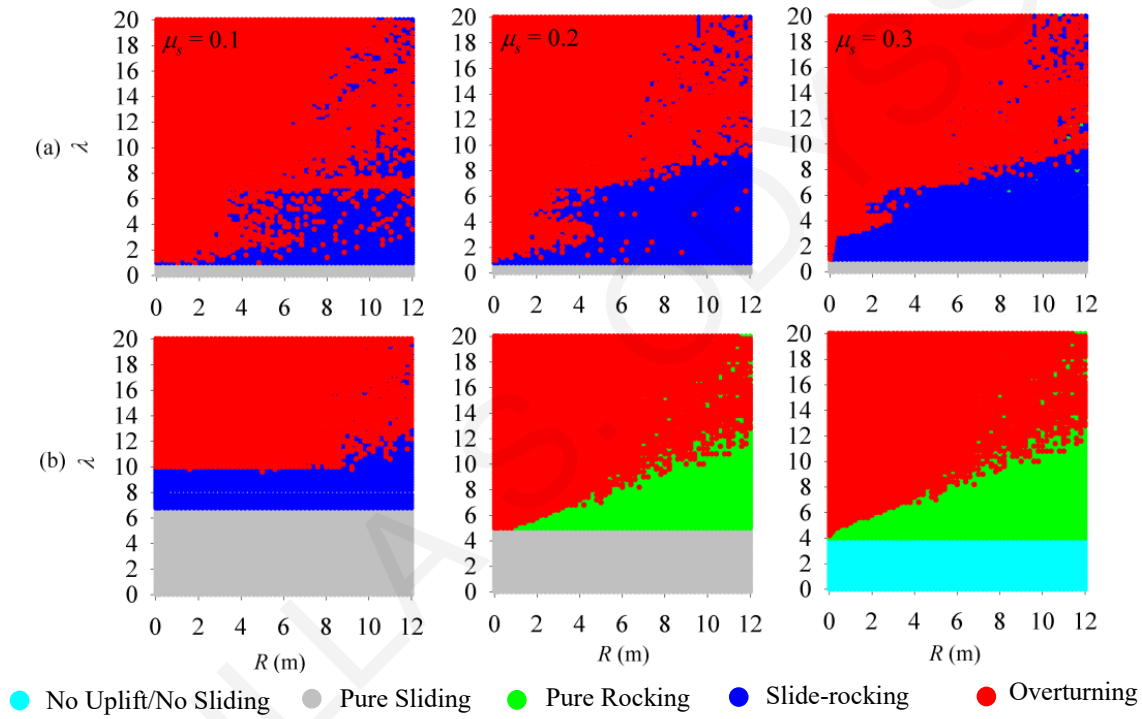

Figure D-1: Response-regime spectra in the $\lambda - R$ space for (a) non-isolated and (b) isolated block of varying geometric characteristics under San Fernando, PCD / SN record ($\rho = 0.5$).

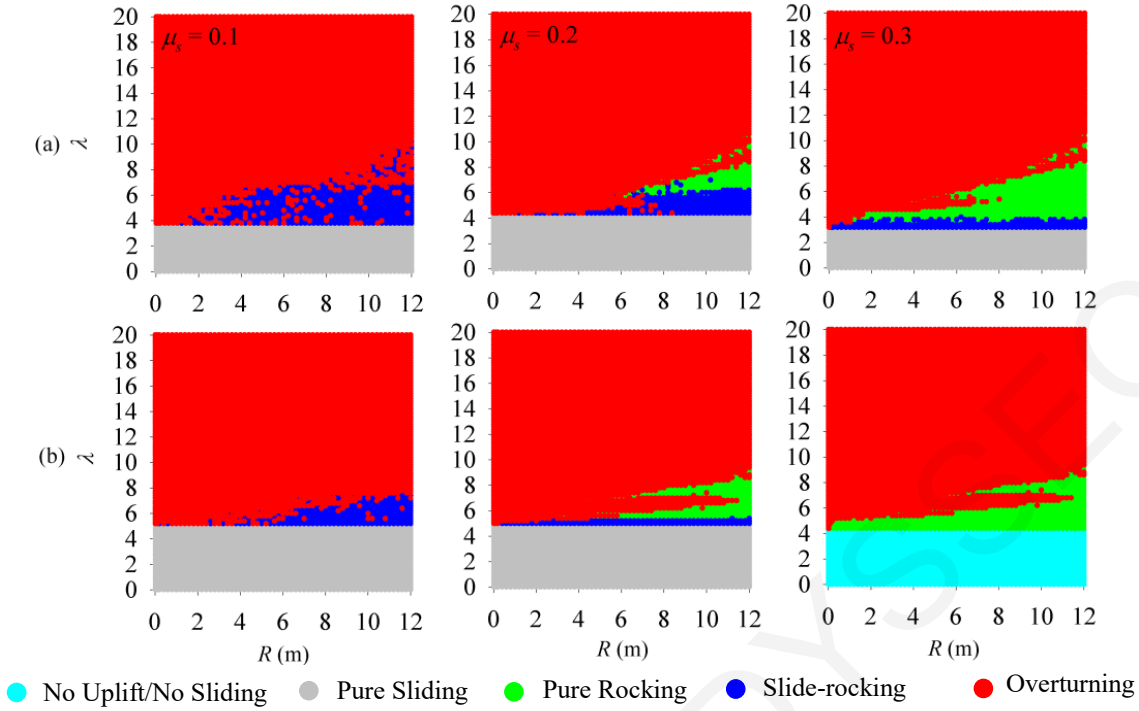

Figure D-2: Response-regime spectra in the $\lambda - R$ space for (a) non-isolated and (b) isolated block of varying geometric characteristics under Northridge, JFA / SN record ($\rho = 0.5$).

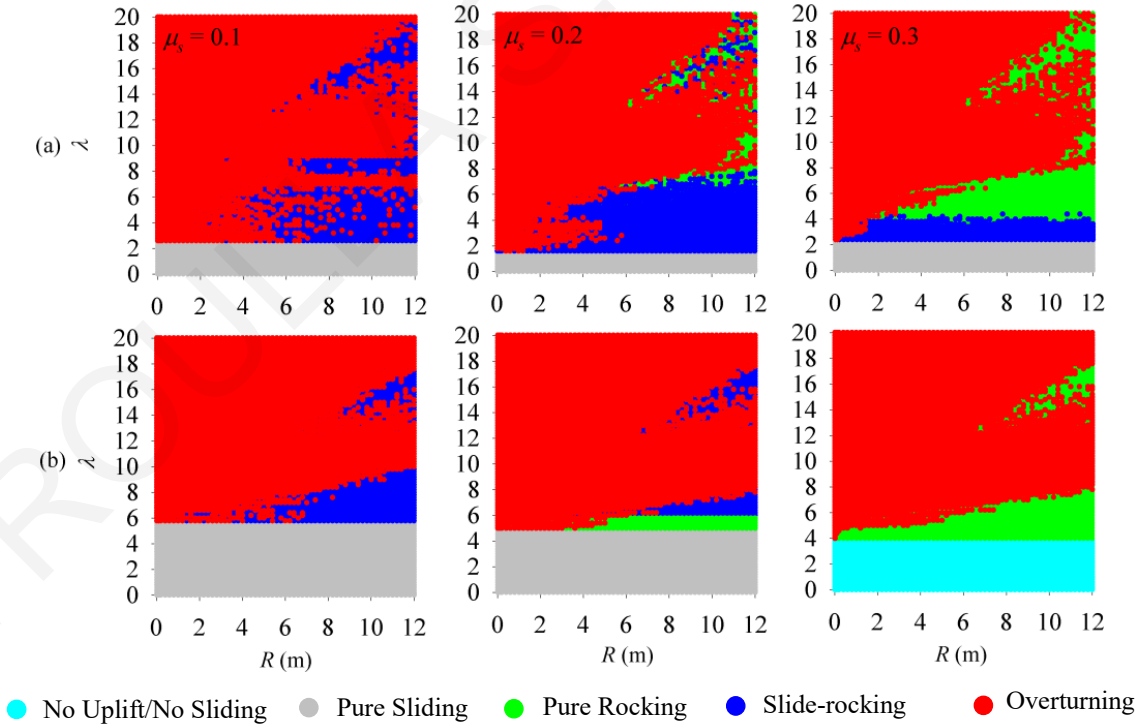

Figure D-3: Response-regime spectra in the $\lambda - R$ space for (a) non-isolated and (b) isolated block of varying geometric characteristics under Northridge, SCH / SN record ($\rho = 0.5$).

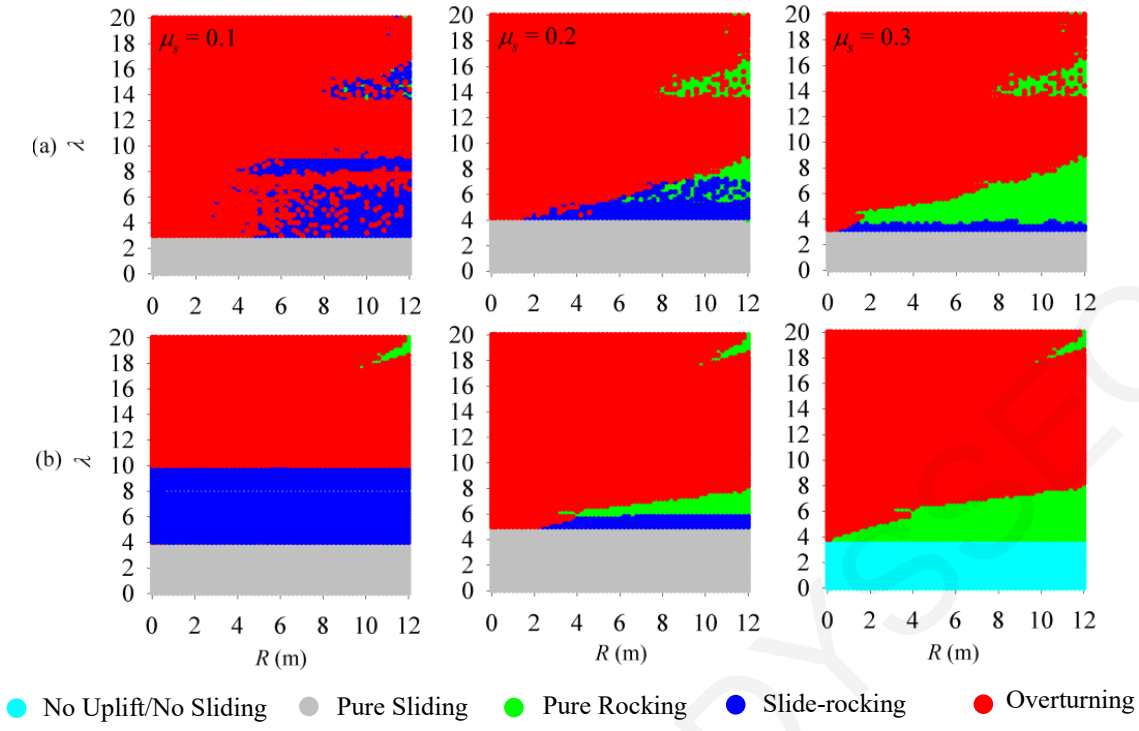

Figure D-4: Response-regime spectra in the $\lambda - R$ space for (a) non-isolated and (b) isolated block of varying geometric characteristics under Northridge, NWS / SN record ($\rho = 0.5$).

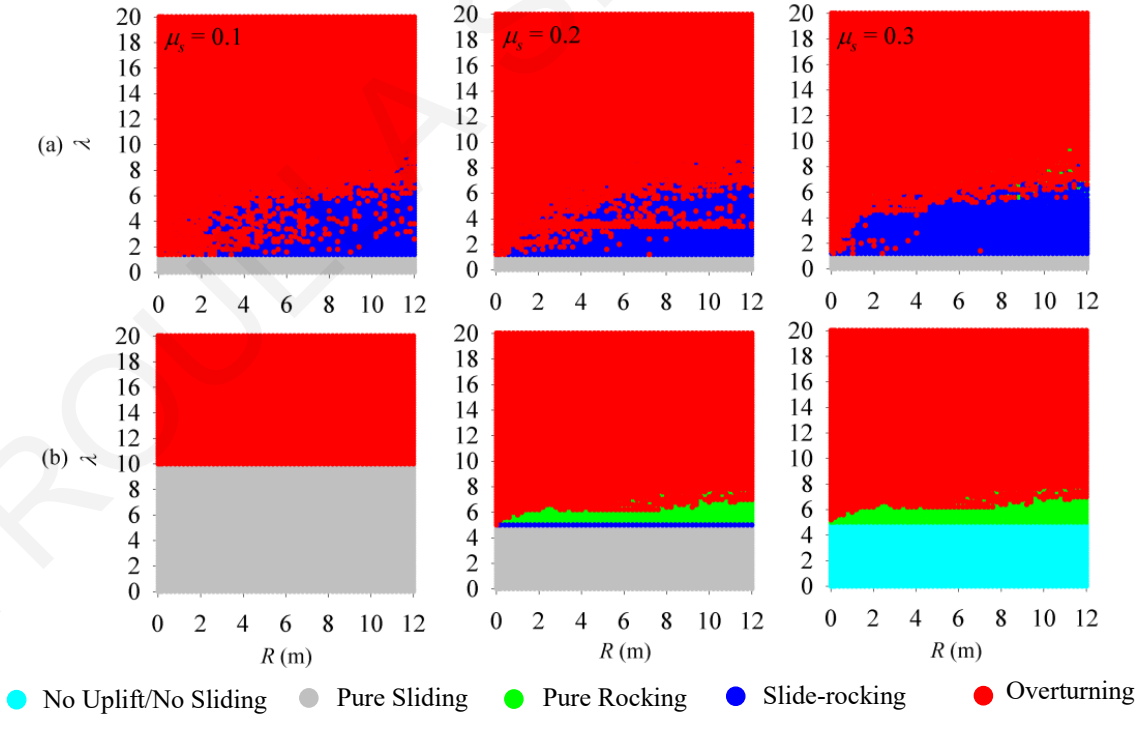

Figure D-5: Response-regime spectra in the $\lambda - R$ space for (a) non-isolated and (b) isolated block of varying geometric characteristics under Tabas, TAB / SP record ($\rho = 0.5$).

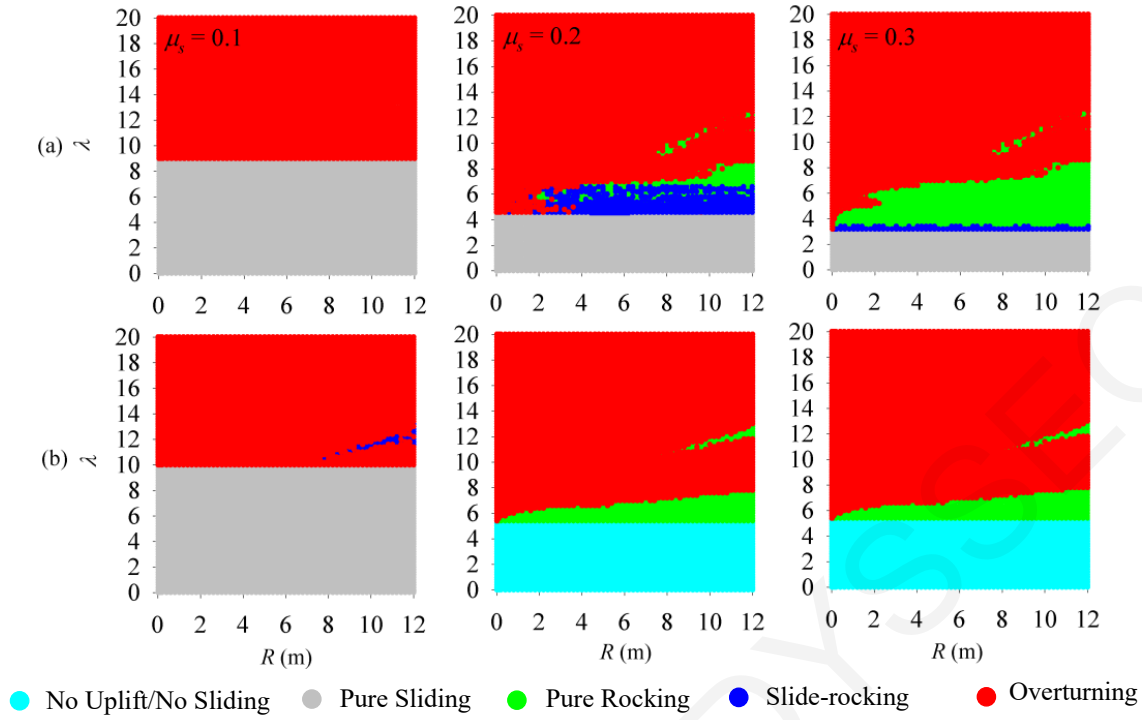

Figure D-6: Response-regime spectra in the $\lambda - R$ space for (a) non-isolated and (b) isolated block of varying geometric characteristics under Imperial Valley, E04 / SN record ($\rho = 0.5$).

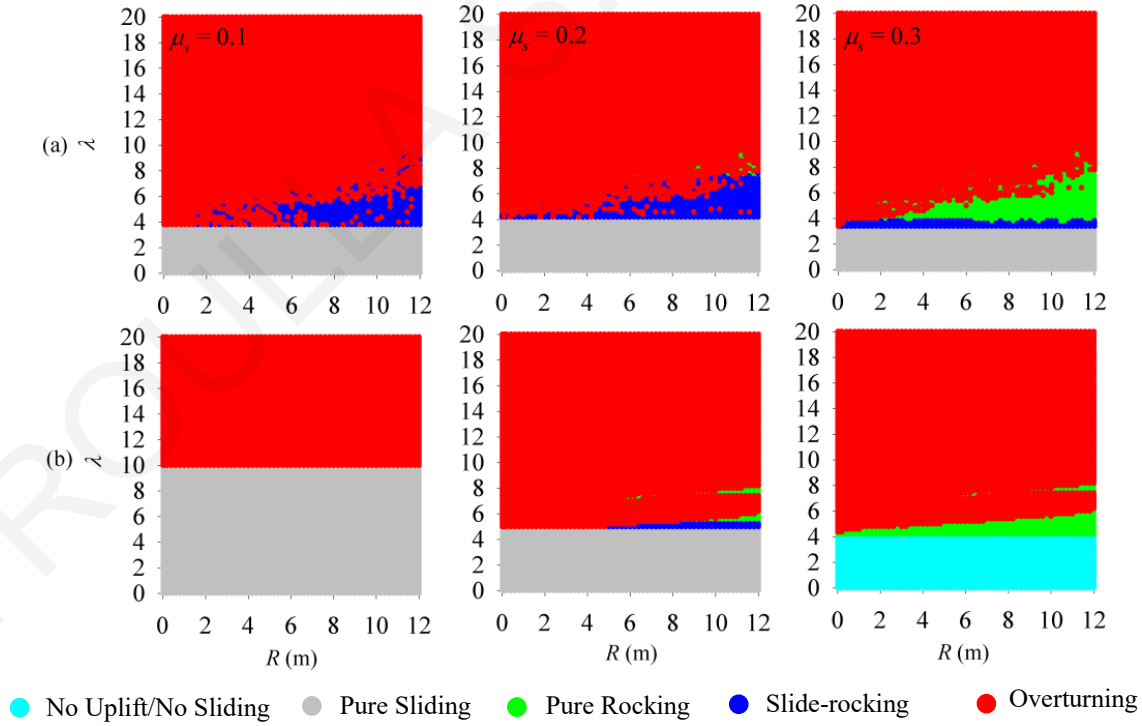

Figure D-7: Response-regime spectra in the $\lambda - R$ space for (a) non-isolated and (b) isolated block of varying geometric characteristics under Imperial Valley, E06 / SN record ($\rho = 0.5$).

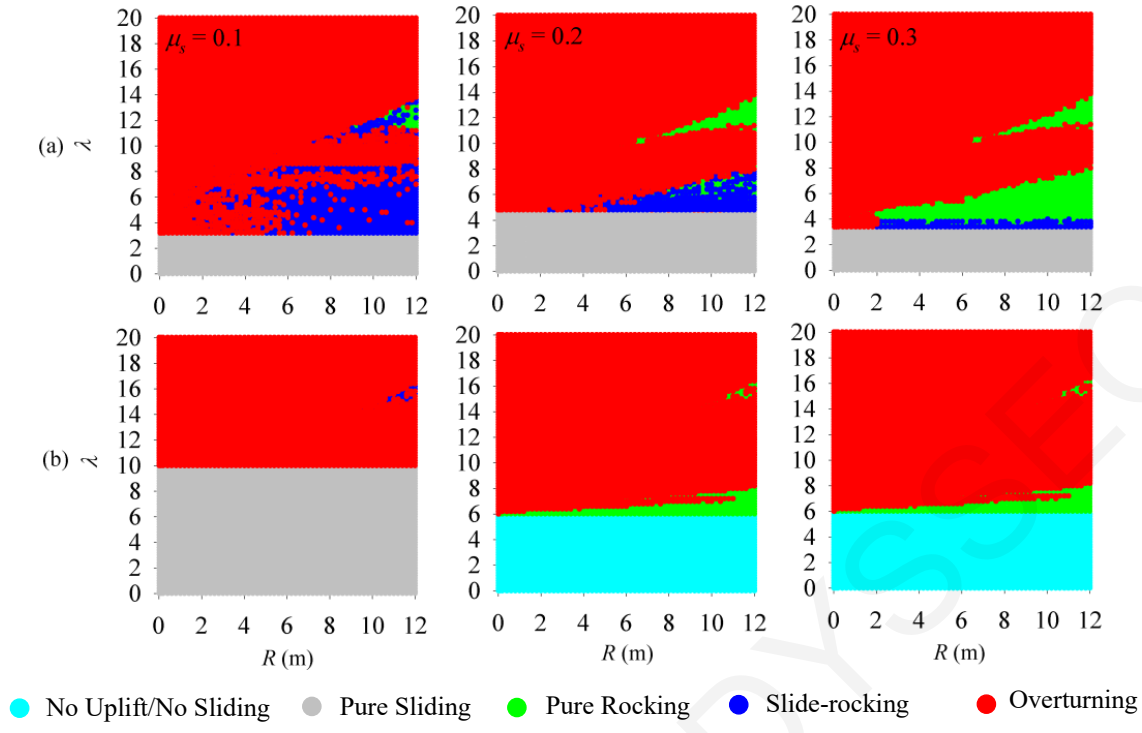

Figure D-8: Response-regime spectra in the $\lambda - R$ space for (a) non-isolated and (b) isolated block of varying geometric characteristics under Imperial Valley, E07 / SN record ($\rho = 0.5$).

APPENDIX E

Multi-Pattern Response-Regime Spectra for Isolated Blocks Using Linear and Nonlinear Isolation Systems

Assuming sliding between the block and the supporting base, entailing a multi-pattern response, this appendix presents a numerous response-regime spectra in the $\lambda - R$ space for isolated rigid blocks of varying geometric characteristics, using different values of the coefficient of friction μ_s. Two types of isolation system are considered in the analysis: (a) a Nonlinear I.S. with a bilinear hysteretic model (typified by friction-pendulum isolator) with parameters $\mu_b = 0.11$ and $R_b = 2.24\text{m}$ (corresponding to $T_b = 3\text{s}$) and (b) a Linear I.S. with viscoelastic model with $T_b = 3\text{s}$.

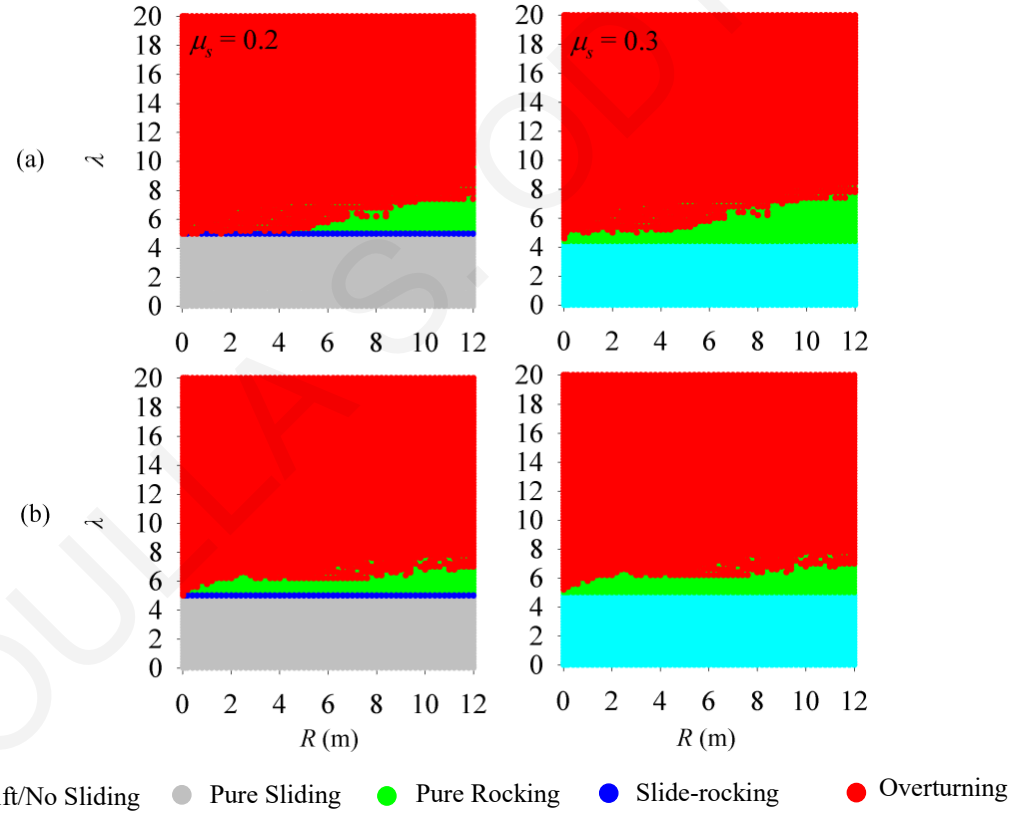

Figure E-1: Response-regime spectra in the $\lambda - R$ space for isolated rigid block of varying geometric characteristics using (a) Nonlinear I.S. and (b) Linear I.S under the SP component of 1978 Tabas, Iran earthquake ($\rho = 0.5$).

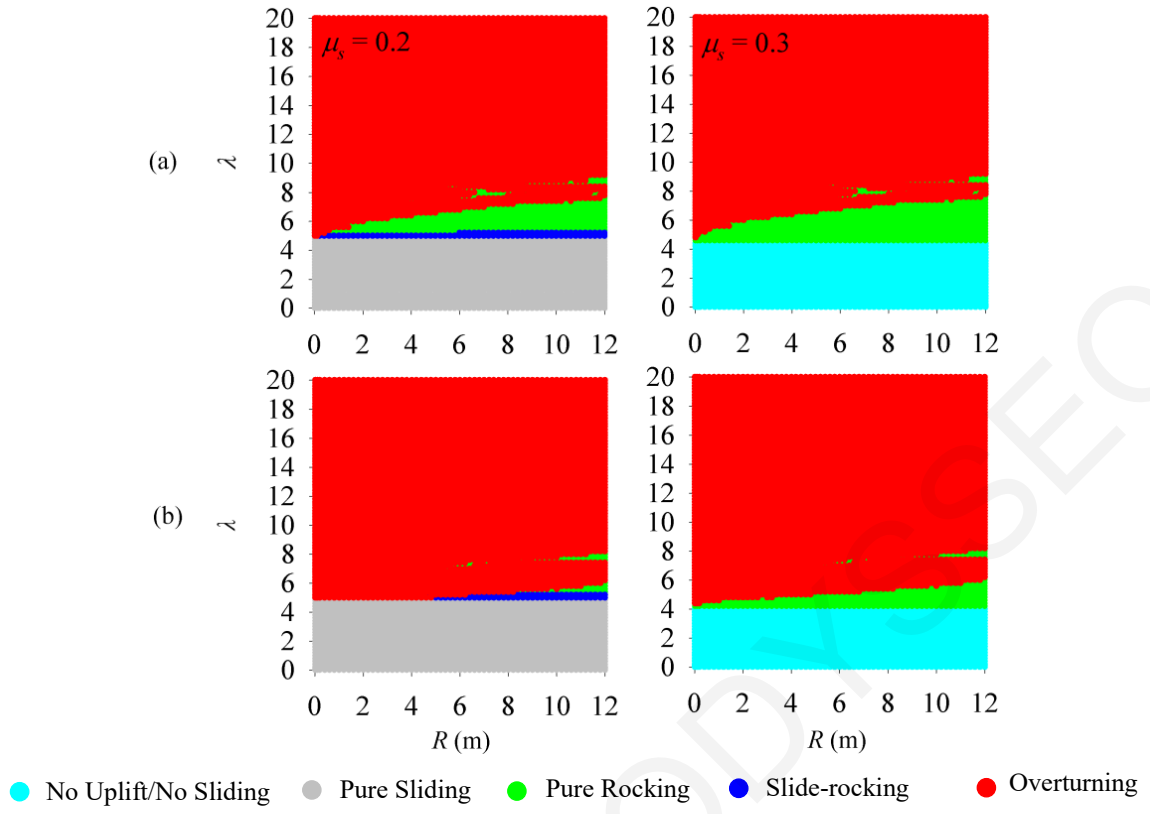

Figure E-2: Response-regime spectra in the $\lambda - R$ space for isolated rigid block of varying geometric characteristics using (a) Nonlinear I.S. and (b) Linear I.S under the SN component of 1979 Imperial Valley, CA, USA earthquake (E06 station) (ρ = 0.5).

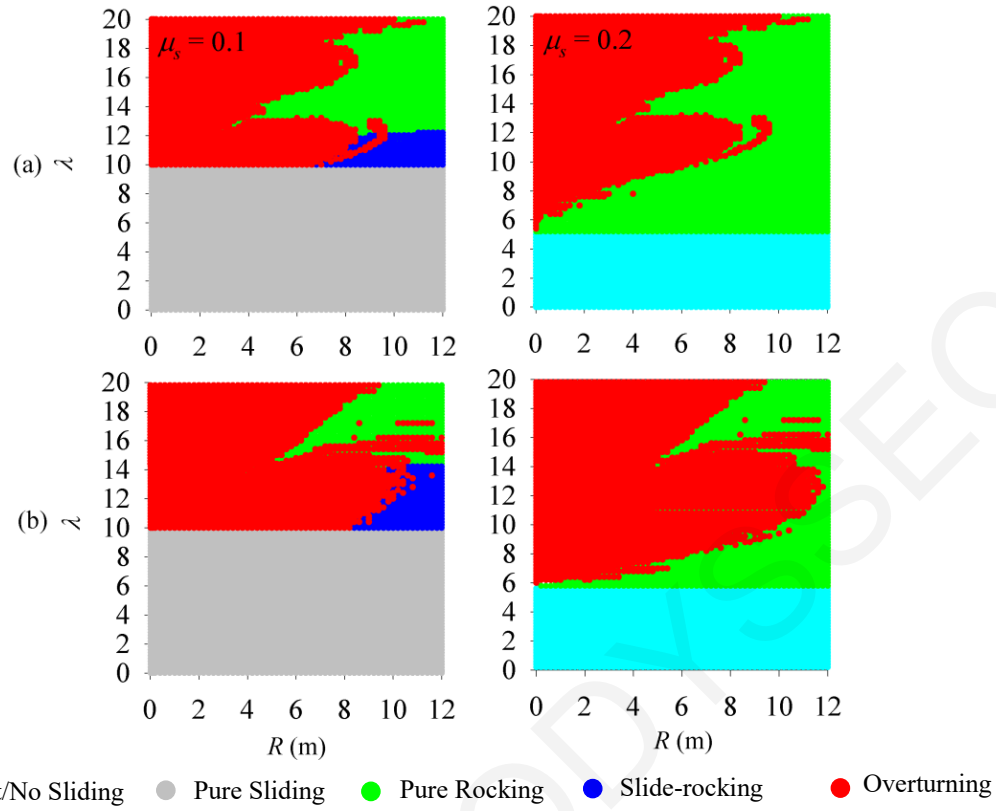

Figure E-3: Response-regime spectra in the $\lambda - R$ space for isolated rigid block of varying geometric characteristics using (a) Nonlinear I.S. and (b) Linear I.S under the SN component of 1977 Bucharest, Romania earthquake ($\rho = 0.5$).

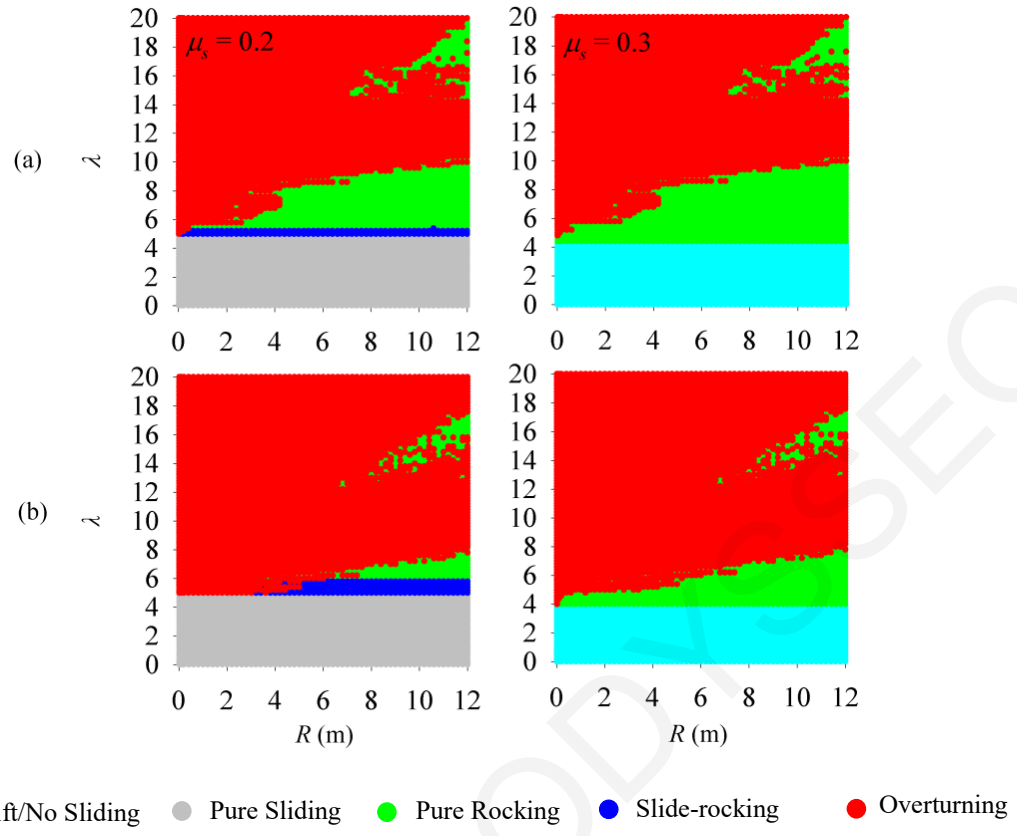

Figure E-4: Response-regime spectra in the $\lambda - R$ space for isolated rigid block of varying geometric characteristics using (a) Nonlinear I.S. and (b) Linear I.S under the SN component of 1994 Northridge, CA, USA earthquake (SCH station) ($\rho = 0.5$).